XXXI. VÝROČNÍ SJEZD
ČESKÉ KARDIOLOGICKÉ
SPOLEČNOSTI

TO NEJLEPŠÍ Z **ČESKÉ KARDIOLOGIE**
ZA ROK 2022

ČESKÁ
KARDIOLOGICKÁ
SPOLEČNOST

Nejlepší původní české práce publikované v roce 2022

Tato sekce prezentuje každoročně na výročním sjezdu ČKS **nejlepší původní vědecké práce členů ČKS**, vzniklé na pracovištích v ČR a publikované v předchozím kalendářním roce v mezinárodních časopisech s impakt faktorem >2,0. Tři nejlepší jsou rovněž **oceněny výborem ČKS**. Práce jsou řazeny dle IF.

Podmínky:

- Práce musí být publikována v časopise s impakt faktorem > 2,0 v průběhu posledního kalendářního roku před sjezdem ČKS, na který je přihlášena
- Práce musí vzniknout na pracovišti v České republice
- Prvním autorem musí být člen ČKS
- Musí jít o původní práci, prezentující vlastní výzkumné výsledky (nemůže se jednat o přehledný článek, editorial, abstrakt ani o kasuistiku)
- Nemůže se jednat ani o práci vzniklou v zahraničí (např. při studijním pobytu českého lékaře)
- Současně s přihlášením práce je autor povinen zaslat do sekretariátu ČKS e–mailem PDF verzi originálního článku s přihlášenou prací. Bez tohoto textu „in extenso" nemůže být práce přijata.

J. Bělohlávek et al.

Effect of Intra-arrest Transport, Extracorporeal Cardiopulmonary Resuscitation, and Immediate Invasive Assessment and Treatment on Functional Neurologic Outcome in Refractory Out-of-Hospital Cardiac Arrest
A Randomized Clinical Trial

JAMA
Impact Factor: 157

rejstřík

JAMA | Original Investigation | CARING FOR THE CRITICALLY ILL PATIENT

Effect of Intra-arrest Transport, Extracorporeal Cardiopulmonary Resuscitation, and Immediate Invasive Assessment and Treatment on Functional Neurologic Outcome in Refractory Out-of-Hospital Cardiac Arrest
A Randomized Clinical Trial

Jan Belohlavek, MD, PhD; Jana Smalcova, MD; Daniel Rob, MD; Ondrej Franek, MD; Ondrej Smid, MD; Milana Pokorna, MD, PhD; Jan Horák, MD; Vratislav Mrazek, MD; Tomas Kovarnik, MD, PhD; David Zemanek, MD, PhD; Ales Kral, MD, PhD; Stepan Havranek, MD, PhD; Petra Kavalkova, PhD; Lucie Kompelentova, MD; Helena Tomková, MD; Alan Mejstrik, MSc; Jaroslav Valasek, MD; David Peran, MSc; Jaroslav Pekara, MSc; Jan Rulisek, MD, PhD; Martin Balik, MD, PhD; Michal Huptych, PhD; Jiri Jarkovsky, PhD; Jan Malik, MD, PhD; Anna Valerianova, MD, PhD; Frantisek Mlejnsky, MSc, PhD; Petr Kolouch, MD; Petra Havrankova, MD, PhD; Dan Romportl, MD; Arnost Komarek, PhD; Ales Linhart, MD, PhD; for the Prague OHCA Study Group

IMPORTANCE Out-of-hospital cardiac arrest (OHCA) has poor outcome. Whether intra-arrest transport, extracorporeal cardiopulmonary resuscitation (ECPR), and immediate invasive assessment and treatment (invasive strategy) is beneficial in this setting remains uncertain.

OBJECTIVE To determine whether an early invasive approach in adults with refractory OHCA improves neurologically favorable survival.

DESIGN, SETTING, AND PARTICIPANTS Single-center, randomized clinical trial in Prague, Czech Republic, of adults with a witnessed OHCA of presumed cardiac origin without return of spontaneous circulation. A total of 256 participants, of a planned sample size of 285, were enrolled between March 2013 and October 2020. Patients were observed until death or day 180 (last patient follow-up ended on March 30, 2021).

INTERVENTIONS In the invasive strategy group (n = 124), mechanical compression was initiated, followed by intra-arrest transport to a cardiac center for ECPR and immediate invasive assessment and treatment. Regular advanced cardiac life support was continued on-site in the standard strategy group (n = 132).

MAIN OUTCOMES AND MEASURES The primary outcome was survival with a good neurologic outcome (defined as Cerebral Performance Category [CPC] 1-2) at 180 days after randomization. Secondary outcomes included neurologic recovery at 30 days (defined as CPC 1-2 at any time within the first 30 days) and cardiac recovery at 30 days (defined as no need for pharmacological or mechanical cardiac support for at least 24 hours).

RESULTS The trial was stopped at the recommendation of the data and safety monitoring board when prespecified criteria for futility were met. Among 256 patients (median age, 58 years; 44 [17%] women), 256 (100%) completed the trial. In the main analysis, 39 patients (31.5%) in the invasive strategy group and 29 (22.0%) in the standard strategy group survived to 180 days with good neurologic outcome (odds ratio [OR], 1.63 [95% CI, 0.93 to 2.85]; difference, 9.5% [95% CI, −1.3% to 20.1%]; P = .09). At 30 days, neurologic recovery had occurred in 38 patients (30.6%) in the invasive strategy group and in 24 (18.2%) in the standard strategy group (OR, 1.99 [95% CI, 1.11 to 3.57]; difference, 12.4% [95% CI, 1.9% to 22.7%]; P = .02), and cardiac recovery had occurred in 54 (43.5%) and 45 (34.1%) patients, respectively (OR, 1.49 [95% CI, 0.91 to 2.47]; difference, 9.4% [95% CI, −2.5% to 21%]; P = .12). Bleeding occurred more frequently in the invasive strategy vs standard strategy group (31% vs 15%, respectively).

CONCLUSIONS AND RELEVANCE Among patients with refractory out-of-hospital cardiac arrest, the bundle of early intra-arrest transport, ECPR, and invasive assessment and treatment did not significantly improve survival with neurologically favorable outcome at 180 days compared with standard resuscitation. However, the trial was possibly underpowered to detect a clinically relevant difference.

TRIAL REGISTRATION ClinicalTrials.gov Identifier: NCT01511666

JAMA. 2022;327(8):737-747. doi:10.1001/jama.2022.1025

Visual Abstract

Supplemental content

Author Affiliations: Author affiliations are listed at the end of this article.

Corresponding Author: Jan Belohlavek, MD, PhD, 2nd Department of Medicine—Department of Cardiovascular Medicine, First Faculty of Medicine, Charles University and General University Hospital, U Nemocnice 2, Prague 2, 128 00, Czech Republic (jan.belohlavek@vfn.cz).

Section Editor: Christopher Seymour, MD, Associate Editor, *JAMA* (christopher.seymour@jamanetwork.org).

Out-of-hospital cardiac arrest (OHCA) is a significant socioeconomic burden to society.[1] In a large trial, 50% of patients who attained stable return of spontaneous circulation (ROSC) during initial resuscitation and were transferred to the hospital for postresuscitation care achieved neurologically favorable survival.[2] However, refractory cardiac arrest (ie, prolonged cardiac arrest and cardiac arrest without ROSC in the field) is associated with poor clinical outcomes.[3] In patients without ROSC, the odds of survival are low when transport to the hospital occurs during ongoing cardiopulmonary resuscitation (CPR), usually less than 4%.[4,5]

Temporary replacement of a failing circulation by extracorporeal life support (ECLS), a method called extracorporeal cardiopulmonary resuscitation (ECPR), has been recognized as a potential approach to refractory cardiac arrest.[6-8] Despite encouraging results of nonrandomized studies, a meta-analysis,[9] and 1 recently published small randomized trial,[10] the benefit of ECPR in refractory OHCA remains uncertain.[11,12] Recent European Resuscitation Guidelines[13] provide a weak recommendation for ECPR, which may be considered as a rescue method when conventional CPR is failing, with very low certainty of evidence.

The purpose of this randomized clinical trial was to compare the bundle of early intra-arrest transport to the hospital using mechanical CPR, ECPR, and immediate invasive assessment and treatment vs standard treatment in refractory OHCA for achieving survival with good neurologic outcome at 180 days.

Key Points

Question In patients with witnessed refractory out-of-hospital cardiac arrest, does early intra-arrest transport, extracorporeal cardiopulmonary resuscitation, and invasive assessment and treatment improve outcomes compared with standard resuscitation?

Findings In this randomized clinical trial that included 256 patients, survival with neurologically favorable outcome (Cerebral Performance Category 1-2) at 180 days occurred in 31.5% in the invasive strategy group and 22.0% in the standard resuscitation group, a difference that was not statistically significant.

Meaning Among patients with refractory out-of-hospital cardiac arrest, the bundle of early intra-arrest transport, extracorporeal cardiopulmonary resuscitation, and invasive assessment and treatment did not significantly improve survival with neurologically favorable outcome at 180 days compared with standard resuscitation, although the trial was possibly underpowered to detect a clinically relevant difference.

Methods

Study Design

This randomized clinical trial was conducted at a single center in Prague, Czech Republic, from March 1, 2013, to October 25, 2020 (with final follow-up on March 30, 2021). The study protocol, including statistical analysis plan (Supplement 1), was published in detail prior to study initiation,[14] and the study was approved by the institutional review board of the General University Hospital and First Faculty of Medicine, Charles University in Prague (192/11S-IV).

Each participant's legal representative was informed of the participant's study enrollment and was asked for written informed consent as soon as possible. All patients who regained normal neurologic function were asked to provide their written consent regarding the use of their data. Consent requirements were waived for patients who died at the scene and never reached the hospital and for participants without known legal representatives. As specified in the protocol, a data and safety monitoring board reviewed the data on patient outcome and complications every 6 months or after every 30 patients enrolled, whichever came first. An independent contract research organization verified and monitored the study data.

Participants

Adults aged 18 to 65 years receiving ongoing resuscitation for witnessed OHCA of presumed cardiac etiology were eligible for enrollment in the trial, given that they had received a minimum of 5 minutes of advanced cardiac life support without ROSC and when the ECPR team was available at the cardiac center. Patients who had unwitnessed cardiac arrest or presumed noncardiac cause, had suspected or confirmed pregnancy, attained ROSC within 5 minutes during initial resuscitation, regained consciousness, had obvious life-limiting comorbidities, bleeding diathesis, known do-not-resuscitate order, or known prearrest Cerebral Performance Category (CPC)[15] 3 or greater were excluded (**Figure 1**; eTable 1 in Supplement 2).

Enrollment and Randomization

Enrollment was conducted with the close cooperation of the Prague Emergency Medical Service dispatch center. The study coordinator in the cardiac center was notified by an automatic Short Message Service alert on every occasion when the dispatch center initiated telephone-assisted bystander chest compressions and activated a rapid response vehicle for a witnessed collapse suspected to be cardiac arrest of presumed cardiac cause. A telephone connection was subsequently established during the ongoing chest compressions between the cardiac center coordinator and the physician or paramedic on scene (randomization call). The coordinator logged into a web-based secured randomization system that was available 24 hours per day and maintained by the Institute of Biostatistics and Analyses, Faculty of Medicine, Masaryk University, Brno. An assigned patient number and intervention group, ie, invasive group or standard group, was recorded. The log-in link was accessible from all computers within the cardiac center and from the smartphone of the coordinator.

For randomization, the patient's estimated age and sex as well as confirmation of the inclusion/exclusion criteria were recorded (eTable 1 in Supplement 2). Randomization into the standard strategy or invasive strategy group was based on 4 strata (men ≤45 years, men >45 years, women ≤45 years,

Figure 1. Prehospital Flow of Participants in a Study of Intra-arrest Transport, Extracorporeal Cardiopulmonary Resuscitation, and Immediate Invasive Assessment and Treatment in Refractory Out-of-Hospital Cardiac Arrest

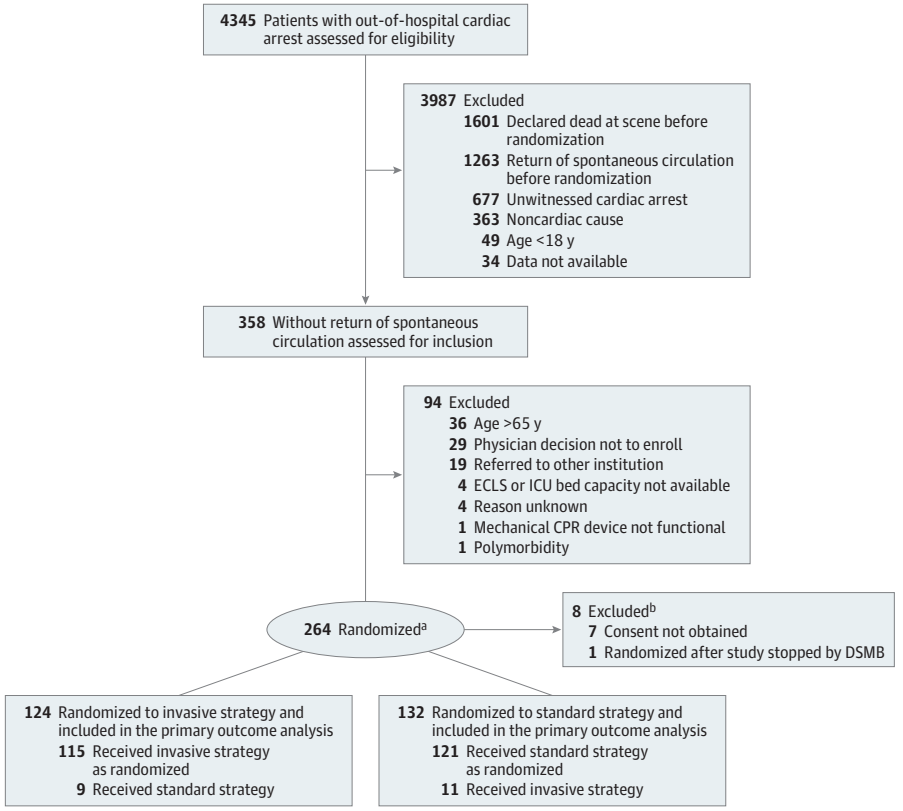

DSMB indicates data and safety monitoring board; ECLS, extracorporeal life support; CPR, cardiopulmonary resuscitation; ICU, intensive care unit; OHCA, out-of-hospital cardiac arrest; ROSC, return of spontaneous circulation.

[a] Randomization into standard strategy and invasive strategy groups was based on 4 strata (men ≤45 years, men >45 years, women ≤45 years, women >45 years), with block size of 8.

[b] Seven patients were excluded after randomization because consent was refused and information was not available as to how many were randomized to each group for analysis.

women >45 years), with block size of 8. The block size was not disclosed to research personnel.

Intervention

Patients randomized to the standard strategy group received continued advanced cardiac life support on site. The use of drugs, further defibrillations, or other interventions followed recommended guidelines.[16,17] If ROSC was achieved (defined as a cardiac electrical activity with palpable pulse), transport to the hospital was initiated and an early invasive strategy (ie, coronary angiography) was encouraged.

A mechanical chest compression device (LUCAS, Lund University Cardiac Arrest System; Physio-Control Inc/Jolife AB, Lund, Sweden) was originally reserved for the invasive strategy group only; however, following the publication of a major trial on mechanical chest compression,[18] the attachment of a mechanical chest compression device was left to the discretion of the emergency physician and was allowed for use at any point during CPR.

In the invasive strategy group, intra-arrest intranasal evaporative cooling via a RhinoChill device (BeneChill Inc) was initiated if feasible (this device became unavailable during the course of the study in 2016) and the patient was immediately transferred directly to the cardiac center catheterization laboratory during ongoing CPR with the intention of proceeding with ECPR if ROSC was not achieved en route or on admission. The use of drugs, further defibrillations en route, or other interventions during transport followed European Resuscitation Council guidelines.[16,17] The team, including study coordinator, intensivist, perfusionist (a specialist responsible for an ECLS), interventional cardiologist, study data manager, and interventional and intensive care unit nurses simultaneously prepared all the necessary equipment. A dry-primed extracorporeal life support machine was ready to be used in the catheterization laboratory when needed.

On admission, the overall status, ROSC presence, and ECLS implantation inclusion/exclusion criteria (eTable 1 in Supplement 2) were evaluated. The ECLS cannulation was performed on the catheterization table during ongoing mechanical CPR using a femoro-femoral approach. After commencement of ECLS and following the completion of the invasive diagnostic and therapeutic procedures (ie, coronary, and eventually pulmonary or aortic angiography and percutaneous coronary intervention, if appropriate), an antegrade perfusion cannula was implanted in the cannulated limb under ultrasound guidance. Patients receiving ECLS were continuously anticoagulated with heparin unless contraindicated, with a target activated partial thromboplastin time of 50 to 70 seconds.

Postresuscitation care was standardized in both study groups. All patients admitted to the hospital had an immediate biochemical evaluation, an urgent bedside echocardiogram, and whole-body computed tomography if feasible and clinically indicated. In-hospital target temperature management to 33 °C was initiated as soon as possible either via ECLS heat exchanger or other routine measures (intravascular or surface feedback device cooling). Following the publication of a target temperature management trial,[19] in cases with early awakening or complications of hypothermia, a strict temperature management to 36 °C was allowed instead of 33 °C. All other postarrest critical care management, including withdrawal of life-sustaining therapy, complied with European Resuscitation Council guidelines and other generally accepted approaches.[16-18,20]

A crossover from the standard strategy group to the invasive strategy group (and vice versa) was allowed in selected patients. In the standard to invasive strategy group, the decision was made based on the request of an emergency physician. At least 2 additional unsuccessful defibrillations were required after randomization before a crossover was accepted by the cardiac center coordinator. The crossover from invasive strategy to standard strategy was accepted when continuing care with invasive measures was deemed to be futile. The termination of resuscitation efforts followed the European Resuscitation Council guidelines,[16,17] although the final decision was based on the discretion of the emergency physician or cardiac intensivist in charge.

Outcomes

Primary Outcome

Primary outcome was 180-day survival with favorable neurologic status defined as no or minimal neurologic impairment (CPC 1 or 2). The CPC schema ranges from 1 (defined as conscious, alert, able to work), 2 (conscious, sufficient cerebral function for independent activities of daily life, able to work in sheltered environment), 3 (conscious, dependent on others for daily support), 4 (comatous, vegetative state) to 5 (brain death).

Neurologic outcome was assessed by a neurologist in a blinded fashion.

Secondary Outcomes

Secondary outcomes included 30-day survival with cardiac recovery (no need for pharmacological or mechanical cardiac support for 24 hours) and neurologic recovery (CPC 1 or 2) at any point within the first 30 days after cardiac arrest.

Exploratory Analyses

Survival to 180 days was assessed as a post hoc outcome. Post hoc subgroup analyses for the primary outcome were performed in the following subgroups: older than 65 years vs 65 years or younger, sex, place of cardiac arrest, initial rhythm, pH below median value vs above, lactate level below median value vs above, and cause of cardiac arrest.

Complications

Bleeding complications were assessed based on Thrombolysis in Myocardial Infarction classification[21] under "major" category, defined as any intracranial hemorrhage (excluding microhemorrhages <10 mm), fatal bleeding directly resulting in death within 7 days, or overt bleeding associated with a decrease in hemoglobin concentration of 5 g/dL or a 15% absolute decrease in hematocrit. Organ lacerations were assessed both by morphological examinations (mainly computed tomography) and during autopsies. Technical complications related to ECLS were gathered and reported by perfusionists.

Power Analysis and Sample Size Calculation

Sample size determination was computed for the statistical superiority of invasive strategy over standard strategy using a 2-tailed test with $\alpha = .05$ and 90% power. A 10% 6-month survival with favorable neurologic outcome in the standard strategy group was expected. Three scenarios were suggested: 10% increase of primary outcome, with 571 patients expected to be enrolled; 15% increase, with 285 patients; and 20% increase, with 176 patients.[14]

Statistical Analysis

A complete case analysis, with no assumptions made for missing data, was performed for primary and secondary outcomes. In the main analysis, patient data were analyzed according to randomization group, and data from patients who crossed over were analyzed by original group assignment. A post hoc analysis pooled all patients treated with ECPR (both those allocated to the invasive strategy group and receiving ECPR and those allocated to the standard strategy group and receiving ECPR after crossover to the invasive strategy group).

Continuous data were evaluated for a normal distribution by Shapiro-Wilk test. Numeric variables are expressed as medians and IQRs. The 2-sided Mann-Whitney test was used to compare cardiac arrest times and laboratory values. Categorical values were compared using the 2-sided Fisher exact test (for 2 × 2 table) or χ^2 test. The primary and secondary outcomes are reported by odds ratios and absolute differences with 95% confidence intervals.

The survival analysis was performed by the Kaplan-Meier analysis and log-rank test and considered patients alive at day 180 regardless of their neurologic status. A subgroup analysis was computed using logistic regression and analysis of interaction between given stratification and study group. Because of the potential for type I error due to multiple comparisons, findings for secondary outcomes and subgroup analyses should be interpreted as exploratory.

A 2-sided $P < .05$ was considered statistically significant. Statistical analyses were performed with MedCalc version 19.7 (MedCalc Software Ltd) and SPSS version 26.0.0.0 (IBM Corp).

Results

The study was terminated on October 25, 2020, at the recommendation of the data and safety monitoring board (Supplement 3) because the standardized test statistics for results of primary end point in the study intersected a prespecified stopping rule for futility at n = 256 (eFigure 1 in Supplement 2).

Table 1. Baseline Demographics and Prehospital Resuscitation Characteristics of Included Patients in a Study of Intra-arrest Transport, Extracorporeal Cardiopulmonary Resuscitation, and Immediate Invasive Assessment and Treatment in Refractory Out-of-Hospital Cardiac Arrest

Characteristics	No. (%)	
	Invasive strategy (n = 124)	Standard strategy (n = 132)
Age, median (IQR), y	59 (48-66)	57 (47-65)
Sex		
Men	102 (82)	110 (83)
Women	22 (18)	22 (17)
Medical history, No./total (%)[a]		
Hypertension	47/108 (44)	42/83 (51)
Diabetes	19/104 (18)	17/83 (21)
Coronary artery disease	17/104 (16)	17/83 (21)
Chronic heart failure	11/106 (10)	5/79 (6)
COPD	8/105 (8)	2/79 (3)
Chronic kidney disease	3/104 (3)	2/79 (3)
Implanted ICD	3/121 (3)	0/89
Location of cardiac arrest		
Public place	44 (36)	54 (41)
Home	42 (34)	34 (26)
EMS	19 (15)	17 (13)
Car	8 (7)	7 (5)
Workplace	5 (4)	14 (11)
Hotel	4 (3)	6 (5)
Health facility	2 (2)	0
Initial rhythm[b]		
Ventricular fibrillation	72 (58)	84 (64)
Asystole	31 (25)	24 (18)
Pulseless electrical activity	21 (17)	24 (18)
Bystander CPR[c]	123 (99)	129 (98)
Telephone-assisted bystander CPR	96 (77)	107 (81)
Time from collapse to EMS arrival, median (IQR), min	8 (7-11)	9 (7-11)
Time from collapse to ACLS, median (IQR), min	10 (7-13)	11 (8-14)
Time to telephone-assisted CPR, median (IQR), min	3 (2-5)	2 (1-4)
Time from collapse to randomization, median (IQR), min	24 (21-30)	26 (19-31)
No. of prehospital epinephrine doses, median (IQR), mg	4 (2-5)	5 (3-7)
No. of prehospital defibrillation attempts, median (IQR)	4 (2-6)	4 (2-7)
Mechanical CPR[d]	114 (92)	104 (79)
Intermittent ROSC[e]	41 (33)	45 (34)
Hypothermia initiated in field[f]	21 (17)	12 (9)

Abbreviations: ACLS, advanced cardiac life support; COPD, chronic obstructive pulmonary disease; CPR, cardiopulmonary resuscitation; EMS, emergency medical service; ICD, implantable cardioverter-defibrillator; ROSC, return of spontaneous circulation.

[a] The information for several categories was obtained later during patient care from EMS, caregivers, relatives, and chart reviews and might not have been available to caregivers during initial treatment.

[b] As determined by EMS.

[c] High rate of bystander CPR consistent with generally high rate in Prague (>80%) as reported in a Eureca 2 study.[27]

[d] Use of LUCAS device (Lund University Cardiac Arrest System; Physio-Control Inc/Jolife AB).

[e] Defined as an unsustained palpable pulse with organized ECG rhythm.

[f] Prehospital hypothermia provided by means of intranasal evaporative cooling was used in the invasive strategy group and those patients in the standard strategy group who crossed over to the invasive approach. This method became unavailable during the course of the study in 2016; therefore, the percentage of use is low.

During the study enrollment period from March 1, 2013, to October 25, 2020, 4345 attended cardiac arrests occurred within the Prague region. After exclusion of those without presumed cardiac cause, those that lacked a witness, patients who achieved ROSC, or patients who died without consideration for study enrollment, 358 patients with arrest refractory to initial resuscitation efforts remained. Of these, 264 were eligible for the study enrollment and randomized. Later, 8 patients were withdrawn; for 7, consent was not obtained from the relatives, and 1 patient was erroneously randomized after the study was already stopped.

In total, 256 patients were analyzed, 124 allocated to the invasive strategy group and 132 to the standard strategy group. Overall, in 20 patients (7.6%), a crossover was accepted. There were 11 crossovers from the standard strategy group to the invasive strategy group (all except 1 involved patients with refractory ventricular fibrillation) and 9 crossovers from the invasive strategy group to the standard strategy group (Figure 1).

Patient and Cardiac Arrest Characteristics

Table 1 reports the main demographics of the study population. The median age was 59 years (IQR, 48-66) for the invasive strategy group and 57 years (IQR, 47-65) for the standard strategy group, and 44 of the 256 patients (17%) were women. Hypertension, diabetes, and coronary artery disease

Table 2. Primary and Secondary Outcomes in a Study of Intra-arrest Transport, Extracorporeal Cardiopulmonary Resuscitation, and Immediate Invasive Assessment and Treatment in Refractory Out-of-Hospital Cardiac Arrest

	No. (%)			
	Invasive strategy (n = 124)	Standard strategy (n = 132)	Absolute difference, % (95% CI)	*P* value
Primary outcome				
Survival with minimal or no neurologic impairment at 180 d[a]	39 (31.5)	29 (22.0)	9.5 (−1.3 to 20.1)	.09
Secondary outcomes				
Survival with minimal or no neurologic impairment at 30 d[a]	38 (30.6)	24 (18.2)	12.4 (1.9 to 22.7)	.02
Cardiac recovery at 30 d[b]	54 (43.5)	45 (34.1)	9.4 (−2.5 to 21)	.12

[a] Defined as Cerebral Performance Category 1 or 2. The Cerebral Performance Category schema ranges from 1 (defined as conscious, alert, able to work), 2 (conscious, sufficient cerebral function for independent activities of daily life, able to work in sheltered environment), 3 (conscious, dependent on others for daily support), 4 (comatous, vegetative state) to 5 (defined as brain death). All patients observed to death or 180 days.

[b] Defined as absence of both pharmacological and mechanical cardiac support for at least 24 hours.

were prevailing comorbidities. The most frequent cause of cardiac arrest was acute coronary syndrome in both the invasive strategy group (64/124 [52%]) and the standard strategy group (63/132 [48%]).

Cardiac arrest occurred most commonly in a public place (44/124 patients [36%] in invasive strategy group, 54/132 [41%] in the standard strategy group). Ventricular fibrillation was the most common initial rhythm (72/124 patients [58%] in the invasive strategy group and 84/132 [64%] in the standard strategy group). Bystander CPR was performed in 123 of 124 cases (99%) in the invasive strategy group and in 129 of 132 (98%) in the standard strategy group, as well as telephone-assisted dispatch center CPR in 96 of 124 (77%) and 107 of 132 (81%), initiated within median of 3 (IQR, 2-5) and 2 (IQR, 1-4) minutes after the collapse in the respective groups. Patients were randomized within a median of 24 (IQR, 21-30) and 26 (IQR, 19-31) minutes after collapse for the invasive strategy and standard strategy groups, respectively.

Primary Outcome

Survival with favorable neurologic outcome at 180 days occurred in 39 of 124 patients (31.5%) in the invasive strategy group and 29 of 132 patients (22%) in the standard strategy group, a difference that was not statistically significant (odds ratio, 1.63 [95% CI, 0.93 to 2.85]; absolute difference, 9.5% [95% CI, −1.3% to 20.1%]; *P* = .09) (**Table 2**). There were no missing data for the primary outcome analysis.

Secondary Outcomes

Neurologic recovery at 30 days occurred in 38 of 124 patients (30.6%) in the invasive strategy group and 24 of 132 (18.2%) in the standard strategy group (odds ratio, 1.99 [95% CI, 1.11 to 3.57]; absolute difference, 12.4% [95% CI, 1.9% to 22.7%]; *P* = .02).

Cardiac recovery at 30 days occurred in 54 of 124 patients (43.5%) in the invasive strategy group and 45 of 132 (34.1%) in the standard strategy group (odds ratio, 1.49 [95% CI, 0.91 to 2.47]; absolute difference, 9.4% [95% CI, −2.5 to 21%]; *P* = .12).

Resuscitation and Hospitalization Procedures and Outcomes

In the invasive strategy group, a median of 4 (IQR, 2-5) epinephrine doses were used, compared with 5 (IQR, 3-7) in the standard strategy group (*P* = .002), while the number of prehospital defibrillations was median of 4 (IQR, 2-6) in the invasive strategy group vs 4 (IQR, 2-7) in the standard strategy group. Intermittent ROSC was identified in 41 of 124 patients (33%) in the invasive strategy group and 45 of 132 (34%) in the standard strategy group.

As **Table 3** describes in detail, more patients in the invasive strategy group were admitted to the hospital after a shorter time of transport from the scene. The overall CPR time was longer in the invasive strategy group (median, 58 [IQR, 43-70] vs 46 [IQR, 33-68] minutes, *P* = .04), as every effort was made to bring the patient to the hospital catheterization laboratory for ECPR.

Among patients admitted to the hospital, target temperature management was used in 117 of 123 patients (95%) in the invasive strategy group and 61 of 87 (70%) in the standard strategy group (*P* < .001). Those who did not receive temperature control (6 in the invasive strategy group and 26 in the standard strategy group) either had contraindications (mainly advanced hemodynamic instability) or died early, before reaching the intensive care unit (eTable 2 in Supplement 2).

An invasive assessment with diagnostic angiography was performed in 120 of 123 admitted patients (98%) in the invasive strategy group and 67 of 87 (77%) in the standard strategy group (*P* < .001), corresponding mainly to coronary angiography. Immediate PCI was performed successfully in 56 of 62 patients (90%) in the invasive strategy group and 24 of 30 (80%) in the standard strategy group (*P* = .20). Of note, in 3 patients, emergency balloon aortic valvuloplasty was performed. On admission, patients in invasive strategy vs standard strategy group had lower pH (median, 6.93 [IQR, 6.8-7.1] vs 7.03 [IQR, 6.9-7.2]; *P* = .001) and higher serum lactate levels (median, 12.5 [IQR, 9.2-16] mmol/L vs 10.4 [IQR, 7.5-13.5] mmol/L; *P* = .01).

Table 3. Additional Outcomes Related to Transport, Hospitalization, and Intervention in a Study of Intra-arrest Transport, Extracorporeal Cardiopulmonary Resuscitation, and Immediate Invasive Assessment and Treatment in Refractory Out-of-Hospital Cardiac Arrest

Prehospital and early hospital events	No. (%)	
	Invasive strategy (n = 124)	Standard strategy (n = 132)
Arrived to hospital	123 (99)	87 (66)
Time from collapse to hospital arrival, median (IQR), min	49 (44-60)	60 (50-69)
Transport time - time from randomization to admission, median (IQR), min	26 (19-33)	33 (25-42)
Prehospital declaration of death	1 (1)	45 (34)
Declaration of death within 1 h of hospital admission	10 (8)	19 (14)
Time of CPR (time to death/ROSC or ECLS), median (IQR), min	58 (43-70)	46 (33-68)
Duration of CPR, min		
<30	14 (11)	26 (20)
≥30 and <45	19 (15)	33 (25)
≥45	91 (73)	73 (55)
Sustained ROSC on admission[a]	34 (27)	58 (44)
Hospitalization events		
Target temperature management used, No./total (%)[b]	117/123 (95)	61/87 (70)
Extracorporeal life support		
ECLS implanted	82 (66)	10 (8)
Time to ECLS, median (IQR), min	61 (55-70) [n = 81]	62 (51-73) [n = 10]
Time of implantation (door to ECLS), median (IQR), min	12 (9-15) [n = 80]	16 (11-17) [n = 10]
Invasive assessment, No./total (%)		
Diagnostic angiography	120/123 (98)	67/87 (77)
Coronary angiography	115/120 (96)	66/67 (99)
Aortography	28/120 (24)	13/67 (19)
Left ventricle angiography	26/120 (22)	21/67 (31)
Pulmonary angiography	22/120 (18)	5/67 (8)
Emergency invasive interventions, No./total (%)		
PCI (both for ACS and CAD)[c]		
Successful	56/62 (90)	24/30 (80)
Unsuccessful	6/62 (10)	6/30 (20)
Balloon valvuloplasty	0/120	3 (4)
Laboratory values on admission		
pH [reference, 7.36-7.44], median (IQR)	6.93 (6.8-7.1)	7.03 (6.9-7.2)
Lactate [reference, 0.5-2.0], median (IQR), mmol/L	12.5 (9.2-16)	10.4 (7.5-13.5)
Cause of cardiac arrest (including autopsy findings)		
Acute coronary syndrome	64 (52)	63 (48)
Coronary artery disease-chronic	14 (11)	18 (14)
Pulmonary embolism	12 (10)	12 (9)
Chronic heart failure	8 (7)	6 (5)
Myocarditis	6 (5)	2 (2)
Accidental hypothermia	3 (2)	1 (1)
Bleeding-other	3 (2)	0
Cardiomyopathy	3 (2)	6 (5)
Unknown	3 (2)	12 (9)
Aortic stenosis	2 (2)	6 (5)
Aortic dissection type A	2 (2)	2 (2)
Pulmonary hypertension	2 (2)	0
Intracranial hemorrhage	1 (1)	2 (2)
Other	1 (1)	1 (1)
Sepsis	0	1 (1)
Cause of death		
No.	84	101
Multiple organ failure	35 (42)	17 (17)
Brain death	21 (25)	9 (9)
Refractory arrest	13 (16)	67 (66)
Cardiogenic shock	10 (12)	4 (4)
Bleeding	4 (5)	0
Unknown	1 (1)	4 (4)
Withdrawal of life-sustaining therapy	21 (17)	14 (11)
Evaluated for organ donation[d]	21 (17)	3 (2)
Accepted for organ donation	13 (11)	2 (2)
Complications/other events, No./total (%)		
Bleeding—any[e]	36/116 (31)	10/69 (15)
Overt	24/36 (67)	8/10 (80)
Intracranial hemorrhage	8/36 (22)	2/10 (20)
Fatal	4/36 (11)	0/10
Organ lacerations	4/114 (4)	3/103 (3)
Technical[f]	3/124 (2)	0/132

Abbreviations: ACS, acute coronary syndrome; CAD, coronary artery disease; CPC, cerebral performance category; CPR, cardiopulmonary resuscitation; ECLS, extracorporeal life support; MOF, multiple organ failure syndrome; PCI, percutaneous coronary intervention; ROSC, return of spontaneous circulation.

[a] Defined as a palpable pulse with organized ECG rhythm for at least 20 minutes.

[b] Target temperature management indicates all cooling categories, including intravascular and surface feedback device cooling and ECLS heat exchanger cooling.

[c] PCI was deemed successful if resulting in residual stenosis of less than 50% with Thrombolysis in Myocardial Infarction grade 2 or 3 flow.

[d] Evaluation by the transplant center as a potential donor.

[e] Bleeding complications were assessed based on Thrombolysis in Myocardial Infarction classification[21] under "major" category, defined as any intracranial hemorrhage (excluding microhemorrhages <10 mm), fatal bleeding directly resulting in death within 7 days, or overt bleeding associated with a decrease in hemoglobin concentration of 5 g/dL or or a 15% absolute decrease in hematocrit.

[f] Any device failures during periresuscitation care, mainly focused on extracorporeal life support components.

Cause of death was different between the groups, with multiple organ failure syndrome being the most frequent cause in the invasive strategy group (35/84 [42%]) and refractory arrest in the standard strategy group (67/101 [66%]).

Withdrawal of life-sustaining therapies occurred in 21 of 124 patients (17%) in the invasive strategy group and 14 of 132 (11%) in the standard strategy group. Organ donation, both considered and accepted, was more frequent in the invasive strategy group (Table 3).

In the invasive strategy group, 11 of 124 patients (9%) were declared dead on scene or during transport or died within 1 hour after admission, compared with 64 of 132 (49%) in the standard strategy group ($P < .001$). Thirty-four of 124 patients (27%) in the invasive strategy group and 58 of 132 (44%) in the standard strategy group achieved sustained ROSC ($P = .01$). For details of resuscitation outcomes, see Table 3 and eFigure 2 in Supplement 2.

Complications

In the invasive strategy group, more major bleeding events were observed (31% vs 15%), including fatal, intracranial, and overt bleeds (Table 3). By contrast, organ lacerations caused by CPR occurred in 4 patients (3.5%) in the invasive strategy group and 3 (2.9%) in the standard strategy group, and technical complications occurred in 3 patients (2.4%) in the invasive strategy group and 0 patients in the standard strategy group (eTables 3 and 4 in Supplement 2). Protocol deviations are described in eTable 5 in Supplement 2.

Additional Analyses

ECPR Outcomes and Crossover Groups

ECPR for ongoing refractory cardiac arrest at admission to the hospital was implemented in 10 patients in the standard strategy group, exclusively in those crossed over to the invasive strategy (10 of 11 crossovers; 1 reached sustained ROSC en route), and in 82 of 124 patients (66%) randomized to the invasive strategy group. Three patients in the invasive strategy group implanted with ECLS died within 1 hour after admission. Among those who ultimately received ECPR, survival with a favorable neurologic outcome at 180 days occurred in 4 of 10 (40%) of those crossed over from the standard strategy group to the invasive strategy group and in 16 of 82 (20%) who were randomized to the invasive group and received ECPR, corresponding to overall neurologically favorable outcome at 180 days of 22% (20/92 patients) when patients who received ECPR from both groups are pooled. All other patients in the standard strategy group who did not obtain stable ROSC and were not crossed over died.

While 5 of 11 patients (45%) who were randomized to the standard strategy and crossed over to the invasive approach had favorable neurologic outcome at 180 days, no patient who was randomized to the invasive strategy group and crossed over to standard resuscitation survived (n = 9).

Survival to 180 Days

Of the 256 participants, 68 (27%) survived to 180 days with favorable neurologic outcome. Comparison of 180-day Kaplan-Meier survival analysis in the entire invasive strategy and standard strategy groups is shown in eFigure 3 in Supplement 2.

Subgroup Analysis

Post hoc subgroup analysis is provided in **Figure 2**. Details of number of patients in different times of CPR subgroups with favorable neurologic outcome are reported in eFigure 4 in Supplement 2.

Discussion

In this single-center randomized clinical trial, an invasive strategy encompassing the bundle of early intra-arrest transport, extracorporeal cardiopulmonary resuscitation, and invasive assessment in refractory out-of-hospital cardiac arrest of presumed cardiac origin did not significantly improve 180-day survival with favorable neurologic outcome compared with standard care. The study was terminated after enrolling 256 patients by the decision of the data and safety monitoring board, while reaching a stopping rule within prespecified scenarios. However, considering wide confidence intervals in the between-group difference for the primary outcome, the study may have been underpowered to detect a clinically important difference in favor of the invasive strategy group.

In the predefined secondary outcome analysis, a significantly improved 30-day neurologic recovery defined as CPC 1 or 2 was shown in favor of invasive strategy, in contrast to cardiac recovery, which was not statistically different between the groups. Invasive approach was associated with an increased risk of bleeding complications, an inherent complication of ECPR.[23]

Prague Emergency Medical Service is a single emergency service that covers the area of Prague, serving 1.25 million individuals, and operates with 1 dispatch center using a rapid response vehicle system with an emergency physician. Approximately 500 to 600 resuscitated cardiac arrests occur in Prague each year,[24] and patients with presumed cardiac etiology who achieve ROSC are distributed to several cardiac centers. During the study period, randomized patients constituted 6% of all persons who experienced cardiac arrest and received CPR (Figure 1). This is comparable to the proportions in Vienna and other studies that have suggested 4% to 6% of OHCAs to be suitable for an intra-arrest transport approach.[25,26] However, in these studies, potential candidates were evaluated retrospectively, whereas in this study, patients were evaluated during ongoing on-scene CPR. More than 90% of bystander CPR in this study affirms previously reported generally high percentage of bystander CPR in Prague,[27] in line with more than 77% of patients receiving concurrently telephone-assisted CPR. Patients were randomized after a median of 24 (IQR, 21-30) and 26 (IQR, 19-31) minutes of ongoing cardiac arrest, thus including approximately 15 minutes of advanced cardiac life support. This is a reasonable time to consider rescue interventions such as ECPR followed by immediate coronary reperfusion.[22,28] Patients experienced true refractory OHCAs, with many being resuscitated for more than 45 minutes in both groups while a still substantial proportion of patients ultimately achieved sustained ROSC.

Until now, to our knowledge, only 1 small, randomized study (ARREST) in refractory OHCA has been published.[10] The study was prematurely stopped after 30 randomized patients based on a recommendation of the data and safety

Figure 2. Post Hoc Analysis, Primary Outcome According to Subgroups in a Study of Intra-arrest Transport, Extracorporeal Cardiopulmonary Resuscitation, and Immediate Invasive Assessment and Treatment in Refractory Out-of-Hospital Cardiac Arrest

	Survival with minimal or no neurologic impairment at 180 d, No./total No. (%)				
	Invasive strategy	Standard strategy	Difference, % (95% CI)	OR (95% CI)	*P* value for interaction
Age, y					
<65	29/89 (32.6)	24/97 (24.7)	7.8 (-5.1 to 20.8)	1.47 (0.78-2.79)	.48
≥65	10/35 (28.6)	5/35 (14.3)	14.3 (-4.6 to 33.2)	2.40 (0.72-7.95)	
Sex					
Men	34/102 (33.3)	24/110 (21.8)	11.5 (-0.5 to 23.5)	1.79 (0.97-3.30)	.46
Women	5/22 (22.7%)	5/22 (22.7)	0.0 (-24.8 to 24.8)	1.00 (0.24-4.10)	
Place of cardiac arrest					
Public	17/44 (38.6)	13/54 (24.1)	14.6 (-3.8 to 32.9)	1.99 (0.83-4.74)	.41
Home	11/42 (26.2)	7/34 (20.6)	5.6 (-13.4 to 24.6)	1.37 (0.47-4.03)	
EMS	3/19 (15.8)	3/17 (17.6)	-1.9 (-26.3 to 22.6)	0.88 (0.15-5.05)	
Other	8/19 (42.1)	6/27 (22.2)	19.9 (-7.3 to 47.1)	2.55 (0.70-9.21)	
Initial rhythm					
Shockable	35/72 (48.6)	28/84 (33.3)	15.3 (0.0 to 30.6)	1.89 (0.99-3.62)	.54
Nonshockable	4/52 (7.7)	1/48 (2.1)	5.6 (-2.7 to 13.9)	3.92 (0.42-36.35)	
pH[a]					
≥6.95	29/54 (53.7)	25/49 (51.0)	2.7 (-16.6 to 22.0)	1.11 (0.51-2.42)	.70
<6.95	10/69 (14.5)	3/30 (10.0)	4.5 (-9.1 to 18.1)	1.53 (0.39-5.99)	
Lactate[a]					
≥11.6 mmol/L	12/70 (17.1)	4/29 (13.8)	3.3 (-12.0 to 18.7)	1.29 (0.38-4.40)	.94
<11.6 mmol/L	27/52 (51.9)	23/49 (46.9)	5.0 (-14.5 to 24.5)	1.22 (0.56-2.67)	
Cardiac arrest cause					
ACS	18/64 (28.1)	14/63 (22.2)	5.9 (-9.2 to 21.0)	1.37 (0.61-3.07)	.12
CAD	9/14 (64.3)	5/18 (27.8)	36.5 (4.0 to 69.0)	4.68 (1.04-21.04)	
CHF	5/8 (62.5)	2/6 (33.3)	29.2 (-21.3 to 79.6)	3.33 (0.36-30.70)	
Other	7/38 (18.4)	8/45 (17.8)	0.6 (-16.0 to 17.3)	1.04 (0.34-3.20)	

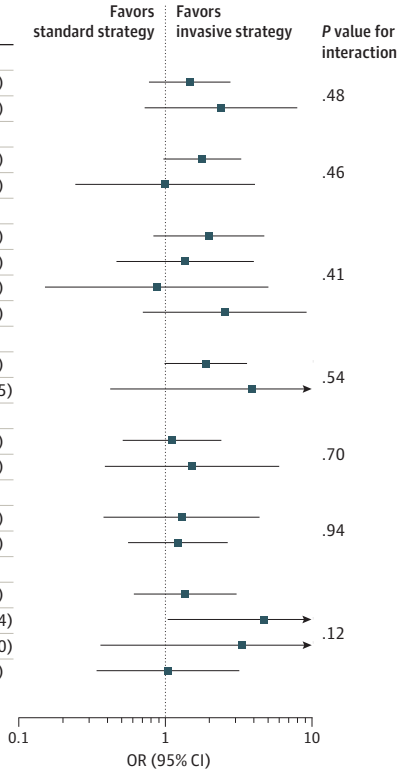

ACS indicates acute coronary syndrome; CAD, coronary artery disease; CHF, chronic heart failure; CPR, cardiopulmonary resuscitation; EMS, emergency medical service; OR, odds ratio; ROSC, return of spontaneous circulation.

[a] For pH and lactate level, the first values after admission are used.

monitoring board because of superiority of early extracorporeal membrane oxygenation (ECMO)-facilitated resuscitation vs standard advanced cardiac life support treatment. The ARREST trial showed that ECMO-facilitated resuscitation for patients with OHCA and refractory ventricular fibrillation significantly improved survival to hospital discharge and functional status compared with patients receiving standard advanced cardiac life support (6/14 patients [43%] vs 1/15 [7%]; risk difference, 36.2% [95% CI, 3.7% to 59.2%]; posterior probability of ECMO superiority, 0.9861). Cumulative 6-month survival was also significantly better in the early ECMO group.[10] The ARREST study differed from the present study mainly in 2 aspects: only patients presenting with shockable rhythms were considered, and patients were randomized after being transferred to the hospital, ie, after approximately 50 minutes of CPR. In contrast, the present study randomized patients during on-scene ongoing CPR, thus comparing different treatment scenarios to consider at the point of impending refractoriness, rather than ultimate rescue option after 50 minutes of unsuccessful CPR, when a standard approach has negligible chance for success.[3,28,29]

An ongoing question related to intra-arrest transport and early invasive treatment for refractory OHCA is the timing of when such an approach should be considered. In this study, the timeline that was adhered to matched the timeline as planned in the protocol and probably represents a realistic timeline in semicrowded urban areas using in-hospital ECPR for OHCA. Patients were admitted within a median of 49 (IQR, 44-60) minutes of collapse in the invasive strategy group, representing approximately 26 minutes of retrieval and transport from the scene to the hospital. The initial decision process to randomize patients after adequate time allowing to achieve ROSC prehospitally thus well correlates with the proposed 16 minutes of professional on-scene CPR[22] and may be considered a satisfactory approach to select truly refractory cases, given that 64% of patients in this study experienced cardiac arrest longer than 45 minutes.

Still, converting on-scene CPR into intra-arrest transport eventually followed by ECPR may not improve outcome.[3,26] Questions remain as to whether it is possible to identify patients early during CPR who may ultimately benefit from such an approach. Several studies have assessed the relationship between the length of cardiac arrest and ECPR treatment.[28-30]

To our knowledge, there have been no other studies in a cardiac arrest population that randomized patients online via a web-based randomization process during ongoing

on-scene CPR. The overall pooled neurologically favorable survival at 180 days of 27% (31.5% in the invasive strategy group, 22% in the standard strategy group, 22% in the pooled ECPR group) is comparable to that in other nonrandomized studies evaluating ECPR (29%[31] and 33%[32]).

If an early invasive approach is to be considered, it should be provided in a well-functioning prehospital system linked to a cooperating ECPR cardiac arrest center.[33]

Studies of refractory OHCA treated by ECPR inherently address potential organ donation[34,35]; potential donors were frequently considered, and organ donations occurred.

Limitations

This study has several limitations. First, the study had a single-center design and limited enrollment. Second, a priori scenarios of expected benefit provided by invasive approach were not reached, presumably because of higher-than-expected survival in the standard strategy group. Third, the study may have thus been underpowered to detect a statistically significant difference for the primary outcome. Fourth, the study design allowed crossover. The trial was designed to represent routine clinical care, and EMS crews thus decided to transport some patients receiving ongoing CPR for ECPR despite being originally randomized to the standard strategy group. For crossover from invasive to standard intervention, patients were apparently deemed not to be candidates for advanced therapies, but such determinations may contain a degree of subjectivity that could influence outcomes. Nonetheless, the rate of crossover was low (7.5%) compared with other studies.[36,37]

Conclusions

Among patients with refractory out-of-hospital cardiac arrest, the bundle of early intra-arrest transport, ECPR, and invasive assessment and treatment did not significantly improve survival with neurologically favorable outcome at 180 days compared with standard resuscitation. However, the trial was possibly underpowered to detect a clinically relevant difference.

ARTICLE INFORMATION

Accepted for Publication: January 20, 2022.

Author Affiliations: 2nd Department of Medicine—Department of Cardiovascular Medicine, First Faculty of Medicine, Charles University in Prague and General University Hospital, Prague, Czech Republic (Belohlavek, Smalcova, Rob, Smid, Horák, Mrazek, Kovarnik, Zemanek, Kral, Havranek, Kavalkova, Linhart); Emergency Medical Service, Prague, Czech Republic (Smalcova, Franek, Pokorna, Kompelentova, Tomková, Mejstrik, Valasek, Peran, Pekara, Kolouch); Department of Anesthesiology, Resuscitation and Intensive Medicine, First Faculty of Medicine, Charles University in Prague and General University Hospital, Prague, Czech Republic (Rulisek, Balik); Czech Institute of Informatics, Robotics and Cybernetics (CIIRC), Czech Technical University, Prague, Czech Republic. (Huptych); Institute of Biostatistics and Analyses, Faculty of Medicine, Masaryk University, Brno, Czech Republic (Jarkovsky); 3rd Department of Medicine, First Faculty of Medicine, Charles University in Prague and General University Hospital, Prague, Czech Republic (Malik, Valerianova); 2nd Department of Surgery, Cardiovascular Surgery, First Faculty of Medicine, Charles University in Prague and General University Hospital, Prague, Czech Republic (Mlejnsky); Department of Neurology, First Faculty of Medicine, Charles University in Prague and General University Hospital, Prague, Czech Republic (Havrankova); Long-term Intensive Care Unit, Etoile, Prague, Czech Republic (Romportl); Department of Probability and Mathematical Statistics, Faculty of Mathematics and Physics, Charles University in Prague, Prague, Czech Republic (Komarek).

Author Contributions: Dr Belohlavek had full access to all of the data in the study and takes responsibility for the integrity of the data and the accuracy of the data analysis.
Concept and design: Belohlavek, Rob, Franek, Horák, Balik, Linhart.
Acquisition, analysis, or interpretation of data: All authors.
Drafting of the manuscript: Belohlavek, Smalcova, Rob, Franek, Linhart.
Critical revision of the manuscript for important intellectual content: All authors.
Statistical analysis: Smalcova, Rob, Smid, Havranek, Kavalkova, Tomková, Pekara, Rulisek, Huptych, Jarkovsky, Havrankova, Komarek.
Obtained funding: Belohlavek, Mrazek, Linhart.
Administrative, technical, or material support: Belohlavek, Rob, Pokorna, Mrazek, Kovarnik, Kral, Valasek, Peran, Balik, Valerianova, Mlejnsky, Kolouch.
Supervision: Belohlavek, Balik, Malik, Linhart.

Conflict of Interest Disclosures: Dr Belohlavek reported receiving lecture honoraria from Maquet Company. No other authors reported disclosures.

Funding/Support: This study was supported by a research grant from the Internal Grant Agency Ministry of Health, Czech Republic (NT 13225-4/2012), by Progres Q38/LF1 and Cooperatio/INCA institutional support. BeneChill Inc provided 8 Rhinochill devices and, for the purpose of this study, provided the application sets and evaporative liquid at a reduced cost. Physio-Control, a division of Medtronic, provided 8 LUCAS devices for the purpose of this study. Maquet provided the MAQUET PLS device for ECLS.

Role of the Funder/Sponsor: The Internal Grant Agency Ministry of Health, BeneChill, Physio-Control, and Maquet had no role in the design and conduct of the study; collection, management, analysis, and interpretation of the data; preparation, review, or approval of the manuscript; and decision to submit the manuscript for publication.

Group Information: A list of the Prague OHCA Study Group members is available in Supplement 4.

Data Sharing Statement: See Supplement 5.

Additional Contributions: We thank the Prague Emergency Medical Service teams and the coronary care unit and the catheterization laboratory teams of the 2nd Department of Internal Medicine, Cardiovascular Medicine, General University Hospital in Prague, for their efforts in providing quality care.

REFERENCES

1. Perkins GD, Graesner JT, Semeraro F, et al; European Resuscitation Council Guideline Collaborators. European Resuscitation Council Guidelines 2021: executive summary. *Resuscitation*. 2021;161:1-60. doi:10.1016/j.resuscitation.2021.02.003

2. Dankiewicz J, Cronberg T, Lilja G, et al; TTM2 Trial Investigators. Hypothermia versus normothermia after out-of-hospital cardiac arrest. *N Engl J Med*. 2021;384(24):2283-2294. doi:10.1056/NEJMoa2100591

3. Grunau B, Kime N, Leroux B, et al. Association of intra-arrest transport vs continued on-scene resuscitation with survival to hospital discharge among patients with out-of-hospital cardiac arrest. *JAMA*. 2020;324(11):1058-1067. doi:10.1001/jama.2020.14185

4. Drennan IR, Lin S, Sidalak DE, Morrison LJ. Survival rates in out-of-hospital cardiac arrest patients transported without prehospital return of spontaneous circulation: an observational cohort study. *Resuscitation*. 2014;85(11):1488-1493. doi:10.1016/j.resuscitation.2014.07.011

5. de Graaf C, Beesems SG, Koster RW. Time of on-scene resuscitation in out of-hospital cardiac arrest patients transported without return of spontaneous circulation. *Resuscitation*. 2019;138:235-242. doi:10.1016/j.resuscitation.2019.03.030

6. Schober A, Sterz F, Herkner H, et al. Emergency extracorporeal life support and ongoing resuscitation: a retrospective comparison for refractory out-of-hospital cardiac arrest. *Emerg Med J*. 2017;34(5):277-281. doi:10.1136/emermed-2015-205232

7. Ortega-Deballon I, Hornby L, Shemie SD, Bhanji F, Guadagno E. Extracorporeal resuscitation for refractory out-of-hospital cardiac arrest in adults: a systematic review of international practices and outcomes. *Resuscitation*. 2016;101:12-20. doi:10.1016/j.resuscitation.2016.01.018

8. Haas NL, Coute RA, Hsu CH, Cranford JA, Neumar RW. Descriptive analysis of extracorporeal cardiopulmonary resuscitation following out-of-hospital cardiac arrest—an ELSO registry study. *Resuscitation*. 2017;119:56-62. doi:10.1016/j.resuscitation.2017.08.003

9. Holmberg MJ, Geri G, Wiberg S, et al; International Liaison Committee on Resuscitation's (ILCOR) Advanced Life Support and Pediatric Task Forces. Extracorporeal cardiopulmonary resuscitation for cardiac arrest: a systematic review. *Resuscitation*. 2018;131:91-100. doi:10.1016/j.resuscitation.2018.07.029

10. Yannopoulos D, Bartos J, Raveendran G, et al. Advanced reperfusion strategies for patients with out-of-hospital cardiac arrest and refractory ventricular fibrillation (ARREST): a phase 2, single centre, open-label, randomised controlled trial. *Lancet*. 2020;396(10265):1807-1816. doi:10.1016/S0140-6736(20)32338-2

11. Dennis M, Lal S, Forrest P, et al. In-depth extracorporeal cardiopulmonary resuscitation in adult out-of-hospital cardiac arrest. *J Am Heart Assoc*. 2020;9(10):e016521. doi:10.1161/JAHA.120.016521

12. Bougouin W, Dumas F, Lamhaut L, et al; Sudden Death Expertise Center investigators. Extracorporeal cardiopulmonary resuscitation in out-of-hospital cardiac arrest: a registry study. *Eur Heart J*. 2020;41(21):1961-1971. doi:10.1093/eurheartj/ehz753

13. Lott C, Truhlář A, Alfonzo A, et al; ERC Special Circumstances Writing Group Collaborators. European Resuscitation Council Guidelines 2021: cardiac arrest in special circumstances. *Resuscitation*. 2021;161:152-219. doi:10.1016/j.resuscitation.2021.02.011

14. Belohlavek J, Kucera K, Jarkovsky J, et al. Hyperinvasive approach to out-of-hospital cardiac arrest using mechanical chest compression device, prehospital intraarrest cooling, extracorporeal life support and early invasive assessment compared to standard of care: a randomized parallel groups comparative study proposal. *J Transl Med*. 2012;10:163. doi:10.1186/1479-5876-10-163

15. Jennett B, Bond M. Assessment of outcome after severe brain damage. *Lancet*. 1975;1(7905):480-484. doi:10.1016/S0140-6736(75)92830-5

16. Nolan JP, Soar J, Zideman DA, et al; ERC Guidelines Writing Group. European Resuscitation Council Guidelines for Resuscitation 2010: section 1: executive summary. *Resuscitation*. 2010;81(10):1219-1276. doi:10.1016/j.resuscitation.2010.08.021

17. Monsieurs KG, Nolan JP, Bossaert LL, et al; ERC Guidelines 2015 Writing Group. European Resuscitation Council Guidelines for Resuscitation 2015: section 1: executive summary. *Resuscitation*. 2015;95:1-80. doi:10.1016/j.resuscitation.2015.07.038

18. Rubertsson S, Lindgren E, Smekal D, et al. Mechanical chest compressions and simultaneous defibrillation vs conventional cardiopulmonary resuscitation in out-of-hospital cardiac arrest: the LINC randomized trial. *JAMA*. 2014;311(1):53-61. doi:10.1001/jama.2013.282538

19. Nielsen N, Wetterslev J, Cronberg T, et al; TTM Trial Investigators. Targeted temperature management at 33°C versus 36°C after cardiac arrest. *N Engl J Med*. 2013;369(23):2197-2206. doi:10.1056/NEJMoa1310519

20. Gaieski DF, Band RA, Abella BS, et al. Early goal-directed hemodynamic optimization combined with therapeutic hypothermia in comatose survivors of out-of-hospital cardiac arrest. *Resuscitation*. 2009;80(4):418-424. doi:10.1016/j.resuscitation.2008.12.015

21. Bovill EG, Terrin ML, Stump DC, et al. Hemorrhagic events during therapy with recombinant tissue-type plasminogen activator, heparin, and aspirin for acute myocardial infarction: results of the Thrombolysis in Myocardial Infarction (TIMI) phase II trial. *Ann Intern Med*. 1991;115(4):256-265. doi:10.7326/0003-4819-115-4-256

22. Grunau B, Reynolds J, Scheuermeyer F, et al. Relationship between time-to-ROSC and survival in out-of-hospital cardiac arrest ECPR candidates: when is the best time to consider transport to hospital? *Prehosp Emerg Care*. 2016;20(5):615-622. doi:10.3109/10903127.2016.1149652

23. Thomas J, Kostousov V, Teruya J. Bleeding and thrombotic complications in the use of extracorporeal membrane oxygenation. *Semin Thromb Hemost*. 2018;44(1):20-29. doi:10.1055/s-0037-1606179

24. Franěk O, Pokorná M, Sukupová P. Pre-hospital cardiac arrest in Prague, Czech Republic—the Utstein-style report. *Resuscitation*. 2010;81(7):831-835. doi:10.1016/j.resuscitation.2010.03.005

25. Poppe M, Weiser C, Holzer M, et al. The incidence of "load&go" out-of-hospital cardiac arrest candidates for emergency department utilization of emergency extracorporeal life support: a one-year review. *Resuscitation*. 2015;91:131-136. doi:10.1016/j.resuscitation.2015.03.003

26. Alm-Kruse K, Sørensen G, Osbakk SA, et al. Outcome in refractory out-of-hospital cardiac arrest before and after implementation of an ECPR protocol. *Resuscitation*. 2021;162:35-42. doi:10.1016/j.resuscitation.2021.01.038

27. Gräsner JT, Wnent J, Herlitz J, et al. Survival after out-of-hospital cardiac arrest in Europe: results of the EuReCa TWO study. *Resuscitation*. 2020;148:218-226. doi:10.1016/j.resuscitation.2019.12.042

28. Wengenmayer T, Rombach S, Ramshorn F, et al. Influence of low-flow time on survival after extracorporeal cardiopulmonary resuscitation (eCPR). *Crit Care*. 2017;21(1):157. doi:10.1186/s13054-017-1744-8

29. Bartos JA, Carlson K, Carlson C, et al. Surviving refractory out-of-hospital ventricular fibrillation cardiac arrest: critical care and extracorporeal membrane oxygenation management. *Resuscitation*. 2018;132:47-55. doi:10.1016/j.resuscitation.2018.08.030

30. Leick J, Liebetrau C, Szardien S, et al. Door-to-implantation time of extracorporeal life support systems predicts mortality in patients with out-of-hospital cardiac arrest. *Clin Res Cardiol*. 2013;102(9):661-669. doi:10.1007/s00392-013-0580-3

31. Maekawa K, Tanno K, Hase M, Mori K, Asai Y. Extracorporeal cardiopulmonary resuscitation for patients with out-of-hospital cardiac arrest of cardiac origin: a propensity-matched study and predictor analysis. *Crit Care Med*. 2013;41(5):1186-1196. doi:10.1097/CCM.0b013e31827ca4c8

32. Bartos JA, Grunau B, Carlson C, et al. Improved survival with extracorporeal cardiopulmonary resuscitation despite progressive metabolic derangement associated with prolonged resuscitation. *Circulation*. 2020;141(11):877-886. doi:10.1161/CIRCULATIONAHA.119.042173

33. Sinning C, Ahrens I, Cariou A, et al. The cardiac arrest centre for the treatment of sudden cardiac arrest due to presumed cardiac cause—aims, function and structure: position paper of the Association for Acute CardioVascular Care of the European Society of Cardiology (AVCV), European Association of Percutaneous Coronary Interventions (EAPCI), European Heart Rhythm Association (EHRA), European Resuscitation Council (ERC), European Society for Emergency Medicine (EUSEM) and European Society of Intensive Care Medicine (ESICM). *Eur Heart J Acute Cardiovasc Care*. 2020;9(4 suppl):S193-S202. doi:10.1177/2048872620963492

34. Ortega-Deballon I, De La Plaza-Horche E. A comprehensive approach to refractory cardiac arrest: saving more lives one way or another. *Heart Lung Vessel*. 2014;6(3):149-151.

35. Ortega-Deballon I, Hornby L, Shemie SD. Protocols for uncontrolled donation after circulatory death: a systematic review of international guidelines, practices and transplant outcomes. *Crit Care*. 2015;19:268. doi:10.1186/s13054-015-0985-7

36. Thiele H, Akin I, Sandri M, et al; CULPRIT-SHOCK Investigators. PCI strategies in patients with acute myocardial infarction and cardiogenic shock. *N Engl J Med*. 2017;377(25):2419-2432. doi:10.1056/NEJMoa1710261

37. Combes A, Hajage D, Capellier G, et al; EOLIA Trial Group, REVA, and ECMONet. Extracorporeal membrane oxygenation for severe acute respiratory distress syndrome. *N Engl J Med*. 2018;378(21):1965-1975. doi:10.1056/NEJMoa1800385

P. Ošťádal et al.

Metabolic risk factors and effect of alirocumab on cardiovascular events after acute coronary syndrome: a post-hoc analysis of the ODYSSEY OUTCOMES randomised controlled trial.

Lancet Diabetes Endocrinol.
Impact Factor: 44.867

Metabolic risk factors and effect of alirocumab on cardiovascular events after acute coronary syndrome: a post-hoc analysis of the ODYSSEY OUTCOMES randomised controlled trial

*Petr Ostadal, Philippe Gabriel Steg, Yann Poulouin, Deepak L Bhatt, Vera A Bittner, Terrence Chua, Rafael Diaz, Shaun G Goodman, Yong Huo, Johan Wouter Jukema, Yuri Karpov, Robert Pordy, Michel Scemama, Michael Szarek, Harvey D White, Gregory G Schwartz, for the ODYSSEY OUTCOMES Investigators**

Summary

Background Many patients with acute coronary syndrome have concurrent metabolic risk factors that affect risk of major adverse cardiovascular events (MACE). We aimed to assess the effects of the PCSK9 inhibitor alirocumab compared with placebo on MACE according to baseline metabolic risk factors.

Methods We performed a post-hoc analysis of the ODYSSEY OUTCOMES trial, which was a multicentre, double-blind, randomised controlled trial done in 1315 hospitals and outpatient clinics in 57 countries. Patients aged 40 years or older with recent acute coronary syndrome (ie, in the past 1–12 months) and elevated concentrations of atherogenic lipoproteins, despite high-intensity or maximum-tolerated statin treatment, were eligible for enrolment. Between Nov 2, 2012, and Feb 9, 2017, patients were randomly assigned (1:1) to 75 mg alirocumab by subcutaneous injection every 2 weeks or matching placebo, beginning 1–12 months after acute coronary syndrome and were followed up for a median of 2·8 years (IQR 2·3–3·4). Patients and investigators were masked to group assignment and treatment dose adjustment. The primary outcome was a composite of death from coronary artery disease, non-fatal myocardial infarction, fatal or non-fatal ischaemic stroke, or unstable angina requiring hospital admission. Analysis of MACE according to an ordinal number of metabolic risk factors was done post hoc. Metabolic risk factors were defined as blood pressure of at least 130/85 mm Hg or treatment with antihypertensive medication, triglyceride concentration of at least 150 mg/dL, HDL cholesterol concentration less than 40 mg/dL for men and 50 mg/dL women, fasting plasma glucose concentration of at least 100 mg/dL or treatment with glucose-lowering medication, and BMI of at least 30 kg/m^2. Risk of MACE and effect of alirocumab were assessed according to the number of metabolic risk factors. ODYSSEY OUTCOMES is registered with ClinicalTrials.gov, number NCT01663402.

Findings Of 18 924 patients, 3882 (41%) of 9462 in the alirocumab group and 3859 (41%) of 9462 in the placebo group had three or more metabolic risk factors. In the placebo group, MACE incidence increased monotonically with each metabolic risk factor from 7·8% (no risk factors) to 19·6% (five risk factors; HR 1·18, 95% CI 1·13–1·24 per metabolic risk factor). Alirocumab decreased relative risk of MACE consistently across categories defined by the number of metabolic risk factors ($p_{interaction}$=0·77), but absolute risk reduction (aRR) increased with the number of metabolic risk factors (no risk factors aRR 0·7%, –1·81 to 3·29 *vs* five risk factors aRR 3·9%, –1·45 to 9·25; $p_{interaction}$<0·001). Similarly, when patients with diabetes were excluded, the incidence of MACE in the placebo group increased from 7·7% in patients with no metabolic risk factors to 14·6% in those with five metabolic risk factors and aRR with alirocumab increased from 0·91% in patients with no metabolic risk factors to 3·82% in those with five factors. Alirocumab was well tolerated in all subgroups defined by the presence of metabolic risk factors.

Interpretation Accumulation of metabolic risk factors was associated with higher risk of MACE in patients with recent acute coronary syndrome. Alirocumab reduced MACE consistently, but aRR increased with number of metabolic risk factors.

Funding Sanofi and Regeneron Pharmaceuticals.

Introduction

Several metabolic factors have been associated with increased risk of major adverse cardiovascular events (MACE), including diabetes or increased fasting plasma glucose concentrations, abdominal obesity, hypertension, low concentrations of HDL cholesterol, and high triglyceride concentrations. A collection of these metabolic risk factors has been termed metabolic syndrome and is associated with elevated risk of MACE and death.[1–4] Current guidelines emphasise the importance of

Lancet Diabetes Endocrinol 2022

Published **Online**
April 1, 2022
https://doi.org/10.1016/S2213-8587(22)00043-2

See **Online/Comment**
https://doi.org/10.1016/S2213-8587(22)00086-9

*Complete list of the ODYSSEY OUTCOMES committee members, investigators, and contributors is provided in the appendix

Na Homolce Hospital, Prague, Czech Republic (Prof P Ostadal MD); **French Alliance for Cardiovascular Trials, Université de Paris, Assistance Publique-Hôpitaux de Paris, and INSERM U1148, Hôpital Bichat, Paris, France** (Prof P G Steg MD); **Imperial College, Royal Brompton Hospital, London, UK** (Prof P G Steg); **IT&M Stats, Paris, France** (Y Poulouin MSc); **Brigham and Women's Hospital Heart & Vascular Center and Harvard Medical School, Boston, MA, USA** (Prof D L Bhatt MD); **Division of Cardiovascular Disease, University of Alabama at Birmingham, Birmingham, AL, USA** (Prof V Bittner MD); **National Heart Centre, Singapore General Hospital, Singapore** (Prof T Chua MD); **Estudios Cardiológicos Latino América, Instituto Cardiovascular de Rosario, Rosario, Argentina** (Prof R Diaz Sr MD); **Canadian VIGOUR Centre, University of Alberta, Edmonton, AB, Canada** (Prof S G Goodman MD); **St Michael's Hospital, University of Toronto, Toronto, ON, Canada** (Prof S G Goodman); **Peking University First Hospital, Beijing, China** (Prof Y Huo MD); **Department of Cardiology, Leiden University**

Medical Center, Leiden, Netherlands (Prof J W Jukema MD); **Netherlands Heart Institute, Utrecht, Netherlands** (Prof J W Jukema); **National Medical Research Centre of Cardiology, Moscow, Russia** (Prof Yuri Karpov MD); **Regeneron Pharmaceuticals, Tarrytown, NY, USA** (R Pordy MD); **Sanofi, Chilly-Mazarin, France** (Michel Scemama MD); **State University of New York, Downstate School of Public Health, Brooklyn, NY, USA** (Prof M Szarek PhD); **CPC Clinical Research and Division of Cardiology, University of Colorado School of Medicine, Aurora, CO, USA** (Prof M Szarek); **Green Lane Cardiovascular Services, Auckland City Hospital, Auckland, New Zealand** (Prof H D White DSc); **Division of Cardiology, University of Colorado School of Medicine, Aurora, CO, USA** (Prof G G Schwartz MD)

Correspondence to: Prof Petr Ostadal, Na Homolce Hospital, 15000 Prague, Czech Republic
ostadal.petr@gmail.com

See Online for appendix

Research in context

Evidence before this study

We searched PubMed from Jan 1, 2010, to June 30, 2021, for articles published in English, investigating the effect of proprotein convertase subtilisin or kexin type 9 inhibitors on cardiovascular events using the terms "alirocumab", "evolocumab", "PCSK9 inhibitor", and "cardiovascular event". Inhibitors of proprotein convertase subtilisin/kexin type 9 (PCSK9) reduce LDL cholesterol concentrations by up to 60% and decrease risk of major adverse cardiovascular events (MACE) in patients with acute coronary syndrome. Many patients with acute coronary syndrome have concurrent metabolic risk factors that affect risk of MACE and efficacy of lipid-lowering therapy. In the cardiovascular outcomes FOURIER trial, the PCSK9 inhibitor evolocumab reduced relative risk of MACE in statin-treated patients with chronic atherosclerotic cardiovascular disease to a similar degree in patients with or without metabolic syndrome, and in patients with or without diabetes. In the placebo-controlled ODYSSEY OUTCOMES trial, patients with acute coronary syndrome on high intensity or maximum-tolerated statin treatment had a reduced relative risk of MACE when randomly assigned to the PCSK9 inhibitor alirocumab regardless of diabetes status. However, the association of metabolic risk factors (hypertension, hypertriglyceridaemia, low HDL cholesterol, hyperglycaemia, obesity) with risk of MACE in patients with acute coronary syndrome on high-intensity or maximum-tolerated statin therapy, and the effect of alirocumab according to the number of metabolic risk factors is unknown.

Added value of this study

In the ODYSSEY OUTCOMES trial, 91·5% of patients with recent acute coronary syndrome (ie, in the past 1–12 months) had at least one metabolic risk factor and 68·8% had two or more. Despite high-intensity or maximum-tolerated statin therapy, each metabolic risk factor (except low HDL cholesterol) remained significantly associated with increased risk of MACE, and accumulation of metabolic risk factors in patients with recent acute coronary syndrome substantially increased risk for further cardiovascular events. Alirocumab reduced relative risk of MACE irrespective of the number of metabolic risk factors, but absolute benefit increased with the number of metabolic risk factors. Absolute risk reduction, and potentially relative risk reduction, appeared more pronounced in patients with at least three metabolic risk factors than in patients with less than three factors, especially in patients without diabetes.

Implications of all the available evidence

Patients with multiple metabolic risk factors, including patients without diabetes, might derive a large absolute benefit of alirocumab treatment after acute coronary syndrome. Counting the number of risk factors could be a simple way for clinicians to identify patients considered for PCSK9 inhibitor therapy after acute coronary syndrome.

managing metabolic syndrome and recommend lifestyle modifications and pharmacological therapy, including lipid-lowering drugs, especially for secondary prevention.[5–7] High-intensity statin therapy has been shown to decrease risk of MACE in patients with metabolic syndrome and chronic coronary artery disease[8] or acute coronary syndrome.[9] Nevertheless, residual risk in individuals with metabolic syndrome remains high.

Inhibitors of proprotein convertase subtilisin/kexin type 9 (PCSK9) reduce concentrations of LDL cholesterol by up to 60% and decrease risk of MACE in patients with chronic atherosclerotic cardiovascular disease[10] or acute coronary syndrome.[9] In the placebo-controlled FOURIER trial, evolocumab reduced relative risk of MACE in statin-treated patients with chronic atherosclerotic cardiovascular disease at similar rates in patients with or without metabolic syndrome and in patients with or without diabetes.[11] In the placebo-controlled ODYSSEY OUTCOMES trial, patients with recent acute coronary syndrome on high intensity or maximum-tolerated statin treatment had a reduced relative risk of MACE when randomly assigned to alirocumab, regardless of diabetes status.[12]

In this post-hoc analysis of the ODYSSEY OUTCOMES trial, we aimed to describe the association of metabolic risk factors with risk of MACE in a population of patients with acute coronary syndrome on high-intensity or maximum-tolerated statin therapy and assess the effect of alirocumab according to the number of metabolic risk factors present.

Methods

Study design and participants

In this study we did a post-hoc analysis of the results of the ODYSSEY OUTCOMES trial. ODYSSEY OUTCOMES was a randomised, double-blind trial[9] that compared the efficacy and safety of alirocumab versus placebo in patients with recent acute coronary syndrome (ie, in the past 1–12 months) on high-intensity or maximum-tolerated statin treatment. The study was done at 1315 hospitals and outpatient clinics in 57 countries, and enrolment occurred between Nov 2, 2012, and Feb 9, 2017. 18 924 patients aged 40 years or older with elevated concentrations of atherogenic lipoproteins (LDL cholesterol ≥70 mg/dL, non–HDL cholesterol ≥100 mg/dL, or apolipoprotein B ≥80 mg/dL), despite high-intensity or maximum-tolerated statin treatment, were eligible for enrolment and randomly assigned to placebo or alirocumab. The study protocol, design, and primary results have been published elsewhere.[9,13] The trial was approved by the institutional review board or ethics committee at each site. All participants provided written informed consent.

Patients were randomly assigned (1:1) to 75 mg alirocumab by subcutaneous injection every 2 weeks or

matching placebo, beginning 1–12 months after acute coronary syndrome and were followed up for a median of 2·8 years (IQR 2·3–3·4). Patients were randomly assigned centrally and stratified by country using an interactive voice-response or web-response system.[9,13]

The aim of the treat-to-target design was to achieve an LDL cholesterol concentration of 25–50 mg/dL in patients receiving alirocumab. Alirocumab was blindly titrated from 75 mg to 150 mg if the LDL cholesterol concentration was 50 mg/dL or more. If LDL cholesterol concentration was less than 15 mg/dL on two consecutive measurements on 75 mg alirocumab, placebo was blindly substituted for the rest of the trial. In patients on 150 mg alirocumab, the dose could be titrated down to 75 mg if LDL cholesterol concentration was less than 15 mg/dL on two consecutive measurements. The trial had a double-blind design, with patients and investigators masked to treatment assignment, dose adjustments, and lipid concentrations.

Outcomes

The primary outcome for this analysis was composite of death from coronary artery disease, non-fatal myocardial infarction, fatal or non-fatal ischaemic stroke, or unstable angina requiring hospital admission. The analysis of subgroups defined by metabolic syndrome status at baseline (ie, presence of three or more metabolic risk factors) was prespecified in a statistical analysis plan, published elsewhere;[9] the analysis of MACE according to ordinal number of metabolic risk factors was done on a

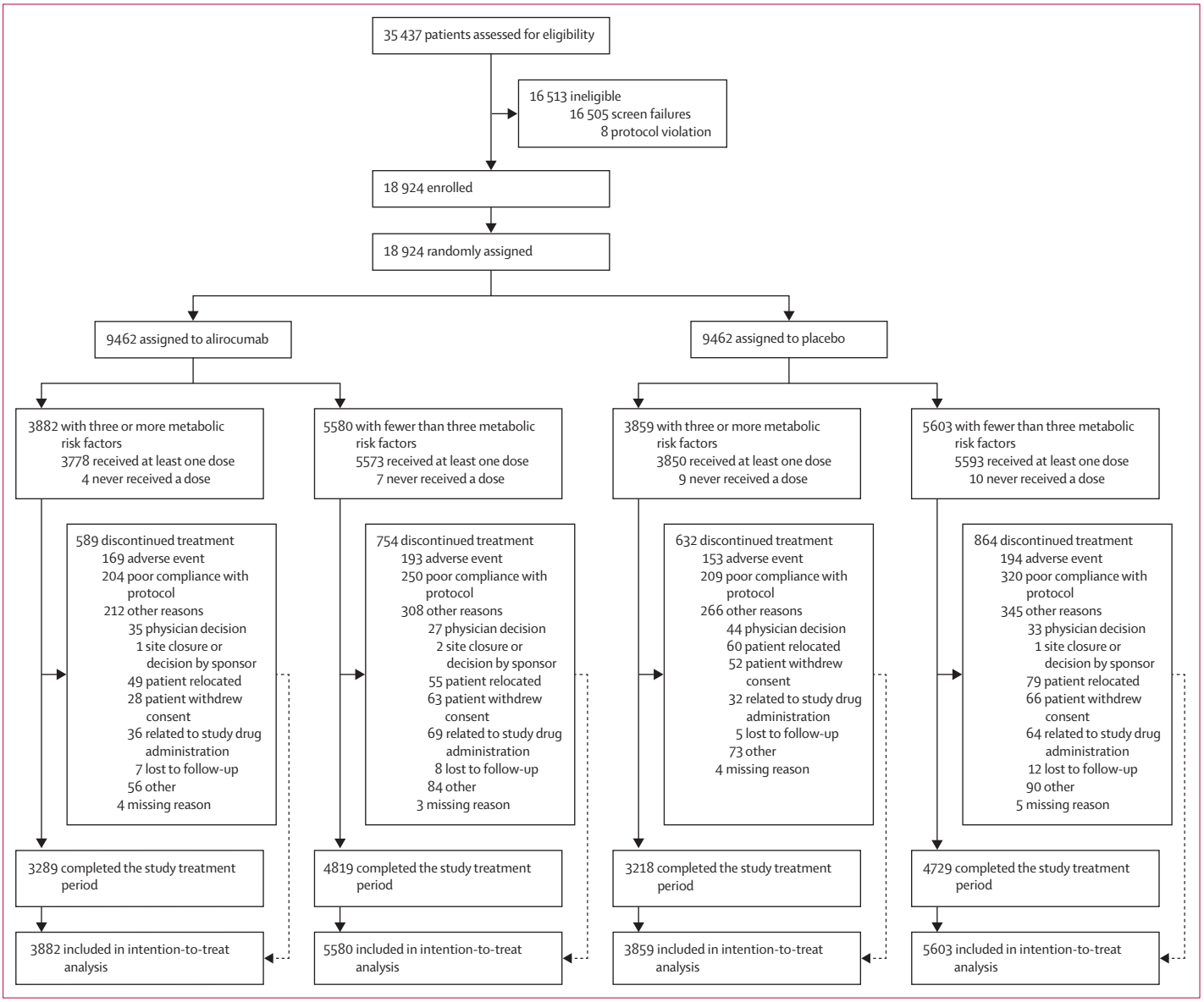

Figure 1: **Profile of the post-hoc analysis**

post-hoc basis. Metabolic risk factors were defined using the following criteria: hypertension (blood pressure of at least 130/85 mm Hg or use of antihypertensive medication; β blocker and angiotensin-converting enzyme inhibitor or angiotensin receptor blocker were considered as antihypertensive therapy only if a hypertension diagnosis was indicated by the investigator); hypertriglyceridaemia (triglycerides ≥150 mg/dL); low HDL cholesterol concentration (<40 mg/dL in men and <50 mg/dL in women); dysglycaemia (fasting plasma glucose concentration ≥100 mg/dL or use of glucose-lowering medication); and obesity (BMI ≥30 kg/m²). An alternative measure of abdominal obesity, waist circumference, was not recorded in the trial.[1,14] Additionally, diabetes was defined as a fasting plasma glucose concentration of at least 125 mg/dL or use of glucose-lowering medication. Patients with missing laboratory or categorical data at baseline were considered as not meeting criteria. The effect of alirocumab was compared across subgroups by ordinal number of metabolic risk factors and between subgroups with at least three and fewer than three metabolic risk factors; patients with at least three metabolic risk factors correspond with the definition of metabolic syndrome when the criterion of waist circumference is substituted by BMI. As diabetes is a strong independent risk factor for cardiovascular events, we aimed to examine burden of risk and benefit of alirocumab by metabolic risk factors in all patients and after exclusion of patients with diabetes.

Statistical analysis

Design assumptions of the ODYSSEY OUTCOMES trial included incidence of the composite primary outcome of 11·4% at 4 years in the placebo group and a median baseline LDL cholesterol concentration of 2·3 mmol/L (90 mg/dL), with an anticipated 50% lower LDL cholesterol concentration in the alirocumab group than in the placebo group,[13] projected to result in an expected 15% lower risk of the primary outcome with alirocumab than with placebo.

The ODYSSEY OUTCOMES trial was not designed to enrol a specific number of patients within each subgroup defined by status of metabolic syndrome at baseline, hence no power calculation has been made on any of the subgroups. Calculations were based on the primary efficacy variable and have been previously described elsewhere.[13,15] In brief, we estimated that in the ODYSSEY OUTCOMES trial 1613 events would be needed to have 90% power (with one-sided log-rank test at the overall 0·025 α level) to show an effect versus placebo assuming 15% risk reduction associated with alirocumab treatment (ie, hazard ratio [HR] 0·85) and considering two interim analyses: a first interim analysis for futility and a second for efficacy.[15]

Controls of type I and type II error were ensured using gamma (–5) spending function for type II error (futility) and gamma (–22) for type I error (efficacy). Analyses presented in this Article are post hoc, hence there was no adjustment for multiplicity.

Kaplan-Meier curves are presented by randomised treatment and subgroups with at least three and fewer than three metabolic risk factors. HR and 95% CI were generated using proportional hazard models, including treatment, region, sex, age, subgroup, and treatment-by-subgroup interaction as covariates. Possible heterogeneity of randomised treatment effects on MACE for selected subgroups was tested by incorporating interaction terms into proportional hazards models for relative risk reductions and by quantitative interactions based on observed incidences for absolute risk reductions. $p_{interaction}$ less than 0·1 was considered a sign of potential treatment interaction. The intention-to-treat population was used for the efficacy analysis.

ODYSSEY OUTCOMES is registered with ClinicalTrials.gov, number NCT01663402.

	All (n=18 924)	Alirocumab group (n=9462)	Placebo group (n=9462)
Metabolic risk factors			
Dysglycaemia*	10 512 (56%)	5262 (56%)	5250 (56%)
Hypertriglyceridemia†	7085 (37%)	3498 (37%)	3587 (38%)
Hypertension‡	9408 (50%)	4797 (51%)	4611 (49%)
Low HDL cholesterol§	8997 (48%)	4480 (47%)	4517 (48%)
BMI ≥30 kg/m²	6262 (33%)	3122 (33%)	3140 (33%)
Number of metabolic risk factors¶			
None	1613 (9%)	813 (9%)	800 (9%)
One	4297 (23%)	2161 (23%)	2136 (23%)
Two	5273 (28%)	2606 (28%)	2667 (28%)
Three	4330 (23%)	2162 (23%)	2168 (23%)
Four	2624 (14%)	1300 (14%)	1324 (14%)
Five	787 (4%)	420 (4%)	367 (4%)

Data are n (%). *Fasting plasma glucose of 100 mg/dL or more, or use of glucose-lowering medication. †Fasting triglycerides of 150 mg/dL or more. ‡Blood pressure of 130/85 mm Hg or more, or use of antihypertensive medication. §HDL cholesterol less than 40 mg/dL in men and less than 50 mg/dL in women. ¶Percentages might not add up to 100% because of rounding.

Table 1: **Patients with each metabolic risk factor in total population and treatment groups**

Role of the funding source

The funders selected the study sites and monitored and supervised data collection, did the statistical analysis, contributed to data interpretation, and provided input on the report. The executive steering committee decided to publish the manuscript and takes responsibility for the completeness and accuracy of the data and the fidelity of the trial to the protocol.

Results

Of 18 924 patients, 3882 (41%) of 9462 in the alirocumab group and 3859 (41%) of 9462 in the placebo group had three or more metabolic risk factors (figure 1, appendix p 10). Overall, 17 311 (92%) patients had at least one metabolic risk factor and 13 014 (69%) had two or more metabolic risk factors. The prevalence of metabolic

risk factors was similar in both groups. At baseline, dysglycaemia was present in 10512 (56%) of patients, hypertriglyceridaemia in 7085 (37%), hypertension in 9408 (50%), low HDL cholesterol in 8997 (48%), and BMI of at least 30 kg/m² in 6262 (33%; table 1; appendix p 2). 11183 patients (59%) had fewer than three factors, and 7741 (41%) had at least three factors (table 1).

Table 2 shows that patients with at least three metabolic risk factors were more likely to be female, reside in North America or Eastern Europe (less likely to reside in Western Europe or Asia), and to have a medical history including heart failure, previous myocardial infarction, or coronary revascularisation procedures compared with those who had fewer than three metabolic risk factors. Although statin treatment was used in almost all patients in both metabolic risk factor groups and use of evidence-based therapies was high overall, a higher percentage among those with at least three metabolic risk factors used β blockers and renin-angiotensin system inhibitors. A more extensive breakdown of baseline characteristics in subgroups with zero to five metabolic risk factors is shown in the appendix (pp 3–5).

Lipid concentrations in patients on alirocumab or placebo in metabolic risk factor groups are shown in the appendix (p 11). The concentration of LDL cholesterol was similar in patients with three or more versus those with fewer than three metabolic risk factors. As expected, patients with three or more metabolic risk factors had higher concentrations of triglyceride, non-HDL cholesterol, and apolipoprotein B, and a lower concentration of HDL cholesterol. Alirocumab had a similar lowering effect on concentrations of total cholesterol, LDL cholesterol, triglycerides, non-HDL cholesterol, and apolipoprotein B, and an increasing effect on HDL cholesterol concentration compared with placebo in both metabolic risk factor groups (appendix p 11).

	Three or more metabolic risk factors		Fewer than three metabolic risk factors	
	Alirocumab (n=3882)	Placebo (n=3859)	Alirocumab (n=5580)	Placebo (n=5603)
Age, years	58·2 (9·1)	58·3 (9·2)	58·7 (9·4)	58·9 (9·5)
Sex				
Female	1156 (30%)	1176 (31%)	1234 (22%)	1196 (21%)
Male	2726 (70%)	2683 (69%)	4346 (78%)	4407 (79%)
Race				
White	3155 (81%)	3137 (81%)	4345 (78%)	4387 (78%)
Black	112 (3%)	113 (3%)	123 (2%)	125 (2%)
Asian	403 (10%)	416 (11%)	848 (15%)	831 (15%)
Other	212 (6%)	193 (5%)	264 (5%)	260 (5%)
Region of enrolment				
North America	697 (18%)	703 (18%)	738 (13%)	733 (13%)
South America	590 (15%)	559 (15%)	703 (13%)	736 (13%)
Western Europe	701 (18%)	734 (19%)	1383 (25%)	1357 (24%)
Eastern Europe	1201 (31%)	1170 (30%)	1518 (27%)	1548 (28%)
Asia	365 (9%)	371 (10%)	785 (14%)	772 (14%)
Rest of world	328 (8%)	322 (8%)	453 (8%)	457 (8%)
Index ACS subtype				
STEMI	1294 (33%)	1203 (31%)	2007 (36%)	2032 (36%)
NSTEMI	1925 (50%)	1969 (51%)	2649 (48%)	2632 (47%)
Unstable angina	656 (17%)	682 (18%)	912 (16%)	932 (17%)
PCI or CABG for ACS index	2765 (71%)	2727 (71%)	4033 (72%)	4151 (74%)
Median time from index ACS event to randomisation, months	3·8 (2·9)	3·7 (2·7)	3·6 (2·8)	3·6 (2·7)
BMI, kg/m²	31·1 (5·1)	31·1 (5·0)	26·7 (3·8)	26·7 (3·8)
Systolic blood pressure, mm Hg	132·3 (15·4)	131·9 (15·8)	124·3 (15·4)	123·9 (15·6)
Diastolic blood pressure, mm Hg	79·7 (9·7)	79·7 (9·9)	75·9 (9·4)	75·5 (9·4)
Heart rate, bpm	68·6 (10·3)	68·5 (10·4)	65·6 (10·1)	65·8 (10·0)
eGFR, mL/min per 1·73 m²	78·8 (20·3)	78·8 (20·4)	80·0 (18·7)	80·5 (18·2)
Fasting glucose (mg/dL)	127·8 (49·1)	128·2 (50·2)	102·7 (29·0)	102·7 (28·7)
HbA_{1c}	6·6% (1·4)	6·6% (1·5)	5·9% (1·0)	5·9% (0·9)
Haemoglobin, g/L	141·9 (14·5)	141·9 (14·4)	142·0 (13·5)	141·9 (13·4)
Total cholesterol, mg/dL	168·9 (39·0)	169·9 (39·7)	164·8 (35·0)	164·3 (35·5)
LDL cholesterol, mg/dL	91·3 (33·2)	91·9 (33·1)	93·2 (29·6)	92·5 (29·1)

(Table 2 continues on next page)

	Three or more metabolic risk factors		Fewer than three metabolic risk factors	
	Alirocumab (n=3882)	Placebo (n=3859)	Alirocumab (n=5580)	Placebo (n=5603)
(Continued from previous page)				
HDL cholesterol, mg/dL	39·6 (9·3)	39·5 (9·2)	47·7 (11·5)	47·4 (11·6)
Triglycerides, mg/dL	191·0 (94·1)	193·7 (102·6)	118·2 (55·0)	120·4 (58·8)
Non-HDL cholesterol, mg/dL	130·7 (38·1)	129·6 (37·3)	117·1 (32·6)	117·4 (32·6)
Apolipoprotein B, g/L	0·884 (0·229)	0·878 (0·227)	0·798 (0·198)	0·797 (0·195)
High-sensitivity C-reactive protein, mg/L	4·30 (6·90)	4·28 (6·88)	3·25 (7·74)	3·13 (7·06)
Previous myocardial infarction	866 (22%)	867 (23%)	924 (17%)	976 (17%)
Previous PCI	804 (21%)	774 (20%)	822 (15%)	841 (15%)
Previous CABG	269 (7%)	255 (7%)	252 (5%)	271 (5%)
Previous stroke	165 (4%)	149 (4%)	141 (3%)	156 (3%)
Family history of premature coronary heart disease	1449 (37%)	1453 (38%)	1959 (35%)	1912 (34%)
Cerebrovascular disease	245 (6%)	225 (6%)	235 (4%)	245 (4%)
Peripheral artery disease	170 (4%)	179 (5%)	203 (4%)	207 (4%)
Hypertension	2984 (77%)	2871 (74%)	3221 (58%)	3173 (57%)
Heart failure	666 (17%)	651 (17%)	699 (13%)	798 (14%)
Diabetes	1597 (41%)	1555 (40%)	708 (13%)	785 (14%)
Cigarette smoking				
Current	915 (24%)	900 (23%)	1367 (25%)	1378 (25%)
Former	1559 (40%)	1625 (42%)	2316 (42%)	2311 (41%)
Never	1408 (36%)	1333 (35%)	1897 (34%)	1914 (34%)
Cardiovascular medication				
β blocker	3378 (87%)	3381 (88%)	4620 (83%)	4611 (82%)
Aspirin	3706 (96%)	3694 (96%)	5344 (96%)	5342 (95%)
P2Y12 inhibitor	3361 (87%)	3349 (87%)	4935 (88%)	4896 (87%)
ACE inhibitor or ARB	3177 (82%)	3158 (82%)	4179 (75%)	4202 (75%)
Statin	3773 (97%)	3755 (97%)	5457 (98%)	5480 (98%)

Data are number (%) or mean (SD). ACE=angiotensin-converting enzyme. ACS=acute coronary syndrome. ARB=angiotensin receptor blocker. CABG=coronary artery bypass grafting. CHD=coronary heart disease. eGFR=estimated glomerular filtration rate. PCI=percutaneous coronary intervention. STEMI=ST-elevated myocardial infarction. NSTEMI=non-ST-elevated myocardial infarction

Table 2: **Baseline characteristics in total population and treatment groups according to presence of at least three or fewer than three metabolic risk factors**

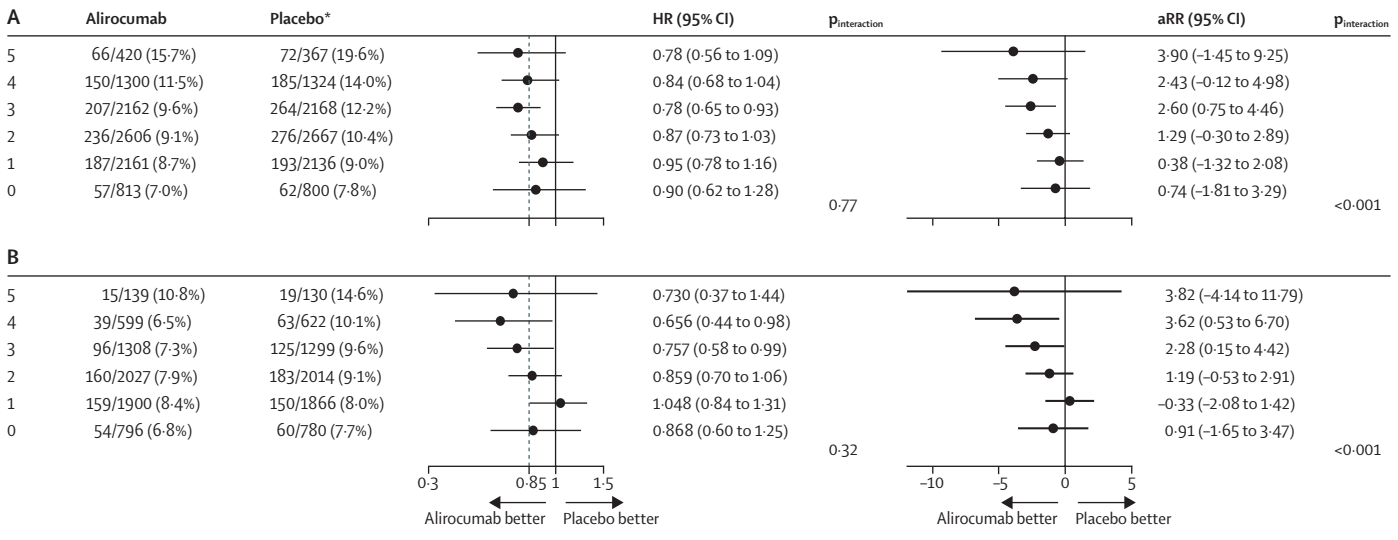

Figure 2: **Effect of alirocumab on MACE in subgroups by number of metabolic risk factors in (A) the overall study population and (B) after exclusion of patients with diabetes**
aRR=absolute risk reduction. MACE=major adverse cardiovascular event. *HR in placebo group 1·18 (95% CI 1·13 to 1·24) per incremental risk factor.

In the placebo group, incidence of MACE increased monotonically with each metabolic risk factor from 7·8% (no risk factors) to 19·6% (five risk factors; overall HR 1·18, 95% CI 1·13–1·24 per metabolic risk factor; figure 2A). The relative risk of MACE in the placebo group associated with the presence of each of the five metabolic risk factors is in the appendix (p 6). Dysglycaemia had the strongest association with risk of MACE (HR 1·43, 95% CI 1·26–1·62), followed by hypertension (HR 1·31, 95% CI 1·16–1·49). In the placebo group, patients with at least three metabolic risk factors (corresponding with presence of metabolic syndrome) had a greater risk of MACE than those with fewer than three risk factors (521 [14%] of 3859 *vs* 531 [10%] of 5603; HR 1·43, 95% CI 1·27–1·62; figure 3A, 4A).

Alirocumab decreased the relative risk of MACE consistently across categories defined by the number of metabolic risk factors ($p_{interaction}$=0·77), but absolute risk reduction (aRR) increased per incremental metabolic risk factor from 0·74% (95% CI –1·81 to 3·29) with 0 risk factors to 3·90% (–1·45 to 9·25) with five risk factors ($p_{interaction}$<0·001; figure 2A; appendix pp 12–16). Similarly, relative reductions in MACE by alirocumab were consistent in patients with at least three versus fewer than three metabolic risk factors (HR 0·80, 95% CI 0·71–0·91 *vs* HR 0·90, 0·79–1·02; $p_{interaction}$=0·22; figures 3A, 4A). However, aRR with alirocumab was greater in patients with at least three metabolic factors than in those with fewer than three factors (aRR 2·60%, 95% CI 1·15–4·06 *vs* aRR 0·87%, –0·19 to 1·94; $p_{interaction}$=0·08; figure 4A). The corresponding number needed to treat for a median of 2·8 years to avoid one primary endpoint event was 38 for patients with at least three metabolic risk factors compared with 115 for patients with fewer than three factors. The effect of alirocumab on MACE remained similar after inclusion of baseline concentration of LDL cholesterol into the model and in on-treatment analysis (appendix pp 17, 18).

An analysis excluding patients with diabetes yielded qualitatively similar results as in the full study population. Incidence of MACE in the placebo groups increased from 7·7% (no metabolic risk factors) to 14·6% (five factors; figure 2B). Alirocumab consistently decreased relative risk of MACE across subgroups defined by ordinal number of metabolic risk factors ($p_{interaction}$=0·32); however, aRR increased with increasing number of metabolic risk factors from none to five (aRR 0·91, 95% CI –1·65 to 3·47 *vs* aRR 3·82, –4·14 to 11·79; $p_{interaction}$<0·001; figure 2B; appendix pp 12–15). In the comparison of subgroups without diabetes who had at least three metabolic risk factors versus fewer than three factors (corresponding with the presence or absence of metabolic syndrome), there was an interaction of the effect of alirocumab on MACE: benefit appeared more pronounced in patients with at least three metabolic risk factors (HR 0·73, 95% CI 0·59–0·90) than in patients with fewer than three metabolic risk factors (HR 0·93, 95% CI 0·81–1·07; $p_{interaction}$=0·05; figures 3B, 4B). Again, the effect of alirocumab on MACE was minimally affected by the inclusion of baseline concentration of LDL cholesterol into the model and in the treatment analysis (appendix pp 17, 18). aRR with alirocumab was higher in patients with at least three metabolic risk factors than in those with fewer than three factors (aRR 2·76%, 95% CI 1·04–4·49 *vs* aRR 0·54%, 95% CI –0·57 to 1·64; $p_{interaction}$=0·04; figure 4B). The corresponding number needed to treat for a median of 2·8 years to avoid one primary endpoint event was 36 for patients with at least three factors versus 185 for patients with fewer than three factors.

Overall alirocumab was well tolerated with incidence of serious adverse events and treatment-emergent adverse events similar to placebo, except for injection site reactions

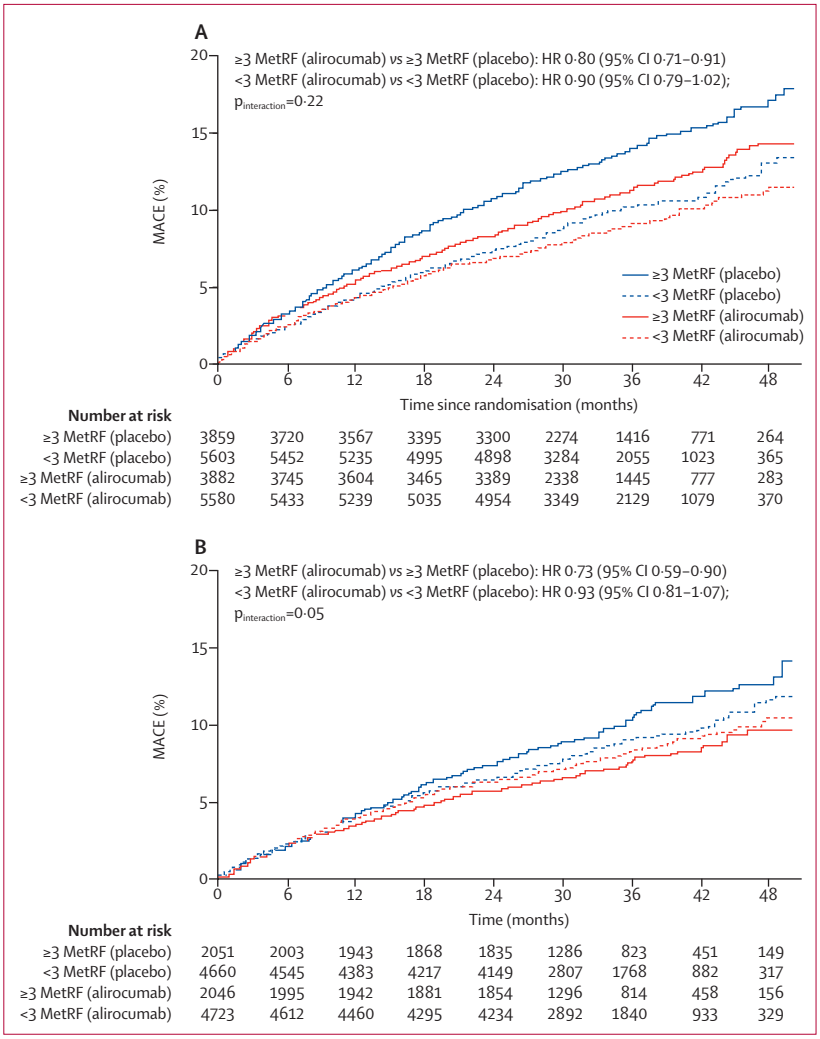

Figure 3: **Kaplan-Meier curves for MACE and effect of alirocumab in subgroups with at least three or fewer than three metabolic risk factors in (A) the overall study population and (B) after exclusion of patients with diabetes**

HR=hazard ratio. MACE=major adverse cardiovascular event. MetRF=metabolic risk factor.

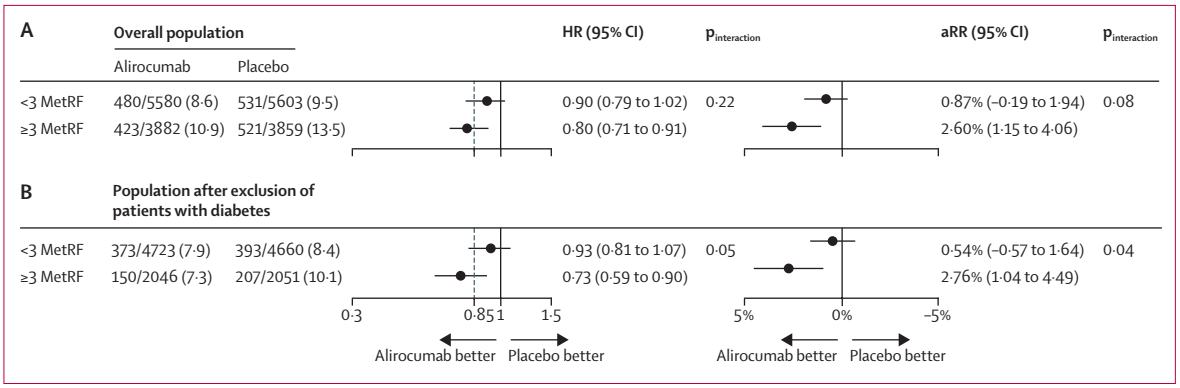

Figure 4: **Effect of alirocumab on MACE in subgroups according to presence of at least three and fewer than three metabolic risk factors in (A) the overall study population and (B) after exclusion of patients with diabetes**

aRR=absolute risk reduction. HR=hazard ratio. MACE=major adverse cardiovascular event. MetRF=metabolic risk factor.

which were more frequent with alirocumab. Treatment emergent adverse events were more common in the group with at least three metabolic risk factors compared to those with fewer than three metabolic risk factors. Incidence of type 2 diabetes in patients without diabetes at baseline was higher in the group with at least three factors than those with fewer than three metabolic risk factors, and in patients with prediabetes at baseline than in those with normoglycaemia (appendix 7). However, the incidence of the new diabetes onset in each subgroup was similar in the alirocumab and placebo groups (appendix p 8).

Discussion

There are three key findings from this post-hoc analysis. First, in the ODDESSY OUTCOMES trial, 91·5% of patients with recent acute coronary syndrome had at least one metabolic risk factor and 68·8% had two or more. Second, despite high-intensity or maximum-tolerated statin therapy, metabolic risk factors (except low concentration of HDL cholesterol) remained associated with increased risk of MACE, and accumulation of metabolic risk factors in patients with past acute coronary syndrome substantially increased risk for further cardiovascular events. Third, alirocumab reduced risk of MACE irrespective of the number of metabolic risk factors, but the absolute benefit increased with the number of risk factors. aRR, and potentially the relative risk reduction, appeared more pronounced in patients with at least three metabolic risk factors (corresponding with the presence of metabolic syndrome) than in those with fewer than three factors, especially in patients without diabetes.

The accumulation of metabolic risk factors and associated metabolic syndrome are known risk factors for MACE.[1–4] High-intensity statin therapy reduces risk in this population.[8,16] Our analysis indicates that accumulation of metabolic risk factors remains associated with increased risk of MACE after acute coronary syndrome, even when patients received evidence-based therapy, including high-intensity or maximum-tolerated statin treatment, use of β blockers, renin-angiotensin system blockers, dual antiplatelet therapy, and coronary revascularisation procedures. Moreover, in the placebo group, each metabolic risk factor except low HDL cholesterol (ie, dysglycaemia, hypertriglyceridaemia, hypertension, and BMI ≥30 kg/m²) was significantly associated with increased risk of MACE. The absence of association of risk after acute coronary syndrome with HDL cholesterol concentration was also observed in an analysis of the dal-OUTCOMES trial, comparing dalcetrapib with placebo in patients with acute coronary syndrome.[17]

Reduction of MACE associated with alirocumab in patients with and without at least three metabolic risk factors in our study was in accordance with other analyses from the ODYSSEY OUTCOMES trial, demonstrating consistent reduction in MACE across various subgroups, with more pronounced aRR in patients at higher risk.[9,12,18–23] Of particular importance was the observation in the ODYSSEY OUTCOMES trial of similar risk of MACE in patients with baseline normoglycaemia and prediabetes compared with markedly increased risk in patients with diabetes.[12] Because dysglycaemia comprises patients with prediabetes or diabetes, we assessed the effect of metabolic risk factors other than diabetes on risk and risk reduction with alirocumab. In patients without diabetes, the risk of MACE remained strongly associated with a larger ordinal number of metabolic risk factors and with at least three factors versus fewer than three factors. Relative reduction in risk of MACE with alirocumab was more pronounced in the subgroup with at least three metabolic risk factors. Importantly, the subgroup of patients without diabetes with at least three factors had more than five-times greater aRR with alirocumab than did the subgroup without diabetes and fewer than three risk factors (2·76% *vs* 0·54%). This suggests that in patients without diabetes, the accumulation of more metabolic risk factors helps to identify individuals in whom a greater absolute benefit of

alirocumab might be expected. The risk of recurrent cardiovascular events in patients with at least three metabolic risk factors remains high despite intensive lipid-lowering therapy with a statin and PCSK9 inhibitor and highly prevalent use of other evidence-based treatments, which indicates a need for additional therapies to improve the prognosis of these patients.

Our results are consistent with a report from the FOURIER trial[11] showing that patients with chronic atherosclerotic cardiovascular disease and metabolic syndrome remain at higher risk of future cardiovascular events despite statin therapy, and that treatment with the PCSK9 inhibitor evolocumab is associated with a reduction in cardiovascular events regardless of the presence or absence of diabetes.

In the ODYSSEY OUTCOMES trial, waist circumference (the criterion for abdominal obesity required for the diagnosis of metabolic syndrome) was not recorded; therefore, patients with strictly defined metabolic syndrome[1] could not be identified. To mitigate this limitation, the presence of obesity was evaluated according to BMI (≥30 kg/m²), another recognised factor associated with increased risk.[14,24–26] and incorporated in some definitions of metabolic syndrome.[27] In clinical practice, weight is measured more commonly than waist circumference.[28] Thus, the present analytical framework might have practical relevance in the decision to treat with a PCSK9 inhibitor. The absence of ethnic-specific thresholds for BMI is a potential source of bias. Baseline lipid concentrations including triglyceride concentrations in the ODYSSEY OUTCOMES trial were measured in patients who already received high-intensity or maximally tolerated dose of statin. Because statins generally reduce triglycerides, the true prevalence of hypertriglyceridaemia according to the definition of metabolic syndrome[1] was probably higher than observed in the present analysis. Median follow-up in the ODYSSEY OUTCOMES trial was 2·8 years. Longer observation might have revealed greater differences in risk between metabolic risk factor groups and greater risk reduction with alirocumab, as has been shown in a subset of the overall study cohort eligible for at least 3 years of observation.[29,30] The safety observations from the present analysis should also be put in the context of a brief follow-up. Although we focused on metabolic risk factors, recognising that other clinical characteristics affect risk of MACE following acute coronary syndrome and that other high-risk subgroups can be defined by those criteria is important.[20–22,31] Statistical inference should be considered in the context of the fact that the trial was not powered for the current subgroup analyses and that there was no allowance for multiplicity of assessments.

Metabolic risk factors remain important factors for subsequent MACE despite high-intensity or maximum-tolerated statin therapy in patients with recent acute coronary syndrome. Alirocumab treatment resulted in a consistent relative reduction in the risk of MACE in patients with or without accumulation of multiple metabolic risk factors, although absolute risk reduction was more pronounced with a greater number of risk factors. Both the relative and absolute effects of alirocumab were more pronounced in patients with at least three factors. Patients with multiple metabolic risk factors, including those without diabetes, might derive a large absolute benefit of alirocumab treatment after acute coronary syndrome. Counting the number of metabolic risk factors could help clinicians to identify patients to be considered for PCSK9 inhibitor therapy after acute coronary syndrome.

Contributors

PO, GS, and GGS conceived and designed the study. PGS and GGS obtained funding and supervised the work. PO, PGS, DLB, VAB, TC, RD, SGG, JWJ, YK, HDW, YH, and GGS acquired, analysed, or interpreted the data. PO drafted the manuscript. YP did the statistical analysis. All authors critically revised the manuscript for important intellectual content. PO, PGS, GGS, and MSz developed the trial protocol and statistical analysis plan in conjunction with the other members of the executive steering committee, which includes representatives of the funders (appendix p 19). PO, PGS, and GGS take responsibility for the integrity of data and accuracy of the data analysis. All authors had full access to all the data in the study and final responsibility for the decision to submit for publication. PO, PGS, GGS and YP have accessed and verified the data.

Declaration of interests

PO reports research grants or speaker and consulting honoraria (or both) from Amgen, AstraZeneca, Edwards, Getinge, Novartis, Promedica, Promedcs, Sanofi, and Servier. PGS reports grants, personal fees, and non-financial support from Sanofi; grants and personal fees from Amarin, Servier and Bayer; personal fees from Amgen, AstraZeneca, BMS, Boehringer Ingelheim, Idorsia, Pfizer, and Novartis; and has patent use of alirocumab to reduce risk after ACS (royalties to Sanofi) pending. YP and MSc are employees of Sanofi. DLB reports grants from Sanofi, Regeneron Pharmaceuticals, Amarin, AstraZeneca, Bristol-Myers Squibb, Eisai, Ethicon, Medtronic, Sanofi Aventis, The Medicines Company, Forest Laboratories/AstraZeneca, Ischemix, Amgen, Lilly, Chiesi, Ironwood, Abbott, Idorsia, Synaptic, Fractyl, Afimmune, Ferring Pharmaceuticals, Lexicon, Contego Medical, Owkin, HLS Therapeutics, 89Bio, and Garmin; is a Board Director at Boston Scientific and Boston VA Research Institute; receives unfunded research collaboration from Merck, FlowCo, and Takeda; is a site co-investigator for Svelte, CSI, Boston Scientific, Philips, St Jude Medical (Abbott), and Biotronik; is on the Advisory Board for Medscape Cardiology and Regado Biosciences; receives a grant from Roche and Pfizer; is a Deputy Editor for Clinical Cardiology; is a Chair at VA; receives grants from and is on the Scientific Advisory Board at Cardax, PLx Pharma, PhaseBio, Novo Nordisk, Cereno Scientific, CellProthera, MyoKardia/BMS, Janssen, Novartis, and NirvaMed; receives personal fees from Duke Clinical Research Institute, Mayo Clinic, Population Health Research Institute, Belvoir Publications, Slack Publications, WebMD, Elsevier, HMP Global, Harvard Clinical Research Institute (Baim Institute for Clinical Research), Journal of the American College of Cardiology, Cleveland Clinic, Mount Sinai School of Medicine, TobeSoft, Bayer, Medtelligence/ReachMD, CSL Behring, MJH Life Sciences, Level Ex, K2P, and the Canadian Medical and Surgical Knowledge Translation Research Group; reports personal fees and non-financial support from, and is a Senior Associate Editor, Chair, and Trustee at American College of Cardiology; reports personal fees and non-financial support from the Society of Cardiovascular Patient Care; non-financial support from American Heart Association; and grants, personal fees, and editorial support services from Boehringer Ingelheim. VAB reports grant support from Sanofi, Regeneron Pharmaceuticals, Astra Zeneca, DalCor, Esperion, and Novartis; consulting fees from Pfizer; honoraria from Medscape; and fees for participating on a Data Safety Monitoring Board or Advisory Board from the National Institutes of Health. RD reports research grants from Sanofi, DalCor Pharmaceuticals, Population Health Research Institute, Duke Clinical

Research Institute, the TIMI group, Amgen, Cirius, Montreal Health Innovations Coordinating Center, and Lepetit, and personal fees, as a member of the Executive Steering Committee, from Amgen and Cirius. SGG reports research grant support (eg, steering committee or data and safety monitoring committee) or speaker and consulting honoraria (or both), from Amgen, AstraZeneca, Bayer, Boehringer Ingelheim, Bristol Myers Squibb, CSL Behring, Daiichi-Sankyo/American Regent, Eli Lilly, Esperion, Ferring Pharmaceuticals, GlaxoSmithKline, HLS Therapeutics, JAMP Pharma, Janssen/Johnson and Johnson, Merck, Novartis, Novo Nordisk A/C, Pendopharm, Pfizer, Regeneron, Sanofi, Servier, Valeo Pharma; and salary support or honoraria from the Heart and Stroke Foundation of Ontario/University of Toronto (Polo) Chair, Canadian Heart Research Centre and MD Primer, Canadian VIGOUR Centre, Cleveland Clinic Coordinating Centre for Clinical Research, Duke Clinical Research Institute, New York University Clinical Coordinating Centre, and PERFUSE Research Institute. YH reports speaker or consulting honoraria from Pfizer, Bayer, Novartis, AstraZeneca, and Sanofi. JWJ reports research grants from the Netherlands Heart Foundation, the Interuniversity Cardiology Institute of the Netherlands, and the European Commission Seventh Framework Programme, and research support from Amgen, Astellas, AstraZeneca, Daiichi- Sankyo, Lilly, Merck-Schering-Plough, Pfizer, Roche, and Sanofi. YK reports payment or honoraria for lectures, presentations, speaker's bureaus, manuscript writing or educational events from Sanofi, Pfizer, Servier, Amgen, Berlin-Chemie, Bayer, Recordati, AstraZeneca, MSD, Takeda, Boeringer Ingelheim, and KRKA; support for attending meetings or travel (or both) from Sanofi-Aventis, Pfizer, Servier, Berlin-Chemie, Bayer, AstraZeneca, and Takeda; and participation on a Data Safety Monitoring Board or Advisory Board for MSD, Servier, AstraZeneca, Sanofi. RP is an employee of Regeneron Pharmaceuticals. MSz reports serving as a consultant or on advisory boards (or both) for CiVi, Resverlogix, Baxter, Esperion, Sanofi, and Regeneron Pharmaceuticals. HDW reports receiving grant support paid to the institution and fees for serving on a steering committee for the ODYSSEY OUTCOMES trial (evaluation of cardiovascular outcomes after an acute coronary syndrome during treatment with alirocumab) from Sanofi-Aventis and Regeneron Pharmaceuticals, for the ACCELERATE study (a study of evacetrapib in high-risk vascular disease) from Eli Lilly, for the STRENGTH trial (outcomes study to assess statin residual risk reduction with EpaNova in high CV risk patients with hypertriglyceridemia) from Omthera Pharmaceuticals, for the SPIRE trial (the evaluation of bococizumab [PF-04950615; RN 316] in reducing the occurrence of major cardiovascular events in high risk subjects) from Pfizer USA, for the HEART-FID study (randomised placebo-controlled trial of FCM as treatment for heart failure with iron deficiency) from American Regent; for the CAMELLIA-TIMI study (a study to evaluate the effect of long-term treatment with BELVIQ [Lorcaserin HC] on the incidence of major adverse cardiovascular events and conversion to type 2 diabetes mellitus in patients with overweight and obesity and with cardiovascular disease or multiple cardiovascular risk factors) from Eisai, for the dal-GenE study (effect of dalcetrapib *vs* placebo on CV risk in a genetically defined population with a recent ACS) from DalCor Pharma UK, for the AEGIS-II study from CSL Behring, for the SCORED trial (effect of sotagliflozin on cardiovascular and renal events in patients with type 2 diabetes and moderate renal impairment who are at cardiovascular risk) and the SOLOIST-WHF trial (effect of sotagliflozin on cardiovascular events in patients with type 2 diabetes post worsening heart failure) from Sanofi-Aventis Australia, and for the CLEAR Outcomes Study (evaluation of major cardiovascular events in patients with, or at high risk for, cardiovascular disease who are statin intolerant treated with bempedoic acid [ETC-1002] or placebo) from esperion therapeutics. HDW was on the Advisory Boards for Acetelion, Sirtex, and Genentech, and received lecture fees from AstraZeneca. GGS reports research grants to the University of Colorado from Resverlogix, Sanofi, The Medicines Company, and Roche, and is coinventor of pending US patent 62/806,313 (Methods for reducing cardiovascular risk) assigned in full to the University of Colorado. TC declares no competing interests.

Data sharing

Individual participant data are not available. The study protocol and statistical analysis plan have been previously published.[9]

Acknowledgments

We thank the patients, study coordinators, and investigators who participated in this trial. Sophie Rushton-Smith (MedLink Healthcare Communications, London) provided editorial assistance in the preparation of the manuscript (limited to editing for style, referencing, and figure and table editing) and was funded by Sanofi, Paris, France. Data in this paper were presented in part at the American College of Cardiology 2021, Atlanta GA, on May 16, 2021.

References

1 Alberti KG, Eckel RH, Grundy SM, et al. Harmonising the metabolic syndrome: a joint interim statement of the International Diabetes Federation Task Force on Epidemiology and Prevention; National Heart, Lung, and Blood Institute; American Heart Association; World Heart Federation; International Atherosclerosis Society; and International Association for the Study of Obesity. *Circulation* 2009; **120:** 1640–45.

2 Ford ES. Risks for all-cause mortality, cardiovascular disease, and diabetes associated with the metabolic syndrome: a summary of the evidence. *Diabetes Care* 2005; **28:** 1769–78.

3 Galassi A, Reynolds K, He J. Metabolic syndrome and risk of cardiovascular disease: a meta-analysis. *Am J Med* 2006; **119:** 812–19.

4 Gami AS, Witt BJ, Howard DE, et al. Metabolic syndrome and risk of incident cardiovascular events and death: a systematic review and meta-analysis of longitudinal studies. *J Am Coll Cardiol* 2007; **49:** 403–14.

5 Grundy SM, Stone NJ, Bailey AL, et al. 2018 AHA/ACC/AACVPR/AAPA/ABC/ACPM/ADA/AGS/APhA/ASPC/NLA/PCNA Guideline on the management of blood cholesterol: Executive Summary: a report of the American College of Cardiology/American Heart Association Task Force on Clinical Practice Guidelines. *Circulation* 2019; **139:** e1046–81.

6 Piepoli MF, Hoes AW, Agewall S, et al. 2016 European Guidelines on cardiovascular disease prevention in clinical practice: The Sixth Joint Task Force of the European Society of Cardiology and Other Societies on Cardiovascular Disease Prevention in Clinical Practice (constituted by representatives of 10 societies and by invited experts) developed with the special contribution of the European Association for Cardiovascular Prevention & Rehabilitation (EACPR). *Eur Heart J* 2016; **37:** 2315–81.

7 Mach F, Baigent C, Catapano AL, et al. 2019 ESC/EAS Guidelines for the management of dyslipidaemias: lipid modification to reduce cardiovascular risk. *Eur Heart J* 2020; **41:** 111–88.

8 Deedwania P, Barter P, Carmena R, et al. Reduction of low-density lipoprotein cholesterol in patients with coronary heart disease and metabolic syndrome: analysis of the Treating to New Targets study. *Lancet* 2006; **368:** 919–28.

9 Schwartz GG, Steg PG, Szarek M, et al. Alirocumab and cardiovascular outcomes after acute coronary syndrome. *N Engl J Med* 2018; **379:** 2097–107.

10 Sabatine MS, Leiter LA, Wiviott SD, et al. Cardiovascular safety and efficacy of the PCSK9 inhibitor evolocumab in patients with and without diabetes and the effect of evolocumab on glycaemia and risk of new-onset diabetes: a prespecified analysis of the FOURIER randomised controlled trial. *Lancet Diabetes Endocrinol* 2017; **5:** 941–50.

11 Deedwania P, Murphy SA, Scheen A, et al. Efficacy and safety of PCSK9 inhibition with evolocumab in reducing cardiovascular events in patients with metabolic syndrome receiving statin therapy: secondary analysis from the FOURIER randomised clinical trial. *JAMA Cardiol* 2021; **6:** 139–47.

12 Ray KK, Colhoun HM, Szarek M, et al. Effects of alirocumab on cardiovascular and metabolic outcomes after acute coronary syndrome in patients with or without diabetes: a prespecified analysis of the ODYSSEY OUTCOMES randomised controlled trial. *Lancet Diabetes Endocrinol* 2019; **7:** 618–28.

13 Schwartz GG, Bessac L, Berdan LG, et al. Effect of alirocumab, a monoclonal antibody to PCSK9, on long-term cardiovascular outcomes following acute coronary syndromes: rationale and design of the ODYSSEY outcomes trial. *Am Heart J* 2014; **168:** 682–89.

14 Song X, Jousilahti P, Stehouwer CD, et al. Comparison of various surrogate obesity indicators as predictors of cardiovascular mortality in four European populations. *Eur J Clin Nutr* 2013; **67:** 1298–302.

15 Schwartz GG, Steg PG, Szarek M, et al. Alirocumab and cardiovascular outcomes after acute coronary syndrome. *N Engl J Med* 2018; **379:** 2097–107.

16 Schwartz GG, Olsson AG, Szarek M, Sasiela WJ. Relation of characteristics of metabolic syndrome to short-term prognosis and effects of intensive statin therapy after acute coronary syndrome: an analysis of the Myocardial Ischemia Reduction with Aggressive Cholesterol Lowering (MIRACL) trial. *Diabetes Care* 2005; **28:** 2508–13.

17 Salahuddin T, Kittelson J, Tardif JC, et al. Association of high-density lipoprotein particle concentration with cardiovascular risk following acute coronary syndrome: a case-cohort analysis of the dal-outcomes trial. *Am Heart J* 2020; **221:** 60–66.

18 Schwartz GG, Steg PG, Szarek M, et al. Peripheral artery disease and venous thromboembolic events after acute coronary syndrome: role of lipoprotein(a) and modification by alirocumab: prespecified analysis of the ODYSSEY OUTCOMES randomised clinical trial. *Circulation* 2020; **141:** 1608–17.

19 Goodman SG, Steg PG, Szarek M, et al. Sustained low-density lipoprotein cholesterol lowering with alirocumab in ODYSSEY OUTCOMES. *J Am Coll Cardiol* 2020; **75:** 448–51.

20 Jukema JW, Szarek M, Zijlstra LE, et al. Alirocumab in patients with polyvascular disease and recent acute coronary syndrome: ODYSSEY OUTCOMES Trial. *J Am Coll Cardiol* 2019; **74:** 1167–76.

21 Tunon J, Steg PG, Bhatt DL, et al. Effect of alirocumab on major adverse cardiovascular events according to renal function in patients with a recent acute coronary syndrome: prespecified analysis from the ODYSSEY OUTCOMES randomised clinical trial. *Eur Heart J* 2020; **41:** 4114–23.

22 Sinnaeve PR, Schwartz GG, Wojdyla DM, et al. Effect of alirocumab on cardiovascular outcomes after acute coronary syndromes according to age: an ODYSSEY OUTCOMES trial analysis. *Eur Heart J* 2020; **41:** 2248–58.

23 Diaz R, Li QH, Bhatt DL, et al. Intensity of statin treatment after acute coronary syndrome, residual risk, and its modification by alirocumab: insights from the ODYSSEY OUTCOMES trial. *Eur J Prev Cardiol* 2021; **28:** 33–43.

24 Darbandi M, Pasdar Y, Moradi S, Mohamed HJJ, Hamzeh B, Salimi Y. Discriminatory capacity of anthropometric indices for cardiovascular disease in adults: a systematic review and meta-analysis. *Prev Chronic Dis* 2020; **17:** e131.

25 Huxley R, Mendis S, Zheleznyakov E, Reddy S, Chan J. Body-mass index, waist circumference and waist:hip ratio as predictors of cardiovascular risk—a review of the literature. *Eur J Clin Nutr* 2010; **64:** 16–22.

26 Song X, Jousilahti P, Stehouwer CD, et al. Cardiovascular and all-cause mortality in relation to various anthropometric measures of obesity in Europeans. *Nutr Metab Cardiovasc Dis* 2015; **25:** 295–304.

27 Alberti KG, Zimmet PZ. Definition, diagnosis and classification of diabetes mellitus and its complications. Part 1: diagnosis and classification of diabetes mellitus provisional report of a WHO consultation. *Diabet Med* 1998; **15:** 539–53.

28 Adab P, Pallan M, Whincup PH. Is BMI the best measure of obesity? *BMJ* 2018; **360:** k1274.

29 Steg PG, Szarek M, Bhatt DL, et al. Effect of alirocumab on mortality after acute coronary syndromes. *Circulation* 2019; **140:** 103–12.

30 Szarek M, White HD, Schwartz GG, et al. Alirocumab reduces total nonfatal cardiovascular and fatal events: the ODYSSEY OUTCOMES Trial. *J Am Coll Cardiol* 2019; **73:** 387–96.

31 Goodman SG, Aylward PE, Szarek M, et al. Effects of alirocumab on cardiovascular events after coronary bypass surgery. *J Am Coll Cardiol* 2019; **74:** 1177–86.

P. Ošťádal et al.

Extracorporeal Membrane Oxygenation in the Therapy of Cardiogenic Shock: Results of the ECMO-CS Randomized Clinical Trial

Circulation
Impact Factor: 39.922

‹ rejstřík

10.1161/CIRCULATIONAHA.122.062949

Extracorporeal Membrane Oxygenation in the Therapy of Cardiogenic Shock: Results of the ECMO-CS Randomized Clinical Trial

Running title: *Ostadal et al.; ECMO in cardiogenic shock*

Petr Ostadal, MD, PhD[1]; Richard Rokyta, MD, PhD[2]; Jiri Karasek, MD, PhD[3,4]; Andreas Kruger, MD, PhD[1]; Dagmar Vondrakova, MD, PhD[1]; Marek Janotka, MD[1]; Jan Naar, MD, PhD[1]; Jana Smalcova, MD[4]; Marketa Hubatova, MSc[4]; Milan Hromadka, MD, PhD[3]; Stefan Volovar, MD[3]; Miroslava Seyfrydova, MD[3]; Jiri Jarkovsky, PhD[5]; Michal Svoboda, MSc[6]; Ales Linhart, MD, PhD[4]; Jan Belohlavek, MD, PhD[4]; for the ECMO-CS Investigators

[1]Department of Cardiology, Na Homolce Hospital, Prague, Czech Republic; [2]Department of Cardiology, University Hospital and Faculty of Medicine Pilsen, Charles University, Czech Republic; [3]Hospital Liberec, Liberec, Czech Republic; [4]2nd Department of Medicine - Department of Cardiovascular Medicine, First Faculty of Medicine, Charles University and General University Hospital, Prague, Czech Republic; [5]Institute of Biostatistics and Analyses, Faculty of Medicine, Masaryk University, Brno, Czech Republic; [6]Institute of Biostatistics and Analyses, Ltd., Brno, Czech Republic

Address for Correspondence:
Prof. Petr Ostadal, MD, PhD
Cardiovascular Center
Na Homolce Hospital
Roentgenova 2, 15000 Prague, Czech Republic
Phone: +420257272208
E-mail: ostadal.petr@gmail.com

*This work was presented as an abstract at AHA Scientific Sessions, November 5-7 2022

Abstract

Background: Veno-arterial extracorporeal membrane oxygenation (VA-ECMO) is increasingly being used for circulatory support in cardiogenic shock patients, although the evidence supporting its use in this context remains insufficient. The aim of the Extracorporeal Membrane Oxygenation in the Therapy of Cardiogenic Shock (ECMO-CS) trial was to compare immediate implementation of VA-ECMO vs. an initially conservative therapy (allowing downstream use of VA-ECMO) in patients with rapidly deteriorating or severe cardiogenic shock .

Methods: This multicenter, randomized, investigator-initiated, academic clinical trial included patients with either rapidly deteriorating or severe cardiogenic shock. Patients were randomly assigned to immediate VA-ECMO or no immediate VA-ECMO. Other diagnostic and therapeutic procedures were performed as per current standard(s) of care. In the early conservative group, VA-ECMO could be used downstream in case of worsening hemodynamic status. The primary endpoint was the composite of death from any cause, resuscitated circulatory arrest, and implementation of another mechanical circulatory support device at 30 days.

Results: A total of 122 patients were randomized; after excluding 5 patients due to the absence of informed consent, 117 subjects were included in the analysis, of whom 58 randomized to immediate VA-ECMO and 59 to no immediate VA-ECMO. The composite primary endpoint occurred in 37 (63.8%) and 42 (71.2%) of patients in the immediate VA-ECMO and the no early VA-ECMO groups, respectively (hazard ratio, 0.72; 95% confidence intervals [CI], 0.46 to 1.12; P=0.21). VA-ECMO was used in 23 (39%) of no early VA-ECMO patients. The 30-day incidence of resuscitated cardiac arrest (10.3.% vs. 13.6%; risk difference [RD], -3.2; 95% CI, -15.0 to 8.5), all-cause mortality (50.0% versus 47.5%; RD, 2.5; 95% CI, -15.6 to 20.7), serious adverse events (60.3% vs. 61.0%; RD, -0.7; 95% CI, -18.4 to 17.0), sepsis, pneumonia, stroke, leg ischemia, and bleeding was not statistically different between the immediate VA-ECMO and the no immediate VA-ECMO groups.

Conclusion: Immediate implementation of VA-ECMO in patients with rapidly deteriorating or severe cardiogenic shock did not improve clinical outcomes compared with an early conservative strategy that permitted downstream use of VA-ECMO in case of worsening hemodynamic status.

Clinical Trial Registration:
URL: https://www.clinicaltrials.gov; Unique identifier NCT02301819.

Nonstandard Abbreviations and Acronyms

VA-ECMO	Veno-arterial extracorporeal membrane oxygenation
ECMO-CS	Extracorporeal Membrane Oxygenation in the Therapy of Cardiogenic Shock Trial
LVEF	Left ventricular ejection fraction
SCAI	Society for Cardiovascular Angiography and Interventions

Clinical Perspective

What is new?

- In the ECMO-CS (Extracorporeal Membrane Oxygenation in the Therapy of Cardiogenic Shock) Trial, immediate implementation of veno-arterial extracorporeal membrane oxygenation (VA-ECMO) did not improve outcomes compared with no immediate VA-ECMO in patients with severe or rapidly deteriorating cardiogenic shock.
- A large proportion (39%) of patients in the no early VA-ECMO group subsequently received VA-ECMO or other mechanical circulatory support due to further hemodynamic deterioration.

What are the Clinical Implications?

- Even in patients with severe or rapidly deteriorating cardiogenic shock, early hemodynamic stabilization using inotropes and vasopressors with implementation of mechanical circulatory support only in case of further hemodynamic deterioration provided outcomes that were not different than immediate insertion of VA-ECMO.

Introduction

Cardiogenic shock is a critical condition with various etiologies, phenotypes, and presentations [1]. Despite advances in cardiovascular acute and intensive care, early mortality from cardiogenic shock remains high [2, 3].

Multiple mechanical circulatory support systems have been developed over the past few decades that can be used for hemodynamic stabilization in this patient population [4]. However, currently available mechanical circulatory support (MCS) devices have not been demonstrated to improve survival in cardiogenic shock. [4]. Veno-arterial extracorporeal membrane oxygenation (VA-ECMO) is increasingly being used in patients with severe circulatory collapse. Compared with other MCS devices VA-ECMO can provide full circulatory support and pulmonary gas exchange and rapidly restore organ perfusion in the case of right-, left-, or bi-ventricular failure. [4]

According to the current guidelines of the European Society of Cardiology, MCS should be considered for hemodynamic stabilization in patients experiencing cardiogenic shock (class of recommendation IIa, level of evidence C). VA-ECMO may also be considered in patients with fulminant myocarditis and other conditions causing severe cardiogenic shock [5]. A position statement of the Acute Cardiovascular Care Association of the European Society of Cardiology recommends the use of VA-ECMO in selected patients with refractory cardiogenic shock caused by acute myocardial infarction [6]. Two scientific statements from the American Heart Association recommend consideration of MCS escalation in appropriately selected patients with clinical hypoperfusion or hemodynamic deterioration while on inotropes, selecting the MCS type of according to the specific hemodynamic condition(s) [7, 8]. However, these recommendations are largely based on data from retrospective studies, registry analyses, and expert opinions. The first small randomized study comparing VA-ECMO and conservative therapy in cardiogenic shock included 42 patients and did not find

significant differences between the study arms [9, 10]. Currently, there are no available data from large, prospective, randomized-controlled trials focusing on the use of VA-ECMO in patients with cardiogenic shock, however several studies are ongoing (Testing the Value of Novel Strategy and Its Cost Efficacy in Order to Improve the Poor Outcomes in Cardiogenic Shock [EURO-SHOCK], Assessment of ECMO in Acute Myocardial Infarction Cardiogenic Shock [ANCHOR], Extracorporeal Life Support in Cardiogenic Shock [11]) [11, 12].

The aim of the Extracorporeal Membrane Oxygenation in the therapy of Cardiogenic Shock (ECMO-CS) trial was to compare immediate implementation of VA-ECMO vs. early conservative therapy allowing downstream use of VA-ECMO in case of hemodynamic deterioration, on the background of standard care.

Methods

Trial organization and overview

The ECMO-CS trial was a multicenter, randomized, investigator-initiated clinical trial conducted at four centers in the Czech Republic. The study protocol was approved by the Ethics Committees of all participating centers. The trial design has been published [13]. The protocol was designed by the first two and the last author, and is available as a full text article at Supplemental Material. All patients provided informed written consent to participate in the study. If patient status did not permit informed consent, it was provided retrospectively after improvement of their clinical condition. If a patient died, remained unconscious, or had significant brain dysfunction, informed consent was obtained from the patient's next of kin. If informed consent was not obtained, all acquired data were removed from the database and were not used for the analysis. Statistical analyses were performed by an independent academic statistical center (Institute of Biostatistics and Analyses, Masaryk University, Brno, Czech Republic). The authors confirm the accuracy and completeness of the data and for the

fidelity of the trial to the protocol. The ECMO-CS trial was supported by a grant from the Czech health research council (No. 15-27994A) and was registered at ClinicalTrials.gov (NCT02301819). The data that support the findings of this study are available from the corresponding author upon reasonable request.

Trial population

Patients were eligible for randomization if they had either rapidly deteriorating or severe cardiogenic shock, defined by echocardiographic, hemodynamic, and metabolic criteria (Table 1). Exclusion criteria include age < 18 years, life expectancy lower than one year, high suspicion of pulmonary emboli or cardiac tamponade as a cause of shock, significant bradycardia or tachycardia that could be responsible for hemodynamic instability and was not treated by pacing or cardioversion, cardiac arrest survivors remaining comatose, hypertrophic obstructive cardiomyopathy, peripheral artery disease precluding arterial cannula insertion in the femoral artery, moderate to severe aortic regurgitation, aortic dissection, uncontrolled bleeding or TIMI major bleeding within last 6 months, and known encephalopathy. Details regarding the inclusion and exclusion criteria are provided in the Supplemental Material.

Trial procedures

Patients who fulfilled the trial entry criteria were randomly assigned in a 1:1 ratio to one of two arms: immediate VA-ECMO or early conservative therapy; the study was unblinded. An automated, web-based system was used for randomization with permuted blocks, with stratification according to the type of cardiogenic shock (rapidly deteriorating or severe), and the trial center. Except for immediate VA-ECMO implementation in the intervention group, all other diagnostic and therapeutic procedures were performed as per current standard(s) of care, including other cardiovascular interventions (i.e., percutaneous coronary or non-coronary intervention, cardiac surgery) or mechanical circulatory support. In the early conservative group, VA-ECMO could be used downstream in case of further worsening of

hemodynamic status, defined as rise of serum lactate by 3 mmol/L in comparison with the lowest value during the past 24 hours. The indications and strategies for left ventricular venting during the VA-ECMO support and also strategies for prevention or treatment of leg ischemia were not defined in the protocol and were left to the discretion of the physicians at the participating centers.

Trial end points

The primary endpoint was the composite of death from any cause, resuscitated circulatory arrest, and implementation of another mechanical circulatory support (including VA-ECMO in the conservative arm) at 30 days. Prespecified secondary endpoints included all-cause mortality at 30 days, neurological outcome (according to the Cerebral Performance Category scale) at 30 days, clinically significant bleeding, leg ischemia, pneumonia, sepsis and technical complications. The endpoints (including the safety endpoints) were reported by investigators without independent adjudication.

Power analysis and sample size calculation

With the sample size of 120 individuals (60 individuals in each arm) the study had 80% power to detect 50% reduction of primary endpoint at two-sided alpha of 0.05.

Statistical analysis

Analyses were performed according to the intention-to-treat principle and included data from all patients and for all events that occurred from the time of randomization until 30 days. Categorical variables are presented as percentages and compared using Pearson Chi Square test or Fisher's exact test. Continuous variables were presented as median (interquartile range) and compared using t-test or Mann-Whitney test.

The time to the occurrence of the primary composite end point (or death) was analyzed using the Kaplan-Meier method and compared using log-rank test. Calculation of the 95% confidence intervals for point estimates of end point occurrence probability are based on the

cumulative risk function (or logarithmic transformation of the survival function). Hazard ratios (HR) with 95% confidence intervals were calculated using a Cox proportional hazard model with Efron approximation for tie holding. Furthermore, multivariate Cox model was used with adjustment for significantly different variables in baseline characteristics. In case that proportionality of risk was not met, sensitivity analysis (Weibull AFT model) was prepared. Differences in end point proportions between the two categories were investigated using risk difference (RD) with 95% confidence intervals. Because of the potential for type 1 error due to multiple comparisons, findings for the secondary outcomes and subgroup analyses should be interpreted as exploratory. The analysis was performed using SPSS version 28 (IBM Corporation, Armonk, NY, USA) and R version 4.2.1 (R Foundation for Statistical Computing, Vienna, Austria). Hypotheses were tested at a significance level of 5%.

Results

Patients

Between September 2014 and January 2022, a total of 122 patients were randomly assigned to immediate VA-ECMO vs no immediate VA-ECMO. After excluding 5 patients due to absence of informed consent (all of them died and informed consent could not be obtained from next of kin) 58 subjects were included in the immediate VA-ECMO group and 59 in the early conservative therapy group (Figure S1). The baseline characteristics of the two study groups at the time of randomization were balanced (Table 2). The median age was 67 (60 to 74) years in the immediate VA-ECMO group and 65 years (58 to 71 years) in the early conservative group. In the immediate VA-ECMO group, fewer patients were smokers. Arterial blood lactate level at randomization was 5.3 mmol/L (3.1 to 8.4 mmol/L) in the immediate VA-ECMO group and 4.7 mmol/L (3.3 to 7.4 mmol/L) in the early conservative group. More than 70% of patients in both groups were on mechanical ventilation.

Furthermore, 86.2% of subjects in the immediate VA-ECMO group and 84.7% in the early conservative group received norepinephrine and a substantial proportion of both groups received dobutamine, milrinone, and vasopressin. The vasoactive-inotropic score was 59.9 (32.8 to 121.5) in the immediate VA-ECMO group and 61.0 (28.0 to 124.9) in the early conservative group (Table 2). The most common cause of cardiogenic shock in both arms was ST-segment elevation acute myocardial infarction followed by decompensation of chronic heart failure (Table 2). Use of therapeutic interventions, including percutaneous coronary intervention and cardiac surgery, did not differ between study groups (Table S1). Although previous cardiac surgery was not an exclusion criterion, finally only primarily non-surgical patients were enrolled in the trial, although some of them subsequently required cardiac surgery during hospitalization.

End points

The composite primary endpoint occurred in 37 (63.8%) patients in the immediate VA-ECMO group and 42 (71.2 %) in the early conservative group (Table 3). The Kaplan–Meier probability estimate at 30 days was 68.9% in the immediate VA-ECMO group and 71.8% in the early conservative group (HR, 0.72; 95% confidence intervals [CI], 0.46 to 1.12; P=0.21) (Figure 1).

All-cause mortality at 30 days was comparable between the two groups (50.0% versus [vs.] 47.5%; HR, 1.110; 95% CI, 0.660 to 1.866) (Table 3, Figure 2). In the immediate VA-ECMO group, fewer patients required another MCS device (17.2% vs. 42.4%, respectively; HR, 0.380; 95% CI, 0.182 to 0.793). Resuscitated cardiac arrest occurred in 10.3% of the immediate VA-ECMO group and 13.6% of the early conservative group (HR, 0.790; 95% CI, 0.274 to 2.277 (Table 3). Similarly, the incidence of death from any cause or resuscitated cardiac arrest, death from any cause, resuscitated cardiac arrest, implementation of another MCS device or serious adverse events were comparable between treatment arms (Table 3).

The results remained similar after adjustment for smoking status with the respect to composite primary endpoint (HR, 0.681; 95 CI, 0.426 to 1.088) and death from any cause (HR, 0.916; 95% CI, 0.528 to 1.590).

In the early conservative group, 23 (39%) patients required downstream VA-ECMO support, of whom 12 (52.2%) died. Of the 36 patients in the early conservative group who did not subsequently receive VA-ECMO 16 (44.4%) died. The mean time from randomization to insertion of VA-ECMO in the early conservative arm was 1.9 days. In the subgroup of 81 patients treated with VA-ECMO in the immediate VA-ECMO arm (58 subjects) or the early conservative arm (23 subjects), 41 (50.6%) patients died, as compared with 16 patients (44.4%) in the early conservative group who did not subsequently receive VA-ECMO ("as-treated" comparison; HR, 1.254; 95% CI, 0.703 to 2.238). Beside the 23 patients with VA-ECMO implementation in the early conservative arm, one patient received long-term MCS (HeartMate, Abbott) and three patients required an Impella (Abiomed, US). In the early VA-ECMO arm two patients received short-term surgical mechanical support (Centrimag, Abbott, US), three patients underwent long-term mechanical support implantation (HeartMate, Abbott, US) and two patients required an Impella (Abiomed, US).

At 30 days, 13 patients in each group remained hospitalized and 7 in each group were discharged home; 9 subjects in the early VA-ECMO group and 11 patients in the early conservative group were transferred to long-term care or rehabilitation (Table S2). Neurological status at 30 days was comparable between the groups (Table S2, Figure S2).

Type and etiology of cardiogenic shock

A total of 45 patients fulfilled the criteria for rapidly deteriorating cardiogenic shock (corresponding to SCAI stage D-E) and 72 experienced severe cardiogenic shock (corresponding to SCAI stage D). The incidence of primary composite end point was 72.2% in those with severe cardiogenic shock and 60.0% in those with rapidly deteriorating

cardiogenic shock (Figure S3); similar results were also observed for all-cause mortality (54.2% vs. 40.0%, respectively) (Figure S4). The incidence of primary end point and all-cause death was comparable between the immediate VA-ECMO and the early conservative therapy groups in both cardiogenic shock types (Figure 3, Table S3).

In the subgroup of 74 patients with cardiogenic shock caused by acute myocardial infarction, the incidence of the primary endpoint and all-cause death was comparable between the immediate VA-ECMO and the early conservative groups (Table S4). Similar results were observed also in the subgroup of 43 subjects with cardiogenic shock of non-myocardial infarction etiology (Table S4).

Safety

Serious adverse events occurred in 35 (60.3%) patients in the immediate VA-ECMO group and 36 (61.0%) in the early conservative group (RD, -0.7; 95% CI, -18.4 to 17.0). The incidence of sepsis and pneumonia were comparable between the two groups; stroke, leg ischemia, and bleeding were numerically higher in the VA-ECMO group (Table 4). Similarly, the incidence of serious adverse events was comparable between the subgroup of 81 patients treated with immediate VA-ECMO in any of the arms and the subgroup of 36 patients in the early conservative arm without downstream VA-ECMO use ("as-treated" analysis) (Table S5).

Discussion

Among patients with rapidly progressing or severe cardiogenic shock, immediate implementation of VA-ECMO did not improve 30 days clinical outcomes. Immediate VA-ECMO therapy was not associated with an increased incidence of adverse events and a substantial proportion of patients in the early conservative therapy group required VA-ECMO later during their hospital stay.

Despite recent advances in diagnostic tools and therapeutic interventions, cardiogenic shock continues to have high mortality. Cardiogenic shock is a clinical syndrome with various etiologies, phenotypes, and presentations [1, 14]. The definitions of cardiogenic shock vary widely based on the presence of hypotension and hypoperfusion, whereas more accurate hemodynamic criteria, confirmation of structural heart disease, or evidence for sufficient heart filling are frequently not required for diagnosis [2, 3, 5, 15]. The severity of cardiogenic shock was recently classified in a statement from the Society for Cardiovascular Angiography and Interventions (SCAI) and endorsed by other major cardiovascular societies [1]. The aim of our study was to compare immediate VA-ECMO with an early conservative therapy in patients with rapidly deteriorating or severe cardiogenic shock, defined according to hemodynamic criteria, evidence of structural heart disease, and parameters of tissue hypoperfusion that best correspond to stage D-E of the SCAI classification. Therefore, the ECMO-CS trial population matches well with the conditions in which mechanical circulatory support may—or should be—considered according to the current guidelines or scientific statements [5-8]. Based on the study protocol, for ethical reasons, VA-ECMO could be used in the early conservative group later in case of clearly defined further hemodynamic worsening, which was also considered a clinically relevant end point. VA-ECMO was used for this indication in a substantial proportion of patients.

Although the incidence of the composite primary end point in our study was higher than anticipated, we failed to demonstrate that immediate implementation of VA-ECMO in severe or rapidly deteriorating cardiogenic shock improved outcomes compared with an early conservative approach. This observation is, in part, in good agreement with the first, small randomized trial reporting equal outcomes with VA-ECMO compared with medical therapy [9, 10]. However, our study compared immediate VA-ECMO implementation with an early conservative therapy and allowed downstream use of VA-ECMO in the early conservative

group. The allowance of VA-ECMO insertion in the early conservative arm in case of further hemodynamic worsening on inotropes and vasopressors makes interpretation of the results more difficult. However, there are ethical reasons to allow MCS if pharmacological stabilization fails, which is a frequent clinical scenario.

Currently, there is no evidence from randomized controlled trials, supporting the use of mechanical circulatory support in cardiogenic shock. The large IABP-Shock II trial (Intra-Aortic Balloon Pump in Cardiogenic Shock II) randomized 600 patients with acute myocardial infarction complicated with cardiogenic shock to routine intra-aortic balloon pump use or conservative care [2]. The use of balloon pump was not associated with a reduction in 30-day all-cause mortality (39.7% versus. 41.3%; P=0.69) [2] and based on these results routine use of balloon pumps is not recommended [5-8]. More evidence for the use of mechanical circulatory support in cardiogenic shock may be derived from the results of the four large ongoing randomized clinical trials (EURO-SHOCK, ANCHOR, ECLS-SHOCK, DanGer Shock) [8, 12, 16, 17]. All these trials are focused on cardiogenic shock caused by acute myocardial infarction. The ECLS-SHOCK and EURO-SHOCK trials compare VA-ECMO and conservative therapy, the ANCHOR trial compares VA-ECMO plus intra-aortic balloon pump and conservative therapy, and DanGer Shock trial compares Impella and conservative therapy. In contrast to our study, VA-ECMO (or Impella) use is not recommended in the conservative arms in these trials [9, 11, 16, 17].

The incidence of adverse events in our study was similar in the early VA-ECMO and early conservative therapy groups. This observation contradicts several other studies reporting a higher occurrence of complication(s) with VA-ECMO in patients with cardiogenic shock [18-21]. However, safety outcomes in the present study could also be influenced by the fact that a substantial proportion of the early conservative group also received VA-ECMO or another MCS device later and the interpretation is difficult due to limited sample size.

Our trial has limitations. First, all patients who participated were white, given that the trial recruited participants exclusively in the Czech Republic, which may limit the generalizability of our results to other racial or ethnic groups. There also was no upper age limit for enrollment but exclusion criteria included life expectancy less than one year. Second, the trial was designed and the sample size was calculated to find a difference in a composite primary outcome. Therefore, all other results must be considered hypothesis generating. The small sample size also precluded subgroup analyses. The sample size was calculated based on the assumption of 54% incidence of the primary end point in the conservative group (assuming 40% mortality [2], 20% incidence of the implantation of another mechanical circulatory of whom 60% would survive, and 2% incidence of successfully resuscitated cardiac arrest without MCS in the conservative group) and 50% reduction of primary endpoint in the VA-ECMO group. We acknowledge that a presumed reduction in the primary endpoint of 50% may be excessive, but considering the meta-analysis reporting a 33% reduction in 30-day mortality with ECMO vs. balloon pump [22] and a lower need for other mechanical support in the early VA-ECMO group we believe it was justified; however, it precludes adequate evaluation of clinically important benefits from early VA-ECMO below this threshold. Thus, larger studies are needed to evaluate smaller, but clinically relevant, degrees of risk reduction with VA-ECMO in patients with cardiogenic shock. Third, as mentioned above, the trial did not compare VA-ECMO with conservative therapy but immediate VA-ECMO with early conservative strategy permitting "bailout" VA-ECMO therapy in case of hemodynamic worsening. The results should, therefore, be interpreted accordingly. Furthermore, the definition of shock progression allowing VA-ECMO placement in the early conservative arm is not perfect. It was based on the rise of lactate that cannot cover all characteristics of the extremely complex hemodynamic situation and is also influenced by lactate clearance. Also, strategies for venting of the possibly overloaded left ventricle by increased afterload caused

by VA-ECMO were not specified in the protocol and these interventions, if needed, were performed at the discretion of the attending physicians and according to local practice at the individual participating centers. Inadequate use of left ventricular unloading might impair the outcomes in the immediate VA-ECMO arm. However, intra-aortic balloon pump was used in 6 patients in the immediate VA-ECMO arm already at randomization and another 7 patients received a percutaneous or surgical left-ventricular assist device later; therefore, a substantial proportion of VA-ECMO-treated patients underwent unloading. Fourth, the trial was unblinded and the end points were not adjudicated. Finally, inclusion criteria for the study were based on shock severity defined by intensity of vasoactive therapy, hemodynamic or metabolic parameters and the evidence of cardiac pump failure, not on the specific etiologies. Exclusion criteria included several specific conditions that may cause or influence cardiogenic shock, including high suspicion of pulmonary embolism, cardiac tamponade, bradycardia, tachycardia, aortic regurgitation, or hypertrophic obstructive cardiomyopathy. Moreover, cardiac arrest survivors remaining comatose were also excluded. Therefore, our results cannot be generalized to all etiologies of shock and to all concomitant conditions and should be interpreted in the context of the inclusion criteria.

In conclusion, immediate implementation of VA-ECMO in patients with rapidly deteriorating or severe cardiogenic shock (corresponding to SCAI stage D-E) was feasible but did not improve clinical outcomes compared with an early conservative approach permitting downstream use of VA-ECMO in cases of hemodynamic worsening.

Acknowledgments

None.

Sources of Funding

The study was supported by a grant from the Czech health research council No. 15-27994A.

Disclosures

Dr. Ostadal received speaker's honoraria from Getinge, Edwards, Xenios. Dr. Belohlavek received speaker's honoraria from Getinge. No other authors reported disclosures.

Supplemental Materials

List of investigators

Inclusion and exclusion criteria

Tables S1-S5

Figures S1-S4

Study protocol

References

1. Naidu SS, Baran DA, Jentzer JC, Hollenberg SM, van Diepen S, Basir MB, Grines CL, Diercks DB, Hall S, Kapur NK, Kent W, Rao SV, Samsky MD, Thiele H, Truesdell AG and Henry TD. SCAI SHOCK Stage Classification Expert Consensus Update: A Review and Incorporation of Validation Studies: This statement was endorsed by the American College of Cardiology (ACC), American College of Emergency Physicians (ACEP), American Heart Association (AHA), European Society of Cardiology (ESC) Association for Acute Cardiovascular Care (ACVC), International Society for Heart and Lung Transplantation (ISHLT), Society of Critical Care Medicine (SCCM), and Society of Thoracic Surgeons (STS) in December 2021. *Journal of the American College of Cardiology*. 2022;79:933-946.
2. Thiele H, Zeymer U, Neumann FJ, Ferenc M, Olbrich HG, Hausleiter J, Richardt G, Hennersdorf M, Empen K, Fuernau G, Desch S, Eitel I, Hambrecht R, Fuhrmann J, Bohm M, Ebelt H, Schneider S, Schuler G and Werdan K. Intraaortic balloon support for myocardial infarction with cardiogenic shock. *N Engl J Med*. 2012;367:1287-96.
3. Thiele H, Akin I, Sandri M, Fuernau G, de Waha S, Meyer-Saraei R, Nordbeck P, Geisler T, Landmesser U, Skurk C, Fach A, Lapp H, Piek JJ, Noc M, Goslar T, Felix SB, Maier LS, Stepinska J, Oldroyd K, Serpytis P, Montalescot G, Barthelemy O, Huber K, Windecker S, Savonitto S, Torremante P, Vrints C, Schneider S, Desch S, Zeymer U and Investigators C-S. PCI Strategies in Patients with Acute Myocardial Infarction and Cardiogenic Shock. *N Engl J Med*. 2017;377:2419-2432.
4. Rob D and Belohlavek J. The mechanical support of cardiogenic shock. *Curr Opin Crit Care*. 2021;27:440-446.
5. McDonagh TA, Metra M, Adamo M, Gardner RS, Baumbach A, Bohm M, Burri H, Butler J, Celutkiene J, Chioncel O, Cleland JGF, Coats AJS, Crespo-Leiro MG, Farmakis D, Gilard M, Heymans S, Hoes AW, Jaarsma T, Jankowska EA, Lainscak M, Lam CSP, Lyon AR, McMurray JJV, Mebazaa A, Mindham R, Muneretto C, Francesco Piepoli M, Price S, Rosano GMC, Ruschitzka F, Kathrine Skibelund A and Group ESCSD. 2021 ESC Guidelines for the diagnosis and treatment of acute and chronic heart failure. *Eur Heart J*. 2021;42:3599-3726.
6. Zeymer U, Bueno H, Granger CB, Hochman J, Huber K, Lettino M, Price S, Schiele F, Tubaro M, Vranckx P, Zahger D and Thiele H. Acute Cardiovascular Care Association position statement for the diagnosis and treatment of patients with acute myocardial infarction complicated by cardiogenic shock: A document of the Acute Cardiovascular Care Association of the European Society of Cardiology. *Eur Heart J Acute Cardiovasc Care*. 2020;9:183-197.
7. Geller BJ, Sinha SS, Kapur NK, Bakitas M, Balsam LB, Chikwe J, Klein DG, Kochar A, Masri SC, Sims DB, Wong GC, Katz JN, van Diepen S, American Heart Association Acute Cardiac C, General Cardiology Committee of the Council on Clinical C, Council on Cardiopulmonary CCP, Resuscitation, Council on Cardiovascular R, Intervention, Council on C, Stroke N, Council on Peripheral Vascular D, Council on Cardiovascular S and Anesthesia. Escalating and De-escalating Temporary Mechanical Circulatory Support in Cardiogenic Shock: A Scientific Statement From the American Heart Association. *Circulation*. 2022;146:e50-e68.
8. Henry TD, Tomey MI, Tamis-Holland JE, Thiele H, Rao SV, Menon V, Klein DG, Naka Y, Pina IL, Kapur NK, Dangas GD, American Heart Association Interventional Cardiovascular Care Committee of the Council on Clinical C, Council on Arteriosclerosis T, Vascular B, Council on C and Stroke N. Invasive Management of Acute Myocardial Infarction Complicated by Cardiogenic Shock: A Scientific Statement From the American Heart Association. *Circulation*. 2021;143:e815-e829.

9. Brunner S, Guenther SPW, Lackermair K, Peterss S, Orban M, Boulesteix AL, Michel S, Hausleiter J, Massberg S and Hagl C. Extracorporeal Life Support in Cardiogenic Shock Complicating Acute Myocardial Infarction. *Journal of the American College of Cardiology*. 2019;73:2355-2357.
10. Lackermair K, Brunner S, Orban M, Peterss S, Orban M, Theiss HD, Huber BC, Juchem G, Born F, Boulesteix AL, Bauer A, Pichlmaier M, Hausleiter J, Massberg S, Hagl C and Guenther SPW. Outcome of patients treated with extracorporeal life support in cardiogenic shock complicating acute myocardial infarction: 1-year result from the ECLS-Shock study. *Clin Res Cardiol*. 2021;110:1412-1420.
11. Thiele H, Freund A, Gimenez MR, de Waha-Thiele S, Akin I, Poss J, Feistritzer HJ, Fuernau G, Graf T, Nef H, Hamm C, Bohm M, Lauten A, Schulze PC, Voigt I, Nordbeck P, Felix SB, Abel P, Baldus S, Laufs U, Lenk K, Landmesser U, Skurk C, Pieske B, Tschope C, Hennersdorf M, Wengenmayer T, Preusch M, Maier LS, Jung C, Kelm M, Clemmensen P, Westermann D, Seidler T, Schieffer B, Rassaf T, Mahabadi AA, Vasa-Nicotera M, Meincke F, Seyfarth M, Kersten A, Rottbauer W, Boekstegers P, Muellenbach R, Dengler T, Kadel C, Schempf B, Karagiannidis C, Hopf HB, Lehmann R, Bufe A, Baumanns S, Oner A, Linke A, Sedding D, Ferrari M, Bruch L, Goldmann B, John S, Mollmann H, Franz J, Lapp H, Lauten P, Noc M, Goslar T, Oerlecke I, Ouarrak T, Schneider S, Desch S, Zeymer U and Investigators E-S. Extracorporeal life support in patients with acute myocardial infarction complicated by cardiogenic shock - Design and rationale of the ECLS-SHOCK trial. *American heart journal*. 2021;234:1-11.
12. Tsangaris A, Alexy T, Kalra R, Kosmopoulos M, Elliott A, Bartos JA and Yannopoulos D. Overview of Veno-Arterial Extracorporeal Membrane Oxygenation (VA-ECMO) Support for the Management of Cardiogenic Shock. *Front Cardiovasc Med*. 2021;8:686558.
13. Ostadal P, Rokyta R, Kruger A, Vondrakova D, Janotka M, Smid O, Smalcova J, Hromadka M, Linhart A and Belohlavek J. Extra corporeal membrane oxygenation in the therapy of cardiogenic shock (ECMO-CS): rationale and design of the multicenter randomized trial. *European journal of heart failure*. 2017;19 Suppl 2:124-127.
14. Berg DD, Bohula EA and Morrow DA. Epidemiology and causes of cardiogenic shock. *Curr Opin Crit Care*. 2021;27:401-408.
15. Hochman JS, Sleeper LA, Webb JG, Sanborn TA, White HD, Talley JD, Buller CE, Jacobs AK, Slater JN, Col J, McKinlay SM and LeJemtel TH. Early revascularization in acute myocardial infarction complicated by cardiogenic shock. SHOCK Investigators. Should We Emergently Revascularize Occluded Coronaries for Cardiogenic Shock. *N Engl J Med*. 1999;341:625-34.
16. Udesen NJ, Moller JE, Lindholm MG, Eiskjaer H, Schafer A, Werner N, Holmvang L, Terkelsen CJ, Jensen LO, Junker A, Schmidt H, Wachtell K, Thiele H, Engstrom T, Hassager C and DanGer Shock i. Rationale and design of DanGer shock: Danish-German cardiogenic shock trial. *American heart journal*. 2019;214:60-68.
17. Banning AS, Adriaenssens T, Berry C, Bogaerts K, Erglis A, Distelmaier K, Guagliumi G, Haine S, Kastrati A, Massberg S, Orban M, Myrmel T, Vuylsteke A, Alfonso F, Van de Werf F, Verheugt F, Flather M, Sabate M, Vrints C, Gershlick AH and Collaborators. Veno-arterial extracorporeal membrane oxygenation (ECMO) in patients with cardiogenic shock: rationale and design of the randomised, multicentre, open-label EURO SHOCK trial. *EuroIntervention*. 2021;16:e1227-e1236.
18. Thiagarajan RR, Barbaro RP, Rycus PT, McMullan DM, Conrad SA, Fortenberry JD, Paden ML and centers Em. Extracorporeal Life Support Organization Registry International Report 2016. *ASAIO J*. 2017;63:60-67.

19. Sy E, Sklar MC, Lequier L, Fan E and Kanji HD. Anticoagulation practices and the prevalence of major bleeding, thromboembolic events, and mortality in venoarterial extracorporeal membrane oxygenation: A systematic review and meta-analysis. *Journal of critical care*. 2017;39:87-96.
20. Nasr DM and Rabinstein AA. Neurologic Complications of Extracorporeal Membrane Oxygenation. *J Clin Neurol*. 2015;11:383-9.
21. Freund A, Jobs A, Lurz P, Feistritzer HJ, de Waha-Thiele S, Meyer-Saraei R, Montalescot G, Huber K, Noc M, Windecker S, Zeymer U, Ouarrak T, Schneider S, Thiele H and Desch S. Frequency and Impact of Bleeding on Outcome in Patients With Cardiogenic Shock. *JACC Cardiovasc Interv*. 2020;13:1182-1193.
22. Ouweneel DM, Schotborgh JV, Limpens J, Sjauw KD, Engstrom AE, Lagrand WK, Cherpanath TGV, Driessen AHG, de Mol B and Henriques JPS. Extracorporeal life support during cardiac arrest and cardiogenic shock: a systematic review and meta-analysis. *Intensive care medicine*. 2016;42:1922-1934.

Table 1. Inclusion criteria

Patients must fulfil criteria for **rapidly deteriorating** or **severe** cardiogenic shock:			
Rapidly deteriorating cardiogenic shock (best corresponds to **SCAI stage D-E**)			
	Defined as progressive hemodynamic instability necessitating repeated bolus administration of vasopressors to maintain mean arterial pressure > 50 mmHg + impaired left ventricle systolic function (Left ventricle ejection fraction (LVEF) < 35% or LVEF 35-55% in case of severe mitral regurgitation or aortic stenosis)		
Severe cardiogenic shock (best corresponds to **SCAI stage D**)			
	All following criteria should be met:		
	1. Hemodynamic:		
		Cardiac Index (CI) < 2.2 L/min/m2 + norepinephrine dose > 0.1 µg/kg/min + dobutamine dose > 5 µg/kg/min	
	or		
		Systolic blood pressure < 100 mmHg + norepinephrine dose > 0.2 µg/kg/min + dobutamine dose > 5 µg/kg/min + (LVEF < 35% or LVEF 35-55% + severe mitral regurgitation or aortic stenosis)	
	2. Metabolic:		
		Lactate – two consecutive values ≥ 3 mmol/L (with at least 30 min between samples), with non-decreasing trend on steady doses of inotropes and/or vasopressors	
	or		
		SvO_2 – two consecutive values < 50% (with at least 30 min between measurements), with non-increasing trend on steady doses of inotropes and/or vasopressors	
	3. Hypovolemia must be excluded:		
		Central venous pressure > 7 mmHg or pulmonary capillary wedge pressure > 12 mmHg	

10.1161/CIRCULATIONAHA.122.062949

Table 2. Baseline characteristics

Characteristic	All	VA-ECMO	Conservative	P-value
	N = 117	N = 58	N = 59	
Sex - no. (%)				
Male	86 (73.5 %)	43 (74.1 %)	43 (72.9 %)	0.878
Female	31 (26.5 %)	15 (25.9 %)	16 (27.1 %)	
Age - years (IQR)	66 (59; 73)	67 (60; 74)	65 (58; 71)	0.356
Medical history - no. (%)				
Chronic coronary syndrome	39 (34.2 %)	21 (37.5 %)	18 (31.0 %)	0.467
Chronic heart failure	27 (23.7 %)	14 (25.0 %)	13 (22.4 %)	0.745
Dilated cardiomyopathy	15 (13.3 %)	6 (10.9 %)	9 (15.5 %)	0.471
Chronic renal failure	16 (14.2 %)	7 (12.5 %)	9 (15.8 %)	0.616
Periphery artery disease	10 (8.8 %)	3 (5.5 %)	7 (11.9 %)	0.324
Hypertension	73 (64.0 %)	35 (62.5 %)	38 (65.5 %)	0.737
Diabetes	37 (32.5 %)	16 (28.6 %)	21 (36.2 %)	0.384
Current smoker	41 (36.9 %)	14 (25.9 %)	27 (47.4 %)	0.019
Clinical parameters at randomization - median (IQR)				
Blood lactate (mmol/L)	5.0 (3.2; 8.0)	5.3 (3.1; 8.4)	4.7 (3.3; 7.4)	0.960
Systolic blood pressure (mmHg)	85.0 (80.0; 100.0)	84.0 (80.0; 95.0)	89.0 (79.5; 105.0)	0.282
Mean arterial pressure (mmHg)	63.3 (55.3; 72.0)	63.3 (56.7; 68.7)	64.5 (54.3; 75.3)	0.289
Heart rate (beats/min)	102.0 (84.0; 120.0)	110.0 (86.5; 130.0)	100.0 (82.0; 110.0)	0.076
Therapy at randomization - no. (%)				
Intra-aortic balloon pump	15 (13.3 %)	6 (10.9 %)	9 (15.5 %)	0.471
Mechanical ventilation	81 (72.3 %)	41 (74.5 %)	40 (70.2 %)	0.605
Renal replacement therapy	7 (6.2 %)	4 (7.3 %)	3 (5.2 %)	0.712
Norepinephrine	100 (85.5 %)	50 (86.2 %)	50 (84.7 %)	
Norepinephrine dose [µg/kg/min]	0.50 (0.23; 1.24)	0.48 (0.23; 1.36)	0.50 (0.27; 1.19)	0.741
Epinephrine	4 (3.4 %)	1 (1.7 %)	3 (5.1 %)	

Epinephrine dose [µg/kg/min]	0.26 (0.14; 0.80)	0.21 (0.21; 0.21)	0.30 (0.07; 1.30)	0.999
Dobutamine	64 (54.7 %)	31 (53.4 %)	33 (55.9 %)	
Dobutamine dose [µg/kg/min]	5.1 (4.9; 8.0)	6.1 (5.0; 9.7)	5.1 (4.7; 7.6)	0.492
Milrinone	38 (32.5 %)	22 (37.9 %)	16 (27.1 %)	
Milrinone dose [µg/kg/min]	0.40 (0.30; 0.50)	0.40 (0.30; 0.50)	0.40 (0.37; 0.51)	0.389
Vasopressin	41 (35.0 %)	19 (32.8 %)	22 (37.3 %)	
Vasopressin dose [U/kg/min]	0.0017 (0.0010; 0.0025)	0.0020 (0.0010; 0.0030)	0.0017 (0.0012; 0.0022)	0.824
Levosimendan	32 (29.4 %)	20 (37.0 %)	12 (21.8 %)	0.081
Vasoactive-inotropic score - median (IQR)	61.0 (30.0; 124.0)	59.9 (32.8; 121.5)	61.0 (28.0; 124.9)	0.976
Cause of cardiogenic shock				
ST-elevation myocardial infarction	59 (50.4 %)	30 (51.7 %)	29 (49.2 %)	0.854
Non-ST-elevation myocardial infarction	14 (12.0 %)	7 (12.1 %)	7 (11.9 %)	0.999
Decompensation of chronic heart failure	27 (23.1 %)	14 (24.1 %)	13 (22.0 %)	0.829
Mechanical complications of myocardial infarction	3 (2.6 %)	1 (1.7 %)	2 (3.4 %)	0.999
Other	14 (12.0 %)	6 (10.3 %)	8 (13.6 %)	0.777

Other causes of cardiogenic shock include myocarditis, aortic stenosis and mitral regurgitation. IQR, interquartile range

10.1161/CIRCULATIONAHA.122.062949

Table 3. Incidence of the composite primary end point, individual components of the composite primary end point and secondary composite outcomes

End point - no. (%)	VA-ECMO	Conservative	Risk difference (95% CI)	Hazard ratio (95% CI)
	N = 58	**N = 59**		
Composite primary outcome - composite of death from any cause, implantation of another mechanical circulatory support, resuscitated cardiac arrest	37 (63.8 %)	42 (71.2 %)	-7.4 (-24.3 to 9.5)	0.721 (0.463; 1.123)
Death	29 (50.0 %)	28 (47.5 %)	2.5 (-15.6 to 20.7)	1.110 (0.660; 1.866)
Another mechanical circulatory support	10 (17.2 %)	25 (42.4 %)	-25.1 (-41.1 to -9.2)	0.380 (0.182; 0.793)
Resuscitated cardiac arrest	6 (10.3 %)	8 (13.6 %)	-3.2 (-15.0 to 8.5)	0.790 (0.274; 2.277)
Composite of death from any cause or resuscitated cardiac arrest	31 (53.4 %)	32 (54.2 %)	-0.8 (-18.9; 17.3)	1.037 (0.633; 1.700)
Composite of death from any cause, implantation of another mechanical circulatory support, resuscitated cardiac arrest and serious adverse event	51 (87.9 %)	50 (84.7 %)	3.2 (-9.2; 15.6)	
CI, confidence interval				

Table 4. Adverse events

Adverse event - no. (%)	VA-ECMO	Conservative	Risk difference (95% CI)	P-value
	N = 58	**N = 59**		
Serious adverse events	**35 (60.3 %)**	**36 (61.0 %)**	**-0.7 (-18.4 to 17.0)**	**0.941**
Bleeding	18 (31.0 %)	12 (20.3 %)	10.7 (-5.0 to 26.4)	0.185
Leg ischemia	8 (13.8 %)	3 (5.1 %)	8.7 (-1.8 to 19.2)	0.107
Stroke	3 (5.2 %)	0 (0.0 %)	5.2 (-0.5 to 10.9)	0.119
Pneumonia	18 (31.0 %)	18 (30.5 %)	0.5 (-16.2 to 17.3)	0.951
Sepsis	23 (39.7 %)	23 (39.0 %)	0.7 (-17.0 to 18.4)	0.941
Technical complications	1 (1.7 %)	0 (0.0 %)	1.7 (-1.6 to 5.1)	0.496
Bleeding, leg ischemia, stroke	22 (37.9%)	14 (23.7%)	14.2 (-2.3; 30.7)	0.096
Number of adverse events				
0	23 (39.7%)	23 (39.0%)		0.179
1	9 (15.5%)	11 (18.6%)		
2	11 (19.0%)	19 (32.2%)		
3	6 (10.3%)	4 (6.8%)		
≥4	8 (13.8%)	2 (3.4%)		

Figure Legends

Figure 1. Cumulative incidence of the composite primary end point.

Figure 2. Cumulative incidence of all-cause death.

Figure 3. Cumulative incidence of primary composite end point and all-cause death according to the type of cardiogenic shock and treatment arms. VA-ECMO, early VA-ECMO arm; CONS, early conservative arm. Rapidly deteriorating CS, rapidly deteriorating cardiogenic shock (corresponds to the SCAI stage D-E); Severe CS, severe cardiogenic shock (corresponds to the SCAI stage D).

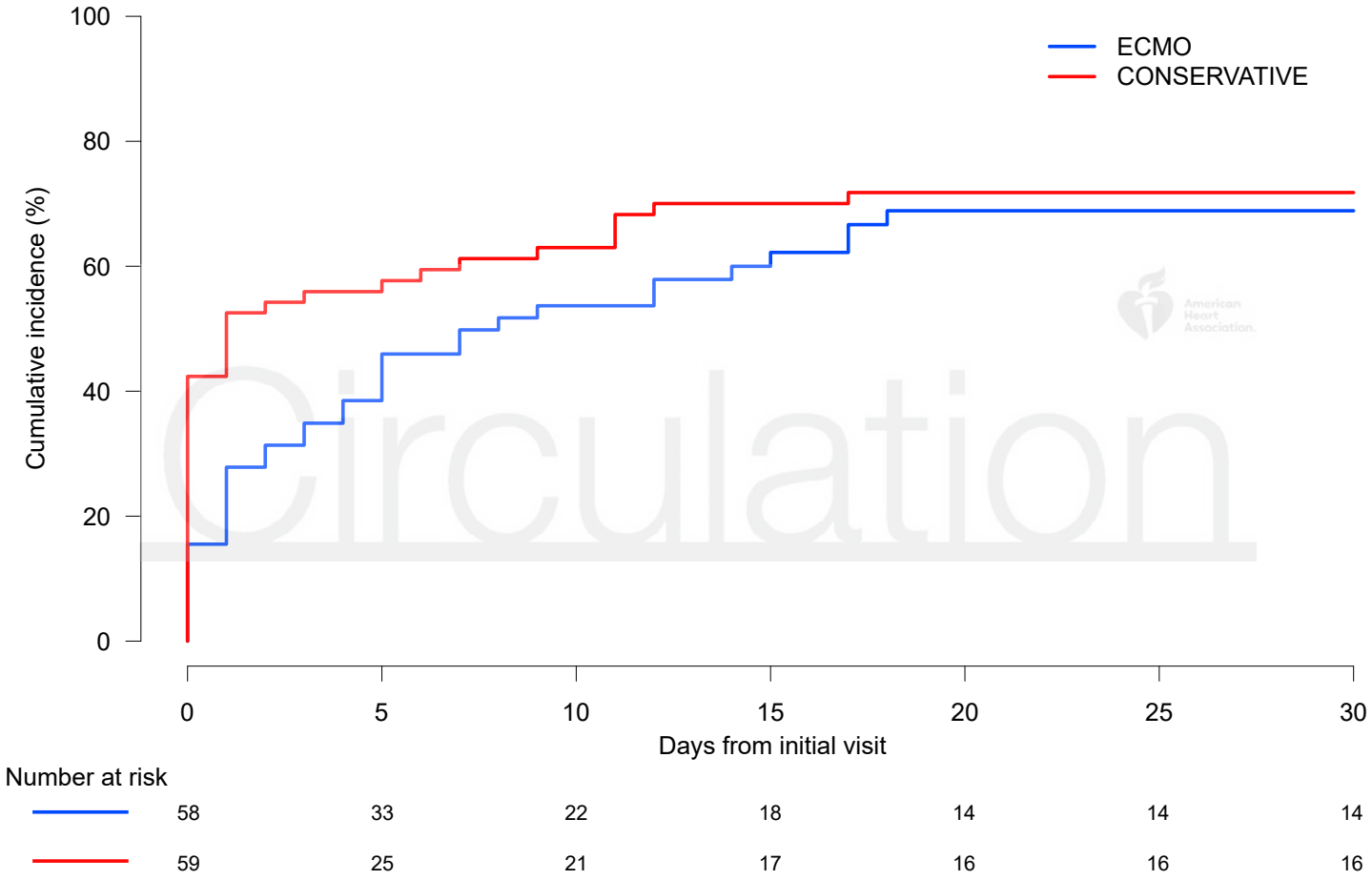

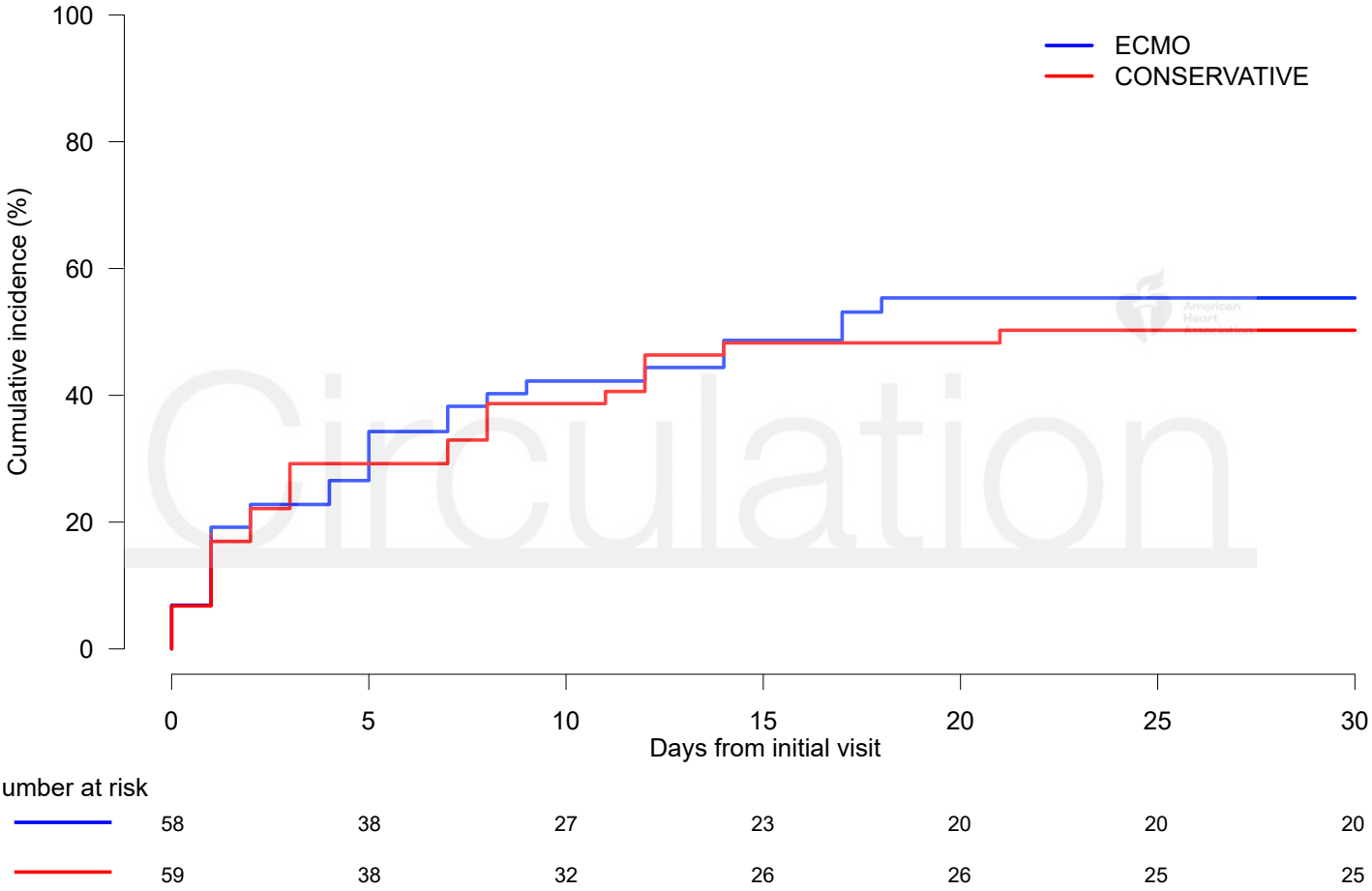

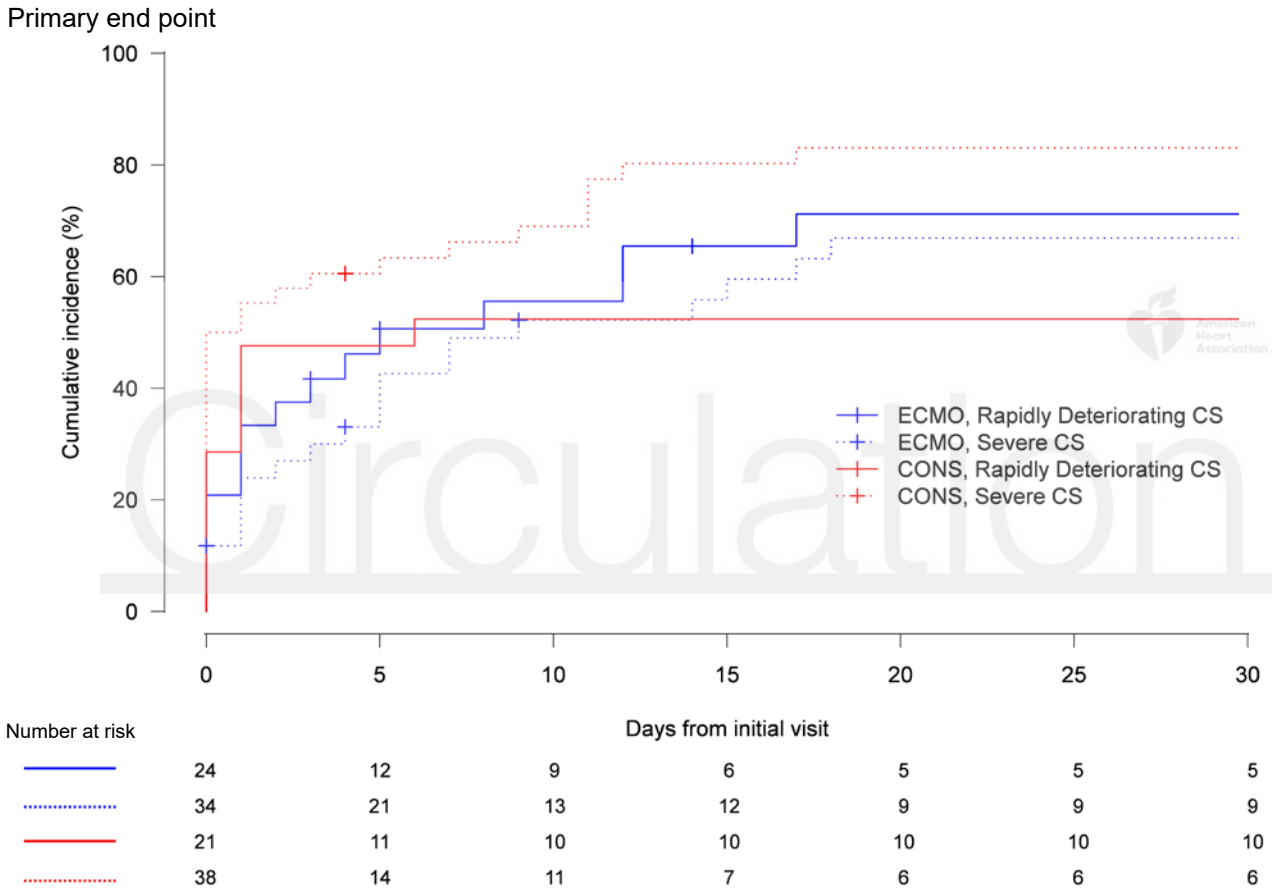

Death from any cause

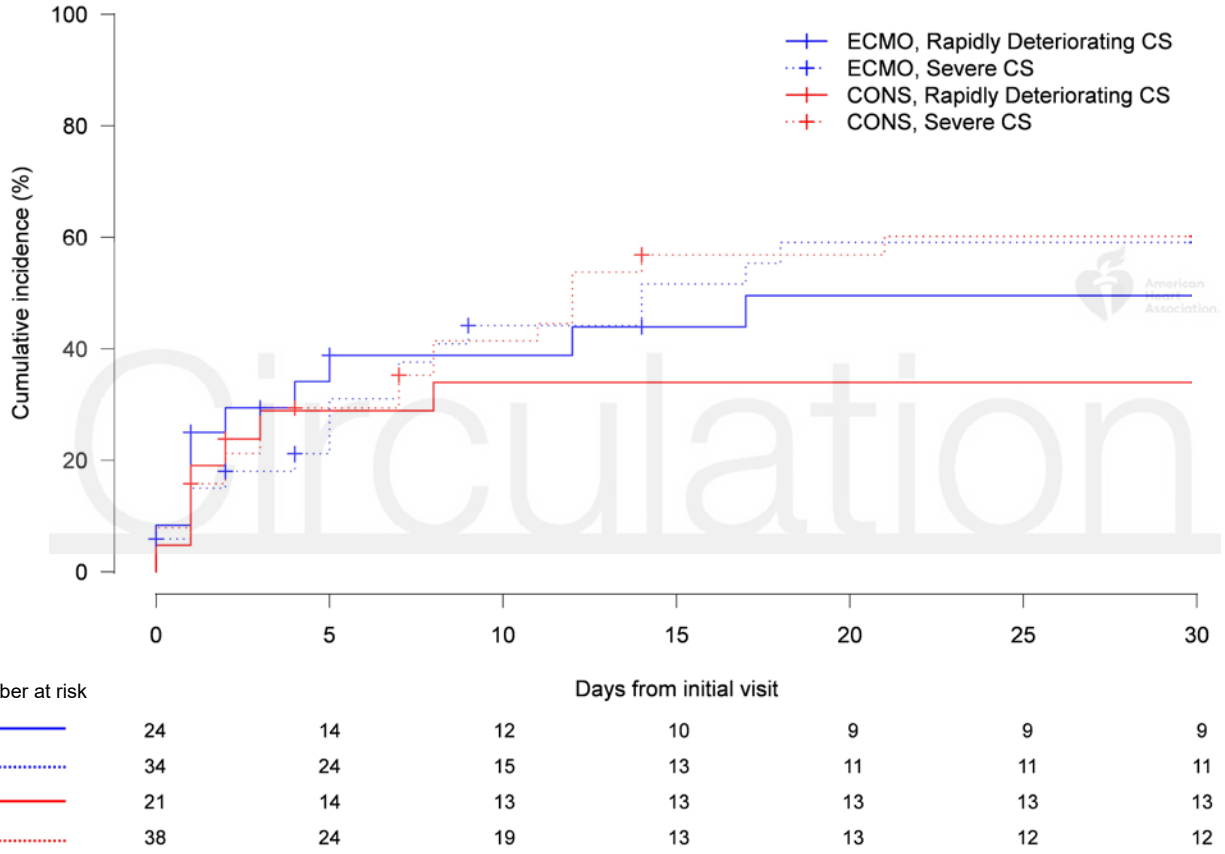

Number at risk

ECMO, Rapidly Deteriorating CS	24	14	12	10	9	9	9
ECMO, Severe CS	34	24	15	13	11	11	11
CONS, Rapidly Deteriorating CS	21	14	13	13	13	13	13
CONS, Severe CS	38	24	19	13	13	12	12

J. Veselka et al.

Outcomes of patients with hypertrophic obstructive cardiomyopathy and pacemaker implanted after alcohol septal ablation

JACC Cardiovasc Intv
Impact Factor: 11.075

JACC: CARDIOVASCULAR INTERVENTIONS VOL. ■, NO. ■, 2022

PUBLISHED BY ELSEVIER

Outcomes of Patients With Hypertrophic Obstructive Cardiomyopathy and Pacemaker Implanted After Alcohol Septal Ablation

Josef Veselka, MD, PhD,[a] Max Liebregts, MD, PhD,[b] Robert Cooper, MBChB, MRCP,[c] Lothar Faber, MD, PhD,[d] Jaroslav Januska, MD,[e] Maksim Kashtanov, MD, PhD,[f] Klara Hulikova Tesarkova, RNDr, PhD,[g] Peter Riis Hansen, MD, DMSc, PhD,[h] Hubert Seggewiss, MD,[i] Eugene Shloydo, MD, PhD,[j] Kirill Popov, MD,[j] Eva Hansvenclova,[a] Jiri Bonaventura, MD, PhD,[a] Jurriën ten Berg, MD, PhD,[b] Rodney Hilton Stables, MA, MD, BM BCH, FRCP,[c] Eva Polakova, MD[a]

ABSTRACT

BACKGROUND Atrioventricular block is a frequent major complication after alcohol septal ablation (ASA).

OBJECTIVES The aim of this study was to evaluate the outcomes of patients with implanted permanent pacemaker (PPM) related to a high-grade atrioventricular block after ASA for hypertrophic obstructive cardiomyopathy.

METHODS We used a multinational registry (the Euro-ASA registry) to evaluate the outcome of patients with PPM after ASA.

RESULTS A total of 1,814 patients were enrolled and followed up for 5.0 ± 4.3 years (median = 4.0 years). A total of 170 (9.4%) patients underwent PPM implantation during the first 30 days after ASA. Using propensity score matching, 139 pairs (278 patients) constituted the matched PPM and non-PPM groups. Between the matched groups, there were no long-term differences in New York Heart Association functional class (1.5 ± 0.7 vs 1.5 ± 0.9, $P = 0.99$) and survival (log-rank $P = 0.47$). Patients in the matched PPM group had lower long-term left ventricular (LV) outflow gradient (12 ± 12 mm Hg vs 17 ± 19 mm Hg, $P < 0.01$), more pronounced LV outflow gradient decrease (81% ± 17% vs 72% ± 35%, $P < 0.01$), and lower LV ejection fraction (64% ± 8% vs 66% ± 8%, $P = 0.02$) and were less likely to undergo reintervention (re-ASA or myectomy) (log-rank $P = 0.02$).

CONCLUSIONS Patients with hypertrophic obstructive cardiomyopathy treated with ASA have a 9% probability of PPM implantation within 30 days after ASA. In long-term follow-up, patients with PPM had similar long-term survival and New York Heart Association functional class but lower LV outflow gradient, a more pronounced LV outflow gradient decrease, a lower LV ejection fraction, and a lower likelihood of reintervention compared with patients without PPM.
(J Am Coll Cardiol Intv 2022;■:■–■) © 2022 by the American College of Cardiology Foundation.

From the [a]Department of Cardiology, Second Medical School, Charles University, University Hospital Motol, Prague, Czech Republic; [b]Department of Cardiology, St. Antonius Hospital Nieuwegein, Nieuwegein, the Netherlands; [c]Institute of Cardiovascular Medicine and Science, Liverpool Heart and Chest Hospital, Liverpool, United Kingdom; [d]Ruhr-University Bochum, Bochum, Germany; [e]Cardiocentre Podlesi, Trinec, Czech Republic; [f]Department of Endovascular Therapy, Sverdlovsk Regional Hospital No. 1 and Ural Federal University, Yekaterinburg, Russian Federation; [g]Department of Demography and Geodemography, Faculty of Science, Charles University, Prague, Czech Republic; [h]Department of Cardiology, Herlev and Gentofte Hospital, Hellerup, Denmark; [i]Comprehensive Heart Failure Centre, University Clinic Wurzburg, Wurzburg, Germany; and the [j]Department of Cardiology, City Hospital No. 2, Saint-Petersburg, Russian Federation.
The authors attest they are in compliance with human studies committees and animal welfare regulations of the authors' institutions and Food and Drug Administration guidelines, including patient consent where appropriate. For more information, visit the Author Center.

Manuscript received March 7, 2022; revised manuscript received June 9, 2022, accepted June 28, 2022.

ISSN 1936-8798/$36.00 https://doi.org/10.1016/j.jcin.2022.06.034

ABBREVIATIONS AND ACRONYMS

ASA = alcohol septal ablation

AV = atrioventricular

BBB = bundle branch block

CCS = Canadian Cardiovascular Society

HOCM = hypertrophic obstructive cardiomyopathy

ICD = implantable cardioverter-defibrillator

LV = left ventricular

NYHA = New York Heart Association

PPM = permanent pacemaker

Alcohol septal ablation (ASA) is used to treat symptomatic patients with hypertrophic obstructive cardiomyopathy (HOCM).[1-4] Because of the proximity of the perfusion territory of the coronary artery septal branches to the cardiac conduction system (especially the right bundle branch), a significant complication of ASA-induced targeted myocardial necrosis is periprocedural atrioventricular (AV) block requiring implantation of a permanent pacemaker (PPM) in 7% to 20% of cases.[5-9]

Currently, very limited evidence is available on the outcomes of these patients.[10,11] Based on a multinational European registry (the Euro-ASA registry) of patients who underwent ASA for HOCM, we determined the short- and long-term outcomes of patients with PPM implanted for high-grade ASA-related AV block. Furthermore, we used propensity score matching analysis to compare the outcomes of patients with and without PPM.

METHODS

DIAGNOSIS AND PATIENTS. The diagnosis of HOCM was established by experienced cardiologists based on typical clinical, electrocardiographic, and echocardiographic features; patients had to have a left ventricular (LV) outflow tract gradient ≥30 mm Hg at rest and/or ≥50 mm Hg after provocation.

TABLE 1 Clinical and Echocardiographic Characteristics of Study Patients at Baseline and at the Last Clinical Checkup

	Unmatched Cohort			Matched Cohort		
	PPM Group (N = 170)	Non-PPM Group (N = 1,644)	*P* Value	PPM Group (N = 139)	Non-PPM Group (N = 139)	*P* Value
Age, years	62.5 ± 12.1	57.5 ± 13.6	<0.001	60.6 ± 11.8	60.1 ± 11.6	0.713
Females	85 (50)	839 (51)	0.809	71 (51)	72 (52)	1.000
ASA alcohol dose, mL	2.2 ± 1.1	2.1 ± 1.2	0.038	2.2 ± 1.1	2.0 ± 1.1	0.059
Alcohol dose during the first ASA, mL	2.1 ± 1.0	2.0 ± 0.9	0.021	2.1 ± 1.0	1.9 ± 0.8	0.031
Bundle branch block before ASA	55 (33)	203 (12)	<0.001	45 (33)	26 (19)	0.013
Basal septum thickness (mm)						
Baseline	20.1 ± 3.3	20.7 ± 3.8	0.101	20.2 ± 3.3	20.0 ± 2.7	0.982
Last clinical checkup	14.9 ± 4.1	15.7 ± 4.0	0.013	15.0 ± 4.1	15.7 ± 3.6	0.069
NYHA functional class						
Baseline	2.8 ± 0.5	2.7 ± 0.6	0.017	2.8 ± 0.5	2.7 ± 0.5	0.497
Last clinical checkup	1.5 ± 0.8	1.4 ± 0.9	0.030	1.5 ± 0.7	1.5 ± 0.9	0.989
NYHA functional class III/IV						
Baseline	129 (77)	1111 (68)	0.018	106 (76)	104 (75)	0.889
Last clinical checkup	17 (11)	141 (11)	0.782	10 (8)	21 (18)	0.021
Angina, CCS class						
Baseline	1.1 ± 1.2	1.0 ± 1.1	0.471	1.2 ± 1.2	1.1 ± 1.1	0.367
Last clinical checkup	0.4 ± 0.7	0.5 ± 0.8	0.089	0.5 ± 0.7	0.5 ± 0.7	0.854
LV outflow gradient at rest, mm Hg						
Baseline	76.6 ± 41.9	67.5 ± 35.1	0.015	71.8 ± 37.5	69.7 ± 34.0	0.737
Last clinical checkup	13.2 ± 20.2	17.6 ± 19.8	<0.001	11.9 ± 12.3	17.1 ± 18.9	0.002
>30 mm Hg	13 (8)	260 (16)	0.003	12 (9)	23 (17)	0.069
Percent LV outflow gradient decrease at last clinical checkup, %	80.9 ± 17.3	70.4 ± 30.8	<0.001	80.8 ± 16.6	71.7 ± 35.2	0.001
LV diameter, mm						
Baseline	44.2 ± 6.3	44.3 ± 6.3	0.857	44.5 ± 6.2	45.5 ± 6.4	0.389
Last clinical checkup	46.7 ± 6.0	46.0 ± 5.9	0.209	46.8 ± 6.1	46.9 ± 5.8	0.986
LV ejection fraction, %						
Baseline	67.7 ± 8.8	69.7 ± 8.4	0.015	68.4 ± 7.9	67.8 ± 8.0	0.395
Last clinical checkup	63.3 ± 9.2	66.5 ± 8.0	<0.001	63.5 ± 8.4	66.1 ± 7.9	0.022
Left atrium diameter, mm						
Baseline	46.8 ± 6.2	45.7 ± 6.4	0.016	46.8 ± 6.1	46.1 ± 5.3	0.205
Last clinical checkup	46.2 ± 7.1	44.6 ± 6.7	0.003	46.3 ± 7.2	45.1 ± 6.3	0.127
Mean follow-up duration, years Median	4.8 ± 4.1 4.0 (1.5, 7.6)	5.0 ± 4.4 4.0 (1.3, 7.8)		4.9 ± 4.1 4.1 (1.9, 7.6)	4.7 ± 4.0 4.0 (1.3, 6.7)	

Values are mean ± SD, n (%), or median (quartile 1, quartile 3).
ASA = alcohol septal ablation; CCS = Canadian Cardiovascular Society; LV = left ventricular; NYHA = New York Heart Association; PPM = pacemaker.

The indication for ASA was intractable clinical symptoms despite maximal pharmacotherapy. The decision regarding septal reduction therapy (ASA vs myectomy) was made after detailed multidisciplinary discussions and shared decision making with the patients.

INTERVENTIONS. Procedures were performed in tertiary invasive centers in 6 European countries. All patients had been prospectively included in institutional registries and subsequently in the Euro-ASA registry.[8] ASA procedures were performed by experienced interventional cardiologists, with only 1 or 2 interventionalists performing all procedures in each center. Details of the technique have been published in the past[4,12]; the indication and procedural technique were at the discretion of the participating centers. There were no major differences in the technique or methodology of performing ASA among sites. The post-ASA patients were observed in the coronary care unit for ≥48 hours. If no episodes of AV block occurred, the periprocedural temporary pacemaker was removed. The indication and technique for PPM implantation was at the discretion of the treating clinicians, and PPMs were usually implanted if high-grade AV block persisted for ≥24 hours or occurred later after the procedure.[5-7,13]

STUDY DESIGN AND OUTCOMES. Clinical, demographic, and echocardiographic data and symptoms were recorded at baseline and during follow-up. Patients underwent a clinical examination 1 to 6 months after ASA and every year thereafter. The follow-up program included recording of symptoms, physical and echocardiographic examination, and electrocardiography. All clinical adverse events were confirmed by reviewing the medical records. The survival of patients treated in the Czech Republic, Russia, and Denmark were confirmed by the National Database of Deaths. The survival of patients treated in the other countries was recently updated by clinical examination, telephone call, or mail communication. The study was performed in compliance with the Declaration of Helsinki.

We identified patients with PPM implanted for high-grade periprocedural AV block (**Table 1**) and used the propensity score to match each patient with a comparable patient without PPM. We then compared both short- and long-term outcomes in all groups of patients.

We assessed the following outcomes: 1) 30-day all-cause mortality rate, 2) long-term all-cause mortality rate, 3) long-term New York Heart Association (NYHA) functional class, 4) long-term LV outflow gradient and percent LV gradient decrease, 5) long-term LV ejection fraction, and 6) long-term rate of reintervention (re-ASA or myectomy).

TABLE 2 Predictors of Pacemaker Implantation During 30 Days After Alcohol Septal Ablation

	Odds Ratio	95% CI	*P* Value
NYHA functional class III/IV (reference category: NYHA functional class I/II)	1.63	1.07-2.49	0.024
Age (per a unit increase [ie, 1 year of age])	1.02	1.00-1.03	0.029
LV ejection fraction at baseline (per a unit increase [ie, 1 percentage point increase])	0.97	0.95-1.00	0.014
IVS thickness at baseline (per a unit increase [ie, 1 mm if thickness increase])	0.94	0.89-0.99	0.026
BBB before ASA (reference category: no BBB before ASA)	3.56	2.38-5.31	<0.001
Alcohol dose during the first ASA (per a unit increase [ie, 1-mL increase])	1.36	1.14-1.63	0.001

BBB = bundle branch block; IVS = interventricular septum; LV = left ventricular; NYHA = New York Heart Association.

STATISTICAL ANALYSIS. All data were assessed and edited by 2 research statisticians. Data are presented as mean ± SD or median and quartiles (Q1, Q3) in case of the follow-up duration and numbers and proportions for categoric variables, respectively. The Mann-Whitney *U* test was used to assess the difference between continuous variables, and the Fisher exact test was used for categoric variables. We compared patients with PPMs implanted during 30 days after ASA (the PPM group) and patients without PPMs implanted during this period (the non-PPM group). We calculated a propensity score for the following baseline variables: sex, age, LV outflow gradient, LV end-diastolic diameter, basal interventricular septum thickness, LV ejection fraction, and NYHA functional class. The propensity score matching was performed using the PSMATCH procedure (SAS software, version 9.4; SAS) (Supplemental Figure 1). Records with missing observations for key variables were not entered into the matching. The calculation yielded 139 patients with PPM (the matched PPM group) and matched them with 139 patients without PPM (the matched non-PPM group). To find risk predictors of all-cause mortality in the matched cohort, the following baseline variables were evaluated in a multivariable model using a backward stepwise algorithm for the Cox proportional hazards survival model: sex, age, LV outflow gradient, LV end-diastolic diameter, interventricular septum thickness, LV ejection fraction, NYHA functional class I/II or III/IV, bundle branch block (BBB) before ASA, total alcohol dose, and distinguishing of the PPM and non-PPM groups of patients. The same variables were used in a logistic regression to find risk predictors of PPM implantation

FIGURE 1 Percent of Permanent Pacemakers (PPMs) Implanted

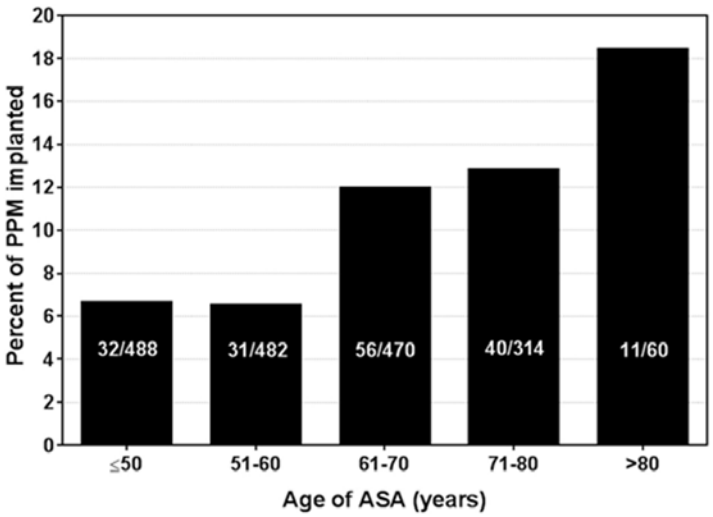

Relationship between the patient's age and the probability of PPM implantation within 30 days after alcohol septal ablation (ASA).

in which the year of ASA also was performed as a predictor in the form of 2 categories (ASA in 1996-2009 and ASA in 2010 and later), and instead of the total alcohol dose, the alcohol dose during the first ASA was used. Estimates for long-term outcomes were performed using the Kaplan-Meier method (including 95% CIs), and differences were assessed by the log-rank test. $P < 0.05$ was considered statistically significant. All reported P values were 2-sided. All analyses were performed using SAS software (version 9.4).

RESULTS

A total of 1,977 consecutive patients with symptomatic HOCM underwent ASA between 1996 and 2021 and were registered in the Euro-ASA registry, which is a multinational European registry of ASA patients.[8] For the analysis, we excluded 163 (8.2%) patients, including 15 (0.8%) patients with myectomy before ASA, 126 (6.4%) patients with a PPM or implantable cardioverter-defibrillator (ICD) implanted before ASA, and 22 (1.1%) patients with an ICD implanted for the prevention of sudden cardiac death during 30 days after ASA. The mean follow-up duration of these patients (n = 163) was 5.3 ± 5 years, and a total of 22 of these patients died, which translated to an all-cause mortality rate of 2.5 per 100 patient-years.

UNMATCHED COHORT. We analyzed 1,814 ASA patients (Table 1). A total of 16 (0.9%) patients died during 30 days after ASA, including 2 (1%) in the PPM group and 14 (0.9%) in the non-PPM group ($P = 0.66$) (Supplemental Table 1).

The PPM group was composed of 170 (9.4%) patients, 150 (88%) of whom received a PPM during the first post-ASA week and 20 (12%) a PPM between day 8 and day 30 after the procedure. Later, PPMs were implanted in a further 56 (3%) patients at a mean of 3.6 ± 3.7 years after ASA.

Patients in the PPM group were older ($P < 0.01$), more often had a BBB before ASA ($P < 0.01$), had a higher NYHA functional class before ASA and at the last clinical checkup ($P = 0.02$ and $P = 0.03$), received a higher total alcohol dose ($P = 0.04$), had a higher LV outflow gradient before ASA ($P = 0.02$) and a lower LV outflow gradient at the last clinical checkup ($P < 0.01$), had a lower basal septum thickness at the last clinical checkup ($P = 0.01$), had a larger left atrial diameter before ASA and at the last clinical checkup ($P = 0.02$ and $P = 0.003$), and a lower LV ejection fraction before ASA and at the last clinical checkup ($P = 0.02$ and $P < 0.01$) (Table 1). In multivariable analysis, the predictors of PPM implantation were older age at baseline, worse NYHA functional class (III/IV), lower LV ejection fraction, lower basal septum thickness, higher alcohol dose during the first ASA, and a BBB before ASA (Table 2). Patients ≤60 years were less likely to undergo PPM implantation than older patients (6.5% vs 12.7%, $P < 0.01$) (Figure 1).

Overall, the mean duration of follow-up was 5.0 ± 4.3 years, and a total of 245 deaths occurred during 9,066 patient-years, which translated to an all-cause mortality rate of 2.7 per 100 patient-years. Freedom from all-cause mortality in the PPM group (N = 170) at 1, 5, and 10 years was 98% (95% CI: 94%-99%), 88% (95% CI: 79%-92%), and 78% (95% CI: 65%-86%), respectively. This observed mortality was comparable with the mortality of the non-PPM group (N = 1,644) (log-rank $P = 0.91$, Central Illustration).

A total of 194 (11%) patients underwent repeated septal reduction procedures (re-ASA or myectomy) attributable to persisting symptoms and/or LV outflow gradient. The Kaplan-Meier curves describing reinterventions rates are shown in Figure 2A; patients in the PPM group were less likely to undergo reinterventions (log-rank $P = 0.03$).

MATCHED COHORT. The matched cohort analysis comprised 278 patients with 139 patients in the matched PPM group and 139 in the matched non-PPM group. One (0.4%) patient died during 30 days after ASA, including 0 patients and 1 patient in the matched PPM group and the non-PPM group ($P = 1.00$), respectively (Supplemental Table 1).

CENTRAL ILLUSTRATION **Survival of Paced Versus Nonpaced Patients After Alcohol Septal Ablation**

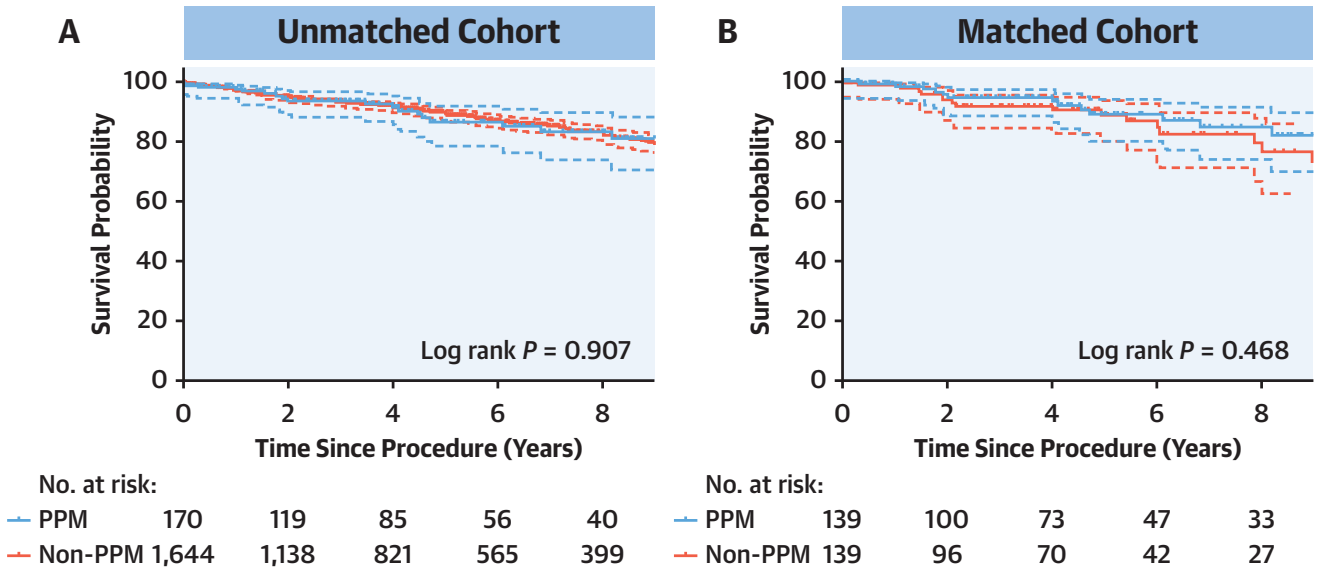

ASA = Alcohol Septal Ablation; PPM = Permanent Pacemaker; Non-PPM = Non Permanent Pacemaker

Veselka J, et al. J Am Coll Cardiol Intv. 2022;■(■):■-■.

Kaplan-Meier survival curves with 95% CIs describing the freedom from all-cause mortality in **(A)** the permanent pacemaker (PPM) versus the non-PPM groups and **(B)** the matched PPM versus the matched non-PPM groups.

Patients in the matched PPM group more often had a BBB before ASA ($P = 0.01$), were treated with a higher dose of alcohol during the first ASA ($P = 0.03$), had a more pronounced reduction of LV outflow gradient and a lower LV outflow gradient at the last clinical checkup ($P < 0.01$ for both), had a lower LV ejection fraction at the last clinical checkup ($P = 0.02$), and had a lower proportion of patients who had NYHA functional class III/IV in comparison to the non-PPM group ($P = 0.02$) (Table 1). The mean duration of follow-up was 4.9 ± 4.1 years, and a total of 33 deaths occurred during 1,335 patient-years, translating to an all-cause mortality rate of 2.5 per 100 patient-years.

Freedom from all-cause mortality in the matched PPM group at 1, 5, and 10 years was 98% (95% CI: 94%-100%), 89% (95% CI: 80%-94%), and 78% (95% CI, 61%-88%), respectively. This observed mortality was comparable with the survival of the matched non-PPM group ($P = 0.47$) (Central Illustration). In multivariable analysis, the predictors of all-cause mortality were older age at baseline ($P < 0.01$) and BBB before ASA ($P = 0.01$). A total of 24 (9%) patients underwent repeated septal reduction procedures. Patients in the matched PPM group were less likely to undergo reinterventions (log-rank $P = 0.02$, Figure 2B).

DISCUSSION

To our knowledge, this is the first study with propensity score matching analysis evaluating short- and long-term outcomes of patients with HOCM who underwent ASA and received a PPM for periprocedural AV block. We report the following principal findings: 1) PPMs were implanted in 9.4% of patients during 30 days after ASA and in addition in 3.1% of patients during follow-up; 2) baseline predictors of PPM implantation within 30 days of ASA were older age, worse NYHA functional class (III/IV), lower LV ejection fraction, lower basal septum thickness, higher alcohol dose during the first ASA, and BBB before ASA; 3) short- and long-term mortality rates were similarly low in all evaluated groups; 4) in the long-term follow-up, patients in the matched PPM group had a lower LV ejection fraction (still in the normal range), lower LV outflow gradient, more pronounced reduction of LV outflow gradient, and a lower proportion of patients had NYHA functional class III/IV in comparison to the non-PPM group; and

FIGURE 2 Repeated Reduction Procedures After Alcohol Septal Ablation

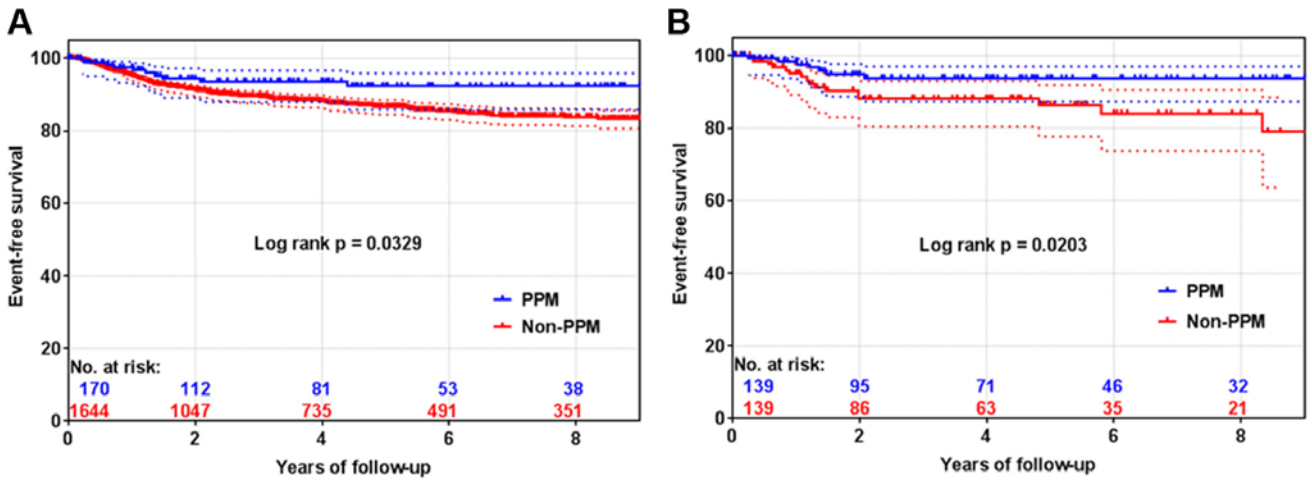

Kaplan-Meier curves with 95% CIs describing the freedom from repeated septal reduction therapy in **(A)** the permanent pacemaker (PPM) versus the non-PPM groups and **(B)** the matched PPM versus the matched non-PPM groups.

5) the rate of reinterventions was significantly lower in the paced patients.

The most frequent significant post-ASA complication is high-grade AV block requiring PPM implantation.[4-8] The cause for this lies in the anatomical proximity of the target perfusion territory of the coronary artery septal branches to the conduction system. In this regard, our current results are in line with previous reports indicating that the occurrence of post-ASA high-grade AV block requiring PPM placement is approximately 10%,[7-9,14] with 97% of these AV blocks occurring within 5 days after ASA.[7,12]

In the past, it has been convincingly shown that certain factors play a key role in the risk of PPM implantation after ASA. Among the most important factors are preprocedural conduction abnormalities, especially a left BBB.[4-6,11] Also, it has been demonstrated that the age of patients is a significant factor contributing to post-ASA conduction disturbances. For example, Batzner et al[15] recently reported ASA-related PPM ratios of 4%, 9%, and 14% in patients <40 years, 40 to 60 years, and ≥60 years of age, respectively. Interestingly, the procedural experience of the center performing ASA may significantly influence these results. Along this line, we have reported that centers with an overall volume >50 ASA procedures implanted fewer postprocedure PPMs than centers with less experience (9% vs 15%, $P < 0.01$).[16] Another factor influencing the likelihood of PPM implantation is the type of financial ownership of the hospital where the procedure is performed. Lam et al[13] identified in the 2010 to 2015 U.S. Nationwide Readmissions Databases 1,296 patients who underwent ASA; 14% of these received PPMs and 11% ICDs during the index hospitalization. Notably, private hospital ownership independently predicted a 2 times increased probability of PPM or ICD implantation. Moreover, both devices were mostly implanted within 3 days after ASA. Thus, a "watch-and-wait" strategy may be used more in governmentally owned hospitals and may reduce the rate of implanted PPM after ASA.[13]

In the present study, we confirmed the results of previous studies regarding the higher risk of ASA-related PPM implantation in elderly patients, and we found that patients ≤60 years of age were almost half as likely to undergo PPM implantation than patients >60 years of age (7% vs 13%). Furthermore, we found additional independent predictors of PPM implantation, including a worse NYHA functional class (III/IV), lower LV ejection fraction, and lower basal septum thickness, respectively. Alcohol dose during the procedure also plays a role because on average a 10% higher dose was used in patients requiring PPMs compared with those who did not receive PPM.

The long-term implications of PPM implantation after ASA are scarcely reported.[10,11,17,18] In terms of long-term outcomes of patients with PPM after ASA, 3 results of the present study are of special importance. First, PPM implantation did not translate into worsened long-term mortality. Second, PPM patients had a more pronounced decrease in the LV outflow gradient during long-term follow-up, which may be caused by both the more aggressive ASA (higher dose of alcohol used during the procedure and smaller

septal thickness, Table 1) and the long-term synergistic effects of PPM pacing on LV hypercontractility and LV ejection fraction.[18] This highlights the difficult clinical choice between more ablation with better gradient reduction but a higher pacemaker rate. Third, the lower LV outflow gradient after ASA in patients with PPM was linked with a lower probability of reintervention.

STUDY LIMITATIONS. The limitations of this study include the following: first, we did not have functional pacing data, but from our previous study of a smaller number of patients, it appears that two-thirds of patients were mostly independent of PPM pacing.[10] Second, although patients in this study were followed for an average of more than 5 years, some complications of PPM can occur later, which could affect future longer-term outcomes. Third, this study was based on the currently largest reported registry of ASA patients. Nevertheless, the sample size of PPM patients (N = 170) was limited, and only 278 patients (139 pairs) were included in propensity score matching. These 2 factors somewhat limit the predictive value of survival-related parameters as well as propensity score matching, which included only 15% of the 1,814 enrolled patients.

CONCLUSIONS

Patients with HOCM treated with ASA have a 9.4% probability of PPM implantation within 30 days after ASA. In this long-term follow-up, patients with PPMs had lower LV outflow gradient, more pronounced LV outflow gradient decrease, lower LV ejection fraction, and lower likelihood of reintervention but similar long-term survival and mean NYHA functional class compared with patients without PPMs.

ACKNOWLEDGMENTS The authors thank the colleagues responsible for the hypertrophic cardiomyopathy clinics in all participating centers.

FUNDING SUPPORT AND AUTHOR DISCLOSURES

The authors have reported that they have no relationships relevant to the contents of this paper to disclose.

ADDRESS FOR CORRESPONDENCE: Dr Josef Veselka, Department of Cardiology, V úvalu 84, Prague 5, 15000, Czech Republic. E-mail: veselka.josef@seznam.cz. Twitter: @josef_veselka.

PERSPECTIVES

WHAT IS KNOWN? Because of the proximity of the perfusion territory of the coronary artery septal branches to the cardiac conduction system, a significant complication of ASA is a periprocedural atrioventricular block requiring implantation of a permanent pacemaker in 7% to 20% of cases. The long-term implications of PPM implantation after ASA are scarcely reported.

WHAT IS NEW? PPMs were implanted in 9% of patients during 30 days after ASA and in addition in 3% of patients during the 5-year follow-up. There were the following baseline predictors of PPM implantation within 30 days of ASA: older age, worse NYHA functional class (III/IV), lower LV ejection fraction, lower basal septum thickness, higher alcohol dose during the first ASA, and BBB before ASA. Patients with and without PPM after ASA did not have different survival rates. However, in the long-term follow-up, patients with PPM had a lower LV ejection fraction (still in the normal range), lower LV outflow gradient, and more pronounced reduction of LV outflow gradient, and a lower proportion of patients had NYHA functional class III/IV. Also, the rate of reinterventions was significantly lower in the paced patients.

WHAT IS NEXT? It should be clarified why PPM patients had a more pronounced decrease in the LV outflow gradient during long-term follow-up.

REFERENCES

1. Maron BJ, Desai MY, Nishimura RA, et al. Management of hypertrophic cardiomyopathy. *J Am Coll Cardiol*. 2022;79:390-414.

2. Elliott PM, Anastakis A, Borger MA, et al. 2014 ESC guidelines on diagnosis and management of hypertrophic cardiomyopathy. *Eur Heart J*. 2014;35:2733-2779.

3. Ommen SR, Mital S, Burke MA, et al. 2020 AHA/ACC guideline for the diagnosis and treatment of patients with hypertrophic cardiomyopathy: executive summary: a report of the American College of Cardiology/American Heart Association Joint Committee on Clinical Practice Guideline. *Circulation*. 2020;142:e533-e557.

4. Rigopoulos AG, Sakellaropoulos S, Ali M, et al. Transcatheter septal ablation in hypertrophic obstructive cardiomyopathy: a technical guide and review of published results. *Heart Fail Rev*. 2018;23:907-917.

5. Talreja DR, Nishimura RA, Edwards WD, et al. Alcohol septal ablation versus surgical septal myectomy: comparison of effects on atrioventricular conduction tissue. *J Am Coll Cardiol*. 2004;44:2329-2332.

6. El-Sabawi B, Nishimura RA, Barsness GW, Cha YM, Geske JB, Eleid MF. Temporal occurrence of arrhythmic complications after alcohol septal ablation. *Circ Cardiovasc Interv*. 2020;13:e008540.

7. Veselka J, Lawrenz T, Stellbrink C, et al. Low incidence of procedure-related major cardiac adverse events after alcohol septal ablation for symptomatic hypertrophic obstructive cardiomyopathy. *Can J Cardiol*. 2013;29:1415-1421.

8. Veselka J, Jensen MK, Liebregts M, et al. Long-term clinical outcome after alcohol septal ablation for obstructive hypertrophic cardiomyopathy: results from the Euro-ASA registry. *Eur Heart J*. 2016;37:1517–1523.

9. Kim LK, Swaminathan RW, Looser P, et al. Hospital volume outcomes after septal myectomy and alcohol septal ablation for treatment of obstructive hypertrophic cardiomyopathy. US Nationwide Inpatient Database, 2003-2011. *JAMA Cardiol*. 2016;1:324–332.

10. Veselka J, Krejčí J, Tomašov P, et al. Outcome of patients after alcohol septal ablation with permanent pacemaker implanted for periprocedural complete heart block. *Int J Cardiol*. 2014;171:e37–e38.

11. Jensen MK, Faber L, Liebregts M, et al. Effect of impaired cardiac conduction after alcohol septal ablation on clinical outcomes: insights from ASEuro registry. *Eur Heart J Qual Care Clin Outcomes*. 2019;5:252–258.

12. Veselka J, Zemánek D, Fiedler J, Šváb P. Real-time myocardial contrast echocardiography for echo-guided alcohol septal ablation. *Arch Med Sci*. 2009;5:271–272.

13. Lam MC, Naidu SS, Kolte D, et al. Cardiac implantable electronic device placement following alcohol septal ablation for hypertrophic cardiomyopathy in the United States. *J Cardiovasc Electrophysiol*. 2020;31:2712–2719.

14. Nagueh SF, Groves BM, Schwartz L, et al. Alcohol septal ablation for the treatment of hypertrophic obstructive cardiomyopathy: a multicenter North American registry. *J Am Coll Cardiol*. 2011;58:2322–2328.

15. Batzner A, Aicha D, Pfeiffer B, Neugebauer A, Seggewiss H. Age-related survival after alcohol septal ablation in hypertrophic obstructive cardiomyopathy. *ESC Heart Fail*. 2022;9:327–336.

16. Veselka J, Faber L, Jensen MK, et al. Effects of institutional experience on outcomes of alcohol septal ablation for hypertrophic obstructive cardiomyopathy. *Can J Cardiol*. 2018;34:16–22.

17. Bleszynski PA, Goldenberg I, Fernandez G, et al. Risk of arrhythmic events after alcohol septal ablation for hypertrophic cardiomyopathy using continuous implantable cardiac monitoring. *Heart Rhythm*. 2021;18:50–56.

18. Daubert C, Gadler F, Mabo P, Linde C. Pacing for hypertrophic obstructive cardiomyopathy: an update and future directions. *Europace*. 2018;20:908–920.

KEY WORDS alcohol septal ablation, permanent pacemaker, prognosis

APPENDIX For supplemental tables and figures, please see the online version of this paper.

R. Kočková et al.

Multiparametric Strategy to Predict Early Disease Decompensation in Asymptomatic Severe Aortic Regurgitation

Circ Cardiovasc Imaging
Impact Factor: 8.589

Circulation: Cardiovascular Imaging

ORIGINAL ARTICLE

Multiparametric Strategy to Predict Early Disease Decompensation in Asymptomatic Severe Aortic Regurgitation

Radka Kočková, MD, PhD; Hana Línková, MD; Zuzana Hlubocká, MD, PhD; Karel Mědílek, MD; Martin Tuna, MD, PhD; Jan Vojáček, MD, PhD; Ivo Skalský, MD, PhD; Štěpán Černý MD, PhD; Jiří Malý, MD, PhD; Jaroslav Hlubocký, MD, PhD; Takuya Mizukami, MD, PhD; Cristina De Colle, MD; Martin Pěnička, MD, PhD

BACKGROUND: Use of the current echocardiography-based indications for aortic regurgitation (AR) surgery might result in late valve replacement at the stage of irreversible myocardial damage. Therefore, we aimed to identify simple models combining multiple echocardiography or magnetic resonance imaging (MRI)–derived indices and natriuretic peptides (BNP [brain natriuretic peptide] or NT-proBNP [N-terminnal pro-B type natriuretic peptide]) to predict early disease decompensation in asymptomatic severe AR.

METHODS: This prospective and multicenter study included asymptomatic patients with severe AR, preserved left ventricular ejection fraction (>50%), and sinus rhythm. The echocardiography and MRI images were analyzed centrally in the CoreLab. The study end point was the onset of indication for aortic valve surgery as per current guidelines.

RESULTS: The derivative cohort consisted of 127 asymptomatic patients (age 45±14 years, 84% males) with 41 (32%) end points during a median follow-up of 1375 (interquartile range, 1041–1783) days. In multivariable Cox regression analysis, age, BNP, 3-dimensional vena contracta area, MRI left ventricular end-diastolic volume index, regurgitant volume, and a fraction were identified as independent predictors of end point (all $P<0.05$). However, a combined model including one parameter of AR assessment (MRI regurgitant volume or regurgitant fraction or 3-dimensional vena contracta area), 1 parameter of left ventricular remodeling (MRI left ventricular end-diastolic volume index or echocardiography 2-dimensional global longitudinal strain or E wave), and BNP showed significantly higher predictive accuracy (area under the curve, 0.74–0.81) than any parameter alone (area under the curve, 0.61–0.72). These findings were confirmed in the validation cohort (n=100 patients, 38 end points).

CONCLUSIONS: In asymptomatic severe AR, multimodality and multiparametric model combining 2 imaging indices with natriuretic peptides, showed high accuracy to identify early disease decompensation. Further prospective studies are warranted to explore the clinical benefit of implementing these models to guide patient management.

REGISTRATION: URL: https://www.clinicaltrials.gov; Unique identifier: NCT02910349

GRAPHIC ABSTRACT: A graphic abstract is available for this article.

Key Words: aortic valve ■ echocardiography ■ magnetic resonance imaging ■ natriuretic peptide, brain ■ prognosis

See Editorial by Fontana and Ioannou

Aortic regurgitation (AR) is the third most common[1–6] valvular heart disease affecting mainly younger males.[1,4] Severe chronic AR may be clinically silent for a long time but eventually leads to heart failure with reduced life expectancy.[1,3,7] It is of note that even before the onset of symptoms or left ventricular (LV) decompensation, severe AR is associated with increased annual mortality.[7–9] This suggests relative insensitivity of current

Correspondence to: Radka Kočková MD, PhD, Center for Congenital Heart Disease in Adults, Na Homolce Hospital, Cardiothoracic Surgery Department, Roentgenova 37/2, Prague, 15030. Email radka.kockova@centrum.cz

Supplemental Material is available at https://www.ahajournals.org/doi/suppl/10.1161/CIRCIMAGING.122.014901.
Continuing medical education (CME) credit is available for this article. Go to http://cme.ahajournals.org to take the quiz.
For Sources of Funding and Disclosures, see page 908.

Circulation: Cardiovascular Imaging is available at www.ahajournals.org/journal/circimaging

CLINICAL PERSPECTIVE

The optimal timing of surgical treatment in asymptomatic patients with chronic severe aortic regurgitation remains challenging. A current approach integrating symptoms, echocardiography-derived aortic regurgitation assessment, and left ventricular remodeling is rather insensitive to detect ongoing myocardial damage and the need for early aortic valve intervention. In the present study of 127 patients the age, serum level of brain natriuretic peptide, echocardiography-derived 3-dimensional vena contracta area, magnetic resonance–derived left ventricular end-diastolic volume index, regurgitant volume and fraction were independent predictors of early disease progression leading aortic valve surgery. However, a multiparametric model combing markers of (1) aortic regurgitation severity, (2) a marker of left ventricular remodeling, and (3) brain natriuretic peptide serum level, showed higher predictive accuracy than any parameter alone. A comprehensive examination of asymptomatic patients with moderate to severe chronic aortic regurgitation using echocardiography, cardiac magnetic resonance, and serum brain natriuretic peptide might be useful. The presented multiparametric model helps to identify patients with a high likelihood of early disease progression and aortic valve surgery. However, further clinical studies are warranted to show if early surgery will result in a better outcome in asymptomatic patients with chronic severe aortic regurgitation and a high risk of early disease progression.

Nonstandard Abbreviations and Acronyms

AR	aortic regurgitation
BNP	brain natriuretic peptide
ECV	extracellular volume
EDVI	end-diastolic volume index
EF	ejection fraction
ESVI	end-systolic volume index
LV	left ventricle
MRI	magnetic resonance imaging
RF	regurgitant fraction
RV	regurgitant volume

guidelines triggers for early aortic valve (AV) intervention.[10–12] Moreover, a non-negligible number of patients undergoing AV surgery have already irreversible myocardial damage with a negative impact on their long-term outcome.[10,13] However, perioperative mortality has decreased with novel surgical techniques and perioperative care.[8,9,11] However, the clinical decision of whether or not to indicate early AV intervention remains challenging.

Cardiac magnetic resonance imaging (MRI) is an accurate and reproducible technique to assess aortic flow and LV remodeling.[6,14] In asymptomatic patients with preserved LV ejection fraction (EF), we have observed high accuracy of the MRI-derived quantification of AR to identify individuals in need of early AV surgery.[15] However, a multiparametric strategy involving not only AR quantification but also an assessment of LV remodeling, natriuretic peptides, or different imaging modalities may be more accurate to guide clinical decisions toward early AV intervention. Therefore, the present study aimed to identify simple models including multiple echocardiographic or MRI-derived indices and natriuretic peptides to predict early disease decompensation in asymptomatic patients with severe AR and preserved LV EF. The accuracy of these models was tested in an external validation cohort.

METHODS

Deidentified data on which this work is based will be available, they can be requested from the corresponding author, upon reasonable request.

Design

The study was a prospective, multicenter, and observational, conducted in six tertiary centers (5 derivation cohorts in the Czech Republic, and 1 external validation cohort in Belgium). In the derivative cohort, analysis of all the echocardiographic and MRI images was performed in a CoreLab located in one of the tertiary cardiology centers (Institute for Clinical and Experimental Medicine, Prague), which is the holder of the European Association of Cardiovascular Imaging Laboratory accreditation for advanced echocardiography. The MRI images were analyzed by a physician holding a European Association of Cardiovascular Imaging Level 3 Diploma in Cardiovascular MRI. The readers were blinded to all other data and outcomes. In the validation cohort, the echocardiography and MRI imaging were performed and analyzed in the Cardiovascular Center Aalst.

Patients

The derivative cohort consisted of consecutive asymptomatic patients (n=127, age 45±14 years, 84% males) with isolated severe AR referred to all 5 participating centers for AR assessment between March 2015 and May 2019. As per study protocol,[15] only adult patients in sinus rhythm with LV EF >50%, LV end-diastolic diameter ≤70 mm, and LV end-systolic diameter ≤25 mm/m^2 with a single valve lesion were included. Patients with poor echocardiographic image quality, contraindications for MRI, or severe comorbidities limiting life expectancy (<3 years) were excluded. The severity of AR was established utilizing an integrative echocardiographic approach according to the American Society of Cardiology and European Association of Cardiovascular Imaging recommendations.[14] The absence of symptoms was validated using exercise testing. The validation cohort consisted of consecutive asymptomatic patients (n=100, age 46±15 years, 82% males) included in the Cardiovascular Center Aalst according to the same eligibility criteria. The study protocol and informed consent were approved by the Ethics committees in all participating centers.[15]

Study Protocol

At baseline, all patients underwent comprehensive 2-dimensional (2D) and 3D echocardiography, exercise testing, and blood sample analysis in the participating centers. All MRI examinations were performed in a single center where the CoreLab was located. A total of 60 (47%) patients underwent MRI on the same day as baseline echocardiography while the remaining patients were referred for MRI within 2 weeks after enrollment. During the follow-up, every 6 months the clinical, biochemical, and echocardiographic data were recorded in each participating center. The decision about further patient management was left to the experienced heart valve team in the particular center. The follow-up data on AV surgery, hospitalization, and mortality were obtained using the hospital database and population registry.

Study end point was the onset of indication for AV surgery as per current guidelines.[1]

Echocardiography

A comprehensive 2D and 3D echocardiography was performed using Vivid 7, Vivid E9, and Vivid E95 (GE Healthcare, Horten, Norway) ultrasound system according to the study protocol described in detail previously.[15] Blood pressure and heart rate were recorded during examination in all patients. At least 3 R-R loops were recorded for each meticulously optimized view, digitally stored, and analyzed offline in the CoreLab. The average measurements from all 3 loops were databased.

Grading of AR Severity

The AR severity was graded utilizing recommended algorithm of the American Society of Cardiology integrating qualitative, semiquantitative, and quantitative measures.[14] The only deviation from this algorithm was in quantitative measurement as the majority of included patients (n=95; 74.8%) had other than a 3-cusp aortic valve with eccentric or multiple jets. A flow convergence method is less accurate in this setting; thus, the stroke volume measurement of regurgitant volume (RV) and a regurgitant fraction (RF) was preferred. In brief, the left ventricular outflow tract area was measured using 3D echocardiography at the annulus during systole and the mitral annulus was measured using 2D echocardiography in 2 perpendicular planes in mid-diastole. The pulsed-wave Doppler signal was recorded at the same level of left ventricular outflow tract and mitral annulus. The RV of AR was calculated from the following equation: $RV = Stroke\,volume_{LVOT} - Stroke\,volume_{Mitral\ annulus}$.[14] Severe AR was defined by the presence of ≥ 4 of the following criteria: flail leaflet, VC width >6 mm, jet width ≥65% of left ventricular outflow tract, large flow convergence, pressure-half-time <200 ms, prominent holodiastolic flow reversal in the descending aorta, and dilated LV with normal function, RV ≥60 mL, and RF ≥50%

Cardiac MRI was performed on a 1.5 Tesla scanner (Magnetom Avanto fit, Siemens). Blood pressure and heart rate were recorded during each examination. A blood sample for hematocrit assessment, needed for extracellular volume calculation (ECV), was drawn just before the examination. All dynamic scans were performed during a breath-hold lasting 10 to 20 s with retrospective electrocardiography-gating. Left ventricular volumes and EF were calculated in a CoreLab using a stack of short-axis steady-state free precession cine sequences (8 mm slice thickness, 0 mm gap) with a thorough correction for the valve position utilizing commercially available software (Segment CMR, Medviso AB 2018, Sweden). Through-plane phase-contrast velocity mapping scans (6 mm slice thickness, 0 mm gap) were performed according to study protocol[15] meticulously perpendicular to blood flow at several levels of the aortic root aiming to be as close as 5 mm above the tips of valve leaflets in systole but avoiding the turbulence. Background velocity offset errors were corrected using the stationary phantom and post-processing correction using software Segment CMR before forward and backward flow calculations. RV and fraction were averaged from 3 measurements. A single breath-hold electrocardiography-triggered phase-sensitive inversion recovery gradient echo sequence was utilized for late gadolinium enhancement 8 to 15 minutes after administration of 0.19 mL/kg of 1-molar gadolinium-based contrast agent (Gadobutrol, GadovistW, Byer, Germany). Modified Look-Locker Inversion recovery sequence (field of view 360×301 mm, matrix 118×256, slice thickness 8 mm, voxel size 1.4 mm×1.4 mm×8 mm, echo time 1.1 ms, repetition time 359 ms, flip angle 35°, bandwidth 1.085 Hz/Pixel) was acquired in basal-to-mid LV short-axis sequence before and 15 minutes after contrast administration for native T1 relaxation time and ECV calculation. A detailed description of the study protocol was published previously.[15,16] The normal value for native T1 relaxation time on the same scanner is 980±22 ms.

Statistical Analysis

Normality distribution of continuous variables was assessed visually with histograms and with the Shapiro-Wilk test. Continuous variables were summarized by using the mean and SD or the median and interquartile range. Categorical variables were presented as frequency counts and percentages. Fisher exact test was used to compare 2 categorical variables, while the Mann-Whitney *U* test was performed for the comparison of 2 continuous ones. Correlation between variables was assessed by Pearson or Spearman test as appropriate. The hazard function was plotted by using spline regression for MRI-derived RV, MRI-derived RF, MRI-derived LV end-diastolic volume index, 3D echocardiography vena contracta area (3D VCA), echocardiography-derived LV global longitudinal strain (GLS), BNP (brain natriuretic peptide), to assess the appropriate GWI cut off points (hazard ratio, 1) for study end point. The Kaplan-Meier analysis and the Log-rank test were used to compare the cumulative incidence of the time-dependent binomial end points between patients with lower and higher MRI-derived RV, MRI-derived RF, MRI-derived LV end-diastolic volume index, BNP, 3D VCA, and transmitral E wave. Cox proportional hazard regression method was used to test the association between baseline variables and end point; results are presented as hazard ratio (95% CI). Proportional hazard assumptions were assessed by Schoenfeld residuals. Univariable and multivariable ROC curves were constructed to derive the area under the curve (AUC) of baseline variables to predict the end point. The backward selection procedure was used for building all multivariate models. The predictive accuracy of these models was tested on an external validation cohort. All statistical tests were considered significant at the $P<0.05$ level. All analyses were performed using the Statistical Package for Social Sciences,

version 25.0 (SPSS, PC version, Chicago, IL) or R software, version 3.6.1 (R Project for Statistical Computing).

RESULTS

Baseline Characteristics

Baseline clinical and imaging characteristics are shown in Tables 1 and 2, respectively. The study sample consisted of 127 patients (age 45±14 years, 84% males). All patients enrolled in the study were asymptomatic, in sinus rhythm, and with preserved LV EF. Using the echocardiography-derived integrative approach, all patients had severe AR, that is, grade III and IV, respectively, in 68 (54%) and 59 (46%) individuals. The cause of AR was a congenitally abnormal bicuspid valve in the majority of patients (n=90; 71%). Four (3%) patients had a history of coronary artery disease. Almost half of the individuals (49%) had hypertension. There were no significant differences in blood pressure and heart rate between the echocardiography and MRI examinations.

Clinical Outcome

During a median follow-up of 1375 (interquartile range, 1041–1783) days, a new indication for AV surgery, that is, study end point, was documented in 41 (32%) participants. The indication for AV surgery was onset of symptoms (n=34; 83%) and LV systolic dysfunction (n=7; 17%). Frequent ventricular ectopy leading to the deterioration of LV function developed in 2 patients. Individuals with versus without end point tended to be older (P=0.10) and were more frequently using thiazide diuretics (P=0.0264). All remaining clinical characteristics including medication were similar (Table 1). Patients with end point showed more advanced LV remodeling as documented by significantly higher BNP, larger LV end-diastolic diameter at echocardiography, LV volumes, and LV mass at MRI (all P<0.05). In contrast, LV EF and

Table 1. Baseline Clinical Characteristics

	Total (n=127)	– End point (n=86)	+ End point (n=41)	*P* value
Age, y	45±14	44±14	49±14	0.10
Male sex, N (%)	107 (84)	73 (85)	34 (83)	0.78
Hypertension, N (%)	60 (47)	38 (45)	22 (54)	0.42
Diabetes, N (%)	6 (5)	5 (6)	1 (2)	0.78
Hyperlipidemia, N (%)	34 (27)	23 (27)	11 (26)	1.00
Smoker, N (%)	20 (16)	16 (19)	4 (10)	0.20
Coronary artery disease, N (%)	4 (3)	3 (3)	1 (2)	1.00
Previous cardiac surgery, N (%)	4 (3)	4 (5)	0 (0)	0.30
Stroke, N (%)	2 (2)	1 (1)	1 (2)	1.00
Aspirin, N (%)	13 (10)	9 (11)	4 (10)	1.00
Oral anticoagulants, N (%)	7 (6)	4 (5)	3 (7)	0.69
ACE inhibitors/ARBs, N (%)	63 (50)	41 (48)	22 (54)	0.59
Beta-blockers, N (%)	31 (24)	21 (24)	10 (24)	1.00
Calcium channel blockers, N (%)	23 (18)	12 (14)	11 (26)	0.14
Thiazide diuretics, N (%)	17 (13)	7 (8)	10 (23)	0.0264
Statins, N (%)	25 (19)	15 (17)	10 (23)	0.48
Height, cm	180±9	180±8	179±9	0.44
Weight, kg	85±14	84±14	85±13	0.58
Systolic blood pressure, mm Hg	135±17	134±16	138±17	0.14
Diastolic blood pressure, mm Hg	71±12	72±11	68±13	0.09
Heart rate, bpm	66±14	65±15	63±11	0.34
Sinus rhythm, N (%)	127 (100)	86 (100)	41 (100)	1.00
Serum creatinine, μmol/L	86±17	86±16	87±18	0.85
Aortic valve morphology				
Trileaflet, N (%)	21 (17)	13 (15)	8 (20)	0.15
Bicuspid, N (%)	90 (71)	65 (76)	25 (61)	
Unicuspid/quadricuspid, N (%)	5 (4)	4 (5)	1 (2)	
Unknown, N (%)	11 (9)	4 (5)	7 (16)	

Values are means±SDs, median (interquartile range), or numbers (percentage). ACE/ARBs indicates angiotensin-converting enzyme/angiotensin receptor blockers.

Table 2. Baseline Imaging Characteristics

	Total (n=127)	− End point (n=86)	+ End point (n=41)	*P* value
LV assessment				
B-natriuretic peptide, ng/L	67 (119)	43 (65)	117 (42)	<0.001
2D ECHO end-diastolic diameter, mm	58±6	57±6	60±6	0.0418
2D ECHO end-systolic diameter, mm	37±5	36±5	38±6	0.16
2D ECHO end-systolic diameter index, mm/m^2	18±3	18±3	18±3	0.29
3D ECHO end-diastolic volume, mL	174±50	168±40	179±54	0.08
3D ECHO end-diastolic volume index, mL/m^2	83±25	81±23	86±23	0.18
3D ECHO end-systolic volume, mL	67±24	65±20	65±28	0.10
3D ECHO end-systolic volume index, mL/m^2	32±11	31±10	31±12	0.32
3D ECHO ejection fraction, %	62±5	62±6	62±6	0.81
2D ECHO global longitudinal strain, %	19±3	19±2	18±2	0.07
Transmitral E wave velocity, cm/s	66±17	68±17	60±14	0.0263
Transmitral E/A wave ratio	1.2±0.5	1.2±0.7	1.1±0.4	0.0289
Septal annular e′, cm/s	9±3	9±3	9±3	0.65
Lateral annular e′, cm/s	12±4	12±4	11±4	0.30
E/e′ ratio	9±3	7±3	8±3	0.67
MRI end-diastolic volume, mL	237±64	217±70	268±71	<0.001
MRI end-diastolic volume index, mL/m^2	116±29	108±24	130±31	<0.001
MRI end-systolic volume, mL	93±33	85±38	107±40	0.0078
MRI end-systolic volume index, mL/m^2	45±15	40±16	52±19	0.0104
MRI ejection fraction, %	61±6	61±7	61±6	0.82
MRI LV mass, g	182±48	172±43	205±50	<0.001
MRI LV mass index, g/m^2	85±24	82±23	99±20	<0.001
MRI native T1 relaxation time, ms	1020±30	1017±31	1025±29	0.12
MRI extracellular volume fraction, %	24±3	24±4	24±2	0.95
Presence of myocardial scar, N (%)	26 (20)	17 (21)	9 (22)	0.92
AR assessment				
Integrative approach				
AR grade IV, N (%)	59 (46)	34 (39)	25 (61)	0.0386
2D ECHO vena contracta width, mm	6.3±1.5	6.1±1.6	6.6±1.5	0.11
Diastolic flow reversal velocity, cm/s	19±4	18±4	21±4	<0.001
2D ECHO regurgitant volume, mL	79±59	73±56	104±64	0.11
2D ECHO regurgitant fraction, %	46±16	45±15	49±16	0.19
3D ECHO vena contracta area, mm^2 (92%)	29±12	25±13	34±14	0.0013
MRI regurgitation volume, mL	47±28	36±24	65±31	<0.001
MRI regurgitation fraction, %	37±16	32±14	46±16	<0.001

Values are means±SDs or numbers (percentage). 2D indicates 2-dimensional; 3D, 3-dimensional; AR, aortic regurgitation; ECHO, echocardiography; LV, left ventricle; and MRI, magnetic resonance imaging.

markers of diffuse myocardial fibrosis were similar. The end point group tended to have lower LV GLS (*P*=0.07) and showed more impaired LV diastolic function (*P*<0.05) than patients without end point (Table 2). We observed a higher prevalence of grade IV AR using an integrative approach, larger 3D VCA, MRI-derived RV, and RF of AR (all *P*<0.05) in the end point group. Out of 41 patients with AV surgery indication, a total of 34 (83%) patients effectively underwent AV surgery, whereas in the remaining ones the surgery was postponed because of patients' refusal or epidemic. Twenty-one (62%) and 13 (38%) patients, respectively, underwent isolated AV surgery and AV surgery plus concomitant aortic root replacement. The AV-sparing surgery was performed in 29% of individuals, while AVR using a bioprosthetic or mechanical valve in 29% or 32%, respectively, and the Ross procedure in 9%. The AV surgery was successful in all patients. Perioperative and 30-day mortality was 0. One patient died 6 months after AV replacement due to early prosthetic infective endocarditis. All the remaining patients were alive at the end of the follow-up. No patient needed redo AV surgery. A total of 32 (78%) surgically treated patients

underwent a follow-up MRI study analyzed in a CoreLab, which showed a significant LV reverse remodeling with a decrease in LVEDVI (123±31 mL/m² vs 78±23 mL/m²; *P*<0.001), LV end-systolic volume index (LVESVI; 48±19 mL/m² vs 36±13 mL/m²; *P*<0.001), and LV mass index (98±22 g/m² vs 75±15 g/m²; *P*<0.001).

Predictors of Clinical Outcome

Figure 1 shows the association between selected parameters and end point using spline curve analysis. In general, indices related to AR assessment versus LV remodeling had a larger area under the curve to identify individuals with future end points (Table 3). In multivariable Cox regression analysis, age, BNP, 3D VCA, MRI-derived LV end-diastolic volume index, RV, and RF were identified as independent predictors of end point (Table 4). However, a combined model including one parameter of AR assessment, one parameter of LV remodeling, and BNP showed significantly higher predictive accuracy than any single parameter alone. Using MRI-derived indices, the largest area under the curve was observed for a combination of either RV (Figure 2A) or RF (Figure 2B) with LVEDVI and BNP. Hazard ratio to predict end point significantly increased with 2 to 3 indices exceeding cutoff values (hazard ratio, 12.45 [95% CI, 2.9–53.38]; *P*=0.0012) compared with only one parameter (hazard ratio, 3.81 [95% CI, 0.81–17.93]; *P*=0.09). At echocardiography,

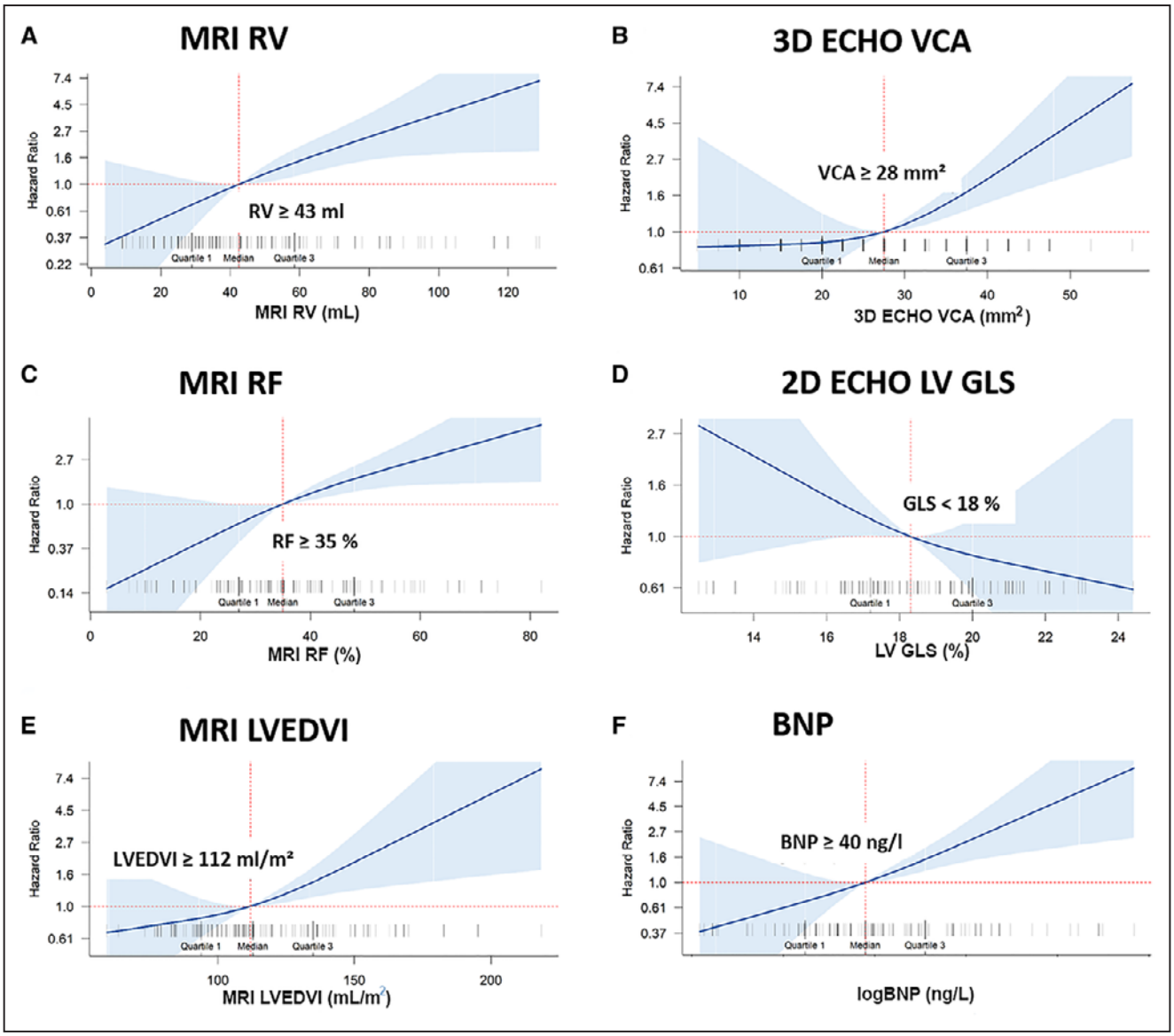

Figure 1. Association between the onset of indication for aortic valve surgery.
A, Magnetic resonance imaging (MRI)-derived regurgitant volume (MRI RV); (**B**) 3-dimensional echocardiography-derived vena contracta area (3D ECHO VCA); (**C**) MRI-derived regurgitant fraction (MRI RF); (**D**) 2-dimensional echocardiography-derived left ventricular (LV) global longitudinal strain (2D ECHO LV GLS); (**E**) MRI-derived LV end-diastolic volume index (MRI LVEDVI); (**F**) Brain natriuretic peptide (BNP). Risk (hazard ratio) increased with MRI RV ≥ 43 ml, MRI RF ≥35%, MRI LVEDVI ≥112 ml/m², 3D ECHO VCA ≥28 mm², 2D ECHO LV GLS <18% and BNP ≥ 40 ng/l.

Table 3. Predictive Accuracy of Selected Parameters to Identify Patients Who Developed AV Surgery Indication

	AUC (95% CI)	Cutoff value	Sensitivity, %	Specificity, %
Age, y	0.61 (0.50–0.72)	45	69	63
BNP, ng/L	0.71 (0.60–0.81)	40	74	63
ECHO LVEDVI, mL/m²	0.58 (0.45–0.71)	92	41	80
2D ECHO GLS, %	0.61 (0.49–0.73)	−17	34	84
Transmitral E wave velocity, cm/s	0.64 (0.53–0.75)	57	50	75
MRI LVEDVI, mL/m²	0.64 (0.51–0.76)	124	59	74
MRI LVESVI, mL/m²	0.61 (0.47–0.74)	54	53	80
MRI LVEDV, mL	0.63 (0.51–0.75)	252	59	66
2D ECHO integrative approach	0.59 (0.49–0.69)	Grade IV AR	59	58
3D VCA, mm²	0.66 (0.54–0.78)	36	50	82
MRI RV, mL	0.71 (0.60–0.81)	45	72	63
MRI RF, %	0.72 (0.62–0.82)	34	78	57

2D indicates 2-dimensional; 3D, 3-dimensional; 3D VCA, 3D echocardiography VCA; AR, aortic regurgitation; AUC, area under the curve; AV, aortic valve; BNP, brain natriuretic peptide; ECHO, echocardiography; GLS, global longitudinal strain; LVEDV, left ventricle end-diastolic volume; LVEDVI, left ventricular end-diastolic volume index; LVESVI, left ventricular end-systolic volume index; MRI, magnetic resonance imaging; MRI LVEDVI, MRI-derived LV end-diastolic volume index; MRI RF, MRI-derived RF; MRI RV, MRI-derived RV; RF, regurgitant fraction; RV, regurgitant volume; and VCA, vena contracta area.

a combined model using 3D VCA, 2D GLS (Figure 3A), or transmitral E wave (Figure 3B), and BNP yielded the largest area under the curve, which was, nevertheless, smaller than that of the MRI-derived models. Figure 4 shows an example of the model combining MRI- and echocardiography-derived parameters with BNP.

Validation in the External Test Cohort

The test cohort included 100 consecutive patients with 38 end points during a median follow-up of 1252 (interquartile range, 902–1534) days. The baseline characteristics between the derivation and the validation cohort were similar (Table S1). Performance of models combining MRI- and/or echocardiography-derived indices and natriuretic peptides to identify patients with early disease progression remained robust in the validation cohort (Table S2). MRI-based models showed higher performance than echocardiography-derived models (AUC, 0.85–0.87 versus 0.72–0.75, respectively).

Reproducibility

Intraobserver and interobserver reproducibility was tested on 10 randomly selected patients' echocardiography and MRI datasets for MRI-derived RV and RF, LVEDVI and LVESVI, 3D VCA, 2D VC width, GLS, native T1 relaxation time using intraclass correlation coefficient. The intraobserver and interobserver intraclass correlation coefficient, respectively, was >0.94 and >0.82 suggesting high reproducibility.

DISCUSSION

In asymptomatic patients with severe AR, preserved LV EF, and LV end-systolic diameter, we have demonstrated

Table 4. Independent Predictors of Aortic Valve Surgery Indication

	Univariable analysis		Multivariable analysis	
	HR (95% CI)	*P* value	HR (95% CI)	*P* value
Age	1.05 (1.00–1.10)	0.0474	1.02 (0.93–1.12)	0.34
Log BNP	4.14 (2.05–8.35)	0.0098	4.67 (1.91–11.31)	<0.001
2D GLS	0.87 (0.75–1.00)	0.05		
Transmitral E wave velocity	0.98 (0.96–1.00)	0.05		
3D VCA	1.05 (1.02–1.09)	<0.001	1.04 (1.01–1.07)	0.0086
MRI LVEDVI	1.02 (1.01–1.03)	0.0043	1.01 (0.99–1.02)	0.55
MRI RV	1.02 (1.01–1.04)	<0.001	1.02 (1.01–1.03)	0.0352
MRI RF	1.04 (1.02–1.06)	<0.001	1.04 (1.01–1.06)	0.0071

2D indicates 2-dimensional; 3D VCA, 3-dimensional echocardiography vena contracta area; BNP, brain natriuretic peptide; GLS, global longitudinal strain; HR, hazard ratio; LVEDVI, left ventricular end-diastolic volume index; MRI, magnetic resonance imaging; MRI LVEDVI, MRI-derived LV end-diastolic volume index; MRI RF, MRI-derived RF; MRI RV, MRI-derived RV; RF, regurgitant fraction; and RV, regurgitant volume.

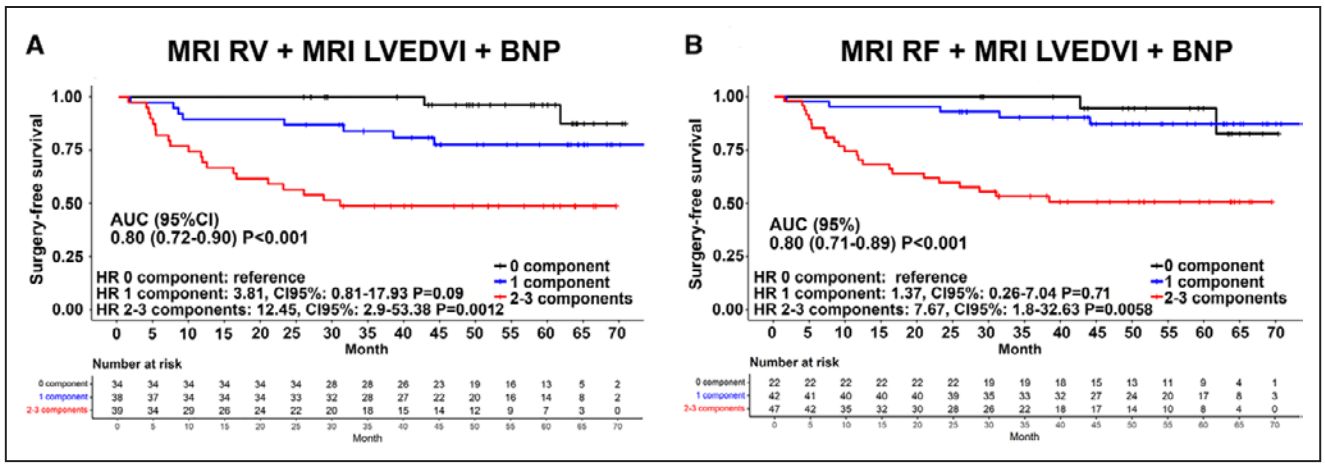

Figure 2. Magnetic resonance imaging (MRI) model combining MRI-derived regurgitant volume (MRI RV; A) or regurgitant fraction (MRI RF; B), left ventricular end-diastolic volume index (LVEDVI) and BNP (brain natriuretic peptide) show a larger area under the curve than any single parameter alone (*P*<0.001).

Hazard ratio (HR) to predict end point significantly increased with 2-3 parameters exceeding cutoff values, derive by using spline curve analysis, compared to any parameter alone. AUC indicates area under curve.

that the multiparametric strategy combining 2 imaging parameters, for example, one to quantify AR severity and another one to assess LV remodeling or subtle LV dysfunction, with natriuretic peptide showed higher accuracy than any parameter alone to identify individuals with early disease progression. In general, parameters of AR severity assessment performed better than indices of LV remodeling or function. Models involving either MRI alone or in combination with echocardiography plus natriuretic peptides showed higher accuracy than models including only echocardiography and natriuretic peptides. MRI showed added value mostly for AR quantification where it outperformed all standard echocardiography measurements with exception of 3D VCA, which is, however, not routinely used. These advocates for the more liberal implementation of MRI in an asymptomatic patient with severe AR at the early stage of the disease.

Management of Severe AR

Chronic AR results in a combined volume and pressure overload of the LV[17,18] leading to LV dilatation, increase in LV mass and, if untreated, LV decompensation resulting in heart failure and/or premature death. In contrast, timely surgical treatment is associated with significant reverse remodeling and perhaps normalization of LV structure and function.[19] However, the currently recommended approach integrating echocardiography-derived AR quantification, LV EF, and LV end-systolic diameter is insensitive to identifying patients with early adverse clinical course.[20,21] This has been demonstrated by several large studies showing, in mainly asymptomatic patients with severe AR and normal LV EF, better both preoperative and postoperative survival in individuals with LV end-systolic diameter indexed (I) below the currently recommended threshold for AV intervention.[10–12,20,22] Corroborating these results,

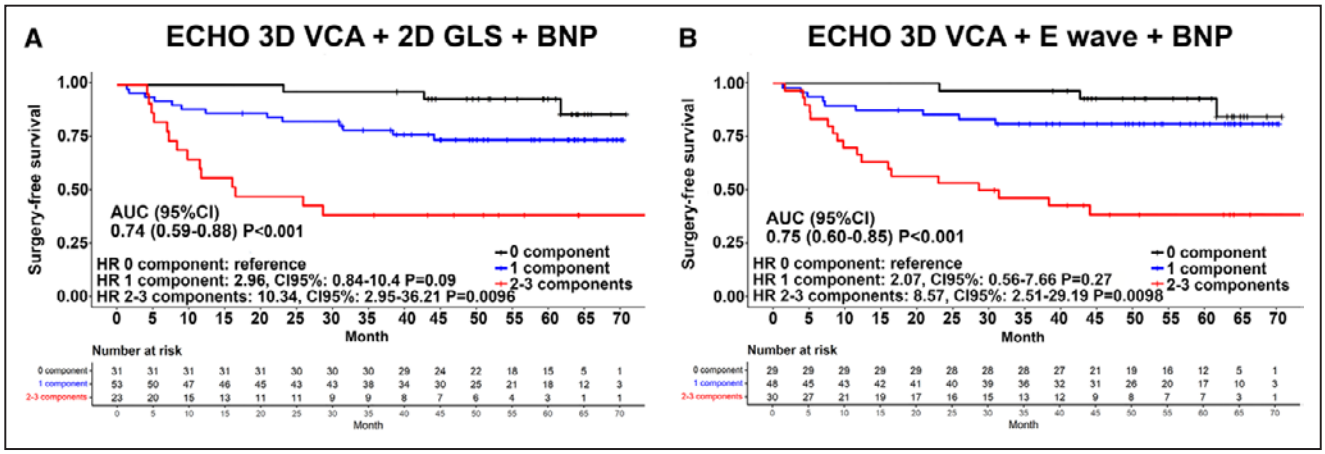

Figure 3. Echocardiography (ECHO) model including ECHO-derived 3-dimensional vena contracta area (ECHO 3D VCA), 2-dimensional global longitudinal strain (2D GLS; A) or transmitral E wave (B) and BNP (brain natriuretic peptide) shows a larger area under the curve than any single parameter alone (*P*<0.001).

Hazard ratio (HR) to predict end point significantly increased with 2–3 parameters exceeding cutoff values, derive by using spline curve analysis, compared to any parameter alone. AUC indicates area under curve.

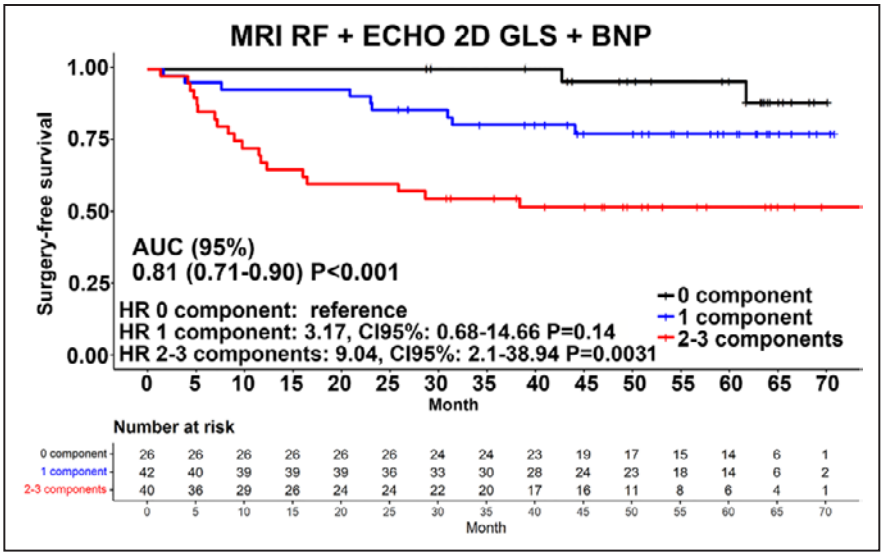

Figure 4. Multimodality model including magnetic resonance imaging–derived regurgitant fraction (MRI RF), 2- dimensional echocardiography-derived global longitudinal strain (ECHO 2D GLS) and BNP (brain natriuretic peptide). AUC indicates area under curve; and HR, hazard ratio.

in the present study, a significant proportion of asymptomatic patients with normal LV EF and ESDI <25 mm/m^2 developed symptoms during relatively a short time. Patients with early disease decompensation had a higher prevalence of grade IV AR per echocardiography integrative approach with a relatively low area under the curve of 0.59 to predict end point. In contrast, MRI-derived RF (AUC, 0.72) and 3D echocardiography VCA (AUC, 0.66) showed the highest accuracy to predict the onset of AV surgery indication. Consistently with previously published data of Myerson et al, [3] Harris et al,[23] and Vejpongsa et al,[24] the prognostically valuable thresholds of MRI-derived RV >45 mL and RF >34% were much lower (Myerson RV >42 mL, RF >33%; Harris RV >50 mL, RF ≥37%; and Vejpongsa RF >35%)[3,23,24] then traditional echocardiography cut off values of severe AR (RV ≥60 mL, RF ≥50%).[6,14] Indices of LV remodeling, both at echocardiography and MRI, had lower predictive accuracy (AUC, 0.58–0.64) to identify early disease decompensation probably reflecting the very early AR stage in our study. In recent studies, myocardial scar, GLS, increased ECV index for body surface area, and BNP have been associated with the early adverse course of reduced survival before or after AV surgery.[7,13,24–28] These markers showed a relatively low predictive value in our patient group comprising a rather younger population with fewer comorbidities at early disease stage. Yet, we observed impaired GLS, diastolic function, the more frequent presence of myocardial scar in late gadolinium enhancement, lower values of T1 relaxation time, and increased BNP in patients with end points implying subtle myocardial damage. In addition, in the present study, 24 patients who underwent a perioperative myocardial biopsy, showed an increased extent of myocardial fibrosis of 16±7%, whereas the normal range is 1% to 7%.[19,29,30] Thus, optimal timing of AV intervention is crucial to prevent irreversible changes and to achieve an optimal long-term outcome. In this regard, single indices of AR quantification showed independent predictive value to identify the onset of symptoms or LV dysfunction, yet their performance remains suboptimal (AUC, 0.72) to guide clinical decision-making between early intervention or watchful waiting strategy. Therefore, a combination of several indices may provide more robust results. In the present study, a simple model including 3 parameters showed a significantly larger area under the curve to predict the end point than any single parameter alone. This suggests that a multiparametric strategy may improve risk stratification in the early stage of AR and facilitate patient management.

Limitations

Cardiac MRI showed the best predictive accuracy out of all tested imaging and biochemical markers in the present study. However, we have to admit that this cardiac imaging method is not routinely available to all cardiology centers. The method is costly and requires expertise and tight collaboration of technologists, cardiologists, and radiologists.

The majority of patients were under 50 years of age, and 71% had a bicuspid AV with frequently presented an eccentric regurgitant jet making the conventional echocardiography AR quantification difficult. This might explain that the best predictive echocardiography marker was 3D VCA instead of traditional echocardiography parameters. Moreover, 3D VCA is not routinely measured in clinical practice and requires a certain level of expertise. However, both availability of MRI/3D echocardiography equipment and expertise within heart valve centers is growing. Thus, these limitations may not significantly hamper the generalizability of these results.

Conclusions

Asymptomatic patients with severe AR, not yet fulfilling guidelines indication for AV intervention, may be at

risk of early disease decompensation. This suggests that the current approach integrating echocardiography-derived AR assessment and LV remodeling is rather insensitive to detecting individuals in need of early AV intervention. In the present study, multimodality and multiparametric model consisting of 3 indices, i.e., one parameter of MRI-derived AR quantification plus one parameter of either MRI- or echocardiography-derived LV dilatation or dysfunction, plus natriuretic peptides, showed high accuracy to identify early disease decompensation. The performance of these models remained robust also in the external validation cohort. This suggests that MRI assessment should be implemented in eligible patients with asymptomatic moderate or severe AR to facilitate clinical decision-making between early AV intervention versus watchful waiting with regular visits at the valve clinic.

ARTICLE INFORMATION

Received September 22, 2022; accepted November 7, 2022.

Affiliations

Cardiothoracic Surgery Department, Na Homolce Hospital, Czech Republic (R.K., I.S., S.C.). Department of Cardiology, Royal Vinohrady University Hospital, Czech Republic (H.L.). Department of Cardiology (Z.H.) and Department of Cardiovascular Surgery (J.H.), General University Hospital, Prague, Czech Republic. 1st Department Medicine - Cardioangiology, University Hospital Hradec Králové, Sokolská Czech Republic (K.M.). Department of Cardiac Surgery, University Hospital Hradec Králové, Hradec Králové, Czech Republic (M.T., J.V.). Institute for Clinical and Experimental Medicine, Prague, Czech Republic (J.M.). Cardiovascular Center Aalst, Belgium (T.M., C.D.C., M.P.). Division of Clinical Pharmacology, Department of Pharmacology, Showa University, Tokyo, Japan (T.M.). Department of Advanced Biomedical Sciences, University Federico II, Naples, Italy (C.D.C.).

Acknowledgments

We are grateful to Dr Marek Malý (National Institute of Public Health, Prague, Czech Republic) for the statistical analysis, and to Prof. David Sedmera (First Faculty of Medicine, Institute of Anatomy, Charles University in Prague) and Matěj Kočka (Medical student of Trinity College Dublin, Ireland) for their invaluable myocardial histology analysis.

Sources of Funding

This study was supported by the Ministry of Health of the Czech Republic 17-28265A.

Disclosures

None.

Supplemental Material

Tables S1–S2

REFERENCES

1. Baumgartner H, Falk V, Bax JJ, De Bonis M, Hamm C, Holm PJ, Iung B, Lancellotti P, Lansac E, Rodriguez Muñoz D, et al. 2017 ESC/EACTS Guidelines for the management of valvular heart disease. *Eur Heart J*. 2017;38:2739–2791. doi: 10.1093/eurheartj/ehx391
2. Iung B. A prospective survey of patients with valvular heart disease in Europe: the Euro Heart Survey on Valvular Heart Disease. *Eur Heart J*. 2003;24:1231–1243. doi: 10.1016/s0195-668x(03)00201-x
3. Myerson SG, d'Arcy J, Mohiaddin R, Greenwood JP, Karamitsos TD, Francis JM, Banning AP, Christiansen JP, Neubauer S. Aortic regurgitation quantification using cardiovascular magnetic resonance: association with clinical outcome. *Circulation*. 2012;126:1452–1460. doi: 10.1161/CIRCULATIONAHA.111.083600
4. Nishimura RA, Otto CM, Bonow RO, Carabello BA, Erwin JP, Fleisher LA, Jneid H, Mack MJ, McLeod CJ, O'Gara PT et al. 2017 AHA/ACC Focused Update of the 2014 AHA/ACC guideline for the management of patients with valvular heart disease: a report of the american college of cardiology/american heart association task force on clinical practice guidelines. *Circulation*. 2017;135:e1159–e1195. doi: 10.1161/CIR.0000000000000503
5. Nkomo VT, Gardin JM, Skelton TN, Gottdiener JS, Scott CG, Enriquez-Sarano M. Burden of valvular heart diseases: a population-based study. *Lancet*. 2006;368:1005–1011. doi: 10.1016/S0140-6736(06)69208-8
6. Steeds RP, Myerson SG. Imaging assessment of mitral and aortic regurgitation: current state of the art. *Heart*. 2020;106:1769–1776. doi:10.1136/heartjnl-2019-316216
7. Alashi A, Khullar T, Mentias A, Gillinov AM, Roselli EE, Svensson LG, Popovic ZB, Griffin BP, Desai MY. Long-term outcomes after aortic valve surgery in patients with asymptomatic chronic aortic regurgitation and preserved lvef: impact of baseline and follow-up global longitudinal strain. *JACC Cardiovasc Imaging*. 2020;13:12–21. doi: 10.1016/j.jcmg.2018.12.021
8. Desai MY. Aortic regurgitation: are we operating too late? *Ann Cardiothorac Surg*. 2019;8:39092–39392. doi: 10.21037/acs.2019.0
9. Dujardin KS, Enriquez-Sarano M, Schaff HV, Bailey KR, Seward JB, Tajik AJ. Mortality and morbidity of aortic regurgitation in clinical practice. A long-term follow-up study. *Circulation*. 1999;99:1851–1857. doi: 10.1161/01.cir.99.14.1851
10. de Meester C, Gerber BL, Vancraeynest D, Pouleur A-C, Noirhomme P, Pasquet A, de Kerchove L, El Khoury G, Vanoverschelde J-L. Do guideline-based indications result in an outcome penalty for patients with severe aortic regurgitation? *JACC Cardiovasc Imaging*. 2019;12:2126–2138. doi: 10.1016/j.jcmg.2018.11.022
11. Mentias A, Feng K, Alashi A, Rodriguez LL, Gillinov AM, Johnston DR, Sabik JF, Svensson LG, Grimm RA, Griffin BP, at al. Long-term outcomes in patients with aortic regurgitation and preserved left ventricular ejection fraction. *J Am Coll Cardiol*. 2016;68:2144–2153. doi: 10.1016/j.jacc.2016.08.045
12. Yang L-T, Michelena HI, Scott CG, Enriquez-Sarano M, Pislaru SV, Schaff HV, Pellikka PA. Outcomes in chronic hemodynamically significant aortic regurgitation and limitations of current guidelines. *J Am Coll Cardiol*. 2019;73:1741–1752. doi: 10.1016/j.jacc.2019.01.024
13. Malahfji M, Senapati A, Tayal B, Nguyen DT, Graviss EA, Nagueh SF, Reardon MJ, Quinones M, Zoghbi WA, Shah DJ. myocardial scar and mortality in chronic aortic regurgitation. *J Am Heart Assoc*. 2020;9:e018731. doi: 10.1161/JAHA.120.018731
14. Zoghbi WA, Adams D, Bonow RO, Enriquez-Sarano M, Foster E, Grayburn PA, Hahn RT, Han Y, Hung J, Lang RM, et al. recommendations for noninvasive evaluation of native valvular regurgitation: a report from the american society of echocardiography developed in collaboration with the society for cardiovascular magnetic resonance. *J Am Soc Echocardiogr*. 2017;30:303–371. doi: 10.1016/j.echo.2017.01.007
15. Kočková R, Línková H, Hlubocká Z, Pravečková A, Polednová A, Súkupová L, Bláha M, Malý J, Honsová E, Sedmera D, et al. new imaging markers of clinical outcome in asymptomatic patients with severe aortic regurgitation. *J Clin Med*. 2019; 8:1654. doi: 10.3390/jcm8101654
16. Kockova R, Kacer P, Pirk J, Maly J, Sukupova L, Sikula V, Kotrc M, Barciakova L, Honsova E, Maly M, et al. Native T1 relaxation time and extracellular volume fraction as accurate markers of diffuse myocardial fibrosis in heart valve disease - comparison with targeted left ventricular myocardial biopsy. *Circ J*. 2016;80:1202–1209. doi: 10.1253/circj.CJ-15-1309
17. Lee JK, Franzone A, Lanz J, Siontis GC, Stortecky S, Gräni C, Roost E, Windecker S, Pilgrim T. Early detection of subclinical myocardial damage in chronic aortic regurgitation and strategies for timely treatment of asymptomatic patients. *Circulation*. 2018;137:184–196. doi: 10.1161/CIRCULATIONAHA.117.0298
18. Carabello BA. The relationship of left ventricular geometry and hypertrophy to left ventricular function in valvular heart disease. *J Heart Valve Dis*. 1995;4 Suppl 2:S132–138; discussion S138-139. doi: 10.1291/hypres.25.191
19. Krayenbuehl HP, Hess OM, Monrad ES, Schneider J, Mall G, Turina M. Left ventricular myocardial structure in aortic valve disease before, intermediate, and late after aortic valve replacement. *Circulation*. 1989;79:744–755. doi: 10.1161/01.cir.79.4.744
20. Vahanian A, Beyersdorf F, Praz F, Milojevic M, Baldus S, Bauersachs J, Capodanno D, Conradi L, De Bonis M, De Paulis R, et al. 2021 ESC/EACTS guidelines for the management of valvular heart disease. *Eur Heart J*. 2022;43:561–632. doi: 10.1093/eurheartj/ehab395

21. Otto CM, Nishimura RA, Bonow RO, Carabello BA, Erwin JP, Gentile F, Jneid H, Krieger EV, Mack M, McLeod C, O'Gara PT, Rigolin VH, Sundt TM, Thompson A, Toly C. 2020 ACC/AHA guideline for the management of patients with valvular heart disease: a report of the american College of Cardiology/American Heart Association Joint Committee on Clinical Practice Guidelines. *Circulation*. 2021;143:e72–e227. doi: 10.1161/CIR.0000000000000923
22. Detaint D, Messika-Zeitoun D, Maalouf J, Tribouilloy C, Mahoney DW, Tajik AJ, Enriquez-Sarano M. Quantitative echocardiographic determinants of clinical outcome in asymptomatic patients with aortic regurgitation: a prospective study. *JACC Cardiovasc Imaging*. 2008;1:1–11. doi: 10.1016/j.jcmg.2007.10.008
23. Harris AW, Krieger EV, Kim M, Cawley PJ, Owens DS, Hamilton-Craig C, Maki J, Otto CM. Cardiac magnetic resonance imaging versus transthoracic echocardiography for prediction of outcomes in chronic aortic or mitral regurgitation. *Am J Cardiol*. 2017;119:1074–1081. doi: 10.1016/j.amjcard.2016.12.017
24. Vejpongsa P, Xu J, Quinones MA, Shah DJ, Zoghbi WA. Differences in cardiac remodeling in left-sided valvular regurgitation. *JACC Cardiovasc Imaging*. 2022;15:1730–1741. doi: 10.1016/j.jcmg.2022.05.006
25. Kammerlander AA, Wiesinger M, Duca F, Aschauer S, Binder C, Zotter Tufaro C, Nitsche C, Badre-Eslam R, Schönbauer R, Bartko P, et al. Diagnostic and prognostic utility of cardiac magnetic resonance imaging in aortic regurgitation. *JACC Cardiovasc Imaging*. 2019;12:1474–1483. doi: 10.1016/j.jcmg.2018.08.036
26. Weber M, Hausen M, Arnold R, Moellmann H, Nef H, Elsaesser A, Mitrovic V, Hamm C. Diagnostic and prognostic value of N-terminal pro B-type natriuretic peptide (NT-proBNP) in patients with chronic aortic regurgitation. *Int J Cardiol*. 2008;127:321–327. doi: 10.1016/j.ijcard.2007.07.174
27. Pizarro R, Bazzino OO, Oberti PF, Falconi ML, Arias AM, Krauss JG, Cagide AM. Prospective validation of the prognostic usefulness of b-type natriuretic peptide in asymptomatic patients with chronic severe aortic regurgitation. *J Am Coll Cardiol*. 2011;58:1705–1714. doi: 10.1016/j.jacc.2011.07.016
28. Senapati A, Malahfji M, Debs D, Yang EY, Nguyen DT, Graviss EA, Shah DJ. Regional replacement and diffuse interstitial fibrosis in aortic regurgitation. *JACC Cardiovasc Imaging*. 2021;14:2170–2182. doi: 10.1016/j.jcmg.2021.04.028
29. Tanaka M, Fujiwara H, Onodera T, Wu DJ, Hamashima Y, Kawai C. Quantitative analysis of myocardial fibrosis in normals, hypertensive hearts, and hypertrophic cardiomyopathy. *Br Heart J*. 1986;55:575–581. doi: 10.1136/hrt.55.6.575
30. Meckel CR, Wilson JE, Sears TD, Rogers JG, Goaley TJ, McManus BM. Myocardial fibrosis in endomyocardial biopsy specimens: do different bioptomes affect estimation? *Am J Cardiovasc Pathol*. 1989;2:309–313. PMID: 2789804

J. Kroupa et al.

A pilot randomised trial of catheter-directed thrombolysis or standard anticoagulation for patients with intermediate-high risk acutepulmonary embolism

EuroIntervention
Impact Factor: 7.728

EuroIntervention 2022;18:e639-e646 published online ahead of print May 2022 ■ published online e-edition October 2022

A pilot randomised trial of catheter-directed thrombolysis or standard anticoagulation for patients with intermediate-high risk acute pulmonary embolism

Josef Kroupa[1]*, MD, PhD; Michal Buk[2], MD; Jiri Weichet[2], MD, PhD; Hana Malikova[2], MD, PhD; Lucie Bartova[1], MSc; Hana Linkova[1], MD, PhD; Oana Ionita[1], MD; Martin Kozel[1], MD, PhD; Zuzana Motovska[1], MD, PhD; Viktor Kocka[1], MD, PhD

1. Department of Cardiology, Third Faculty of Medicine, Charles University, University Hospital Královské Vinohrady, Prague, Czech Republic; 2. Department of Radiology, Third Faculty of Medicine, Charles University, University Hospital Královské Vinohrady, Prague, Czech Republic

KEYWORDS

- miscellaneous
- pulmonary embolism
- pulmonary hypertension
- thrombus-containing lesion

Abstract

Background: Intermediate-high risk acute pulmonary embolism (PE) remains associated with substantial mortality despite anticoagulation therapy.

Aims: The aim of this randomised pilot study was to compare catheter-directed thrombolysis to standard anticoagulation therapy.

Methods: Intermediate-high risk acute PE patients were admitted to a tertiary care centre (November 2019 to April 2021) and randomised in a 1:1 ratio to catheter-directed thrombolysis (CDT) or standard anticoagulation. Two catheters were used for the infusion of alteplase (1 mg/hr/catheter; total dose 20 mg) in the CDT group. The primary efficacy endpoint targeted improvement of right ventricular (RV) function, a decrease in pulmonary pressure, and a reduction of thrombus burden.

Results: Twenty-three patients were included (12 in the CDT group and 11 in the standard care group). The primary efficacy endpoint was achieved more frequently in the CDT group than in the standard care group (7 of 12 patients vs 1 of 11 patients, p=0.0004). An RV/left ventricular ratio reduction ≥25% (evident on computed tomography angiography) was achieved in 7 of 12 patients in the CDT group vs 2 of 11 patients in the standard care group (p=0.03). A systolic pulmonary artery pressure decrease of ≥30% or normotension at 24 hrs after randomisation was present in 10 of 12 patients in the CDT group vs 2 of 11 patients in the standard care group (p=0.001). There was no intracranial or life-threatening bleeding (type 5 or 3c bleeding, according to the Bleeding Academic Research Consortium classification).

Conclusions: CDT for intermediate-high risk acute PE appears to be safe and effective. Further research is warranted to assess clinical endpoints.

**Corresponding author: Department of Cardiology, Third Faculty of Medicine, Charles University, University Hospital Královské Vinohrady, Šrobárova 50, 10034 Prague, Czech Republic. E-mail: josef.kroupa@fnkv.cz*

SUBMITTED ON 10/12/2021 - REVISION RECEIVED ON 1st 21/02/2022 / 2nd 26/03/2022 - ACCEPTED ON 19/04/2022

DOI: 10.4244/EIJ-D-21-01080

Abbreviations

CDT	catheter-directed thrombolysis
CTA	computed tomography angiography
LMWH	low-molecular-weight heparin
LV	left ventricle
PE	pulmonary embolism
PESI	pulmonary embolism severity index
RV	right ventricle
sPAP	systolic pulmonary artery pressure
SPESI	simplified pulmonary embolism severity index
USAT	ultrasound-assisted local thrombolysis

Introduction

Acute pulmonary embolism (PE) is a common and life-threatening condition (60/100,000 population annually)[1] that is associated with high mortality in certain subgroups[2]. It is essential to identify patients at high risk of early death when selecting the optimal therapeutic management. The current European Society of Cardiology guidelines for the diagnosis and management of acute PE implement risk stratification based on haemodynamic instability and the assessment of other prognostic criteria (principally right ventricular [RV] dysfunction) and other potentially aggravating factors (e.g., comorbidities)[3]. Intermediate-high risk patients constitute one subgroup of acute PE patients, in which the early mortality rate is 6.0-7.7%[4]. Previous efforts to decrease mortality in this subgroup via systemic administration of thrombolytic agents have failed; such treatments were associated with an increased rate of extra- and intracranial bleeding[5,6]. Thus, systemic thrombolysis is not recommended for such patients, and anticoagulation remains the mainstay of acute PE therapy without any progress over the last several decades.

CATHETER-DIRECTED THROMBOLYSIS: THE RATIONALE

Catheter-directed thrombolysis (CDT) in the treatment of patients with acute PE seeks to rapidly reduce the thrombotic load that obstructs the pulmonary arteries, while improving RV function. RV dysfunction is a major predictor of poor prognosis in such patients[7]. Low-dose thrombolytic therapy does not appear to be associated with an increased risk of intracranial bleeding[8-10]. Ultrasound-assisted local thrombolysis (USAT) was recently introduced; it has yielded promising results but is expensive and, thus, infrequently used[9-11]. Simple CDT (i.e., without ultrasound) is potentially a low-cost alternative[12] with similar efficacy, as suggested by the SUNSET sPE Trial[13]. Data from prospective randomised trials comparing CDT to anticoagulation alone are lacking[14].

The main goal of our randomised pilot study was to introduce a safe and simple method of CDT in the treatment of patients with intermediate-high risk acute PE and to compare it to a standard anticoagulation therapy.

Methods

STUDY POPULATION AND DESIGN

Patients >18 years of age with acute PE, who were admitted to our tertiary care centre from November 2019 to April 2021, were enrolled if they met the inclusion criteria but not the exclusion criteria **(Table 1)**. All patients provided written informed consent to participate. The study was approved by our local ethics committee and adhered to the tenets of the Declaration of Helsinki.

Table 1. Inclusion and exclusion criteria.

Inclusion criteria
1. Age >18 years
2. Computed tomography angiography (CTA)-verified proximal* PE AND symptom onset <14 days prior.
3. Intermediate-high risk PE with a SPESI score ≥1 AND RV dysfunction** AND an elevated biomarker *** (hs-troponin I or NT-proBNP) level.
Exclusion criteria
1. Active clinically significant bleeding.
2. Any haemorrhagic stroke OR a recent (<6 months) ischaemic stroke/transient ischaemic attack.
3. Recent (<3 months) cranial trauma OR another active intracranial/intraspinal process.
4. Major surgery within 7 days prior.
5. RV/LV ratio <0.7 on transthoracic echocardiography or CTA.
6. Active malignancy OR other severe illness with expected survival <2 years.
7. Haemoglobin level <80 g/l; international normalised ratio >2.0, platelet count ≤100×10^9; creatinine level >200 µmol/l.
8. Pregnant or breastfeeding, fertility without previous exclusion of gravidity.
9. Allergic to thrombolytics or heparin or low-molecular-weight heparin (LMWH), contrast allergy, a history of heparin-induced thrombocytopaenia.
10. Participation in another clinical trial.
*A perfusion defect in at least one main or one lobar pulmonary artery evident on CTA. **RV/LV ratio ≥0.9 on transthoracic echocardiography or CTA. ***hs-troponin I (TnI) >53 ng/l (men) or >34 ng/l (women); NT-proBNP level >600 pg/ml. LV: left ventricular; PE: pulmonary embolism; RV: right ventricular; SPESI: simplified pulmonary embolism severity index

After CDT in five patients (feasibility evaluation), all subsequent patients were randomised using a simple envelope method to CDT and standard care (anticoagulation only) in a 1:1 ratio.

CDT

All procedures were performed by experienced interventional cardiologists (V. Kocka, J. Kroupa). All procedures were performed as soon as possible, but within normal working hours. After the exclusion of deep vein thrombosis via ultrasound or computed tomography (CT), venous access was obtained under ultrasound guidance (via the common femoral vein) and a double-lumen 8 Fr introducer was inserted (Fast-Cath Duo Hemostasis Introducer 8 Fr; St. Jude Medical/Abbott). The pulmonary thrombus was crossed using a standard diagnostic catheter (Radifocus Optitorque TIG 4 Fr; Terumo) by employing either a standard soft J-wire (EMERALD Guidewire, Exchange J-Tip 0.81 mm, 260 cm; Cordis) or a hydrophilic wire (Radifocus Guidewire M, Stiff type [angled]; Terumo). Thrombolytic catheters (Cragg-McNamara

Valved Infusion Catheter 4 Fr; Medtronic) were placed in each of the right and left interlobar pulmonary arteries with a short overlap in the main pulmonary artery. The catheters featured a 10 cm infusion zone; thus, thrombolytic concentrations were high. Fused computed tomography angiography (CTA) and real-time fluoroscopy were used to guide the catheter placement; no contrast was employed. After the catheter placement, a continuous infusion of alteplase (Actilyse; Boehringer Ingelheim) at 1 mg/hr/catheter was commenced and continued for 10 hrs (total dose 20 mg). Intravenous unfractionated heparin was continued to a target activated partial thromboplastin time (aPTT) of 50-60 secs. After the local thrombolysis was complete, the catheters were removed and anticoagulation with unfractionated heparin (without a bolus) was continued to a target aPTT of 70-90 secs. The 8 Fr sheath was removed from the femoral vein 60 mins after the alteplase infusion had ended, and the access site was manually compressed for 10 min.

ANTICOAGULATION

Before randomisation, all patients received intravenous unfractionated heparin (to a target aPTT of 70-90 secs) or subcutaneous low-molecular-weight heparin (LMWH; the full therapeutic dose). For patients in the CDT group, the anticoagulation treatment was as described above; among CDT patients who received LMWH, the procedure was postponed for 8 hrs after the last dose of LMWH. Patients in the standard care group continued therapeutic anticoagulation with either unfractionated heparin or LMWH.

CTA, ECHOCARDIOGRAPHY AND LABORATORY TESTS

Diagnostic CTA was a component of routine clinical care. A second CTA was performed 48 hrs after randomisation in both groups. All CTA were performed in the Department of Radiology, University Hospital Královské Vinohrady, using a Somatom Drive and a Somatom Definition AS (both Siemens). CT scans were acquired using a standardised protocol that employed 60-100 ml of contrast fluid (Iomeron 400; Bracco). Acquisition was not electrocardiogram (ECG)-gated. All CT measurements were performed by experienced radiologists and a biomedical engineer (J. Weichet, M. Buk, L. Bartova) who had been blinded to group assignment, using proprietary Siemens software and Fluoro-CT software (Circle Cardiovascular Imaging, version 3.2).

RV AND LV DIAMETER MEASUREMENT

Using Fluoro-CT 3D reconstruction software, the standard four-chamber view was identified. The distance between the atrioventricular groove and the left ventricular apex was measured; the basal third of the interventricular septum was identified **(Figure 1A)**. At this point, the LV and RV diameters were measured in the plane perpendicular to the mid-septum in both the short-axis and four-chamber views **(Figure 1B)**. The severity of the pulmonary artery tree obstruction was scored using the Qanadli method[15].

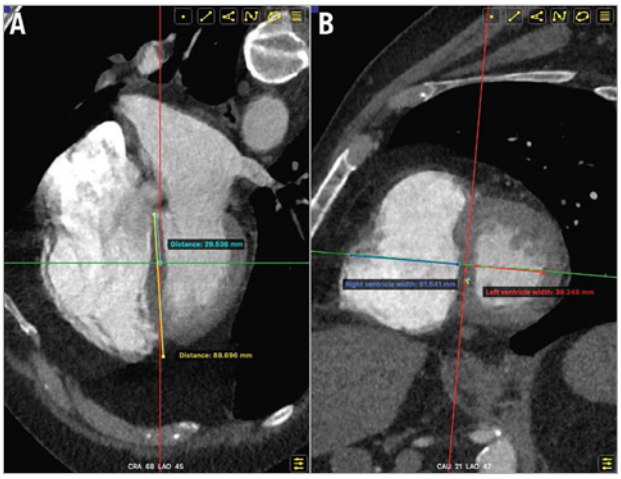

Figure 1. *RV and LV measurements via CTA. A) Identification of the basal one-third of the interventricular septum in the four-chamber view. B) Measurement of RV and LV diameters in the plane perpendicular to the mid-septum on both the short-axis and four-chamber views. CTA: computed tomography angiography; LV: left ventricle; RV: right ventricle*

Echocardiography was performed at the time of randomisation, then repeated 24 hrs later. Standard measurements were performed in accordance with the European Society of Cardiology recommendations[16,17]. The subannular RV/LV ratio was derived as suggested by the ULTIMA study[10]; in brief, end-diastolic dimensions of the RV and LV were measured 1 cm above the tricuspid annular plane. All measurements were performed in our local echo lab by experienced cardiologists (H. Linkova, O. Ionita) who had been blinded to group assignment.

Laboratory tests were performed at the time of randomisation (creatinine, troponin hsTnI, and NT-proBNP; a blood count; and the aPTT and international normalised ratio [INR] coagulation tests) and 48 hrs after randomisation. In CDT patients, additional tests (blood count, coagulation parameters) were performed 6 hrs after the commencement of local thrombolysis.

ENDPOINTS

PRIMARY ENDPOINTS

1) Effectiveness of CDT, defined as improved RV function (where at least two of the following criteria were met):
   a. Reduction of the RV/LV ratio by 25% between admission and 48 hrs post-randomisation, as revealed by CTA.
   b. Reduction of the systolic pulmonary artery pressure (sPAP) by 30% from baseline or attainment of normotension (≤35 mmHg sPAP), as revealed by echocardiography at 24 hrs post-randomisation.
   c. Reduction of the Qanadli score[15] by 30% between admission and 48 hrs post-randomisation, as revealed by CTA.
2) Safety of CDT, defined as the absence of intracranial or life-threatening bleeding according to the Bleeding Academic Research Consortium (BARC) classification[18] (i.e., type 5 or 3c bleeding) within 72 hrs post-randomisation.

SECONDARY ENDPOINTS

1) Technical success of CDT: successful catheter placement followed by continuous infusion of alteplase.
2) All bleeding complications (scored using the BARC classification).
3) Haemodynamic instability during hospitalisation.
4) Length of hospitalisation.
5) In-hospital mortality.

STATISTICAL ANALYSIS

Statistical analysis was performed using IBM SPSS software version 23.0 (IBM). Independent samples t-tests were used to compare the CDT and standard care groups. P-values <0.05 were considered statistically significant. Continuous variables are expressed as means (± standard deviations [SD]) and categorical variables are expressed as numbers (with percentages).

Results

Twenty-three patients with an intermediate-high risk acute PE were randomised (12 into the CDT group and 11 into the standard care group). The baseline demographic and clinical characteristics are summarised in **Table 2**.

PROCEDURAL CHARACTERISTICS

CDT was successful (i.e., no periprocedural complications) in all 12 patients. The mean time from admission to intervention was 25.1 (±12.1) hrs; the mean procedural duration was 44.5 (±8.8) mins (commencing with the venous puncture). The mean fluoroscopy time was 12.8 (±8.4) mins and the mean dose area product was 26.5 (±16.1) Gy·cm^2. Two catheters were used in all patients – one in each of the right and left interlobar pulmonary arteries for bilateral thrombolysis.

CTA, ECHOCARDIOGRAPHY AND LABORATORY RESULTS

All data are shown in **Table 3**.

CTA proceeded without complications in all patients; the standard dose of contrast agent was 80 ml. At baseline, the RV/LV ratios were 1.35 (±0.45) in the CDT group and 1.75 (±0.44) in the standard care group (p=0.97). Forty-eight hours after randomisation, the RV/LV ratio was significantly lower in the CDT group than in the standard care group (0.88±0.16 vs 1.42±0.44, p=0.013). The Qanadli index fell 17.3% in the CDT group and 11.6% in the standard care group (p=0.45).

Echocardiography did not reveal any significant between-group differences. The sPAP tended to be lower 24 hrs after randomisation in the CDT group than in the standard care group (33.3±9.1 vs 52.7±17.1 mmHg, p=0.18).

The baseline levels of hsTnI and NT-proBNP were elevated in both groups **(Table 3)**. The NT-proBNP levels were higher in the standard care group than in the CDT group at baseline (6,594.6±6,198.1 vs 3,848.1±2,524.6 ng/l, p=0.01) and 48 hrs after randomisation (5,731.2±5,874.1 vs 1,586.6±2,098.6 ng/l, p=0.003). The NT-proBNP level improved to a greater extent 48 hrs after randomisation in the CDT group than in the standard care group (–2,261.5±1,242.6 vs –863.5±2,790.8 ng/l, p=0.02) **(Figure 2)**. There were no between-group differences in any other laboratory parameters (creatinine, haemoglobin, platelet, or fibrinogen level; the aPTT; or the INR)

PRIMARY ENDPOINT ANALYSIS

The combined endpoint "effectiveness of catheter-directed thrombolysis" was better in the CDT group than in the standard care group (7 of 12 patients vs 1 of 11 patients, p=0.0004). An RV/LV reduction ≥25% (on CTA) was achieved in 7 of

Table 2. Baseline demographic and clinical characteristics.

	CDT group (n=12)	Standard care group (n=11)	*p*-value
Characteristic			
Age (years)	60.6 (±14.3)	63.5 (±15.1)	0.87
Men (%)	8 (66.7%)	5 (45.5%)	0.33
Body mass index (kg/m^2)	31.3 (±5.9)	30.9 (±3.9)	0.35
Comorbidities			
Arterial hypertension	9 (75%)	6 (54.5%)	0.10
Diabetes mellitus	0 (0%)	3 (27.3%)	<0.001
Coronary artery disease	0 (0%)	1 (9.1%)	0.03
Thromboembolism history	1 (8.3%)	3 (27.3%)	0.02
Malignancy	2 (16.7%)	3 (27.3%)	0.25
Immobilisation	2 (16.7%)	1 (9.1%)	0.30
Previous antithrombotic therapy	2 (16.7%)	2 (18.2%)	0.86
Smoking	3 (25%)	3 (27.3%)	0.82
Clinical characteristics			
Systolic BP on admission (mmHg)	141.6 (±22.4)	140.2 (±22.1)	0.87
PESI score	89.8 (±32.4)	102.6 (±19.9)	0.16

BP: blood pressure; CDT: catheter-directed thrombolysis; PESI: pulmonary embolism severity index

Table 3. CT angiography, echocardiography and laboratory tests.

	CDT group (n=12)	Standard care group (n=11)	*p*-value
CT angiography			
RV diameter (baseline), mm	45.4 (±6.2)	46.8 (±5.5)	0.71
RV diameter (at 48 hrs), mm	38.0 (±8.2)	42.3 (±5.9)	0.66
LV diameter (baseline), mm	36.2 (±10.2)	28.4 (±7.9)	0.50
LV diameter (at 48 hrs), mm	43.4 (±6.5)	32.0 (±8.0)	0.62
RV/LV ratio (baseline)	1.35 (±0.45)	1.75 (±0.44)	0.97
RV/LV ratio (at 48 hrs)	0.88 (±0.16)	1.42 (±0.44)	0.013
RV/LV ratio change (baseline vs 48 hrs after randomisation [%])	–29.1 (±24.8)	–16.1 (±24.4)	0.22
Qanadli score (baseline)	21.1 (±10.7)	22.3 (±8.0)	0.38
Qanadli score (at 48 hrs)	16.4 (±8.9)	19.2 (±6.8)	0.20
Qanadli score (mean difference from baseline to 48 hrs after randomisation [%])	–17.3 (±19.8)	–11.6 (±14.2)	0.45
Echocardiography			
RV diameter (baseline), mm	48.6 (±6.2)	47.8 (±4.7)	0.21
RV diameter (at 24 hrs), mm	44.5 (±4.8)	46.9 (±4.2)	0.32
LV diameter (baseline), mm	46.4 (±7.0)	36.7 (±4.9)	0.36
LV diameter (at 24 hrs), mm	48.3 (±7.0)	40.6 (±3.7)	0.18
RV/LV ratio (baseline)	1.1 (±0.1)	1.3 (±0.1)	0.83
RV/LV ratio (at 24 hrs)	0.9 (±0.1)	1.2 (±0.2)	0.76
sPAP (baseline), mmHg	51.7 (±11.1)	52.1 (±12.7)	0.89
sPAP (at 24 hrs), mmHg	33.3 (±9.1)	52.7 (±17.1)	0.18
TAPSE (baseline), mm	16.3 (±1.9)	14.6 (±3.5)	0.10
TAPSE (at 24 hrs), mm	22.0 (±3.4)	18.3 (±3.6)	0.84
S' TDI (baseline), cm/s	12.0 (±2.1)	9.8 (±2.3)	0.75
S' TDI (at 24 hrs), cm/s	13.3 (±3.0)	12.2 (±3.8)	0.91
Laboratory tests	**(ng/l)**	**(ng/l)**	
Troponin hsTnI (baseline)	244.5 (±241)	365.2 (±329.6)	0.24
Troponin hsTnI (at 48 hrs)	115.2 (±160.9)	93.4 (±75.6)	0.28
Troponin (mean difference from baseline to 48 hrs after randomisation)	–129.2 (±249.6)	–271.7 (±270.6)	0.54
NT-proBNP (baseline)	3,848.1 (±2524.6)	6,594.6 (±6,198.1)	0.01
NT-proBNP (at 48 hrs)	1,586.6 (±2098.6)	5,731.2 (±5,874.1)	0.003
NT-proBNP (mean difference from baseline to 48 hrs after randomisation)	–2,261.5 (±1242.6)	–863.5 (±2790.8)	0.02
aPTT (baseline), secs	80.8 (±56.2)	97.2 (±58.9)	0.50
aPTT (at 48 hrs), secs	61.2 (±28.9)	87.6 (±44.7)	0.13

aPTT: activated partial thromboplastin time; CDT: catheter-directed thrombolysis; CT: computed tomography; LV: left ventricular; PE: pulmonary embolism; RV: right ventricular; S' TDI: tissue Doppler imaging-derived tricuspid lateral annular systolic velocity; sPAP: systolic pulmonary artery pressure; TAPSE: tricuspid annular plane systolic excursion

12 patients in the CDT group vs 2 of 11 patients in the standard care group (p=0.03). An sPAP decrease of ≥30% or the attainment of pulmonary artery normotension at 24 hrs after randomisation was evident in 10 of 12 CDT patients vs 2 of 11 standard care patients (p=0.001). Qanadli score reductions ≥30% were achieved by 3 of 12 patients in the CDT group vs 2 of 11 patients in the standard care group (p=0.45) **(Central illustration)**. The "safety of CDT" endpoint was achieved in all patients; no intracranial or life-threatening bleeding (BARC type 5 or 3c) was observed in any study participant.

SECONDARY ENDPOINT ANALYSIS

One local bleeding complication developed in the CDT group (an access site haematoma of BARC type 2). There were two bleeding complications in the standard care group (haematuria in one patient [BARC type 2] and renal parenchymal haemorrhage [BARC type 3a] in one patient with acute kidney ischaemia caused by a paradoxical renal artery embolism during hospitalisation).

No haemodynamic instability was observed in any patient. Positive trends toward a shorter intensive care unit stay (99.3±61.1 vs 153.5±96.0 hrs; p=0.29) and hospitalisation time (189.8±65.3

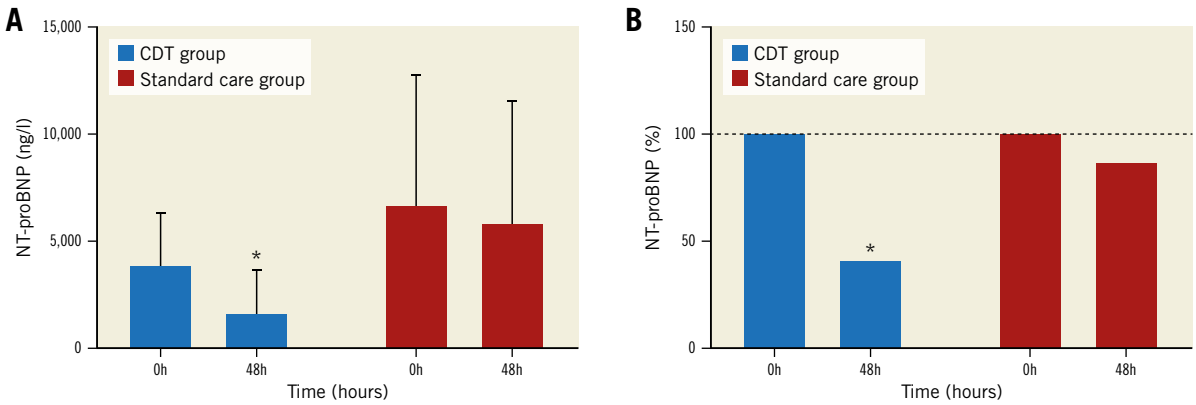

Figure 2. *NT-proBNP levels in the CDT and standard care groups at baseline and 48 hrs post-randomisation. A) Absolute values; B) Relative reductions. *significant difference with p-value <0.05. CDT: catheter-directed thrombolysis*

vs 234.6±98.6 hrs; p=0.16) were more apparent in the CDT group, compared to the standard care group. Two patients in the standard care group underwent rescue local thrombolysis on clinical grounds at 72 and 53 hrs post-randomisation; this led to clinical improvement and reduction of the RV size in both patients. There was zero mortality and no hospital readmission at 30-day follow-up.

Discussion

Both primary endpoints were achieved. The combined endpoint "effectiveness of catheter-directed thrombolysis" was more common in the CDT group than in the standard care group, and there were no safety concerns, with no occurrence of intracranial or life-threatening bleeding according to the BARC classification in our study.

Patients included in our study appear to be similar to patients in the non-randomised PERFECT and USAT CDT studies[8-11], despite differences in the high-risk stratifications between the European Society of Cardiology and the American College of Cardiology/American Heart Association. Our study was conducted in a large tertiary care centre, as were the cited works. Patients treated in high-volume centres represent approximately half of all patients with acute PE[19]. The remaining patients (including patients at intermediate-high risk) are usually treated (via anticoagulation

EuroIntervention

CENTRAL **ILLUSTRATION** Combined primary endpoint effectiveness of catheter-directed thrombolysis.

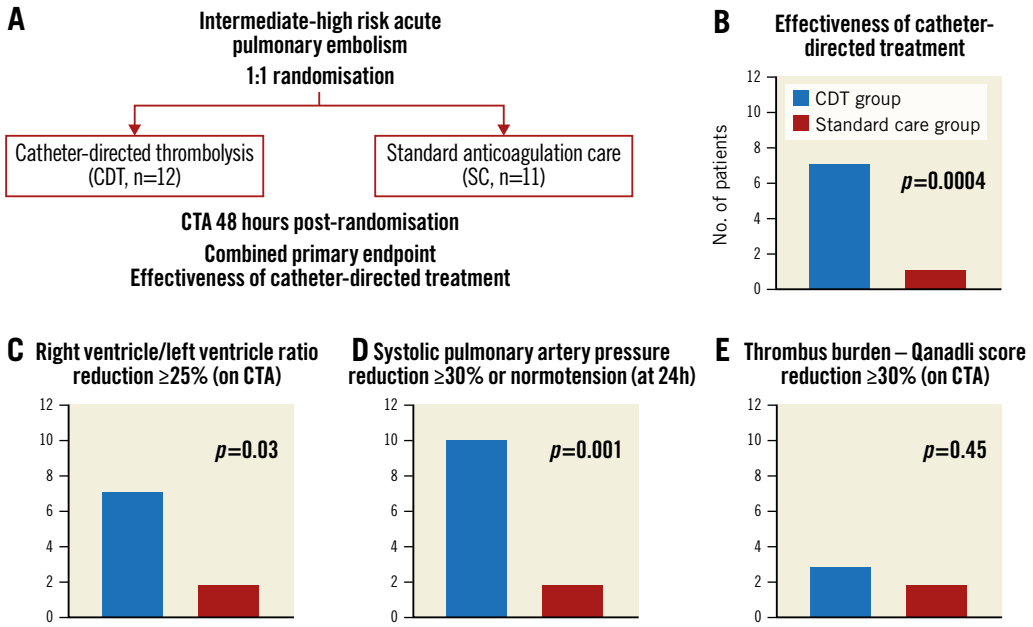

A) Study design. B) Combined primary endpoint effectiveness of catheter-directed treatment – at least two of three predefined criteria – per C), D), E) had to be met. CDT: catheter-directed thrombolysis; CTA: computed tomography angiography; SC: standard care

rejstřík

therapy) in low-volume centres. Patients at intermediate-high risk might benefit from transfers to large tertiary care centres where other treatment options are available.

Our CDT philosophy was the simplest possible approach. The introduction of two 4 Fr catheters via a single dual-lumen introducer was safe and patient-friendly. The fusion of CTA and real-time fluoroscopy eliminated any need for contrast, reducing the risk of kidney injury. In contrast to the previously published papers[8-11], we have described the standardised methodology of CDT. Radiation time and dose were non-negligible, but a large field of view was required; the exposure is reasonable considering the clinical severity of intermediate-high risk acute PE.

To our knowledge, no prospective randomised comparison of CDT (local thrombolysis alone) with standard anticoagulation has been published[14]. In our pilot study, patients undergoing CDT exhibited a greater RV/LV ratio reduction and a greater sPAP decrease than patients in the standard care group, without any serious bleeding. The dose of the thrombolytic agent and infusion duration varied across the studies[8-11]. Our thrombolytic choice was alteplase; the use of one 20 mg vial per patient was practical and economical. It may be useful to individualise the dose and duration of local thrombolytic therapy (based on treatment effects) in future studies.

The study was not powered nor prospectively designed to analyse cost-effectiveness, but a simple financial assessment is possible. The cost of a standard thrombolytic catheter (approximately 120 USD) is significantly lower than the cost of an ultrasound-assisted thrombolytic EKOS catheter (Boston Scientific). Furthermore, the intensive care unit and total hospitalisation times tended to be shorter in the CDT group. The cost savings afforded by two fewer days in the intensive care unit would compensate for the cost of 20 mg alteplase (approximately 260 USD). Future CDT studies will need to include formal cost-effectiveness analysis with quality-of-life evaluation.

Several important issues remain open to further research. A large randomised comparison of CDT and anticoagulation therapy alone, with well-defined clinical endpoints, is required to verify the effectiveness of our approach. The optimal thrombolytic dose and infusion duration should be clarified. Formal cost-effectiveness analysis of different treatment modalities (anticoagulation alone vs CDT local thrombolysis vs ultrasound-assisted local thrombolysis) should be performed.

Limitations

Our sample size was obviously insufficient to allow us to draw definitive conclusions including long-term outcomes (quality of life, mortality, etc.). However, the study was randomised, so the data can facilitate sample size calculation for subsequent larger studies with clinical endpoints. The minor differences in baseline characteristics are likely attributable to chance; they are unlikely to influence our (principally image-based) endpoints. The study was performed in a tertiary care cardiac centre; we lacked information concerning the need for patient transfer. The timing of CDT might have had an impact on the study outcome; the average delay of 24 hrs might lead to selection bias. We sought to be maximally practical; thus, we did not invasively measure pulmonary pressures after local thrombolysis was concluded. However, transthoracic echocardiography with an estimation of sPAP was performed at 24 hrs post-randomisation. Our data appear similar to the findings in previous studies[8-10] **(Figure 3)**. No formal interobserver comparisons of CT or echocardiography measurements were performed; difficulties were resolved by discussion among observers.

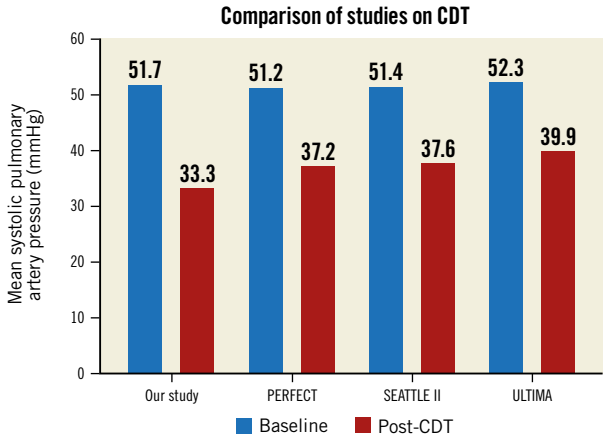

Figure 3. *Comparison of studies on CDT. Comparison of our study with previous studies on CDT for patients with acute PE: mean systolic pulmonary artery pressures at baseline and post-CDT. PERFECT[8], SEATTLE II[9], ULTIMA[10]. CDT: catheter-directed thrombolysis*

Conclusions

CDT for intermediate-high risk acute PE patients appears simple and safe; it improves known predictors of poor patient prognosis. Further research featuring carefully chosen clinical endpoints is warranted.

Impact on daily practice

Simple catheter-directed local thrombolysis might offer a safe and effective treatment option for patients with intermediate-high risk acute PE.

Acknowledgements

This work was supported by the Charles University Research Program Q 38 and the Interventional Treatment of Life-Threatening Cardiovascular Diseases (INTERCARDIS) EU project CZ. 02.1.01/0.0/0.0/16_026/0008388. All authors agree with the submission of the manuscript. Data are available from the corresponding author on request.

Funding

This work was funded by the Charles University Research Program Q 38 and the Interventional Treatment of Life-Threat-

ening Cardiovascular Diseases (INTERCARDIS) EU project CZ.02.1.01/ 0.0/0.0/16_026/0008388.

Conflict of interest statement

V. Kocka received consultation fees from Medtronic related to work on another structural intervention (TAVI). J. Kroupa received consultation fees from B. Braun for work in a different area (related to coronary interventions). The other authors have no conflicts of interest to declare.

References

1. Andersson T, Söderberg S. Incidence of acute pulmonary embolism, related comorbidities and survival; analysis of a Swedish national cohort. *BMC Cardiovasc Disord.* 2017;17:155.

2. Goldhaber SZ, Visani L, De Rosa M. Acute pulmonary embolism: Clinical outcomes in the International Cooperative Pulmonary Embolism Registry (ICOPER). *Lancet.* 1999;353:1386-9.

3. Konstantinides SV, Meyer G, Becattini C, Bueno H, Geersing GJ, Harjola VP, Huisman MV, Humbert M, Jennings CS, Jiménez D, Kucher N, Lang IM, Lankeit M, Lorusso R, Mazzolai L, Meneveau N, Ní Áinle F, Prandoni P, Pruszczyk P, Righini M, Torbicki A, Van Belle E, Zamorano JL; ESC Scientific Document Group. 2019 ESC Guidelines for the diagnosis and management of acute pulmonary embolism developed in collaboration with the European Respiratory Society (ERS). *Eur Heart J.* 2020;41:543-603.

4. Becattini C, Agnelli G, Lankeit M, Masotti L, Pruszczyk P, Casazza F, Vanni S, Nitti C, Kamphuisen P, Vedovati MC, De Natale MG, Konstantinides S. Acute pulmonary embolism: Mortality prediction by the 2014 European Society of Cardiology risk stratification model. *Eur Respir J.* 2016;48:780-6.

5. Steering Committee. Single-bolus tenecteplase plus heparin compared with heparin alone for normotensive patients with acute pulmonary embolism who have evidence of right ventricular dysfunction and myocardial injury: rationale and design of the Pulmonary Embolism Thrombolysis (PEITHO) trial. *Am Heart J.* 2012;163:33-8.

6. Meyer G, Vicaut E, Danays T, Agnelli G, Becattini C, Beyer-Westendorf J, Bluhmki E, Bouvaist H, Brenner B, Couturaud F, Dellas C, Empen K, Franca A, Galiè N, Geibel A, Goldhaber SZ, Jimenez D, Kozak M, Kupatt C, Kucher N, Lang IM, Lankeit M, Meneveau N, Pacouret G, Palazzini M, Petris A, Pruszczyk P, Rugolotto M, Salvi A, Schellong S, Sebbane M, Sobkowicz B, Stefanovic BS, Thiele H, Torbicki A, Verschuren F, Konstantinides SV; PEITHO Investigators. Fibrinolysis for patients with intermediate-risk pulmonary embolism. *N Engl J Med.* 2014;370:1402-11.

7. Quiroz R, Kucher N, Schoepf UJ, Kipfmueller F, Solomon SD, Costello P, Goldhaber SZ. Right ventricular enlargement on chest computed tomography: prognostic role in acute pulmonary embolism. *Circulation.* 2004;109:2401-4.

8. Kuo WT, Banerjee A, Kim PS, DeMarco FJ Jr, Levy JR, Facchini FR, Unver K, Bertini MJ, Sista AK, Hall MJ, Rosenberg JK, De Gregorio MA. Pulmonary Embolism Response to Fragmentation, Embolectomy, and Catheter Thrombolysis (PERFECT): Initial Results From a Prospective Multicenter Registry. *Chest.* 2015;148:667-73.

9. Piazza G, Hohlfelder B, Jaff MR, Ouriel K, Engelhardt TC, Sterling KM, Jones NJ, Gurley JC, Bhatheja R, Kennedy RJ, Goswami N, Natarajan K, Rundback J, Sadiq IR, Liu SK, Bhalla N, Raja ML, Weinstock BS, Cynamon J, Elmasri FF, Garcia MJ, Kumar M, Ayerdi J, Soukas P, Kuo W, Liu PY, Goldhaber SZ; SEATTLE II Investigators. A Prospective, Single-Arm, Multicenter Trial of Ultrasound-Facilitated, Catheter-Directed, Low-Dose Fibrinolysis for Acute Massive and Submassive Pulmonary Embolism: The SEATTLE II Study. *JACC Cardiovasc Interv.* 2015;8:1382-92.

10. Kucher N, Boekstegers P, Müller OJ, Kupatt C, Beyer-Westendorf J, Heitzer T, Tebbe U, Horstkotte J, Müller R, Blessing E, Greif M, Lange P, Hoffmann RT, Werth S, Barmeyer A, Härtel D, Grünwald H, Empen K, Baumgartner I. Randomized, controlled trial of ultrasound-assisted catheter-directed thrombolysis for acute intermediate-risk pulmonary embolism. *Circulation.* 2014;129:479-86.

11. Tapson VF, Sterling K, Jones N, Elder M, Tripathy U, Brower J, Maholic RL, Ross CB, Natarajan K, Fong P, Greenspon L, Tamaddon H, Piracha AR, Engelhardt T, Katopodis J, Marques V, Sharp ASP, Piazza G, Goldhaber SZ. A Randomized Trial of the Optimum Duration of Acoustic Pulse Thrombolysis Procedure in Acute Intermediate-Risk Pulmonary Embolism: The OPTALYSE PE Trial. *JACC Cardiovasc Interv.* 2018;11:1401-10.

12. Rao G, Xu H, Wang JJ, Galmer A, Giri J, Jaff MR, Kolluri R, Lau JF, Selim S, Weinberg I, Weinberg MD. Ultrasound-assisted versus conventional catheter-directed thrombolysis for acute pulmonary embolism: A multicenter comparison of patient-centered outcomes. *Vasc Med.* 2019;24:241-7.

13. Avgerinos ED, Jaber W, Lacomis J, Markel K, McDaniel M, Rivera-Lebron BN, Ross CB, Sechrist J, Toma C, Chaer R; SUNSET sPE Collaborators. Randomized Trial Comparing Standard Versus Ultrasound-Assisted Thrombolysis for Submassive Pulmonary Embolism: The SUNSET sPE Trial. *JACC Cardiovasc Interv.* 2021;14:1364-73.

14. Klein AJ, Shishehbor MH. Ultrasound-assisted catheter directed therapy (CDT) for pulmonary embolism versus standard CDT: Sounds of a cry for data! *Vasc Med.* 2019;24:248-50.

15. Qanadli SD, El Hajjam M, Vieillard-Baron A, Joseph T, Mesurolle B, Oliva VL, Barré O, Bruckert F, Dubourg O, Lacombe P. New CT index to quantify arterial obstruction in pulmonary embolism: comparison with angiographic index and echocardiography. *AJR Am J Roentgenol.* 2001;176:1415-20.

16. Galderisi M, Cosyns B, Edvardsen T, Cardim N, Delgado V, Di Salvo G, Donal E, Sade LE, Ernande L, Garbi M, Grapsa J, Hagendorff A, Kamp O, Magne J, Santoro C, Stefanidis A, Lancellotti P, Popescu B, Habib G; 2016-2018 EACVI Scientific Documents Committee. Standardization of adult transthoracic echocardiography reporting in agreement with recent chamber quantification, diastolic function, and heart valve disease recommendations: an expert consensus document of the European Association of Cardiovascular Imaging. *Eur Heart J Cardiovasc Imaging.* 2017;18:1301-10.

17. Lang RM, Badano LP, Mor-Avi V, Afilalo J, Armstrong A, Ernande L, Flachskampf FA, Foster E, Goldstein SA, Kuznetsova T, Lancellotti P, Muraru D, Picard MH, Rietzschel ER, Rudski L, Spencer KT, Tsang W, Voigt JU. Recommendations for cardiac chamber quantification by echocardiography in adults: an update from the American Society of Echocardiography and the European Association of Cardiovascular Imaging. *J Am Soc Echocardiogr.* 2015;28:1-39.

18. Mehran R, Rao SV, Bhatt DL, Gibson CM, Caixeta A, Eikelboom J, Kaul S, Wiviott SD, Menon V, Nikolsky E, Serebruany V, Valgimigli M, Vranckx P, Taggart D, Sabik JF, Cutlip DE, Krucoff MW, Ohman EM, Steg PG, White H. Standardized bleeding definitions for cardiovascular clinical trials: a consensus report from the Bleeding Academic Research Consortium. *Circulation.* 2011;123:2736-47.

19. Jiménez D, Bikdeli B, Quezada A, Muriel A, Lobo JL, de Miguel-Diez J, Jara-Palomares L, Ruiz-Artacho P, Yusen RD, Monreal M; RIETE investigators. Hospital volume and outcomes for acute pulmonary embolism: multinational population based cohort study. *BMJ.* 2019;366:l4416.

M. Pazderník et al.

Surgery and outcome of infective endocarditis in octogenarians: prospective data from the ESC EORP EURO-ENDO registry

Infection
Impact Factor: 7.455

Infection (2022) 50:1191–1202
https://doi.org/10.1007/s15010-022-01792-0

ORIGINAL PAPER

Surgery and outcome of infective endocarditis in octogenarians: prospective data from the ESC EORP EURO-ENDO registry

Michal Pazdernik[1,2] · Bernard Iung[3] · Bulent Mutlu[4] · François Alla[5] · Robert Riezebos[6] · William Kong[7] · Maria Carmo Pereira Nunes[8] · Luc Pierard[9] · Ilija Srdanovic[10] · Hirotsugu Yamada[11] · Andrea De Martino[12] · Marcelo Haertel Miglioranza[13] · Julien Magne[14] · Cornelia Piper[15] · Cécile Laroche[16] · Aldo P. Maggioni[16,17] · Patrizio Lancellotti[18] · Gilbert Habib[19,20] · Christine Selton-Suty[21,22] on behalf of the EURO-ENDO Investigators group

Received: 6 November 2021 / Accepted: 24 February 2022 / Published online: 15 March 2022

Abstract

Purpose High mortality and a limited performance of valvular surgery are typical features of infective endocarditis (IE) in octogenarians, even though surgical treatment is a major determinant of a successful outcome in IE.

Methods Data from the prospective multicentre ESC EORP EURO-ENDO registry were used to assess the prognostic role of valvular surgery depending on age.

Results As compared to < 80 yo patients, ≥ 80 yo had lower rates of theoretical indication for valvular surgery (49.1% vs. 60.3%, $p < 0.001$), of surgery performed (37.0% vs. 75.5%, $p < 0.001$), and a higher in-hospital (25.9% vs. 15.8%, $p < 0.001$) and 1-year mortality (41.3% vs. 22.2%, $p < 0.001$). By multivariable analysis, age per se was not predictive of 1-year mortality, but lack of surgical procedures when indicated was strongly predictive (HR 2.98 [2.43–3.66]). By propensity analysis, 304 ≥ 80 yo were matched to 608 < 80 yo patients. Propensity analysis confirmed the lower rate of indication for valvular surgery (51.3% vs. 57.2%, $p = 0.031$) and of surgery performed (35.3% vs. 68.4%, $p < 0.0001$) in ≥ 80 yo. Overall mortality remained higher in ≥ 80 yo (in-hospital: HR 1.50[1.06–2.13], $p = 0.0210$; 1-yr: HR 1.58[1.21–2.05], $p = 0.0006$), but was not different from that of < 80 yo among those who had surgery (in-hospital: 19.7% vs. 20.0%, $p = 0.4236$; 1-year: 27.3% vs. 25.5%, $p = 0.7176$).

Conclusion Although mortality rates are consistently higher in ≥ 80 yo patients than in < 80 yo patients in the general population, mortality of surgery in ≥ 80 yo is similar to < 80 yo after matching patients. These results confirm the importance of a better recognition of surgical indication and of an increased performance of surgery in ≥ 80 yo patients.

Keywords Infective endocarditis · Elderly · Prognosis · Surgery · Propensity analysis

Introduction

Characteristics of patients with infective endocarditis (IE) have dramatically changed over recent decades, with a high prevalence and specific features of IE in elderly population [1–8]. Old age leads to surgical hesitancy by referring physicians, surgeons and patients themselves [9]. Furthermore, frequent associated comorbidities also influence the outcome of this fragile cohort [6]. As a result, increased mortality and less-frequent performance of valvular surgery are hallmarks of IE episodes in elderly as compared to younger patients. This is especially true in octogenarians who represent a growing part of IE population, who are often limited to medical therapy without being discussed for surgery just

The original online version of this article was revised: In this article the "EURO-ENDO Investigators group" member U. Y. Sinan was incorrectly written as U. S. Yasar.

A complete list of the EURO-ENDO Investigators Group is provided in Supplementary Material Appendix 1.

✉ Christine Selton-Suty
c.suty-selton@chru-nancy.fr

Extended author information available on the last page of the article

because of their age, even though surgical treatment is a well-known determinant of successful outcome in IE.

To date, the impact of age and associated comorbidities on prognosis have, however, been poorly investigated, as the rare studies published on the subject were limited by retrospective design, single-centre recruitment, and/or small numbers of patients. A recent study based on the Swedish population between 2006 and 2017 emphasized the fact that surgery is underused in elderly. A propensity analysis to match patients according to the performance of surgery was used and showed significantly higher one-year mortality in patients who did not undergo surgery [10].

The ESC EORP Euro-Endo registry is a comprehensive prospective observational cohort that included 3113 patients with IE which is based on contemporary practices (2016–2018) in a wide range of countries and centres [11]. It aimed to assess how the 2015 ESC guidelines on the management of IE [12], which were endorsed by the European Association for Cardio-Thoracic Surgery (EACTS), and the European Association of Nuclear Medicine (EANM), were implemented in clinical practice. It therefore provides a unique opportunity to investigate the current influence of patients' age on the demographic, clinical, therapeutic, and prognostic profile of IE, taking into account the numerous confounding factors with an appropriate statistical power. The aim of our study was to describe the specific features of IE in octogenarians, with a special focus on the respective contribution of age, IE characteristics and comorbidities on surgical decision and outcome.

Methods

Study design and data collection

All patients from the prospective multicentre ESC EORP EURO-ENDO registry, apart from three patients, who retrospectively withdrew an informed consent, were included in our ancillary study. The detailed methodology of EURO-ENDO has *previously* been reported [11]. All consecutive patients aged ≥ 18 years with definite or possible IE *according to the ESC 2015 diagnostic criteria* [12] were included *during a one-year period in each centre* between January 2016 and March 2018. All participants signed informed consent. In total, 3113 index cases of IE from 156 centres across 40 countries were collected. Patients' management was supposed to be performed according to the 2015 ESC guidelines and main therapeutic decisions were supposed to be taken from a multidisciplinary approach including cardiologists, surgeons, ID specialists and microbiologists among Endocarditis Teams [12].

Baseline and follow-up data

Baseline data included clinical characteristics, biological and microbiological data, imaging data, treatment before admission and during hospitalization, complications under therapy, theoretical indication for valvular surgery, in-hospital valvular surgery performed, in-hospital mortality and 1-year follow-up.

Theoretical indication for valvular surgery was defined as the existence of any type of theoretical indication listed in the ESC guidelines (haemodynamic, embolic, infectious and/or other), as acknowledged by the practitioners taking care of the patients regardless of operative risk. This definition allowed us to classify patients in 3 subgroups regarding valvular surgery: patients without theoretical indication of surgery, patients with theoretical indication and surgery performed and patients with theoretical indication and surgery not performed.

Statistical analysis

Continuous and categorical variables were reported as mean ± SD or as median (interquartile range) as appropriate, and as absolute values and related percentages, respectively. Between-groups differences were tested with Kruskal–Wallis test and with chi-square test or Fisher's exact test for continuous and categorical variables, respectively.

Subjects were stratified into two groups: ≥ 80 years old (≥ 80 yo group) and < 80 years old (< 80 yo group) at inclusion.

Univariable and multivariable logistic regression were performed to analyse factors associated with actual performance of valvular surgery with age and gender forced in the model. Variables with $p < 0.10$ in univariable analysis were entered in the multivariable logistic model with a backward selection procedure and a significance level of $p = 0.05$.

Survival curves according to age and gender were calculated using Kaplan–Meier method and compared using the log-rank test.

Univariable analysis of mortality was performed with a Cox proportional hazards model. Variables with $p < 0.10$ and age and gender were entered in a multivariable adjusted Cox proportional hazards model with a backward selection procedure and a significance level of $p = 0.05$. The following variables were not included in the Cox multivariable model: Charlson comorbidity index due to collinearity with age, vegetation length due to missing data, cerebral complications, fistula and para-prosthetic regurgitation due to incidence < 10% in overall population. Goodness of fit, concordance and Schoenfeld residual tests were calculated to verify the adequacy of the models.

A propensity analysis was then performed to account for the imbalance in patient characteristics between ≥ 80 yo and < 80 yo patients. A propensity score was fitted using a non-parsimonious multivariable logistic model including variables usually recognised as linked to surgery and to prognosis (gender, history of heart failure, device therapy, previous stroke, chronic renal failure, diabetes mellitus, history of cancer, aortic/mitral location of IE, prosthetic valve IE, presence of an abscess, *Staphylococcus aureus* or viridans streptococci as responsible micro-organisms, cerebral embolic event and congestive heart failure as complications of IE; Supplementary Table 1). The options to perform the propensity dataset were the following: the calliper was 0.30, the gender should match exactly, the 2:1 matching was without replacement and no missing imputation was performed on baseline data. Because of missing data, 71 subjects were not included in the propensity analysis and 304 patients ≥ 80 yo were finally matched with 608 < 80 yo patients according to the closest propensity score (Fig. 1). Rates of theoretical surgical indications, of surgical performance were compared using McNemar's test for binary variables. In-hospital and 1-year mortality rates were compared using Cox proportional hazard model stratifying on matched pairs for time to event data. Same analyses were then performed among patients with only definite IE. A low number of patients with possible IE over 80 yo ($n = 56$) did not allow us to perform a propensity analysis with the same matching variables as for the whole population or the population of definite IE, and we matched the cases only on the following variables: gender but without exact matching, prosthetic valve IE, presence of an abscess, *Staphylococcus aureus* as responsible micro-organisms, congestive heart failure as complication of IE.

A two-sided p value < 0.05 was considered statistically significant. All analyses were performed using SAS statistical software version 9.4.

One author (CL) had full access to all the data in the study and takes responsibility for its integrity and the data analysis.

Results

Comparison of IE characteristics according to age groups

Demographic and baseline characteristics

Among the 3113 patients included in the Euro-Endo registry, median age was 63.0 (46.0–73.0), 375 (12.0%) were ≥ 80 yo and 2378 were < 80 yo. Female patients were more frequent in the ≥ 80 yo group (44.0%).

Characteristics of the patients are displayed in Supplementary Table 2. Previous valvular surgery or cardiac

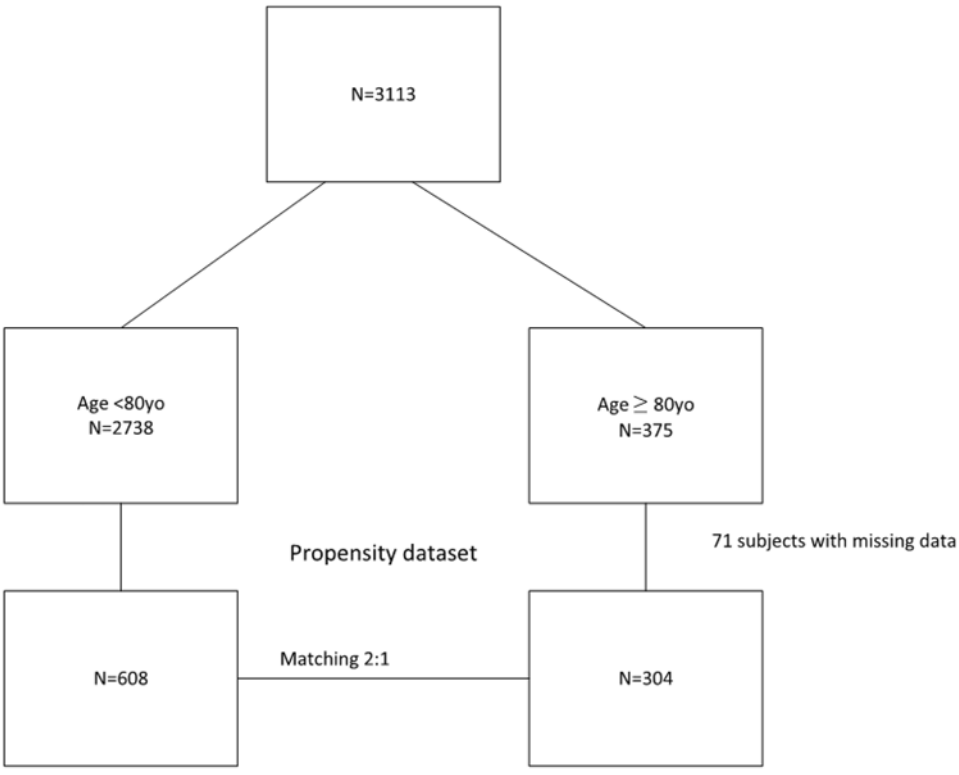

Fig. 1 Flow chart depicting how the propensity score dataset was formed

implantable electronic devices (CIED) were more frequent in ≥ 80 yo than in < 80 yo.

Characteristics of IE

The proportion of definite and possible IE as well as that of community-acquired/health care-related IE was not significantly different among the two groups (Supplementary Table 3).

IE was more often located on prosthetic/repaired valves ($p < 0.0001$) or on CIED ($p < 0.0001$) in ≥ 80 yo patients. Embolic events both at admission (15.5% vs. 26.8%, $p < 0.0001$) and under therapy (12.8% vs. 21.7%, < 0.0001) were less frequent in the ≥ 80 yo. Blood cultures were more often positive (85.9% vs. 78.0%, $p = 0.0005$) with a higher proportion of micro-organisms of gastrointestinal tract in the ≥ 80 yo.

FDG PET/CT scan was more frequently used in the ≥ 80 yo (21.3% vs. 16.0%, $p = 0.0093$). Echocardiography was less frequently positive in ≥ 80 yo (66.9% vs. 80.2%, $p < 0.0001$), mostly because of less-frequent vegetations ($p < 0.0001$).

Therapy and outcome in the overall population

A theoretical indication for surgery was reported in 61% of the patients and surgery was finally performed in 44% of the overall population. Theoretical indication for valvular surgery was less frequently reported in ≥ 80 yo than in < 80 yo (49.1% vs. 60.3%, $p < 0.001$) (Table 1). Furthermore, among those with a theoretical indication, valvular surgery was less often performed in ≥ 80 yo (37.0% vs. 75.5%, $p < 0.0001$) (Supplementary Fig. 1A) and less often in female than in male patients in each group of age. Time delay between diagnosis and performance of surgery was similar in the two groups, as was the distribution between emergent, urgent, early and elective surgery as defined by the guidelines [11]. The proportion of patients with definite IE, who would have been classified as possible IE if they had not been operated on because of lack of the main pathological/microbiological criteria of IE) is quite low, 7% in the < 80 yo and 3.5% in the ≥ 80 yo group (Supplementary Table 4). 1-year mortality was 24% in the global population, 17% among those who were surgically treated and 32% among those who were medically treated, higher in those with theoretical indication who were not operated on (54%) than in those without surgical indication (20%). In-hospital and 1-year mortality were significantly higher in ≥ 80 yo (in-hospital: 25.9% vs. 15.8%; 1 year: 41.3% vs. 22.2%, $p < 0.0001$) (Supplementary Fig. 1B).

Therapy and outcome in the propensity score model

Propensity matching enabled baseline covariates to be equally balanced between ≥ 80 yo and < 80 yo (Supplementary Table 1). In the propensity score-matched analysis (Table 2), theoretical indication of valvular surgery remained significantly less frequent in ≥ 80 yo than in matched < 80 yo patients (51.3% vs. 57.2%, $p = 0.030$). The performance of valvular surgery when theoretically indicated was also significantly less frequent in ≥ 80 yo (35.3% vs. 68.4%, $p < 0.0001$).

In-hospital mortality and 1-year mortality were significantly higher in ≥ 80 yo (in-hospital: 26.0% vs. 20.4%, hazard ratio [HR] 1.50, 95% confidence interval [CI] 1.06–2.13, $p = 0.0210$; 1-year mortality: 41.8% vs. 29.1%, HR 1.58, 95% [CI] 1.21–2.05, $p = 0.0006$). However, when having a look on subgroups of patients related to indication and performance of valvular surgery, short- and long-term mortality in ≥ 80 yo were no longer significantly different from < 80 yo (Fig. 2). This was the case among patients with valvular surgery indicated but not performed where mortality rates were high in both groups and also in patients with no surgical indication. In those two subgroups, mortality rates tended nevertheless to be higher in ≥ 80 yo. Among those who were operated on, mortality rates were really similar in both groups (in-hospital: 19.7% vs. 20.0%, $p = 0.4236$; 1-year: 27.3% vs. 25.5%, $p = 0.7176$). Results were similar among patients with only definite IE (Supplementary Table 5). Results among the two propensity-matched groups of patients with possible IE are displayed in Supplementary Table 6. Of note, the higher mortality among operated patients in the ≥ 80 yo in this subgroup is related to the fact that only three patients with possible IE were operated on with one post-operative death (33% mortality).

Factors associated with valvular surgery according to age groups

The factors associated with the performance of valvular surgery during acute IE in multivariable analysis are displayed in Table 3. Older age and female gender were associated with a less-frequent use of valvular surgery. Definite IE and the presence of abscess were associated with more frequent surgery in the whole population and in both age groups.

Role of age in the multivariable prediction of death

The results of the univariable and multivariable analyses (Supplementary Table 7) (Fig. 3) in the whole population showed that neither age nor female gender were significant predictors of 1-year mortality. Regarding valvular surgery, the performance of surgery was associated with lower mortality (HR 0.77, 95% CI 0.62–0.97, $p = 0.0260$), whereas

Table 1 Comparison of therapy and outcome of infective endocarditis according to the two groups of age

	< 80 years old ($n = 2738$)	≥ 80 years old ($n = 375$)	*p*-value
Risk score			
Euroscore II (*N*)	2334	298	
Median (IQR)	4.5 (1.8–11.3)	12.4 (5.5–25.2)	< 0.0001
Theoretical indication for valvular surgery			
Indication	1724/2737 (63.0%)	184/375 (49.1%)	< 0.001
Indication—surgery performed	1301/1724 (75.5%)	68/184 (37.0%)	< 0.001
Indication—no surgery performed	423/1724 (24.5%)	116/184 (63.0%)	< 0.001
Reasons for not performing surgery when indicated			
Patient refusal	76/423 (18.0%)	25/116 (21.6%)	0.381
Surgical risk	217/423 (51.3%)	93/116 (80.2%)	< 0.001
Death before surgery	102/423 (24.1%)	16/116 (13.8%)	0.017
Absence of surgery in the hospital	32/423 (7.6%)	3/116 (2.6%)	0.054
Neurological complication	53/423 (12.5%)	10/116 (8.6%)	0.246
Other	97/423 (22.9%)	16/116 (13.8%)	0.032
Indication			
Haemodynamic	892/1724 (51.7%)	83/184 (45.1%)	0.087
Embolic	606/1724 (35.2%)	52/184 (28.3%)	0.062
Infectious	1075/1724 (62.4%)	113/184 (61.4%)	0.802
Other	147/1724 (8.5%)	11/184 (6.0%)	0.233
Timing of surgery			
Median time between diagnosis and surgery (IQR) (days)	13.0 (6.0–26.0)	13.0 (8.0–23.0)	0.8016
Emergency surgery*	93/1416 (6.6%)	9/97 (9.3%)	0.1384
Urgent surgery†	359/1416 (25.4%)	15/97 (15.5%)	
Early surgery‡	448/1416 (31.6%)	36/97 (37.1%)	
Elective surgery§	516/1416 (36.4%)	37/97 (38.1%)	
In-hospital follow-up			
Death	432/2738 (15.8%)	97/375 (25.9%)	< 0.0001
Cause of death			
Cardiovascular	122/431 (28.3%)	29/97 (29.9%)	0.4400
Non-cardiovascular	122/431 (28.3%)	34/97 (35.1%)	
Cardiovascular + non-cardiovascular	161/431 (37.4%)	30/97 (30.9%)	
Unknown	26/431 (6.0%)	4/97 (4.1%)	
If surgery performed			
Death post valvular surgery	135/432 (31.3%)	15/97 (15.5%)	0.002
If patient alive, cardiac status			
Heart failure	299/2301 (13.0%)	71/278 (25.5%)	< 0.0001
Valve or prosthetic dysfunction	376/2304 (16.3%)	63/278 (22.7%)	0.0078
One-year follow-up			
Death	609/2738 (22.2%)	155/375 (41.3%)	< 0.0001
Among pts with valvular surgery	208/1301 (16.0%)	21/68 (30.9%)	0.001
Among medically treated patients	401/1437 (27.9%)	134/307 (43.6%)	< 0.001
With theoretical valvular surgical indication	215/423 (50.8%)	74/116 (63.8%)	0.013
Without theoretical valvular surgical indication	186/1013 (18.4%)	60/191 (31.4%)	< 0.001

IQR Interquartile range

*Emergency surgery: surgery performed within 24 h after diagnosis

†Urgent surgery within a few days

‡Early surgery within 1 week

§Elective surgery after at least 1–2 weeks of antibiotic therapy

Table 2 Comparison of therapy and outcome of infective endocarditis among the two propensity-matched subgroups (< 80 yo and ≥ 80 yo)

	Total ($n=912$)	< 80 years old ($n=608$)	≥ 80 years old ($n=304$)	p value
Theoretical indication of valvular surgery	504/912 (55.3%)	348/608 (57.2%)	156/304 (51.3%)	0.0302
Indication				
Haemodynamic	250/504 (49.6%)	180/348 (51.7%)	70/156 (44.9%)	0.0151
Embolic	125/504 (24.8%)	86/348 (24.7%)	39/156 (25.0%)	0.6419
Infectious	310/504 (61.5%)	214/348 (61.5%)	96/156 (61.5%)	0.9183
Other	46/504 (9.1%)	36/348 (10.3%)	10/156 (6.4%)	0.2230
Valvular surgery performed when indicated	293/504 (58.1%)	238/348 (68.4%)	55/156 (35.3%)	< 0.0001
Overall population				
In-hospital mortality	203/912 (22.3%)	124/608 (20.4%)	79/304 (26.0%)	
HR [95%CI]*		Reference	1.50 [1.06–2.13]	0.0210
1-year mortality	304/912 (33.3%)	177/608 (29.1%)	127/304 (41.8%)	
HR [95%CI]		Reference	1.58 [1.21–2.05]	0.0006
Patients with valvular surgery indicated but not performed				
In-hospital mortality	85/211 (40.3%)	41/110 (37.3%)	44/101 (43.6%)	
HR [95%CI]		Reference	1.19 [0.48–2.95]	0.7008
1-year mortality	121/211 (57.3%)	56/110 (50.9%)	65/101 (64.4%)	
HR [95%CI]		Reference	0.90 [0.42–1.95]	0.7929
Patients with no indication for surgery				
In-hospital mortality	60/408 (14.7%)	36/260 (13.8%)	24/148 (16.2%)	
HR [95%CI]		Reference	2.17 [0.82–5.78]	0.1205
1-year mortality	104/408 (25.5%)	56/260 (21.5%)	48/148 (32.4%)	
HR [95%CI]		Reference	2.00 [1.00–4.00]	0.0499
Patients with valvular surgery performed				
In-hospital mortality	58/293 (19.8%)	47/238 (19.7%)	11/55 (20.0%)	
HR [95%CI]		Reference	2.00 [0.37–10.92]	0.4236
1-year mortality	79/293 (27.0%)	65/238 (27.3%)	14/55 (25.5%)	
HR [95%CI]		Reference	1.22 [0.42–3.51]	0.7176

*HR [95%CI]—hazard ratio [95% confidence interval]

non-performance of surgery despite theoretical indication was highly associated with mortality (HR 2.98, 95% CI 2.43–3.66, $p < 0.0001$).

Discussion

The main age-related features of IE among the ESC EORP EURO-ENDO registry are the following: (1) specific features are confirmed regarding underlying heart disease, responsible micro-organisms and complications of IE in ≥ 80 yo patients; (2) theoretical indication of valvular surgery is less often recognised and, in particular, valvular surgery is less often performed in ≥ 80 yo than in < 80 yo patients; (3) in the overall population, both short- and long-term mortality are higher in ≥ 80 yo patients, as are mortality rates of operated patients and of non-operated patients with or without theoretical surgical indication; (4) multivariable and propensity score-matching analyses consistently show that significant differences in theoretical indication of surgery and in its actual performance are present among the two groups and strongly influence prognosis; (5) although mortality remains significantly higher in ≥ 80 yo patients after propensity matching, mortality rates of operated patients are no longer significantly different among age groups; (6) age per se is not a prognostic factor of mortality in multivariable analysis in the overall population.

Using an 80 yo limit for this study may be considered as arbitrary as age is a continuum and elderly population is very heterogeneous. However, this age was chosen with regard to surgery, as patients < 80 yo are quite easily referred to surgeon if necessary while this becomes less and less the case when age progressively increases over 80.

This large series of IE patients over 80 yo confirms that IE in the elderly have several peculiarities. As expected, elderly more often had comorbidities and previous non-cardiac

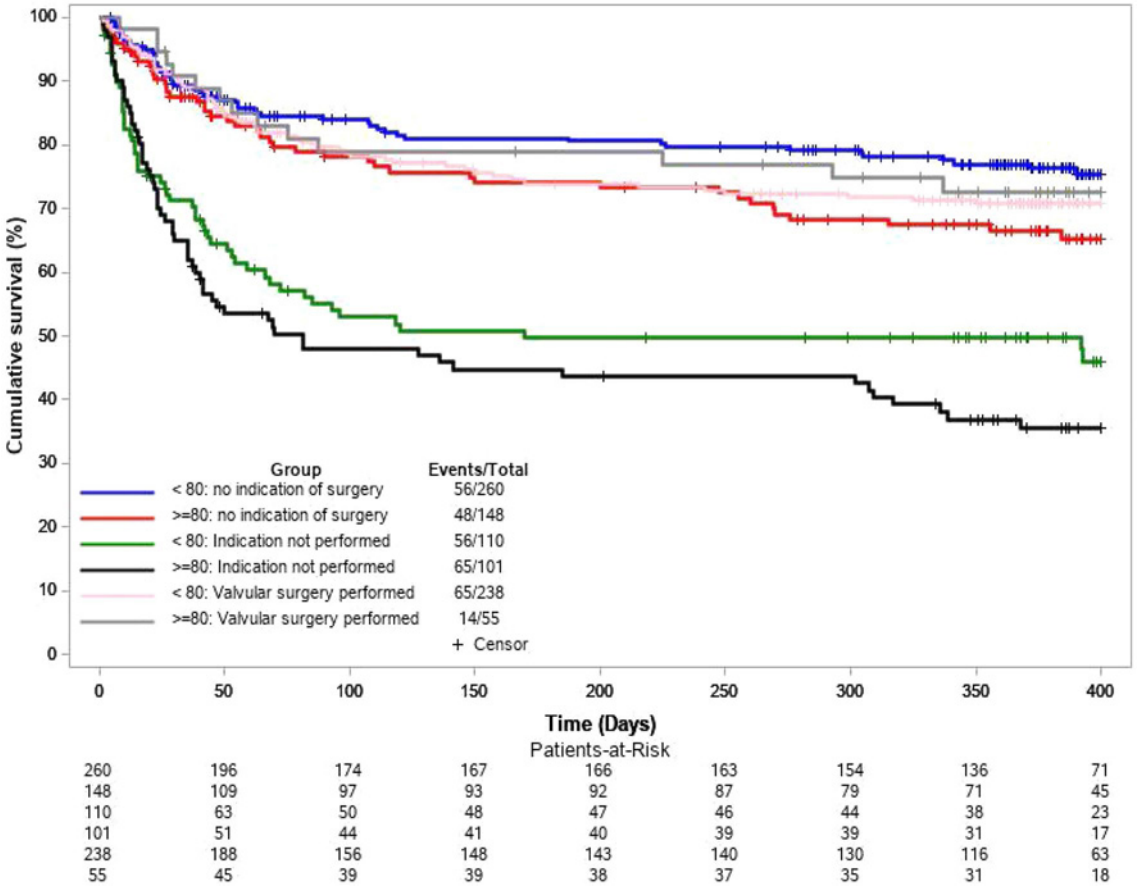

Fig. 2 Comparison of outcome of infective endocarditis among the 2 propensity-matched subgroups (< 80 yo and ≥ 80 yo) according to the indication and actual performance of surgery

procedures. Notably, and in contrast to what has been described in an Australian population-based study, there was no significant difference in the origin of IE (community or health care-associated) depending on age [13]. Nevertheless, IE on CIED and on valvular prosthesis/repair were more frequent in the elderly resulting from increasing use of more complex devices in old patients [14]. As previously reported, embolic events were less common in ≥ 80 yo patients, both before and after admission [4, 7].

Regarding responsible micro-organisms, *Staphylococcus aureus* was less frequent in elderly. Among **Streptococcaceae**, those colonizing the gastro-intestinal tract were more frequent in elderly, with a rate as high as 24% of enterococci. These results are consistent with most of previous series reporting an increased frequency of enterococcus from 10% in patients aged < 65 to > 20% in octogenarians [5, 15] and a 25% rate of *Enterococcus faecalis* in IE after aortic valve implantation [16]. However, a recent Swedish study reported a different repartition of responsible micro-organisms according to age, with a higher rate of *Staphylococcus aureus* in the ≥ 80 group and no significant difference in the frequency of enterococci among age groups [10].

Contemporary data indicate that surgery is now undertaken in approximately 50% of patients with acute IE [17, 18]. Theoretical indication according to the automated application of the guidelines has been reported to be present in more than 70% of patients in a French cohort [19]. In the Euro-Endo registry, the theoretical indication was the one recognised by the responsible practitioner, which is not exactly the same definition, and was reported in 61% of the whole population, less frequently in elderly (49% vs 63%). In the same manner, valvular surgery itself was less often performed when indicated in the elderly than in younger patients (37% vs 75%).

Of note, as per results shown in Supplementary Table 4, the proportion of patients classified as definite IE because of the main pathological/microbiological criteria defining the anatomically definite IE is a little bit lower among ≥ 80 yo than among < 80 yo suggesting that patients > 80 yo who are operated on have more other positive diagnostic criteria (imaging, clinical and microbiological criteria) than younger ones, i.e. that more objective criteria are mandatory in elderly to take a decision of surgery.

Propensity analysis gave us a unique opportunity to better analyse the actual performance of valvular surgery and the

Table 3 Multivariable analysis of predictors of valvular surgery during hospital stay stratified on age groups

		Whole population			< 80 years old			≥ 80 years old		
	Effect	OR*	95% CI†	*p* Wald	OR	95% CI	*p* Wald	OR	95% CI	*p* Wald
Age and gender	Female < 80 yo	1								
	Female ≥ 80 yo	0.29	[0.18–0.47]	< 0.0001						
	Male < 80 yo	1.43	[1.17–1.75]	0.0005						
	Male ≥ 80 yo	0.36	[0.23–0.56]	< 0.0001						
Gender	Male				1.43	[1.17–1.75]	0.0004	1.48	[0.79–2.79]	0.2197
Type of IE	Native	1			1			1		
	PM/ICD‡	0.06	[0.03–0.11]	< 0.0001	0.06	[0.03–0.11]	< 0.0001	0.08	[0.01–0.62]	0.0157
	Prosthesis + Repair	0.70	[0.57–0.85]	0.0004	0.69	[0.56–0.85]	0.0005	0.70	[0.37–1.34]	0.2805
Classification	Definite IE§	1.92	[1.48–2.49]	< 0.0001	1.80	[1.38–2.36]	< 0.0001	3.65	[1.07–12.43]	0.0385
Source of infection	Community	1								
	Non-nosocomial	0.78	[0.58–1.05]	0.0985	0.83	[0.61–1.13]	0.2418			
	Nosocomial	0.66	[0.51–0.86]	0.0020	0.63	[0.48–0.83]	0.0009			
Staph. aureus	Yes	0.58	[0.46–0.73]	< 0.0001	0.58	[0.46–0.74]	< 0.0001			
Abscess	Yes	2.20	[1.63–2.96]	< 0.0001	2.11	[1.54–2.89]	< 0.0001	3.24	[1.39–7.55]	0.0063
Heart failure	Yes	0.69	[0.54–0.88]	0.0023	0.66	[0.51–0.85]	0.0011			
COPD‖/asthma	Yes	0.70	[0.52–0.94]	0.0189				0.16	[0.04–0.74]	0.0191
IVDU#	Yes	0.50	[0.36–0.70]	< 0.0001	0.53	[0.38–0.74]	0.0002			
Diabetes mellitus	Yes	0.79	[0.63–0.99]	0.0380						
Previous stroke/TIA**	Yes							2.24	[1.07–4.72]	0.0333

*OR odds ratio

†*CI* confidence interval

‡*PM/ICD* pacemaker/implantable cardioverter defibrillator

§*IE* infective endocarditis

‖COPD—chronic obstructive pulmonary disease

#*IVDU* intravenous drug abuse

**TIA transient ischemic attack

prognosis of octogenarians in this large cohort of patients. By matching on most of the classical factors of severity of IE, influencing both surgical indication and prognosis, we could better analyse the direct impact of age on surgery and outcome. We chose not to include baseline variables, such as frailty or surgical score, as they were strongly related to age and not to IE itself.

Propensity analysis was also used in a recent paper on data from the Swedish registry on Infective Endocarditis but from a different point of view [10]. Although variables used for matching were globally similar to ours, matching was performed between surgical and non-surgical patients, and those two groups were subsequently separated according to age (with a limit of age of 75 years old), to estimate whether the effect of age differed between the surgery and the non-surgery groups. The mortality rate was significantly lower between the ages of 55 and 82 years in patients who underwent surgery compared with patients who did not undergo surgery. Surgery was also associated with better long-term survival in matched patients who were ≥ 75 years (hazard ratio, 0.36; 95% CI, 0.24–0.54, $p < 0.001$). However, this study did not take into account the indication bias and the factors that may have influenced whether the patient would undergo surgery or not. Furthermore, surgery was performed in only 6% of the elderly patients, which is a lower rate than in our series (18%).

In our study, despite similar features of IE and similar risk factors obtained by propensity matching, differences regarding surgical indication and performance remained significant with less often recognised indication for surgery (51% vs 57%), and far less often surgery performed when indicated (35% vs. 68%). Overall mortality rates also remained significantly higher in elderly group after propensity matching. When looking at the three subgroups of surgery, there remained a non-significant trend toward higher mortality for elderly among patients without indication for surgery and among patients with indication but without surgery. However, interestingly, mortality of surgically treated patients was remarkably similar in the two groups of age.

So, these two propensity analyses, one matching patients according to the performance or not of surgery, the other matching patients according to age groups, allow us to conclude that surgery is associated with better survival than

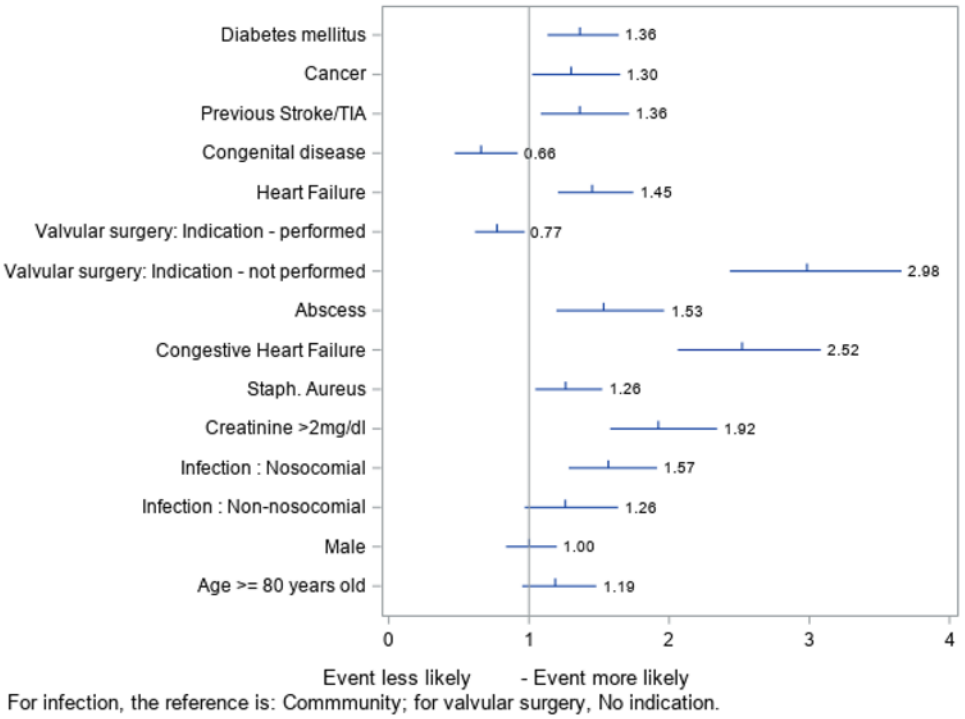

Fig. 3 Cox Regression Analysis for all causes of 1-year mortality with age and gender forced in the model

non-performance of surgery in older patients, and that survival is similar to that of younger patients among operated patients after matching on most of the classical risk factors.

Frail condition, nutritional status and comorbidities obviously predispose elderly patients to higher morbidity and mortality. Nevertheless, neither age nor female gender was independent predictor of mortality in multivariable analysis, although comorbidities frequently associated with age were independent predictors of death. The strongest predictor of mortality by multivariate analysis was the non-performance of valvular surgery despite theoretical indication, whereas the actual performance of valvular surgery was associated with improved survival.

The consistent results of multivariable analysis and propensity score matching strongly suggest that less-frequent indications and interventions in elderly cannot be attributed only to more frequent comorbidities, *but also to a lack of recognition of indication in some cases*. The recognition of a theoretical indication by the responsible cardiologist is probably partly influenced by the subjective appreciation of the feasibility of surgery. Elderly population appears quite heterogeneous, from healthy people to bedridden ones, and general health status further rapidly deteriorates after hospitalisation [6]. Women gender, more frequent among elderly, also negatively influences surgical management, as shown in this study. The fact that theoretical indication for surgery remains significantly less frequent in the elderly even after propensity matching clearly indicates that age itself influences our clinical judgement and recognition of theoretical surgical indication. Similarly, age influences the performance of invasive diagnostic procedures, such as transesophageal echocardiography, which is not more frequently performed in elderly despite higher rates of intra-cardiac material.

At the very end, the decision not to perform surgery despite indication is also linked to several factors including not only age of the patient, but also survival-risk benefit, appreciation of future quality of life, refusal of the patient, local socioeconomic factors, etc. Lopez et al. already noted that the percentage of patients with surgical indications who were rejected for surgery increased significantly with age, due to several factors including frailty but also life's choice of the patient [7]. However, the French study also insisted on the fact that non-performance of surgery whatever the age was due to a non-recognition of the indication in half of the cases of non-operated patients despite theoretical indication *as defined by an automated application of the* guidelines [17].

These findings suggest that performance of surgery in well-selected elderly patients might increase their chance for survival. Our results are in concordance with previous smaller studies, which found that mortality in operated octogenarians was not higher compared to younger age groups [5, 20]. Lower rate of surgery in old patients is a well-described phenomenon [18–20]. So, the observed higher mortality in elderly suffering from IE could be, at least in part, a consequence of non-recognition of surgical indication and of a non-performance of surgery when

indicated. This also partially explains the higher mortality of medically treated patients without surgical indication, as this group probably includes both patients without indication and patients with non-recognized indication.

Study limitations

These results were extracted from a large European and worldwide voluntary registry which has inherent limitations and is not a population-based sample; representativeness is therefore sub-optimal and selection bias cannot be excluded. However, since 3113 index cases from 156 hospitals were included, this represents a mean of 20 patients per centre per year which is a quite high number for such a rare disease. Furthermore, recruiting centres were mostly tertiary centres, inducing a referral bias, in particular, because older and/or inoperable patients are not transferred to tertiary centres.

No specific rules were given regarding the identification of responsible microorganisms. Microbiology analysis was performed according to the usual manners/rules of each institution; hence, we cannot exclude the theoretical possibility that other related bacterial species (such as *Aerococcus* spp.) could have been misidentified as viridans group streptococci, etc.

We chose to include not only definite but also possible cases of IE, as surgical therapy may be discussed in all patients. Furthermore, when surgery is not performed, macroscopic and histologic examinations that would have transformed a possible into a definite case are not available. Finally, part of our analysis is based on theoretical indication of valvular surgery as recognized by the responsible practitioner, which is in part subjective and not a "true" theoretical indication based on an automated analysis of specific IE features leading to indication according to guidelines.

Conclusion

This large study on IE in patients older than 80 years further confirms the strong influence of age on the demographic, clinical, therapeutic, and prognostic profile of IE. Non-recognition of surgical indication and non-performance of surgery when indicated are frequent in old patients and are strong predictors of mortality while age per se is not. After propensity matching on many prognostic factors of IE, mortality of surgically treated patients in octogenarians is not different from that of younger patients, suggesting that recognition of indication and performance of surgery in well-selected elderly patients might increase their chance for survival. Hence, the issue of surgery in elderly must be thoroughly discussed among Endocarditis Teams including geriatricians and considering not only the crude age of the patients to avoid underuse of surgery in that population.

Supplementary Information The online version contains supplementary material available at https://doi.org/10.1007/s15010-022-01792-0.

Acknowledgements EORP Oversight Committee, Registry Executive and Steering Committees. The Data collection was conducted by the EORP department of the ESC: Emanuela Fiorucci, as Project Officer; Viviane Missiamenou, Florian Larras, and Rachid Mir Hassaine, as Data Managers. Statistical analyses were performed by Cécile Laroche of the EURObservational Research Programme, European Society of Cardiology, France. Overall activities were coordinated and supervised by Doctor Aldo P. Maggioni (EORP Scientific Coordinator). Special thanks to the EACVI (European Association of CardioVascular Imaging), to the ESC Working Group on Valvular Heart Disease and to the AEPEI (Association pour l'Etude et la Prévention de l'Endocardite Infectieuse) for their support.

Funding This work was supported by Abbott Vascular Int. (2011–2021), Amgen Cardiovascular (2009–2018), AstraZeneca (2014–2021), Bayer AG (2009–2018), Boehringer Ingelheim (2009–2019), Boston Scientific (2009–2012), The Bristol Myers Squibb and Pfizer Alliance (2011–2019), Daiichi Sankyo Europe GmbH (2011–2020), The Alliance Daiichi Sankyo Europe GmbH and Eli Lilly and Company (2014–2017), Edwards (2016–2019), Gedeon Richter Plc. (2014–2016), Menarini Int. Op. (2009–2012), MSD-Merck & Co. (2011–2014), Novartis Pharma AG (2014–2020), ResMed (2014–2016), Sanofi (2009–2011), SERVIER (2009–2021), Vifor (2019–2022).

Declarations

Informed consent Informed consent was obtained from all individual participants included in the study. Our study complies with the Declaration of Helsinki, the research protocol has been approved by the locally appointed ethics committee; informed consent has been obtained from all the subjects (or their legally authorized representative).

Ethical approval Our study complies with all ethical standards.

Conflict of interest François Alla, Ilija Srdanović, Robert Riezebos, William KF Kong, Maria Carmo Pereira Nunes, Michal Pazderník, Luc Pierard, Bülent Mutlu, Hirotsugu Yamada, Andrea De Martino, Marcelo Haertel Miglioranza, Julien Magne, Cornelia Piper, Cécile Laroche, Patrizio Lancellotti, Gilbert Habib, Christine Selton-Suty have nothing to disclose. Bernard Iung reports personal fees from Edwards Lifesciences, other from Boehringer Ingelheim, outside the submitted work. Aldo P. Maggioni reports personal fees from Bayer, personal fees from Fresenius, personal fees from Novartis, outside the submitted work.

References

1. Habib G, Erba PA, Iung B, Donal E, Cosyns B, Laroche C, Popescu BA, Prendergast B, Tornos P, Sadeghpour A, Oliver L, Vaskelyte J-J, Sow R, Axler O, Maggioni AP, Lancellotti P, EURO-ENDO Investigators. Clinical presentation, aetiology and outcome of infective endocarditis. Results of the ESC-EORP EURO-ENDO (European infective endocarditis) registry: a prospective cohort study. Eur Heart J. 2019;40:3222–32.
2. Murdoch DR, Corey GR, Hoen B, Miro JM, Fowler VG, Bayer AS, Karchmer AW, Olaison L, Pappas PA, Moreillon P, Chambers ST, Chu VH, Falco V, Holland DJ, Jones P, Klein JL, Raymond NJ, Read KM, Tripodi MF, Utili R, Wang A, Woods CW, Cabell CH. Clinical presentation, etiology, and outcome of infective

endocarditis in the 21st century: the International Collaboration on Endocarditis-Prospective Cohort Study. Arch Intern Med. 2009;169:463–73.
3. Slipczuk L, Codolosa JN, Davila CD, Romero-Corral A, Yun J, Pressman GS, Figueredo VM. Infective endocarditis epidemiology over five decades: a systematic review. PLoS ONE. 2013;8:e82665.
4. Durante-Mangoni E, Bradley S, Selton-Suty C, Tripodi MF, Barsic B, Bouza E, Cabell CH, Ramos AI, Fowler V, Hoen B, Konecny P, Moreno A, Murdoch D, Pappas P, Sexton DJ, Spelman D, Tattevin P, Miro JM, van der Meer JT, Utili R. Current features of infective endocarditis in elderly patients: results of the International Collaboration on Endocarditis Prospective Cohort Study. Arch Intern Med. 2008;168:2095–103.
5. Oliver L, Lavoute C, Giorgi R, Salaun E, Hubert S, Casalta J-P, Gouriet F, Renard S, Saby L, Avierinos J-F, Maysou L-A, Riberi A, Grisoli D, Casalta A-C, Collart F, Raoult D, Habib G. Infective endocarditis in octogenarians. Heart. 2017;103:1602–9.
6. Forestier E, Roubaud-Baudron C, Fraisse T, Patry C, Gavazzi G, Hoen B, Carauz-Paz P, Moheb-Khosravi B, Delahaye F, Sost G, Paccalin M, Nazeyrollas P, Strady C, Alla F, Selton-Suty C. Comprehensive geriatric assessment in older patients suffering from infective endocarditis. A prospective multicentric cohort study. Clin Microbiol Infect. 2019;25:1246–52.
7. Lopez J, Revilla A, Vilacosta I, Sevilla T, Villacorta E, Sarria C, Pozo E, Rollan MJ, Gomez I, Mota P, San Roman JA. Age-dependent profile of left-sided infective endocarditis: a 3-center experience. Circulation. 2010;121:892–7.
8. Selton-Suty C, Hoen B, Grentzinger A, Houplon P, Maignan M, Juilliere Y, Danchin N, Canton P, Cherrier F. Clinical and bacteriological characteristics of infective endocarditis in the elderly. Heart. 1997;77:260–3.
9. Ghanta RK, Pettersson GB. Surgical treatment of infective endocarditis in elderly patients: the importance of shared decision making. J Am Heart Assoc. 2021;10(19): e022186. https://doi.org/10.1161/JAHA.121.022186 (**Epub 2021 Sep 24. PMID: 34558288**).
10. Ragnarsson S, Salto-Alejandre S, Ström A, Olaison L, Rasmussen M. Surgery is underused in elderly patients with left-sided infective endocarditis: a nationwide registry study. J Am Heart Assoc. 2021;10(19): e020221. https://doi.org/10.1161/JAHA.120.020221 (**Epub 2021 Sep 24. PMID: 34558291**).
11. Habib G, Lancellotti P, Erba P-A, Sadeghpour A, Meshaal M, Sambola A, Furnaz S, Citro R, Ternacle J, Donal E, Cosyns B, Popescu B, Iung B, Prendergast B, Laroche C, Tornos P, Pazdernik M, Maggioni A, Gale CP, EURO-ENDO Investigators. The ESC-EORP EURO-ENDO (European Infective Endocarditis) registry. Eur Heart J Qual Care Clin Outcomes. 2019;5:202–7.
12. Habib G, Lancellotti P, Antunes MJ, Bongiorni MG, Casalta JP, Del Zotti F, Dulgheru R, El Khoury G, Erba PA, Iung B, Miro JM, Mulder BJ, Plonska-Gosciniak E, Price S, Roos-Hesselink J, Snygg-Martin U, Thuny F, Tornos Mas P, Vilacosta I, Zamorano JL; ESC Scientific Document Group (2015) 2015 ESC Guidelines for the management of infective endocarditis: the task force for the management of infective endocarditis of the European Society of Cardiology (ESC). Endorsed by: European Association for Cardio-Thoracic Surgery (EACTS), the European Association of Nuclear Medicine (EANM). Eur Heart J. 2015;36(44):3075–128. doi: https://doi.org/10.1093/eurheartj/ehv319. Epub 2015 Aug 29. PMID: 26320109.
13. Sy RW, Kritharides L. Health care exposure and age in infective endocarditis: results of a contemporary population-based profile of 1536 patients in Australia. Eur Heart J. 2010;31:1890–2187.
14. Polyzos KA, Konstantelias AA, Falagas ME. Risk factors for cardiac implantable electronic device infection: a systematic review and meta-analysis. Europace. 2015;17:767–77.
15. Chirouze C, Athan E, Alla F, Chu VH, Ralph Corey G, Selton-Suty C, Erpelding M-L, Miro JM, Olaison L, Hoen B, International Collaboration on Endocarditis Study Group. Enterococcal endocarditis in the beginning of the 21st century: analysis from the International Collaboration on Endocarditis-Prospective Cohort Study. Clin Microbiol Infect. 2013;19:1140–7.
16. Summers MR, Leon MB, Smith CR, Kodali SK, Thourani VH, Herrmann HC, Makkar RR, Pibarot P, Webb JG, Leipsic J, Alu MC, Crowley A, Hahn RT, Kapadia SR, Tuzcu EM, Svensson L, Cremer PC, Jaber WA. Prosthetic valve endocarditis after TAVR and SAVR: insights from the PARTNER trials. Circulation. 2019;140:1984–94.
17. Cahill TJ, Baddour LM, Habib G, Hoen B, Salaun E, Pettersson GB, Schäfers HJ, Prendergast BD. Challenges in infective endocarditis. J Am Coll Cardiol. 2017;69:325–44.
18. Chu VH, Park LP, Athan E, Delahaye F, Freiberger T, Lamas C, Miro JM, Mudrick DW, Strahilevitz J, Tribouilloy C, Durante-Mangoni E, Pericas JM, Fernández-Hidalgo N, Nacinovich F, Rizk H, Krajinovic V, Giannitsioti E, Hurley JP, Hannan MM, Wang A, International Collaboration on Endocarditis (ICE) Investigators. Association between surgical indications, operative risk, and clinical outcome in infective endocarditis: a prospective study from the International Collaboration on Endocarditis. Circulation. 2015;131:131–40.
19. Iung B, Doco-Lecompte T, Chocron S, Strady C, Delahaye F, Le Moing V, Poyart C, Alla F, Cambau E, Tattevin P, Chirouze C, Obadia J-F, Duval X, Hoen B, AEPEI Study Group. Cardiac surgery during the acute phase of infective endocarditis: discrepancies between European Society of Cardiology guidelines and practices. Eur Heart J. 2016;37:840–8.
20. López-Wolf D, Vilacosta I, San Román JA, Fernández C, Sarriá C, López J, Revilla A, Manchado R. Infective endocarditis in octogenarian patients. Rev Esp Cardiol. 2011;64:329–33.

Authors and Affiliations

Michal Pazdernik[1,2] · Bernard Iung[3] · Bulent Mutlu[4] · François Alla[5] · Robert Riezebos[6] · William Kong[7] · Maria Carmo Pereira Nunes[8] · Luc Pierard[9] · Ilija Srdanovic[10] · Hirotsugu Yamada[11] · Andrea De Martino[12] · Marcelo Haertel Miglioranza[13] · Julien Magne[14] · Cornelia Piper[15] · Cécile Laroche[16] · Aldo P. Maggioni[16,17] · Patrizio Lancellotti[18] · Gilbert Habib[19,20] · Christine Selton-Suty[21,22] on behalf of the EURO-ENDO Investigators group

Michal Pazdernik
michal.pazdernik@email.cz

Bernard Iung
bernard.iung@aphp.fr

Bulent Mutlu
mutlub@gmail.com

François Alla
francois_alla@yahoo.fr

Robert Riezebos
r.k.riezebos@olvg.nl

William Kong
william_kong@nuhs.edu.sg

Maria Carmo Pereira Nunes
mcarmo@waymail.com.br

Luc Pierard
lpierard@chu.ulg.ac.be

Ilija Srdanovic
ilijasrd@gmail.com

Hirotsugu Yamada
yamadah@tokushima-u.ac.jp

Andrea De Martino
and.demartino@libero.it

Marcelo Haertel Miglioranza
marcelohaertel@gmail.com

Julien Magne
jumagne8@gmail.com

Cornelia Piper
cpiper@hdz-nrw.de

Patrizio Lancellotti
plancellotti@chu.ulg.ac.be

Gilbert Habib
gilbert.habib3@gmail.com

[1] Institute for Clinical and Experimental Medicine (IKEM), Prague, Czech Republic

[2] Department of Cardiology, Second Medical School, Charles University, University Hospital Motol, Prague, Czech Republic

[3] Cardiology Department, Bichat Hospital, APHP, Université de Paris, Paris, France

[4] Department of Cardiology, Marmara University Hospital, Pendik, Istanbul, Turkey

[5] CHU de Bordeaux, Bordeaux, France

[6] Heart Center, OLVG, Amsterdam, Netherlands

[7] National University Heart Centre Singapore, Singapore, Singapore

[8] Federal University of Minas Gerais, Belo Horizonte, Brazil

[9] University Hospital Sart Tilman, University of Liege, Liege, Belgium

[10] Medical Faculty University, Novi Sad, Serbia

[11] Tokushima University Graduate School of Biomedical Sciences, Tokushima, Japan

[12] University Hospital of Pisa, Pisa, Italy

[13] Brasil Institute of Cardiology/University Foundation, Porto Alegre, Brazil

[14] Cardiology Dept, CHU Limoges, INSERM 1094, University Hospital Dupuytren, 87042 Limoges, France

[15] Herz- und Diabeteszentrum NRW, Universitätsklinikum der Ruhr-Universität Bochum, Bad Oeynhausen, Germany

[16] EURObservational Research Programme, European Society of Cardiology, Biot, France

[17] Maria Cecilia Hospital, GVM Care and Research, Cotignola, Italy

[18] University Hospital of Liege (CHU), Liege, Belgium

[19] Cardiology Dept, APHM, La Timone Hospital, Marseille, France

[20] Aix Marseille Univ, IRD, APHM, MEPHI, IHU-Méditerranée Infection, Marseille, France

[21] Cardiology Dept, CIC-ECCHU Nancy-Brabois, 54000 Nancy, France

[22] Association pour l'Etude et la Prevention de l'Endocardite Infectieuse (AEPEI), Paris, France

P. Šedová et al.

The decline in stroke hospitalization due to COVID-19 is unrelated to COVID-19 intensity

Eur J Neurol
Impact Factor: 6.288

‹ rejstřík

Received: 21 September 2022 | Accepted: 8 December 2022

DOI: 10.1111/ene.15664

european journal of neurology
the official journal of the european academy of neurology

ORIGINAL ARTICLE

The decline in stroke hospitalization due to COVID-19 is unrelated to COVID-19 intensity

Petra Sedova[1,2,3,4] | Julia Anna Kent[5] | Tomas Bryndziar[2,4] | Jiri Jarkovsky[6,7] | Ales Tomek[8] | Martin Sramek[8] | Ondrej Skoda[9,10] | Tereza Sramkova[8] | Kateřina Pokorová[6,7] | Simona Littnerova[6,7] | Robert D. Brown Jr[1] | Robert Mikulik[2,4]

[1]Department of Neurology, Mayo Clinic, Rochester, Minnesota, USA

[2]International Clinical Research Center, St Anne's University Hospital, Brno, Czech Republic

[3]Department of Internal Medicine and Cardiology, University Hospital Brno and Faculty of Medicine, Masaryk University, Brno, Czech Republic

[4]Department of Neurology, St Anne's University Hospital, and Faculty of Medicine, Masaryk University, Brno, Czech Republic

[5]Faculty of Medicine, Masaryk University, Brno, Czech Republic

[6]Institute of Health Information and Statistics of the Czech Republic, Prague, Czech Republic

[7]Faculty of Medicine, Institute of Biostatistics and Analyses, Masaryk University, Brno, Czech Republic

[8]Department of Neurology, Charles University in Prague, and Second Faculty of Medicine and Motol University Hospital, Prague, Czech Republic

[9]Neurological Department and Stroke Unit, Jihlava Hospital, Jihlava, Czech Republic

[10]Department of Neurology, University Hospital Kralovske Vinohrady and Charles University in Prague, Prague, Czech Republic

Correspondence
Petra Sedova, International Clinical Research Center, St Anne's University Hospital, Pekarska 53, Brno 65691, Czech Republic.
Email: kofronova.petra@mayo.edu

Funding information
COST (European Cooperation in Science and Technology) Association, project No. CA18118; IRENE COST Action - Implementation Research Network in Stroke Care Quality and by the project No. LQ1605 from the National Program of Sustainability II; IRIS-TEPUS Project No. LTC20051 from the INTER-EXCELLENCE INTER-COST program of the Ministry of Education, Youth and Sports of the Czech Republic

Abstract

Background and Purpose: During the coronavirus disease 2019 (COVID-19) pandemic many countries reported a decline in stroke volumes. The aim of this study was to analyze if the decline was related to the intensity of the COVID-19 pandemic.

Methods: The first pandemic year (1 March 2020 to 28 February 2021) overall and during the three COVID-19 waves were compared with the preceding year. Volumes of acute ischaemic stroke (AIS), subarachnoid hemorrhage, intracerebral hemorrhage and recanalization treatments (intravenous thrombolysis [IVT] and mechanical thrombectomy [MT]) were obtained from the National Register of Reimbursed Health Services. Door-to-needle time, onset-to-door time and National Institutes of Health Stroke Scale at admission were obtained from the Registry of Stroke Care Quality.

Results: During the pandemic year compared to the preceding year there were 26,453 versus 28,771 stroke admissions, representing an 8.8% decline ($p < 0.001$). The declines (−10%, −11%, −19%) appeared in COVID-19 waves (spring 2020, autumn 2020, winter 2021) except for an increase (2%) during summer 2020. Admissions for AIS declined by 10.2% ($p < 0.001$), whilst hemorrhagic stroke volumes were minimally decreased. The absolute volumes of IVT and MT decreased by 9.4% ($p < 0.001$) and 5.7% ($p = 0.16$), respectively. However, the proportions of ischaemic stroke patients receiving IVT (18% vs. 18%; $p = 0.72$) and MT (6% vs. 6%; $p = 0.28$) remained unchanged.

Petra Sedova and Julia Anna Kent contributed equally to this work.

Conclusions: There was a decline in stroke admissions, but such decline was not related to COVID-19 incidence. The frequency of use of recanalization procedures (IVT, MT) and times (onset-to-door time, door-to-needle time) in AIS were preserved in the Czech Republic during the first year of the pandemic.

KEYWORDS
COVID-19, Czech Republic, intravenous thrombolysis, mechanical thrombectomy, stroke

INTRODUCTION

For over 2 years the coronavirus disease 2019 (COVID-19) pandemic has challenged hospitals worldwide. Many studies [1–14] reported a decline in the number of stroke code activations and hospital admission rates during the first wave of the pandemic (March–May/June 2020) [15–28]. Consequently, a decline in the number of recanalization procedures (mechanical thrombectomy [MT] [18–20, 25, 29, 30] and intravenous thrombolysis [IVT] [10, 14, 16, 18–20, 23, 25–27, 30]) was observed. Furthermore, changes in stroke severity and indicators of acute ischaemic stroke (AIS) care quality (door-to-needle time [DNT], onset-to-door time [ODT]) have been noted in many countries, with more severe strokes at admission [5, 6, 27, 30] and higher stroke mortality rates [3, 9, 25].

In the Czech Republic (CR), a state of national emergency was declared on 12 March 2020. During the first coronavirus wave (March–May 2020), the CR was amongst the countries with the lowest incidence rate; however, the opposite was true for the later phases (September 2020 to February 2021), during which the CR was one of the most affected countries in the world.

Our initial report covering the first wave of the COVID-19 pandemic (March–May 2020) demonstrated a decline in stroke admission volumes and recanalization procedures in the CR [20].

It is unknown how the surge in COVID-19 cases in later phases and the following governmental protective measures influenced stroke admissions and management. In this study the impact of the COVID-19 pandemic on stroke volume and stroke management (recanalization therapy, DNT, ODT) during the first full year of the pandemic is evaluated.

METHODS

Study design

Data related to all stroke patients occurring in the CR were retrieved from the National Register of Reimbursed Health Services (NRRHS) for the years 2019, 2020 and 2021. DNT, ODT and stroke severity at admission (National Institutes of Health Stroke Scale, NIHSS) were obtained from the Registry of Stroke Care Quality (RES-Q) for March 2019, October 2019, April 2020 and October 2020. Only patients who were diagnosed with the following stroke types were included: subarachnoid hemorrhage (SAH), intracerebral hemorrhage (ICH) and ischaemic stroke (International Classification of Diseases, 10th revision, codes I60, I61 and I63, respectively). The occurrence of each stroke type, the utilization of recanalization procedures (IVT, MT) and demographic parameters (age, sex) during the first pandemic year (1 March 2020 to 28 February 2021) overall and during the three COVID-19 waves within that year were compared with the preceding year (1 March 2019 to 29 February 2020).

Czech Republic

In the CR, there is a public health insurance system. All health care services reimbursed from the public health insurance system by health insurance companies are reported to the NRRHS. Thus, the NRRHS collects and stores all data reported to health insurance companies by every healthcare provider.

Registry of Stroke Care Quality (RES-Q)

Data on all stroke patients discharged with a stroke diagnosis from all accredited stroke centers in the CR are collected in the international RES-Q for 2 months every year (March or April and October). Further, RES-Q includes stroke management data including time to initiation of reperfusion therapy (DNT, ODT) and stroke severity as reflected by the NIHSS score.

COVID epidemic in the CR

The CR was one of the least affected countries by the COVID-19 pandemic during the spring wave of 2020. By 31 May 2020, a total of only 9268 people (i.e., 881 cases per million) had tested positive for severe acute respiratory syndrome coronavirus 2 (SARS-CoV-2) (incidence 3.6 per million, 30 deaths per million) [31]. This success was followed by a significant surge in cases and the CR turned out to be one of the most heavily affected countries in the world in autumn 2020 and winter 2021. By 31 December 2020, 718,661 people (i.e., 68,373 cases per million) had tested positive, and by the end of February 2021 the total COVID-19 cases reached 1.24 million (i.e., 117,544 cases per million) [31]. Moreover, there was a substantial rise in case mortality, as the total number of deaths increased to 11,580 by 31 December 2020, and it had nearly doubled to 20,339 (1935 per million) by 28 February 2021 [31].

Study periods

The COVID-19 pandemic year (March 2020 to February 2021) was compared with the immediately preceding year (March 2019 to February 2020). The pandemic year was divided into four periods according to COVID-19 incidence and compared to corresponding pre-pandemic months: spring (March–May 2020) first wave but with low COVID-19 incidence, summer (June–August 2020) with low COVID-19 incidence, autumn (September–December 2020) second wave with high COVID-19 incidence, and winter (January–February 2021) third wave with high COVID-19 incidence.

Statistical analysis

Categorical variables are reported as absolute numbers and percentages. Continuous variables are presented as mean and standard deviation or median and interquartile range. The comparisons between years were performed using Fisher's exact test or the Mann–Whitney test, as appropriate. For overall volume analysis, the *p* value is based on two-sided Poisson means test. A *p* value of <0.05 was considered statistically significant. All statistical analyses were produced using R Statistical Software (version 4.0.3).

Statement of Ethics

The present study conforms to the guidelines issued in the Declaration of Helsinki. Informed consent requirement was waived by the institutional ethics committees for this retrospective study using anonymized clinical data, with no direct patient contact. The ethics committee of St Anne's University Hospital determined that this study does not constitute clinical research and is thus exempt from ethics committee review (communication received on 13 January 2021).

RESULTS

The decrease in stroke admissions appeared in all COVID-19 waves (spring 2020, autumn 2020, winter 2021), and the decrease was greater as time and COVID-19 incidence progressed (−10.2%, −11.7%, −18.9%, respectively), except for the unexpected rise (+2%) in stroke admissions in summer 2020, when the COVID-19 pandemic was considered to potentially be over.

During the pandemic year 2020 compared to the prior year, the overall number of patients with stroke admitted to hospitals fell from 28,771 to 26,453 (8.8%, $p < 0.001$). Hemorrhagic stroke admissions remained stable, with only a slight decrease in the number of admitted patients with SAH and ICH, 1057–1024 (3.2%, $p = 0.48$) for SAH and 3286 to 3261 (0.8%, $p = 0.77$) for ICH. Only the decline observed in admissions for AIS reached statistical significance, as their number during the pandemic fell from 24,428 to 22,168 (10.2%, $p < 0.001$) in comparison to the pre-pandemic year (Table 1).

Comparing the first pandemic year to the previous year, the age of the admitted ischaemic stroke patients and the relative proportion of male patients remained unchanged for all stroke types.

Hospital admission rates for AIS fell significantly during all COVID-19 waves (Figure 1). The decline observed during the

TABLE 1 Hospital admissions for all stroke types during the first year of the pandemic compared to the previous year

	1 year	Low incidence wave	Summer "zero" COVID-19	High incidence waves	
	1 year March 2020 to February 2021 [March 2019 to February 2020]	First wave March–May 2020 [2019]	June–August 2020 [2019]	Second wave September–December 2020 [2019]	Third wave January–February 2021 [2020]
Stroke total					
N	26,453 [28,771]	6615 [7290]	7084 [6940]	8716 [9738]	4038 [4803]
Relative change (*p* value)	−8.8% (<0.001)	−10.2% (<0.001)	2.0% (0.23)	−11.7% (<0.001)	−18.9% (<0.001)
SAH (I60)					
N	1024 [1057]	262 [283]	301 [229]	335 [380]	126 [165]
Relative change (*p* value)	−3.2% (0.48)	−8.0% (0.39)	23.9% (0.00)	−13.4% (0.10)	−31.0% (0.03)
ICH (I61)					
N	3261 [3286]	865 [863]	713 [711]	1125 [1152]	558 [560]
Relative change (*p* value)	−0.8% (0.77)	0.2% (0.98)	0.3% (0.98)	−2.4% (0.59)	−0.4% (0.98)
AIS (I63)					
N	22,168 [24,428]	5488 [6144]	6070 [6000]	7256 [8206]	3354 [4078]
Relative change (*p* value)	−10.2% (<0.001)	−12.0% (<0.001)	1.2% (0.53)	−13.1% (<0.001)	−21.6% (<0.001)

Abbreviations: AIS, acute ischaemic stroke; ICH, intracerebral hemorrhage; SAH, subarachnoid hemorrhage.

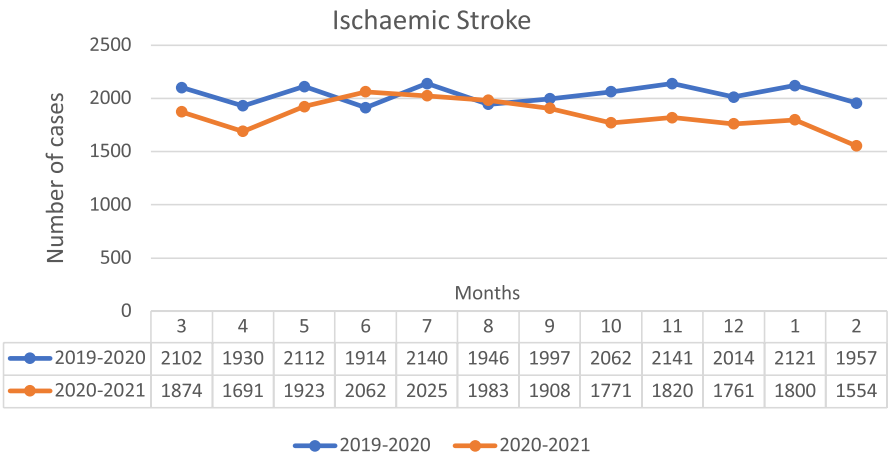

FIGURE 1 Number of acute ischaemic stroke cases during the first pandemic year and the pre-pandemic year

autumn wave (−13.1%, $p<0.001$) with higher COVID-19 incidence was slightly greater compared to the decline during the spring wave (12.0%, $p<0.001$) with lower COVID-19 incidence. The most significant reduction was observed during the winter 2021 wave with the highest number of COVID-19 cases, as hospitalizations decreased by 21.6% ($p<0.001$) in comparison to the previous year.

Probably related to the reduction in the number of admitted AIS patients there was also a reduction in the volume of IVT procedures, with the most notable decline during the autumn wave (16.8%, $p<0.001$) and winter wave 2021 (11.9%, $p=0.041$), when COVID-19 cases were peaking, whilst there was a return to pre-pandemic levels (−0.4%) during the summer months when COVID-19 occurrence was low. A similar but not significant decline was reported for MT procedures, with the sharpest decline during the spring (12.5%, $p=0.151$) and winter 2021 waves (13.3%, $p=0.211$). During the first year of the COVID-19 pandemic, similar to the decrease in admission rates, there was a reduction in the volume of MT and IVT procedures in AIS patients, with numbers falling from 1350 to 1277 (5.7%, $p=0.160$) and 4322 to 3950 (9.4%, $p<0.001$), respectively, At the same time, the relative proportion of patients receiving recanalization procedures remained relatively stable compared to the pre-COVID year (Table 2).

For SAH, the decline in the number of admitted patients during the autumn (−13.4%, $p=0.1$) and winter waves (−31%, $p=0.03$) with high COVID-19 incidence was greater than during the first wave (−8.0%, $p=0.48$).

Using the RES-Q, the time to initiation of reperfusion therapy remained unchanged during the spring COVID-19 wave (DNT, 24 vs. 24 min, $p=0.5$; and ODT, 160 vs. 158 min, $p=0.23$) with improvement in ODT during the autumn wave (147 vs. 172 min; $p=0.009$). Stroke severity at admission did not differ comparing the years (NIHSS 6 vs. 6, $p=0.5$; NIHSS 6 vs. 6; $p=0.15$) (Table 3).

More detailed information on stroke type admission volumes and stroke management is presented in Tables 1–3 and Figures 1–3.

DISCUSSION

Using nationwide data, the effect of the COVID-19 pandemic on hospital admission rates and ischaemic stroke acute care quality in the CR during the first pandemic year was evaluated. A significant reduction in the total number of admitted stroke patients (8.8%, $p<0.001$) during the pandemic was observed compared to the previous year. However, only the decline in AIS reached statistical significance (10.2%, $p<0.001$), whilst ICH and SAH were unchanged. The most relevant results of our analysis are twofold. First, a significant decline in hospitalizations for total stroke during all COVID-19 waves regardless of COVID-19 incidence was found. Secondly, stroke hospital admissions returned to pre-pandemic levels during summer 2020, when the COVID-19 cases were low and the pandemic was considered to be over. The observed decline in AIS was accompanied by a decrease in the volume of recanalization procedures compared to the previous year, with an unchanged relative proportion of patients receiving IVT and MT. The time to initiation of reperfusion therapy was unchanged, suggesting that stroke management quality in the earliest stages of AIS was preserved.

No change in stroke severity at admission was observed, suggesting that people avoided hospitals regardless of stroke severity. Others have reported more severe strokes at admission during the pandemic [5, 6, 27, 30], indicating that patients with mild to moderate stroke or a transient ischaemic attack (TIA) did not seek medical help as consistently. Possible reasons proposed have included the fear of contracting the virus in the hospital setting [2, 3, 6, 12–14, 21–24, 27–29, 32] and the restrictive measures adopted during lockdown periods leading to social distancing, leading to more mild strokes or TIAs being unintentionally overlooked by the patients' relatives [5, 8, 12, 14, 16, 21, 22, 24, 27, 32].

To date, few studies have reported changes in hospitalization rates and stroke care quality during the second wave of the pandemic [22, 25, 33–35]. Our findings are in line with a recently published study by Katsouras et al. [35] (Greece, second wave November–December 2020), who observed a decline in acute stroke and acute coronary syndrome admission rates by 33.7% and 33.3%, respectively, compared to the same period in 2019.

In the CR the COVID-19 incidence rate was higher during the second wave in autumn 2020, which was accompanied by a sharper decline in stroke admission rates compared to the first wave of spring 2020 (11.8% vs. 10.2%). Yu et al. [25] (Ontario, Canada)

TABLE 2 Demographic variables, recanalization procedures and mortality rates for acute ischaemic stroke patients

	1 year		Low incidence wave		Summer "zero" COVID-19		High incidence waves			
	March 2020 to February 2021	March 2019 to February 2020	March–May 2020	March–May 2019	June–August 2020	June–August 2019	September–December 2020	September–December 2019	January–February 2021	January–February 2020
Mean age ± SD	73.48 ± 12.35	73.61 ± 12.41	73.58 ± 12.40	73.92 ± 12.32	73.30 ± 12.61	73.16 ± 12.71	73.38 ± 12.19	73.45 ± 12.16	73.87 ± 12.13	74.14 ± 12.55
Men, *n* (%)	10,742 (48.5 %)	12,039 (49.3 %)	2648 (48.3 %)	3017 (49.1 %)	2991 (49.3 %)	2945 (49.1 %)	3482 (48.0 %)	4060 (49.5 %)	1621 (48.3 %)	2017 (49.5 %)
Relative change (*p* value)	−12.1 % (<0.001)		−13.9 % (<0.001)		1.5 % (0.559)		−16.6 % (<0.001)		−24.4 % (<0.001)	
IVT, *n* (%)	3950 (17.8 %)	4322 (17.7 %)	976 (17.8 %)	1056 (17.2 %)	1071 (17.6 %)	1075 (17.9 %)	1265 (17.4 %)	1477 (18.0 %)	638 (19.0 %)	714 (17.5%)
Relative change (*p* value)	−9.4 % (<0.001)		−8.2 % (0.080)		−0.4 % (0.948)		−16.8 % (<0.001)		−11.9 % (0.041)	
MT, *n* (%)	1277 (5.76 %)	1350 (5.53 %)	296 (5.39 %)	333 (5.42 %)	327 (5.39 %)	310 (5.17 %)	451 (6.22 %)	477 (5.81 %)	203 (6.05 %)	230 (5.64 %)
Relative change (*p* value)	−5.7 % (0.160)		−12.5 % (0.151)		5.2 % (0.526)		−5.8 % (0.412)		−13.3 % (0.211)	

Abbreviations: IVT, intravenous thrombolysis; MT, mechanical thrombectomy.

reported that the number of stroke patients visiting the emergency department did not drop to the degree of that noted during the first lockdown in the spring of 2020. Similarly, Richter et al. [33] (Germany) showed there was a greater decrease in admission rates for AIS during the first wave of spring 2020 compared to the second wave of autumn 2020, leading to possible explanations such as better public awareness about the detrimental effects of not seeking medical help in the case of stroke and a reduction in fear of contracting the virus. A study from Denmark reported a decrease in the number of stroke patients and stroke mimics during the first lockdown in Denmark (13 March 2020 to 17 May 2020) compared to the pre-pandemic year (1 January 2019 to 12 March 2020) [22]. At the same time, if the first pandemic year (13 March 2020 to 28 February 2021) was compared to the pre-pandemic year an increase in the total number of stroke patients was noted, with an increase in AIS cases but an unchanged number of ICH patients. These findings suggest that after the first lockdown period the number of stroke patients has been on the rise [22].

Whilst no change in demographic characteristics was observed, Richter et al. [33] reported a more significant decline in females with AIS during both waves compared to the pre-pandemic year, with only the change during the second wave being statistically significant. The authors attributed the observed difference to German women representing a greater proportion of care facility residents, one of the most vulnerable parts of the population during the pandemic, as well as to women being more serious about the severity of the pandemic and more inclined to follow restrictive measures [33].

Due to lower admission rates during the pandemic, the absolute volume of IVT procedures also decreased (but with a preserved relative proportion of AIS patients receiving such procedures) in all COVID-19 waves and returned to pre-pandemic levels during summer 2020. Comparable results were reported from Canada [25] and from Germany [33]. In our analysis a decline in the number of MTs in AIS patients (but with a stable percentage of AIS patients) during all time periods except for the summer 2020 was found. These results contradict the observed increase of MT procedures during the pandemic year in Germany [33]. On the other hand, data from Denmark [22] showed no change in the number of IVT and MT procedures during the pandemic; however, the authors hypothesized that these findings might be due to the smaller study cohort or the possible prevalence of milder strokes during the pandemic, even though no data regarding the NIHSS were reported.

The observed decrease in admission rates of stroke patients during the second wave in autumn 2020 and the third wave in winter 2021 was comparable to the decline noted during the first wave of spring 2020 although the infection rate in the CR was higher at the later stages of the first pandemic year. These findings indicate that during the later waves people with stroke did not seek medical assistance in a similar manner compared to the first wave, whilst in other countries the decline was not as great [33], or stroke cases even rose [22]. Strict political measures leading to social distancing could have led to more TIAs being overlooked by the patients' relatives. People might have had ongoing fear of contracting the virus. Due to the

TABLE 3 Parameters of stroke care in ischaemic stroke patients (I63) in 2019 and 2020 using RES-Q

	March 2019	April 2020	*p* value	October 2019	October 2020	*p* value
DNT (min), median (IQR)	24 (15–35)	24 (16–34)	0.52	23 (15–33)	22 (16–30)	0.46
ODT (min), median (IQR)	158 (85–375.5)	160 (84–387)	0.52	172 (85–430)	147 (80–336)	0.009*
NIHSS at admission median (IQR)	6 (3–13)	6 (3–12)	0.49	6 (3–12)	6 (3–13)	0.15

Abbreviations: DNT, door-to-needle time; IQR, interquartile range; NIHSS, National Institutes of Health Stroke Scale; ODT, onset-to-door time.
*p value of <0.05 was considered statistically significant.

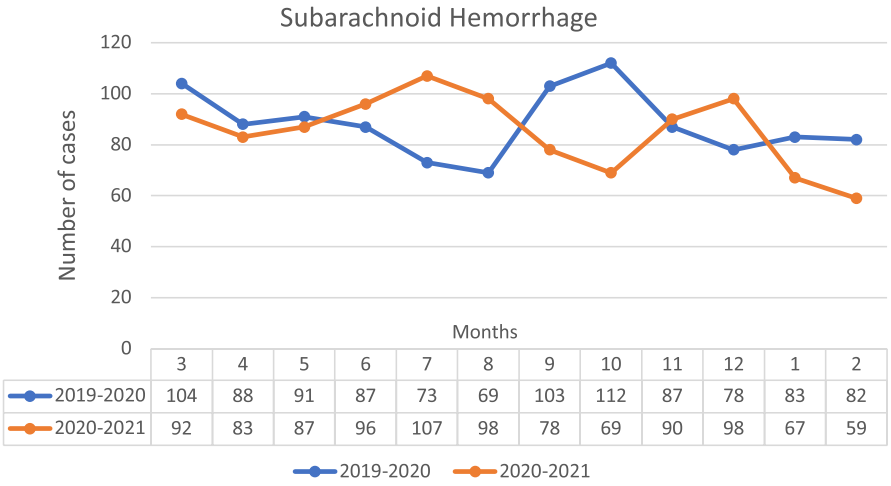

FIGURE 2 Number of subarachnoid hemorrhage cases during the first pandemic year and the pre-pandemic year

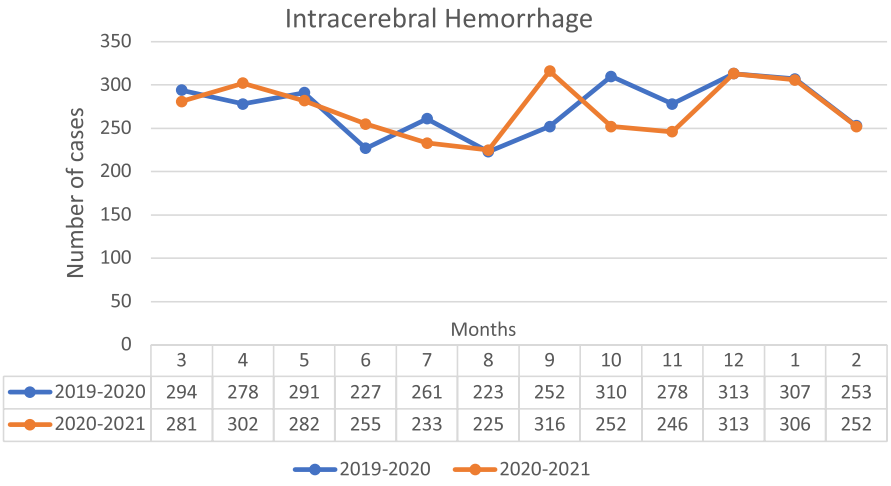

FIGURE 3 Number of intracerebral hemorrhage cases during the first pandemic year and the pre-pandemic year

current study design, it could not be determined whether the drop in admission rates was due to the stroke incidence decline during the pandemic or patients with stroke being less likely to seek medical assistance. Our results also suggest that during the pandemic acute stroke care in the CR remained widely accessible and the quality of the earliest stages of ischaemic stroke care was preserved, as the relative proportion of patients receiving recanalization procedures was comparable to the pre-pandemic year and recanalization times remained stable.

One of the biggest strengths of this study is the nationwide data coverage. Furthermore, to date this is one of the few studies to evaluate the impact of the pandemic on stroke admission rates and care quality at the earliest stages of AIS during the entire first year of the pandemic.

CONCLUSION

In this nationwide study in the CR the effect of the SARS-CoV-2 pandemic on stroke hospitalization and frequency of use of IVT and MT for AIS during the first COVID-19 pandemic year was evaluated. An 8.8% drop in stroke hospitalizations was found, with a statistically significant decrease only being noted in ischaemic stroke. The decline in stroke admissions occurred regardless of the level of COVID-19 incidence with a return to normal levels during pandemic "disappearance" in the summer months of 2020. The decline in ischaemic stroke admission rates was accompanied by a decrease in the absolute volumes of recanalization procedures (IVT, MT) but with a stable relative proportion of AIS patients receiving the procedures. Preserved recanalization times (DNT, ODT)

suggest stable acute management quality for ischaemic stroke. The unchanged NIHSS at admission would be consistent with the avoidance of hospital visits irrespective of stroke severity. As the pandemic continues, it is imperative that the public has increased awareness of the consequences of untreated serious medical conditions like stroke.

FUNDING INFORMATION

Petra Sedova and Robert Mikulik were supported by the COST (European Cooperation in Science and Technology) Association, project no. CA18118, IRENE COST Action–Implementation Research Network in Stroke Care Quality and by the project no. LQ1605 from the National Program of Sustainability II and by the IRIS-TEPUS Project No. LTC20051 from the INTER-EXCELLENCE INTER-COST program of the Ministry of Education, Youth and Sports of the Czech Republic. Petra Sedova was supported by Ministry of Health, Czech Republic - conceptual development of research organization (FNBr, 65269705).

CONFLICT OF INTEREST

Tomas Bryndziar reports former employment at Bristol-Myers Squibb outside the submitted work.

DATA AVAILABILITY STATEMENT

The data that support the findings of this study are available upon request from the corresponding author.

ORCID

Petra Sedova https://orcid.org/0000-0002-1379-0203
Tomas Bryndziar https://orcid.org/0000-0001-7651-4778
Robert Mikulik https://orcid.org/0000-0002-7458-5166

REFERENCES

1. Esenwa C, Parides MK, Labovitz DL. The effect of COVID-19 on stroke hospitalizations in New York City. *J Stroke Cerebrovasc Dis*. 2020;29(10):105114.
2. Romoli M, Eusebi P, Forlivesi S, et al. Stroke network performance during the first COVID-19 pandemic stage: a meta-analysis based on stroke network models. *Int J Stroke*. 2021;16(7):771-783.
3. Richter D, Eyding J, Weber R, et al. Analysis of nationwide stroke patient care in times of COVID-19 pandemic in Germany. *Stroke*. 2021;52(2):716-721.
4. de Havenon A, Yaghi S, Majersik JJ, et al. Acute coronary syndrome and ischemic stroke discharges in the United States during the COVID-19 pandemic. *Stroke*. 2021;52(6):e239-e241.
5. Kristoffersen ES, Jahr SH, Thommessen B, Rønning OM. Effect of COVID-19 pandemic on stroke admission rates in a Norwegian population. *Acta Neurol Scand*. 2020;142(6):632-636.
6. Katsanos AH, Palaiodimou L, Zand R, et al. Changes in stroke hospital care during the COVID-19 pandemic: a systematic review and meta-analysis. *Stroke*. 2021;52(11):3651-3660.
7. Bres Bullrich M, Fridman S, Mandzia JL, et al. COVID-19: stroke admissions, emergency department visits, and prevention clinic referrals. *Can J Neurol Sci*. 2020;47(5):693-696.
8. Bersano A, Kraemer M, Touzé E, et al. Stroke care during the COVID-19 pandemic: experience from three large European countries. *Eur J Neurol*. 2020;27(9):1794-1800.
9. Douiri A, Muruet W, Bhalla A, et al. Stroke care in the United Kingdom during the COVID-19 pandemic. *Stroke*. 2021;52(6):2125-2133.
10. Uchino K, Kolikonda MK, Brown D, et al. Decline in stroke presentations during COVID-19 surge. *Stroke*. 2020;51(8):2544-2547.
11. Altersberger VL, Stolze LJ, Heldner MR, et al. Maintenance of acute stroke care service during the COVID-19 pandemic lockdown. *Stroke*. 2021;52(5):1693-1701.
12. Diegoli H, Magalhães PSC, Martins SCO, et al. Decrease in hospital admissions for transient ischemic attack, mild, and moderate stroke during the COVID-19 era. *Stroke*. 2020;51(8):2315-2321.
13. Gdovinová Z, Vitková M, Baráková A, Cvopová A. The impact of the COVID-19 outbreak on acute stroke care in Slovakia: data from across the country. *Eur J Neurol*. 2021;28(10):3263-3266.
14. Nogueira RG, Qureshi MM, Abdalkader M, et al. Global impact of COVID-19 on stroke care and IV thrombolysis. *Neurology*. 2021;96(23):e2824-e2838.
15. Rudilosso S, Laredo C, Vera V, et al. Acute stroke care is at risk in the era of COVID-19: experience at a Comprehensive Stroke Center in Barcelona. *Stroke*. 2020;51(7):1991-1995.
16. Sacco S, Ricci S, Ornello R, Eusebi P, Petraglia L, Toni D. Reduced admissions for cerebrovascular events during COVID-19 outbreak in Italy. *Stroke*. 2020;51(12):3746-3750.
17. Siegler JE, Heslin ME, Thau L, Smith A, Jovin TG. Falling stroke rates during COVID-19 pandemic at a comprehensive stroke center. *J Stroke Cerebrovasc Dis*. 2020;29(8):104953.
18. Zhao J, Li H, Kung D, Fisher M, Shen Y, Liu R. Impact of the COVID-19 epidemic on stroke care and potential solutions. *Stroke*. 2020;51(7):1996-2001.
19. Kerleroux B, Fabacher T, Bricout N, et al. Mechanical thrombectomy for acute ischemic stroke amid the COVID-19 outbreak: decreased activity, and increased care delays. *Stroke*. 2020;51(7):2012-2017.
20. Sedova P, Brown RD Jr, Bryndziar T, et al. Treat COVID-19, but not only COVID-19: stroke matters as well. *Cerebrovasc Dis*. 2022;51(1):52-59.
21. Rinkel LA, Prick JCM, Slot RER, et al. Impact of the COVID-19 outbreak on acute stroke care. *J Neurol*. 2021;268(2):403-408.
22. Drenck N, Grundtvig J, Christensen T, et al. Stroke admissions and revascularization treatments in Denmark during COVID-19. *Acta Neurol Scand*. 2022;145(2):160-170.
23. Ghoreishi A, Arsang-Jang S, Sabaa-Ayoun Z, et al. Stroke care trends during COVID-19 pandemic in Zanjan Province, Iran. From the CASCADE initiative: statistical analysis plan and preliminary results. *J Stroke Cerebrovasc Dis*. 2020;29(12):105321.
24. De Marchis GM, Wright PR, Michel P, et al. Association of the COVID-19 outbreak with acute stroke care in Switzerland. *Eur J Neurol*. 2022;29(3):724-731.
25. Yu AYX, Lee DS, Vyas MV, et al. Emergency department visits, care, and outcome after stroke and myocardial infarction during the COVID-19 pandemic phases. *CJC Open*. 2021;3(10):1230-1237.
26. Raymaekers V, Demeestere J, Bellante F, et al. The impact of COVID-19 on acute stroke care in Belgium. *Acta Neurol Belg*. 2021;121(5):1251-1258.
27. Ortega-Gutierrez S, Farooqui M, Zha A, et al. Decline in mild stroke presentations and intravenous thrombolysis during the COVID-19 pandemic: the Society of Vascular and Interventional Neurology Multicenter Collaboration. *Clin Neurol Neurosurg*. 2021;201:106436.
28. Tanisaka LS, Paiva LDS, Werneck de Carvalho LE, et al. Stroke hospital admissions during the COVID-19 outbreak in São Paulo, Brazil. *Cerebrovasc Dis*. 2022;51(5):686-689.
29. Markus HS, Martins S. COVID-19 and stroke—understanding the relationship and adapting services. A global world stroke organisation perspective. *Int J Stroke*. 2021;16(3):241-247.
30. Benali F, Stolze LJ, Rozeman AD, et al. Impact of the lockdown on acute stroke treatments during the first surge of the COVID-19 outbreak in the Netherlands. *BMC Neurol*. 2022;22(1):22.

31. Ritchie H ME, Rodés-Guirao L, Appel C, Giattino C, Ortiz-Ospina E, Hasell J, Macdonald B, Beltekian D, Roser M. Czechia: coronavirus pandemic country profile. https://ourworldindata.org/coronavirus/country/czech-republic. Published 2020. Accessed September 19, 2022.
32. Demaerschalk BM. Where in the world have all the strokes gone? *Neurology*. 2021;96(23):1069-1070.
33. Richter D, Eyding J, Weber R, et al. A full year of the COVID-19 pandemic with two infection waves and its impact on ischemic stroke patient care in Germany. *Eur J Neurol*. 2022;29(1):105-113.
34. Fuentes B, Alonso de Leciñana M, Rigual R, et al. Fewer COVID-19-associated strokes and reduced severity during the second COVID-19 wave: the Madrid stroke network. *Eur J Neurol*. 2021;28(12):4078-4089.
35. Katsouras C, Tsivgoulis G, Papafaklis M, et al. Persistent decline of hospitalizations for acute stroke and acute coronary syndrome during the second wave of the COVID-19 pandemic in Greece: collateral damage unaffected. *Ther Adv Neurol Disord*. 2021;14:17562864211029540.

How to cite this article: Sedova P, Kent JA, Bryndziar T, et al. The decline in stroke hospitalization due to COVID-19 is unrelated to COVID-19 intensity. *Eur J Neurol*. 2022;00:1-8. doi:10.1111/ene.15664

Š. Havránek et al.

Initial rhythm and survival in refractory out-ofhospital cardiac arrest. Post-hoc analysis of the Prague OHCA randomized trial

Resuscitation
Impact Factor: 6.251

rejstřík

RESUSCITATION 181 (2022) 289–296

Available online at ScienceDirect

Resuscitation

journal homepage: www.elsevier.com/locate/resuscitation

Clinical paper

Initial rhythm and survival in refractory out-of-hospital cardiac arrest. Post-hoc analysis of the Prague OHCA randomized trial

Stepan Havranek[a,*], *Zdenka Fingrova*[a,*], *Daniel Rob*[a], *Jana Smalcova*[a], *Petra Kavalkova*[a], *Ondrej Franek*[b], *Ondrej Smid*[a], *Michal Huptych*[c], *Milan Dusik*[a], *Ales Linhart*[a], *Jan Belohlavek*[a]

Abstract

Background: The prognosis of refractory out-of-hospital cardiac arrest (OHCA) is generally poor. A recent Prague OHCA study has demonstrated that an invasive approach (including extracorporeal cardiopulmonary resuscitation, ECPR) is a feasible and effective treatment strategy in refractory OHCA. Here we present a post-hoc analysis of the role of initial rhythm on patient outcomes.

Methods: The study enrolled patients who had a witnessed OHCA of presumed cardiac cause without early recovery of spontaneous circulation. The initial rhythm was classified as either a shockable or a non-shockable rhythm. The primary outcome was a composite of 180 day-survival with Cerebral Performance in Category 1 or 2.

Results: 256 (median age 58y, 17% females) patients were enrolled. The median (IQR) duration of resuscitation was 52 (33–68) minutes. 156 (61%) and 100 (39%) of patients manifested a shockable and non-shockable rhythm, respectively. The primary outcome was achieved in 63 (40%) patients with a shockable rhythm and in 5 (5%) patients with a non-shockable rhythm ($p < 0.001$). When patients were analyzed separately based on whether the treatment was invasive (n = 124) or standard (n = 132), the difference in the primary endpoint between shockable and non-shockable initial rhythms remained significant (35/72 (49%) vs 4/52 (8%) in the invasive arm and 28/84 (33%) vs 1/48 (2%) in the standard arm; $p < 0.001$).

Conclusion: An initial shockable rhythm and treatment with an invasive approach is associated with a reasonable neurologically favorable survival for 180 days despite refractory OHCA. Non-shockable initial rhythms bear a poor prognosis in refractory OHCA even when ECPR is readily available.

Keywords: Resuscitation, Cardiac arrest, Extracorporeal circulation, Invasive approach

Introduction

Out-of-hospital cardiac arrest (OHCA) is a significant burden to society.[1] Survival at the level of a hospital discharge with neurological and functional recovery after OHCA is low.[2] It has been reported that a good clinical outcome of treated ventricular fibrillation (VF) or pulseless ventricle tachycardia arrest is far more favorable than asystole or pulseless electrical activity (PEA).[2–6] However, half of the patients with OHCA and VF which exhibited refractory arrhythmia

Abbreviations: OHCA, out-of-hospital cardiac arrest, ECPR, extracorporeal cardiopulmonary resuscitation, VF, ventricular fibrillation, PEA, pulseless electrical activity, ROSC, recovery of spontaneous circulation, CPR, cardiopulmonary resuscitation, CA, cardiac arrest, ECR, European Resuscitation Council, LUCAS, Lund University Cardiac Arrest System, S, standard, I, invasive, CPC, Cerebral Performance Category, IQR, interquartile range, ICD, impantable cardioverter-defibrilator, EMS, emergency medical service, ACLS, advanced cardiac life support, TTM, target temperature management, MODS, multiorgan dysfunction syndrome, WLST, withdrawal of life-sustaining therapy, HR, hazard ratio, CI, confidence interval

* Corresponding author at: 2nd Department of Medicine – Department of Cardiovascular Medicine, General University Hospital and First Faculty of Medicine, Charles University, U Nemocnice 2, Prague 2 128 00, Czech Republic.

E-mail address: stepan.havranek@vfn.cz (S. Havranek).

https://doi.org/10.1016/j.resuscitation.2022.10.006

Received 22 August 2022; Received in Revised form 26 September 2022; Accepted 4 October 2022

and were unresponsive to initial standard treatment, had a poor prognosis.[3,7] In patients who didn't have a recovery of spontaneous circulation (ROSC), the chance of survival when being transported to the hospital while still undergoing cardiopulmonary resuscitation (CPR) is low, usually less than 4% when using standard measures.[8,9]

The temporary replacement of failing circulation by extracorporeal cardiopulmonary resuscitation (ECPR), has been recognized as a promising approach to refractory cardiac arrest (CA).[10–14] Recently, a Prague OHCA study has demonstrated that an invasive approach (early transport to the hospital under mechanical CPR, ECPR, and immediate invasive assessment and therapy) is a feasible and effective treatment strategy in refractory OHCA. The trial suggested the beneficial effects of the invasive approach in the results of 30-day neurological outcome and 180-day mortality/180-day survival with a favorable neurological outcome.[15]

To date, only retrospective studies analysed the role of initial rhythms in refractory OHCA and ECPR. These data suggest poor outcomes for patients with non-shockable rhythms treated with ECPR. Many OHCA centers, therefore, reserve ECPR for VF patients only. Prague OHCA study was the first randomized refractory OHCA trial which also included patients with non-shockable rhythms.

Therefore, we hereby present an analysis on the role of the initial rhythm on patient outcomes in the refractory CA population of the Prague OHCA trial. The secondary objective was to identify the impact of the initial rhythm on the clinical outcome relating to treatment strategy approach, i.e. invasive vs standard. We hypothesized that a shockable rhythm is associated with favorable 180 days survival in refractory OHCA regardless of the treatment strategy. Further, we also hypothesized, that an invasive approach followed by ECPR might have neurologically favorable survival benefits.

Methods

The current study is a post-hoc analysis of the Prague OHCA study, a randomized controlled trial comparing the invasive approach (early transport to hospital under mechanical CPR, ECPR, and immediate invasive assessment and therapy) to standard treatment in the refractory OHCA population.[15,16] The study was performed according to good clinical practice and in compliance with the Helsinki declaration. The Prague OHCA study was approved by the Ethics committee of the General University Hospital in Prague (192/11 S-IV).

Study population

A detailed protocol of the main study has been described previously in detail.[15,16] In brief, the study enrolled adults over 18 years of age, with a witnessed OHCA of a presumed cardiac etiology, who were given a minimum of 5 minutes of advanced cardiac life support without ROSC and who remained unconscious. The patients were randomized in a 1:1 ratio into two study arms: invasive (I) or standard (S). Patients who attained ROSC during initial resuscitation, regained consciousness, or had a known or obvious life-limiting comorbidity, or bleeding diathesis were excluded. The termination of resuscitation efforts followed the valid European Resuscitation Council (ERC) guidelines.[17,18]

Intervention

Patients who were randomized to the S arm were managed on site by continued advanced cardiac life support. The use of drugs, further defibrillations, or other interventions followed the available ERC guidelines.[17,18] If ROSC was achieved (defined as cardiac electrical activity with a palpable pulse), transportation to hospital was initiated and an early invasive strategy was encouraged, namely a coronary angiography.

The mechanical chest compression device LUCAS (Lund University Cardiac Arrest System; Physio-Control Inc./Jolife AB, Lund, Sweden) was originally reserved exclusively for the I arm. However, following the publication of a major trial on mechanical chest compression,[19] the attachment of a LUCAS device was left to the discretion of the emergency physician and was allowed for use at any point during CPR.

In the I arm, the patient was immediately transferred directly to the cardiac center catheterization laboratory (Cathlab) during ongoing CPR with the intention of proceeding with ECPR if ROSC was not achieved en route or on admission. The use of drugs, further defibrillations, or other interventions during transportation followed the ERC guidelines.[17,18] Post-resuscitation care was standardized in both study arms.

Initial rhythm

For the present study, the initial rhythm was defined as the first documented rhythm by the medical emergency system. For further evaluation, initial rhythm was classified as either a shockable rhythm or a non-shockable rhythm. A shockable rhythm included VF or pulseless ventricular tachycardia, the non-shockable group consisted of asystole and PEA. The team in the intensive care unit was unblinded regarding the initial heart rhythm.

Outcomes

The primary outcome was the composite of a 180 day-survival rate with a favorable neurological status, defined as no or minimal neurological impairment (Cerebral Performance Category, CPC, 1 or 2). Secondary outcomes included a 30 day-survival rate with cardiac recovery (no need for pharmacological or mechanical cardiac support for at least 24 hours) and a neurological recovery (CPC 1 or 2) at any time within the first 30 days following the CA. Survival up to 180 days, CPC distribution, and differences in favorable survival in relationship to the length of the CA as well as adverse events incidence were also determined.

Statistical analysis

The CA time and other numeric variables are expressed as medians and interquartile ranges (IQR). The 2-sided Mann-Whitney test was used to compare the CA times and laboratory values between the shockable and non-shockable initial rhythm. The categorical values were compared using the Fisher's exact test (for 2x2 table) or the chi-square test. All presented p-values are two-tailed. We used the Fisher exact test with doubled one-sided p-value. The Cox regression model was used for multivariable survival analysis. Two models were designed. First using available variables on hospital admission. Second model included known variables or completed interventions after initial in-hospital evaluation (one hour after admission). Selection of variables included in both models was based on a significance in an univariate analysis and its clinical relevance. $P < 0.05$ was considered as statistically significant. Statistical analyses were performed with MedCalc® Statistical Software version 19.7 (MedCalc Software Ltd, Ostend, Belgium; 2021) and RStudio 2022.07.2 + 576 (RStudio Team (2020). RStudio: Integrated Development for R. RStudio, PBC, Boston, MA URL http://www.rstudio.com/).

Table 1 – Baseline demographical and prehospital data.

Parameter	Shockable rhythm (*N* = 156)	Non-shockable rhythm (*N* = 100)	*P*
Age (years)	56 (45–64)	60 (51–66)	0.03
Sex			
Female	15 (10%)	29 (29%)	<0.001
Male	141 (90%)	71 (71%)	
Medical history			
Hypertension	57/126 (45%)	32/65 (49%)	0.65
Coronary artery disease	26/125 (21%)	8/62 (13%)	0.23
Chronic heart failure	10/123 (8%)	6/62 (10%)	0.78
Diabetes mellitus	18/120 (15%)	18/62 (29%)	0.03
Chronic kidney disease	2/122 (2%)	3/61 (5%)	0.34
Chronic obstructive pulmonary disease	7/122 (6%)	3/62 (5%)	1.00
ICD implanted	1/134 (1%)	2/76 (3%)	0.30
Bystander CPR	154 (99%)	98 (98%)	1.00
Time from collapse to EMS arrival (min)	9 (6–11)	9 (7–12)	0.54
Time from collapse to ACLS (physician arrival) (min)	10 (8–13)	11 (6–14)	0.87
Dispatcher assisted CPR	133 (85%)	70 (70%)	0.006
Time until or of dispatcher assisted CPR began (min)	3 (2–4)	3 (1–5)	0.97
Time from collapse to randomization (min)	25 (20–30)	24 (20–32)	0.98
Number of adrenaline doses prehospitally (mg)	4 (2–6)	5 (4–7)	<0.001
Intermittent ROSC	56 (36%)	30 (30%)	0.40
Randomised to			
Standard	84 (54%)	48 (48%)	0.44
Invasive	72 (46%)	52 (52%)	

Note: Data is expressed as median (IQR) or *N* (%). ICD – implantable cardioverter-defibrillator; CPR – cardiopulmonary resuscitation; EMS – emergency medical service; ACLS – advanced cardiac life support; ROSC – recovery of spontaneous circulation.

Results

Baseline clinical data, prehospitalization phase

During the study period, 256 patients (median age 58 years, 17% females) were enrolled and analyzed. The baseline demographic and clinical data are described in Table 1. Out of the entire study cohort, 156 (61%) patients manifested VF as an initial rhythm. The rest of the patients had an initially non-shockable rhythm: PEA in 45 (18%) and asystole in 55 (21%) cases. Not a single patient exhibited pulseless VT. Patients with VF were slightly younger, predominantly male, and less prevalently had diabetes mellitus than those without a shockable rhythm. In the VF group, telephone assisted CPR was more frequently performed and a lower number of adrenaline doses were used.

Hospitalization phase, procedures, and interventions

As Table 2 describes in detail, less patients in the shockable group died prior to admission to the hospital or within the first hour after admission, and more frequently had a sustained ROSC on admission. In-hospital target temperature management was applied more frequently in patients with VF. An invasive assessment by diagnostic angiography was performed in 93% and 81% of admitted patients in the VF and non-shockable groups, respectively, with a different spectrum of invasive procedures according to the initial rhythm. Upon admission, the VF group manifested less advanced metabolic derangement, i.e. lower lactates and higher pH. Acute coronary syndromes were more frequently identified as a cause of the CA in the VF group (89 (57%) vs 38 (38%)). The second most frequent cause of CA in the VF group was chronic coronary artery disease. On the contrary, pulmonary embolism was more frequently found in non-VF patients. Patients with a shockable rhythm were less likely to manifest organ lacerations due to CPR.

Clinical outcome

Overall, 68 (27%) patients in the whole study reached the primary outcome of neurologically favorable survival at 180 days represented by 63 (40%) patients with an initially documented VF and 5 (5%) patients with an initially non-shockable rhythm ($p < 0.001$), Table 3.

Compared to patients with a non-shockable rhythm, a higher probability of secondary outcomes of cardiac and neurological recovery at 30 days occurred in VF patients. When patients in the I and S arms were analyzed separately, the difference in primary and secondary endpoints between shockable and non-shockable initial rhythms remained significant (Table 3). Of all the patients with VF, patients treated with an invasive strategy more frequently recovered neurologically at 30 days than those in the S arm (34 (47%) vs 24 (29%); $p = 0.03$). However, the difference in the proportion of surviving patients with CPC 1 or 2 after 180 days and VF between the I and S arms was not different (35 (49%) vs 28 (33%); $p = 0.08$; Fig. 1.

In the first cox regression model (including variables known at the time of hospital admission), see Table 4, model A, a shockable initial rhythm and sustained ROSC were independently associated with a lower probability of unfavorable clinical outcome (the absence of 180 day-survival with favorable neurological outcome). The second cox regression analysis, see Table 4, model B, included variables known after initial in-hospital evaluation (within the first hour of admission). Unfavorable clinical outcome was associated with CPR > 45 minutes and not having initial shockable rhythm. Other variables such as age, gender, dispatcher assisted CPR, and acute coronary syndromes were not significantly associated with the outcome.

Table 2 – Hospitalization phase, procedures, and interventions.

Parameter	Shockable rhythm (*N* = 156)	Non-shockable rhythm (*N* = 100)	*P*
Admitted to hospital	136 (87%)	74 (74%)	0.01
Time to hospital admission (min)	55 (46–64)	51 (41–63)	0.12
Time from randomization to admission (min)	30 (23–37)	28 (20–35)	0.20
Declared dead	33 (21%)	42 (42%)	<0.001
Prehospitally	20/33 (61%)	26/33 (62%)	1.00
Within 1 hour of admission	13/33 (39%)	16/33 (38%)	
Time of CPR (time to death/ROSC or ECLS) (min)	54 (33–69)	51 (39–68)	0.33
Time of CPR subgroups			
<30 min	31 (20%)	9 (9%)	0.06
≥30 and <45 min	29 (19%)	23 (23%)	
≥45 min	96 (62%)	68 (68%)	
Sustained ROSC on admission	67 (43%)	25 (25%)	0.005
TTM used	122/136 (90%)	66/74 (76%)	0.01
ECLS			
ECLS implanted	57 (37%)	35 (35%)	0.91
Time to ECLS (min)	62 (57–73)	60 (50–66)	0.09
Invasive assessment			
Coronary angiography	126/127 (99%)	55/62 (89%)	0.002
Pulmonary angiography	8/127 (6%)	19/62 (31%)	<0.001
Aortography	22/127 (17%)	19/62 (31%)	0.06
Left ventricle angiography	29/127 (23%)	18/62 (29%)	0.37
Laboratory values on admission			
pH	7.00 (6.87–7.17)	6.85 (6.75–6.97)	<0.001
Lactate (mmol/L)	10.7 (7.8–13.8)	13.8 (10.5–17.0)	<0.001
Cause of cardiac arrest (including autopsy findings)			
Acute coronary syndrome	89 (57%)	38 (38%)	<0.001
Coronary artery disease – chronic	29 (19%)	3 (3%)	
Pulmonary embolism	1 (1%)	23 (23%)	
Chronic heart failure	8 (5%)	6 (6%)	
Cardiomyopathy	7 (5%)	2 (2%)	
Myocarditis	5 (3%)	3 (3%)	
Aortic stenosis	5 (3%)	3 (3%)	
Aortic dissection type A	1 (1%)	3 (3%)	
Intracranial haemorrhage	1 (1%)	2 (2%)	
Bleeding – other	0 (0%)	3 (3%)	
Accidental hypothermia	3 (2%)	1 (1%)	
Pulmonary hypertension	0 (0%)	2 (2%)	
Sepsis	0 (0%)	1 (1%)	
Other	1 (1%)	1 (1%)	
Unknown	6 (4%)	9 (9%)	
Cause of death			
Refractory arrest	34/91 (37%)	46/94 (49%)	0.36
Brain death	14/91 (15%)	16/94 (17%)	
MODS	30/91 (33%)	22/94 (23%)	
Cardiogenic shock	9/91 (10%)	5/94 (5%)	
Unknown	3/91 (3%)	2/94 (2%)	
Bleeding	1/91 (1%)	3/94 (3%)	
WLST	18 (12%)	17 (17%)	0.29
Complications			
Bleeding -any	29/123 (24%)	17/62 (27%)	0.69
Fatal	1 (3%)	3 (18%)	0.23
Intracranial haemorrhage	6 (21%)	4 (24%)	
Overt	22 (76%)	10 (59%)	
Shock gut	44/123 (36%)	17/57 (30%)	0.54
Organ lacerations	1/132 (1%)	6/83 (7%)	0.03
Technical	2 (1%)	1 (1%)	1.00

Note: Data is expressed as median (IQR) or *N* (%). CPR – cardiopulmonary resuscitation; ROSC – recovery of spontaneous circulation; TTM – Target temperature management; ELCS – extracorporeal life support; MODS – multiorgan dysfunction syndrome; WLST – withdrawal of life-sustaining therapy.

Table 3 – Clinical outcome.

	All patients			Invasive therapy			Standard therapy		
Initial rhythm	Shockable (*N* = 156)	Non-shockable (*N* = 100)	*P*	Shockable (*N* = 72)	Non-shockable (*N* = 52)	*P*	Shockable (*N* = 84)	Non-shockable (*N* = 48)	*P*
Primary outcome									
Survival with CPC at 180 days									
1 or 2	63 (40%)	5 (5%)	<0.001	35 (49%)	4 (8%)	<0.001	28 (33%)	1 (2%)	<0.001
≥3	93 (60%)	95 (95%)		37 (51%)	48 (92%)		56 (67%)	47 (98%)	
Secondary outcomes									
Cardiac recovery at 30 days									
Yes	84 (54%)	15 (15%)	<0.001	43 (60%)	11 (21%)	<0.001	41 (49%)	4 (8%)	<0.001
No	72 (46%)	85 (85%)		29 (40%)	41 (79%)		43 (51%)	44 (92%)	
Neuro recovery at 30 days									
Yes	58 (37%)	4 (4%)	<0.001	34 (47%)	4 (8%)	<0.001	24 (29%)	0 (0%)	<0.001
No	98 (63%)	96 (96%)		38 (53%)	48 (92%)		60 (17%)	48 (100%)	

Note: Data is expressed as N (%). CPC – Cerebral Performance Category.

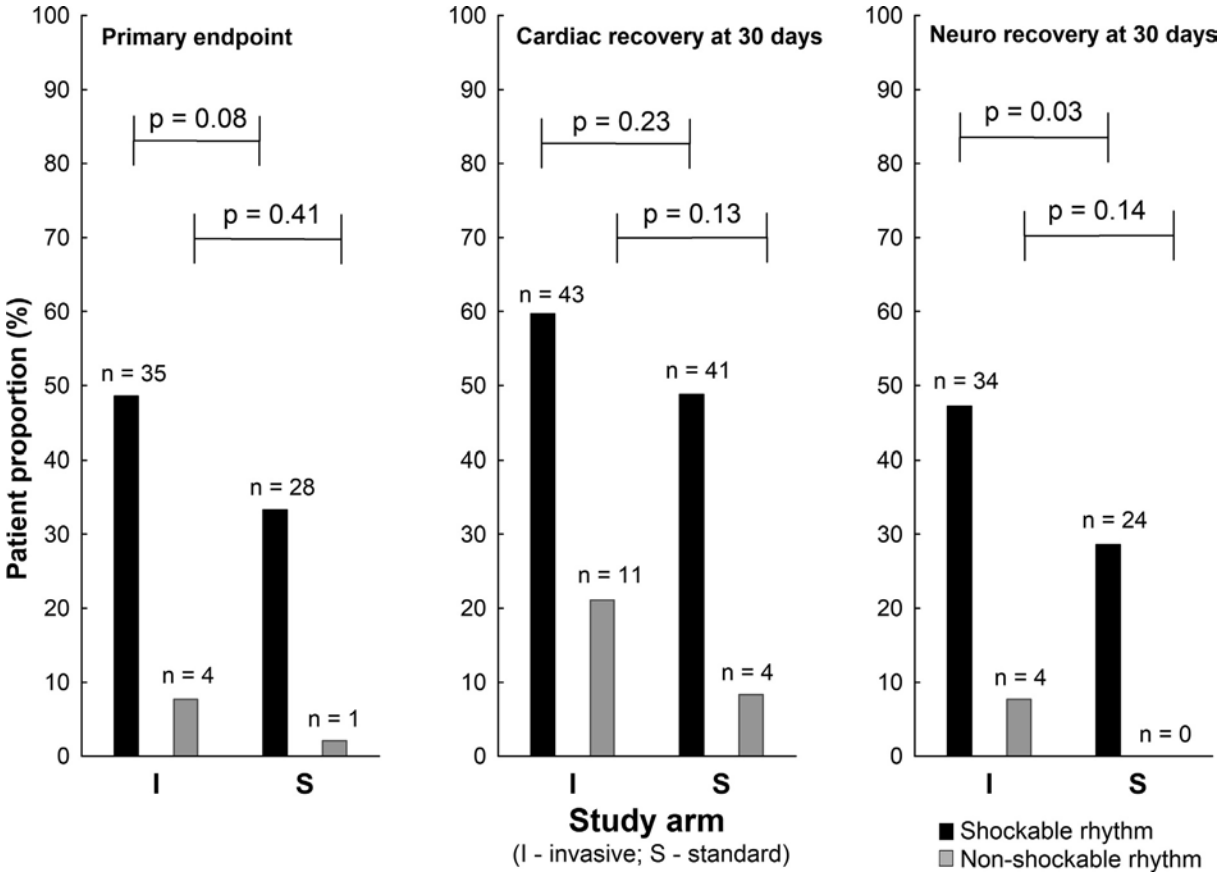

Fig. 1 – Clinical outcome of patients with shockable and non-shockable rhythm in standard and invasive treatment arms. Notes: A shockable rhythm had 72 patients in the invasive and 84 patients in the standard arm. A non-shockable rhythm had 52 patients in the invasive and 48 patients in the standard arm. Two-tailed Fisher's exact test. Presented p-values are for the superiority of the invasive arm (separately for a shockable and a non-shockable rhythm).

Table 4 – Cox regression analysis in the prediction of an unfavorable clinical outcome.

	Model A (Admitted to hospital) (n = 210)			Model B (After the initial in-hospital evaluation) (n = 181)		
Covariate	HR	95% CI	P	HR	95% CI	P
Age ≥ 65 years	0.92	0.63–1.34	0.67	0.87	0.57–1.34	0.53
Sex = women	0.96	0.62–1.49	0.86	1.17	0.73–1.85	0.52
Sustained ROSC on admission = yes	0.35	0.24–0.51	<0.001	0.69	0.41–1.15	0.15
Length CPR > 45 min = yes	–	–	–	1.97	1.16–3.32	0.01
Telephone assisted bystander CPR = yes	1.19	0.8–1.77	0.39	1.31	0.82–2.1	0.26
Acute coronary syndrome = yes	–	–	–	1.29	0.86–1.94	0.22
Shockable rhythm = yes	0.32	0.22–0.46	<0.001	0.27	0.18–0.41	<0.001

HR – hazard ratio; CI – confidence interval; ROSC – recovery of spontaneous circulation; CPR – cardiopulmonary resuscitation; ELCS – extracorporeal life support.

Discussion

This post-hoc analysis of the Prague OHCA study contains several important findings. A shockable initial rhythm is associated with a better chance of a 180 day-survival rate with a favorable neurological outcome, an improved secondary 30 day-neurological outcome and a 30 day-survival in refractory OHCA. This prognostically beneficial effect applies regardless of the invasive or standard treatment strategies used. The second important finding indicates that patients with an initial shockable rhythm who were treated with invasive strategy including ECPR more likely recovered their neurological function at 30 days.

Our findings for favorable outcomes in OHCA for those who presented with a shockable rhythm are not surprising and are in accordance with previously published data.[2,3,6] However, first, this analysis was based on a randomized population, and second, we enrolled truly refractory patients with prolonged resuscitations reaching 58 and 46 minutes in the invasive and standard arms with a reasonably overall favorable neurological survival.[15]

Currently, there is very limited data elucidating the impact of initial rhythm on the clinical outcome in refractory OHCA. Prior to the Prague OHCA study, only one small, randomized study focusing on refractory OHCA, which only considered patients manifesting a shockable rhythm, had been published.[20] Other non-randomised or retrospective studies also analysed prolonged and refractory OHCA. However, those only involved patients with shockable rhythms,[21,22] or included not only refractory CA,[11,23,24] or were performed in a cohort of in-hospital CA,[25] or the initial rhythm analysis was not shown.[26] Our data is in accordance with the retrospective analysis published by Kim et al.[27] In their study, which also included some patients treated with ECPR, an initial shockable rhythm seemed to be a favorable phenotype in patients with prolonged CA. One other retrospective study investigated the efficacy of rapid-response ECMO and intra-arrest coronary intervention in patients with CA which was complicated by acute coronary syndrome who were unresponsive to conventional CPR.[11] They observed a trend toward a higher rate of initial recorded shockable rhythm among patients who survived up to 30 days, but the difference was not statistically significant (68% versus 48%; p = 0.08). However, this study also enrolled non-OHCA patients.

Why are shockable rhythms better?

Patients who presented shockable rhythms represent > 85% of all CA survivors, probably due to a high prevalence of reversible causes of arrest.[28–30] It is generally accepted that the vast majority of VF arrests are related to an underlying cardiac disorder. Cardiac causes are less frequent in patients with asystole or PEA, even after excluding obvious non-cardiac causes such as a drug overdose, trauma, exsanguination, and primary respiratory failure.[31–33]

Our data showed overall higher number of declared prehospital death and death within the first hour after admission in patients with non-shockable rhythm. This is reflected in lower chance to achieve prehospital ROSC in patients with a non-shockable rhythm. The higher number of adrenalin doses and higher rate of organ lacerations most likely reflect difficulties during CPR and apprehension of inferior outcome of those patients. We speculate, that the absence of telephone assisted CPR might be a relevant cause of insufficient CPR and could therefore be linked to progression of some shockable rhythms to asystole. Target temperature management was less frequently applied in patients with a non-shockable rhythm. The reasons for non-starting or premature termination of target temperature management in our study (data not shown) are higher number of contraindications, mainly the haemodynamic instability.

Some authors considered VF to be a dependent rather than an independent variable and excluded initial rhythm from the logistic regression models.[6,34,35] It has been shown that variables which contributed to VF are similar to those covariates that predicted survival (i.e. bystander CPR, age, Firemen/Police-performed CPR, bystander-witnessed arrest).[6] However, in our study, the Cox regression analyses showed that an initial shockable rhythm was an independent predictor of survival with favorable neurological outcome similar to a shorter duration of CPR or a presence of sustained ROSC on admission. The inclusion of VF to the predictive models also has another purpose. In routine practice, the medical staff usually has very limited information about the patient's status and initial rhythm is one of very few available and easily recognisable parameters. Initial rhythm has also been identified as an independent parameter in some predictive models to rapidly determine the risk of the ischemic aetiology of CA.[36] All those aspects warrant the inclusion of initial rhythm to the final analysis. Acute coronary syndromes were responsible for a significant proportion of VF in the Prague OHCA

cohort. However, multivariable models did not identify acute coronary syndrome as an independent predictor of favorable outcome.

Some authors also reported that patients with non-shockable rhythms demonstrated poor overall outcomes, with the longest time-to-ROSC in a survivor of just less than 30 min.[3] Data from our standard arm showed that prolonged CPR in non-shockable rhythm does not yield more survivors. We have also shown, that ECPR in patients with a non-shockable rhythm does not improve survival with a good neurological outcome markedly. In contrast to patients with a non-shockable rhythm, our data have proven that patients with VF had better neurological recovery at 30 days when invasive approach including ECPR was applied. However, this encouraging secondary outcome was not followed with clearly higher neurologically favorable survival of VF patients after 180 days in the invasive arm most likely due to the fact, that the study was overall underpowered to show this difference.

Study limitations

The main limitation of this study was the single-centre design with limited sample size which does not allow us to study differences between PEA and asystole. This data is the post-hoc (not predefined) analysis. In some cases, the initial rhythm was not optimally recorded and easily analysable, and data were based on medical emergency system staff reports.

Conclusion

In the Prague OHCA study, an initial shockable rhythm is associated with neurologically favorable survival at 180 days even in prolonged refractory OHCA. The survival with favorable neurological outcome was not influenced by invasive treatment strategy. Non-shockable initial rhythms bear a poor prognosis in refractory OHCA even when ECPR is readily available.

Conflict of interest

None.

CRediT authorship contribution statement

Stepan Havranek: Conceptualization, Methodology, Writing – original draft. **Zdenka Fingrova:** Conceptualization, Methodology, Writing – original draft. **Daniel Rob:** Investigation, Data curation, Validation, Writing – review & editing. **Jana Smalcova:** Investigation, Data curation, Writing – review & editing. **Petra Kavalkova:** Investigation, Project administration, Data curation, Validation, Writing – review & editing. **Ondrej Franek:** Investigation, Data curation, Validation. **Ondrej Smid:** Investigation, Data curation. **Michal Huptych:** Formal analysis, Data curation. **Milan Dusik:** Investigation, Data curation, Validation. **Ales Linhart**: Writing - review & editing. **Jan Belohlavek:** Writing – review & editing, Supervision.

Acknowledgments

The authors express their immense gratitude to the Prague Emergency Medical Service teams and the Cath Lab and Coronary Care Unit teams of the 2nd Department of Medicine - Department of Cardiovascular Medicine, General University Hospital in Prague, for their inexhaustible efforts in providing superb quality care. Without their continuous commitment, it would not have been possible to perform this study. The authors also express their thanks to Valeria Reeves for language editing.

Funding sources

This study has been supported by Ministry of Health, Czech Republic – conceptual development of research organisation (General University Hospital in Prague – VFN, 00064165, and by the Charles University Research program „Cooperatio – Intensive Care Medicine“.

Author details

[a]*2nd Department of Medicine - Department of Cardiovascular Medicine, First Faculty of Medicine, Charles University in Prague and General University Hospital in Prague, Czech Republic* [b]*Emergency Medical Service Prague, Czech Republic* [c]*Czech Institute of Informatics, Robotics and Cybernetics (CIIRC), Czech Technical University in Prague, Czech Republic*

REFERENCES

1. Perkins GD, Graesner JT, Semeraro F, et al. European Resuscitation Council Guidelines 2021: Executive summary. Resuscitation 2021;161:1–60.
2. Nichol G, Thomas E, Callaway CW, et al. Regional variation in out-of-hospital cardiac arrest incidence and outcome. JAMA 2008;300:1423–31.
3. Grunau B, Reynolds JC, Scheuermeyer FX, et al. Comparing the prognosis of those with initial shockable and non-shockable rhythms with increasing durations of CPR: Informing minimum durations of resuscitation. Resuscitation 2016;101:50–6.
4. Hollenberg J, Herlitz J, Lindqvist J, et al. Improved survival after out-of-hospital cardiac arrest is associated with an increase in proportion of emergency crew–witnessed cases and bystander cardiopulmonary resuscitation. Circulation 2008;118:389–96.
5. Iwami T, Nichol G, Hiraide A, et al. Continuous improvements in “chain of survival” increased survival after out-of-hospital cardiac arrests: a large-scale population-based study. Circulation 2009;119:728–34.
6. Stiell IG, Wells GA, DeMaio VJ, et al. Modifiable factors associated with improved cardiac arrest survival in a multicenter basic life support/defibrillation system: OPALS Study Phase I results. Ontario Prehospital Advanced Life Support. Ann Emerg Med 1999;33:44–50.
7. Kjaergaard J, Nielsen N, Winther-Jensen M, et al. Impact of time to return of spontaneous circulation on neuroprotective effect of targeted temperature management at 33 or 36 degrees in comatose survivors of out-of hospital cardiac arrest. Resuscitation 2015;96:310–6.
8. Drennan IR, Lin S, Sidalak DE, Morrison LJ. Survival rates in out-of-hospital cardiac arrest patients transported without prehospital return of spontaneous circulation: an observational cohort study. Resuscitation 2014;85:1488–93.
9. Wampler DA, Collett L, Manifold CA, Velasquez C, McMullan JT. Cardiac arrest survival is rare without prehospital return of spontaneous circulation. Prehosp Emerg Care 2012;16:451–5.

10. Haas NL, Coute RA, Hsu CH, Cranford JA, Neumar RW. Descriptive analysis of extracorporeal cardiopulmonary resuscitation following out-of-hospital cardiac arrest-An ELSO registry study. Resuscitation 2017;119:56–62.
11. Kagawa E, Dote K, Kato M, et al. Should we emergently revascularize occluded coronaries for cardiac arrest?: rapid-response extracorporeal membrane oxygenation and intra-arrest percutaneous coronary intervention. Circulation 2012;126:1605–13.
12. Ortega-Deballon I, Hornby L, Shemie SD, Bhanji F, Guadagno E. Extracorporeal resuscitation for refractory out-of-hospital cardiac arrest in adults: A systematic review of international practices and outcomes. Resuscitation 2016;101:12–20.
13. Schober A, Sterz F, Herkner H, et al. Emergency extracorporeal life support and ongoing resuscitation: a retrospective comparison for refractory out-of-hospital cardiac arrest. Emerg Med J 2017;34:277–81.
14. Wallmuller C, Sterz F, Testori C, et al. Emergency cardio-pulmonary bypass in cardiac arrest: seventeen years of experience. Resuscitation 2013;84:326–30.
15. Belohlavek J, Smalcova J, Rob D, et al. Effect of Intra-arrest Transport, Extracorporeal Cardiopulmonary Resuscitation, and Immediate Invasive Assessment and Treatment on Functional Neurologic Outcome in Refractory Out-of-Hospital Cardiac Arrest: A Randomized Clinical Trial. JAMA 2022;327:737–47.
16. Belohlavek J, Kucera K, Jarkovsky J, et al. Hyperinvasive approach to out-of hospital cardiac arrest using mechanical chest compression device, prehospital intraarrest cooling, extracorporeal life support and early invasive assessment compared to standard of care. A randomized parallel groups comparative study proposal. "Prague OHCA study". J Transl Med 2012;10:163.
17. Monsieurs KG, Nolan JP, Bossaert LL, et al. European Resuscitation Council Guidelines for Resuscitation 2015: Section 1. Executive summary. Resuscitation 2015;95:1–80.
18. Nolan JP, Soar J, Zideman DA, et al. Group ERCGW. European Resuscitation Council Guidelines for Resuscitation 2010 Section 1. Executive summary. Resuscitation 2010;81:1219–76.
19. Rubertsson S, Lindgren E, Smekal D, et al. Mechanical chest compressions and simultaneous defibrillation vs conventional cardiopulmonary resuscitation in out-of-hospital cardiac arrest: the LINC randomized trial. JAMA 2014;311:53–61.
20. Yannopoulos D, Bartos J, Raveendran G, et al. Advanced reperfusion strategies for patients with out-of-hospital cardiac arrest and refractory ventricular fibrillation (ARREST): a phase 2, single centre, open-label, randomised controlled trial. Lancet 2020;396:1807–16.
21. Alm-Kruse K, Sorensen G, Osbakk SA, et al. Outcome in refractory out-of-hospital cardiac arrest before and after implementation of an ECPR protocol. Resuscitation 2021;162:35–42.
22. Nas J, Thannhauser J, van Dijk E, et al. Coronary angiography findings in patients with shock-resistant ventricular fibrillation cardiac arrest. Resuscitation 2021;164:54–61.
23. Grunau B, Kime N, Leroux B, et al. Association of Intra-arrest Transport vs Continued On-Scene Resuscitation With Survival to Hospital Discharge Among Patients With Out-of-Hospital Cardiac Arrest. JAMA 2020;324:1058–67.
24. Reynolds JC, Frisch A, Rittenberger JC, Callaway CW. Duration of resuscitation efforts and functional outcome after out-of-hospital cardiac arrest: when should we change to novel therapies? Circulation 2013;128:2488–94.
25. Chen YS, Lin JW, Yu HY, et al. Cardiopulmonary resuscitation with assisted extracorporeal life-support versus conventional cardiopulmonary resuscitation in adults with in-hospital cardiac arrest: an observational study and propensity analysis. Lancet 2008;372:554–61.
26. Chen YS, Yu HY, Huang SC, et al. Extracorporeal membrane oxygenation support can extend the duration of cardiopulmonary resuscitation. Crit Care Med 2008;36:2529–35.
27. Kim SJ, Jung JS, Park JH, Park JS, Hong YS, Lee SW. An optimal transition time to extracorporeal cardiopulmonary resuscitation for predicting good neurological outcome in patients with out-of-hospital cardiac arrest: a propensity-matched study. Crit Care 2014;18:535.
28. Adabag S, Hodgson L, Garcia S, et al. Outcomes of sudden cardiac arrest in a state-wide integrated resuscitation program: Results from the Minnesota Resuscitation Consortium. Resuscitation 2017;110:95–100.
29. Spaulding CM, Joly LM, Rosenberg A, et al. Immediate coronary angiography in survivors of out-of-hospital cardiac arrest. N Engl J Med 1997;336:1629–33.
30. Yannopoulos D, Bartos JA, Aufderheide TP, et al. The Evolving Role of the Cardiac Catheterization Laboratory in the Management of Patients With Out-of-Hospital Cardiac Arrest: A Scientific Statement From the American Heart Association. Circulation 2019;139: e530–52.
31. Kurkciyan I, Meron G, Sterz F, et al. Spontaneous subarachnoid haemorrhage as a cause of out-of-hospital cardiac arrest. Resuscitation 2001;51:27–32.
32. Kurkciyan I, Meron G, Sterz F, et al. Pulmonary embolism as a cause of cardiac arrest: presentation and outcome. Arch Intern Med 2000;160:1529–35.
33. Meron G, Kurkciyan I, Sterz F, et al. Non-traumatic aortic dissection or rupture as cause of cardiac arrest: presentation and outcome. Resuscitation 2004;60:143–50.
34. Cummins RO, Eisenberg MS, Hallstrom AP, Litwin PE. Survival of out-of-hospital cardiac arrest with early initiation of cardiopulmonary resuscitation. Am J Emerg Med 1985;3:114–9.
35. Wilcox-Gok VL. Survival from out-of-hospital cardiac arrest. A multivariate analysis. Med Care 1991;29:104–14.
36. Bascom KE, Dziodzio J, Vasaiwala S, et al. Derivation and Validation of the CREST Model for Very Early Prediction of Circulatory Etiology Death in Patients Without ST-Segment-Elevation Myocardial Infarction After Cardiac Arrest. Circulation 2018;137:273–82.

P. Stojadinović et al.

Autonomic Changes Are More Durable After Radiofrequency Than Pulsed Electric Field Pulmonary Vein Ablation

J Am Coll Cardiol EP
Impact Factor: 6.124

JACC: CLINICAL ELECTROPHYSIOLOGY VOL. ■, NO. ■, 2022

PUBLISHED BY ELSEVIER

Autonomic Changes Are More Durable After Radiofrequency Than Pulsed Electric Field Pulmonary Vein Ablation

Predrag Stojadinović, MD,[a] Dan Wichterle, MD, PhD,[a] Petr Peichl, MD, PhD,[a] Hiroshi Nakagawa, MD, PhD,[b] Robert Čihák, MD, PhD,[a] Jana Hašková, MD,[a] Josef Kautzner, MD, PhD[a]

ABSTRACT

OBJECTIVES We investigated whether PVI by a PEF compared with RF energy will result in less prominent alteration of the cardiac autonomic nervous system.

BACKGROUND Pulmonary vein isolation (PVI) by radiofrequency (RF) energy is associated with a collateral ganglionated plexi ablation. Pulsed electric field (PEF) is a nonthermal energy source that preferentially affects the myocardial cells and spares neural tissue.

METHODS A total of 31 patients with atrial fibrillation underwent PVI using a novel lattice-tip catheter and PEF energy (n = 18) or a conventional irrigated-tip catheter and RF energy (n = 13). The response of the sinoatrial node and atrioventricular node to extracardiac high-frequency, high-output, right vagal nerve stimulation was evaluated at baseline and during and at the end of the ablation procedure. Substantial reduction in responsiveness was arbitrarily defined as stimulation-inducible pause <1.5 seconds.

RESULTS Reduced response of the sinoatrial node was documented in 13 of 13 (100%) and 6 of 18 (33%) patients ($P = 0.0001$) in RF and PEF groups, respectively. Reduced response of the atrioventricular node was found in 10 of 11 (93%) and 6 of 18 (33%) patients ($P = 0.002$) in RF and PEF groups, respectively. The major effects were observed predominantly during ablation around the right pulmonary veins. Early recovery of ganglionated plexi function was noticed only in the PEF ablation group. RF ablation resulted in higher acceleration of the sinus rhythm compared with PEF ablation (20 ± 13 beats/min vs 12 ± 10 beats/min; $P = 0.04$).

CONCLUSIONS PEF compared with RF energy used for PVI induces significantly weaker and less durable suppression of cardiac autonomic regulations. (J Am Coll Cardiol EP 2022;■:■–■) © 2022 by the American College of Cardiology Foundation.

Catheter ablation is a well-established treatment modality for rhythm control in patients with drug-refractory atrial fibrillation (AF).[1,2] Contemporary ablative energy sources such as radiofrequency (RF) energy, cryoenergy, and laser energy cause nonselective thermal destruction of the target tissue. Recently, a novel technique of nonthermal energy called a pulsed electric field (PEF) has been introduced.[3-5] This method uses short direct-current electric field pulses to create pores in cardiomyocyte cell membranes resulting in apoptosis (irreversible electroporation). The advantage of this method is a short duration of the energy delivery and low potential for collateral damage caused by the high sensitivity of cardiomyocytes compared with surrounding cells, including the phrenic nerve and esophagus. On the other hand, PEF ablation may not significantly influence autonomic

From the [a]Institute for Clinical and Experimental Medicine, Prague, Czech Republic; and the [b]Department of Cardiovascular Medicine, Cleveland Clinic, Cleveland, Ohio, USA.
The authors attest they are in compliance with human studies committees and animal welfare regulations of the authors' institutions and Food and Drug Administration guidelines, including patient consent where appropriate. For more information, visit the Author Center.

Manuscript received December 28, 2021; revised manuscript received March 28, 2022, accepted April 24, 2022.

ISSN 2405-500X/$36.00 https://doi.org/10.1016/j.jacep.2022.04.017

ABBREVIATIONS AND ACRONYMS

AF = atrial fibrillation

AV = atrioventricular

AVN = atrioventricular node

ECVS = extracardiac vagal stimulation

GPs = ganglionated plexi

HRV = heart rate variability

PEF = pulsed electric field

PV = pulmonary vein

PVI = pulmonary vein isolation

RF = radiofrequency

SAN = sinoatrial node

innervation to the heart that would be comparable to pulmonary vein isolation (PVI) performed by thermal energy. Ablation of ganglionated plexi (GP) by RF energy during PVI is believed by many to contribute to the overall clinical effect of the catheter ablation procedure.[6-9] Whether PEF applications can affect cardiac autonomic ganglia remains unknown. In the present study, we hypothesized that PVI by PEF compared with RF energy will result in less prominent acute alteration of the cardiac autonomic nervous system (ANS).

METHODS

A single-center, prospective, parallel-arm, nonrandomized study was conducted at our institution. A study was approved by the institutional ethical committee and conducted in accordance with the Declaration of Helsinki.

STUDY POPULATION. We enrolled all (n = 18) consecutive patients undergoing point-by-point PEF ablation and a random sample (n = 13) of comparable patients undergoing standard RF ablation. All patients signed informed consent with the study procedures.

CATHETER ABLATION PROCEDURE. Ablation procedures were performed on uninterrupted oral anticoagulation and under general anesthesia. Administration of parasympatholytic drugs was prohibited during the procedure. General anesthesia was induced by sufentanil and propofol and was maintained with volatile agent desflurane. Patients were relaxed using rocuronium bromide when needed. Patients who presented with AF were cardioverted. Unfractionated heparin was administered before transseptal puncture as an initial bolus and continuous infusion was adjusted to maintain the activated clotting time between 300 and 350 seconds. One decapolar catheter was deployed into the coronary sinus. The left atrium was accessed via a single or double transseptal puncture that was facilitated by intracardiac echocardiography (AcuNav, Siemens Medical Solutions). In all patients, left pulmonary veins (PVs) were isolated first.

PULSED ELECTRIC FIELD ABLATION. PVI was performed using a novel 3-dimensional electroanatomical mapping/ablating system that has been described previously (Affera, Inc).[10] The 8-F ablation catheter is equipped with a 9-mm expandable lattice tip that contains 9 microelectrodes and 9 thermocouples, distributed equally on the surface of the lattice-tip (Sphere-9, Affera, Inc).[10,11] PEF is delivered in a point-by-point manner to achieve circumferential ipsilateral PVI. A dedicated PEF generator (HexaPulse, Affera, Inc) was used, and PEF (24-32 Amps, biphasic pulses) was applied in short microsecond-scale pulses over 4 seconds (synchronized to either atrial or ventricular depolarization) between the lattice-tip and a skin patch position on the patient's back during saline irrigation of 15 mL/min. Bidirectional conduction block across the ablation line was confirmed by pacing from the PVs.

RF ABLATION. PVI was navigated using a 3-dimensional electroanatomic mapping system CARTO 3 (Biosense Webster) and guided by intracardiac echocardiography. PVs were isolated using a 3.5-mm irrigated-tip catheter (NaviStar ThermoCool, Biosense Webster). Circumferential lesions were created around PV ostia in a point-by-point fashion. During saline irrigation of 17 mL/min, RF energy was delivered using SmartAblate generator (Biosense Webster) in power-controlled mode with output set at 25-30 W on the anterior wall and 20-25 W at the posterior wall of the left atrium, respectively. Duration of each application at a single spot varied between 25 and 35 seconds. PVI was confirmed by a 10-pole circular Lasso catheter (Biosense Webster) positioned at the ostial level of PVs.

ELECTROPHYSIOLOGICAL STUDY. Twelve-lead surface electrocardiograms and bipolar intracardiac electrograms were recorded on the CardioLab system (GE Healthcare). A programmable cardiac stimulator EPS320 (MicroPace EP Inc) was used to deliver electrical impulses as appropriate. The mean sinus rate (over the 10 consecutive cycles), sinus node recovery time, and Wenckebach point were assessed at baseline and at the end of the procedure. Extracardiac vagal stimulation (ECVS) using the Neurostimulator Pachon was performed as described in detail in the study by Pachon et al.[12] Briefly, the second decapolar catheter (with electrode spacing of 2-5-2 mm) was introduced into the right internal jugular vein to the level of upper wisdom tooth with the posteromedial bend via the 7-F/90-cm Super Arrow-Flex® sheath (Teleflex) from the groin access (**Central Illustration**). The bipolar stimulation between the distal and third electrode (with mutual distance of 7 mm) was accomplished with a frequency of 50 Hz, a pulse width of 0.05 ms, an output of 1 V/kg (<70 V), and a train duration of 5 seconds. The catheter position was slightly adjusted to maximize the response of the sinus and atrioventricular node (AVN). Once reached, this position was recorded on the x-ray system and used as a reference for repeated stimulation during the study. The response of sinoatrial node (SAN) and

AVN to ECVS were recorded before, immediately after the left and the right PVI and after 20 minutes from the last energy application, and it was quantified by the longest ECVS-induced pause, ie, maximum P-P interval during the sinus rhythm and maximum R-R interval during atrial pacing. Substantial reduction in responsiveness at the end of the procedure was arbitrarily defined as a maximum inducible pause ≤1.5 seconds.

STATISTICAL ANALYSIS. The statistical analyses were conducted using a combination of SPSS (version 23, SPSS Inc) and R (R Foundation). Continuous variables were described as means with SDs and compared with a 2-tailed *t-test* for independent samples. Variables with non-normal distribution were compared by the nonparametric Mann-Whitney test. Categorical variables were compared by Fisher exact test. Within-patient time-dependent data were analyzed using analysis of variance for repeated measures. Post hoc tests were performed using Bonferroni corrections. A P value < 0.05 was considered statistically significant.

RESULTS

PVI was achieved in all PVs in all patients, representing 62 electrically complete circular lesions around ipsilateral veins. No major clinical complications, including cardiac tamponade, stroke, phrenic nerve injury, and esophageal injury, occurred. The baseline clinical characteristics were comparable in both groups (Table 1). However, patients scheduled for ablation using RF energy were more likely to be in sinus rhythm on admission and had lower body mass index.

At baseline, physiological response to ECVS (long sinus arrest and/or atrioventricular [AV] block) was apparent in most of the patients in both groups.

RF ABLATION GROUP. In the RF ablation group, isolation of the left-sided PVs had an inconsistent but, on the average, neutral impact on SAN and AVN response to ECVS. In contrast, isolation of the right-sided PVs abolished the response almost completely, and this effect persisted until the end of the procedure (Figure 1, top).

PEF ABLATION GROUP. In the PEF group, both SAN and AVN responses to ECVS progressively attenuated during the ablation of all PVs with perceptible effects already after the left-sided PVI and additive effect of right-sided PVI. However, the cardiac ANS function markedly recovered during the 20-minute waiting period (Figure 1, bottom).

TABLE 1 Baseline Characteristics

	Radiofrequency Group (n = 13)	Pulsed Electric Field Group (n = 18)	*P* Value
Age, y	53 ± 16	59 ± 10	0.2
Male	7 (54)	15 (83)	0.11
Body mass index, kg/m^2	26 ± 3.6	31 ± 5.3	0.008
Arterial hypertension	8 (62)	11 (61)	1
Diabetes mellitus	1 (8)	2 (11)	1
Coronary artery disease	1 (8)	2 (11)	1
Transient ischemic attack or stroke	0 (0)	2 (11)	1
Left ventricular ejection fraction, %	59 ± 1	57 ± 5	0.07
Left atrium volume index, ml/m^2	34 ± 10	39 ± 9	0.10
Atrial fibrillation duration, months	36 ± 53	28 ± 23	0.60
Beta-blockers	9 (69)	15 (83)	0.41
Antiarrhythmic drugs[a]	8(61)	14 (77)	0.43
Sinus rhythm on admission	12 (92)	9 (50)	0.01

Values are mean ± SD or n (%). [a]Propafenone or amiodarone.

COMPARISON OF PEF VS RF ABLATION GROUPS. Immediately after PVI, the responsiveness of SAN to ECVS was influenced significantly less after PEF compared with RF ablation ($P = 0.001$), whereas the between-group difference in AV node responsiveness was not significant ($P = 0.48$). However, as a result of the rapid recovery of neural tissue during the waiting period, the difference between the RF and PEF ablation groups fully manifested at the end of the procedure (Figure 2).

Final effects on responsiveness in the categorical evaluation were also significantly weaker after PEF vs RF ablation (Figure 3). Substantial reduction in the responsiveness of the SAN was demonstrated in 13 of 13 (100%) and 6 of 18 (33%) patients ($P = 0.0001$) in RF and PEF groups, respectively. Analogically, reduced responsiveness of the AVN was observed in 10 of 11 (93%) and 6 of 18 (33%) patients ($P = 0.002$) in RF and PEF groups, respectively (Figure 3). In the same line, RF ablation was accompanied by significantly higher acceleration of the sinus rhythm (20.3 ± 13.2 vs 12.1 ± 9.9; $P = 0.04$) compared with PEF ablation (Table 2). The durations of the procedures were 170 ± 40 minutes and 152 ± 24 minutes in the RF and PEF groups, respectively ($P = 0.15$).

DISCUSSION

We quantified for the first time the impact of the PEF PVI on the vagal innervation of the SAN and AVN using ECVS. We confirmed that RF PVI alone is highly efficient in eliminating vagal responses at the level of both SAN and AVN and that this effect, which is primarily achieved by ablation around right PVs, is

FIGURE 1 **Time Course of SAN and AVN Responsiveness to ECVS During the RF and PEF Ablation Procedure**

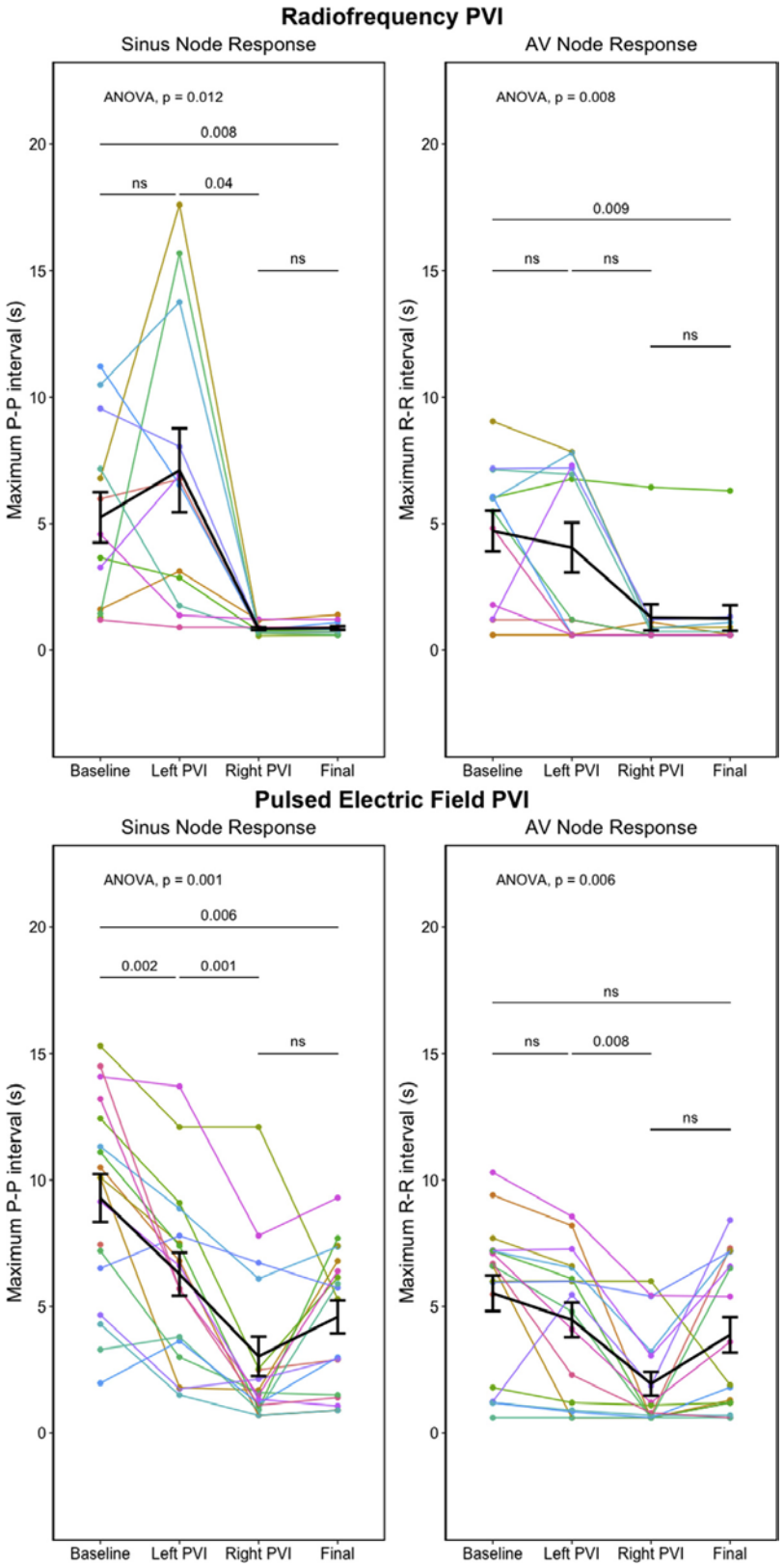

Continued on the next page

FIGURE 2 SAN and AVN Responsiveness to ECVS at the End of the Procedure: Continuous Variable Evaluation

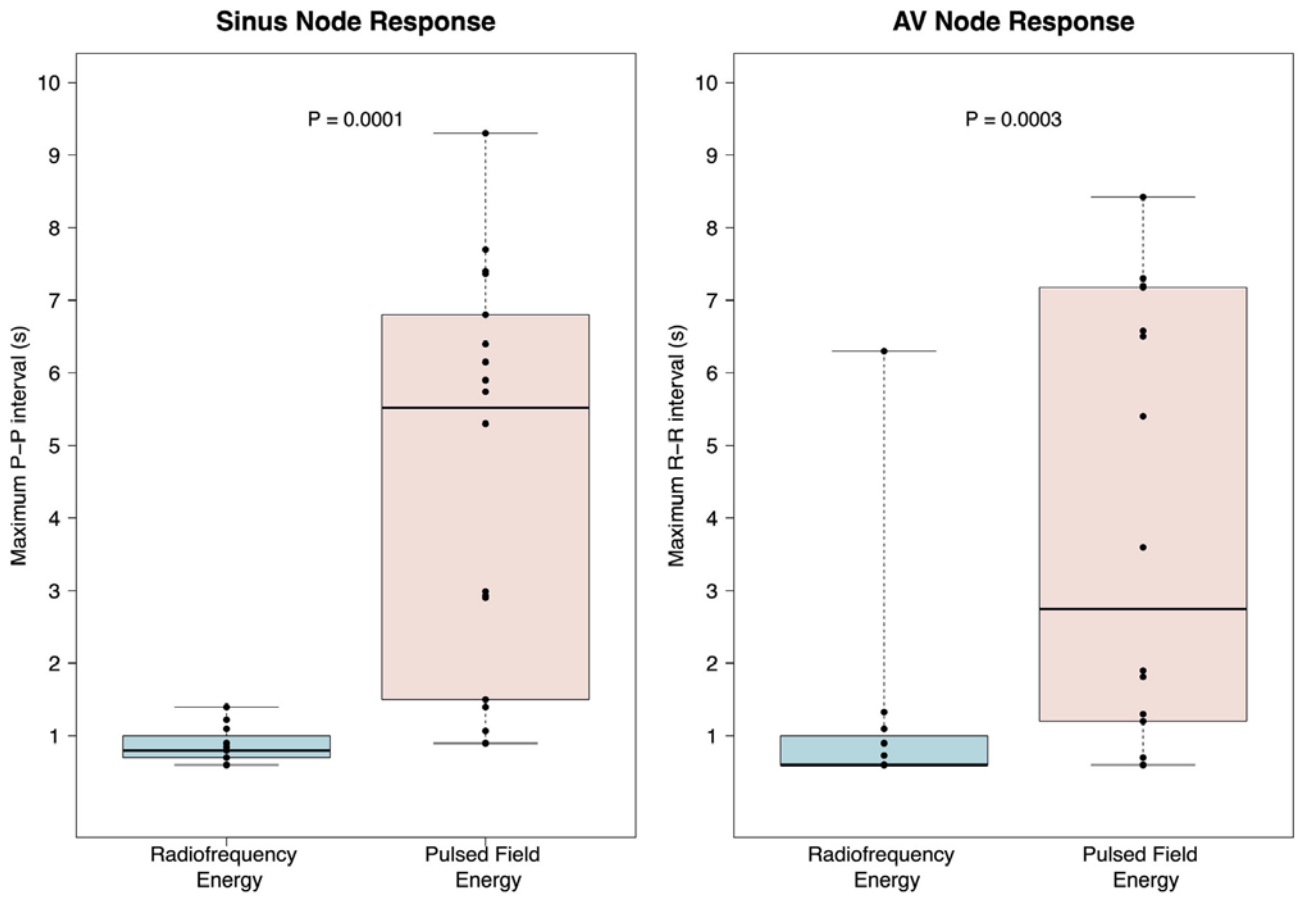

The maximum P-P interval in sinus rhythm **(left)** and R-R interval while atrial pacing **(right)** induced by ECVS is compared between RF **(red)** and PEF **(cyan)** ablation groups. **Boxes** indicate medians and IQR. The **whiskers** indicate the maximum and minimum values. Abbreviations as in Figure 2.

intraprocedurally durable. We newly revealed that the PEF PVI results in significantly weaker abolition of the vagal responses and that early recovery can be observed within the range of a few minutes (Central Illustration).

The results must be seen in the context of the potential role of vagal action in the pathogenesis of AF and the efficacy of catheter ablation.

ABLATION OF GPs. ANS plays an important role in regulation of cardiac functions.[13,14] Earlier observations have suggested that parasympathetic attenuation after RF PVI might play a role in preventing late arrhythmia recurrence.[6-9] Ablation of GPs occurs as "collateral damage" during PVI and the effect is more durable after large antral compared with ostial lesions.[15] Although some studies have shown a benefit of adding intrinsic ANS modulation to PVI,[7,8] others have not.[14,16] The ablation of GPs alone has never been superior to PVI.[17-19] Nevertheless, if the thermal ablation of GPs has an adjuvant

FIGURE 1 Continued

(Top) RF and **(bottom)** PEF ablation procedure. The maximum induced P-P interval in sinus rhythm **(left)** or R-R interval while atrial pacing **(right)** is plotted at baseline, after left- and right-sided PVI, and after 20 minutes of waiting period (final). The **colored lines** depict the trend in individual patients. **Black lines with error bars** are for group means and SEs. ANOVA = analysis of variance; AV = atrioventricular; AVN = atrioventricular node; ECVS = extracardiac vagal stimulation; PEF = pulsed electric field; PVI = pulmonary vein isolation; RF = radiofrequency; SAN = sinoatrial node.

FIGURE 3 **SAN and AVN Responsiveness to ECVS at the End of the Procedure: Categorical Evaluation**

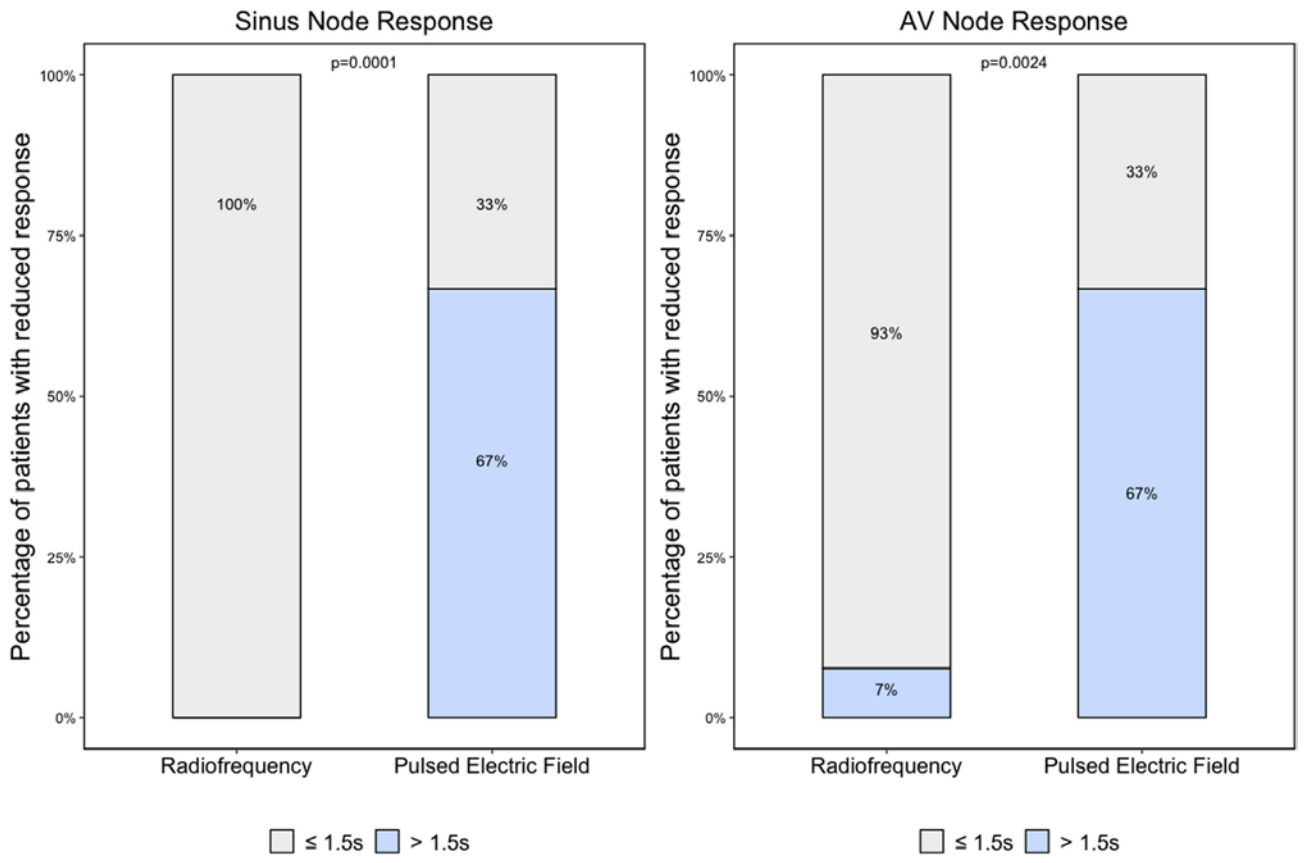

The maximum P-P interval <1.5 seconds in sinus rhythm **(left)** and maximum R-R interval <1.5 seconds while atrial pacing **(right)** induced by ECVS define substantial reduction of responsiveness to parasympathetic stimuli. RF and PEF ablation groups are compared. Abbreviations as in Figure 1.

effect on suppression of AF, PEF ablation with the limited collateral damage of neural tissue may be theoretically handicapped in terms of efficacy compared to RF ablation.

Ablation of GPs can be targeted anatomically, guided by endocardial high-frequency stimulation[20] or single-photon emission computed tomography imaging.[21] In our study, PV ostia were ablated circumferentially without selective targeting of GPs. It is well known, however, that PV antrum isolation by thermal energy results in a profound reduction of responsiveness of both sinus and AV nodes to vagal stimulation. Therefore, patients undergoing RF energy ablation served as a suitable comparator group for investigating the hypothesis that PEF ablation is associated with a lower effect on parasympathetic innervation of both nodes.

ASSESSMENT OF CARDIAC ANS FUNCTION. Previous studies have shown a significant impact of RF ablation for AF on cardiac ANS function, with an increase of mean heart rate (around 10 beats/min) postablation.[22-24] The increase was found to be positively associated with a significantly lower rate of AF recurrences.[25] However, such an observation may not be causal. A higher elevation of heart rate after PVI because of higher parasympathetic modulation at baseline might be an epiphenomenon of younger age and/or absence of comorbidities in patients who are principally less prone to AF recurrences. We observed a much higher increase in heart rate in our patients after RF ablation (around 20 beats/min) because this change was investigated intraprocedurally when its magnitude is the highest, whereas the effect weakens during the follow-up.

Attenuated heart rate variability (HRV) is another marker of reduced cardiac ANS activity. This was also reported to be associated with a better outcome of AF ablation.[23,24,26] Various HRV measures can be used, including the simple time-domain indexes, advanced frequency domain measures, descriptors of heart rate

TABLE 2 Changes of Electrophysiological Parameters

	Radiofrequency Ablation (n = 13)			Pulsed Electric Field Ablation (n = 18)			
	Before PVI	After PVI[a]	Change	Before PVI	After PVI[a]	Change	*P* Value RF vs PEF
Heart rate, beats/min[b]	60.5 ± 8.7	80.8 ± 8.8	+20.3 ± 13.2[c]	55 ± 11.5	67.1 ± 9.9	+12.1 ± 9.9[c]	0.04
Heart rate, beats/min[d]	55 ± 8.2	73.3 ± 15.5	+18.6 ± 11.9[c]	49.2 ± 9.0	60.7 ± 15.5	+11.5 ± 13.4[c]	0.06
Sinus node recovery time, ms	1,322 ± 301	1,116 ± 309	−205 ± 338[e]	1,794 ± 650	1,500 ± 484	−294 ± 586[e]	0.7
Wenckebach point, beats/min	155 ± 23	156 ± 25	+1.5 ± 12[f]	126 ± 22	132 ± 22	+5.7 ± 21[f]	0.6

Values are mean ± SD. [a]At the end of the procedure (after the waiting period). [b]Mean heart rate from standard surface electrocardiogram recorded at the ward. [c]$P < 0.005$ (for the statistical significance of the change within the study groups). [d]Mean heart rate recorded during the ablation procedure. [e]$P \leq 0.05$. [f]$P > 0.05$.
PVI = pulmonary vein isolation.

turbulence, heart rate recovery, or acceleration/deceleration capacity of the heart rate by sophisticated signal-processing technology.[26] The disadvantage of all of these methods is that they require several hours (or at least several minutes) of electrocardiogram recording, so they are not suitable for the assessment of intraprocedural dynamics of HRV.

UTILITY OF THE ECVS. To overcome this, we have used the ECVS technique proposed by Pachon et al,[27] which was already used in previous studies for the quantification of acute reduction of parasympathetic innervation during cryoballoon ablation.[28] The ECVS can be repeatedly assessed during the procedure with almost instant assessment of temporal evolution of cardiac vagal innervation (including trends to recovery during the waiting period). Another advantage of the ECVS is that, unlike HRV, which is limited to analysis of the behavior of SAN, the parasympathetic innervation of AVN can be assessed with the help of atrial pacing. Such a systematic investigation of vagal modulation of both nodes in the setting of PVI was performed for the first time in our study.

We stimulated the right vagal nerve because access to the right vs left jugular vein is considerably easier. As the right vagal nerve innervates predominantly the SAN, stronger responses of SAN vs AVN were observed at baseline. We do not consider this to be a limitation because we used the right ECVS consistently in all patients and primarily investigated the relative change of vagal responses during the ablation procedure.

COLLATERAL AF ABLATION EFFECTS. Known effects of ablation on cardiac ANS were derived mainly from studies that used RF energy. However, comparable modulation of cardiac ANS was also reported after cryoballoon-based PVI[29,30] and is probably present in all thermal energy ablations. Interestingly, the RF PVI resulted in complete loss of responsiveness of both SAN and AVN to ECVS in all but 1 patient (with persistent AVN innervation only), even if specific sites of GPs were ablated merely because of spatial coincidence within PV antra or were not targeted at all (namely those responsible for AVN innervation). Perhaps, the major attenuation of vagal responses was associated with isolation of right-sided PVs, and this was in agreement with results of previous studies.[22,29] Although the reduction in responsiveness was weaker after PEF ablation, it was rather concordant with RF ablation in terms of the higher impact of right PVI.

Until now, it was not possible to differentiate whether the modulation of cardiac ANS is required for the prevention of AF recurrences or whether it is only a bystander effect.

Given the high selectivity of PEF ablation for cardiomyocytes compared with neural cells, not only is PEF ablation promising in overcoming the drawbacks of RF or cryo-based approaches to PVI, but it may also serve as an investigational tool that yields highly durable PVI with a limited extent of GPs ablation. Our observations confirm for the first time that PEF results in transient abolition of the vagal responses with subsequent early recovery, probably because of the neural stunning effect. Whether this will be reflected by lower efficacy of ablation in the maintenance of sinus rhythm has to be verified. In this respect, a recent study has shown a high clinical success rate of 84% in patients undergoing PEF PVI at 1 year follow-up.[31] In addition, the role of parasympathetic modulation of the heart in the prevention of AF recurrence is not well established. Although attenuation of vagal innervation may have a protective role, the opposite intervention—intermittent low-level transcutaneous stimulation of the auricular branch of the vagal nerve—was shown to lower the median AF burden in a randomized trial.[32] This suggests that elimination of parasympathetic innervation may not be necessary for successful AF elimination. Whether adjuvant modulation of the cardiac ANS may play a role in selective patient subpopulation remains to be elucidated by upcoming studies.

CENTRAL ILLUSTRATION **Acute Change of Responsiveness of Sinoatrial Node and Atrioventricular Node to Extracardiac Vagal Stimulation After Pulmonary Vein Isolation**

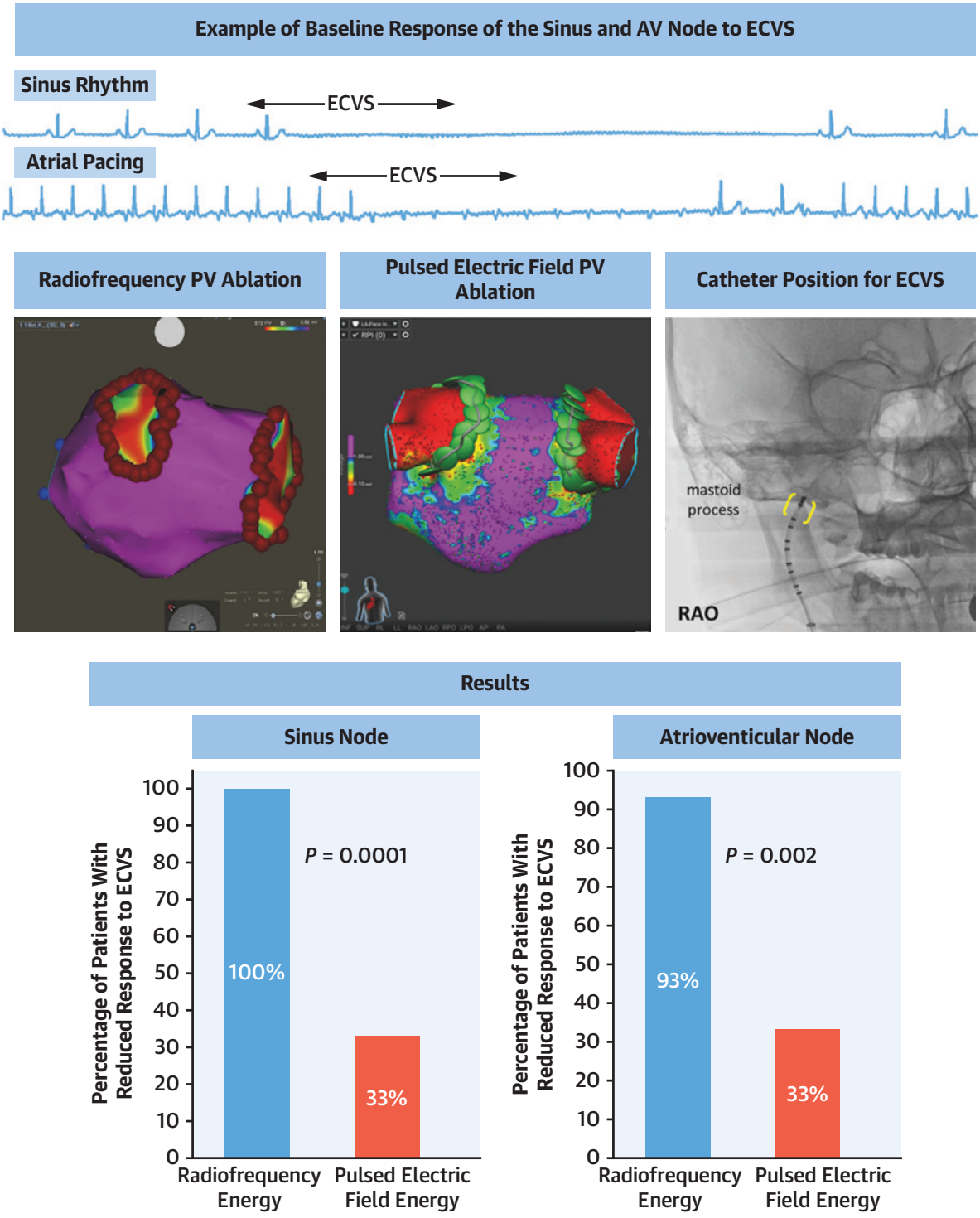

Stojadinović P, et al. J Am Coll Cardiol EP. 2022;■(■):■-■.

Example of baseline response to extracardiac vagal stimulation during sinus rhythm and atrial stimulation **(top)**. Voltage remaps after pulmonary vein isolation performed by radiofrequency and pulsed electric field energy and the x-ray of the skull with decapolar catheter position used for extracardiac vagal stimulation **(middle)**. The results are shown on the **bottom**.

STUDY LIMITATIONS. First, only acute effects of PVI were investigated. Even if there was a significant recovery of the parasympathetic branch of cardiac ANS after PEF ablation within the first 20 minutes of the waiting period, we cannot speculate whether this is followed by further restoration, with a theoretical return to preablation level. Second, the small number of patients were allocated to treatment strategies in a nonrandomized fashion, limiting the direct comparison between groups, subgroup analyses, and applicability of results. Third, although the differences between study groups were not significant for the majority of baseline variables (because of the small sample size), the patients in the PEF group had more advanced disease with a higher proportion of patients on beta-blockers and antiarrhythmic therapy, lower proportion of patients in sinus rhythm on admission, and lower baseline sinus rate. All of these factors could contribute to between-group differences in the PVI-induced suppression of cardiac ANS function. Fourth, a longer duration of general anesthesia in the RF group could hypothetically potentiate the gradual suppression of cardiac ANS. However, both sudden change in cardiac ANS function after the right PVI and a trend toward recovery in the waiting period in the PEF group go against this concept. Fifth, we investigated merely the innervation of SAN and AVN, which is not equivalent to overall atrial innervation. In addition, recent studies[33,34] have shown that there is significant discordance between the location of GPs that either cause bradycardia responses or trigger atrial ectopy that may initiate or perpetuate AF. The outcome measure in our study was based on the functional assessment of bradycardia-related GPs. Sixth, the acute effect of ablation on cardiac sympathetic innervation was not assessed because of the absence of a clinically suitable surrogate measure. A certain degree of loss of sympathetic innervation can be expected because previous studies demonstrated that adrenergic and cholinergic nerves are highly colocated close to the PV-LA junction.[35] Finally, the efficacy of PEF ablation is conditioned by ablation catheter type, pulse energy and duration, and many other PEF characteristics. Our data are relevant for a specific mapping and ablating system with a lattice-tip ablation catheter introduced by the Affera company.

CONCLUSIONS

PEF ablation provides a unique opportunity to test in the clinical setting the hypothesis of whether ablation of GPs during PVI contributes to the effectiveness of AF ablation. Our data suggest that cardiac vagal response is preserved in a considerable proportion of AF patients after PEF ablation, which is in contrast to a significantly stronger effect of RF energy. Therefore, it would be important to analyze the freedom from AF during the follow-up in both study groups.

FUNDING SUPPORT AND AUTHOR DISCLOSURES

This work has received institutional support from the project (Ministry of Health, Czech Republic) for development of research organization 00023001 (IKEM, Czech Republic). Dr Peichl has received speaker honoraria from St. Jude Medical (Abbott); and has served as a consultant for Biotronik and Boston Scientific. Dr Nakagawa has served as a consultant of Affera, Inc, Biosense Webster, and Gallaxy Medical, Inc. Dr Kautzner has received personal fees from Bayer, Biosense Webster, Boehringer Ingelheim, Medtronic, and St. Jude Medical (Abbott) for participation in scientific advisory boards; and has received speaker honoraria from Bayer, Biosense Webster, Biotronik, Boehringer Ingelheim, Daiichi Sankyo, Medtronic, Merck Sharp and Dohme, Mylan, Pfizer, ProMed, and St. Jude Medical (Abbott). All other authors have reported that they have no relationships relevant to the contents of this paper to disclose.

ADDRESS FOR CORRESPONDENCE: Dr Predrag Stojadinović, Institute for Clinical and Experimental Medicine (IKEM), Vídeňská 1958/9, Prague 140 21, Czech Republic. E-mail: stop@ikem.cz.

PERSPECTIVES

COMPETENCY IN MEDICAL KNOWLEDGE: Significant alteration of cardiac ANS functions has been described as a collateral effect of PVI. Previous studies suggested that targeted ablation of GPs on top of PVI may have a beneficial effect in terms of the clinical outcome of the procedure. Our data suggest that cardiac vagal response is preserved in a considerable proportion of AF patients after PEF ablation, which is in contrast to a significantly stronger effect of RF energy ablation.

TRANSLATIONAL OUTLOOK: Further studies are needed to elucidate whether a stronger alteration of cardiac ANS after PVI is associated with a better clinical outcome of the procedure.

REFERENCES

1. Hindricks G, Potpara T, Dagres N, et al. 2020 ESC guidelines for the diagnosis and management of atrial fibrillation developed in collaboration with the European Association for Cardio-Thoracic Surgery (EACTS). *Eur Heart J*. 2021;42(5):373–498.

2. Calkins H, Hindricks G, Cappato R, et al. 2017 HRS/EHRA/ECAS/APHRS/SOLAECE expert consensus statement on catheter and surgical ablation of atrial fibrillation: executive summary. *Europace*. 2018;20(1):157–208.

3. Reddy VY, Neuzil P, Koruth JS, et al. Pulsed field ablation for pulmonary vein isolation in atrial fibrillation. *J Am Coll Cardiol*. 2019;74(3):315–326.

4. Koruth JS, Kuroki K, Iwasawa J, et al. Endocardial ventricular pulsed field ablation: a proof-of-concept preclinical evaluation. *Europace*. 2020;22(3):434–439.

5. Neven K, Van Es R, Van Driel V, et al. Acute and long-term effects of full-power electroporation ablation directly on the porcine esophagus. *Circ Arrhythmia Electrophysiol*. 2017;10(5):e004672.

6. Pappone C, Santinelli V, Manguso F, et al. Pulmonary vein denervation enhances long-term benefit after circumferential ablation for paroxysmal atrial fibrillation. *Circulation*. 2004;109(3):327–334.

7. Katritsis DG, Giazitzoglou E, Zografos T, Pokushalov E, Po SS, Camm AJ. Rapid pulmonary vein isolation combined with autonomic ganglia modification: a randomized study. *Heart Rhythm*. 2011;8(5):672–678.

8. Katritsis DG, Pokushalov E, Romanov A, et al. Autonomic denervation added to pulmonary vein isolation for paroxysmal atrial fibrillation: a randomized clinical trial. *J Am Coll Cardiol*. 2013;62(24):2318–2325.

9. Lin YJ, Chang SL, Lo LW, et al. A prospective, randomized comparison of modified pulmonary vein isolation versus conventional pulmonary vein isolation in patients with paroxysmal atrial fibrillation. *J Cardiovasc Electrophysiol*. 2012;23(11):1155–1162.

10. Reddy VY, Anter E, Rackauskas G, et al. Lattice-tip focal ablation catheter that toggles between radiofrequency and pulsed field energy to treat atrial fibrillation: a first-in-human trial. *Circ Arrhythmia Electrophysiol*. 2020;13(6):e008718.

11. Anter E, Neužil P, Rackauskas G, et al. A lattice-tip temperature-controlled radiofrequency ablation catheter for wide thermal lesions: First-in-human experience with atrial fibrillation. *J Am Coll Cardiol EP*. 2020;6(5):507–519.

12. Pachon JC, Pachon EI, Cunha Pachon MZ, Lobo TJ, Pachon JC, Santillana TG. Catheter ablation of severe neurally meditated reflex (neurocardiogenic or vasovagal) syncope: cardioneuroablation long-term results. *Europace*. 2011;13(9):1231–1242.

13. Hanna P, Buch E, Stavrakis S, et al. Neuroscientific therapies for atrial fibrillation. *Cardiovasc Res*. 2021;117(7):1732–1745.

14. Hanna P, Dacey MJ, Brennan J, et al. Innervation and neuronal control of the mammalian sinoatrial node a comprehensive atlas. *Circ Res*. 2021;128(9):1279–1296.

15. Bauer A, Deisenhofer I, Schneider R, et al. Effects of circumferential or segmental pulmonary vein ablation for paroxysmal atrial fibrillation on cardiac autonomic function. *Heart Rhythm*. 2006;3:1428–1435.

16. Gelsomino S, Lozekoot P, La Meir M, et al. Is ganglionated plexi ablation during Maze IV procedure beneficial for postoperative long-term stable sinus rhythm? *Int J Cardiol*. 2015;192:40–48.

17. Berger W, Neefs J, van den Berg N, et al. Additional ganglion plexus ablation during thoracoscopic surgical ablation of advanced atrial fibrillation: intermediate follow-up of the AFACT study. *J Am Coll Cardiol EP*. 2019;5(3):343–353.

18. Katritsis D, Giazitzoglou E, Sougiannis D, Goumas N, Paxinos G, Camm AJ. Anatomic approach for ganglionic plexi ablation in patients with paroxysmal atrial fibrillation. *Am J Cardiol*. 2008;102(3):330–334.

19. Sandler B, Kim MY, Sikkel MB, et al. Targeting the ectopy-triggering ganglionated plexuses without pulmonary vein isolation prevents atrial fibrillation. *J Cardiovasc Electrophysiol*. 2021;32(2):235–244.

20. Po S, Nakagawa H, Jackman WM. Localization of left atrial ganglionated plexi in patients with atrial fibrillation. *J Cardiovasc Electrophysiol*. 2009;20(10):1186–1189.

21. Stirrup J, Gregg S, Baavour R, et al. Hybrid solid-state SPECT/CT left atrial innervation imaging for identification of left atrial ganglionated plexi: technique and validation in patients with atrial fibrillation. *J Nucl Cardiol*. 2020;27(6):1939–1950.

22. Ketels S, Houben R, Van Beeumen K, Tavernier R, Duytschaever M. Incidence, timing, and characteristics of acute changes in heart rate during ongoing circumferential pulmonary vein isolation. *Europace*. 2008;10(12):1406–1414.

23. von Olshausen G, Saluveer O, Schwieler J, et al. Sinus heart rate post pulmonary vein ablation and long-term risk of recurrences. *Clin Res Cardiol*. 2021;110(6):851–860.

24. Goff ZD, Laczay B, Yenokyan G, et al. Heart rate increase after pulmonary vein isolation predicts freedom from atrial fibrillation at 1 year. *J Cardiovasc Electrophysiol*. 2019;30(12):2818–2822.

25. Yu HT, Kim TH, Uhm JS, et al. Prognosis of high sinus heart rate after catheter ablation for atrial fibrillation. *Europace*. 2017;19(7):1132–1139.

26. Kang KW, Kim TH, Park J, et al. Long-term changes in heart rate variability after radiofrequency catheter ablation for atrial fibrillation: 1-year follow-up study with irrigation tip catheter. *J Cardiovasc Electrophysiol*. 2014;25(7):693–700.

27. Pachon MJC, Pachon MEI, Santillana PTG, et al. Simplified method for vagal effect evaluation in cardiac ablation and electrophysiological procedures. *J Am Coll Cardiol EP*. 2015;1(5):451–460.

28. Osório TG, Coutiño HE, Iacopino S, et al. Quantification of acute parasympathetic denervation during cryoballoon ablation by using extracardiac vagal stimulation. *J Cardiovasc Med (Hagerstown)*. 2019;20(3):107–113.

29. Oswald H, Klein G, Koenig T, Luesebrink U, Duncker D, Gardiwal A. Cryoballoon pulmonary vein isolation temporarily modulates the intrinsic cardiac autonomic nervous system. *J Interv Card Electrophysiol*. 2010;29(1):57–62.

30. Tang LYW, Hawkins NM, Ho K, et al. Autonomic alterations after pulmonary vein isolation in the CIRCA-DOSE (Cryoballoon vs Irrigated Radiofrequency Catheter Ablation) Study. *J Am Heart Assoc*. 2021;10(5):e018610.

31. Reddy VY, Dukkipati SR, Neuzil P, et al. Pulsed field ablation of paroxysmal atrial fibrillation: 1-year outcomes of IMPULSE, PEFCAT, and PEFCAT II. *J Am Coll Cardiol EP*. 2021;7(5):614–627.

32. Stavrakis S, Stoner JA, Humphrey MB, et al. TREAT AF (Transcutaneous Electrical Vagus Nerve Stimulation to Suppress Atrial Fibrillation): a randomized clinical trial. *J Am Coll Cardiol EP*. 2020;6(3):282–291.

33. Kim MY, Sikkel MB, Hunter RJ, et al. A novel approach to mapping the atrial ganglionated plexus network by generating a distribution probability atlas. *J Cardiovasc Electrophysiol*. 2018;29(12):1624–1634.

34. Kim MY, Sandler BC, Sikkel MB, et al. Anatomical distribution of ectopy-triggering plexuses in patients with atrial fibrillation. *Circ Arrhythm Electrophysiol*. 2020;13(9):e008715.

35. Tan AY, Li H, Wachsmann-Hogiu S, et al. Autonomic innervation and segmental muscular disconnections at the human pulmonary vein-atrial junction. *J Am Coll Cardiol*. 2006;48:132–143.

KEY WORDS **atrial fibrillation, autonomic regulation, catheter ablation, ganglionated plexi, pulsed electric field**

M. Pešl et al.

Aminophylline Induces Two Types of Arrhythmic Events in Human Pluripotent Stem Cell – Derived Cardiomyocytes

Front. Pharmacol.
Impact Factor: 5.988

‹ rejstřík

frontiers in Pharmacology

ORIGINAL RESEARCH
published: 17 January 2022
doi: 10.3389/fphar.2021.789730

Aminophylline Induces Two Types of Arrhythmic Events in Human Pluripotent Stem Cell–Derived Cardiomyocytes

Simon Klimovic[1,2,3†], Martin Scurek[4,5†], Martin Pesl[2,6,7†], Deborah Beckerova[2,6], Sarka Jelinkova[2], Tomas Urban[2,7], Daniil Kabanov[1,2,3], Zdenek Starek[6,7], Marketa Bebarova[8], Jan Pribyl[1], Vladimir Rotrekl[2,6] and Kristian Brat[4,5,6†]*

[1]CEITEC, Masaryk University, Brno, Czechia, [2]Department of Biology, Faculty of Medicine, Masaryk University, Brno, Czechia, [3]Department of Biochemistry, Faculty of Science, Masaryk University, Brno, Czechia, [4]Department of Respiratory Diseases, University Hospital Brno, Brno, Czechia, [5]Faculty of Medicine, Masaryk University, Brno, Czechia, [6]International Clinical Research Center, St. Anne's University Hospital, Brno, Czechia, [7]First Department of Internal Medicine—Cardioangiology, Faculty of Medicine, St. Anne's University Hospital, Masaryk University, Brno, Czechia, [8]Department of Physiology, Faculty of Medicine, Masaryk University, Brno, Czechia

OPEN ACCESS

Edited by:
Paulo Correia-de-Sá, University of Porto, Portugal

Reviewed by:
Bruno Bragança, Centro Hospitalar do Tâmega e Sousa, Portugal, Portugal
Jean-Sebastien Rougier, University of Bern, Switzerland

***Correspondence:**
Kristian Brat
Brat.Kristian@fnbrno.cz

[†]These authors have contributed equally to this work

Specialty section:
This article was submitted to Cardiovascular and Smooth Muscle Pharmacology, a section of the journal Frontiers in Pharmacology

Received: *05 October 2021*
Accepted: *17 November 2021*
Published: *17 January 2022*

Citation:
Klimovic S, Scurek M, Pesl M, Beckerova D, Jelinkova S, Urban T, Kabanov D, Starek Z, Bebarova M, Pribyl J, Rotrekl V and Brat K (2022) Aminophylline Induces Two Types of Arrhythmic Events in Human Pluripotent Stem Cell–Derived Cardiomyocytes. Front. Pharmacol. 12:789730. doi: 10.3389/fphar.2021.789730

Cardiac side effects of some pulmonary drugs are observed in clinical practice. Aminophylline, a methylxanthine bronchodilator with documented proarrhythmic action, may serve as an example. Data on the action of aminophylline on cardiac cell electrophysiology and contractility are not available. Hence, this study was focused on the analysis of changes in the beat rate and contraction force of human pluripotent stem cell–derived cardiomyocytes (hPSC-CMs) and HL-1 cardiomyocytes in the presence of increasing concentrations of aminophylline (10 µM–10 mM in hPSC-CM and 8–512 µM in HL-1 cardiomyocytes). Basic biomedical parameters, namely, the beat rate (BR) and contraction force, were assessed in hPSC-CMs using an atomic force microscope (AFM). The beat rate changes under aminophylline were also examined on the HL-1 cardiac muscle cell line via a multielectrode array (MEA). Additionally, calcium imaging was used to evaluate the effect of aminophylline on intracellular Ca^{2+} dynamics in HL-1 cardiomyocytes. The BR was significantly increased after the application of aminophylline both in hPSC-CMs (with 10 mM aminophylline) and in HL-1 cardiomyocytes (with 256 and 512 µM aminophylline) in comparison with controls. A significant increase in the contraction force was also observed in hPSC-CMs with 10 µM aminophylline (a similar trend was visible at higher concentrations as well). We demonstrated that all aminophylline concentrations significantly increased the frequency of rhythm irregularities (extreme interbeat intervals) both in hPSC-CMs and HL-1 cells. The occurrence of the calcium sparks in HL-1 cardiomyocytes was significantly increased with the presence of 512 µM aminophylline. We conclude that the observed aberrant cardiomyocyte response to aminophylline suggests an arrhythmogenic potential

Abbreviations: sAFM, atomic force microscope; bpm, beats per minute; CBBs, cell-based biosensors; CCTL, center for cell therapy line; CM, cardiomyocyte; EB, embryoid body; ECC, excitation–contraction coupling; hESC, human embryonic stem cell; hiPSC, human-induced pluripotent stem cell; hPSC, human pluripotent stem cell (hESC and hiPSC); hPSC-CMs, pluripotent stem cell–derived cardiomyocytes.

of the drug. The acquired data represent a missing link between the arrhythmic events related to the aminophylline/theophylline treatment in clinical practice and describe cellular mechanisms of methylxanthine arrhythmogenesis. An AFM combined with hPSC-CMs may serve as a robust platform for direct drug effect screening.

Keywords: aminophylline, IPSC, hESC, cardiomyocytes, drug cardiotoxicity, atomic force microscopy, arrhythmogenic effects, methylxanthines

INTRODUCTION

Theophylline (1,3-dimethylxanthine) and its more soluble form aminophylline (a complex of two theophylline molecules and ethylenediamine) are well-known bronchodilators used mostly for therapy of chronic obstructive pulmonary disease (COPD) and asthma. These drugs are also recommended for the treatment of emphysema (Zatloukal et al., 2020). Other indications have been suggested, for example, treatment of apnea in premature neonates (Ye et al., 2019). Unfortunately, a narrow therapeutic range and frequent adverse effects make their use controversial (Singh et al., 2019). An increased mortality rate in theophylline users has been reported by multiple research teams (Lee et al., 2009; Horita et al., 2016). A higher percentage of cardiovascular deaths was observed in asthma patients who received aminophylline (Suissa et al., 1996), as well as in patients with COPD (Lee et al., 2009), and also in a general patient population overdosed with theophylline (Shannon, 1999).

The adverse effects of theophylline/aminophylline include arrhythmias, even at their therapeutic plasma concentrations (Bittar and Friedman, 1991). In a meta-analysis of several randomized clinical trials, 13% incidence of arrhythmias or palpitations after intravenous aminophylline infusion has been observed (Nair et al., 2012). More than 20% of patients experience cardiac arrhythmias during an aminophylline overdose episode (Shannon, 1999). Supraventricular arrhythmias have been observed most frequently, usually represented by atrial fibrillation (AF) (Varriale and Ramaprasad, 1993; Huerta et al., 2005). Concurrently, COPD is an independent risk factor of AF (Goudis, 2017). The risk of arrhythmias is further enhanced by hypokalemia (Hoppe et al., 2018), which may develop as a side effect of aminophylline treatment, particularly occurring in cases of intentional overdose (Ellis, 1985; Charytan and Jansen, 2003).

Mechanisms of theophylline-/aminophylline-induced arrhythmias are not clear. It is well known that methylxanthines non-specifically inhibit phosphodiesterases (hence increasing the cAMP level) and adenosine receptors (Ukena et al., 1993). These effects may explain the sinus tachycardia often observed in clinical practice. In contrast, this does not explain the origin of AF associated with aminophylline treatment. Effects of theophylline/aminophylline on cardiac electrophysiology were studied mostly in animal models (Komadina et al., 1992; Onodera et al., 2001; Shamsuzzaman et al., 2016). However, a conclusive explanation of their proarrhythmic action has not been provided, and data from human cardiomyocytes (CMs) embedded in cardiac syncytia have been missing completely.

This study was aimed to reveal changes of basic functional characteristics (contraction force and beat rate) of human cardiac tissues induced by aminophylline at a wide range of concentrations. A clinically relevant model was employed, for example, 3D structures called embryoid bodies (EBs) derived from human pluripotent stem cells subsequently differentiated into cardiomyocytes (hPSC-CMs). The model was originally described in previous studies (Burridge et al., 2012; Pesl et al., 2014). Its functional properties were further validated using atomic force microscopy (Liu et al., 2012; Dinarelli et al., 2018; Pribyl et al., 2019), a method enabling real-time monitoring of contractions and thus also beating properties of single cardiomyocytes or cardiac cell clusters, alone or in combination with other methods such as microelectrode array (Caluori et al., 2019b) or calcium imaging (Odstrcilik et al., 2015; Caluori et al., 2019a). This model was recently used for disease modeling in studies by Acimovic et al., 2018; Jelinkova et al., 2019. The effects of aminophylline were further validated on an independent model of HL-1 cardiomyocyte cells. The overall scheme of all experiments within this study is presented in **Figure 1**. This approach has provided the first experimental data well-corresponding with the aminophylline-induced arrhythmias observed in clinical medicine.

MATERIALS AND METHODS

Cell Cultivation

The hESC line CCTL14 (46 XX) derived at Masaryk University, Brno, and previously characterized (International Stem Cell Initiative et al., 2007) was routinely maintained on a feeder layer of mitotically inactivated mouse embryonic fibroblasts as previously described (Dvorak et al., 2005; Krutá et al., 2014; Jelinkova et al., 2020).

Differentiation into CMs via embryoid bodies (EBs) and measurements by an AFM were performed as previously described (Pesl et al., 2014), with minor modifications. Briefly, hESC colonies were collected 4 days after seeding and subsequently broken down into smaller clumps which were seeded into the EB medium (86% KO DMEM, 10% FBS, 1% L-glutamine, 1% penicillin/streptomycin, 1% non-essential amino acids, 0.1 mM 2-mercaptoethanol, and 10 µg/ml ascorbic acid) with 10 ng/ml BMP4 (R&D) and placed in hypoxic conditions (5% O_2, 5% CO_2,) where they spontaneously formed EBs. After 3 days, the medium was removed and replaced with fresh EB medium supplemented with 5 ng/ml FGF2 (Peprotech), 10 ng/ml BMP4, and 6 ng/ml activin A (R&D) for a 4-day incubation. A 3-day incubation in EB

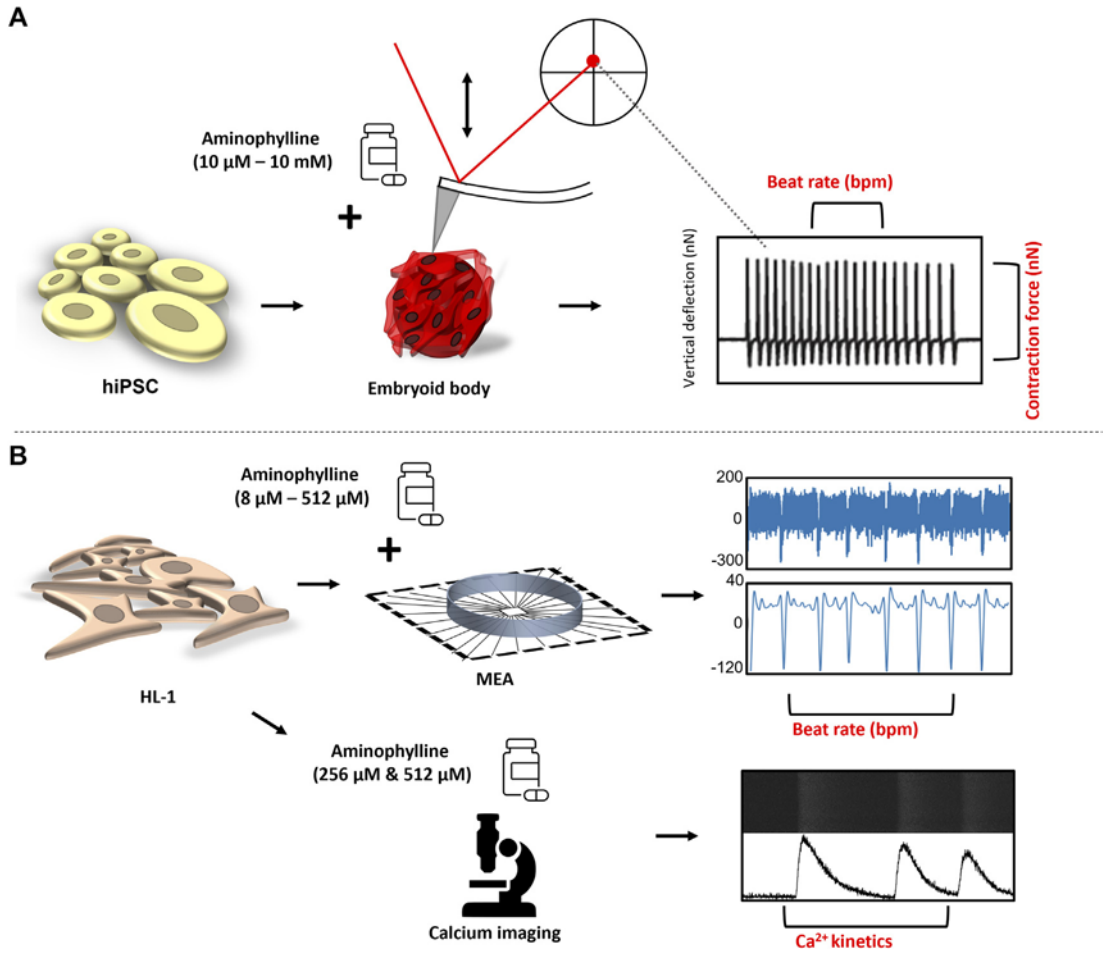

FIGURE 1 | Experimental design: **(A)** hPSCs were differentiated in the form of EBs into contracting 3D clusters of cardiomyocytes, and under the influence of increasing concentrations of aminophylline, the mechanocardiogram (MCG) was recorded was recorded by an atomic force microscope. The BR and contraction force values of each contractive event were further analyzed and compared. **(B)** Field potential by the multielectrode array (MEA) system, together with intrinsic Ca^{2+} kinetics via Fluo-8 AM, a calcium-binding dye, was assessed on HL-1 cells to further confirm the arrhythmogenic effect of aminophylline.

medium supplemented with 10 ng/ml VEGF (R&D) and 10 µM IWR1 (R&D). The next induction medium was the EB medium supplemented with 10 ng/ml VEGF and 5 ng/ml FGF2, with a medium exchange every 4 days. After four days in this medium (day 14 of differentiation), the EBs were transferred into a normoxic incubator (21% O_2, 5% CO_2) for the remaining 8 days of this induction period. From then onward, EBs remained in normoxia and were fed with the EB medium every 4 days until analysis. Beating EBs were selected and transferred on a gelatin-coated PM3 dish to adhere to for measurement. These cellular constructs of the cardiac syncytium were coupled to an AFM force sensor to perform a high-fidelity contraction pattern as an hPSC-CM–based biosensor (Pesl et al., 2014). The constant size of clusters of hPSC-CMs allows comparable and stable beating pattern evaluation allowing for force- and rhythm-related drug effect tracking.

For the immunocytochemistry experiment, either whole or dissociated EBs attached on coverslips were fixed with 4% PFA, blocked and permeabilized by 1% BSA (Sigma) in 0,1% Triton-X (Sigma) or 0,05% TWEEN (Sigma) in PBS, and incubated with anti–troponin T antibody (1:5,000, Cell Signaling, 5,593, Rb) overnight in 4 C. Anti-rabbit Alexa 594 (1:500, Invitrogen) was left to incubate for an hour at room temperature, and the slips were mounted on slides with Mowiol containing DAPI (Sigma). The images were obtained using a Zeiss LSM 700 confocal microscope.

The contracting clusters were previously checked for expression and checked by immunostaining for cardiac troponin T (cTnT) and ryanodine receptor RyR2 as described elsewhere (Pesl et al., 2014; Souidi et al., 2021). The expression of myosin heavy chain MYH6/7 and MYH7, RyR2, and the striated pattern of cTnT in dissociated cardiomyocytes was used to assess the progress in CM maturation. The clusters consisted of all three CM subtypes as described elsewhere; in brief, nodal-like CMs had an AP duration at 90% of repolarization shorter than 100 ms (about 16%), slightly more frequent were atrial-like cells, and recorded AP mainly demonstrated a typical ventricular-like

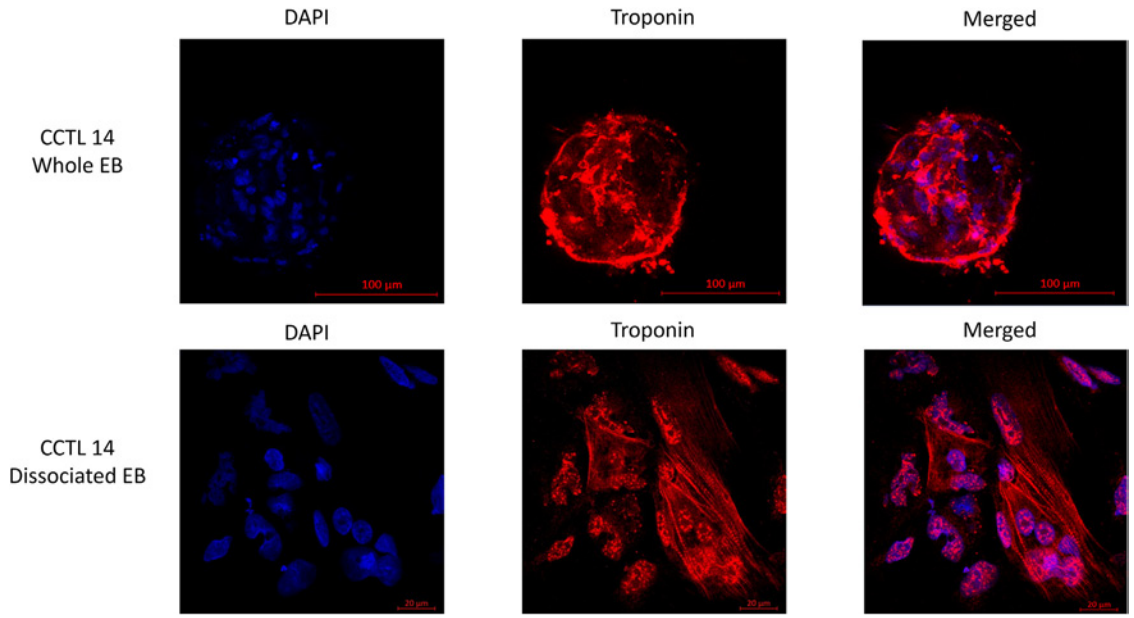

FIGURE 2 | Fluorescence staining of whole and dissociated CCTL14 EBs (cell cluster) illustrates the presence of matured cardiomyocytes identified by the presence of troponin T (red color); cells are localized with DAPI staining of the nucleus (blue color).

shape (Acimovic et al., 2018). EB responses to basic heart modulators, such as β adrenoceptor agonist and blocker, isoproterenol, and metoprolol, were previously measured (**Supplementary Figure S1**).

EBs from the same cultivation batch were checked for the presence of cTnT in the clusters as well as in the dissociated EBs by immunostaining to demonstrate the batch-to-batch differentiation consistency (**Figure 2**).

The HL-1 Cardiac Muscle Cell Line (Sigma) was routinely maintained on fibronectin-coated dishes in Claycomb medium (Sigma) supplemented with 10% FBS, 100 U/ml:100 µg/ml penicillin:streptomycin, 0.1 mM norepinephrine, and 2 mM L-glutamine. The cells were passaged with trypsin after reaching full confluency, usually every 3–4 days, in a ratio of 1:3. For experiments with MEA, the HL-1 cells were cultivated on MEA chips coated with fibronectin in 0.02% gelatin (5 mg/ml; Sigma). The HL-1 response to β-adrenoceptor agonist isoproterenol was measured (**Supplementary Figure S1**).

Atomic Force Microscopy Measurements

NanoWizard 3 AFM (Bruker-JPK) combined with inverted light microscope IX-81 (Olympus) was used to obtain mechanocardiograms (MCGs) of beating EBs as previously described (Pesl et al., 2014; Caluori et al., 2019b; Pribyl et al., 2019).

Drug response tests were performed after initial equilibration of EBs in Tyrode's solution (composition in mM: NaCl 135, KCl 5.4, $MgCl_2$ 0.9, $CaCl_2$ 1.8, HEPES 10, NaH_2PO_4 0.33, and glucose 5.5; pH 7.4 adjusted with 3M NaOH) (Bébarová et al., 2017). The addition of increasing concentrations of aminophylline (10 µM, 100 µM, 1 mM, and 10 mM; Fagron) followed. Each concentration was prepared in Tyrode's solution from 1 mM stock solution of aminophylline. The MCG was recorded for further analysis; each measurement point consisted of 10 min of stabilization time, followed by 10 min of measurement. Control experiments were conducted in the same setting without aminophylline in the treatments.

The contraction of beating EBs was recorded as a force value in time (MCG). In-house built MATLAB-based script located R and S peaks for each contractive event and their respective vertical deflection and time values. From these values, R-R (sec), R-S (contraction force; nN), and BR (beat rate; beats per minute) were calculated, averaged, and normalized to the respective baseline values recorded in Tyrode's solution.

Multielectrode Array Measurements

The field potential of the HL-1 cells was measured using MEA2100-mini-60 (Multi Channel Systems). Drug responses were measured after initial equilibration in Claycomb medium, followed by the increasing concentrations of aminophylline in Claycomb medium (8, 16, 32, 64, 128, 256, and 512 µM). Measurement points consisted of 3 min of stabilization time, followed by 5 min of measurement. As a monolayer, HL-1 cells are more sensitive to a treatment than hPSC-CM clusters. Therefore, treatment measurement times and concentration ranges were modified.

MEA recordings were analyzed using Multi-Channel Analyzer software and in-house Python script, which processed the data in a similar way; however, the resulting parameters were only R-R (sec) and BR (beat rate; beats per minute). R-S (amplitude; µV) values in case of MEA recordings do not correlate with R-S values measured *via* AFM; therefore, they were not used in this study. Noisy and non-representative MEA channels were eliminated, and at least 3 channels were then used for calculations.

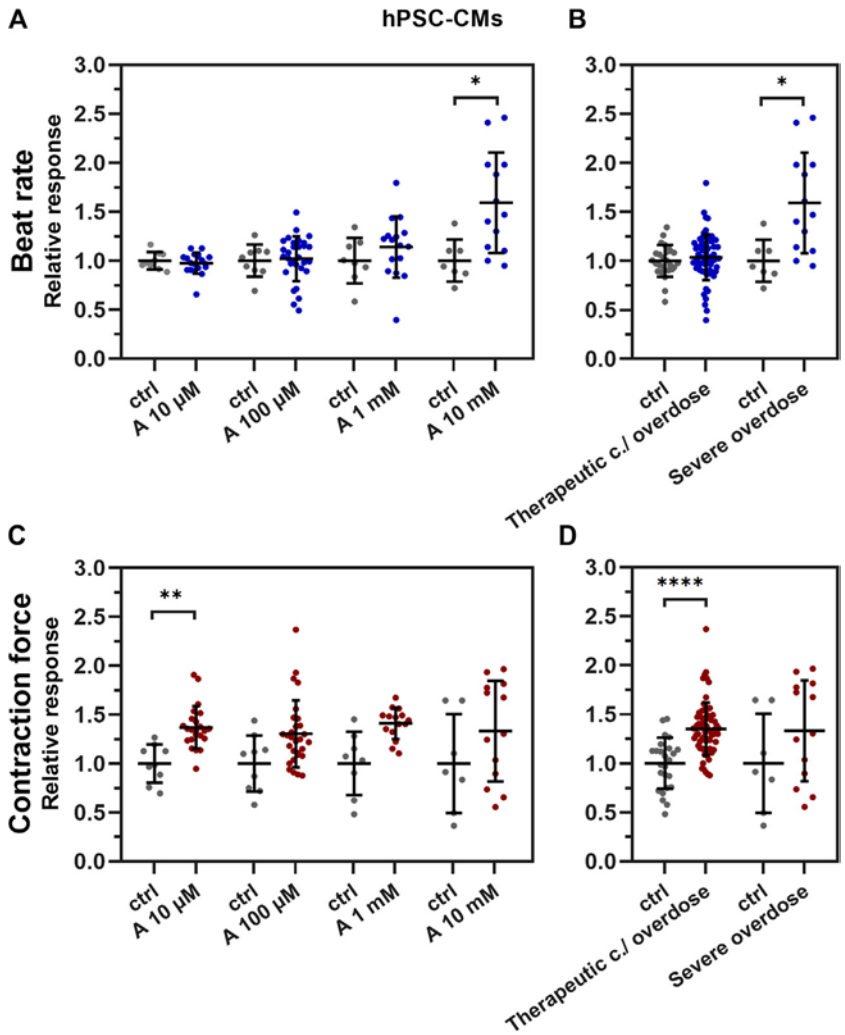

FIGURE 3 | Effect of aminophylline (A) on contractile properties of 3D cardiac clusters. Scatterplots (mean ± standard deviation) of the BR (blue) and contraction force (red) overall changes, normalized to a baseline measurement (relative response) and to control measurement means (n = 19 for A 10 µM, n = 30 for A 100 µM, n = 16 for A 1 mM, n = 13 for A 10 mM, n = 9 for BR ctrl and n = 7 for contraction force ctrl). At least four biological repetitions were used in each column. **(A)** BR of the measured EBs with 10 mM aminophylline (A 10 mM) was significantly increased compared to that of the control ($p < 0.05$). **(B)** Similarly, the BR of EBs treated with 10 mM concentration of aminophylline was significantly increased over that of the controls ($p < 0.05$). **(C)** Contraction force of EBs with 10 µM aminophylline treatment was significantly increased over that of the control ($p < 0.05$), with a similar trend in higher concentrations. **(D)** Group analyses then showed a strong statistically significant effect of therapeutic concentration / overdose (10 µM and 100 µM and 1 mM) aminophylline over the controls. (Brown–Forsythe and Welch ANOVA tests were used in all analyses).

Measurements of Intracellular Cytosolic Ca^{2+}

HL-1 cells were passaged and seeded onto an imaging dish with a polymer coverslip bottom (Ibidi) and allowed to adhere. Fluo-8 (490/525; AAT Bioquest) was added into the medium (final concentration 2 µM; stock solution in DMSO 2 mM), and the cells were incubated for 20 min at 37°C. After the incubation, the solution was replaced with fresh medium, and the cells were placed on the heated stage (37°C) of an inverted microscope. Ca^{2+} images in the line-scan (line size 3.37 µm, 100 Hz) mode were recorded using a laser scanning confocal microscope Olympus FL1200 (Olympus) with a ×40 water immersion objective, in the x–y mode. Kinetic properties of intracellular Ca^{2+} were analyzed *via* the in-house Python-based script (Kabanov, 2021).

Measurement of HL-1 Viability

The HL-1 cells were passaged and mixed with PBS containing aminophylline (final concentration 512 µM) or only PBS for control. The cells were incubated for 8 min after which their viability was analyzed via the trypan blue dye exclusion method (Vicell-XR, Beckman Coulter).

Statistical Analyses

Statistical evaluation was carried out with the use of GraphPad Prism 8.5 software (GraphPad Software). All data were tested for

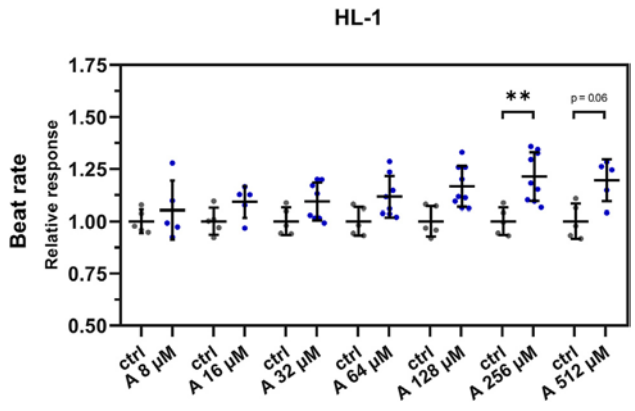

FIGURE 4 | Effect of aminophylline (A) on the BR of HL-1 cells. Scatterplots (mean ± standard deviation) of the BR (blue) normalized to a baseline measurement (relative response) and to control measurement means (n = 5 for A 8 and 16 µM, n = 8 for 32 and 64 µM, n = 9 for 128 and 256 µM, n = 5 for 512 µM and n = 5 for ctrl). At least three biological repetitions were used in each column. Results showed linear increase of BR correlating with a higher concentration of aminophylline, with statistically significant and partially significant changes of BR 256 and 512 µM measurements compared that of the control (A 256 vs. ctlr $p < 0.01$, A 526 vs. ctlr $p = 0.06$, ordinary one-way ANOVA).

outliers by the ROUT (Q = 1%) method, and available normality tests were performed for the obtained data. In case of hPSC-CM measurements, Brown–Forsythe ANOVA with Games–Howell multiple comparisons test was used to assess the statistical significance of the differences on normally distributed group pairs. In the case of arrhythmia analysis, R-R for each contractive event was extracted *via* processing scripts as mentioned before. R-R values over 1 or 3 s (cut-off) in HL-1 and hPSC-CMs, respectively, were quantified in all treatment groups and compared to controls. Choice of the cut-off value for hPSC-CMs was based on clinical experience with arrhythmia in human patients. The cut-off value for HL-1 was reduced with respect to the fact that HL-1 is a murine cell line with a higher overall beat rate. The resulting contingency tables were statistically evaluated by using the chi-square test with Yates's correction. The use of the individual statistical test is specified in appropriate figure legends and in Supplementary Data. Additionally, datasets containing complete raw data from all measurements are available at the online open-access repository (Klimovic et al., 2021).

RESULTS

Positive Chronotropic and Inotropic Effects of Aminophylline on hPSC-CMs

In the case of hPSC-CMs, two groups of treatment concentrations were determined according to the literature (Aslaksen et al., 1981; Goldberg et al., 1986; Rowe et al., 1988; Higgins et al., 1995; Shannon, 1999). The "therapeutic concentration/overdose" group consisted of 10 µM, 100 µM, and 1 mM of aminophylline treatments, while the 10-mM aminophylline treatment was considered "severe overdose" concentration. Consistent presence of troponin-positive cardiomyocytes in whole and dissociated embryoid bodies (EBs) was confirmed by immunostaining (representative example shown in **Figure 2**).

The positive chronotropic effect of aminophylline on hPSC-CMs was seen only in the 10 mM concentration of aminophylline (**Figures 3A,B**; $p < 0.05$; the remaining p-values are given in **Supplementary Table S1** and **Supplementary Table S2**). The positive inotropic effect was evident by a significantly increased contraction force of EBs in lower concentrations of aminophylline that was in contrast to its chronotropic effect (**Figure 3D**; $p < 0.0001$; the remaining p-values are given in **Supplementary Table S3**). Statistical analysis showed that this effect was significant in 10 µM concentration, with a similar trend in the concentrations of 100 µM and 1 mM (**Figure 3C**; $p < 0.01$; the remaining p-values are given in **Supplementary Table S4**). Linear regression analysis showed that the beat rate increase correlates with the concentration of aminophylline (**Supplementary Figure S2A,B**, $p < 0.0001$). On the contrary, this relationship was not proven in case of contraction force (**Supplementary Figure S2A,B**). To further strengthen the presented results, the washout experiment was performed on hPSC-CMs. The results showed that the BR of EBs increases significantly after administration of aminophylline; however, it decreased again during the washout period, suggesting that the chronotropic and inotropic effects is likely due to the effect of aminophylline and not due to irreversible cellular damage (**Supplementary Figure S3**).

In order to further explain molecular mechanisms, hPSC-CM cells were treated with 1 µM adenosine, followed by a combination of 1 µM adenosine and 1 mM aminophylline, a well-known non-selective adenosine receptor antagonist. The results showed an insignificant trend toward the adenosine-antagonizing aminophylline effect (**Supplementary Figure S3B**).

Positive Chronotropic Effect of Aminophylline on HL-1

To test whether chronotropic effects of aminophylline are model-independent, field potential measurements of the HL-1 cardiac cell line treated with aminophylline were conducted. The concentrations of aminophylline in a range of 8 up to 512 µM were used. Higher concentrations turned out to be toxic for the cells, which can be explained by higher treatment efficacy on the cellular monolayer of HL-1, as opposed to the cellular cluster of hPSC-CMs. Non-toxicity of selected concentrations was experimentally tested by trypan blue staining (**Supplementary Figure S3C**).

The results of these experiments showed a similar positive chronotropic effect with increasing concentration of aminophylline. Compared to controls, the BR was significantly increased only in the cells treated with 256 µM aminophylline; however, we observed a similar non-significant trend also in the case of the 512-µM treatment (**Figure 4**; 256 µM aminophylline vs. the control $p < 0.05$; 512 µM aminophylline vs. the control $p < 0.06$; the remaining p-values are given in **Supplementary Table S5**).

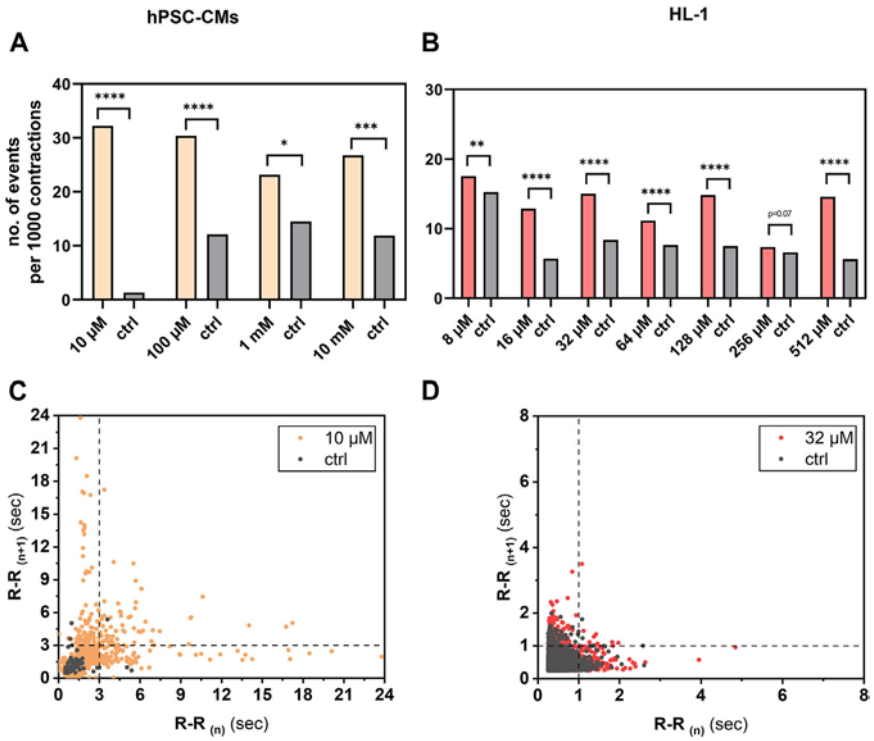

FIGURE 5 | Analysis of arrhythmogenic effect of aminophylline on hPSC-CMs and HL-1 cells. R-R values over 3 s in case of hPSC-CM measurements or 1 s in case of HL-1 of aminophylline and control measurements were subtracted, and the resulting contingency tables were statistically analyzed. Column graphs show sums of cutoff R-R values (arrhythmic events) per 1,000 contractions in each treatment group and controls of **(A)** hPSC-CMs and **(B)** HL-1 experiments (chi-square test with Yates' correction). Results show significant or partially significant higher frequency of aminophylline group cutoff values compared to that of the control. Poincaré plots of R-R values of representative concentration for **(C)** hPSC-CMs and **(D)** HL-1 experiments with visible cutoff lines.

Exposure to Aminophylline Causes Spontaneous Ca^{2+} Releases Leading to Arrhythmia

Among the adverse effects of aminophylline apparent in clinical practice, arrhythmias are most frequent. To test whether this effect is also present in our *in vitro* hPSC-CM model and HL-1 cardiomyocytes, we assessed the number of R-R intervals (inter-beat interval length) over 3 s or 1 s, respectively. Our results showed that the frequency of cutoff R-R values in measurements with aminophylline was significantly higher than that in controls in both models (**Figure 5**; *p*-values in **Supplementary Table S6** and **Supplementary Table S7**).

To further investigate this effect, intracellular cytosolic Ca^{2+} events were measured on HL-1 cells in the presence of 256 and 512 µM aminophylline. A significantly higher number of Ca^{2+} sparks was detected in the presence of 512 µM aminophylline than the control (**Figure 6,** 512 µM aminophylline vs. the control $p < 0.0001$). A similar effect was not detected in the presence of 256 µM aminophylline. Higher concentrations of aminophylline cause arrhythmic events presented by calcium leakage events (sparks). This is in good agreement with the measurement of electrical activity of cells (**Figure 5B**), where the concentration of 256 µM did not cause a significantly higher occurrence of arrhythmia; however, the concentration of 512 µM leads to rhythm irregularities. Last, the time to peak and decay time of main calcium waves were analyzed. While aminophylline caused no change in time to peak, the decay time significantly decreased, corresponding to an increased BR (**Figures 6B,C**).

DISCUSSION

This is the first study demonstrating the proarrhythmic action of aminophylline on human cardiomyocytes *in vitro*. To monitor aminophylline's effect at a wide range of concentrations, AFM was used on cell clusters [embryoid bodies (EBs)] formed by aggregation of human pluripotent stem cell–derived cardiomyocytes. Furthermore, the effect of aminophylline was investigated *via* a multielectrode array and by means of intracellular cytosolic Ca^{2+} measurement on HL-1 cells. Despite the differences between the models such as monolayer growth, cellular populations, or the fact that it is a murine cell type, HL-1 cells are considered a standard drug screening platform; therefore, we chose them to confirm our findings.

A missing link between the previous experimental data and aminophylline-induced arrhythmias observed in clinical practice was identified. Our most important finding was that aminophylline had two principal actions of arrhythmogenicity, the first being concentration-dependent ("deterministic") and the

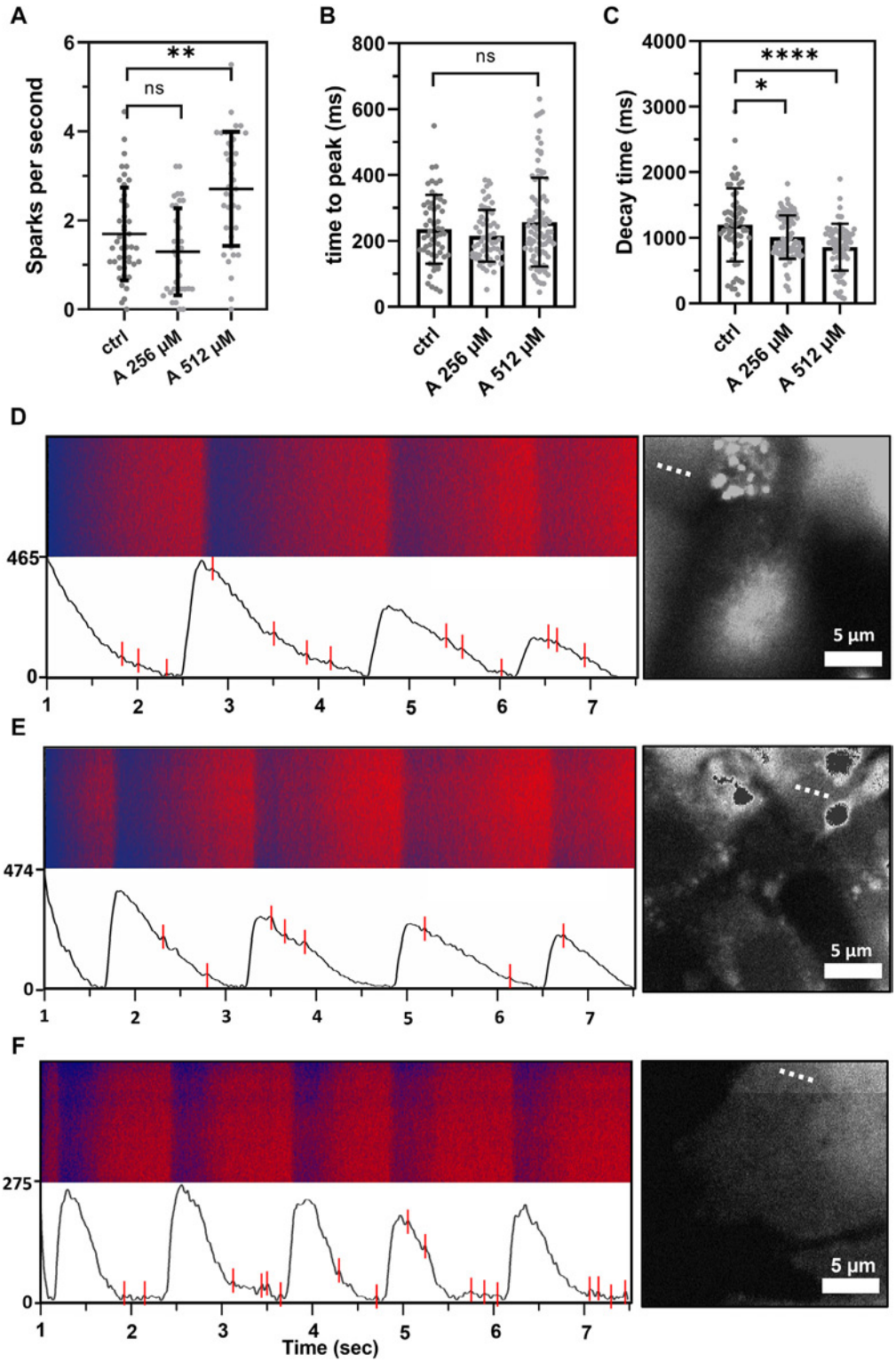

FIGURE 6 | Calcium sparks measured as extra events in the fluorescence in-time signal, showing leakage of calcium from the sarcoplasmic reticulum. **(A)** Scatterplot (mean ± standard deviation) showing calcium leakage events in a one-second period in control cells compared to the treatment by 256 and 512 µM aminophylline (A; $n = 43$ for ctlr, $n = 33$ for 256 µM and $n = 37$ for 512 µM). The frequency of calcium leakage events of cells treated with 512 µM aminophylline was significantly higher than that of the control (A 512 vs. ctlr $p < 0.01$, ordinary one-way ANOVA). **(B,C)** Scatterplots (mean ± standard deviation) showing times to peak and decay times of the control compared to the treatments. Aminophylline caused no significant change to time to peak compared to the control; however, decay time

(*Continued*)

FIGURE 6 | significantly decreased in a linear trend (n = 65 for ctrl, n = 89 for A 256 μM, n = 77 for A 512 μM; ctlr vs. A 256 μM $p < 0.05$, ctlr vs. A 512 μM $p < 00.001$; Kruskal–Wallis test). **(D–F)** Fluorescence line profiles were measured in time, typical recordings together with fluorescence–time curves were filtered for the presence of noise, and calcium sparks were found—labeled as red lines (B = control, C = 256 μM, D = 512 μM). Each recording is accompanied with a fluorescence image showing the exact location of line scan on the cell (dashed line).

second one concentration-independent ("stochastic"). First, we observed a linear concentration-dependent positive chronotropic effect with increasing aminophylline concentrations in hPSC-CMs (**Figures 3A,B** and **Supplementary Figure S2A,B**). Moreover, this effect was also confirmed to an extent on the HL-1 cellular line (**Figure 4**). This may be related to previous clinical findings that demonstrated that theophylline's higher plasmatic levels were associated with an increased heart rate (sinus tachycardia); the relationship was linear and concentration-dependent (Vestal et al., 1983; Nadkarni et al., 1988). This effect is sometimes used to treat severe, atropine-resistant bradycardia (Pasnoori and Leesar, 2004) or other indications (Conte et al., 2017). The inotropic effect was non-linear in our study. An increased inotropic effect was present only in lower aminophylline concentrations. This response may be attributed to reaching peak-shortening amplitude, as a physical parameter of cells and cluster, respectively, and partial immaturity may be responsible for lower number of present sarcomeres and, thus, lower shortening capability of the cells (Fraticelli et al., 1989).

In parallel to the "deterministic" effect, we observed a second arrhythmogenic action of aminophylline expressed as a concentration-independent occurrence of RR interval abnormities. This action was stochastic, independent of the applied aminophylline concentration. It consisted of repeated tachycardia-like periods followed by bradycardia-like periods (not illustrated), which is reflected by the extreme R-R intervals in **Figure 5** that occurred significantly more often in the cells exposed to aminophylline. Even though certain beat rate variability was present in spontaneously beating hPSC-derived CMs in previous studies (Mandel et al., 2012; Binah et al., 2013; Niehoff et al., 2019), similar events have never been previously described to our best knowledge. We speculate that this effect may be an experimental equivalent to the sick sinus syndrome (Tse et al., 2017) or to tachy–brady alternating episodes in patients with AF, an arrhythmia that was previously observed both in aminophylline overdose cases and at therapeutic levels of the drug (Laaban et al., 1988; Bittar and Friedman, 1991; Varriale and Ramaprasad, 1993).

Attempts to reveal mechanisms of the arrhythmogenic action of aminophylline/theophylline have been performed previously, using various animal models. In rats, aminophylline induced tachycardia and elevated blood pressure and potential cardiac ischemia (Shamsuzzaman et al., 2016), which may be related to theophylline-induced myocardial fibrosis found as a long-term concentration-/dose-dependent side effect in a notable portion of rats (Onodera et al., 2001). In a canine model, aminophylline significantly enhanced AV nodal and His–Purkinje conduction; this effect was potentiated in combined therapy with metaproterenol (Komadina et al., 1992).

Studies published so far have not provided a clear clue to the genesis of proarrhythmic effects of aminophylline/theophylline, namely, AF. Aminophylline effects (likely an equivalent of the sinus tachycardia in patients) may be explained by the effect of elevated cAMP and the absence of the inhibitory effect of adenosine (Belardinelli et al., 1995) on cardiac ionic currents (see insignificant trend in **Supplementary Figure S3B**).

As studied in detail by Kong et al. (2008), caffeine (another type of methylxanthine), aminophylline, and theophylline preferentially potentiated luminal Ca^{2+} activation of the ryanodine type 2 (RyR2) receptor, reduced the threshold for spontaneous Ca^{2+} release, and increased the basal activity, inducing repeated quantal Ca^{2+} releases. As is well-known, the accumulation of Ca^{2+} in the cytoplasm may result in delayed afterdepolarizations, which can trigger arrhythmia. Considering the increased occurrence of Ca^{2+} sparks in HL-1 cardiomyocytes treated with 512 μM aminophylline (**Figure 6**), the concentration-independent "stochastic" effect of aminophylline observed in our study may be a consequence of microdomain cAMP level–related diastolic release of Ca^{2+} *via* independent clusters of RyR2 receptors (Berisha et al., 2021). Such transient Ca^{2+} accumulation may induce an increased BR and, following Ca^{2+} depletion, results in a pause in the investigated cardiac cell's beating clusters. Such chain of events might also be amplified by the local cAMP level–induced alteration of the current amplitude *via* modulation of hERG potassium channel phosphorylation (Cui et al., 2000). Detailed subcellular mechanisms of this effect should be studied in the future.

To our best knowledge, this is the first study reporting results of experiments with aminophylline conducted on human cardiomyocytes derived from hPSCs. As such, this set of experiments showed that our comprehensive monitoring system is a unique and valuable tool for cardiotoxicity vs. safety testing of various molecules or drugs. Our results may present the missing link between the described subcellular mechanisms of methylxanthine arrhythmogenesis and the clinical variability of arrhythmic events related to the theophylline treatment in clinical practice.

CONCLUSION/SUMMARY

We conclude that aminophylline had two parallel arrhythmogenic mechanisms of action on EBs: a concentration-dependent ("deterministic") effect, presenting with an increased beat rate (potential clinical correlate: sinus tachycardia), and a concentration-independent ("stochastic") effect, which was characterized by tachycardia-like episodes alternating with long pauses (potential clinical correlate: atrial fibrillation). Our comprehensive monitoring system is a unique

and valuable tool for cardiotoxicity vs. safety testing of various molecules or drugs.

STUDY LIMITATIONS

The study presents the effect of aminophylline on contractile properties of human hPSC-CMs along with results of field potential measurements on the HL-1 cardiac cell line that further confirmed the effects. First, it has to be considered that hPSC-derived CMs represented immature/neonatal phenotype possibly affecting drug effect kinetics [e.g., altered IK1 levels which may affect resting potential, repolarization, and depolarization dynamics (Sartiani et al., 2007)]. Second, if different hPSC lines are used to generate embryoid bodies, it is likely that there will be different degrees of maturity and the effect of aminophylline might also differ. The last limitation is that field potential measurements can generate information about the BR but not about contraction force; therefore, the results with HL-1 cells confirmed only the chronotropic effect of aminophylline.

DATA AVAILABILITY STATEMENT

The original contributions presented in the study are included in the article/**Supplementary Material**; further inquiries can be directed to the corresponding author.

AUTHOR CONTRIBUTIONS

All the authors have contributed to manuscript writing and corrections and were included substantially in the project preparation, conceptualization, and evaluation. MP, VR, and KB prepared the experimental design. DB, TU, and SJ have differentiated the cardiomyocytes; DB and DK maintained the HL-1 cell line; and SJ performed the immunostaining. SK and MS analyzed the data, interpreted them, prepared the figures, and wrote the manuscript draft. SK and JP performed the AFM measurements and evaluated AFM data; ZS and VR supervised the project, interpreted the obtained results, and corrected the manuscript; MB drafted additional explanations to experimental findings and commented on the manuscript; KB was responsible for the coordination and supervision; and SK, MS, and MP contributed equally to the study. DK performed the MEA measurments and analyzed the MEA data.

FUNDING

This study was funded by the Ministry of Health of the Czech Republic (Research Grant No. NU20-06-00156).

ACKNOWLEDGMENTS

We acknowledge further support by the European Regional Development Fund-Project ENOCH (No. CZ.02.1.01/0.0/0.0/16_019/0000868) and the Specific University Research Grants of the Masaryk University MUNI/A/1246/2020, MUNI/A/1700/2020, and MUNI/A/1133/2021 provided by the Ministry of Education, Youth and Sports of the Czech Republic. We also acknowledge the support by the Internal grant agency of Masaryk University - Project MUNI/IGA/1428/2020. CIISB, Instruct-CZ Centre of the Instruct-ERIC EU consortium, funded by the MEYS CR infrastructure project LM2018127, is gratefully acknowledged for the financial support of the measurements at the CF Nanobiotechnology.

SUPPLEMENTARY MATERIAL

The Supplementary Material for this article can be found online at: https://www.frontiersin.org/articles/10.3389/fphar.2021.789730/full#supplementary-material

REFERENCES

Acimovic, I., Refaat, M. M., Moreau, A., Salykin, A., Reiken, S., Sleiman, Y., et al. (2018). Post-translational Modifications and Diastolic Calcium Leak Associated to the Novel RyR2-D3638a Mutation Lead to CPVT in Patient-specific hiPSC-Derived Cardiomyocytes. *J. Clin. Med.* 7, 423. doi:10.3390/jcm7110423

Aslaksen, A., Bakke, O. M., and Vigander, T. (1981). Comparative Pharmacokinetics of Theophylline and Aminophylline in Man. *Br. J. Clin. Pharmacol.* 11, 269–273. doi:10.1111/j.1365-2125.1981.tb00533.x

Bébarová, M., Matejovič, P., Švecová, O., Kula, R., Šimurdová, M., and Šimurda, J. (2017). Nicotine at Clinically Relevant Concentrations Affects Atrial Inward Rectifier Potassium Current Sensitive to Acetylcholine. *Naunyn-schmiedeberg's Arch. Pharmacol.* 390, 471–481. doi:10.1007/s00210-017-1341-z

Belardinelli, L., Shryock, J. C., Song, Y., Wang, D., and Srinivas, M. (1995). Ionic Basis of the Electrophysiological Actions of Adenosine on Cardiomyocytes. *FASEB J.* 9, 359–365. doi:10.1096/fasebj.9.5.7896004

Berisha, F., Götz, K. R., Wegener, J. W., Brandenburg, S., Subramanian, H., Molina, C. E., et al. (2021). cAMP Imaging at Ryanodine Receptors Reveals β2-Adrenoceptor Driven Arrhythmias. *Circ. Res.* 129, 81–94. doi:10.1161/CIRCRESAHA.120.318234

Binah, O., Weissman, A., Itskovitz-Eldor, J., and Rosen, M. R. (2013). Integrating Beat Rate Variability: from Single Cells to Hearts. *Heart Rhythm* 10, 928–932. doi:10.1016/j.hrthm.2013.02.013

Bittar, G., and Friedman, H. S. (1991). The Arrhythmogenicity of Theophylline. A Multivariate Analysis of Clinical Determinants. *Chest* 99, 1415–1420. doi:10.1378/chest.99.6.1415

Burridge, P. W., Keller, G., Gold, J. D., and Wu, J. C. (2012). Production of De Novo Cardiomyocytes: Human Pluripotent Stem Cell Differentiation and Direct Reprogramming. *Cell Stem Cell* 10, 16–28. doi:10.1016/j.stem.2011.12.013

Caluori, G., Pribyl, J., Cmiel, V., Pesl, M., Potocnak, T., Provaznik, I., et al. (2019a). Simultaneous Study of Mechanobiology and Calcium Dynamics on hESC-Derived Cardiomyocytes Clusters. *J. Mol. Recognit.* 32, e2760. doi:10.1002/jmr.2760

Caluori, G., Pribyl, J., Pesl, M., Jelinkova, S., Rotrekl, V., Skladal, P., et al. (2019b). Non-invasive Electromechanical Cell-Based Biosensors for Improved Investigation of 3D Cardiac Models. *Biosens. Bioelectron.* 124-125 (125), 129–135. doi:10.1016/j.bios.2018.10.021

Charytan, D., and Jansen, K. (2003). Severe Metabolic Complications from Theophylline Intoxication. *Nephrology (Carlton)* 8, 239–242. doi:10.1046/j.1440-1797.2003.00181.x

Conte, L., Pugliese, N. R., and Giannoni, A. (2017). Reversal of Ticagrelor-Induced Arrhythmias and Cheyne-Stokes Respiration with Aminophylline Infusion. *J. Cardiovasc. Pharmacol.* 70, 290–292. doi:10.1097/FJC.0000000000000518

Cui, J., Melman, Y., Palma, E., Fishman, G. I., and McDonald, T. V. (2000). Cyclic AMP Regulates the HERG K(+) Channel by Dual Pathways. *Curr. Biol.* 10, 671–674. doi:10.1016/s0960-9822(00)00516-9

Kabanov, D. (2021). DaniilKabanov/CardioScripts. Available at: https://github.com/DaniilKabanov/CardioScripts [Accessed September 14, 2021].

Dinarelli, S., Girasole, M., Spitalieri, P., Talarico, R. V., Murdocca, M., Botta, A., et al. (2018). AFM Nano-Mechanical Study of the Beating Profile of hiPSC-Derived Cardiomyocytes Beating Bodies WT and DM1. *J. Mol. Recognit* 31, e2725. doi:10.1002/jmr.2725

Dvorak, P., Dvorakova, D., Koskova, S., Vodinska, M., Najvirtova, M., Krekac, D., et al. (2005). Expression and Potential Role of Fibroblast Growth Factor 2 and its Receptors in Human Embryonic Stem Cells. *Stem Cells* 23, 1200–1211. doi:10.1634/stemcells.2004-0303

Ellis, E. F. (1985). Theophylline Toxicity. *J. Allergy Clin. Immunol.* 76, 297–301. doi:10.1016/0091-6749(85)90645-1

Fraticelli, A., Josephson, R., Danziger, R., Lakatta, E., and Spurgeon, H. (1989). Morphological and Contractile Characteristics of Rat Cardiac Myocytes from Maturation to Senescence. *Am. J. Physiol.* 257, H259–H265. doi:10.1152/ajpheart.1989.257.1.H259

Goldberg, M. J., Park, G. D., and Berlinger, W. G. (1986). Treatment of Theophylline Intoxication. *J. Allergy Clin. Immunol.* 78, 811–817. doi:10.1016/0091-6749(86)90066-7

Goudis, C. A. (2017). Chronic Obstructive Pulmonary Disease and Atrial Fibrillation: An Unknown Relationship. *J. Cardiol.* 69, 699–705. doi:10.1016/j.jjcc.2016.12.013

Higgins, R. M., Hearing, S., Goldsmith, D. J., Keevil, B., Venning, M. C., and Ackrill, P. (1995). Severe Theophylline Poisoning: Charcoal Haemoperfusion or Haemodialysis. *Postgrad. Med. J.* 71, 224–226. doi:10.1136/pgmj.71.834.224

Hoppe, L. K., Muhlack, D. C., Koenig, W., Carr, P. R., Brenner, H., and Schöttker, B. (2018). Association of Abnormal Serum Potassium Levels with Arrhythmias and Cardiovascular Mortality: a Systematic Review and Meta-Analysis of Observational Studies. *Cardiovasc. Drugs Ther.* 32, 197–212. doi:10.1007/s10557-018-6783-0

Horita, N., Miyazawa, N., Kojima, R., Inoue, M., Ishigatsubo, Y., and Kaneko, T. (2016). Chronic Use of Theophylline and Mortality in Chronic Obstructive Pulmonary Disease: A Meta-Analysis. *Arch. Bronconeumol* 52, 233–238. doi:10.1016/j.arbres.2015.02.021

Huerta, C., Lanes, S. F., and García Rodríguez, L. A. (2005). Respiratory Medications and the Risk of Cardiac Arrhythmias. *Epidemiology* 16, 360–366. doi:10.1097/01.ede.0000158743.90664.a7

International Stem Cell InitiativeAdewumi, O., Adewumi, O., Aflatoonian, B., Ahrlund-Richter, L., Amit, M., Andrews, P. W., et al. (2007). Characterization of Human Embryonic Stem Cell Lines by the International Stem Cell Initiative. *Nat. Biotechnol.* 25, 803–816. doi:10.1038/nbt1318

Jelinkova, S., Fojtik, P., Kohutova, A., Vilotic, A., Marková, L., Pesl, M., et al. (2019). Dystrophin Deficiency Leads to Genomic Instability in Human Pluripotent Stem Cells via NO Synthase-Induced Oxidative Stress. *Cells* 8. doi:10.3390/cells8010053

Jelinkova, S., Vilotic, A., Pribyl, J., Aimond, F., Salykin, A., Acimovic, I., et al. (2020). DMD Pluripotent Stem Cell Derived Cardiac Cells Recapitulate *In Vitro* Human Cardiac Pathophysiology. *Front. Bioeng. Biotechnol.* 8, 535. doi:10.3389/fbioe.2020.00535

Klimovic, S., Scurek, M., Pesl, M., Beckerova, D., Jelinkova, S., Urban, T., et al. (2021). *Aminophylline Induces Two Types of Arrhythmic Events in Human Pluripotent Stem Cell-Derived Cardiomyocytes - Dataset*. doi:10.5281/zenodo.4552607

Komadina, K. H., Carlson, T. A., Strollo, P. J., and Navratil, D. L. (1992). Electrophysiologic Study of the Effects of Aminophylline and Metaproterenol on Canine Myocardium. *Chest* 101, 232–238. doi:10.1378/chest.101.1.232

Krutá, M., Šeneklová, M., Raška, J., Salykin, A., Zerzánková, L., Pešl, M., et al. (2014). Mutation Frequency Dynamics inHPRTLocus in Culture-Adapted Human Embryonic Stem Cells and Induced Pluripotent Stem Cells Correspond to Their Differentiated Counterparts. *Stem Cell Dev.* 23, 2443–2454. doi:10.1089/scd.2013.0611

Laaban, J. P., Iung, B., Chauvet, J. P., Psychoyos, I., Proteau, J., and Rochemaure, J. (1988). Cardiac Arrhythmias during the Combined Use of Intravenous Aminophylline and Terbutaline in Status Asthmaticus. *Chest* 94, 496–502. doi:10.1378/chest.94.3.496

Lee, T. A., Schumock, G. T., Bartle, B., and Pickard, A. S. (2009). Mortality Risk in Patients Receiving Drug Regimens with Theophylline for Chronic Obstructive Pulmonary Disease. *Pharmacotherapy* 29, 1039–1053. doi:10.1592/phco.29.9.1039

Liu, J., Sun, N., Bruce, M. A., Wu, J. C., and Butte, M. J. (2012). Atomic Force Mechanobiology of Pluripotent Stem Cell-Derived Cardiomyocytes. *PLoS ONE* 7, e37559. doi:10.1371/journal.pone.0037559

Mandel, Y., Weissman, A., Schick, R., Barad, L., Novak, A., Meiry, G., et al. (2012). Human Embryonic and Induced Pluripotent Stem Cell-Derived Cardiomyocytes Exhibit Beat Rate Variability and Power-Law Behavior. *Circulation* 125, 883–893. doi:10.1161/CIRCULATIONAHA.111.045146

Nadkarni, S., Hay, A. W., Faye, S., and Congdon, P. J. (1988). The Relationship between Theophylline, Caffeine and Heart Rate in Neonates. *Ann. Clin. Biochem.* 25 (Pt 4) (Pt 4), 408–410. doi:10.1177/000456328802500415

Nair, P., Milan, S. J., and Rowe, B. H. (2012). Addition of Intravenous Aminophylline to Inhaled Beta(2)-Agonists in Adults with Acute Asthma. *Cochrane Database Syst. Rev.* 12, CD002742. doi:10.1002/14651858.CD002742.pub2

Niehoff, J., Matzkies, M., Nguemo, F., Hescheler, J., and Reppel, M. (2019). The Effect of Antiarrhythmic Drugs on the Beat Rate Variability of Human Embryonic and Human Induced Pluripotent Stem Cell Derived Cardiomyocytes. *Sci. Rep.* 9, 14106. doi:10.1038/s41598-019-50557-7

Odstrcilik, J., Cmiel, V., Kolar, R., Ronzhina, M., Baiazitova, L., Pesl, M., et al. (2015). "Computer Analysis of Isolated Cardiomyocyte Contraction Process via Advanced Image Processing Techniques," in 2015 Computing in Cardiology Conference (CinC) (Nice, France: IEEE), 453–456. doi:10.1109/CIC.2015.7408684

Onodera, K., Shibata, M., Kojima, J., Wachi, M., Sogawa, N., Furuta, H., et al. (2001). Toxicity of Theophylline Depends on Plasma Concentration by Single and Also Repeated Dosing in Rats. *Pharmacol. Res.* 44, 81–87. doi:10.1006/phrs.2001.0831

Pasnoori, V. R., and Leesar, M. A. (2004). Use of Aminophylline in the Treatment of Severe Symptomatic Bradycardia Resistant to Atropine. *Cardiol. Rev.* 12, 65–68. doi:10.1097/01.crd.0000096418.72821.fa

Pesl, M., Acimovic, I., Pribyl, J., Hezova, R., Vilotic, A., Fauconnier, J., et al. (2014). Forced Aggregation and Defined Factors Allow Highly Uniform-Sized Embryoid Bodies and Functional Cardiomyocytes from Human Embryonic and Induced Pluripotent Stem Cells. *Heart Vessels* 29, 834–846. doi:10.1007/s00380-013-0436-9

Pribyl, J., Pešl, M., Caluori, G., Acimovic, I., Jelinkova, S., Dvorak, P., et al. (20191886). Biomechanical Characterization of Human Pluripotent Stem Cell-Derived Cardiomyocytes by Use of Atomic Force Microscopy. *Methods Mol. Biol.* 1886, 343–353. doi:10.1007/978-1-4939-8894-5_20

Rowe, D. J., Watson, I. D., Williams, J., and Berry, D. J. (1988). The Clinical Use and Measurement of Theophylline. *Ann. Clin. Biochem.* 25 (Pt 1), 4–26. doi:10.1177/000456328802500102

Sartiani, L., Bettiol, E., Stillitano, F., Mugelli, A., Cerbai, E., and Jaconi, M. E. (2007). Developmental Changes in Cardiomyocytes Differentiated from Human Embryonic Stem Cells: a Molecular and Electrophysiological Approach. *Stem Cells* 25, 1136–1144. doi:10.1634/stemcells.2006-0466

Shamsuzzaman, M., Kavita, G., and Arunabha, R. (2016). Methylxanthine Induced Cardiotoxicity and its Mechanisms: An Experimental Study. *MJMS* 1, 10.

Shannon, M. (1999). Life-threatening Events after Theophylline Overdose: a 10-year Prospective Analysis. *Arch. Intern. Med.* 159, 989–994. doi:10.1001/archinte.159.9.989

Singh, D., Agusti, A., Anzueto, A., Barnes, P. J., Bourbeau, J., Celli, B. R., et al. (2019). Global Strategy for the Diagnosis, Management, and Prevention of Chronic Obstructive Lung Disease: the GOLD Science Committee Report 2019. *Eur. Respir. J.* 53. doi:10.1183/13993003.00164-2019

Souidi, M., Sleiman, Y., Acimovic, I., Pribyl, J., Charrabi, A., Baecker, V., et al. (2021). Oxygen Is an Ambivalent Factor for the Differentiation of Human Pluripotent Stem Cells in Cardiac 2D Monolayer and 3D Cardiac Spheroids. *Ijms* 22, 662. doi:10.3390/ijms22020662

Suissa, S., Hemmelgarn, B., Blais, L., and Ernst, P. (1996). Bronchodilators and Acute Cardiac Death. *Am. J. Respir. Crit. Care Med.* 154, 1598–1602. doi:10.1164/ajrccm.154.6.8970341

Tse, G., Liu, T., Li, K. H., Laxton, V., Wong, A. O., Chan, Y. W., et al. (2017). Tachycardia-bradycardia Syndrome: Electrophysiological Mechanisms and Future Therapeutic Approaches (Review). *Int. J. Mol. Med.* 39, 519–526. doi:10.3892/ijmm.2017.2877

Ukena, D., Schudt, C., and Sybrecht, G. W. (1993). Adenosine Receptor-Blocking Xanthines as Inhibitors of Phosphodiesterase Isozymes. *Biochem. Pharmacol.* 45, 847–851. doi:10.1016/0006-2952(93)90168-v

Varriale, P., and Ramaprasad, S. (1993). Aminophylline Induced Atrial Fibrillation. *Pacing Clin. Electrophysiol.* 16, 1953–1955. doi:10.1111/j.1540-8159.1993.tb00987.x

Vestal, R. E., Eiriksson, C. E., Musser, B., Ozaki, L. K., and Halter, J. B. (1983). Effect of Intravenous Aminophylline on Plasma Levels of Catecholamines and Related Cardiovascular and Metabolic Responses in Man. *Circulation* 67, 162–171. doi:10.1161/01.cir.67.1.162

Ye, C., Miao, C., Yu, L., Dong, Z., Zhang, J., Mao, Y., et al. (2019). Factors Affecting the Efficacy and Safety of Aminophylline in Treatment of Apnea of Prematurity in Neonatal Intensive Care Unit. *Pediatr. Neonatol* 60, 43–49. doi:10.1016/j.pedneo.2018.03.008

Zatloukal, J., Brat, K., Neumannova, K., Volakova, E., Hejduk, K., Kocova, E., et al. (2020). Chronic Obstructive Pulmonary Disease - Diagnosis and Management of Stable Disease; a Personalized Approach to Care, Using the Treatable Traits Concept Based on Clinical Phenotypes. Position Paper of the Czech Pneumological and Phthisiological Society. *Biomed. Pap. Med. Fac. Univ. Palacky Olomouc Czech Repub* 164, 325–356. doi:10.5507/bp.2020.056

Conflict of Interest: The authors declare that the research was conducted in the absence of any commercial or financial relationships that could be construed as a potential conflict of interest.

Publisher's Note: All claims expressed in this article are solely those of the authors and do not necessarily represent those of their affiliated organizations, or those of the publisher, the editors, and the reviewers. Any product that may be evaluated in this article, or claim that may be made by its manufacturer, is not guaranteed or endorsed by the publisher.

J. Rubáčková Popelová et al.

Long-Term Survival of Adult Patients With Atrial Septal Defect With Regards to Defect Closure and Pulmonary Hypertension

Front. Cardiovasc. Med.
Impact Factor: 5.846

frontiers | Frontiers in Cardiovascular Medicine

BRIEF RESEARCH REPORT
published: 28 April 2022
doi: 10.3389/fcvm.2022.867012

Long-Term Survival of Adult Patients With Atrial Septal Defect With Regards to Defect Closure and Pulmonary Hypertension

Jana Rubáčková Popelová[1,2†], Markéta Tomková[1,3†], Jakub Tomek[1,4] and Renata Živná[1]*

[1] Department of Cardiac Surgery, Na Homolce Hospital, Prague, Czechia, [2] Faculty Hospital Motol, Pediatric Heart Centre, Prague, Czechia, [3] Department of Biochemistry and Molecular Medicine, School of Medicine, University of California, Davis, Davis, CA, United States, [4] Department of Pharmacology, School of Medicine, University of California, Davis, Davis, CA, United States

OPEN ACCESS

Edited by:
Gerhard-Paul Diller, University Hospital Münster, Germany

Reviewed by:
Steve Bibevski, Joe DiMaggio Children's Hospital, United States
Giuseppe Mascia, San Martino Hospital (IRCCS), Italy

***Correspondence:**
Jana Rubáčková Popelová
jana.popelova@homolka.cz

†These authors share first authorship

Specialty section:
This article was submitted to General Cardiovascular Medicine, a section of the journal Frontiers in Cardiovascular Medicine

Received: *31 January 2022*
Accepted: *06 April 2022*
Published: *28 April 2022*

Citation:
Rubáčková Popelová J, Tomková M, Tomek J and Živná R (2022) Long-Term Survival of Adult Patients With Atrial Septal Defect With Regards to Defect Closure and Pulmonary Hypertension. Front. Cardiovasc. Med. 9:867012. doi: 10.3389/fcvm.2022.867012

Background: Atrial septal defect (ASD) is the most common congenital heart disease (CHD) in adults and pulmonary hypertension (PH) is an established risk factor. A decision whether to perform ASD closure, especially in elderly patients with PH, is a complex dilemma. The aim of our study was to compare long-term survival in patients with closed and open ASD.

Methods: A retrospective cohort study was performed on 427 patients with ASD (median age at diagnosis 38 years, IQR 18–56) out of which 186 patients (44%) manifested PH. ASD closure in patients with PH was only considered in patients without Eisenmenger syndrome with pulmonary vascular resistance < 5 WU. Median follow-up duration was 18 years (IQR 9–31 years). Kaplan-Meier and Cox proportional hazards survival analyses were performed to evaluate 12 potential predictors of survival.

Results: Defect closure was associated with improved long-term survival in ASD patients both with ($P < 0.001$) and without PH ($P = 0.01$) and this association was present also in patients over 40 years. The 20-year survival since diagnosis was significantly higher in patients with PH and closed ASD compared to those with PH and open ASD (65% vs. 41%). ASD closure was a significant independent predictor of long-term survival ($P = 0.003$) after accounting for age at diagnosis, PH, NYHA class, Eisenmenger syndrome, and mitral regurgitation. Significant negative independent predictors of survival were older age at diagnosis ($P < 0.001$), Eisenmenger syndrome ($P < 0.001$), and PH ($P = 0.03$).

Conclusion: ASD closure appears to be associated with improved long-term survival independently of age, PH, and other clinical variables.

Keywords: atrial septal defect, long-term survival, pulmonary hypertension, defect closure, congenital heart disease

INTRODUCTION

Atrial septal defect (ASD) is the most common congenital heart disease (CHD) in adults and is often diagnosed late in adulthood. Identification of patients who would benefit from a closure of atrial septal defect (ASD) in adulthood remains a crucial, but complicated question (1). One particularly important group with unclear closure benefit comprises patients with pulmonary hypertension (PH). ASD closure appears safe in young patients without PH or even with PH meeting the criteria for defect closure (2–6). However, the presence of PH in older patients is associated with increased mortality following ASD closure compared to patients without PH (3, 4). It is not known whether the poor prognosis of the PH patients results from the ASD closure itself, or if their outcome would have been similar or even worse if the ASD closure was not carried out. As highlighted in the latest ESC guidelines, the impact of shunt closure on long-term outcome of patients with PH remains an area of uncertainty and requires further research (6).

We therefore sought to compare long-term survival of adults with and without ASD closure, with respect to PH, age, and other clinical variables.

METHODS

Patients

Following institutional ethics committee approval, we performed a retrospective observational cohort analysis of isolated ASD patients in our database. The consecutive patient data were collected between 1995 and 2020. Mortality data were obtained from the national mortality register. The inclusion criteria were: adults with ASD type secundum, sinus venosus or coronary sinus defect diagnosed in adulthood or childhood, with accessible information concerning presence of PH and defect closure. The exclusion criteria were: ASD type primum, patent foramen ovale, missing data on ASD closure or on PH, or presence of another hemodynamically important congenital heart disease.

Clinical Variables

For the purpose of this analysis, pulmonary hypertension (PH) was defined as mean pulmonary arterial pressure $\geq$ 25 mmHg, as determined by catheterization (if available) or echocardiography (7, 8). Patients suspected to have moderate or severe PH based on echocardiography have undergone right heart catheterization (RHC) with pulmonary vascular resistance (PVR) assessment. ASD size was measured by transesophageal echocardiography in 74% patients. The contraindications for ASD closure were: (a) Eisenmenger syndrome or non-indexed PVR > 5 Wood Units (WU) not responding to vasodilatation testing with epoprostenol or advanced therapy treatment (5, 6), (b) an increase in left atrial mean pressure during temporary balloon occlusion > 10 mmHg compared to baseline (9). In some patients, ASD was not closed in accordance with their wish.

Statistical Analysis

Comparisons between cohorts (with and without PH) were performed with the Fisher's exact test for binary variables and Mann-Whitney *U*-test for continuous variables, with Benjamini-Hochberg correction for multiple testing (false-discovery rate 0.05) applied on the reported *P*-values. Kaplan-Meier estimates and Cox proportional hazards model were used to analyze survival. All covariates were assessed that they fulfill the proportional hazards assumption, using the MATLAB fitcox function, which is based on the scaled Schoenfeld residuals, as derived by Grambsch and Therneau (10). The following variables were included in the univariable model: ASD closure, age at diagnosis, sex, New York Heart Association (NYHA) functional class, PH, moderate or severe mitral regurgitation (MR), Eisenmenger syndrome, ASD types (ASD secundum, sinus venosus, coronary sinus defect), ASD size, and advanced pulmonary vasodilator therapy. NYHA was used as a binary variable (NYHA > 2) to fulfill the proportional hazards assumption. The variables significant in univariable Cox proportional hazards model were then included in a multivariable model. Both the Kaplan-Meier and the multivariable Cox proportional hazards analyses were performed first in all patients (model A) and second in patients without Eisenmenger syndrome (model B). Values of $P < 0.05$ were considered statistically significant ($^{***}P < 0.001$; $^{**}P < 0.01$; $^{*}P < 0.05$). Statistical tests were two-sided. Data were analyzed using MATLAB (R2021b).

RESULTS

Patient Characteristics

Data analysis was performed in 427 patients from our database meeting the inclusion criteria. Median age at diagnosis of the whole group was 38 (IQR 18–56) years and 74% of patients were female (**Table 1**). The age at diagnosis was higher in patients with PH compared to patients without PH: 50 (IQR 30–60) vs. 29 (IQR 13–46) years for closed defects ($P < 0.001$) and 53 (IQR 29–70) vs. 39 (IQR 28–57) for open defects ($P = 0.3$), (**Table 1**). Median follow-up was 18 years (IQR 9–31). Sinus venosus defect was present in 77 patients (18%) and coronary sinus defect in 8 patients (2%). Catheterization was performed in 60% of patients with PH and in 22% of patients without PH, altogether in 166 patients. ASD closure was performed in 367 patients (86%); out of which 58% by sternotomy, 14% video-assisted mini-thoracotomy, 10% robotic cardiac surgery, and 17% transcatheter.

Pulmonary Hypertension

PH was present in 186 patients (44%), out of which 150 have undergone ASD closure (81%) and 36 have not (19%), (**Table 1**). The group of 36 patients with PH and open ASD comprised 12 patients who refused a recommended ASD closure (7 of them died), 7 patients with Eisenmenger syndrome (5 of them died), 4 patients with high PVR without Eisenmenger syndrome (3 died), 2 patients with small defects and PH (1 died), and 11 patients with various reasons for leaving ASD open (lung

TABLE 1 | Patient characteristics.

Feature	No PH closed (*n* = 223)	PH closed (*n* = 144)	*P*-value closed no PH vs. PH	No PH open (*n* = 25)	PH open (*n* = 35)	*P*-value open no PH vs. PH	All (*n* = 427)
Age at diag. (years)	29 [13–46] (*n* = 217)	50 [30–60] (*n* = 150)	1×10^{-8} (***)	39 [28–57] (*n* = 24)	53 [29–70] (*n* = 36)	0.3	38 [18–56] (*n* = 427)
NYHA > 2	11.5% (25/217)	54.7% (82/150)	3×10^{-18} (***)	16.7% (4/24)	61.1% (22/36)	0.007 (**)	31.1% (133/427)
MR	12.0% (26/217)	28.9% (43/149)	1×10^{-4} (***)	12.5% (3/24)	31.4% (11/35)	0.2	19.5% (83/425)
Eisenmenger	*NA*	0.0% (0/150)	1	*NA*	19.4% (7/36)	0.1	1.6% (7/427)
ASD secundum	82.9% (180/217)	80.7% (121/150)	0.7	95.8% (23/24)	80.6% (29/36)	0.2	82.7% (353/427)
Sinus venosus	17.5% (38/217)	19.3% (29/150)	0.8	4.2% (1/24)	25.0% (9/36)	0.1	18.0% (77/427)
Coronary sinus	0.5% (1/217)	2.7% (4/150)	0.2	0.0% (0/24)	8.3% (3/36)	0.4	1.9% (8/427)
ASD size	16 [11–20] (*n* = 147)	20 [14–25] (*n* = 126)	0.001 (**)	6 [4–12] (*n* = 16)	19 [12–28] (*n* = 25)	9×10^{-4} (***)	18 [12–23] (*n* = 314)
Advanced therapy	0.0% (0/217)	4.7% (7/150)	0.003 (**)	0.0% (0/24)	8.3% (3/36)	0.4	2.3% (10/427)
Sex (male)	28.1% (61/217)	22.0% (33/150)	0.3	20.8% (5/24)	30.6% (11/36)	0.7	25.8% (110/427)
10-year survival	98.2% (166/169)	86.5% (109/126)	2×10^{-4} (***)	90.5% (19/21)	63.6% (21/33)	0.1	90.3% (315/349)
20-year survival	94.8% (110/116)	65.1% (56/86)	2×10^{-7} (***)	69.2% (9/13)	40.6% (13/32)	0.2	76.1% (188/247)
40-year survival	80.5% (33/41)	44.3% (27/61)	5×10^{-4} (***)	0.0% (0/5)	23.3% (7/30)	0.4	48.9% (67/137)
TVP	7.8% (17/217)	40.7% (61/150)	5×10^{-13} (***)	*NA*	*NA*	*NA*	*NA*
MVP + MVR	6.5% (14/217)	20.7% (31/150)	2×10^{-4} (***)	*NA*	*NA*	*NA*	*NA*
antiarrhythmic MAZE + CTI	4.6% (10/217)	24.0% (36/150)	2×10^{-7} (***)	*NA*	*NA*	*NA*	*NA*

*Binary variables are given as percentage (positive/all cases). Continuous variables are given as median [interquartile range] (n), where n is the number of patients in the group with available data. ASD, atrial septal defect; MR, moderate or severe mitral regurgitation; NYHA, New York Heart Association class; PH, pulmonary hypertension; TVP, tricuspid valvuloplasty; MVP, mitral valvuloplasty; MVR, mitral valve replacement; CTI, ablation of cavo-tricuspid isthmus. (***P < 0.001; **P < 0.01; *P < 0.05).*

disease, left heart failure with high pulmonary capillary wedge pressure (PCW), age or increased PVR between 3 and 5 WU), 10 of them died.

Concomitant Surgical Procedures

Concomitant surgical procedures were performed in moderate or severe valve regurgitations: tricuspid valve repair (TVP), mitral valve repair (MVP) or replacement (MVR) or documented supraventricular arrhythmias: MAZE procedure or cryo-ablation of cavo-tricuspid isthmus (CTI). The concomitant surgical procedures were significantly more frequent in the group of 150 closed defects with PH compared to the group of 217 closed defects without PH (TVP: 41% vs. 8%, MVP/MVR: 21% vs. 6%, MAZE/CTI: 24% vs. 5%, respectively, **Table 1**).

Advanced Pulmonary Vasodilator Therapy

Advanced pulmonary vasodilator therapy was administered to 10 patients with ASD and PH in our study (5.4%): three patients with Eisenmenger syndrome and open ASD, six patients after ASD closure (all with persistent PH and PVR $\geq$ 2.9 WU), and one patient with PVR > 5 WU received the therapy both before and after the ASD closure. The remaining 4 patients with Eisenmenger syndrome died before the specific therapy was available.

Pulmonary Hypertension and Atrial Septal Defect Closure as Predictors of Mortality

As expected, PH was associated with higher all-cause mortality of ASD patients with closed defects (log-rank $P < 0.001$) as well as with open defects (log-rank $P = 0.01$ for model A and log-rank $P = 0.006$ for model B with Eisenmenger patients excluded) (**Figure 1A** and **Supplementary Figure 1A**). At the same time, defect closure was associated with improved survival not only in patients without PH (log-rank $P = 0.01$), but also in patients with PH and PVR < 5 WU (log-rank $P < 0.001$ for model A and log-rank $P < 0.001$ for model B) (**Figure 1A** and **Supplementary Figure 1**). Finally, this difference was present also in patients older than 40 years at diagnosis (**Figure 1B** and **Supplementary Figure 1B**).

The 20-year survival since diagnosis was higher in closed ASD than open ASD both in patients with PH (65% vs. 41%, $P = 0.02$) and without PH (95% vs. 69%, $P = 0.01$).

Univariable Analysis of Mortality Prediction

Six variables significantly predicted mortality in a univariable model. While defect closure was negatively associated with mortality (hazard ratio 0.2, 95% confidence interval 0.1–0.4, $P < 0.001$), positive association with mortality was found for

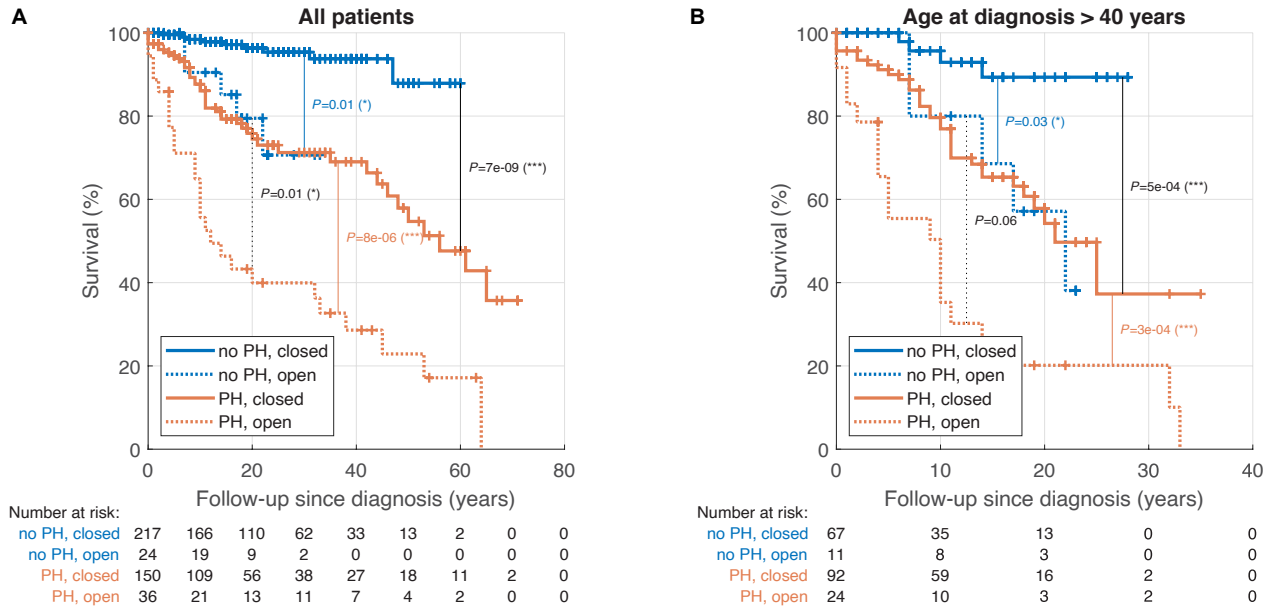

FIGURE 1 | Kaplan-Meier survival analysis of atrial septal defect (ASD) patients stratified by pulmonary hypertension (PH) and ASD closure; all patients (model A). **(A)** Patients of all ages. **(B)** Patients diagnosed at the age above 40. ASD, atrial septal defect; MR, moderate or severe mitral regurgitation; NYHA, New York Heart Association class; PH, pulmonary hypertension.

older age at diagnosis, PH, Eisenmenger syndrome, NYHA class, and MR (**Table 2** and **Figure 2A**). The remaining variables were not significantly predictive of mortality: ASD secundum, sinus venosus defect, coronary sinus defect, advanced therapy, ASD size, and sex.

Multivariable Analysis of Mortality Prediction

The six variables significant in univariable analysis were subsequently included in a multivariable model A, in which four of them remained significantly predictive of mortality: ASD closure negatively (P = 0.003), while older age at diagnosis (P < 0.001), Eisenmenger syndrome (P < 0.001), and PH (P = 0.03) positively (**Table 2** and **Figure 2B**). Finally, even when patients with Eisenmenger syndrome (as they are contraindicated for ASD closure) were completely excluded from this analysis (multivariable model B), the better long-term survival in patients with closed defects remained significant (P = 0.003) (**Table 2**).

DISCUSSION

The decision concerning ASD closure is particularly difficult in elderly patients with PH given the increased mortality risk in this group after ASD closure compared to young patients or patients without PH (3, 4, 11, 12).

The previous studies were missing a control group of patients without ASD closure, and thus could not distinguish whether the worsened survival is due to ASD closure itself, or PH and older age (3). Other previous studies have indicated that older patients with moderate or severe PH benefit from transcatheter closure of ASD with regards to improvement of symptoms and reduction of PH; however, these studies did not report a survival analysis (9, 13, 14).

A study of ASD and trisomy 21 showed a significantly higher mortality in uncorrected ASD including those with severe pulmonary vascular disease (PVD) compared to those with ASD closure. However, this study comprised only children and the group with PH before ASD closure was not analyzed (15).

Here, we conducted a retrospective study comparing long-term mortality in ASD patients with and without defect closure, with respect to PH, age, and other clinical variables. In line with previous studies (3, 4), we observed PH to be associated with higher all-cause mortality. The frequency of PH was high in our cohort (44%). This reflects the fact that our patients were older with late ASD diagnosis (they were followed-up since 1995). There could be also a selection bias resulting from the fact that high-risk patients with PH were sent to our tertiary referral center, while simple ASD patients were frequently treated at the local level.

A key finding of our study is that ASD closure (with adherence to the contraindication criteria) is associated with improved long-term survival in patients with or without PH and this holds also for patients over 40 years of age. ASD closure was a significant independent predictor of survival even after adjusting for age at diagnosis, PH, NYHA, MR, and Eisenmenger syndrome (which was present only in patients with open defects). In particular, ASD patients with PH had significantly better long-term survival after defect closure (65% after 20 years since diagnosis) compared to patients with PH and open ASD (41% after 20 years since diagnosis). Therefore, our data do not support the hypothesis that closure itself increases mortality risk for patients at high

TABLE 2 | Cox-proportional hazards models for mortality prediction.

	Univariable analysis (*n* = 427)		Multivariable model A (*n* = 425)		Multivariable model B (*n* = 418)	
Feature	**Hazard ratio**	***P*-value**	**Hazard ratio**	***P*-value**	**Hazard ratio**	***P*-value**
Age at diag. (decades)	2.9 [2.4–3.5]	1×10^{-27} (***)	2.8 [2.3–3.5]	7×10^{-22} (***)	2.7 [2.2–3.4]	6×10^{-20} (***)
Eisenmenger	4.3 [1.7–10.8]	0.002 (**)	16.4 [4.9–54.3]	3×10^{-06} (***)		
ASD closure	0.2 [0.1–0.4]	2×10^{-10} (***)	0.5 [0.3–0.8]	0.003 (**)	0.5 [0.3–0.8]	0.003 (**)
PH	6.2 [3.4–11.1]	8×10^{-10} (***)	2.0 [1.1–3.8]	0.03 (*)	2.0 [1.0–3.7]	0.03 (*)
NYHA > 2	4.6 [2.9–7.4]	8×10^{-11} (***)	1.3 [0.8–2.2]	0.2	1.4 [0.8–2.3]	0.2
MR	2.1 [1.3–3.4]	0.001 (**)	1.4 [0.9–2.3]	0.2	1.4 [0.9–2.3]	0.2
ASD secundum	1.9 [1.0–3.8]	0.06				
Sinus venosus	0.7 [0.4–1.2]	0.2				
Coronary sinus	2.0 [0.6–6.6]	0.2				
Advanced therapy	0.9 [0.2–3.8]	0.9				
ASD size	1.0 [1.0–1.0]	0.4				
Sex (male)	1.0 [0.6–1.6]	1				

*In the univariable analysis, all variables were assessed independently, and the significant variables were then included in the multivariable analysis (models A and B). In the multivariable model A, all 425 patients with non-missing values for the seven variables were included. In the multivariable model B, patients with Eisenmenger syndrome were excluded and all 418 patients with non-missing values for the remaining six variables were included. ASD, atrial septal defect; MR, moderate or severe mitral regurgitation; NYHA, New York Heart Association class; PH, pulmonary hypertension. (***P < 0.001; **P < 0.01; *P < 0.05).*

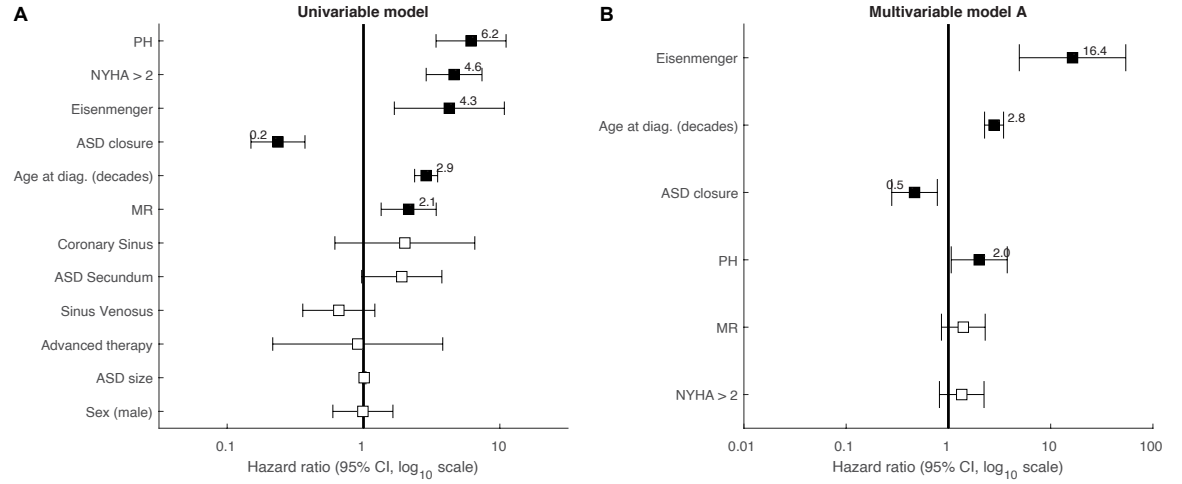

FIGURE 2 | Forest plot of Cox-proportional hazards survival analysis in ASD patients. **(A)** univariable analysis. **(B)** Multivariable analysis (all patients, i.e., model A). The forest plot shows the hazard ratios and their 95% confidence intervals at a $\log_{10}$ scale. Significant variables are highlighted by a filled black square. ASD, atrial septal defect; MR, moderate or severe mitral regurgitation; NYHA, New York Heart Association class; PH, pulmonary hypertension.

age or with PH, but rather that these patients are at high risk even without the closure. Our finding of the benefit of ASD closure is in line with results of a large nationwide study showing that patients with closed ASD have lower mortality compared to patients with open ASD (16).

It should be emphasized that the association of improved survival with ASD closure is relevant only for patients who fulfill the indication criteria for defect closure, with PVR $\leq$ 5 WU at baseline or after pulmonary vasodilator therapy (5, 6). Patients with PVR above 5 WU were shown to develop pulmonary arterial hypertension (PAH) late after defect closure, with poor prognosis (17). However, some case reports in the literature and also one of our patients suggest the possibility of "treat and repair" strategy with the use of advanced pulmonary vasodilator therapy in ASD patients with higher baseline PVR than 5 WU (18).

Patients with Eisenmenger syndrome are rare in ASD (1.6% in our study). Since Eisenmenger syndrome is a contradiction for defect closure, we designed our analysis with a special care to account for this potential confounding factor and performed all analyses with and without inclusion of patients with Eisenmenger syndrome. In our study, Eisenmenger syndrome was a strong predictor of mortality in univariable as well as in multivariable analysis (**Table 2**). However, ASD closure was a significant independent predictor of survival both in the analysis with Eisenmenger syndrome patients included (model A) and excluded (model B).

The presence of PH is sometimes erroneously considered to be a contraindication for defect closure on the basis of the study by Manes et al. (19). The authors observed the worst survival in patients with closed defects and PH, while the best survival was observed in Eisenmenger syndrome with open defects (most of them treated by advanced therapy). On the contrary, in our study, the highest long-term mortality was observed in open ASD with PH, including Eisenmenger syndrome. Eisenmenger syndrome, age at diagnosis, and PH were independent positive predictors of mortality in our study, while defect closure was a significant independent negative predictor of mortality. The discrepancy between the studies may be explained by the fact that the study of Manes et al. comprised predominantly post-tricuspid defects with unknown and potentially high preoperative PVR due to PAH and PVD. Therefore, the conclusions of Manes study are not applicable to ASD patients with PH and PVR $\leq$ 5 WU considered for closure. Moreover, the favorable long-term survival in patients with Eisenmenger syndrome in Manes et al. study could have been influenced by the use of advanced pulmonary vasodilator therapy. This therapy could only be used in a minority of our patients. While we observed general stabilization of clinical state in patients treated with advanced therapy, the numbers were too low to evaluate a potential significant benefit in the survival analysis.

The results of our study support the strategy of active screening of the ASD in adults with timely closure of hemodynamically significant defects early after diagnosis. ASD closure should be performed even in asymptomatic patients and on the other side even in older patients with PH if they comply with the indication criteria for ASD closure specified in the guidelines (5, 6). Transcatheter closure is preferred because of its lower invasiveness; however, if a patient with ASD and PH has concomitant severe tricuspid or MR or large defect without appropriate rims, we believe there is still place for surgery as recommended by the guidelines (5, 20).

High-risk patients should always be assessed for risks and benefits of ASD closure in a specialized expert center (6). ASD closure may prevent further deterioration of PH and improve survival, however in patients with severe PH and advanced PVD, the shunt closure may be detrimental. Therefore, the catheterization with PVR assessment is crucial (5, 6, 21). The current recommended cut-off value of PVR for ASD closure is 5 WU (6). In high-risk patients with PAH, a small fenestration may be useful to prevent right heart failure after ASD closure. In postcapillary and combined PH, we aimed to remove the cause of postcapillary PH (mitral regurgitation, coronary artery disease, left heart failure, etc.) before or during the ASD closure and to leave a small fenestration to prevent left heart failure.

Mortality and morbidity (stroke or heart failure) are significantly increased by atrial arrhythmias (22). The risk of atrial arrhythmias and stroke is increased in patients with ASD (23, 24) and the prevalence of atrial arrhythmias in ASD increases with age (22). In our study, we performed the antiarrhytmic surgery (MAZE and/or CTI) in the case of documented atrial arrhythmias. This procedure was significantly more frequent in patients with PH compared to defects without PH (24% vs. 5%, $p < 0.001$). Close long-term follow-up of patients with open as well as closed ASD is important. It should include clinical examination with assessment of symptoms, especially arrhythmias, repeated echocardiogram, and ECG monitoring. Some of the small defects may increase their hemodynamic relevance with increasing age and such defects should be closed in time.

Our study confirmed that ASD patients with PH had higher mortality and suffered more often from mitral and tricuspid regurgitation and arrhythmias, compared to patients without PH. This is in line with the literature; patients with PH had more comorbidities, were older and had a significantly higher risk of developing major cardiac and cerebrovascular adverse events after transcatheter ASD closure (25).

In conclusion, our study on 427 ASD patients identified ASD closure as a positive independent predictor of survival. In contrast, older age at diagnosis, Eisenmenger syndrome, and PH were independent negative predictors of survival. Patients with PH and closed ASD had significantly lower long-term mortality compared to patients with PH and open defects. ASD closure thus appears to be beneficial even in older patients with PH and PVR < 5 WU, who are not contraindicated for closure for other reasons.

LIMITATIONS OF THE STUDY

(A) Due to the retrospective nature of our study, the groups with and without ASD closure could not be matched. Patients with open ASD and PH formed a heterogenous group comprising patients contraindicated for ASD closure (Eisenmenger syndrome, small defects with severe PH), and patients who refused ASD closure despite PVR < 5 WU. However, the mortality was high in all subgroups of open ASD and PH patients. (B) While the long-term follow-up (and data collection since 1995) is of a general advantage of our study, it brings two inherent limitations. First, catheterization was not performed in all patients, but preferentially in those with suspicion of moderate or severe PH based on echocardiography. Second, not all patients with high PVR had the possibility of advanced pulmonary vasodilator therapy treatment. However, as soon as the advanced therapy was accessible, it was administered to all patients with Eisenmenger syndrome or high PVR who were still alive. The impact of advanced vasodilator therapy on the long-term survival of ASD patients with high PVR and open or closed defects therefore remains to be assessed in future research.

DATA AVAILABILITY STATEMENT

The raw data supporting the conclusions of this article will be made available by the authors, without undue reservation.

ETHICS STATEMENT

The studies involving human participants were reviewed and approved by Ethics Committee of Na Homolce Hospital, project

5.6.2019/25 and 26. Written informed consent for participation was not required for this study in accordance with the national legislation and the institutional requirements.

AUTHOR CONTRIBUTIONS

JR conceived the study, collected the patient data, and was the guarantor of the study. RŽ contributed to data collection. MT and JT carried out data analysis and visualization. MT and JR wrote the initial draft, with all authors subsequently carrying out critical revisions.

FUNDING

This study was supported by the Ministry of Health, Czech Republic – Conceptual Development of Research Organization, Nemocnice Na Homolce – NNH, Prague, Czech Republic (00023884, IG160201) and University Hospital Motol, Prague, Czech Republic (00064203).

ACKNOWLEDGMENTS

We thank the surgeons (Štěpán Černý, Ivo Skalský, Roman Gebauer, and Petr Pavel) and the interventional cardiologists (Karel Hlaváček, Martin Mates, Petr Kmoníček, and Karel Kopřiva) for their contribution.

SUPPLEMENTARY MATERIAL

The Supplementary Material for this article can be found online at: https://www.frontiersin.org/articles/10.3389/fcvm.2022.867012/full#supplementary-material

REFERENCES

1. Opotowsky AR. Clinical evaluation and management of pulmonary hypertension in the adult with congenital heart disease. *Circulation.* (2015) 131:200–10. doi: 10.1161/CIRCULATIONAHA.114.006976
2. Cuypers JAAE, Opiæ P, Menting ME, Utens EMWJ, Witsenburg M, Helbing WA, et al. The unnatural history of an atrial septal defect: longitudinal 35 year follow up after surgical closure at young age. *Heart.* (2013) 99:1346–52. doi: 10.1136/heartjnl-2013-304225
3. Ranard LS, Mallah WE, Awerbach JD, Abernethy A, Halane M, Qureshi AM, et al. Impact of pulmonary hypertension on survival following device closure of atrial septal defects. *Am J Cardiol.* (2019) 124:1460–4. doi: 10.1016/j.amjcard.2019.07.042
4. Murphy JG, Gersh BJ, McGoon MD, Mair DD, Porter CJ, Ilstrup DM, et al. Long-Term outcome after surgical repair of isolated atrial septal defect follow-up at 27 to 32 years. *N Engl J Med.* (1990) 323:1645–50. doi: 10.1056/NEJM199012133232401
5. Baumgartner H, Bonhoeffer P, De Groot NMSS, de Haan F, Deanfield JE, Galie N, et al. ESC Guidelines for the management of grown-up congenital heart disease (new version 2010). *Eur Heart J.* (2010) 31:2915–57. doi: 10.1093/eurheartj/ehq249
6. Baumgartner H, De Backer J, Babu-Narayan SV, Budts W, Chessa M, Diller G-P, et al. 2020 ESC Guidelines for the management of adult congenital heart disease. *Eur Heart J.* (2020) 42:1–83. doi: 10.1093/eurheartj/ehaa554
7. Galiè N, Humbert M, Vachiery JL, Gibbs S, Lang I, Torbicki A, et al. 2015 ESC/ERS guidelines for the diagnosis and treatment of pulmonary hypertension. *Eur Heart J.* (2016) 37:67–119. doi: 10.1093/eurheartj/ehv317
8. Parasuraman S, Walker S, Loudon BL, Gollop ND, Wilson AM, Lowery C, et al. Assessment of pulmonary artery pressure by echocardiography-a comprehensive review. *Int J Cardiol Hear Vasc.* (2016) 12:45–51. doi: 10.1016/j.ijcha.2016.05.011
9. Humenberger M, Rosenhek R, Gabriel H, Rader F, Heger M, Klaar U, et al. Benefit of atrial septal defect closure in adults: Impact of age. *Eur Heart J.* (2011) 32:553–60. doi: 10.1093/eurheartj/ehq352
10. Grambsch PM, Therneau TM. Proportional hazards tests and diagnostics based on weighted residuals. *Biometrika.* (1994) 81:515. doi: 10.2307/2337123
11. Kaemmerer H, Apitz C, Brockmeier K, Eicken A, Gorenflo M, Hager A, et al. Pulmonary hypertension in adults with congenital heart disease: updated recommendations from the cologne consensus conference 2018. *Int J Cardiol.* (2018) 272:79–88. doi: 10.1016/j.ijcard.2018.08.078
12. Lammers AE, Bauer LJ, Diller GP, Helm PC, Abdul-Khaliq H, Bauer UMM, et al. Pulmonary hypertension after shunt closure in patients with simple congenital heart defects. *Int J Cardiol.* (2020) 308:28–32. doi: 10.1016/j.ijcard.2019.12.070
13. Yong G, Khairy P, De Guise P, Dore A, Marcotte F, Mercier LA, et al. Pulmonary arterial hypertension in patients with transcatheter closure of secundum atrial septal defects a longitudinal study. *Circ Cardiovasc Interv.* (2009) 2:455–62. doi: 10.1161/CIRCINTERVENTIONS.108.826560
14. Zwijnenburg RD, Baggen VJM, Geenen LW, Voigt KR, Roos-Hesselink JW, van den Bosch AE. The prevalence of pulmonary arterial hypertension before and after atrial septal defect closure at adult age: a systematic review. *Am Heart J.* (2018) 201:63–71. doi: 10.1016/j.ahj.2018.03.020
15. Lammers AE, Stegger J, Koerten MA, Helm PC, Bauer UM, Baumgartner H, et al. Secundum type atrial septal defect in patients with trisomy 21—therapeutic strategies, outcome, and survival: a nationwide study of the German national registry for congenital heart defects. *J Clin Med.* (2021) 10:3807. doi: 10.3390/jcm10173807
16. Nyboe C, Karunanithi Z, Nielsen-Kudsk JE, Hjortdal VE. Long-term mortality in patients with atrial septal defect: a nationwide cohort-study. *Eur Heart J.* (2018) 39:993–8. doi: 10.1093/eurheartj/ehx687
17. D'Alto M, Romeo E, Argiento P, Correra A, Santoro G, Gaio G, et al. Hemodynamics of patients developing pulmonary arterial hypertension after shunt closure. *Int J Cardiol.* (2013) 168:3797–801. doi: 10.1016/j.ijcard.2013.06.036
18. Kim Y-H, Yu JJ, Yun T-J, Lee Y, Kim YB, Choi HS, et al. Repair of atrial septal defect with Eisenmenger syndrome after long-term sildenafil therapy. *Ann Thorac Surg.* (2010) 89:1629–30. doi: 10.1016/j.athoracsur.2009.10.027
19. Manes A, Palazzini M, Leci E, Bacchi Reggiani ML, Branzi A, Galiè N. Current era survival of patients with pulmonary arterial hypertension associated with congenital heart disease: a comparison between clinical subgroups. *Eur Heart J.* (2014) 35:716–24. doi: 10.1093/eurheartj/eht072
20. Stout KK, Daniels CJ, Aboulhosn JA, Bozkurt B, Broberg CS, Colman JM, et al. 2018 AHA/ACC Guideline for the management of adults with congenital heart disease: executive summary: a report of the american college of cardiology/american heart association task force on clinical practice guidelines. *J Am Coll Cardiol.* (2019) 73:1494–563. doi: 10.1016/j.jacc.2018.08.1028
21. Steele PM, Fuster V, Cohen M, Ritter DG, McGoon DC. Isolated atrial septal defect with pulmonary vascular obstructive disease - long-term follow-up and prediction of outcome after surgical correction. *Circulation.* (1987) 76:1037–42. doi: 10.1161/01.CIR.76.5.1037
22. Bouchardy J, Therrien J, Pilote L, Ionescu-Ittu R, Martucci G, Bottega N, et al. Atrial arrhythmias in adults with congenital heart disease. *Circulation.* (2009) 120:1679–86. doi: 10.1161/CIRCULATIONAHA.109.866319
23. Nyboe C, Olsen MS, Nielsen-Kudsk JE, Johnsen SP, Hjortdal VE. Risk of pneumonia in adults with closed versus unclosed atrial septal defect (from a Nationwide Cohort Study). *Am J Cardiol.* (2014) 114:105–10. doi: 10.1016/j.amjcard.2014.03.063

24. Nyboe C, Olsen MS, Nielsen-Kudsk JE, Hjortdal VE. Atrial fibrillation and stroke in adult patients with atrial septal defect and the long-term effect of closure. *Heart.* (2015) 101:706–11. doi: 10.1136/heartjnl-2014-306552
25. Akseer S, Abrahamyan L, Lee DS, Huszti E, Meier LM, Osten M, et al. Long-Term outcomes in adult patients with pulmonary hypertension after percutaneous closure of atrial septal defects. *Circ Cardiovasc Interv.* (2022) 15:e011110. doi: 10.1161/CIRCINTERVENTIONS.121.011110

Conflict of Interest: The authors declare that the research was conducted in the absence of any commercial or financial relationships that could be construed as a potential conflict of interest.

Publisher's Note: All claims expressed in this article are solely those of the authors and do not necessarily represent those of their affiliated organizations, or those of the publisher, the editors and the reviewers. Any product that may be evaluated in this article, or claim that may be made by its manufacturer, is not guaranteed or endorsed by the publisher.

J. Rubáčková Popelová et al.

Normalization of Four Different Types of Pulmonary Hypertension After Atrial Septal Defect Closure

Front. Cardiovasc. Med.
Impact Factor: 5.846

‹ rejstřík

frontiers | Frontiers in Cardiovascular Medicine

BRIEF RESEARCH REPORT
published: 10 June 2022
doi: 10.3389/fcvm.2022.876755

Normalization of Four Different Types of Pulmonary Hypertension After Atrial Septal Defect Closure

Jana Rubáčková Popelová[1,2*†], *Jakub Tomek*[1,3†], *Markéta Tomková*[1,4] *and Renata Živná*[1]

[1] Department of Cardiac Surgery, Na Homolce Hospital, Prague, Czechia, [2] Pediatric Heart Centre, Motol University Hospital, Prague, Czechia, [3] Department of Pharmacology, School of Medicine, University of California, Davis, Davis, CA, United States, [4] Department of Biochemistry and Molecular Medicine, School of Medicine, University of California, Davis, Davis, CA, United States

Pulmonary hypertension (PH) is an established risk factor in patients with atrial septal defect (ASD), and its persistence after ASD closure is associated with increased mortality. Therefore, predictors for PH normalization after defect closure are needed. Multiple hemodynamic types of PH exist, but little is known about their prevalence and prognostic value for PH normalization after ASD closure. We carried out a retrospective study on 97 patients (76% female, median age at ASD closure 58 years) with four types of PH determined predominantly by right heart catheterization: hyperkinetic, pulmonary arterial hypertension, isolated post-capillary, and combined pre- and post-capillary. We investigated the frequency of the PH types and their prognostic significance for PH normalization after ASD closure. Frequency of PH types before ASD closure in our study was: hyperkinetic 55%, pulmonary arterial hypertension 10%, isolated post-capillary PH 24%, and combined PH 11%. Hyperkinetic PH type was positively associated with PH normalization after ASD closure (78% patients normalized), remaining a significant independent predictor when adjusted for age at closure, sex, heart failure, and NYHA. Hyperkinetic PH patients also had significantly better survival prognosis versus patients with other PH types ($p = 0.04$). Combined PH was negatively associated with PH normalization, with no patients normalizing. Pulmonary arterial hypertension and isolated post-capillary PH had intermediate rates of normalization (60 and 52%, respectively). In summary, all four hemodynamic types of PH are found in adult patients with ASD, and they can be used to stratify patients by their likelihood of PH normalization and survival after ASD closure.

Keywords: pulmonary hypertension, atrial septal defect, hemodynamic type of pulmonary hypertension, normalization, reversibility, mortality

OPEN ACCESS

Edited by:
Astrid Lammers, University of Münster, Germany

Reviewed by:
Mona Mostafa Rayan, Ain Shams University, Egypt
Anggoro Budi Hartopo, Gadjah Mada University, Indonesia

***Correspondence:**
Jana Rubáčková Popelová
jana.popelova@homolka.cz

†These authors share first authorship

Specialty section:
This article was submitted to General Cardiovascular Medicine, a section of the journal Frontiers in Cardiovascular Medicine

Received: *15 February 2022*
Accepted: *23 May 2022*
Published: *10 June 2022*

Citation:
Rubáčková Popelová J, Tomek J, Tomková M and Živná R (2022) Normalization of Four Different Types of Pulmonary Hypertension After Atrial Septal Defect Closure. Front. Cardiovasc. Med. 9:876755. doi: 10.3389/fcvm.2022.876755

INTRODUCTION

Pulmonary hypertension (PH) represents an important risk factor associated with reduced functional capacity and increased mortality in patients with atrial septal defect (ASD) (1–6). Moreover, persistence of PH after ASD closure is strongly associated with increased mortality (4, 7, 8). On the other hand, patients with normalization of PH after ASD closure have similar outcome as patients without PH (7). The decision of whether to close ASD in patients with PH

presents a complex clinical dilemma (9, 10). Therefore, it is highly important to predict in which patients with ASD and PH the defect closure will lead to PH normalization and in which patients the closure may be detrimental with right heart failure and persistence or even progression of PH.

The guidelines give limits for safe defect closure for pulmonary vascular resistance (PVR) < 3 Wood Units (WU) or 4 WU × m^2 and contraindication of defect closure for PVR more than 5 WU or 8 WU × m^2 (2, 11, 12). However, the guidelines do not specify the probability of PH normalization after defect closure, an important factor for survival (4, 7, 8). Moreover, many studies (including guidelines) deal only with pulmonary arterial hypertension (PAH) in congenital shunt lesions (2, 3, 13, 14), although it is just one of four hemodynamic types of PH in adults with ASD (9, 15). We hypothesized that the hemodynamic types of PH may be predictive of normalization of PH following ASD closure.

Existing ESC/ERS guidelines for the diagnosis and treatment of PH recognize pre-capillary PH, isolated post-capillary PH (IpcPH), and combined pre- and post-capillary PH (CpcPH) (2, 15). Pre-capillary PH involves pulmonary arterial hypertension (PAH), defined by elevated pulmonary vascular resistance (PVR ≥ 3 WU). One of the causes of PAH can be congenital heart disease (CHD) with shunt (2). Although most studies on ASD with PH focus just on PAH (3, 14, 16), hyperkinetic PH (H-PH), characterized by normal or only modestly increased PVR (<3 WU) and normal pulmonary capillary wedge pressure (PCW ≤15 mmHg), is another type of PH described in ASD (9, 17, 18). Interestingly, hyperkinetic PH is currently not discussed in ESC/ERS guidelines for the diagnosis and treatment of pulmonary hypertension (2, 15). IpcPH is characterized by increased left atrial pressure or PCW (>15 mmHg), which can in some cases worsen after defect closure (10, 19). Little is known about CpcPH in patients with ASD.

The objective of this study was to characterize the frequency of the four types of PH (H-PH, PAH, IpcPH, and CpcPH) as determined predominantly by right heart catheterization (RHC) in adults with ASD, to assess their prognostic value for predicting PH normalization after defect closure, and to evaluate patient mortality in the four PH types.

METHODS

Patients

Following institutional ethics committee approval (Na Homolce Hospital), we performed a retrospective observational study including all the adult patients in our database with the diagnosis of ASD (type secundum, sinus venosus or coronary sinus defect) with PH who underwent defect closure, with known PH type before defect closure. Patients with incomplete atrioventricular septal defects (ASD type primum) or ASD combined with other hemodynamically important CHD were excluded. PH was defined for the purpose of this study as mean pulmonary arterial pressure (mPAP) ≥ 25 mmHg (2). The contraindications for ASD closure were: PVR > 5 WU not responding to advanced therapy or (previously) to acute vasodilation testing which is not recommended any more (11, 12). Another contraindication for ASD closure was increase in left atrial mean pressure during temporary balloon occlusion > 10 mmHg compared to baseline in patients with postcapillary PH (19). Mortality data were obtained from the national mortality register. Processing of human data was carried out in accordance with institutional guidelines.

Catheterization

During right heart catheterization (RHC) the right atrial pressure, sPAP, mPAP, pulmonary capillary wedge pressure (PCW), and left atrial pressure were measured. Cardiac output (pulmonary flow) was measured by Fick method preferentially with measured oxygen consumption, but also with estimated oxygen consumption or dye-dilution or thermodilution, according to the cath-lab facilities. PVR was calculated, and the shunt was quantified by oximetry. Left heart catheterization with coronary angiography was performed according to the usual criteria. Re-catheterization after defect closure was performed in the case of suspected moderate or severe PH from echocardiography.

For the purpose of this study, the four investigated hemodynamic types of PH were defined as specified in **Table 1** (2, 15, 17, 18). IpcPH and CpcPH were distinguished by PVR, not by diastolic pressure gradient (15).

Echocardiography

The size of the ASD was assessed by transesophageal echocardiography. In addition to RHC-determined hemodynamic types of PH, 19 out of the 97 patients (all 19 with H-PH) were diagnosed by echocardiography (20–22). These patients had only mild PH (mPAP 25–30 mHg), with no signs of left heart disease, high pulmonary flow and near-normal PVR (assessed by echocardiographic method which has good correlation with invasive PVR) (21). Therefore, we consider the diagnosis of H-PH in these patients as reliable. All other 78 patients had diagnosis of the type of PH assessed by RHC.

PH normalization was assessed by echocardiography using the method of mPAP assessment described by Aduen et al. (22). Mean PAP = mean pressure difference between right ventricle and right atrium, which is derived from the velocity-time integral (VTI) of the tricuspid regurgitation and the estimated right atrial pressure (RAP) is added. This method correlates closely with invasive measurements (22). Only in the rare case of absence of tricuspid regurgitation we used the alternative method of peak Doppler velocity of the pulmonary regurgitation, mPAP = $4V^2$ + RAP. Both methods are recommended in a review article by Parasurman (20). When PH was suspected after defect closure, RHC was used for the diagnostics. PH was considered normalized when mPAP was < 25 mmHg (2).

Statistical Methods

Kruskal-Wallis ANOVA was used to compare clinical features between PH types (**Table 2**). Cox proportional-hazards ratio was used to study the association between clinical features and PH normalization (**Table 3**). One exception within **Table 3** is the CpcPH, where the zero rate of normalization

TABLE 1 | Definition of hemodynamic types of PH in ASD.

	mPAP (mmHg)	PCW (mmHg)	PVR (WU)
Hyperkinetic (H-PH)	≥ 25	≤15	<3
Pulmonary arterial hypertension (PAH)	≥ 25	≤15	≥3
Isolated post-capillary PH (IpcPH)	≥ 25	>15	<3
Combined pre- and post-capillary PH (CpcPH)	≥ 25	>15	≥3

mPAP, mean pulmonary arterial pressure; PCW, pulmonary capillary wedge pressure; PVR, pulmonary vascular resistance.

TABLE 2 | Cohort summary.

Clinical variable	H-PH ($n = 53$)	PAH ($n = 10$)	IpcPH ($n = 23$)	CpcPH ($n = 11$)	All ($n = 97$)	p-value
PH normalization	78% (35/45)	60% (6/10)	52% (12/23)	0% (0/11)	60% (53/89)	$4.8{\cdot}10^{-5}$
Sex (female)	77% (41/53)	90% (9/10)	57% (13/23)	100% (11/11)	76% (74/97)	0.025
Age at diagnosis (years)	47.0 [34.0–59.0] ($n = 53$)	59.0 [37.0–60.0] ($n = 10$)	50.0 [10.0–65.0] ($n = 23$)	66.0 [52.8–72.0] ($n = 11$)	50.0 [28.0–61.0] ($n = 97$)	0.18
Age at closure (years)	52.0 [42.0–61.3] (n =53)	59.0 [51.0–65.0] (n =10)	60.0 [51.0–70.8] (n =23)	69.0 [58.0–74.0] (n =11)	58.0 [46.8–65.0] (n =97)	0.009
NYHA before closure	2.0 [2.0–3.0] (n =53)	3.0 [2.0–3.5] (n =10)	3.0 [2.6–3.0] (n =23)	3.0 [2.6–3.0] (n =11)	2.5 [2.0–3.0] (n =97)	$2.4{\cdot}10^{-5}$
ASD size (mm)	20.0 [16.5–25.5] (n =48)	28.0 [20.0–39.3] (n =7)	15.5 [11.0–21.0] (n =20)	19.5 [14.0–22.5] (n =8)	20.0 [15.0–24.8] (n =83)	0.06
Qp/Qs	2.4 [1.8–3.0] (n =48)	2.0 [1.7–2.5] (n =9)	2.2 [1.6–2.6] (n =18)	2.5 [2.2–2.7] (n =6)	2.3 [1.8–3.0] (n =81)	0.63
HF before closure	13% (7/53)	40% (4/10)	35% (8/23)	55% (6/11)	26% (25/97)	0.011
mPAP before closure (mmHg)	30.0 [27.0–33.8] (n =51)	32.0 [28.0–40.0] (n =10)	33.5 [28.0–44.0] (n =22)	37.5 [35.0–45.0] (n =10)	32.0 [28.0–36.3] (n =93)	0.009
sPAP before closure (mmHg)	44.0 [39.8–50.0] (n =53)	47.5 [45.0–63.0] (n =10)	50.0 [42.0–59.8] (n =23)	55.0 [52.0–69.5] (n =11)	47.0 [41.0–55.0] (n =97)	0.0006
Surgical closure	77% (41/53)	100% (10/10)	100% (23/23)	64% (7/11)	84% (81/97)	0.012
PH follow-up length (months)	14.5 [9.0–48.5] (n =44)	14.0 [10.0–40.0] (n =10)	31.0 [12.0–60.8] (n =23)	13.0 [4.0–84.3] (n =11)	16.0 [10.0–51.0] (n =88)	0.74

Binary variables are given as percentage (positive/all cases in the PH type). Numerical variables are given as median [interquartile range] (n), where n is the number of patients in the PH group with available data. Qp/Qs, pulmonary-to-systemic flow; HF, heart failure; sPAP, systolic PAP; mPAP, mean PAP; H-PH, hyperkinetic PH; PAH, pulmonary arterial hypertension; IpcPH, Isolated post-capillary PH; CpcPH, combined pre- and post-capillary PH. "Surgical closure" corresponds to sternotomy, minithoracotomy, or robotic thoracoscopy (in the other cases, transcatheter closure was used).

precludes the use of the Cox proportional-hazards ratio, and a Fisher test was used instead on the underlying contingency table to obtain the p-value. We verified that all covariates in the Cox model fulfill the proportional hazards assumption, using the MATLAB fitcox function, which is based on the scaled Schoenfeld residuals, as derived by Grambsch and Therneau (23). The variables significant in univariable Cox proportional hazard ratio model and sex and age at closure and the NYHA class were then included in a multivariable model. Kaplan-Meier survival analysis was used to compare survival rates in the four PH types (**Figure 1**). Wilcoxon rank-sum test was used to assess the difference in NYHA in PH-normalized vs. PH-persisting patients. Only patients with data available on normalization were included in the Cox proportional-hazards and Kaplan-Meier analyses. Hypothesis testing was two-sided and $p < 0.05$ was considered statistically significant. Data were analyzed using MATLAB (R2021b).

RESULTS

A total of 97 adult patients after ASD closure (70% *via* sternotomy, 8% *via* minithoracotomy, 5% *via* robotic thoracoscopy, 17% *via* transcatheter) were included in the study. The median age at the ASD closure was 58 years [47–65 IQR] and 76% of the patients were female. Before defect closure, 53 (55%) patients had H-PH, 10 (10%) PAH, 23 (24%) IpcPH, and 11 (11%) CpcPH. During long-term follow-up for PH normalization after ASD closure (median 16 months, IQR 10–51), PH normalized in 53 patients out of 89 (60%) for whom the data on normalization were available.

PH normalization differed significantly between the hemodynamic types ($p = 4.8{\cdot}10^{-5}$, **Table 2**). Patients with H-PH manifested the greatest rate of normalization (78%), while normalization was lowest in patients with CpcPH (0%). Other features significantly different between

TABLE 3 | Univariable and multivariable Cox proportional-hazards analysis for association of PH normalization and clinical features.

Univariable Cox proportional-hazards models				
Feature	**PH normalized ($n = 53$)**	**PH persisting ($n = 36$)**	**Hazard ratio [CI]**	***p*-value**
Sex (female)	81% (43/53)	69% (25/36)	1.633 [0.819–3.258]	0.16
Age at diagnosis (years)	49.0 [33.5–60.0] (n =53)	57.5 [18.0–66.0] (n =36)	1.008 [0.996–1.021]	0.19
Age at closure (years)	53.0 [42.0–62.3] (n =53)	60.5 [54.5–69.5] (n =36)	1.003 [0.984–1.022]	0.74
NYHA before closure	2.0 [2.0–3.0] (n =53)	3.0 [2.0–3.0] (n =36)	0.685 [0.449–1.047]	0.08
ASD size	20.0 [14.3–24.8] (n =47)	20.0 [16.3–23.3] (n =29)	1.003 [0.969–1.038]	0.86
Qp/Qs	2.2 [1.8–3.0] (n =44)	2.3 [1.9–3.5] (n =29)	0.895 [0.637–1.255]	0.52
HF before closure	17% (9/53)	42% (15/36)	0.456 [0.221–0.942]	0.034
H-PH	66% (35/53)	28% (10/36)	2.414 [1.344–4.338]	0.003
PAH	11% (6/53)	11% (4/36)	1.236 [0.526–2.904]	0.63
IpcPH	23% (12/53)	31% (11/36)	0.610 [0.313–1.188]	0.15
CpcPH	0% (0/53)	31% (11/36)	N/A	$1.6{\cdot}10^{-5}$
mPAP before closure (mm Hg)	30.0 [27.0–33.8] (n =51)	35.0 [29.0–40.0] (n =34)	0.991 [0.955–1.029]	0.65
sPAP before closure (mm Hg)	45.0 [40.0–52.3] (n =53)	50.0 [45.0–61.5] (n =36)	0.995 [0.971–1.019]	0.67
Surgical closure	85% (45/53)	78% (28/36)	1.230 [0.576–2.628]	0.5924
Multivariable Cox proportional-hazards model				
Model	**Feature**	**Hazard ratio [CI]**	**p-value**	
H- PH adjusted for age at closure, sex, HF, and NYHA	Hyperkinetic PH	2.37 [1.22–4.6]	0.01	
	Age at closure (years)	1.0 [0.99–1.03]	0.56	
	Sex	1.43 [0.7–2.94]	0.33	
	HF before closure	0.53 [0.23–1.22]	0.13	
	NYHA before closure	1.12 [0.64–1.96]	0.68	

Binary variables are given as percentage (positive/all cases). Numerical variables are given as median [interquartile range] (n). Distinct PH types were represented as four separate binary variables (1=presence of the PH type). Hazard ratios (HR) are expressed with regards to PH normalization, i.e., hazard ratio > 1 means a positive association between the feature and PH normalization. Qp/Qs, pulmonary-to-systemic flow; HF, heart failure; sPAP, systolic PAP; mPAP, mean PAP; H-PH, hyperkinetic PH; PAH, pulmonary arterial hypertension; IpcPH, Isolated post-capillary PH; CpcPH, combined pre- and post-capillary PH. In the case of CpcHP, the Cox proportional-hazards analysis cannot be applied given the zero normalization rate; the Fisher-test was used to calculate the p-value from the underlying contingency table instead.

hemodynamic types were: sex, age at closure, NYHA class before closure, presence of heart failure (HF) before closure, the measurements of sPAP (systolic PAP) and mPAP (mean PAP) before closure, and the proportion of surgical closure (as opposed to transcatheter closure) (**Table 2**).

Three clinical variables were significantly predictive of PH normalization (**Table 3**, top). While H-PH type was positively predictive of PH normalization ($p = 0.003$, HR = 2.4 [1.34–4.34]), CpcPH type was negatively predictive ($p = 1.6{\cdot}10^{-5}$). Presence of HF before closure was negatively predictive of normalization [$p = 0.034$, HR = 0.46 (0.22–0.94)]. In addition, the NYHA class was borderline nonsignificantly negatively predictive of PH normalization [$p = 0.08$; HR = 0.69 (0.45–1.05)].

Next, we used a multivariable Cox proportional-hazards model for the H-PH, further accounting for age at closure, sex, heart failure, and the NYHA class. H-PH remained a significant independent predictor of PH normalization ($p = 0.01$) (**Table 3**, bottom). Given the zero normalization rate in the CpcPH group, a similar analysis could not be carried out for this hemodynamic type.

In addition, we compared the improvement in NYHA class after ASD closure between PH-normalized and PH-persisting patients. The PH-normalized patients showed a significantly increased improvement in NYHA class compared to PH-persisting patients (mean improvement of 0.85 vs. 0.28; $p = 0.007$).

Finally, we compared survival of patients in the four hemodynamic types using Kaplan-Meier survival analysis (**Figure 1A**). H-PH type showed the best survival ($p = 0.04$; logrank test compared to other PH types) with a 10-year survival of 92% (**Figure 1B**). PAH and IpcPH types had intermediate 10-year survival (77 and 66%, respectively). The survival was lowest in CpcPH type with a 10-year survival of 61%.

Due to the exclusion criterion PVR > 5 WU in our study, advanced therapy (bosentan and sildenafil) was used in 7 (7%) of our ASD patients only (6 after defect closure, one before and after closure). Majority of patients with advanced therapy (5 out of 7) did not normalize PH (3x CpcPH, 1x PAH, 1x H-PH). The patient with H-PH had PVR 2.7 WU before closure and developed CpcPH after ASD closure with PVR 5 WU and died due to heart failure with severe left ventricular dysfunction 12 years after ASD closure.

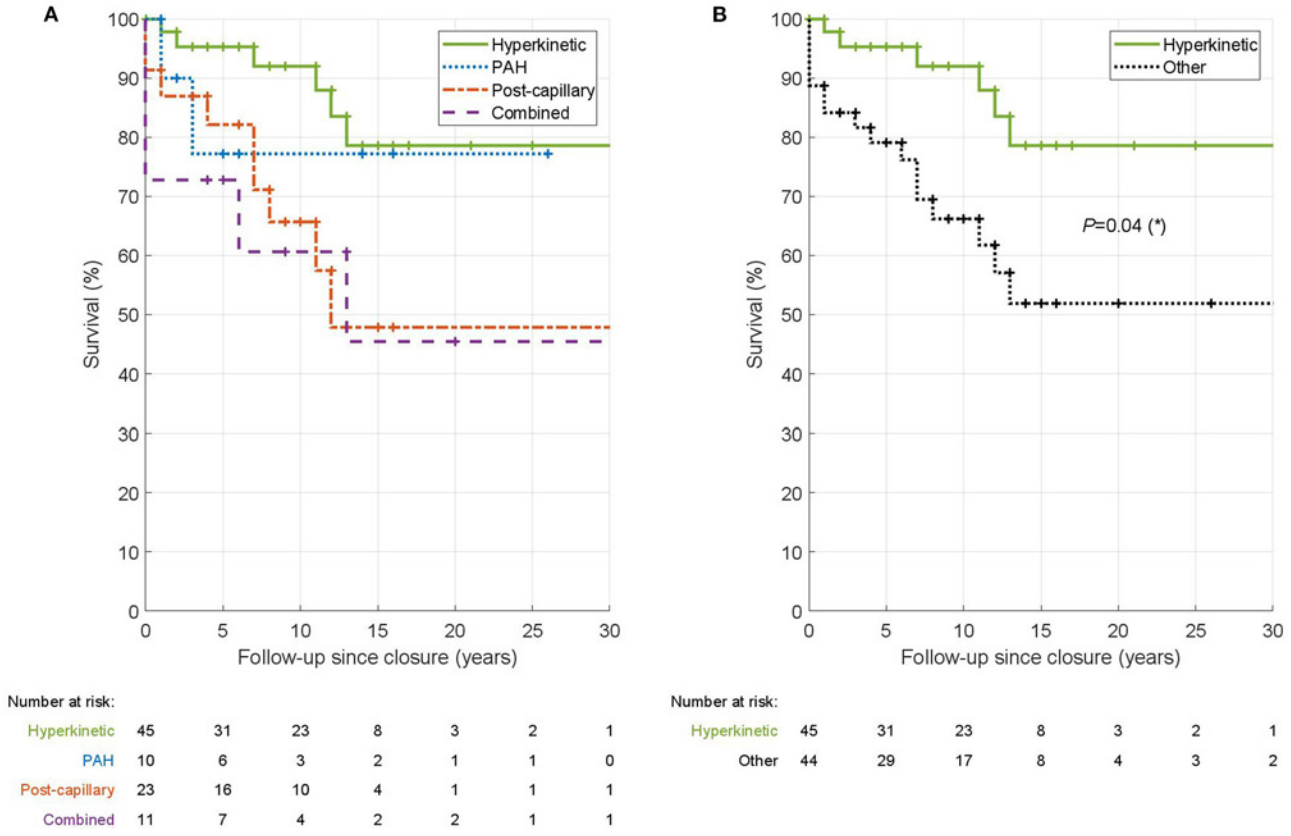

FIGURE 1 | Kaplan-Meier survival analysis of hemodynamic types of PH in ASD. In the left panel **(A)** is shown the comparison of survival among the four hemodynamic types. In the right panel **(B)** is the comparison of H-PH patients vs. patients with other PH types pooled together. The tables underneath the Kaplan-Meier curves give the number of patients who were alive and followed at the given time point. The log-rank test was used to test the significance of survival difference between hyperkinetic patients and all other patients.

DISCUSSION

This study is the first to evaluate the frequency of the four different types of PH in ASD patients, as well as their predictive value for PH normalization and mortality. We observed that the PH types are highly predictive of PH normalization after ASD closure, with H-PH being a significant positive predictor, even after adjusting for age, sex, NYHA class, and presence of heart failure. Conversely, CpcPH was a significant negative predictor of PH normalization. Moreover, we observed a substantially higher improvement in NYHA class after ASD closure in PH-normalized patients compared to PH-persisting patients. Our study therefore shows the importance of assessing the hemodynamic PH type for the risk stratification and design of treatment strategy of ASD patients. The RHC is recommended for PH type diagnosis; the echocardiography-based studies cannot usually conclusively determine the hemodynamic type of PH, particularly in more severe PH.

The reversibility of PH is known to be affected by the severity of pulmonary vascular disease (PVD) and the extent of remodeling of the pulmonary vasculature (14). In the past, the prediction of PH normalization was assessed by histology from open lung biopsies; however, it was abandoned for risk of the procedure and non-uniform distribution of histological changes. More recently, non-invasive predictors of PH normalization have been suggested, reporting age at closure, NYHA class, degree of tricuspid regurgitation, and baseline PAP as significant predictors (4, 16, 24).

Interestingly, women comprised the vast majority of patients with PVR $\geq$ 3 WU (PAH and CpcPH, **Table 2**) in our study, although there was no significant difference in the rate of PH normalization between men and women. On the contrary, the hazard ratio for PH normalization was non-significantly better for women (HR = 1.6; $p = 0.16$), (**Table 3**).

Hyperkinetic PH

Hyperkinetic PH (H-PH) in ASD is a consequence of increased pulmonary blood flow due to the left-to-right shunt on the atrial level. Volume overload of the highly distensible pulmonary vascular bed in young patients may or may not lead to increased PAP. If the increased pulmonary pressure is proportional to the increased pulmonary flow, the PVR is low with no pulmonary vascular disease (PVD). With time, excess pulmonary blood flow can lead to early PVD changes with marked remodeling of the

distal pulmonary vasculature and loss of the elastic properties and stiffening of the large proximal pulmonary arteries. High pulmonary flow leads to upregulation of flow-sensitive genes with endothelial cell dysfunction and neomuscularization, which is reversible when the high pulmonary flow is normalized (13). In the case of progression of pulmonary vascular bed remodeling, PVR increases. If PVR exceeds 3 WU, the H-PH turns to PAH, suggesting the presence of a significant PVD. It is worth mentioning that the cut-off of 3 WU is relatively arbitrary, and PVR > 2 WU could be also considered abnormal (15). The impact of mildly increased PVR (2.5–3 WU) on patient prognosis in H-PH remains to be assessed.

In our study, H-PH was the most frequent PH type (55% patients). It was an independent positive predictor of PH normalization after ASD closure, manifesting the greatest normalization rate of 78%. Patients with H-PH had also significantly better long-term survival after defect closure compared to other types of PH, with a 10-year survival of 92%. This is in line with the mild PVD in H-PH, as well as high pulmonary pressure proportional to high pulmonary flow, resulting in normal or mildly increased PVR.

More attention therefore needs to be paid to the hyperkinetic type of PH in ASD. Some patients with high PAP due to H-PH may be erroneously considered inoperable by inexperienced cardiologists, even though their prognosis after ASD closure might have been very good with PH normalization. In addition, hyperkinetic PH patients misdiagnosed as having PAH may be prescribed expensive advanced therapy with no evidence of its utility for hyperkinetic PH. Therefore, consultation in specialized expert centers including RHC is important for patients with signs of moderate or severe PH according to echocardiography.

Pulmonary Arterial Hypertension

While being the most studied PH type in connection with shunt CHD, PAH was the least frequent type in our study (present in 10% patients with ASD). It showed 60% PH normalization rate and 77% 10-year survival rate after ASD closure. PAH is characterized by increased PVR (≥ 3 WU) and more severe PVD (2, 15). This includes not only the medial hypertrophy and intimal hyperplasia but also resistance to apoptosis, neointimal fibrosis with vascular lumen occlusion, and plexiform lesions (13). While high likelihood of irreversible changes in pulmonary vascular bed can be expected in patients with PVR above 5 WU (2, 11, 12, 25), such patients are contraindicated for ASD closure and therefore not a part of this study. However, more precise prediction of PH normalization in PAH patients with PVR of 3–5 WU is needed. The role of new methods such as nuclear imaging, circulating biomarkers, or specific genetic mutations should be evaluated in the future (13). Advanced pulmonary vasodilator therapy, before and/or after ASD closure, may be helpful in stabilization of the clinical state with NYHA improvement and lowering of PAP and PVR, even if not leading to complete PH normalization. Advanced therapy may lower PVR below 5 WU in some patients and thus allow ASD closure, usually with fenestration (treat-and-repair strategy) if significant left-to right shunt is still present (Qp:Qs > 1.5) (12).

Isolated Post-capillary PH

IpcPH was the second most frequent PH type (24% patients) with 52% normalization rate and 66% 10-year survival rate since ASD closure. IpcPH is a consequence of left heart failure with increased filling pressures and PCW ≥ 15 mmHg. The reason may be the co-incidence of ASD with mitral regurgitation or stenosis or with left ventricular (LV) systolic dysfunction. IpcPH may be also a consequence of LV diastolic dysfunction resulting from altered geometry of the LV due to severely dilated right ventricle. In post-capillary PH, the defect serves as a pop-off valve alleviating the risk of pulmonary edema in the case of high left atrial pressure. It is therefore important to exclude further increase of filling pressures after defect closure. Based on literature and our experience, temporary occlusion testing, fenestrated closure, heart failure treatment before defect closure and correction of valvular heart disease and arrhythmias are important and recommended (7, 19, 26).

Combined Pre- and Post-capillary PH

Little is known about clinical and physiological characteristics of CpcPH generally (27) and in connection with ASD. In our study, CpcPH was present in 11% patients with ASD. It was a significant negative predictor of PH normalization in our study (no patients normalized) and resulted in the lowest 10-year survival of 61%. Patients with this PH type also had the highest mPAP and sPAP and the highest rate of heart failure before ASD closure (55%). Patients with ASD and CpcPH were the oldest (median age of 66 and 69 years at diagnosis and defect closure, respectively). Patients with CpcPH develop more severe PVD than patients with IpcPH and resemble PAH in hemodynamic and genetic characteristics (27). Design of an optimal treatment strategy in these patients needs further research. In our experience, measures should be applied beyond ASD closure (if PVR is below 5 WU), such as heart failure treatment, concomitant valvular or antiarrhythmic surgery, fenestrated closure or pulmonary vasodilator treatment in individual cases and individual dosage before and/or after defect closure (27).

Patients with ASD and IpcPH or CpcPH due to left heart disease (mitral valve disease, left ventricular dysfunction, etc.) are sometimes excluded from research studies concerning ASD (14, 16). Consequently, information on their prognosis and treatment strategies is lacking. Our results demonstrate substantial differences between normalization rates and prognosis in IpcPH (52% normalized) vs. CpcPH (0% normalized), highlighting these as two functionally highly distinct types.

Summary

In conclusion, we investigated four different hemodynamic types of PH based on RHC, which may accompany ASD in adulthood. They differed in frequency within the studied cohort, likelihood of normalization following ASD closure, and in mortality. The high frequency and strong prognostic value of hyperkinetic PH suggests that this PH type is worth including and discussing in future ESC/ERS guidelines (2, 15). The knowledge of the PH type in ASD can help to guide a tailored treatment strategy.

LIMITATIONS OF THE STUDY

We used an older cut-off value for the diagnosis of PH with mPAP $\geq$ 25 mmHg in our study, based on the guidelines from the time of data collection and study design (2). According to our experience, inclusion of patients with mPAP 20–24 mmHg would only increase the number of patients with mild hyperkinetic PH who did not have RHC.

Given the retrospective nature of the study, certain clinical variables are missing in some of the patients. However, **Tables 2**, **3** contain the patient counts for each comparison so that the number of available measurements is clear.

Due to the exclusion criterion PVR > 5 WU in this study, advanced therapy was used only in 7 of our ASD patients with PH, which does not allow detailed analysis.

DATA AVAILABILITY STATEMENT

The raw data supporting the conclusions of this article will be made available by the authors, without undue reservation.

ETHICS STATEMENT

The studies involving human participants were reviewed and approved by Ethical Committee of the Na Homolce hospital. Written informed consent for participation was not required for this study in accordance with the national legislation and the institutional requirements.

AUTHOR CONTRIBUTIONS

JR conceived the study, collected the patient data, and is the guarantor of the study. RŽ contributed to data collection. JT and MT carried out data analysis. JT and JR wrote the initial draft, with all authors subsequently carrying out critical revisions. All authors contributed to the article and approved the submitted version.

FUNDING

This work was supported by Ministry of Health, Czech Republic–conceptual development of research organization, Nemocnice Na Homolce–NNH, Prague, Czech Republic, 00023884, IG160201 and Motol University Hospital, Prague, Czech Republic 00064203, IG6004.

ACKNOWLEDGMENTS

We thank the invasive cardiologists (A/Prof. Karel Hlaváček, MD, A/Prof. Martin Mates, MD, PhD, Petr Kmoníček, MD, Karel Kopřiva, MD) for their contribution.

REFERENCES

1. Murphy JG, Gersh BJ, McGoon MD, Mair DD, Porter CJ, Ilstrup DM, et al. Long-term outcome after surgical repair of isolated atrial septal defect. *N Engl J Med.* (1990) 323:1645–50. doi: 10.1056/NEJM199012133232401
2. Galiè N, Humbert M, Vachiery JL, Gibbs S, Lang I, Torbicki A, et al. 2015 ESC/ERS Guidelines for the diagnosis and treatment of pulmonary hypertension. *Eur Heart J.* (2016) 37:67–119. doi: 10.1016/j.rec.2016.01.002
3. Engelfriet P, Meijboom F, Boersma E, Tijssen J, Mulder B. Repaired and open atrial septal defects type II in adulthood: an epidemiological study of a large European cohort. *Int J Cardiol.* (2008) 126:379–85. doi: 10.1016/j.ijcard.2007.04.044
4. Gabriels C, De Meester P, Pasquet A, De Backer J, Paelinck BP, Morissens M, et al. A different view on predictors of pulmonary hypertension in secundum atrial septal defect. *Int J Cardiol.* (2014). doi: 10.1016/j.ijcard.2014.08.009
5. Akseer S, Abrahamyan L, Lee DS, Huszti E, Meier LM, Osten M, et al. Long-term outcomes in adult patients with pulmonary hypertension after percutaneous closure of atrial septal defects. *Circ Cardiovasc Interv.* (2022) 15:e011110. doi: 10.1161/CIRCINTERVENTIONS.121.011110
6. Rubáčková Popelová J, Tomková M, Tomek J, Živná R. Long-term survival of adult patients with atrial septal defect with regards to defect closure and pulmonary hypertension. *Front Cardiovasc Med.* 9:867012. doi: 10.3389/fcvm.2022.867012
7. Ranard LS, Mallah WE, Awerbach JD, Abernethy A, Halane M, Qureshi AM, et al. Impact of pulmonary hypertension on survival following device closure of atrial septal defects. *Am J Cardiol.* (2019) 124:1460–4. doi: 10.1016/j.amjcard.2019.07.042
8. Lammers AE, Bauer LJ, Diller GP, Helm PC, Abdul-Khaliq H, Bauer UMM, et al. Pulmonary hypertension after shunt closure in patients with simple congenital heart defects. *Int J Cardiol.* (2020) 308:28–32. doi: 10.1016/j.ijcard.2019.12.070
9. Opotowsky AR. Clinical evaluation and management of pulmonary hypertension in the adult with congenital heart disease. *Circulation.* (2015) 131:200–10. doi: 10.1161/CIRCULATIONAHA.114.006976
10. Jain S, Dalvi B. Atrial septal defect with pulmonary hypertension: when/how can we consider closure? *J Thorac Dis.* (2018) 10:S2890–8. doi: 10.21037/jtd.2018.07.112
11. Baumgartner H, Bonhoeffer P, De Groot NMSS, de Haan F, Deanfield JE, Galie N, et al. ESC Guidelines for the management of grown-up congenital heart disease (new version 2010). *Eur Heart J.* (2010) 31:2915–57. doi: 10.1016/j.repce.2012.05.004
12. Baumgartner H, De Backer J, Babu-Narayan SV, Budts W, Chessa M, Diller G-P, et al. 2020 ESC Guidelines for the management of adult congenital heart disease: the Task Force for the management of adult congenital heart disease of the European Society of Cardiology (ESC). *Eur Heart J.* (2020) 42:ehaa554. doi: 10.15829/1560-4071-2021-4702
13. Van Der Feen DE, Bartelds B, De Boer RA, Berger RMF. Assessment of reversibility in pulmonary arterial hypertension and congenital heart disease. *Heart.* (2019) 105:276–82. doi: 10.1136/heartjnl-2018-314025
14. Van Riel ACMJ, Schuuring MJ, Van Hessen ID, Zwinderman AH, Cozijnsen L, Reichert CLA, et al. Contemporary prevalence of pulmonary arterial hypertension in adult congenital heart disease following the updated clinical classification. *Int J Cardiol.* (2014) 174:299–305. doi: 10.1016/j.ijcard.2014.04.072
15. Simonneau G, Montani D, Celermajer DS, Denton CP, Gatzoulis MA, Krowka M, et al. Haemodynamic definitions and updated clinical classification of pulmonary hypertension. *Eur Respir J.* (2019) 53:1801913. doi: 10.1183/13993003.01913-2018
16. Yong G, Khairy P, De Guise P, Dore A, Marcotte F, Mercier LA, et al. Pulmonary arterial hypertension in patients with transcatheter closure of secundum atrial septal defects a longitudinal study. *Circ Cardiovasc Interv.* (2009) 2:455–62. doi: 10.1161/CIRCINTERVENTIONS.108.826560
17. Wood P. The Eisenmenger syndrome or pulmonary hypertension with reversed central shunt. *Br Med J.* (1958) 2:755–62. doi: 10.1136/bmj.2.5099.755
18. Newman JH. Pulmonary hypertension by the method of Paul Wood. *Chest.* (2020) 158:1164–1171. doi: 10.1016/j.chest.2020.02.035

19. Humenberger M, Rosenhek R, Gabriel H, Rader F, Heger M, Klaar U, et al. Benefit of atrial septal defect closure in adults: impact of age. *Eur Heart J.* (2011) 32:553–560. doi: 10.1093/eurheartj/ehq352
20. Parasuraman S, Walker S, Loudon BL, Gollop ND, Wilson AM, Lowery C, et al. Assessment of pulmonary artery pressure by echocardiography-A comprehensive review. *Int J Cardiol Hear Vasc.* (2016) 12:45–51. doi: 10.1016/j.ijcha.2016.05.011
21. Abbas AE, Franey LM, Marwick T, Maeder MT, Kaye DM, Vlahos AP, et al. Noninvasive assessment of pulmonary vascular resistance by Doppler echocardiography. *J Am Soc Echocardiogr.* (2013) 26:1170–7. doi: 10.1016/j.echo.2013.06.003
22. Aduen JF, Castello R, Lozano MM, Hepler GN, Keller CA, Alvarez F, et al. An alternative echocardiographic method to estimate mean pulmonary artery pressure: diagnostic and clinical implications. *J Am Soc Echocardiogr.* (2009) 22:814–819. doi: 10.1016/j.echo.2009.04.007
23. Grambsch PM, Therneau TM. Proportional hazards tests and diagnostics based on weighted residuals. *Biometrika.* (1994) 81:515. doi: 10.1093/biomet/81.3.515
24. Zwijnenburg RD, Baggen VJM, Witsenburg M, Boersma E, Roos-Hesselink JW, van den Bosch AE. Risk factors for pulmonary hypertension in adults after atrial septal defect closure. *Am J Cardiol.* (2019) 123:1336–42. doi: 10.1016/j.amjcard.2019.01.011
25. D'Alto M, Romeo E, Argiento P, Correra A, Santoro G, Gaio G, et al. Hemodynamics of patients developing pulmonary arterial hypertension after shunt closure. *Int J Cardiol.* (2013) 168:3797–3801. doi: 10.1016/j.ijcard.2013.06.036
26. Warnes CA, Williams RG, Bashore TM, Child JS, Connolly HM, Dearani JA, et al. ACC/AHA 2008 guidelines for the management of adults with congenital heart disease. *J Am Coll Cardiol.* (2008) 52:1890–1947. doi: 10.1016/j.jacc.2008.10.001
27. Assad TR, Hemnes AR, Larkin EK, Glazer AM, Xu M, Wells QS, et al. Clinical and biological insights into combined post- and pre-capillary pulmonary hypertension. *J Am Coll Cardiol.* (2016) 68:2525–2536. doi: 10.1016/j.jacc.2016.09.942

Conflict of Interest: The authors declare that the research was conducted in the absence of any commercial or financial relationships that could be construed as a potential conflict of interest.

Publisher's Note: All claims expressed in this article are solely those of the authors and do not necessarily represent those of their affiliated organizations, or those of the publisher, the editors and the reviewers. Any product that may be evaluated in this article, or claim that may be made by its manufacturer, is not guaranteed or endorsed by the publisher.

J. Piťha et al.

Cardiovascular, Metabolic and Inflammatory Changes after Ovariectomy and Estradiol Substitution in Hereditary Hypertriglyceridemic Rats

Int J Mol Sci.
Impact Factor: 5.542

‹ rejstřík

International Journal of
Molecular Sciences

MDPI

Article

Cardiovascular, Metabolic and Inflammatory Changes after Ovariectomy and Estradiol Substitution in Hereditary Hypertriglyceridemic Rats

Jan Pitha [1,*], Martina Huttl [2], Hana Malinska [2], Denisa Miklankova [2], Hana Bartuskova [3,4], Tomas Hlinka [3,5,6] and Irena Markova [2]

1 Cardiology Department, Cardiac Centre, Institute for Clinical and Experimental Medicine, 140 21 Prague, Czech Republic
2 Laboratory for Diabetes Pathology, Experimental Medicine Centre, Institute for Clinical and Experimental Medicine, 140 21 Prague, Czech Republic; mabw@ikem.cz (M.H.); haml@ikem.cz (H.M.); mild@ikem.cz (D.M.); irma@ikem.cz (I.M.)
3 Atherosclerosis Research Laboratory, Experimental Medicine Centre, Institute for Clinical and Experimental Medicine, 140 21 Prague, Czech Republic; kubh@ikem.cz (H.B.); hlit@ikem.cz (T.H.)
4 Department of Physiology, Faculty of Science, Charles University, 128 44 Prague, Czech Republic
5 Internal Department, 2nd Medical Faculty, Charles University Prague, 150 06 Prague, Czech Republic
6 Faculty Hospital Motol Prague, 150 06 Prague, Czech Republic
* Correspondence: jan.pitha@ikem.cz

Abstract: Background: If menopause is really independent risk factor for cardiovascular disease is still under debate. We studied if ovariectomy in the model of insulin resistance causes cardiovascular changes, to what extent are these changes reversible by estradiol substitution and if they are accompanied by changes in other organs and tissues. Methods: Hereditary hypertriglyceridemic female rats were divided into three groups: ovariectomized at 8th week (n = 6), ovariectomized with 17-β estradiol substitution (n = 6), and the sham group (n = 5). The strain of abdominal aorta measured by ultrasound, expression of vascular genes, weight and content of myocardium and also non-cardiac parameters were analyzed. Results: After ovariectomy, the strain of abdominal aorta, expression of nitric oxide synthase in abdominal aorta, relative weight of myocardium and of the left ventricle and circulating interleukin-6 decreased; these changes were reversed by estradiol substitution. Interestingly, the content of triglycerides in myocardium did not change after ovariectomy, but significantly increased after estradiol substitution while adiposity index did not change after ovariectomy, but significantly decreased after estradiol substitution. Conclusion: Vascular and cardiac parameters under study differed in their response to ovariectomy and estradiol substitution. This indicates different effects of ovariectomy and estradiol on different cardiovascular but also extracardiac structures.

Keywords: ovariectomy; cardiovascular changes; estradiol substitution; insulin resistance; hereditary hypertriglyceridemic rat

Citation: Pitha, J.; Huttl, M.; Malinska, H.; Miklankova, D.; Bartuskova, H.; Hlinka, T.; Markova, I. Cardiovascular, Metabolic and Inflammatory Changes after Ovariectomy and Estradiol Substitution in Hereditary Hypertriglyceridemic Rats. *Int. J. Mol. Sci.* **2022**, *23*, 2825. https://doi.org/10.3390/ijms23052825

Academic Editor: Ioanna Andreadou

Received: 31 January 2022
Accepted: 28 February 2022
Published: 4 March 2022

1. Introduction

It is still matter of debate whether menopause is an independent cardiovascular risk factor. However, cardiovascular disease (CVD) caused mainly by atherosclerosis is the primary and underscored cause of morbidity and mortality in women [1,2]. Moreover, in addition to traditional risk factors for atherosclerotic disease and subsequent cardiovascular events, insulin resistance associated with metabolic syndrome was definitely proved to be risk factor for atherosclerosis and menopause could further aggravate and, potentially, also even trigger unfavorable vascular changes. In addition, if female sex hormone substitution therapy after menopause could reverse unfavorable vascular changes remains very controversial topic which is intensively investigated on experimental and human

level [3–5]. Several studies indicated that if hormonal substitution therapy is started early after menopause, it could have favorable vascular effects. This is in contrast to previous unsuccessful studies which initiated hormone substitution therapy later after menopause [6,7]. However, despite many studies focused on the timing of hormone substitution therapy after menopause, less data is available regarding the effect of such intervention on traditional atherosclerotic risk factors and other cardiovascular parameters but especially few data exist regarding effect of hormone substitution therapy on extracardiac organs and tissues. In particular, there are only few data available, to what extent exactly are atherosclerotic and, in general, cardiovascular changes reversible by hormone substitution therapy, which factors could be associated with (un)favorable changes of involved organs and if these changes are associated with changes in other organs and tissues. This topic is of high importance, because the presence of metabolic and other atherosclerotic and cardiovascular risk factors before menopause could strongly determine success of hormonal substitution therapy after menopause. Such interaction between hormone substitution therapy and presence of risk factors or already present vascular pathology could potentially determine future development of CVD in women [8]. Regarding optimal timing of potential intervention, in our previous cross-sectional study of population sample of middle-aged women, we detected much stronger impact of smoking on preclinical atherosclerosis defined as carotid intima media thickness in perimenopausal women than in pre- and postmenopausal women [9], potentially partly mediated by remnant lipoproteins [10]. In addition, in our experimental study in hamster model [11] the hypolipidemic treatment with simvastatin substantially decreased the prevalence of atherosclerotic changes after ovariectomy, but otherwise did not change concentration of atherogenic LDL cholesterol. Nevertheless, statin treatment improved proportions of pro- and antiatherogenic serum lipids by the increase of HDL cholesterol. Therefore, antiatherogenic effect of statin treatment in this study was not mediated by decrease of concentration of LDL cholesterol, but by the increase of concentration of HDL cholesterol. Notably, in this model, the timing of simvastatin treatment had no significant effect on prevention of atherosclerotic changes or lipid parameters. More complex changes after menopause beyond circulating lipoproteins should be, therefore, studied.

In general, development of cardiovascular disease after menopause is a complex and challenging process and the research in this field is focused on unfavorable arterial changes at early stages of cardiovascular disease. Recently the use of non-invasive imaging strategies, such as ultrasound studies of cardiac, but also aortic, cerebral, and peripheral vascular disease models in rodents is widely implemented and ultrasound detection of vascular disease is expanding methodology which allows longitudinal studies of different vascular and cardiac structures in living animals [12]. This could be specifically applicable for studying the effect of menopause on cardiovascular structures prospectively also in animal models.

In the recent study, we focused on the more complex effect of ovariectomy and estradiol substitution on vascular, cardiac, but also extravascular and extracardiac organs and tissues, and metabolic, genetic and inflammatory parameters in already well-established experimental model of insulin resistance, dyslipidemia, mild hypertension and low-grade inflammation, particularly in hereditary hypertriglyceridemic (HHTg) female rats [13].

The main aim was to investigate cardiovascular, metabolic and inflammatory changes caused by ovariectomy in the terrain of insulin resistance, i.e., mimicking menopause in women with already present metabolic and inflammatory burden. We also studied to what extent are these changes reversible with female sex hormone substitution, namely with estradiol. In addition, we analyzed vascular parameters through repeated examination of vascular system by ultrasound, but also structure and content of extravascular and extracardiac organs and tissues.

2. Results

At the start of the experiments, study groups (sham, ovariectomized and ovariectomized with estradiol substitution) did not differ in weight and, no pathological changes in abdominal aorta were detected by ultrasound before start of the study. Body weight increased in ovariectomized group during the study and remained stable in the group with estradiol substitution. In addition, food intake increased in ovariectomized females without estradiol substitution compared to other two groups.

2.1. Changes of Cardiovascular Parameters after Ovariectomy and Estradiol Substitution

At the end of the study, the strain of suprarenal aorta after ovariectomy was non-significantly lower in suprarenal and significantly lower in infrarenal aorta and in ovariectomized females with estradiol substitution the strain of suprarenal and infrarenal aorta was significantly higher than in ovariectomized females without estradiol substitution; in suprarenal aorta, the strain after estradiol substitution was higher not only than in ovariectomized rats (p = 0.002) but also than in the sham group (p = 0.02) (Figure 1, Table A1/Appendix A); even more pronounced increase was detected for the strain in suprarenal aorta, but it was partly caused by higher diameter of this segment measured at the start of the study (data not shown). Similar pattern was found for heart rate. The heart rate at baseline was 297.0 ± 18.0, 324.7 ± 30.0, and 372.0 ± 22.5 beats per minute in sham, ovariectomized group and in ovariectomized group with estradiol substitution, respectively (one-way ANOVA: $p < 0.001$). The heart rate at the end of the study was 319.4 ± 29.7, 284.2 ± 25.9, and 285.0 ± 30.3 beats per minute in sham, ovariectomized group and in ovariectomized group with estradiol substitution, respectively (one-way ANOVA: $p < 0.881$). This means that in ovariectomized rats and in ovariectomized rats with estradiol substitution heart rate significant decreased (Figure A1/Appendix A).

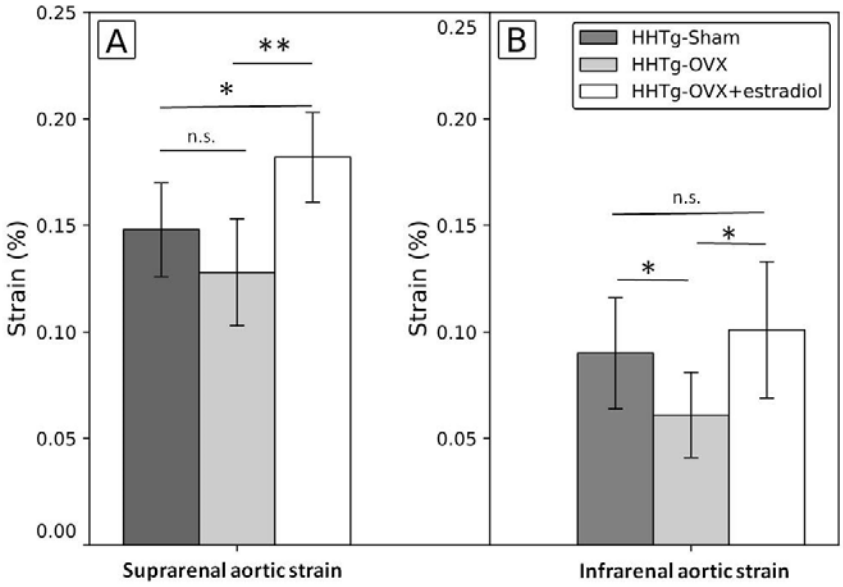

Figure 1. Differences in the strain of the abdominal aorta after ovariectomy and estradiol substitution in HHTg rats in suprarenal (**A**) and infrarenal (**B**) segments. Legend: Strain: (systolic-diastolic aortic diameter)/diastolic aortic diameter; HHTg: hereditary hypetriglyceridemic; HHTg-Sham: sham group, n = 5; HHTg-OVX: Ovx: ovariectomy (n = 6); HHTg-OVX + estradiol: ovariectomy followed by estradiol substitution (n = 6). Data are expressed as mean ± SD and evaluated by one-way ANOVA and Fisher LSD post-hoc test; n.s.: nonsignificant, * $p < 0.05$, ** $p < 0.01$.

In addition, the expression of the gene for nitric oxide synthase 3 (*Nos3*) measured in the whole abdominal aorta irrespectively of supra/infrarenal segment was significantly lower after ovariectomy while in ovariectomized females treated with estradiol it was similar to the sham group. No significant between-group differences were observed for

connexin 37 (*Cx37*) gene expression measured also in the whole abdominal aorta (Figure 2). No between group differences were detected for circulating nitric oxide synthase (NOS) (Table A1/Appendix A). The correlation between *Nos3* and *Cx37* gene expression was r = 0.459 in the whole group, r = 0.752, r = 0.183, and r = 0.624 for the sham group, ovariectomized rats, and ovariectomized rats with estradiol substitution, respectively.

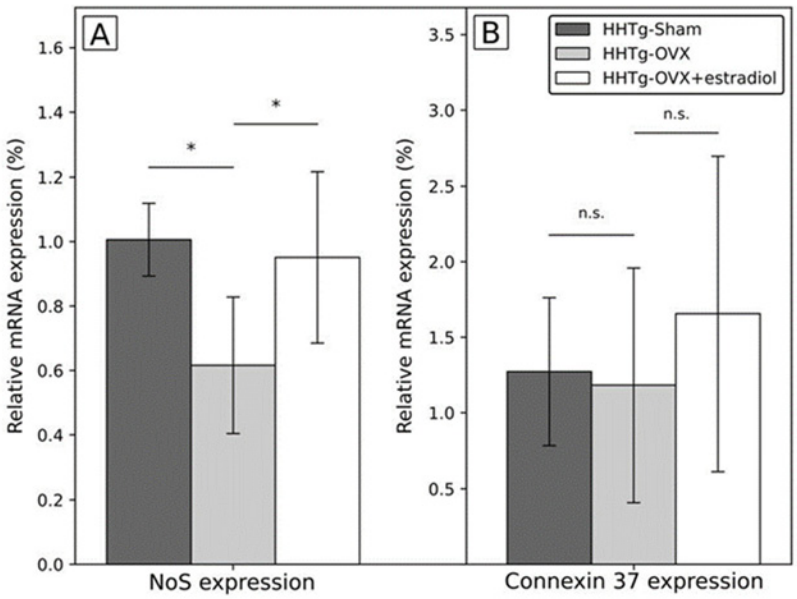

Figure 2. Differences in the expression of genes in abdominal aorta after ovariectomy and estradiol substitution in HHTg rats. Legend: HHTg: hereditary hypetriglyceridemic; HHTg-Sham: sham group, $n = 5$; HHTg-OVX: Ovx: ovariectomy ($n = 6$); HHTg-OVX + estradiol: ovariectomy followed by estradiol substitution ($n = 6$). (**A**) NoS expression: expression of the gene for *nitric oxid synthase*, (**B**) Connexin 37 expression: expression of the gene for *connexin 37*. Data are expressed as mean ± SD and evaluated by one-way ANOVA and Fisher LSD post-hoc test; n.s.: nonsignificant, * $p < 0.05$.

Regarding cardiac parameters, relative weight of myocardium and the weight of the left ventricle were significantly lower in ovariectomized females than in the sham group at the end of the experiment while in ovariectomized females with estradiol substitution they were similar to the sham group. Different pattern was observed for the content of triglycerides in the myocardium which was similar in ovariectomized females at the end of the study as in the sham group, but significantly higher in ovariectomized females with estradiol substitution than in other two groups (Figure 3). However, no between group differences were found in the expression of genes potentially responsible for triglyceride and/or other lipid content in the heart, oxidative stress and other pathophysiological pathways/homeostatic mechanisms: namely lipoprotein lipase, stearoyl-CoA-desaturase-1, nuclear factor E2-related factor 2 and connexin 43 (data not shown).

2.2. Changes in Other Organs after Ovariectomy and Estradiol Substitution

Changes of these parameters are shown in Table 1. Body weight was significantly higher in ovariectomized females than in the sham group, and similar in ovariectomized females with estradiol substitution as in the sham group at the end of the study. In addition, relative and absolute weight of uterus was lower in ovariectomized females than in the sham group, and similar in ovariectomized females with estradiol substitution as in the sham group. Interestingly, the adiposity index was similar in ovariectomized females as in the sham group, but in ovariectomized females substituted with estradiol it was significantly lower than in other two groups; in other words, reversed pattern compared to the content of triglycerides in myocardial tissue was observed. Relative liver weight was significantly lower in ovariectomized females than in the sham group and was found to be

higher in ovariectomized rats with estradiol substitution than in the sham group. Similar patterns for the effect of ovariectomy and ovariectomy with estradiol substitution were found for: increased and decreased content of triglycerides in the liver tissue, increased and decreased content of cholesterol in the liver tissue, decreased and increased relative weight of kidneys, and increased and decreased content of triglycerides in the renal cortex, respectively. No between group differences were detected for the content of triglycerides in the skeletal muscle.

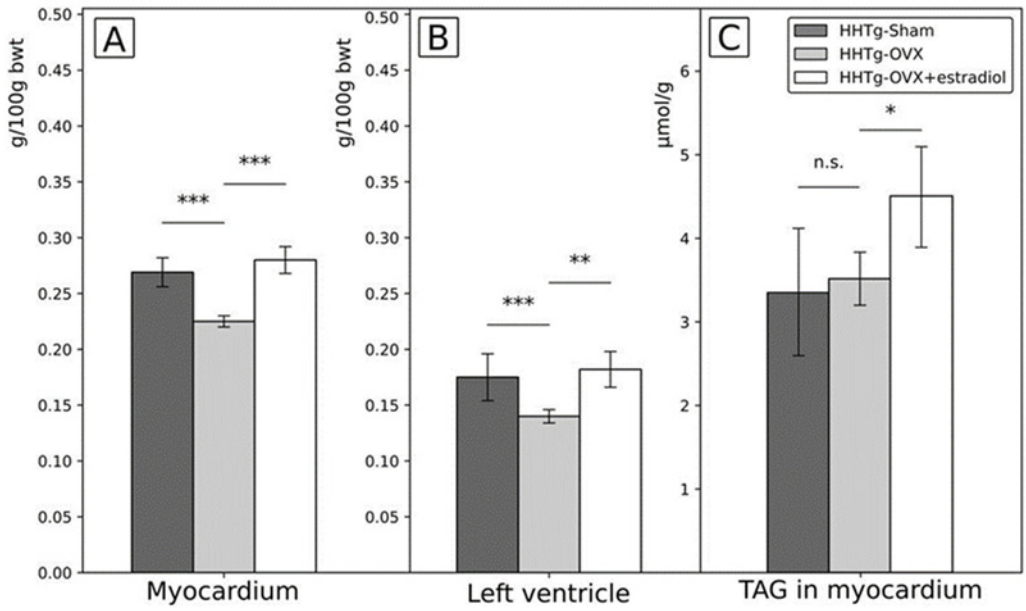

Figure 3. Differences in the relative weight of myocardium (**A**) and the left ventricle (**B**) and triglycerides content of the myocardium (**C**) after ovariectomy and estradiol substitution in HHTg rats. Legend: HHTg: hereditary hypetriglyceridemic; HHTg-Sham: sham group, $n = 5$; HHTg-OVX: Ovx: ovariectomy ($n = 6$); HHTg-OVX + estradiol: ovariectomy followed by estradiol substitution ($n = 6$). Data are expressed as mean ± SD and evaluated by one-way ANOVA and Fisher LSD post-hoc test; n.s.: nonsignificant, * $p < 0.05$, ** $p < 0.01$, *** $p < 0.001$.

Table 1. Differences after Ovariectomy and Estradiol Substitution in Hereditary Hypertriglyceridemic Rats in the Relative Weight and Lipid Content of Extracardiac Tissues and Organs.

	Sham $n = 5$	**Ovx** $n = 6$	**Ovx + Estradiol** $n = 6$	**One-Way ANOVA**	***p*** **Ovx vs. Sham**	***p*** **Ovx + E vs. Ovx**
Body weight (g)	242.4 ± 8.2	272.2 ± 12.9	238.0 ± 12.9	0.001	0.001	0.001
Uterus (g/100 g bwt)	0.226 ± 0.029	0.098 ± 0.034	0.290 ± 0.069	0.001	0.001	0.001
Adiposity index (g/100 g bwt)	2.051 ± 0.453	2.253 ± 0.397	1.620 ± 0.336	0.05	n.s.	0.05
Liver (g/100 g bwt)	3.283 ± 0.095	2.556 ± 0.042	3.769 ± 0.094	0.001	0.001	0.001
Hepatic content of triglycerides (µmol/g)	7.885 ± 1.853	12.970 ± 1.533	10.215 ± 0.851	0.001	0.001	0.01
Hepatic content of cholesterol (µmol/g)	6.581 ± 0.826	9.950 ± 0.593	6.763 ± 1.029	0.001	0.001	0.001
Kidneys (g/100 g bwt)	0.570 ± 0.015	0.438 ± 0.009	0.620 ± 0.027	0.001	0.001	0.001
Content of triglycerides in the renal cortex (µmol/g)	0.771 ± 0.067	1.075 ± 0.112	0.824 ± 0.049	0.001	0.001	0.001
Content of triglycerides in the skeletal muscles (µmol/g)	1.223 ± 0.242	1.467 ± 0.205	1.491 ± 0.621	n.s.	n.s.	n.s.

Legend: Data are given as the mean ± SD. One-way ANOVA and Fisher LSD post-hoc test were used. Ovx: ovariectomy, Ovx + E: Ovariectomy and estradiol substitution. Data are expressed as mean ± SD and evaluated by one-way ANOVA and Fisher LSD post-hoc test; n.s.: non.significant.

2.3. Circulating Metabolic, Inflammatory and Hormonal Parameters after Ovariectomy and Estradiol Substitution

Serum estradiol was significantly lower in ovariectomized females than in the sham group, and was significantly higher in ovariectomized females with estradiol substitution, in the latter group reaching very high values. Progesterone was significantly lower in

ovariectomized females than in the sham group and remained at the same level in ovariectomized females substituted with estradiol as in ovariectomized females without estradiol substitution. No between group differences were detected for circulating Anti-Mullerian hormone (AMH). Regarding serum cholesterol, no differences were found between study groups. Serum triglycerides were significantly lower in the ovariectomized females than in the sham group while in the ovariectomized females with estradiol substitution they were at the same level as in the sham group. Serum HDL cholesterol was significantly higher in ovariectomized females than in the sham group, and in ovariectomized females with estradiol substitution it was higher than in other two groups. No between group differences were detected for circulating free fatty acids (FFA), non-fasting glucose, insulin and glucagon. The concentration of liver enzymes (AST, ALT) was higher in ovariectomized females than in the sham group, and in ovariectomized females after estradiol substitution it stayed at similar level as in ovariectomized rats. Serum concentration of interleukin 6 (IL-6) was significantly lower in ovariectomized females than in the sham group, and was significantly higher in ovariectomized females with estradiol substitution, in the latter group, the concentration of IL-6 was even higher than in the sham group ($p = 0.001$).

2.4. Summary of Changes of Parameters with Regard to Ovariectomy and Estradiol Substitution

Significant changes after ovariectomy reversed by estradiol substitution were increased body weight, decreased expression of *Nos3* in the abdominal aorta, decreased relative weight of myocardium, decreased relative weight of the left ventricle, and changes in the liver and kidney parameters including decreased relative organ weight, increased content of cholesterol and triglycerides in particular organs and tissues, and decreased circulating triglycerides. Significant changes after ovariectomy modified by estradiol substitution to the levels significantly different than were in the sham group was decreased strain of infrarenal segment of the abdominal aorta, increased serum HDL cholesterol and decreased circulating IL-6. Significant changes after ovariectomy not reversed by estradiol substitution were decreased serum progesterone level and increased liver enzymes. No effect of ovariectomy and of the ovariectomy followed by estradiol substitution was observed for AMH, NOS, expression of *Cx37*, circulating FFA, non-fasting glycemia, serum insulin, and glucagon. No effect of ovariectomy but significant changes after ovariectomy with estradiol substitution were observed for the increased triglycerides content in myocardium, increased strain of suprarenal aorta, and decreased adiposity index.

3. Discussion

Regarding vascular parameters under study, the main finding was that aortic strain moderately decreased after ovariectomy but increased significantly if ovariectomy was followed by estradiol substitution; in the suprarenal segment estradiol substitution after ovariectomy led even to significantly higher levels of the aortic strain than in the sham group (Figure 1, Table A1/Appendix A). These vascular changes were accompanied by changes in the expression of *Nos3* gene which demonstrated similar pattern; it decreased after ovariectomy and increased to the levels similar as in the sham group if ovariectomy was followed by estradiol substitution. On one hand, these findings demonstrated unfavorable effect of decrease of sex female hormones, on the other hand, favorable effect of estradiol substitution on the vasculature already was detected as in already detected in human and experimental studies [14–17]. Moreover, our findings indicate mechanisms potentially more or less involved in the vascular effects of sex hormones, in this case estradiol. In contrast to the favorable effect of estradiol on aortic strain and expression of *Nos3*, there was no effect of the ovariectomy and/or estradiol substitution on the expression of also "cardiovascular" gene for *Cx37* [18,19], which is potential target for intervention in cardiovascular disease [20] and described as important for cardiovascular disease in previous (but not all) studies [21–24]. The explanation for this negative finding could be that the change of *Cx37* gene expression was not yet detectable relatively soon after ovariectomy and could be relatively delayed compared to the change of the expression of gene for

Nos3. In addition, changes of *Cx37* activity and gap junctions were described mainly in the smaller vessels including mice and dependent on changes of shear stress [25,26]. Therefore, in abdominal aorta, the changes of shear stress in rats compared to mice could be less pronounced in this location due simply to larger diameter and in contrast to *Nos3* gene, *Cx37* gene could be less sensitive to these changes. Another explanation comes from our pilot experimental study in which the expression of *Cx37* gene was significantly lower in the suprarenal than in the infrarenal segment in four Prague hypercholesterolemic females on standard diet (suprarenal segment of abdominal aorta: 1.009 ± 0.152 vs. infrarenal segment: 2.011 ± 0.297; $p = 0.015$; unpublished data). Notably, it was not observed on hypercholesterolemic diet. Therefore, if we can suppose similar situation in HHTg rats in which we measured *Cx37* gene expression in the whole abdominal aorta, we could miss segment specific differences in expression of particular genes including gene for *Cx37*. We noted, that changes after ovariectomy/estradiol substitution both in *Cx37* gene expression, but also in circulating NOS were similar to changes of aortic strain and of *Nos3* but were not statistically significant (Figure 2, Table A1/Appendix A). In this particular study, Cx37 was involved in basal nitric oxide release, release of cyclooxygenase products and the regulation of the sensitivity for acetylcholine in contrast to connexin 40. We found rather strong correlation between *Nos3* and *Cx37* gene expression which was not present in the ovariectomized group in contrast to the sham group and ovariectomized group with estradiol substitution, but because of relatively low numbers of animals in each group we are cautious to interpret these data on biological grounds.

Regarding cardiac parameters, the relative weight of myocardium and of the left ventricle decreased significantly after ovariectomy and were completely reversed by estradiol substitution to values similar as in the sham group. These findings could be explained by rapid decrease of myocardial mass due also at least partly to rapid decrease of sex hormones and decreased number of estradiol receptors in cardiac tissue after ovariectomy and their restoration after estradiol substitution [27,28]. Changes levels of estradiol could be also the cause of the significant changes of the heart rate, this could be caused also by changes in estradiol receptors function and their impact on sensitivity of the heart to stress. In addition, in recent study it has been shown in mice that cellular content of the heart is dependent on and can be rapidly changed by endocrine factors, particularly gonadal hormones [28–31]. In previous study estrogen (and also testosterone) were shown to have direct interactions with ion channels and were able to transcriptionally alter ion channel expression in a regionally dependent manner, in rabbit heart [32]. Changes of sex hormone could, therefore, lead to different stress responses of the heart, but it should be noted, that estradiol can have discordant cardiac effects based on the experimental models used. However, in our study rather the rate of change of estradiol concentration was of importance, because similar pattern, decrease of heart rate, was detected both in ovariectomized females and in ovariectomized females with estradiol substitution. Nevertheless, because of different values of heart rates detected at the beginning of the study in our study groups, we are also cautious in the interpretation of these data. Moreover, no between group differences were found in myocardial tissue for the expression of genes which could be potentially responsible for impaired homeostatis especially in lipid metabolism.

In contrast to changes of myocardial mass, content of triglycerides in myocardium changed after ovariectomy differently; the content of triglycerides in myocardium was not affected by ovariectomy but it increased significantly if ovariectomy was followed by estradiol substitution even above the values in the sham group. Increased content of triglycerides in heart muscle is recently under investigation and considered to be unfavorable process [33–35], however, which might be modified [36,37]. In this respect and with respect to findings in other tissues, the favorable effect of estradiol in this case is questionable and it seems that estradiol could cause also unfavorable shifts of fat content between different body compartments [37], including myocardial tissue. Therefore, the evaluation also of other organs and tissues in our study was important. Interesting finding in this respect was the changes of adiposity index (Table 1) as the marker for central fat; it was

not affected by ovariectomy but decreased when ovariectomy was followed by estradiol treatment. Therefore, it followed reverse pattern as observed in the content of triglycerides in myocardial tissue (Figure 3); IL-6 could also modify this process as discussed later. In addition, also changes in the liver and renal cortex reflected significant increase in the content of triglycerides after ovariectomy reversed when ovariectomy was followed by estradiol substitution (Table 1). Notably, these rather robust changes in the mass and content of organs and tissues were not accompanied by changes in circulating FFA, and cholesterol, non-fasting glycemia, circulating insulin and glucagon. The explanation could be from previous experimental study in Wistar rats [38] indicating that organ changes after ovariectomy could precede changes in circulating factors, in this case not only changes of circulating lipids but also of parameters associated with glucose homeostasis. Regarding changes in circulating serum lipids, triglycerides decreased after ovariectomy and increased when estradiol was substituted after ovariectomy. It means that changes of serum triglycerides were in opposite direction compared to changes of the content of triglycerides in the liver and in the renal cortex (Tables 1 and 2). Therefore, changing levels of estradiol were associated with redistribution between serum triglycerides and triglycerides in these organs. In addition, concentration of HDL cholesterol increased significantly after ovariectomy and increased even further if ovariectomy was followed by estradiol substitution. It should be noted, that neither in human plasma serum/plasma concentration of HDL cholesterol exactly reflect structure or mechanisms of the real metabolic activity of HDL particles [39]. In addition, in rodents HDL cholesterol could play different roles than in humans [40]. Therefore, changes of HDL cholesterol concentrations after ovariectomy and ovariectomy followed by estradiol treatment definitely could not be definitely defined as favorable, i.e., concentration of HDL cholesterol does not reflect only positive effects. Notably, HDL cholesterol could interact also with non-cardiovascular structures [41] and also changes of HDL cholesterol concentration caused by ovariectomy and/or estradiol treatment are rather complex [42].

Table 2. Differences after Ovariectomy and Estradiol Substitution in Circulating Metabolic and Inflammatory Parameters in Serum in Hereditary Hypertriglyceridemic Rats.

	Sham $n = 5$	**Ovx** $n = 6$	**Ovx + Estradiol** $n = 6$	**One-Way ANOVA**	***p*** **Ovx vs. Sham**	***p*** **Ovx + E vs. Ovx**
17β-estradiol (pg/mL)	35.16 ± 4.40	23.37 ± 3.58	314.95 ± 104.33	0.001	n.s.	0.001
Progesterone (ng/mL)	1.542 ± 0.366	0.417 ± 0.083	0.563 ± 0.061	0.001	0.001	n.s.
Anti-Mullerian hormone (ng/mL)	6.725 ± 1.645	6.654 ± 2.201	5.884 ± 0.636	n.s.	n.s.	n.s.
Cholesterol (mmol/L)	1.564 ± 0.265	1.795 ± 0.181	2.027 ± 0.244	0.01	n.s.	n.s.
Triglycerides (mmol/L)	4.826 ± 1.073	2.220 ± 0.706	4.187 ± 0.698	0.001	0.001	0.01
HDL-cholesterol (mmol/L)	0.808 ± 0.085	1.025 ± 0.138	1.230 ± 0.078	0.001	0.01	0.01
Free fatty acids (mmol/L)	0.520 ± 0.132	0.625 ± 0.109	0.528 ± 0.091	n.s.	n.s.	n.s.
Non-fasting glucose (mmol/L)	8.260 ± 0.666	8.350 ± 0.709	8.317 ± 0.741	n.s.	n.s.	n.s.
Insulin (nmol/L)	0.191 ± 0.059	0.160 ± 0.034	0.151 ± 0.030	n.s.	n.s.	n.s.
Glucagon (pg/mL)	201.8 ± 25.5	214.1 ± 37.1	219.2 ± 18.6	n.s.	n.s.	n.s.
Alanine aminotransferase (μkat/L)	0.960 ± 0.082	1.250 ± 0.096	1.222 ± 0.118	0.001	0.001	n.s.
Aspartate aminotransferase, (μkat/L)	2.540 ± 0.179	3.202 ± 0.309	2.977 ± 0.226	0.01	0.001	n.s.
Circulating Interleukin 6 (pg/mL)	106.65 ± 7.47	72.73 ± 14.98	173.31 ± 22.06	0.001	0.01	0.001

Legend: Data are given as the mean ± SD, One-way ANOVA and Fisher LSD post-hoc test were used. Ovx: ovariectomy, Ovx + E: Ovariectomy and estradiol substitution. Data are expressed as mean ± SD and evaluated by one-way ANOVA and Fisher LSD post-hoc test; n.s.: nonsignificant.

The last interesting finding was the change of supposedly pro-inflammatory factor, circulating IL-6 (Table 2). These changes were of similar pattern as changes in aortic vascular strain, myocardial, liver and kidney mass and of reverse pattern than was observed in adiposity index. It means IL-6 significantly decreased after ovariectomy and increased to concentration significantly higher than in the sham group if ovariectomy was followed by estradiol substitution. Such change of IL-6 seems to be counterintuitive, but IL-6 in the early stages of vascular impairment could play more ambiguous and even protective role on the vessel wall [43]. From previous findings, the role of the IL-6 is really ambiguous and could exert different effects on cardiovascular system especially in the terrain of fluctuating sex

hormones [44,45]. Additionally, it cannot be excluded that IL-6 could be involved also in the shift of lipids between various organs and tissues including myocardial muscle [46,47].

Limitation of our study is the absence of blood pressure values at the time of ultrasound measurements of aortic strain; blood pressure at the time of measurements is very tightly associated with this parameter. Nevertheless, invasive methods, the most reliable methods for blood pressure measurements in experimental models to date, can adversely affect obtained results; changes in aortic strain were logical and offered biological plausibility. In addition, in our study we were focused not only on the arterial properties but also on cardiac and non-cardiac changes. Another limitation could be the focus on the abdominal aorta only and not on the other vessels, experimental studies in this area are focused mainly on the model of abdominal aneurysm [48]. The evaluation of the whole vasculature could be now possible with ultrasound studies.

Another potential limitation to be discussed is the dosage of estradiol and its relatively high concentration after substitution. In our study, the concentration of estradiol after supplementation was much higher than in the sham group (315 $\pm$ 57 pg/mL vs. 35 pg/mL). In this respect, the dosage of estradiol was based on the information from previous studies and was similar as in other published experiments. Dosage of estradiol 3 µg/day administered through pump device, produced concentration of estradiol after 6 weeks in serum 242 $\pm$ 89 pg/mL [49]. Polito et al. [50] administered doses 0.003 and 0.03 mg of estradiol/kg per day in their experimental study without determined consequent estradiol levels in circulation. In general, in available literature, in rat females is the concentration of estradiol dependent on estrus and fluctuates in the range of 145–2100 pg/mL. In some papers it could fluctuate in the range of 20–60 pg/mL. From vascular point of view, higher doses of estradiol were studied intensively in the cerebral circulation and, interestingly, proved to be protective irrespectively of ovariectomy [51]. However, the effects of estradiol could be also dependent on the route of administration [52].

The strength of our study is specific design of repeated ultrasound measurements of vascular changes in the same animal before and after intervention focused on functional arterial properties and, more importantly complex assessment not only of cardiovascular but also extracardiac parameters with possibility to study potential interactions between cardiac, vascular and other organs and tissues after ovariectomy and estradiol substitution in the terrain of insulin resistance. Another advantage of this study is the focus on reciprocal interactions between multiple organs after mimicking menopause and hormonal substitutional therapy; as to our best knowledge, such approach was very rarely applied.

The main message from this study is that not all cardiovascular changes after estradiol substitution after ovariectomy need to be favorable especially at the background of already present metabolic disorders including insulin resistance accompanied by the inflammatory status. These findings highlight need to assess changes after menopause and hormonal substitution therapy in a complex manner including also assessment of the role of extravascular and extracardiac structures and the complex status of organism at the time of rapid hormonal changes induced by menopause but also by sex hormone substitution. In another words, effects of estradiol substitution after menopause really need not to be favorable in all aspects and in all individuals.

4. Materials and Methods

4.1. Animals and Diet

Design/flowchart of the study is presented in Figure 4. HHTg female rats were included in the study as optimal model for prediabetes and insulin resistance [13]. This strain is characterized by the presence of genetically determined hypertriglyceridemia, insulin resistance of peripheral tissues and hepatic steatosis but with the absence of obesity and fasting hyperglycemia. All animals used in the present study were bred at the animal house of the Center of Experimental Medicine, Institute for Clinical and Experimental Medicine (IKEM, Prague, Czech Republic). All of the experiments were performed in agreement with the Animal Protection Law of the Czech Republic (311/1997), which is in

compliance with European Community Council recommendations (86/609/ECC) for the use of laboratory animals, and were approved by the Ethics Committee of the Institute for Clinical and Experimental Medicine, Project No. 6/2020. Rats were kept at a temperature of 22 °C and humidity-controlled conditions under a 12/12 h light/dark cycle with free access to a standard chow diet (Altromin, Maintenance diet for rats and mice, Lage, Germany) and drinking water. At the beginning of the study female rats were randomly divided into three experimental groups (n = 6), with measurements taken for body weight, serum glucose and triglycerides. At 8 weeks of age, were anesthetized with ketamine (70 mg/kg) and xylazine (10 mg/kg) administered intraperitoneally and then bilaterally ovariectomized using a midline incision (W-OVX). Sham-operated animals underwent the entire surgery, except for the removal of ovaries. Animals were saturated with oxygen throughout the procedure followed by subcutaneous analgesia (meloxicam 1 mg/kg). The health status of animals was monitored post-surgery. Two weeks after ovariectomy, 17-β estradiol subcutaneous therapy, in a dose 12.5 µg of 17-β estradiol (Sigma-Aldrich, St. Louis, MO, USA)/ kg body weight per day, was started in HHTg group supplemented with estradiol after ovariectomy. Food intake was measured weekly over a 4-month period to ensure the likely development of metabolic disorders associated with postmenopausal metabolic syndrome, as reported in previous studies [53]. At the end of the experiment, rats were sacrificed by decapitation after light anaesthetization (zoletil 5 mg/kg b.wt.) in a postprandial state. Aliquots of serum and tissue samples were collected and stored at −80 °C for further analysis.

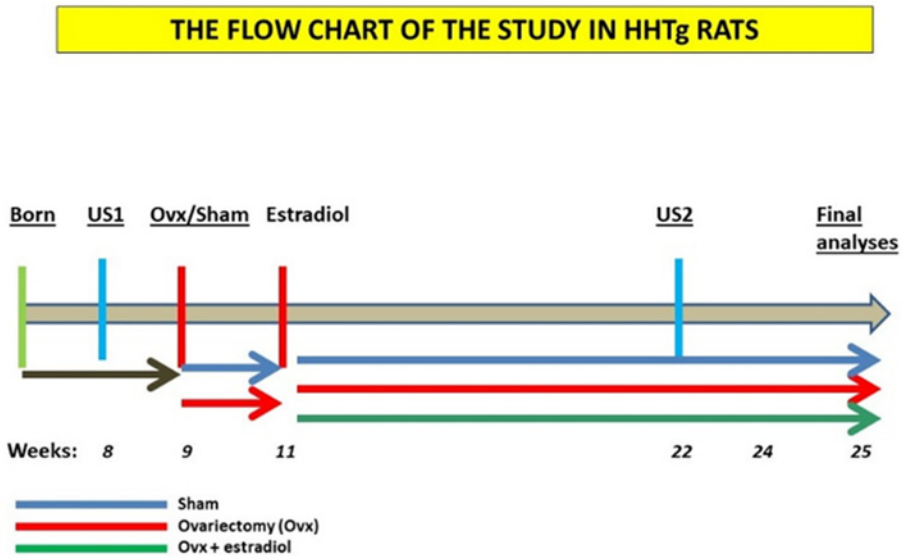

Figure 4. Flow chart of the experiment. HHTg: hereditary hypetriglycerdiemic, US1—first ultrasound examination of abdominal aorta, US2—second ultrasound examination of abdominal aorta, Ovx: ovariectomy.

4.2. Ultrasound Studies

Animal experiments were performed under a protocol approved by the Committee of the Institute. Rats were examined by a high-resolution US imaging system (Vevo 2100, FUJIFILM VisualSonics Inc., Toronto, Canada). The rats were anesthetized with isoflurane using an induction chamber connected with a scavenger canister. After induction, each animal was placed on a temperature-controlled board, and the four limbs coated with conductive paste and taped on the ECG electrodes. During the examination, the animals were maintained under gaseous anesthesia by a nose cone (1.5–2% isoflurane in 0.4–0.8 L/min in pure oxygen) and heart rate, respiration frequency and electrocardiogram were monitored. The abdomen was shaved and coated with acoustic coupling gel. M-mode images of abdominal aorta directly above and under the origin of renal arteries were obtained with Vevo 2100 high-resolution in vivo microimaging system using MS

250S transducer (20 MHz) (FUJIFILM VisualSonics Inc., Toronto, Canada) held in position by a hand and/or mechanical arm was used for the image acquisitions. B-mode images were obtained placing the US probe above the abdominal aorta to obtain cross-sectional images with the region of interest located in the focal zone of the transducer. Screening of aorta including aortic dilation was assessed by ultrasound 5 days prior surgery and 14 weeks after surgery (i.e., after 12 weeks of hormone replacement therapy) as a surrogate marker of aortic elasticity. Examiners and readers were blinded to the status of animals. Three consecutive cycles (maximal and minimal aortic diameter) were measured in three separate recordings for both, abdominal aorta above and under the origin of renal arteries. Aortic dilation was calculated as a difference between the averages of maximal and minimal aortic diameters gated by ECG in systole and diastole. Data were evaluated in a blinded fashion. Strain in abdominal aorta was calculated as previously described in carotid arteries [54–56]. In short, the strain was expressed as percent change in the arterial diameter: strain = (SD − DD)/DD, where SD was the systolic and DD the diastolic aortic diameter. The main principle of the measurement of abdominal dilation used for aortic strain calculation is shown in Figure 5.

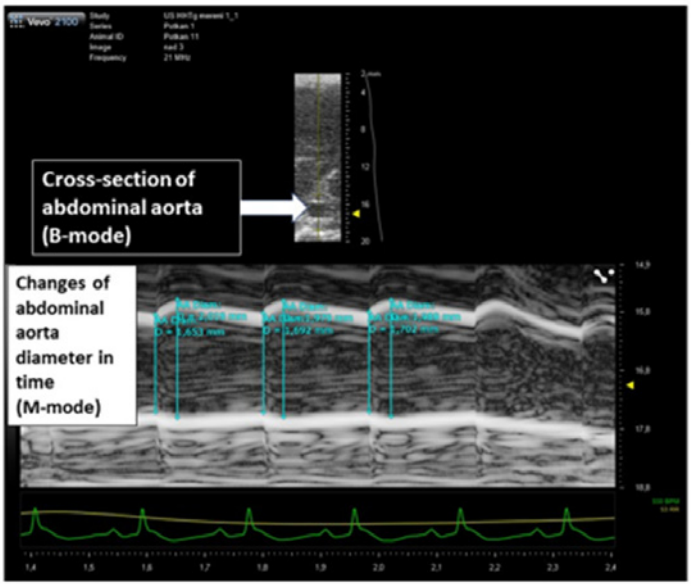

Figure 5. The principle of the assessment of abdominal aortic dilation in HHtg rats (ultrasound/M-mode measurements) for aortic strain calculation.

4.3. Analytical Methods and Biochemical Analyses

Serum levels of triglycerides (Kit number: TG250, BLT00059), glucose (Kit number: GOD 1500, 132410), total and HDL cholesterol (Kit number: CHOL250, BLT00036 and HDLC4, 07528566), ALT (Kit number: 94973UN18), AST (Kit number: 73201UN19), and FFA (Kit number: half micro test, 11383175001) were measured using commercially available kits (Erba Lachema, Brno, Czech Republic, and Roche Diagnostics, Mannheim, Germany). Serum insulin (Kit number: 10-1250-01), glucagon (Kit number: YK90), IL-6 (Kit number: MBS 701221), AMH (Kit number: MBS 264077) and NOS (Kit number: MBS 261741) concentrations were determined using the rat ELISA kit (Mercodia AB, Uppsala, Sweden; Yanaihara Institute Inc., Fujinomiya-shi, Japan, MyBioSource, San Diego, CA, USA). Serum 17β-estradiol (Kit number: DLS 4800) and 17β-hydroxyprogesterone (Kit number: IM 1452) were analyzed using rat RIA kits (Immunotech, Prague, Czech Republic). To determine triglyceride and cholesterol content in tissues, samples were extracted using a chloroform/methanol mixture. The resulting pellet was dissolved in isopropyl alcohol, with triglyceride content determined by enzymatic assay (Erba-Lachema, Brno, Czech Republic). Perimetrial fat pads (Figure 6) were removed and weighed to assess adiposity index according to already established methodology [57] and the adiposity was determined

by the adiposity index (the sum of the weight of perimetrial inguinal and perimetrial white adipose tissue divided by body weight).

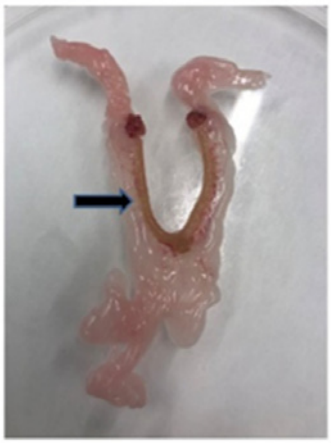

Figure 6. Perimetrial fat (black arrow) obtained for evaluation of the adiposity index (rat uterus).

4.4. Gene Expression

Total RNA were isolated from abdominal aorta and myocardial tissue using RNA Blue (Top-Bio, Vestec, Czech Republic). Reverse transcription and quantitative real-time PCR analysis was performed using the TaqMan RNA-to-C_T 1-Step Kit and TaqMan Gene Expression Assay (Applied Biosystems, Waltham, MA, USA). Relative expressions of *Nos3* (Assay ID: Rn02132634_s1) and *Cx37* (Assay ID: Rn00572193s1) were determined after normalization against *Hprt* gene as an internal reference and calculated using 2-ΔΔCt method, with results run in triplicate.

4.5. Statistical Analyses

Data are given as the mean ± SD. One-way ANOVA was applied to analyze the parameters describing the differences between variables before and after ovariectomy and before and after estradiol treatment and Fisher LSD post-hoc test was used. When comparing difference in suprarenal aortic strain of the group after ovariectomy and estradiol substitution with the sham group, unpaired Student's t-test was used. Statistical significance was defined as $p < 0.05$. Statistical analysis was performed using BMDP Statistical Software.

5. Conclusions

Ovariectomy in HHTg rats caused robust changes of the properties of abdominal aorta and also of the mass and the structure of the heart. Most vascular and cardiac changes after ovariectomy were reversed by estradiol treatment and some parameters reached values even different from sham group. In addition, some parameters were changed by estradiol supplementation irrespectively of ovariectomy. Moreover, vascular and cardiac changes were accompanied by similar or reverse changes in other organs and tissues including central adiposity, liver and kidney. In summary, these findings indicate different effects of ovariectomy and estradiol on different cardiovascular but also extravascular and extracardiac systems and structures and should be taken into account and studied in parallel.

Author Contributions: Conceptualization, J.P. and M.H.; methodology, M.H., H.M., I.M. and D.M.; validation, J.P., H.B. and D.M.; formal analysis, J.P., M.H., H.M., I.M., D.M., T.H. and H.B.; investigation, J.P., M.H., H.M., I.M., D.M., T.H. and H.B.; resources, J.P. and I.M.; data curation, J.P., M.H., H.M., I.M., D.M., T.H. and H.B.; writing—original draft preparation, J.P. and M.H.; writing—review and editing, J.P., M.H., H.M., I.M., D.M., T.H. and H.B.; visualization, J.P. and M.H.; supervision, J.P. and H.M.; project administration, J.P., I.M., M.H. and H.M.; funding acquisition, J.P. and I.M. All authors have read and agreed to the published version of the manuscript.

Funding: This work was supported by Ministry of Health of the Czech Republic, grant No. NU20-01-00083 and by Ministry of Health of the Czech Republic under its conceptual development of the research organization program (Institute for Clinical and Experimental Medicine—IKEM, IN 00023001. All rights reserved.

Institutional Review Board Statement: Animal Protection Law of the Czech Republic (311/1997) and with European Community Council recommendations (86-609/ECC) for the use of laboratory animals and approved by the Ethics Committee of the Institute for Clinical and Experimental Medicine, Prague.

Informed Consent Statement: Not applicable.

Data Availability Statement: All datasets generated for this study are included in the article.

Conflicts of Interest: The authors declare no conflict of interest.

Abbreviations

ALT	Alanine aminotransferase
AMH	Anti-Mullerian hormone
AST	Aspartate aminotransferase
CVD	cardiovascular disease
Cx37	Connexin 37
FFA	Free fatty acids
HDL	High density lipoprotein
HHTg	Hereditary Hypertriglyceridemic
IL-6	Interleukin 6
LDL	Low density lipoprotein
NOS	Nitric oxide synthase (circulating)
Nos3	Nitric oxide 3 synthase (gene)
Ovx	Ovariectomy
Ovx + E	Ovariectomy followed by estradiol substitution
TAG	Triacylglycerols
US	Ultrasound

Appendix A

Table A1. Differences after Ovariectomy and Estradiol Substitution in Cardiovascular Parameters in Hereditary Hypertriglyceridemic Rats.

	Sham $n = 5$	**Ovariectomy** $n = 6$	**Ovariectomy + Estradiol** $n = 6$	**One-Way ANOVA**	p **Ovx vs. Sham**	p **Ovx + E vs. Ovx**
Strain in suprarenal aorta	0.148± 0.022	0.128 ± 0.025	0.182 ± 0.021	0.01	0.197	0.002 (0.020 vs. Sham)
Strain infrarenal aorta	0.090 ± 0.026	0.061 ± 0.020	0.101± 0.032	0.01	0.067	0.027
Nitric oxide synthase 3 gene expression in abdominal aorta	1.006 ± 0.113	0.616 ± 0.212	0.951 ± 0.266	0.01	0.05	0.05
Connexin 37 gene expression in abdominal aorta	1.272 ± 0.490	1.183 ± 0.775	1.656 ± 1.043	n.s.	n.s.	n.s.
Circulating Nitric oxide synthase	6.746 ± 1.149	5.246 ± 1.873	6.284 ± 0.806	n.s.	n.s.	n.s.
Myocardium (g/100 g bwt)	0.269 ± 0.013	0.225 ± 0.005	0.280 ± 0.012	0.001	0.001	0.001
Left ventricle (g/100 g bwt)	0.175 ± 0.021	0.140 ± 0.006	0.182 ± 0.016	0.001	0.01	0.001
The content of triglycerides in the myocardium (μmol/g)	3.350 ± 0.762	3.509 ± 0.317	4.487 ± 0.602	0.01	n.s.	0.05

Legend: Strain = difference between systolic and diastolic diameter/diastolic diameter. Ovx: ovariectomy, Ovx + E: Ovariectomy and estradiol substitution. Data are expressed as mean ± SD and evaluated by one-way ANOVA and Fisher LSD post-hoc test; n.s.: nonsignificant.

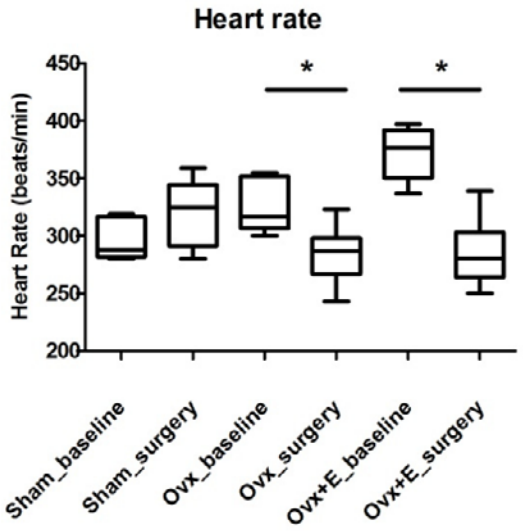

Figure A1. Heart rate in Hereditary hypertriglyceridemic rats at baseline vs. values at the end of the study. Legend: Sham_baseline: sham group before surgery; sham_surgery: sham group after surgery (n = 5); Ovx_baseline: ovariectomized group before surgery; Ovx_surgery: ovariectomized group after surgery (n = 6); Ovx+E_baseline: ovariectomized group with estradiol substitution before surgery; Ovx+E_surgery: ovariectomized group with estradiol substitution after surgery (n = 6). Evaluated by one-way ANOVA and Fisher LSD post-hoc test; n.s.: nonsignificant, * $p < 0.05$.

References

1. Vogel, B.; Acevedo, M.; Appelman, Y.; Merz, C.N.B.; Chieffo, A.; Figtree, G.A.; Guerrero, M.; Kunadian, V.; Lam, C.S.P.; Maas, A.H.E.M.; et al. The Lancet women and cardiovascular disease Commission: Reducing the global burden by 2030. *Lancet* **2021**, *397*, 2385–2438. [CrossRef]
2. Woodward, M. Cardiovascular Disease and the Female Disadvantage. *Int. J. Environ. Res. Public Health* **2019**, *16*, 1165. [CrossRef] [PubMed]
3. Clarkson, T.B. Estrogen effects on arteries vary with stage of reproductive life and extent of subclinical atherosclerosis progression. *Menopause* **2018**, *25*, 1262–1274. [CrossRef]
4. Hodis, H.N.; Mack, W.J. The Timing Hypothesis and Hormone Replacement Therapy: A Paradigm Shift in the Primary Prevention of Coronary Heart Disease in Women. Part 1: Comparison of Therapeutic Efficacy. *J. Am. Geriatr. Soc.* **2013**, *61*, 1005–1010. [CrossRef]
5. Hodis, H.N.; Mack, W.J.; Henderson, V.W.; Shoupe, D.; Budoff, M.J.; Hwang-Levine, J.; Li, Y.; Feng, M.; Dustin, L.; Kono, N.; et al. Vascular Effects of Early versus Late Postmenopausal Treatment with Estradiol. *N. Engl. J. Med.* **2016**, *374*, 1221–1231. [CrossRef] [PubMed]
6. Grady, D.; Herrington, D.; Bittner, V.; Blumenthal, R.; Davidson, M.; Hlatky, M.; Hsia, J.; Hulley, S.; Herd, A.; Khan, S.; et al. Cardiovascular Outcomes During 6.8 Years of Hormone Therapy: Heart and Estrogen/Progestin Replacement Study Follow-Up (HERS II). *JAMA* **2002**, *57*, 678. [CrossRef]
7. Rossouw, J.E.; Anderson, G.L.; Prentice, R.L.; LaCroix, A.Z.; Kooperberg, C.; Stefanick, M.L.; Jackson, R.D.; Beresford, S.A.; Howard, B.V.; Johnson, K.C.; et al. Writing Group for the Women's Health Initiative I: Risks and benefits of estrogen plus progestin in healthy postmenopausal women: Principal results From the Women's Health Initiative randomized controlled trial. *JAMA* **2002**, *288*, 321–333.
8. Mack, W.J.; Hameed, A.B.; Xiang, M.; Roy, S.; Slater, C.C.; Stanczyk, F.Z.; Lobo, R.A.; Liu, C.R.; Liu, C.H.; Hodis, H.N. Does elevated body mass modify the influence of postmenopausal estrogen replacement on atherosclerosis progression: Results from the estrogen in the prevention of atherosclerosis trial. *Atherosclerosis* **2003**, *168*, 91–98. [CrossRef]
9. Pitha, J.; Lesná, K.; Sekerkova, A.; Poledne, R.; Kovář, J.; Lejsková, M.; Dvořáková, H.; Adámková, S.; Lánská, V.; Bobak, M. Menopausal transition enhances the atherogenic risk of smoking in middle aged women. *Int. J. Cardiol.* **2013**, *168*, 190–196. [CrossRef]
10. Pitha, J.; Kovar, J.; Skodova, Z.; Cifkova, R.; Stavek, P.; Cervenka, L.; Sejda, T.; Lanska, V.; Poledne, R. Association of in-tima-media thickness of carotid arteries with remnant lipoproteins in men and women. *Physiol. Res.* **2015**, *64*, S377–S384. [CrossRef]
11. Pitha, J.; Bobková, D.; Kovar, J.; Havlíčková, J.; Poledne, R. Antiatherogenic effect of simvastatin is not due to decrease of ldl cholesterol in ovariectomized golden syrian hamster. *Physiol. Res.* **2010**, *59*, 401–406. [CrossRef] [PubMed]
12. Lin, J.B.; Phillips, E.H.; Riggins, T.E.; Sangha, G.S.; Chakraborty, S.; Lee, J.Y.; Lycke, R.J.; Hernandez, C.L.; Soepriatna, A.H.; Thorne, B.R.; et al. Imaging of small animal peripheral artery disease models: Recent advancements and translational potential. *Int. J. Mol. Sci.* **2015**, *16*, 11131–11177. [CrossRef] [PubMed]

13. Vrana, A.; Kazdova, L. The hereditary hypertriglyceridemic nonobese rat: An experimental model of human hypertriglyceridemia. *Transpl. Proc.* **1990**, *22*, 2579. [PubMed]
14. Zhang, L.; Li, C.; Yang, L.; Adzika, G.K.; Machuki, J.O.; Shi, M.; Sun, Q.; Sun, H. Estrogen Protects Vasomotor Functions in Rats During Catecholamine Stress. *Front. Cardiovasc. Med.* **2021**, *8*, 679240. [CrossRef]
15. Bourassa, P.A.; Milos, P.M.; Gaynor, B.J.; Breslow, J.L.; Aiello, R.J. Estrogen reduces atherosclerotic lesion development in apolipoprotein E-deficient mice. *Proc. Natl. Acad. Sci. USA* **1996**, *93*, 10022–10027. [CrossRef]
16. Bendale, D.S.; Karpe, P.A.; Chhabra, R.; Shete, S.P.; Shah, H.; Tikoo, K. 17-beta Oestradiol prevents cardiovascular dys-function in post-menopausal metabolic syndrome by affecting SIRT1/AMPK/H3 acetylation. *Br. J. Pharmacol.* **2013**, *170*, 779–795. [CrossRef]
17. Ceylan-Isik, A.F.; Erdogan-Tulmac, O.B.; Ari, N.; Ozansoy, G.; Ren, J. Effect of 17beta-oestradiol replacement on vascular responsiveness in ovariectomized diabetic rats. *Clin. Exp. Pharmacol. Physiol.* **2009**, *36*, e65–e71. [CrossRef]
18. Reed, K.E.; Westphale, E.M.; Larson, D.M.; Wang, H.Z.; Veenstra, R.D.; Beyer, E.C. Molecular cloning and functional expression of human connexin37, an endothelial cell gap junction protein. *J. Clin. Investig.* **1993**, *91*, 997–1004. [CrossRef]
19. Wu, Z.; Lou, Y.; Jin, W.; Liu, Y.; Lu, L.; Chen, Q.; Zhang, R. The Connexin37 gene C1019T polymorphism and risk of coronary artery disease: A meta-analysis. *Arch. Med. Res.* **2014**, *45*, 21–30. [CrossRef]
20. Guo, S.; Yang, Y.; Yang, Z.; You, H.; Shi, Y.; Hu, Z.; Meng, Z.; Xiao, J. Improving myocardial fractional flow reserve in coronary atherosclerosis via CX37 gene silence: A preclinical validation study in pigs. *Interact. Cardiovasc. Thorac. Surg.* **2017**, *26*, 139–145. [CrossRef]
21. Derouette, J.-P.; Wong, C.; Burnier, L.; Morel, S.; Sutter, E.; Galan, K.; Brisset, A.C.; Roth, I.; Chadjichristos, C.E.; Kwak, B.R. Molecular role of Cx37 in advanced atherosclerosis: A micro-array study. *Atherosclerosis* **2009**, *206*, 69–76. [CrossRef] [PubMed]
22. Pitha, J.; Kralova Lesna, I.; Hubacek, J.A.; Sekerkova, A.; Lanska, V.; Adamkova, V.; Dorobantu, M.; Nicolescu, R.; Steiner, R.; Ivic, V.; et al. Smoking impairs and circulating stem cells favour the protective effect of the T allele of the con-nexin37 gene in ischemic heart disease—A multinational study. *Atherosclerosis* **2016**, *244*, 73–78. [CrossRef] [PubMed]
23. Pitha, J.; Hubácek, J.A.; Cífková, R.; Skodová, Z.; Stávek, P.; Lánská, V.; Kovar, J.; Poledne, R. The association between subclinical atherosclerosis in carotid arteries and Connexin 37 gene polymorphism (1019C>T.; Pro319Ser) in women. *Int. Angiol.* **2011**, *30*, 221–226. [PubMed]
24. Hubacek, J.A.; Staněk, V.; Gebauerová, M.; Pilipčincová, A.; Poledne, R.; Aschermann, M.; Skalická, H.; Matoušková, J.; Kruger, A.; Pěnička, M.; et al. Lack of an association between connexin-37, stromelysin-1, plasminogen activator-inhibitor type 1 and lymphotoxin-alpha genes and acute coronary syndrome in Czech Caucasians. *Exp. Clin. Cardiol.* **2010**, *15*, e52.
25. Looft-Wilson, R.C.; Billig, J.E.; Sessa, W.C. Shear Stress Attenuates Inward Remodeling in Cultured Mouse Thoracodorsal Arteries in an eNOS-Dependent, but Not Hemodynamic Manner, and Increases Cx37 Expression. *J. Vasc. Res.* **2019**, *56*, 284–295. [CrossRef]
26. Pfenniger, A.; Meens, M.J.; Pedrigi, R.M.; Foglia, B.; Sutter, E.; Pelli, G.; Rochemont, V.; Petrova, T.V.; Krams, R.; Kwak, B.R. Shear stress-induced atherosclerotic plaque composition in ApoE(-/-) mice is modulated by connexin37. *Atherosclerosis* **2015**, *243*, 1–10. [CrossRef]
27. Bozdogan, O.; Bozcaarmutlu, A.; Kaya, S.T.; Sapmaz, C.; Ozarslan, T.O.; Eksioglu, D.; Yasar, S. Decreasing myocardial estrogen receptors and antioxidant activity may be responsible for increasing ischemia- and reperfusion-induced ventricular arrhythmia in older female rats. *Life Sci.* **2021**, *271*, 119190. [CrossRef]
28. Aryan, L.; Younessi, D.; Zargari, M.; Banerjee, S.; Agopian, J.; Rahman, S.; Borna, R.; Ruffenach, G.; Umar, S.; Eghbali, M. The Role of Estrogen Receptors in Cardiovascular Disease. *Int. J. Mol. Sci.* **2020**, *21*, 4314. [CrossRef]
29. Murphy, E. Estrogen Signaling and Cardiovascular Disease. *Circ. Res.* **2011**, *109*, 687–696. [CrossRef]
30. Matarrese, P.; Maccari, S.; Vona, R.; Gambardella, L.; Stati, T.; Marano, G. Role of β-Adrenergic Receptors and Estrogen in Cardiac Repair after Myocardial Infarction: An Overview. *Int. J. Mol. Sci.* **2021**, *22*, 8957. [CrossRef]
31. Squiers, G.T.; McLellan, M.A.; Ilinykh, A.; Branca, J.; Rosenthal, N.; Pinto, A.R. Cardiac cellularity is dependent upon biological sex and is regulated by gonadal hormones. *Cardiovasc. Res.* **2020**, *117*, 2252–2262. [CrossRef] [PubMed]
32. Yang, X.; Chen, G.-J.; Papp, R.; DeFranco, D.B.; Zeng, F.; Salama, G. Oestrogen upregulates L-type Ca^{2+} channels via oestrogenreceptor-α by a regional genomic mechanism in female rabbit hearts. *J. Physiol.* **2012**, *590*, 493–508. [CrossRef] [PubMed]
33. Wei, J.; Nelson, M.D.; Szczepaniak, E.W.; Smith, L.; Mehta, P.K.; Thomson, L.E.; Berman, D.S.; Li, D.; Bairey Merz, C.N.; Szczepaniak, L.S. Myocardial steatosis as a possible mechanistic link between diastolic dysfunction and coronary microvascular dysfunction in women. *Am. J. Physiol. Heart Circ. Physiol.* **2016**, *310*, H14–H19. [CrossRef] [PubMed]
34. Zhou, Y.-T.; Grayburn, P.; Karim, A.; Shimabukuro, M.; Higa, M.; Baetens, D.; Orci, L.; Unger, R.H. Lipotoxic heart disease in obese rats: Implications for human obesity. *Proc. Natl. Acad. Sci. USA* **2000**, *97*, 1784–1789. [CrossRef]
35. Varela, R.; Rauschert, I.; Romanelli, G.; Alberro, A.; Benech, J.C. Hyperglycemia and hyperlipidemia can induce morphophysiological changes in rat cardiac cell line. *Biochem. Biophys. Rep.* **2021**, *26*, 100983.
36. Wang, S.; Wong, L.-Y.; Neumann, D.; Liu, Y.; Sun, A.; Antoons, G.; Strzelecka, A.; Glatz, J.F.; Nabben, M.; Luiken, J.J. Augmenting Vacuolar H+-ATPase Function Prevents Cardiomyocytes from Lipid-Overload Induced Dysfunction. *Int. J. Mol. Sci.* **2020**, *21*, 1520. [CrossRef]
37. Miklankova, D.; Markova, I.; Hüttl, M.; Zapletalova, I.; Poruba, M.; Malinska, H. Metformin Affects Cardiac Arachidonic Acid Metabolism and Cardiac Lipid Metabolite Storage in a Prediabetic Rat Model. *Int. J. Mol. Sci.* **2021**, *22*, 7680. [CrossRef]
38. Malinská, H.; Hüttl, M.; Miklánková, D.; Trnovská, J.; Zapletalová, I.; Poruba, M.; Marková, I. Ovariectomy-Induced Hepatic Lipid and Cytochrome P450 Dysmetabolism Precedes Serum Dyslipidemia. *Int. J. Mol. Sci.* **2021**, *22*, 4527. [CrossRef]

39. Huang, J.; Wang, D.; Huang, L.H.; Huang, H. Roles of Reconstituted High-Density Lipoprotein Nanoparticles in Cardi-ovascular Disease: A New Paradigm for Drug Discovery. *Int. J. Mol. Sci.* **2020**, *21*, 739. [CrossRef]
40. Oschry, Y.; Eisenberg, S. Rat plasma lipoproteins: Re-evaluation of a lipoprotein system in an animal devoid of cholesteryl ester transfer activity. *J. Lipid Res.* **1982**, *23*, 1099–1106. [CrossRef]
41. Kjeldsen, E.; Nordestgaard, L.; Frikke-Schmidt, R. HDL Cholesterol and Non-Cardiovascular Disease: A Narrative Review. *Int. J. Mol. Sci.* **2021**, *22*, 4547. [CrossRef]
42. Agacayak, E.; Basaranoglu, S.; Tunc, S.; Kaplan, I.; Evliyaoglu, O.; Gul, T.; Icen, M.S.; Findik, F.M. Oxidant/antioxidant status, paraoxonase activity, and lipid profile in plasma of ovariectomized rats under the influence of estrogen, estrogen combined with progesterone, and genistein. *Drug Des. Dev. Ther.* **2015**, *9*, 2975–2982. [CrossRef] [PubMed]
43. Reiss, A.B.; Siegart, N.M.; De Leon, J. Interleukin-6 in atherosclerosis: Atherogenic or atheroprotective? *Clin. Lipidol.* **2017**, *12*, 14–23.
44. Rachon, D.; Mysliwska, J.; Suchecka-Rachon, K.; Wieckiewicz, J.; Mysliwski, A. Effects of oestrogen deprivation on in-terleukin-6 production by peripheral blood mononuclear cells of postmenopausal women. *J. Endocrinol.* **2002**, *172*, 387–395. [CrossRef] [PubMed]
45. Kim, O.Y.; Chae, J.S.; Paik, J.K.; Seo, H.S.; Jang, Y.; Cavaillon, J.-M.; Lee, J.H. Effects of aging and menopause on serum interleukin-6 levels and peripheral blood mononuclear cell cytokine production in healthy nonobese women. *AGE* **2011**, *34*, 415–425. [CrossRef]
46. Khoa, N.D.; Montesinos, M.C.; Reiss, A.B.; Delano, D.L.; Awadallah, N.W.; Cronstein, B. Inflammatory Cytokines Regulate Function and Expression of Adenosine A2A Receptors in Human Monocytic THP-1 Cells. *J. Immunol.* **2001**, *167*, 4026–4032. [CrossRef]
47. Palomer, X.; Salvado, L.; Barroso, E.; Vazquez-Carrera, M. An overview of the crosstalk between inflammatory process-es and metabolic dysregulation during diabetic cardiomyopathy. *Int. J. Cardiol.* **2013**, *168*, 3160–3172. [CrossRef]
48. Knipp, B.S.; Ailawadi, G.; Sullivan, V.V.; Roelofs, K.J.; Henke, P.K.; Stanley, J.C.; Upchurch, G.R., Jr. Ultrasound meas-urement of aortic diameters in rodent models of aneurysm disease. *J. Surg. Res.* **2003**, *112*, 97–101. [CrossRef]
49. Long, T.; Yao, J.K.; Li, J.; Kirshner, Z.Z.; Nelson, D.; Dougherty, G.G.; Gibbs, R.B. Estradiol and selective estrogen receptor agonists differentially affect brain monoamines and amino acids levels in transitional and surgical menopausal rat models. *Mol. Cell Endocrinol.* **2019**, *496*, 110533. [CrossRef]
50. Polito, F.; Marini, H.; Bitto, A.; Irrera, N.; Vaccaro, M.; Adamo, E.B.; Micali, A.; Squadrito, F.; Minutoli, L.; Altavilla, D. Genistein aglycone, a soy-derived isoflavone, improves skin changes induced by ovariectomy in rats. *Br. J. Pharmacol.* **2011**, *165*, 994–1005. [CrossRef]
51. Buleon, M.; Cuny, M.; Grellier, J.; Charles, P.Y.; Belliere, J.; Casemayou, A.; Arnal, J.F.; Schanstra, J.P.; Tack, I. A single dose of estrogen during hemorrhagic shock protects against Kidney Injury whereas estrogen restoration in ovariectomized mice is ineffective. *Sci. Rep.* **2020**, *10*, 17240. [CrossRef] [PubMed]
52. Strom, J.O.; Theodorsson, E.; Holm, L.; Theodorsson, A. Different methods for administering 17beta-estradiol to ovari-ectomized rats result in opposite effects on ischemic brain damage. *BMC Neurosci.* **2010**, *11*, 39. [CrossRef] [PubMed]
53. Medina-Contreras, J.; Villalobos-Molina, R.; Zarain-Herzberg, A.; Balderas-Villalobos, J. Ovariectomized rodents as a menopausal metabolic syndrome model. A minireview. *Mol. Cell. Biochem.* **2020**, *475*, 261–276. [CrossRef] [PubMed]
54. Rosenberg, A.J.; Lane-Cordova, A.D.; Wee, S.O.; White, D.W.; Hilgenkamp, T.I.M.; Fernhall, B.; Baynard, T. Healthy aging and carotid performance: Strain measures and β-stiffness index. *Hypertens. Res.* **2018**, *41*, 748–755. [CrossRef]
55. Iino, H.; Okano, T.; Daimon, M.; Sasaki, K.; Chigira, M.; Nakao, T.; Mizuno, Y.; Yamazaki, T.; Kurano, M.; Yatomi, Y.; et al. Usefulness of Carotid Arterial Strain Values for Evaluating the Arteriosclerosis. *J. Atheroscler. Thromb.* **2019**, *26*, 476–487. [CrossRef]
56. Saito, M.; Okayama, H.; Inoue, K.; Yoshii, T.; Hiasa, G.; Sumimoto, T.; Nishimura, K.; Ogimoto, A.; Higaki, J. Carotid arterial circumferential strain by two-dimensional speckle tracking: A novel parameter of arterial elasticity. *Hypertens. Res.* **2012**, *35*, 897–902. [CrossRef]
57. Li, H.; Matheny, M.; Nicolson, M.; Tumer, N.; Scarpace, P.J. Leptin gene expression increases with age independent of increasing adiposity in rats. *Diabetes* **1997**, *46*, 2035–2039. [CrossRef]

J. Hašková et al.

Repeated stereotactic radiotherapy of recurrent ventricular tachycardia: reasons, feasibility, and safety

Front Cardiovasc Med.
Impact Factor: 5,05

frontiers in Cardiovascular Medicine

CASE REPORT
published: 28 March 2022
doi: 10.3389/fcvm.2022.845382

Case Report: Repeated Stereotactic Radiotherapy of Recurrent Ventricular Tachycardia: Reasons, Feasibility, and Safety

Jana Haskova[1], Petr Peichl[1], Marek Šramko[1], Jakub Cvek[2,3], Lukáš Knybel[2], Otakar Jiravský[4], Radek Neuwirth[4,5] and Josef Kautzner[1]*

[1] Department of Cardiology, Institute for Clinical and Experimental Medicine (IKEM), Prague, Czechia, [2] Department of Oncology, University Hospital Ostrava, Ostrava, Czechia, [3] Department of Oncology, Ostrava University Medical School, Ostrava, Czechia, [4] Department of Cardiology, Podlesí Hospital Trinec, Trinec, Czechia, [5] Department of Cardiology, Masaryk University Medical School, Brno, Czechia

OPEN ACCESS

Edited by:
Maria Lucia Narducci, Catholic University of the Sacred Heart, Italy

Reviewed by:
Ji Hyun Chang, Seoul National University Hospital, South Korea
Mahmut Ozsahin, Centre Hospitalier Universitaire Vaudois (CHUV), Switzerland
Ravi Ranjan, The University of Utah, United States

***Correspondence:**
Jana Haskova
hasj@ikem.cz

Specialty section:
This article was submitted to Cardiac Rhythmology, a section of the journal Frontiers in Cardiovascular Medicine

Received: *29 December 2021*
Accepted: *24 February 2022*
Published: *28 March 2022*

Citation:
Haskova J, Peichl P, Šramko M, Cvek J, Knybel L, Jiravský O, Neuwirth R and Kautzner J (2022) Case Report: Repeated Stereotactic Radiotherapy of Recurrent Ventricular Tachycardia: Reasons, Feasibility, and Safety. Front. Cardiovasc. Med. 9:845382. doi: 10.3389/fcvm.2022.845382

Stereotactic body radiotherapy (SBRT) has been reported as an attractive option for cases of failed catheter ablation of ventricular tachycardia (VT) in structural heart disease. However, even this strategy can fail for various reasons. For the first time, this case series describes three re-do cases of SBRT which were indicated for three different reasons. The purpose in the first case was the inaccuracy of the determination of the treatment volume by indirect comparison of the electroanatomical map and CT scan. A newly developed strategy of co-registration of both images allowed precise targeting of the substrate. In this case, the second treatment volume overlapped by 60% with the first one. The second reason for the re-do of SBRT was an unusual character of the substrate–large cardiac fibroma associated with different morphologies of VT from two locations around the tumor. The planned treatment volumes did not overlap. The third reason for repeated SBRT was the large intramural substrate in the setting of advanced heart failure. The first treatment volume targeted arrhythmias originating in the basal inferoseptal region, while the second SBRT was focused on adjacent basal septum without significant overlapping. Our observations suggested that SBRT for VT could be safely repeated in case of later arrhythmia recurrences (i.e., after at least 6 weeks). No acute toxicity was observed and in two cases, no side effects were observed during 32 and 22 months, respectively. To avoid re-do SBRT due to inaccurate targeting, the precise and reproducible strategy of substrate identification and co-registration with CT image should be used.

Keywords: stereotactic body radiotherapy, ventricular tachycardia, electroanatomical mapping, failed catheter ablation, safety

INTRODUCTION

Current strategies of catheter ablation are effective in the prevention of recurrences of ventricular tachycardias (VTs) (1–3). Not frequently, catheter ablation may fail due to the inability to reach the critical part of the substrate (4, 5). The reasons include deep intramural location or failure to negotiate epicardial access (usually after previous surgery). Among the alternative treatment

strategies, stereotactic body radiotherapy (SBRT) was first reported in case reports or case series as an attractive option (6–8).

The experience with SBRT is gradually growing and several other case reports and prospective clinical studies documented a significant decrease in VT occurrences (9–19). However, even this strategy can fail for various reasons. Hence, the goal of this report was to describe a case series of re-do SBRT for VT recurrences, which is the first time in the literature.

METHODS

Since we used the same strategy of SBRT in all sessions, a brief description was provided here. The MultiPlan treatment planning system with sequential dose optimization and the CyberKnife radiosurgery system (both from Accuray, Inc., Sunnyvale, CA, USA) were employed as described previously (12). After image registration with two ECG-gated CT scans (in both systole and diastole), the internal target volume was calculated to account for heart contractions. For compensation of respiratory movements, the existing implantable cardioverter-defibrillator (ICD) lead was used as a surrogate marker. The tracking mode relevant to SBRT for VT is Synchrony using "fiducials". Based on the target surrogate, which is an ICD lead tip, in this case, a correlation respiratory motion model was created before the treatment. Such model was based on lead 3D locations extracted from a series of X-ray image pairs and corresponding respiratory phase signals from LED markers placed on the patient's chest. The created model was then used during dose delivery to control radiation source position and orientation to move together with the target (surrogate) while the beam was on. During treatment, the correlation model was updated with every new pair of X-ray images. In principle, this technology required minimum target volume expansion to cover respiratory motion-related target position variation during breathing so it has relatively better potency to spare normal tissue from dose.

CASE SERIES

Case 1

The first case was reported recently in detail as a case report, illustrating the need for precision in planned target volume (PTV) determination (20). Briefly, a 66-year-old man with a

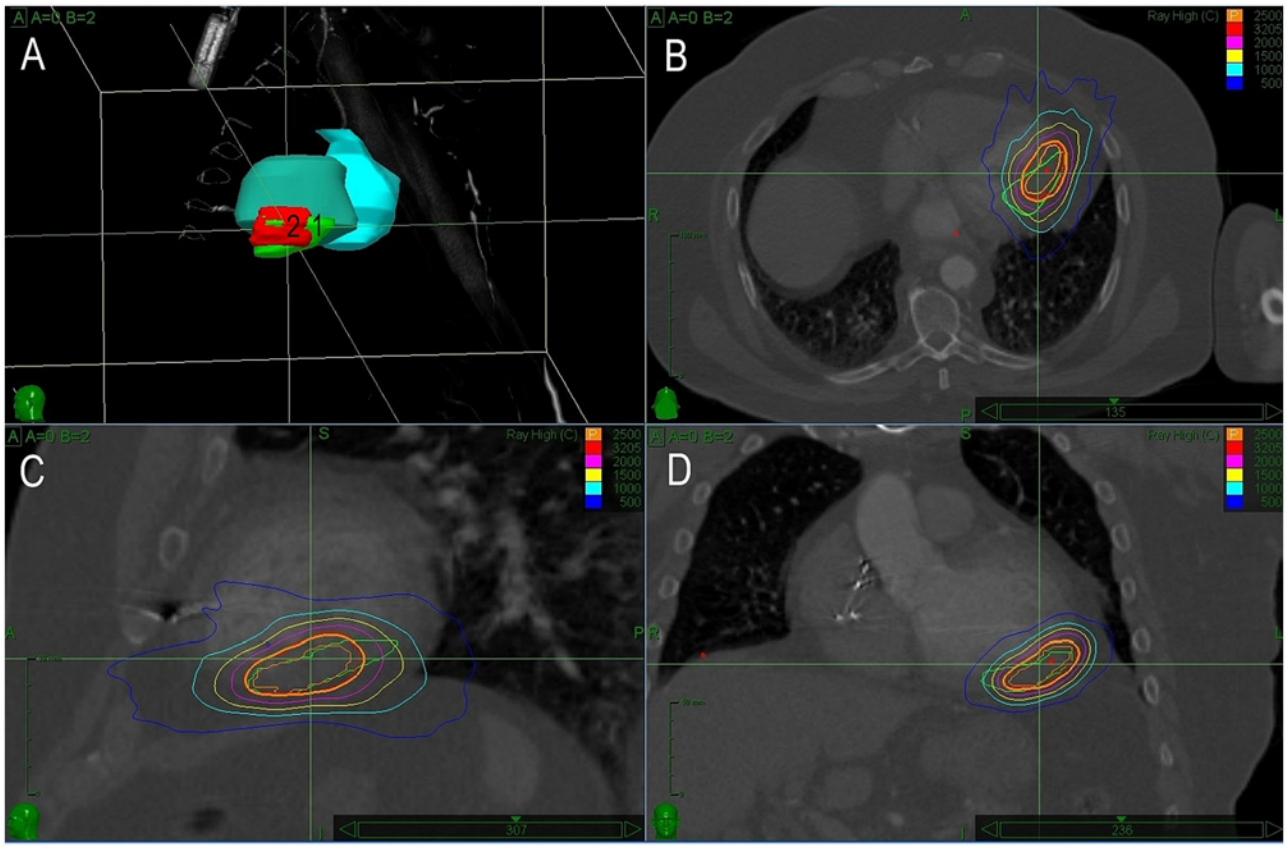

FIGURE 1 | A treatment plan for Case 1. **(A)** 3D reconstruction of planned treatment volumes for the first (1) and second (2) radiotherapy. **(B–D)** Depict sagittal, coronal, and axial views with isodose lines for both sessions of radiotherapy (green line shows target volume for the first and red for the second session). In this case, there is a significant overlap of both treatment volumes caused by inaccuracy in the planning of the first session.

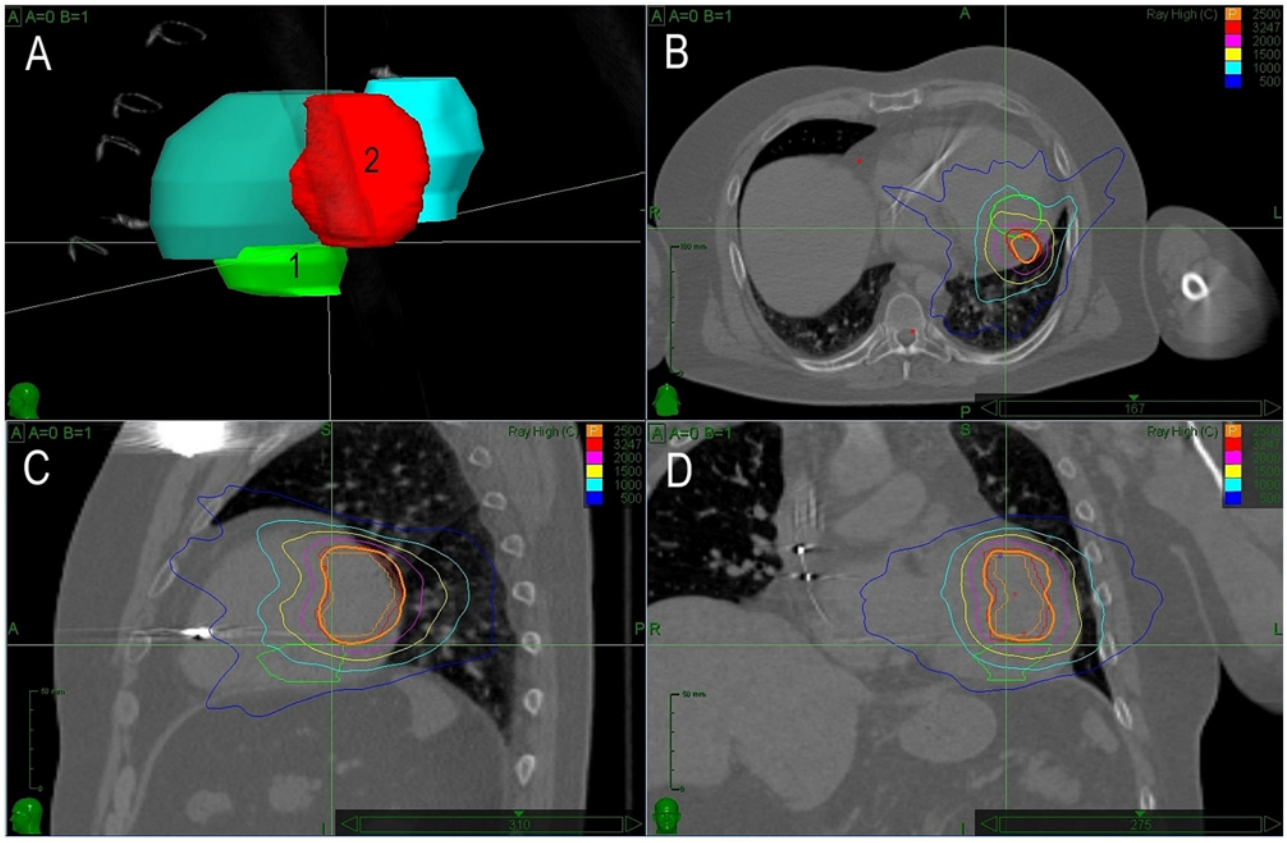

FIGURE 2 | The treatment plan for Case 2. Description of **(A–D)** is identical as in **Figure 1**. In this case, the second planned target volume covers an entirely different region.

history of coronary artery bypass graft surgery and primary prophylactic ICD implant (left ventricular ejection fraction of 35%) underwent catheter ablation for recurrences of slow VT. Clinical VT originated from a small reentrant circuit located intramurally and/or epicardially below the base of the posteromedial papillary muscle. Despite multiple endocardial ablation attempts, VT remained inducible and an attempt for percutaneous epicardial approach failed because of severe adhesions from previous cardiac surgery. The first SBRT session was planned based on a visual alignment of the presumed origin of VT from electroanatomical maps and CT images. A single fraction of 25Gy was delivered. For recurrences of VT episodes of the same ECG morphology, the patient underwent the second electrophysiology study and remapping 14 months later. Based on the electroanatomical mapping, the low voltage area caused by the previous SBRT was adjacent to the site of the earliest endocardial activity during VT. Additional RF ablation failed again to prevent the inducibility of VT and we used a newly developed co-registration method for the precise targeting of the SBR (20). Detailed maps were presented in a previously published case report (20). Briefly, there was only a small bipolar low voltage area after the first SBRT which was adjacent to the true exit of VT. Precise co-registration of the target in the second SBRT allowed to establish a smaller PTV amounting to 18 ml, including an additional 3 mm margin. The dice overlap of previous and new PTV was 0.68. The second session was performed 19 months after the first one. The same dose of 25 Gy was delivered (**Figure 1**). After transient early recurrences of slow VT, arrhythmias gradually disappeared within 3 months and the patient became arrhythmia-free for 32 months. No adverse effect of SBRT was observed during this period.

Case 2

The second case of a patient with cardiac fibroma triggering recurrent VTs of different morphologies was reported after the first successful SBRT in 2017 (10). Briefly, it was a 34-year-old patient diagnosed with an intramyocardial tumor (60 x 40 x 25 mm) located in the inferolateral wall of the left ventricle. The patient presented with several morphologies of VT. The patient underwent exploratory surgery, but the excision of the tumor was impossible for its size. Only far-field signals were recorded above and around the tumor. Empirical epicardial cryoablation around the tumor was performed with transient suppression of VTs. Subsequent electroanatomical mapping and pace mapping identified two regions responsible for two residual clinical VTs. One had a reentrant character with an exit in the lateral wall, which was close to the summit. This VT was non-inducible after catheter ablation. The other VT became

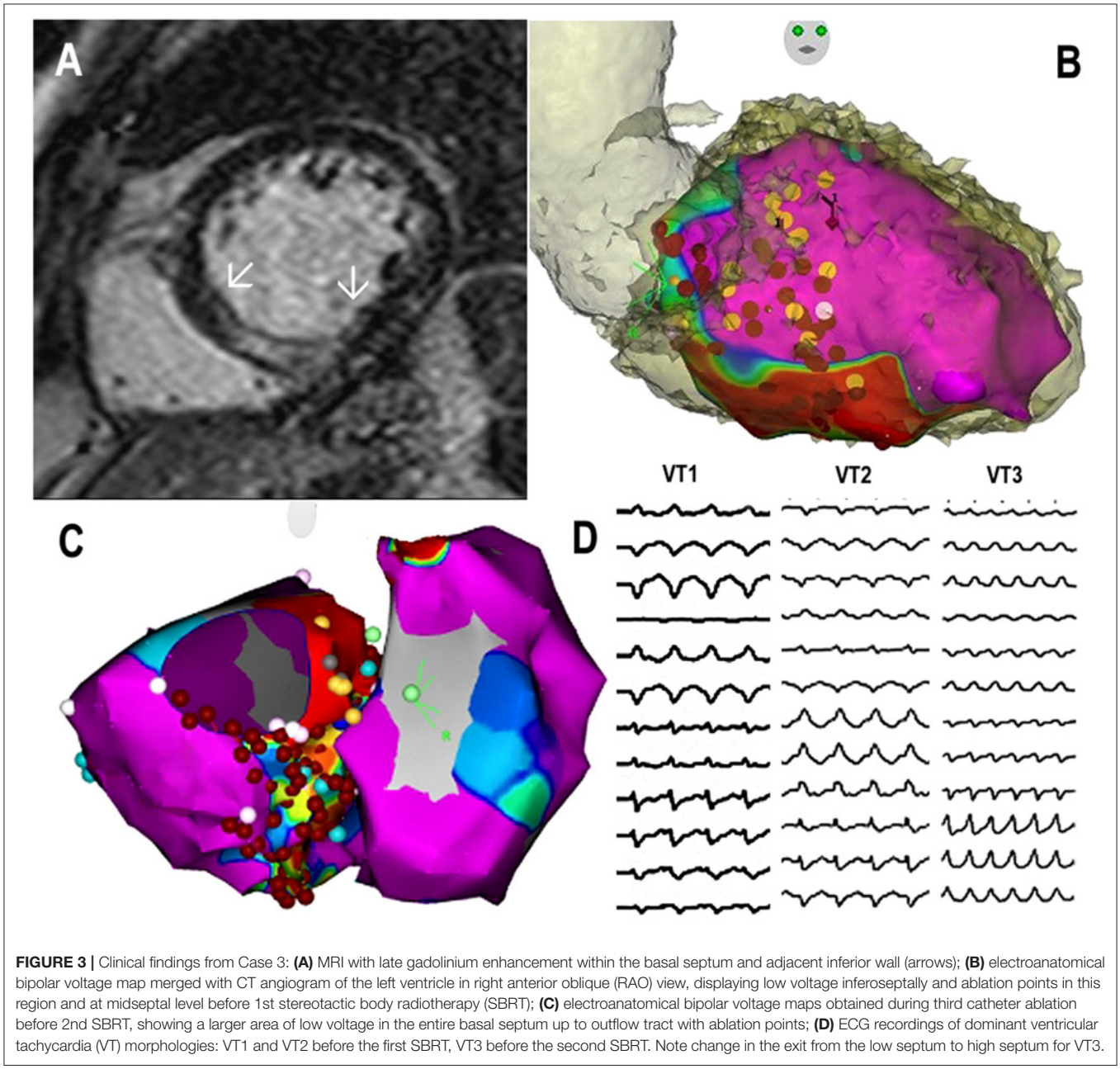

FIGURE 3 | Clinical findings from Case 3: **(A)** MRI with late gadolinium enhancement within the basal septum and adjacent inferior wall (arrows); **(B)** electroanatomical bipolar voltage map merged with CT angiogram of the left ventricle in right anterior oblique (RAO) view, displaying low voltage inferoseptally and ablation points in this region and at midseptal level before 1st stereotactic body radiotherapy (SBRT); **(C)** electroanatomical bipolar voltage maps obtained during third catheter ablation before 2nd SBRT, showing a larger area of low voltage in the entire basal septum up to outflow tract with ablation points; **(D)** ECG recordings of dominant ventricular tachycardia (VT) morphologies: VT1 and VT2 before the first SBRT, VT3 before the second SBRT. Note change in the exit from the low septum to high septum for VT3.

incessant and originated in a region between the septum and posteromedial papillary muscle. It had characteristics of focal VT with a source located deep in the wall, adjacent to the tumor. The patient was referred for SBRT. PTV was determined based on tumor location and visual comparison with electroanatomical maps. SBRT was performed with 25 Gy to the 75% isodose line. After the procedure, VT disappeared gradually within 6 months. The patient was without any arrhythmia for the next 22 months. However, the patient remained on amiodarone which had to be stopped due to amiodarone-related thyrotoxicosis. After successful treatment of this condition, the patient was without arrhythmias for the next 10 months. Then, the patient returned with an electrical storm and one morphology of VT. Electrophysiological study induced sustained VT from the anterolateral basal part of the ventricle. Electroanatomical bipolar voltage map showed normal values and pacing revealed slowed conduction in this region. Ablation did not prevent the inducibility of VT due to the deep location of the substrate. The second session of SBRT was planned and conducted based on precise integration of data from electroanatomical mapping and CT. PTV for the second SBRT was applied on the opposite side of the tumor and there was no overlap with the first radiotherapy site. The size of the tumor remained the same. After the second SBRT (25 Gy, PTV 62.2 ml; **Figure 2**), the patient

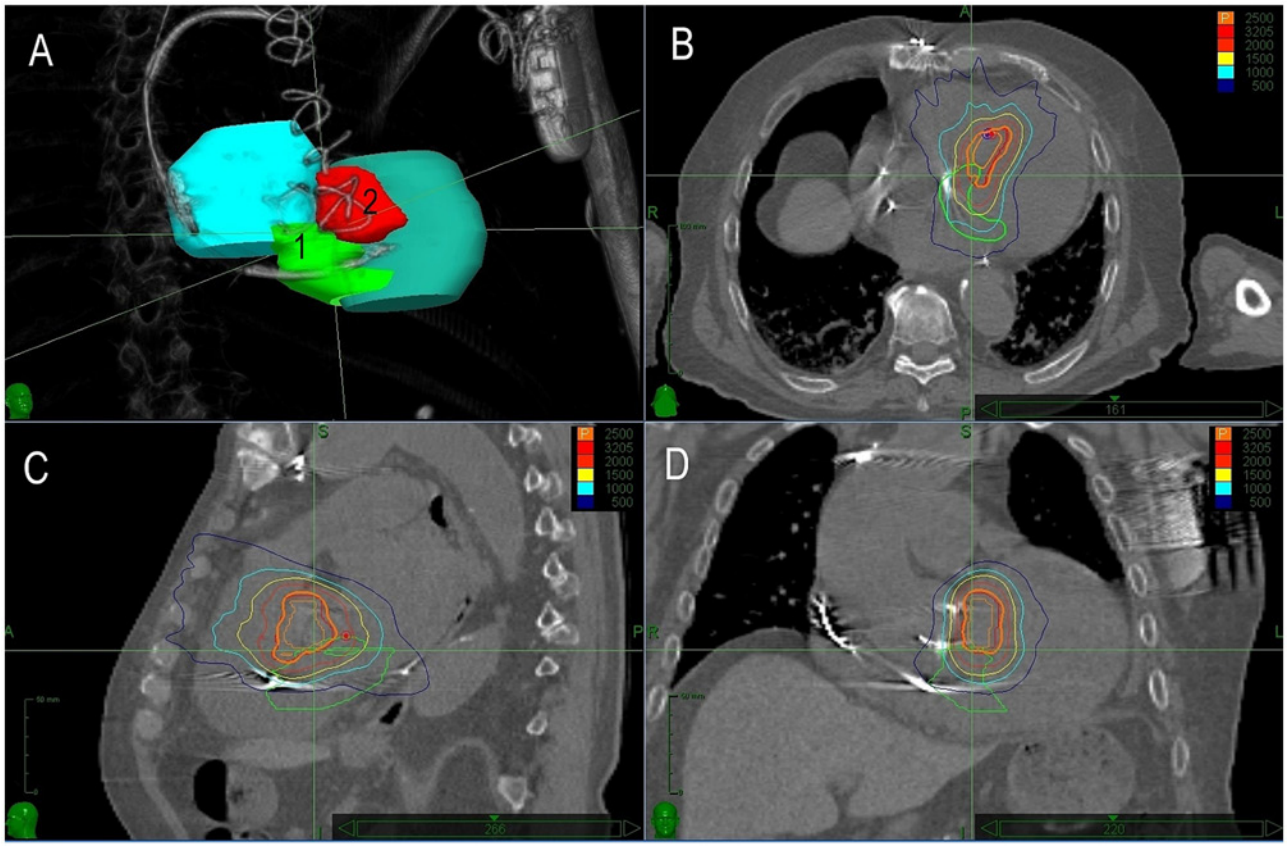

FIGURE 4 | The treatment plan for Case 3. Description of **(A–D)** is identical as in **Figure 1**. In this case, the second planned volume covered extensive substrate within the basal septum.

remained without VTs and did not gain any adverse effects for 22 months.

Case 3

The third patient was a 77-year-old man with a diagnosis of non-ischemic cardiomyopathy and intramural location of fibrosis in the basal region of the left ventricle. The patient presented with ventricular arrhythmias for several years and was implanted with a single chamber ICD. Later, aortic valve replacement with mechanical prosthesis was performed for aortic regurgitation together with a concomitant MAZE procedure. After 3 years, the device was upgraded to cardiac resynchronization therapy-defibrillators (CRT-D). At that time, the patient presented with an electrical storm. They underwent electroanatomical mapping and substrate ablation in the inferoseptal region of the left ventricle two times. For sporadic recurrences of VT, the patient was referred for SBRT 1 month later (**Figure 3**). A 25 Gy dose was applied to the basal inferoseptal region. After temporary improvement, the patient presented with recurrent VTs and underwent 2 months later another electrophysiology study. Three different VTs were induced, all with the exit in the septum above the initially irradiated region. The entire basal septum showed decreased bipolar voltage and catheter ablation covered it all. No VT was inducible at the end of the procedure. The patient was readmitted for decompensated heart failure due to incessant VT with an exit in the upper septum and was indicated to re-do SBRT. The septal region adjacent to the initial PTV was delineated as a new PTV with minimal spatial overlap. The second SBRT was performed 4 months after the first one (**Figure 4**). After SBRT, the patient continued to present with slow VT (CL around 600 ms) which necessitated another catheter ablation from both sides of the interventricular septum. Non-inducibility of VT was achieved. Although the patient was without VT, their overall clinical status gradually deteriorated and then eventually died due to the progression of heart failure 1 month later. No autopsy was performed.

Timelines of treatment for all three patients are listed in **Table 1**. Dose-volume parameters of organs at risk (OAR) and PTVs are enumerated in **Table 2**.

DISCUSSION

This case series is the first of this kind that reports on the feasibility and acute and mid-term safety of re-do SBRT in patients with recurrent VTs. The reason for repeated SBRT was different in all three subjects. One reason was the inaccuracy of targeting when using indirect comparison of electroanatomical

TABLE 1 | Timelines.

Case 1	
Index date	A 66-year-old male with ischemic cardiomyopathy and recurrent VTs requiring therapy from ICD
1,5,11 months	Repeated ineffective catheter ablations due to intramural location of the substrate
18 months	First SBRT with continuing recurrences of VT
34 months	Remapping after the first SBRT
38 months	Second SBRT, after 3 months VT disappeared
69 months	Last follow-up visit, no arrhythmias
Case 2	
Index date	A 34-year-old patient with an intramyocardial fibroma (60 x 40 x 25 mm) in the inferolateral wall of the left ventricle and recurrent VTs of different morphologies
6 months	Empirical circumferential epicardial cryoablation around the tumor, 6 months without recurrences of VT
13 months	Catheter ablation for recurrences of 2 morphologies of VT, one non-inducible, other almost incessant
14 months	First SBRT, within 6 months all arrhythmias gradually disappeared
38 months	v Re-do catheter ablation, without elimination of VT due to intramural substrate located in the opposite side of the tumor
38 months	Second SBRT, within 3 months VT disappeared
60 months	Last follow-up visit, no arrhythmias
Case 3	
Index date	A77-year-old male with non-ischemic cardiomyopathy, aortic valve replacement and fibrosis in basal region of left ventricle and sporadic interventions of ICD
70 months	Repeated catheter ablation for electrical storm
71 months	First SBRT, arrhythmias less frequent
73 months	Re-do catheter ablation for VT recurrences in basal septal region above the previous SBRT, non-inducibility
75 months	Second SBRT for incessant VT, leading to slowing VT to 100 bpm
76 months	Re-do catheter ablation in the basal septum, non-inducibility
77 months	Progression of heart failure and cachexia, death

TABLE 2 | Parameters of organs at risk (OAR) and planning target volume (PTV).

OAR and PTV volume parameter	Case 1	Case 2	Case 3
Heart D15 ml (Gy)	46.3	42.4	42.9
Heart D0,035 ml (Gy)	61.0	51.3	50.0
Heart Dmean (Gy)	4.8	13.5	14.5
Lung Left Dmean (Gy)	1.8	7.7	2.1
Esophagus D5 ml (Gy)	5.9	4.9	13.3
Esophagus D0,035 ml (Gy)	8.6	7.1	21.9
Stomach D10 ml (Gy)	10.4	7.3	6.5
Stomach D5 ml (Gy)	12.2	8.0	8.7
Stomach D0,035 ml (Gy)	18.3	11.6	14.3
PTV (mL)	21.2	23.4	43.4
PTVredo (mL)	18.3	62.2	20.0
PTVxPTVredo (mL)	11.3	0.1	0.4
PTVxPTVredo (%)	61.7	0.2	2.2
PTVxPTVredo Dmax (Gy)	32.1	25.6	25.8
PTVxPTVredo D0,035 ml(Gy)	31.9	24.5	25.6
PTVxPTVredo Dmean (Gy)	28.8	24	25.2

Dose-volume parameters are based on integrated isodose plans calculation from the first and second SBRT sessions. Both CT series from simulation were registered according to the heart region and summation of dose distribution was performed. D—abbreviation for dose; D5 ml, D10 ml, and D15 ml represents the dose to 5, 10, and 15 ml of relevant OAR, respectively. D.035 ml represents near-maximum dose, "x" means the intersection of volumes, redo means second irradiation.

maps with pretreatment CT. The second reason for re-do SBRT was an unusual character of the substrate, wherein there is an inoperable cardiac fibroma associated with several morphologies of VT from different regions of the tumor. The third reason for repeated SBRT was the large intramural basal septal substrate in the setting of dilated cardiomyopathy and advanced heart failure.

Regarding the safety of re-do SBRT, it is important to keep in mind that the risk of cardiovascular complications associated with chest radiotherapy can persist for many years (21, 22). Studies on the relationship between the dose and adverse outcomes show up to 16% relative risk of heart disease and major cardiac events per Gy of the mean heart dose (23, 24). In addition, other studies showed correlations between radiation doses to specific cardiac regions and cardiac morbidity and mortality (21). In the case of repetition of SBRT, the likelihood of severe toxicity may increase. Since no radiation-related adverse events were observed in our patients, we were not able to comment about the relationship between the dose to organs at risk dose and the occurrence of side effects.

Another fear may concern the further worsening of left ventricular ejection fraction after the second SBRT. Importantly, we did not observe a significant change in this parameter nor the significant increase of cardiac troponin after the second SBRT. Additionally, our patients had no clinical symptoms or signs of pericarditis or pneumonitis. The third patient died of terminal heart failure which was not in our opinion in relation to the second SBRT. One explanation for the good tolerability of the repeated SBRT may reflect the fact that our strategy of SBRT uses relatively small PTV, covering the critical region of the substrate (12).

We found only one case of re-do SBRT description in the literature. It was in a series by Lloyd et al. (15) who reported on outcomes of SBRT in 10 patients with advanced heart failure and VTs. One patient in this group who had no response to SBRT underwent a second SBRT ineffective treatment 90 days later. The patient was considered an outlier and ultimately underwent heart transplantation for recurrent VTs despite all therapies. No more details were available.

For a discussion on the indication to re-do SBRT and its safety, it is important to recall that the tissue effect of SBRT for VT in humans remains largely unknown, and also the time window to

clinical effect is highly variable. Most of the experimental studies suggested that electrophysiological effects are rather delayed and that the development of fibrosis is important for clinical effect (25, 26). Our recent report analyzing 3 post-mortem hearts after SBRT is in line with the above experimental data on early apoptosis and delayed fibrosis (27). Furthermore, the clinical effect of SBRT was delayed and a similar pattern was observed also in the current series (28, 29). In the largest published clinical study of Encore VT, the blanking period of 6 weeks was used to avoid counting early recurrences of VT (9). It appeared that in the majority of cases, the clinical effect should be observed after 2–3 months. Later recurrences or incessant VT could be considered either for re-do catheter ablation or repeated SBRT.

However, anecdotal cases described the immediate clinical effect of SBRT resulting in acute termination of an electrical storm (11, 13, 14, 16). Some recent experimental studies suggested that the clinical effect of SBRT is not necessarily related to the development of fibrosis and even deconstruct fibrosis as the main antiarrhythmic mechanism. A study by Zhang DM et al. demonstrated that postmortem heart specimens from four patients, with a substantial reduction of VT after SBRT, did not exhibit transmural fibrosis within the timeframe of VT reduction (30). In an experimental study, electrophysiologic assessment of irradiated murine hearts revealed a persistent supraphysiologic electrical phenotype, mediated by increases in components of the Natrium channel and Cx43. Additionally, increased $Na_V1.5$ expression was also found in the explanted human heart from the said clinical study. The authors offered an alternative explanation of the effect of SBRT—increased cardiac conduction. Interestingly, another experimental study suggested a different mechanism for the early effect of SBRT (31). In the rat model of SBRT, the authors found acute structural changes, such as interstitial and subsarcolemmal edema, widening of intercalated discs, and microvascular inflammatory responses. These acute structural changes resulted in the slowing of intracardiac conduction on ECG, which might be an alternative explanation of the effect of SBRT. These observations may suggest that an even shorter time window than 2–3 months could be employed to consider a failure of SBRT and re-do procedure.

Our first case emphasized the need for using the accurate and reproducible strategy of planned target volume delineation. Using the novel method of co-registration of electroanatomical maps with pretreatment CT, we were able to correct the previous treatment plan and deliver successfully therapy (20). More recently, we showed reproducibility of this strategy (32). The other important issue related to accuracy and safety is how to minimalize the treatment volume with respiratory compensation. We used ICD lead tracking as described above. The other possibility is the use of continuous real-time imaging and tracking of the moving target during treatment with gated irradiation using MR-guided radiotherapy (33). Therefore, with current strategies of accurate targeting of the critical substrate region and motion mitigation, the main reason for considering re-do SBRT should be either extensive substrate or development of a new substrate in a different region of the heart.

CONCLUSION

Our observations suggest that SBRT for VT could be repeated in case of arrhythmia recurrences with good acute and mid-term safety. Long-term safety remains to be further documented. The clinical effect of SBRT appears to be predominantly delayed and re-do procedures should be considered after a 2–3 month period. For earlier indications, there is still limited evidence. With current strategies of accurate targeting of the critical substrate region and precise delivery of SBRT, the main reason for considering re-do SBRT should be either extensive substrate or development of the new substrate in a different region of the heart.

DATA AVAILABILITY STATEMENT

The original contributions presented in the study are included in the article/supplementary material, further inquiries can be directed to the corresponding author.

ETHICS STATEMENT

The studies involving human participants were reviewed and approved by Ethical Committee of the Institute for Clinical and Experimental Medicine, Prague, Czechia. The patients/participants provided their written informed consent to participate in this study. Written informed consent was obtained from the individual(s) for the publication of any potentially identifiable images or data included in this article.

AUTHOR CONTRIBUTIONS

JH: preparation of the manuscript and organization. PP: catheter ablation, organization, and correction of manuscript. MŠ: development of co-registration strategy and correction of manuscript. JC: radiotherapist and reading manuscript. LK: radiotherapy planning and figure preparation. OJ: catheter ablation. RN: organization, leading part of project, and preparation of manuscript. JK: catheter ablation, leading project, and final corrections to manuscript. All authors contributed to the article and approved the submitted version.

FUNDING

This work was supported by grant project AZV NU20-02-00244 from the Ministry of Health of the Czech Republic and by funding from the European Union's Horizon 2020 research and innovation program under grant agreement No 945119.

REFERENCES

1. Briceño DF, Romero J, Patel K, Liaqat W, Zhang XD, Alviz I, et al. First-line ablation of ventricular tachycardia in ischemic cardiomyopathy: stratification of outcomes by left ventricular function. *J Interv Card Electrophysiol*. (2021) 62:391–400. doi: 10.1007/s10840-020-00912-w
2. Vergara P, Tung R, Vaseghi M, Brombin C, Frankel DS, Di Biase L, et al. Successful ventricular tachycardia ablation in patients with electrical stormreduces recurrences and improves survival. *Heart Rhythm*. (2018) 15:48–55. doi: 10.1016/j.hrthm.2017.08.022
3. Tung R, Vaseghi M, Frankel DS, Vergara P, Di Biase L, Nagashima K, et al. Freedom from recurrent ventricular tachycardia after catheter ablation is associated with improved survival in patients with structural heart disease: An International VT Ablation Center Collaborative Group study. *Heart Rhythm*. (2015) 12:1997–2007. doi: 10.1016/j.hrthm.2015.05.036
4. Kumar S, Barbhaiya CR, Sobieszczyk P, Eisenhauer AC, Couper GS, Nagashima K, et al. Role of alternative interventional procedures when endo- and epicardial catheter ablation attempts for ventricular arrhythmias fail. *Circ Arrhythm Electrophysiol.* (2015) 8:606–15. doi: 10.1161/CIRCEP.114.002522
5. Tokuda M, Kojodjojo P, Tung S, Tedrow UB, Nof E, Inada K, et al. Acute failure of catheter ablation for ventricular tachycardia due to structural heart disease: causes and significance. *J Am Heart Assoc*. (2013) 2:e000072. doi: 10.1161/JAHA.113.000072
6. Cvek J, Neuwirth R, Knybel L, Molenda L, Otahal B, Pindor J, et al. Cardiac Radiosurgery for Malignant Ventricular Tachycardia. *Cureus*. (2014) 6:e190. doi: 10.7759/cureus.190
7. Loo BW Jr, Soltys SG, Wang L, Lo A, Fahimian BP, Iagaru A, et al. Stereotactic ablative radiotherapy for the treatment of refractory cardiac ventricular arrhythmia. *Circ Arrhythm Electrophysiol.* (2015) 8:748–50. doi: 10.1161/CIRCEP.115.002765
8. Cuculich PS, Schill MR, Kashani R, Mutic S, Lang A, Cooper D, et al. Noninvasive cardiac radiation for ablation of ventricular tachycardia. *N Engl J Med*. (2017) 377:2325–36. doi: 10.1056/NEJMoa1613773
9. Robinson CG, Samson PP, Moore KMS, Hugo GD, Knutson N, Mutic S, et al. Phase I/II Trial of Electrophysiology-Guided Noninvasive Cardiac Radioablation for Ventricular Tachycardia. *Circulation.* (2019) 139:313–21. doi: 10.1161/CIRCULATIONAHA.118.038261
10. Haskova J, Peichl P, Pirk J, Cvek J, Neuwirth R, Kautzner J. Stereotactic radiosurgery as a treatment for recurrent ventricular tachycardia associated with cardiac fibroma. *HeartRhythm Case Rep*. (2018) 5:44–47. doi: 10.1016/j.hrcr.2018.10.007
11. Jumeau R, Ozsahin M, Schwitter J, Vallet V, Duclos F, Zeverino M, et al. Rescue procedure for an electrical storm using robotic non-invasive cardiac radio-ablation. *Radiother Oncol.* (2018) 128:189–91. doi: 10.1016/j.radonc.2018.04.025
12. Neuwirth R, Cvek J, Knybel L, Jiravsky O, Molenda L, Kodaj M, et al. Stereotactic radiosurgery for ablation of ventricular tachycardia. *Europace.* (2019) 21:1088–95. doi: 10.1093/europace/euz133
13. Scholz EP, Seidensaal K, Naumann P, André F, Katus HA, Debus J. Risen from the dead: Cardiac stereotactic ablative radiotherapy as last rescue in a patient with refractory ventricular fibrillation storm. *HeartRhythm Case Rep*. (2019) 5:329–32. doi: 10.1016/j.hrcr.2019.03.004
14. Bhaskaran A, Downar E, Chauhan VS, Lindsay P, Nair K, Ha A, et al. Electroanatomical mapping-guided stereotactic radiotherapy for right ventricular tachycardia storm. *HeartRhythm Case Rep.* (2019) 5:590–2. doi: 10.1016/j.hrcr.2019.09.007
15. Lloyd MS, Wight J, Schneider F, Hoskins M, Attia T, Escott C, et al. Clinical experience of stereotactic body radiation for refractory ventricular tachycardia in advanced heart failure patients. *Heart Rhythm.* (2020) 17:415–22. doi: 10.1016/j.hrthm.2019.09.028
16. Park JS, Choi Y. Stereotactic cardiac radiation to control ventricular tachycardia and fibrillation storm in a patient with apical hypertrophic cardiomyopathy at burnout stage: case report. *J Korean Med Sci.* (2020) 35:e200. doi: 10.3346/jkms.2020.35.e200
17. Martí-Almor J, Jiménez-López J, Rodríguez de Dios N, Tizón H, Vallés E, Algara M. Noninvasive ablation of ventricular tachycardia with stereotactic radiotherapy in a patient with arrhythmogenic right ventricular cardiomyopathy. *Rev Esp Cardiol (Engl Ed).* (2020) 73:97–9. doi: 10.1016/j.rec.2019.06.004
18. Lee J, Bates M, Shepherd E, Riley S, Henshaw M, Metherall P, et al. Cardiac stereotactic ablative radiotherapy for control of refractory ventricular tachycardia: initial UK multicentre experience. *Open Heart*. (2021) 8:e001770. doi: 10.1136/openhrt-2021-001770
19. Carbucicchio C, Andreini D, Piperno G, Catto V, Conte E, Cattani F, et al. Stereotactic radioablation for the treatment of ventricular tachycardia: preliminary data and insights from the STRA-MI-VT phase Ib/II study. *J Interv Card Electrophysiol.* (2021) 62:427–39. doi: 10.1007/s10840-021-01060-5
20. Peichl P, Sramko M, Cvek J, Kautzner. A case report of successful elimination of recurrent ventricular tachycardia by repeated stereotactic radiotherapy: the importance of accurate target volume delineation. *Eur Heart J Case Rep*. (2020) 5:ytaa516. doi: 10.1093/ehjcr/ytaa516
21. Bergom C, Bradley JA, Ng AK, Samson P, Robinson C, Lopez-Mattei J, et al. Past, present, and future of radiation-induced cardiotoxicity: refinements in targeting, surveillance, and risk stratification. *JACC CardioOncol.* (2021) 3:343–59. doi: 10.1016/j.jaccao.2021.06.007
22. Borkenhagen JF, Bergom C, Rapp CT, Klawikowski SJ, Rein LE, Gore EM. Dosimetric predictors of cardiotoxicity in thoracic radiotherapy for lung cancer. *Clin Lung Cancer*. (2019) 20:435–41. doi: 10.1016/j.cllc.2019.05.014
23. van den Bogaard VA, Ta BD, van der Schaaf A, Bouma AB, Middag AM, Bantema-Joppe EJ, et al. Validation and modification of a prediction model for acute cardiac events in patients with breast cancer treated with radiotherapy based on three-dimensional dose distributions to cardiac substructures. *J Clin Oncol*. (2017) 35:1171–8. doi: 10.1200/JCO.2016.69.8480
24. Taylor C, Correa C, Duane FK, Aznar MC, Anderson SJ, Bergh J, et al. Early Breast Cancer Trialists' Collaborative Group. Estimating the risks of breast cancer radiotherapy: evidence from modern radiation doses to the lungs and heart and from previous randomized trials. *J Clin Oncol.* (2017) 35:1641–9. doi: 10.1200/JCO.2016.72.0722
25. Lehmann HI, Graeff C, Simoniello P, Constantinescu A, Takami M, Lugenbiel P, et al. Feasibility study on cardiac arrhythmia ablation using high-energy heavy ion beams. *Sci Rep.* (2016) 6:38895. doi: 10.1038/srep38895
26. Suzuki A, Deisher AJ, Rettmann ME, Lehmann HI, Hohmann S, Wang S, et al. Catheter-free arrhythmia ablation using scanned proton beams: electrophysiologic outcomes, biophysics, and characterization of lesion formation in a porcine model. *Circ Arrhythm Electrophysiol.* (2020) 13:e008838. doi: 10.1161/CIRCEP.120.008838
27. Kautzner J, Jedlickova K, Sramko M, Peichl P, Cvek J, Knybel L, et al. Radiation-induced changes in ventricular myocardium after stereotactic body radiotherapy for recurrent ventricular tachycardia. *JACC Clin Electrophysiol*. (2021) 21:S2405-500X(21)00687-3. doi: 10.1016/j.jacep.2021.07.012
28. Chin R, Hayase J, Hu P, Cao M, Deng J, Ajijola O, et al. Non-invasive stereotactic body radiation therapy for refractory ventricular arrhythmias: an institutional experience. *J Interv Card Electrophysiol.* (2021) 61:535–43. doi: 10.1007/s10840-020-00849-0
29. Gianni C, Rivera D, Burkhardt JD, Pollard B, Gardner E, Maguire P, et al. Stereotactic arrhythmia radioablation for refractory scar-related ventricular tachycardia. *Heart Rhythm.* (2020) 17:1241–8. doi: 10.1016/j.hrthm.2020.02.036
30. Zhang DM, Navara R, Yin T, Szymanski J, Goldsztejn U, Kenkel C, et al. Cardiac radiotherapy induces electrical conduction reprogramming in the absence of transmural fibrosis. *Nat Commun.* (2021) 12:5558. doi: 10.1038/s41467-021-25730-0
31. Cha MJ, Seo JW, Kim HJ, Kim MK, Yoon HS, Jo SW, et al. Early changes in rat heart after high-dose irradiation: implications for antiarrhythmic effects of cardiac radioablation. *J Am Heart Assoc.* (2021) 10:e019072. doi: 10.1161/JAHA.120.019072
32. Abdel-Kafi S, Sramko M, Omara S, de Riva M, Cvek J. Peichl P, et al. Accuracy of electroanatomical mapping-guided cardiac radiotherapy for ventricular tachycardia: pitfalls and solutions. *Europace.* (2021) 23:1989–97. doi: 10.1093/europace/euab195
33. Mayinger M, Kovacs B, Tanadini-Lang S, Ehrbar S, Wilke L, Chamberlain M, et al. First magnetic resonance imaging-guided cardiac radioablation

of sustained ventricular tachycardia. *Radiother Oncol.* (2020) 152:203–7. doi: 10.1016/j.radonc.2020.01.008

Conflict of Interest: JH received speaker honoraria from ProMed, PP has received speaker honoraria from Abbott and ProMed. JK reports personal fees from Bayer, Biosense Webster, Boehringer Ingelheim, Medtronic, and Abbott for participation in scientific advisory boards, and has received speaker honoraria from Bayer, Biosense Webster, Biotronik, Boehringer Ingelheim, Medtronic, Mylan, Pfizer, ProMed, and Abbott.

The remaining authors declare that the research was conducted in the absence of any commercial or financial relationships that could be construed as a potential conflict of interest.

Publisher's Note: All claims expressed in this article are solely those of the authors and do not necessarily represent those of their affiliated organizations, or those of the publisher, the editors and the reviewers. Any product that may be evaluated in this article, or claim that may be made by its manufacturer, is not guaranteed or endorsed by the publisher.

J. Beneš et al.

Metformin treatment is associated with improved outcome in patients with diabetes and advanced heart failure (HFrEF)

Scientific reports
Impact Factor: 4.997

scientific reports

Check for updates

OPEN

Metformin treatment is associated with improved outcome in patients with diabetes and advanced heart failure (HFrEF)

Jan Benes[1]✉, Martin Kotrc[1], Katerina Kroupova[1], Peter Wohlfahrt[1], Jan Kovar[1], Janka Franekova[1], Marketa Hegarova[1], Lenka Hoskova[1], Eva Hoskova[1], Terezie Pelikanova[1], Petr Jarolim[2], Josef Kautzner[1] & Vojtech Melenovsky[1]

The role of metformin (MET) in the treatment of patients with advanced HFrEF and type 2 diabetes mellitus (DM) is not firmly established. We studied the impact of MET on metabolic profile, quality of life (QoL) and survival in these patients. A total of 847 stable patients with advanced HFrEF (57.4 ± 11.3 years, 67.7% NYHA III/IV, LVEF 23.6 ± 5.8%) underwent clinical and laboratory evaluation and were prospectively followed for a median of 1126 (IQRs 410; 1781) days for occurrence of death, urgent heart transplantation or mechanical circulatory support implantation. A subgroup of 380 patients (44.9%) had DM, 87 of DM patients (22.9%) were treated with MET. Despite worse insulin sensitivity and more severe DM (higher BMI, HbA1c, worse insulin resistance), MET-treated patients exhibited more stable HF marked by lower BNP level (400 vs. 642 ng/l), better LV and RV function, lower mitral and tricuspid regurgitation severity, were using smaller doses of diuretics (all $p < 0.05$). Further, they had higher eGFR (69.23 vs. 63.34 ml/min/1.73 m^2) and better QoL (MLHFQ: 36 vs. 48 points, $p = 0.002$). Compared to diabetics treated with other glucose-lowering agents, MET-treated patients had better event-free survival even after adjustment for BNP, BMI and eGFR ($p = 0.035$). Propensity score-matched analysis with 17 covariates yielded 81 pairs of patients and showed a significantly better survival for MET-treated subgroup ($p = 0.01$). MET treatment in patients with advanced HFrEF and DM is associated with improved outcome by mechanisms beyond the improvement of blood glucose control.

Type 2 diabetes mellitus (DM) is a common and severe comorbidity in patients with heart failure with reduced ejection fraction (HFrEF), but optimal treatment modality has not yet been clarified. Biguanides including metformin (MET) had long been considered contraindicated in HF patients due to concerns about lactic acidosis, that was observed with phenformin, an older biguanide with less favorable pharmacological profile[1]. Large meta-analysis, however, has not demonstrated an association between MET therapy and increased risk of lactic acidosis[2], so MET has been used even in HF population. Observational studies showed not only MET safety in HF subjects[3–5] but some studies even suggested a survival benefit associated with this drug[6–8]. However, there is only one study analyzing MET specifically in patients with HFrEF[9] and the absence of a randomized trial is a major limitation for MET use. Moreover, registry-based retrospective studies lack a precise characterization of analyzed patients (echocardiography, laboratory analysis including metabolic profile). Therefore, the mechanism of MET action in this population is speculative.

The aim of the present study was to evaluate the association between MET treatment and metabolic profile, quality of life and outcome in prospectively followed advanced HFrEF patients.

Methods

Patients. Patients with stable HFrEF (LVEF < 40%) of least 6-month duration receiving a stable medication for at least 3 months were enrolled in the study between 2008 and 2016 in a prospectively defined registry. Subjects with potentially reversible LV dysfunction (planned valve surgery, revascularization, or tachycardia-induced

[1]Department of Cardiology, Institute for Clinical and Experimental Medicine-IKEM, Videnska 1958/9, 140 21 Praha 4, Czech Republic. [2]Department of Pathology, Brigham and Women's Hospital, Harvard Medical School, Boston, MA, USA. ✉email: jan.benes@ikem.cz

cardiomyopathy) were excluded. Patients were followed until July 2019. DM was diagnosed according to current recommendation[10]. The investigation conforms with the principles outlined in the Declaration of Helsinki, the study protocol was approved by the Institutional Ethics Committee and all subjects signed an informed consent. At the study enrollment, patients completed a Minnesota Living with Heart Failure Questionnaire (MLHFQ) and had anthropometric tests and underwent an echocardiographic study (Vivid-7; General Electric, Milwaukee, Wisconsin). LV function and dimensions were measured according to recommendations[11]. RV dysfunction was quantified in four grades (0–3). Mitral and tricuspid regurgitations were assessed semiquantitatively and expressed in 3 grades (mild, moderate, significant). An adverse outcome was defined as the combined endpoint of death, urgent heart transplantation (HTx) or mechanical circulatory support (MCS) implantation[12]. Patients who received a non-urgent HTx were censored as having no adverse event at the day of HTx.

Statistical analysis. Data are presented as mean ± standard deviation, median with interquartile ranges (IQRs), or frequency (percent). Unpaired t-test or Mann–Whitney test were used to compare continuous variables between groups as appropriate. The effect of biomarker concentration on prognosis was tested using univariate and multivariable Cox model. Event-free survival of patients was analyzed by Kaplan–Meier analysis with log-rank test comparison between groups. Propensity score matching was used to account for differences in characteristics of patients with and without MET. The propensity score for each patient was calculated using a multivariable logistic regression model in which the MET use was regressed on 17 characteristics (see "Results" section) that might influence the selection of MET therapy or that have been shown to influence prognosis of patients with advanced HF. All tests were 2-sided, and p values < 0.05 were considered significant. Calculations were performed using JMP 11 (SAS Institute Inc., Cary, NC) and R (Vienna, Austria). Methods in detail can be found in the Online Supplement.

Ethics approval and consent to participate. The ethical committee of the Institute for Clinical and Experimental Medicine-IKEM and Thomayer hospital in Prague approved the study protocol. Written, informed consent for participation in the study was obtained from all the subjects. The study was performed in accordance with the Helsinki Declaration of 1964, and its later amendments.

Results

Patients. A total of 847 advanced HFrEF patients (67.7% were in with NYHA III/IV, average LV-ejection fraction was 23.6%, 44.9% had moderate/severe RV dysfunction), were enrolled in the study (Fig. 1 in the Online supplement). Enrolled patients achieved high level of guideline-recommended HF pharmacotherapy and device therapy (Table 1). Patients were prospectively followed for a median of 1126 (IQRs 410; 1781) days. During follow-up, 515 patients (60.8%) experienced an adverse outcome.

A total of 380 patients (44.9%) were found to have DM, 467 patients (55.1%) were DM free. All DM patients had type 2 DM; none of the patients had type 1 DM. DM patients were older, had more often CAD as underlying HF etiology, larger body mass index, worse renal function (Table 1) and worse cumulative survival—269 (70.8%) DM vs. 246 (52.7%) non-DM patients experienced an adverse outcome, median time to event was 879 days (IQRs 312; 1631) for DM patients compared with 1270 (IQRs 467; 2010) days for non-DM counterparts. Kaplan–Meier curves are provided in Fig. 2 in the Online Supplement.

Diabetes treatment. Out of 380 DM patients, 153 patients (40.3%) were treated with diet only, 87 patients (22.9%) with MET, 67 patients (17.6%) with sulfonylurea (SU) derivatives, 108 patients (28.4%) with insulin, 26 patients (6.8%) with DPPIV-inhibitors, 3 patients (0.8%) with repaglinide and 1 patient (0.3%) was treated with liraglutide. In 3 patients the information about the treatment was missing. None of the patients was treated with thiazolidinediones, acarbose or SGLT2-inhibitors. 31 patients (8.2%) were treated with more than one peroral antidiabetics (PAD), 26 patients (6.8%) with the combination of PAD and insulin. More detailed information about DM treatment is given in Table 1 and Fig. 3 in the Online Supplement.

In patients treated with MET, the most widely used MET dose was 1000 mg (29 patients, 33.3%). 18 patients (20.7%) were taking a dose lower than 1000 mg, 14 patients (16.1%) a dose between 1000 and 2000 mg and 25 patients (28.8%) were taking 2000 mg daily or higher. The information about MET daily dose was missing in 1 patient (1.1%). Distribution of MET daily dose is in Fig. 4 in the Online Supplement.

Compared with MET-free counterparts, MET-treated DM patients had better LV function (LVEF), RV function and lower both mitral and tricuspid regurgitation severity, better renal function and larger BMI. They were using smaller diuretic doses but achieved similar level of guideline-recommended HF pharmacotherapy, had comparable rate of ICD and CRT treatment and similar hemodynamic profile (Table 1). MET-treated patients were more often treated with SU derivatives and DPPIV-inhibitors; no significant difference was found for insulin treatment.

Metabolic profile of MET-treated patients. Analysis of metabolic parameters revealed that compared with MET-free counterparts, MET-treated patients had similar levels of fasting glycemia and insulin secretion (C-peptide level), but larger Hb1Ac level, higher insulin and glucagon level and more pronounced insulin resistance (HOMA-IR), Table 1 and Fig. 1. Further, MET-treated patients had higher level of beta-hydroxybutyrate but similar level of GDF-15 (Fig. 1).

Diabetes treatment and quality of life. No significant difference was found in QoL between patients with and without DM (Table 1). In DM subgroup, pharmacotherapy with neither insulin, SU derivatives nor

	Whole cohort (n = 847)	Non-DM (n = 467)	DM (n = 380)	P (non-DM vs. DM)	DM MET-free (n = 290)	DM MET-treated (n = 87)	P (MET-free vs. MET-treated)
Age (years)	57.40 ± 11.28	55.03 ± 11.94	60.31 ± 9.65	**< 0.0001**	60.14 ± 9.63	60.92 ± 9.85	0.51
Males (%)	82.8	81.6	84.2	0.31	83.5	86.2	0.53
HF etiology (% CAD)	50.2	41.6	60.8	**< 0.0001**	59.4	65.1	0.34
BMI (kg/m^2)	27.82 ± 5.09	26.94 ± 4.55	28.9 ± 5.50	**< 0.0001**	28.27 ± 5.31	30.98 ± 5.61	**< 0.0001**
NYHA (2–4, %)	32.2/60.3/7.4	35.1/58.9/6.0	28.7/62.1/9.2	0.11	25.5/63.5/11.0	40.2/56.3/3.5	**0.02**
BNP (ng/l)	466 (208; 1077)	381 (162; 948)	613 (264; 1187)	**< 0.0001**	642 (334; 1354)	400 (148; 920)	**0.0002**
Hemoglobin (g/l)	140.85 ± 18.18	142.00 ± 18.36	139.49 ± 17.90	**0.049**	140.09 ± 18.13	138.00 ± 16.39	0.34
eGFR (ml/min 1.73/m^2)	68.91 ± 22.50	72.55 ± 22.55	64.59 ± 21.69	**< 0.0001**	63.34 ± 22.12	69.26 ± 19.76	**0.03**
CRP (mg/l)	4.5 (1.9; 9.9)	3.5 (1.5; 8.1)	5.5 (2.5; 11.4)	**< 0.0001**	5.5 (2.9; 11.3)	5.3 (2.1; 13.2)	0.70
Diabetes and metabolism							
Glucagon (mIU/ml)	97 (77; 125)	90.8 (73.83; 116.2)	105.7 (82.5; 132.8)	**< 0.0001**	102.35 (80.35; 128.73)	116.30 (92.10; 145.70)	**0.015**
C-peptid (nmol/l)	1.38 (0.958; 1.942)	1.27 (0.92; 1.76)	1.52 (1.03; 2.16)	**< 0.0001**	1.50 (1.02; 2.12)	1.56 (1.08; 2.26)	0.90
Free fatty acids (mmol/l)	0.53 (0.37; 0.72)	0.49 (0.35; 0.69)	0.59 (0.40; 0.79)	**0.0008**	0.61 (0.39; 0.80)	0.57 (0.42; 0.79)	0.74
Biomarkers							
Hs-TnT[&] (ng/l)	23.86 (14.46; 40.72)	20.05 (11.98; 33.41)	28.18 (18.71; 49.03)	**< 0.0001**	29.3 (18.8; 49.2)	25.3 (17.6; 43.1)	0.49
Cardiac morphology and function							
SBP (mmHg)	116.33 ± 19.10	115.3 ± 19.2	117.6 ± 18.9	0.07	116.08 ± 18.89	122.78 ± 18.00	**0.004**
Heart rate (min^{-1})	75.72 ± 14.54	74.22 ± 14.77	77.55 ± 14.07	**0.002**	77.66 ± 14.26	77.43 ± 13.61	0.90
LVEDD (mm)	69.41 ± 9.11	69.82 ± 9.72	68.90 ± 8.28	0.14	69.04 ± 8.47	68.31 ± 7.68	0.47
LVEF (%)	23.59 ± 5.80	23.57 ± 5.80	23.63 ± 5.79	0.88	23.05 ± 5.82	25.60 ± 5.30	**0.0003**
RVD1 (mm)	40.62 ± 7.94	39.64 ± 8.11	41.81 ± 7.58	**< 0.0001**	41.93 ± 7.81	41.40 ± 6.89	0.57
RV dysfunction grade (0–3, %)	32.3 22.8/33.5/11.4	38.5/23.8/28.6/9.1	24.7/21.6/39.5/14.2	**< 0.0001**	19.9/21.4/42.8/15.9	42.2/21.7/27.7/8.4	**0.002**
Mitral regurgitation (1–3, %)	25.2/40.5/34.3	27.0/40.3/32.7	22.9/40.8/36.3	0.32	18.3/44.1/37.6	39.1/28.7/32.2	**0.0004**
Tricuspid regurgitation (1–3, %)	44.6/39.0/16.3	48.9/37.4/13.7	39.4/41.0/19.6	**0.001**	34.0/44.5/21.5	57.5/31.0/11.5	**0.0004**
Estimated systolic pulmonary pressure (mmHg)	45.11 ± 13.65	43.46 ± 13.93	46.98 ± 13.10	**0.002**	46.97 ± 12.95	47.60 ± 13.05	0.74
IVC (mm)	19.55 ± 5.74	18.93 ± 5.58	20.31 ± 5.86	**0.0006**	20.45 ± 5.81	19.54 ± 5.36	0.21
Quality of life							
MLHFQ sum	44 (26; 60)	43 (24; 59)	44 (28; 61)	0.25	48 (30; 62)	36 (16; 51)	**0.002**
MLHFQ somatic	21 (12; 28)	21 (12; 27)	22 (12; 28)	0.59	23 (14; 29)	17 (10; 24)	**0.0007**
MLHFQ emotional	6 (2; 11)	6 (1; 12)	6 (2; 11)	0.86	6 (3; 12)	5 (1; 10)	0.09
Hemodynamics[Δ]							
RA pressure (mmHg)	9 (6; 13)	8 (5; 12)	10 (6; 16)	**0.0009**	10 (6; 16)	9 (7; 14)	0.56
Systolic PA pressure (mmHg)	53 (38; 65)	47 (34; 62)	57 (44; 68)	**< 0.0001**	57 (44; 69)	60 (45; 68)	0.89
Diastolic PA pressure (mmHg)	24 (18; 31)	22 (16; 29.5)	27 (20; 32)	**0.005**	27 (19.5; 32)	26.5 (19.75; 32.25)	0.92
Mean PA pressure (mmHg)	35 (26; 43)	32 (23; 42)	37 (30; 45)	**0.0003**	37 (30; 45)	38 (32; 44)	0.99
PCWP (mmHg)	24 (17; 29)	23 (16; 28)	25 (19; 30)	**0.02**	24.5 (19; 30	25 (16; 31)	0.73
CI (l/min/1.73 m^2)	1.84 (1.58; 2.15)	1.90 (1.59; 2.18)	1.80 (1.55; 2.14)	0.14	1.75 (1.51; 2.13)	1.96 (1.73; 2.32)	0.06
Therapy							
ACEi/ARB (%)	78.65	79.83	77.31	0.37	77.51	79.31	0.72
BB (%)	87.66	88.20	87.07	0.62	88.58	82.76	0.17
MRA (%)	76.99	75.32	78.89	0.22	79.93	75.86	0.42
Furosemide daily dose (mg)	80 (40; 125)	60 (40; 120)	80 (40; 125)	**< 0.0001**	80 (40; 131.25)	60 (40; 125)	**0.03**
ICD any (%)	59.4	57.8	61.4	0.29	61.70	61.45	0.97
CRT any (%)	32.0	31.5	32.6	0.73	35.11	24.10	0.06
Amiodarone (%)	18.3	17.9	18.8	0.73	19.66	16.09	0.45
Insulin (%)	–	–	28.4	–	30.34	22.99	0.18
Insulin daily dose	–	–	48 (31; 66)*	–	46 (31; 63.5)	54.5 (31.5; 80)	0.29

Continued

	Whole cohort (n = 847)	Non-DM (n = 467)	DM (n = 380)	P (non-DM vs. DM)	DM MET-free (n = 290)	DM MET-treated (n = 87)	P (MET-free vs. MET-treated)
SU derivatives (%)	–	–	17.6	–	15.17	26.44	**0.02**
DPP-IV inhibitors (%)	–	–	6.8	–	4.83	13.79	**0.007**
Outcome							
Death (%)	324 (38.3%)	134 (28.7%)	190 (50.0%)	–	152 (52.4%)	37 (42.5%)	–
Urg. HTx (%)	107 (12.6%)	63 (13.5%)	44 (11.6%)	–	39 (13.5%)	4 (4.6%)	–
Norm. HTx (%)	35 (4.1%)	23 (4.9%)	12 (3.2%)	–	10 (3.5%)	2 (2.3%)	–
MCSi (%)	83 (9.8%)	48 (10.3%)	35 (9.2%)	–	28 (9.7%)	6 (6.9%)	–

Table 1. Patients characteristics. Data are shown as mean ± SD or median with IQRs. [&]Available in 450 patients only. [Δ]Available in 385 patients only. *Calculated for only 108 patients treated with insulin. Information about DM treatment was missing in 3 patients. Significant values are in bold.

with DPPIV-inhibitors was associated with better QoL (Table 1 in the Online Supplement). On the contrary, MET treatment was associated with a better QoL (Table 1).

Multivariable regression analysis identified MET treatment together with BNP and BMI, but not eGFR, SU derivatives treatment, DPPIV-inhibitors treatment or insulin treatment to be independently associated with MLHFQ score (Table 2 in the Online Supplement). Similar results were obtained for the somatic component of MLHFQ whereas no association of MET treatment with emotional component of the MLHFQ score was found (data not shown).

Diabetes treatment and outcome. Kaplan–Meier analysis showed that MET-treated diabetic patients had better survival compared to MET-free counterparts. Other therapeutic regimes were not associated with any difference in event-free survival (Fig. 2). Similarly, Cox proportional hazard model identified MET treatment to be associated with improved outcome. No such relationship was observed for therapy with insulin, SU derivatives or DPPIV-inhibitors (Table 3 in the Online Supplement).

Next, we have analyzed whether there was any subgroup having altered benefit from MET treatment. No significant interaction was found between MET therapy and NYHA functional class, LVEF, RV dysfunction grade, BNP level, eGFR, ACEi/ARB treatment, beta-blocker treatment, presence of ICD, or CRT (all p for interaction ≥ 0.20, Table 4 in the Online Supplement). This suggests that the benefit from MET therapy is preserved regardless of HF severity and independent of HF treatment. Similarly, no significant interaction was found between MET therapy and insulin or DPPIVi treatment (p for interaction = 0.35 and 0.95, respectively). However, borderline interaction was found for SU derivatives treatment (p for interaction = 0.054). Kaplan–Meier analysis showed borderline worse survival of patients treated with MET and SU derivatives compared with MET without SU derivatives (p (log-rank) = 0.08).

Adjustment for confounders, propensity score-matched analysis. Although MET-treated DM patients had better cardiac function, renal function and larger BMI, Cox proportional hazard model analysis revealed that MET treatment was associated with a significantly better outcome even after the adjustment for BNP, eGFR and BMI (Table 2).

Finally, we have performed propensity score matched analysis that matched the patients for 17 variables that might influence the selection of MET therapy or that have been shown to influence prognosis of patients with advanced heart failure (age, sex, NYHA functional class, BMI, estimated glomerular filtration rate, LVEF, RV dysfunction grade, mitral and tricuspid regurgitation severity, BNP level, beta-blockers use, renin-angiotensin system inhibitors use, ICD therapy, CRT therapy, uric acid levels, treatment with other PAD/incretins and treatment with insulin). Propensity score matching yielded 81 pairs of patients. Standardized mean differences of matched covariates ranged from 0 to 0.23, with a standardized median difference of 0.06 (IQR 0.029–0.076). Significantly better survival for MET-treated group was showed both using the McNemar (p = 0.04), as well as Cox proportional hazard model (p = 0.01, Fig. 3).

Discussion

The results of this study can be summarized as follows: (i) despite worse insulin sensitivity and worse DM compensation in MET-treated patients, MET-treatment was independently associated with both better quality of life and improved outcome in advanced HFrEF patients with DM; (ii) MET treatment was associated with better outcome regardless of HF severity or compensation of diabetes.

Optimal treatment modality in patients with advanced HF and DM is not well established, which is mirrored by the large variability of treatment strategies observed in our study.

Only 22.9% of our patients were treated with MET, which is likely a consequence of previous recommendations to avoid this drug in HF because of concerns regarding lactic acidosis risk[13]. Nevertheless, MET was used in clinical practice and data on MET use in HF patients with DM eventually emerged. One recently published study showed lower risk of hospitalization for HF in MET-treated DM patients[14]. Thirteen studies have been published describing the association between MET treatment on outcome in patients with established HF and DM[6,7,9,15–24]. However, the majority of studies are retrospective and based on administrative or disease records[7,17–21,23,24]. Only five of them reported LV-ejection fraction[6,7,9,17,22] and only one study focused specifically on patients with

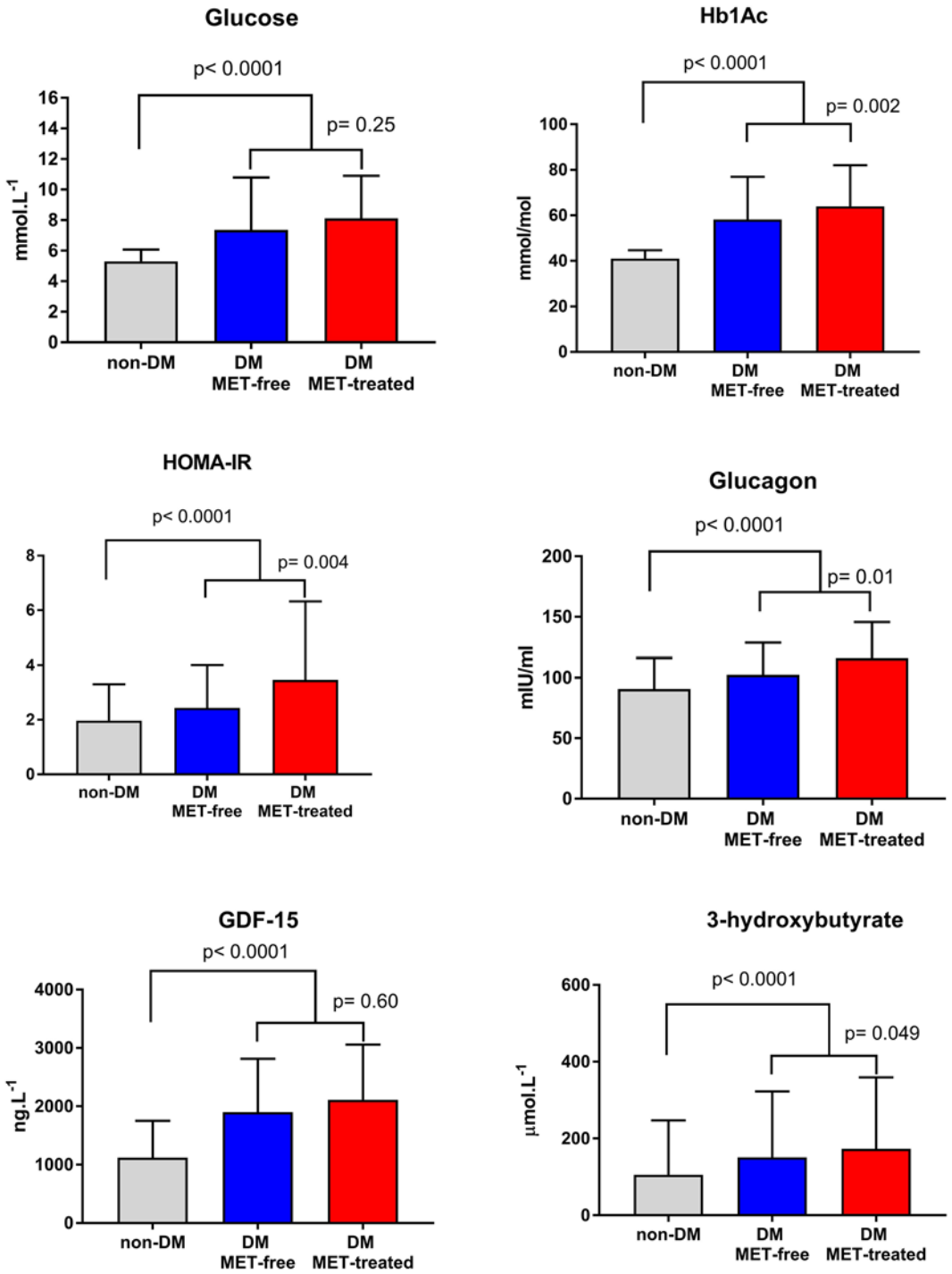

Figure 1. Metabolic profile. For Glucose and Hb1Ac, data are shown as mean ± SD, for HOMA-IR, Glucagon, GDF-15 and 3-hydroxybutyrate as median ± IQRs. For HOMA-IR, only patients without insulin treatment were evaluated (n = 196 DM MET-free, n = 61 DM MET-treated).

LVEF < 40%[9]. Although meta-analyses of these studies reported mostly better outcome in patients treated with MET[3,4], the heterogeneity of studied populations and approaches leave many questions unanswered. None of the studies focused specifically on patients with advanced HF and no study HFrEF patients employed propensity-matching approach. As large randomized controlled trials with MET in HF patients with DM are unlikely to be carried out[25], our data offering a prospective observational design of well-characterized cohort employing propensity matching analysis offers the strongest evidence possible. In the propensity matching analysis, we have adjusted the cohort for seventeen possible confounders and our data thus strongly suggest that despite differences between MET-treated and MET-free patients, observed difference in outcome between these groups is indeed attributable to MET therapy.

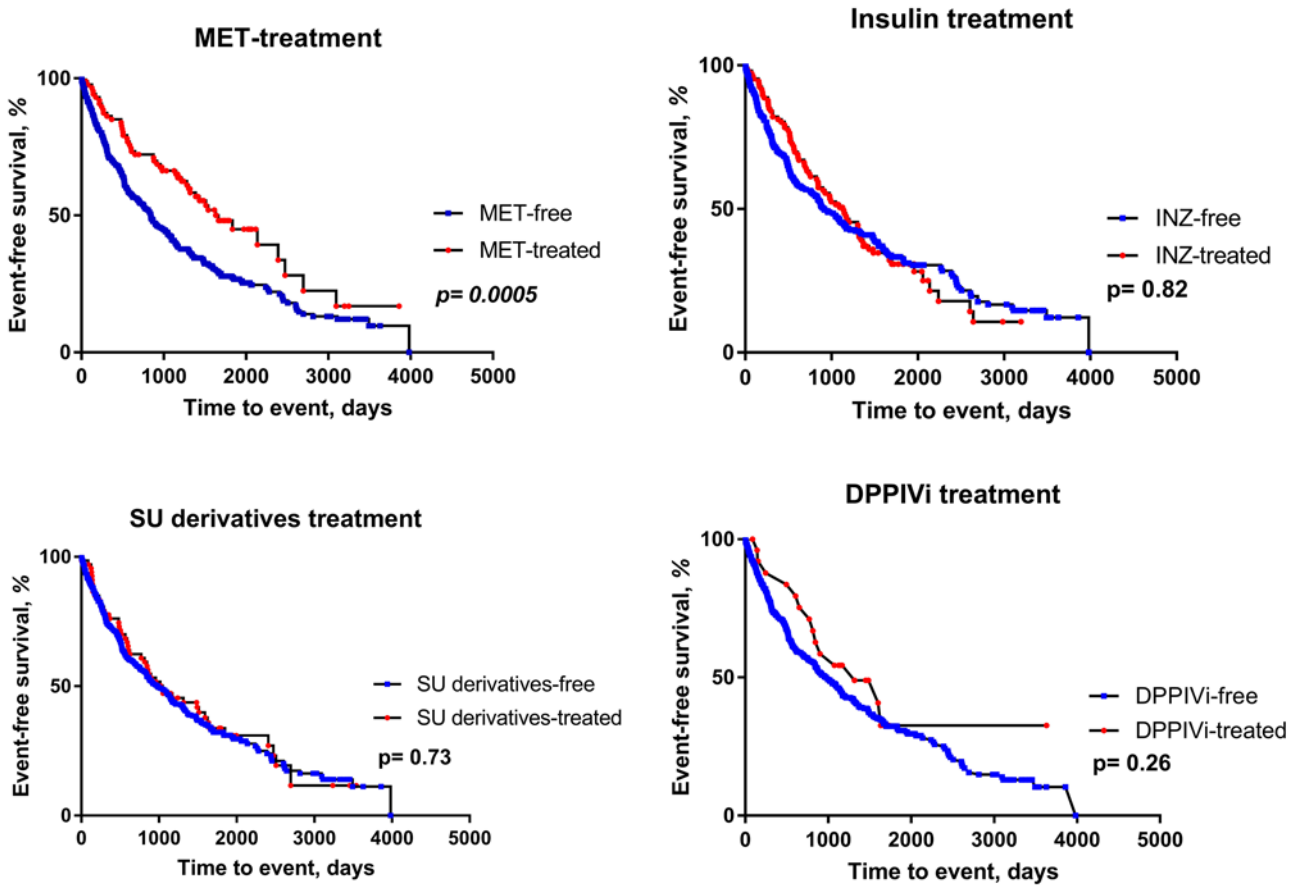

Figure 2. Event-free survival DM patients according DM treatment; MET-treated DM patients had significantly better survival, no significant difference in survival was observed among patients treated with other glucose-lowering agents.

		HR	95% CI	p
Model 1	MET (present vs. absent)	0.57	0.41–0.78	**0.0003**
Model 2	MET (present vs. absent)	0.63	0.45–0.87	**0.004**
	BMI (kg/m^2)	0.97	0.94–0.99	**0.005**
Model 3	MET (present vs. absent)	0.64	0.46–0.88	**0.007**
	BMI (kg/m^2)	0.97	0.94–0.99	**0.01**
	eGFR (ml/min 1.73/m^2)	0.995	0.989–1.0006	0.08
Model 4	MET (present vs. absent)	0.70	0.50–0.98	**0.035**
	BNP (ng/l)	1.00056	1.0004–1.0007	**< 0.0001**
	BMI (kg/m^2)	0.99	0.97–1.018	0.51
	eGFR (ml/min 1.73/m^2)	0.996	0.991–1.002	0.24

Table 2. Metformin and outcome, Cox proportional hazard analysis. MET treatment was associated with lower risk of an adverse outcome even after the adjustment for BNP, eGFR and BMI. *HR* hazard ratio, *CI* confidence interval. Significant values are in bold.

The mechanism of action of MET is a subject of intense debate. Beneficial effect of MET was first explained by an inhibition of mitochondrial complex I[26,27] and by an increase in ADP/ATP ratio that activates AMP-dependent protein kinase (AMPK). However, the mechanism of action of MET is likely to be more pleiotropic; MET enhances cardiac autophagy[28], improves myocardial efficiency and reduces myocardial energy consumption[29], and directly modulates the growth and function of gut microbiota[30]. MET has been also shown to have potent effect on cancer prevention and recurrence[31,32] and its anti-cancer effect might be also clinically relevant in HF patients as they are consistently reported to have higher risk of malignancies[33,34].

Although our study was not designed to unveil the mechanism responsible for overall benefit from MET therapy, our data suggest that the cardioprotection of MET is independent on glycemic control. This is in line with results of the post UKPDS-trial follow-up that showed significant risk reduction by MET in diabetes-related

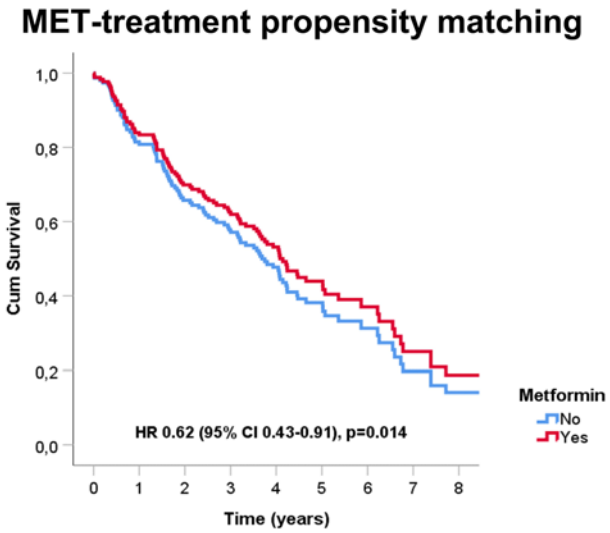

Figure 3. Survival of MET-treated patients, propensity-score matched analysis. *BMI* body mass index, *eGFR* estimated glomerular filtration rate, *LVEF* left ventricle ejection fraction, *RV* right ventricle, *BNP* B-type natriuretic peptide, *RAAi* renin-angiotensin system inhibitors, *ICD* implantable cardioverter/defibrillator, *CRT* cardiac resynchronization, therapy, *PAD* peroral antidiabetics.

endpoints despite of the loss of between-group differences in glycated hemoglobin[35]. Experimental studies have similarly shown anti-inflammatory properties of MET irrespective of DM status[36].

Metabolic abnormalities are observed early in the course of cardiac pathologies. When subjected to pressure overload, the ventricular myocardium shifts from fatty acids to glucose as its main source for energy; this precedes the development of LV hypertrophy[36]. The excessive glucose metabolism in the cardiomyocytes causes glucose-6-phosphate (G6P) accumulation. G6P activates mammalian target of rapamycin complex 1 (mTORC1), which induces hypertrophy. MET activates AMPK, which inhibits mTROC1, thus preventing LV hypertrophy[36]. This explains that MET treatment has also been shown to induce regression of LV-hypertrophy and exert antioxidant effects even in non-diabetic patients[37]. Similarly, LV reverse remodeling has been observed in other drugs that activate AMPK such as SGLT2-inhibitors[38].

In non-HF subjects, MET was shown to mediate its effect on body weight and energy balance through GDF-15[39]. We have not observed increased GDF-15 level in MET-treated compared with MET-free patients in our study, which can be explained by worse cardiac and renal function in MET-free patients. Both cardiac as well as renal dysfunction are associated with higher GDF-15 levels[40]. MET-treated patients have increased ketone body beta-hydroxybutyrate, a metabolic substrate that is readily utilized by failing heart and that may have favorable effects on bioenergetics[41]. Infusion of ketone bodies in HFrEF patients was shown to improve cardiac output and LV-ejection fraction[42]. Interestingly, despite patients on MET had lower neurohumoral activation, we observed higher levels of stress hormone glucagon in MET-treated patients. Is was shown that MET administration to prediabetic subjects resulted in an increase of glucagon[43]. Higher glucagon in MET-treated patients may be protective against hypoglycemia that is a feared complication of DM treatment and was linked to arrhythmias and increased mortality[44].

Although QoL was independent of DM status in our study, we have observed a better QoL in MET-treated DM patients and MET was significantly associated with QoL also in multivariable linear regression suggesting its independent effect on QoL. To our best knowledge, this is the first study that analyzed the QoL with respect to MET treatment using a validated tool[45]. It has been recently demonstrated that QoL in HF patients is driven by HF itself, not by associated comorbidities[46]. MET-induced improvement in myocardial efficiency[29] suggests that the effect of MET on QoL in HF is rather due to an improvement in HF, not due to improvement in blood glucose control.

Beneficial effects of MET documented in high risk advanced HF population suggest that MET should be more widely used in management of HF. Even in studies with SGLT2 inhibitors in HF patients, a substantial proportion of DM+ patients were treated with biguanides (metformin). In DAPA-HF trial, 41.8% of patients had DM and 51% of DM+ patients were treated by biguanides (predominantly MET)[47]. EMPEROR-Reduced trial reports also a 49.8% prevalence of DM and 46.4% of DM+ patients were treated with biguanides[48,49]. Our data strongly suggest that MET should be a frontline drug for the treatment of diabetic patients with HFrEF. Combination

therapy with MET and SGLT2i has been shown safe and efficacious in patients with DM[50]. Combined therapy of these patients with MET and SGLT2 inhibitors warrants further research.

Limitations. Our study was performed in a heart center offering a complex cardiovascular program including MCS implantation and HTx. Since this could introduce bias related to the analysis of prognostic value, urgent HTx and MCS implantation were considered adverse outcomes, while the patients receiving non-urgent HTx were censored as having no adverse outcome on the day of transplantation[12]. In addition, it was a single-center study with a substantial predominance of males. Our study cohort included patients with advanced HFrEF, the results thus might not be fully applicable to patients with milder HF or to older patients. Data about HF re-hospitalizations were not available in all patients so this endpoint could have not been included in the analysis. The information about DM duration and MET exposure time before entering the study were not available in all subjects, therefore it was not possible to address these variables in the propensity-matching analysis. The cause of death was not available in all patients, so we were not able to distinguish between cardiovascular and non-cardiovascular mortality. QoL was analyzed only at baseline and is likely a result of a various time of preceding MET therapy; the time of MET treatment before baseline exam or during follow-up is unknown. Data about plasmatic MET concentration are not available; similarly, lactate was not measured. None of the patients was treated by sacubitril-valsartan or SGLT2 inhibitors. Therefore, it is impossible to analyze potentially additional effect of MET and these agents. Only a subset of patients had serial echocardiographic examinations, so it was not possible to analyze the impact of MET-treatment of cardiac reverse remodeling.

Conclusion

Metformin treatment in advanced HFrEF patients with DM is associated with better outcome by mechanisms beyond the improvement of blood glucose control. Metformin should stay among frontline drugs for the management of HFrEF patients with DM.

Data availability

The datasets analyzed during the current study are available from the corresponding author on reasonable request (jan.benes@ikem.cz).

Received: 20 February 2022; Accepted: 25 July 2022
Published online: 29 July 2022

References

1. Lu, H. C., Parikh, P. P. & Lorber, D. L. Phenformin-associated lactic acidosis due to imported phenformin. *Diabetes Care* **19**, 1449–1450. https://doi.org/10.2337/diacare.19.12.1449 (1996).
2. Salpeter, S. R., Greyber, E., Pasternak, G. A. & Salpeter, E. E. Risk of fatal and nonfatal lactic acidosis with metformin use in type 2 diabetes mellitus. *Cochrane Database Syst. Rev.* **2010**, CD002967. https://doi.org/10.1002/14651858.CD002967.pub4 (2010).
3. Eurich, D. T. *et al.* Comparative safety and effectiveness of metformin in patients with diabetes mellitus and heart failure: Systematic review of observational studies involving 34,000 patients. *Circ. Heart Fail.* **6**, 395–402. https://doi.org/10.1161/circheartfailure.112.000162 (2013).
4. Crowley, M. J. *et al.* Clinical outcomes of metformin use in populations with chronic kidney disease, congestive heart failure, or chronic liver disease: A systematic review. *Ann. Intern. Med.* **166**, 191–200. https://doi.org/10.7326/m16-1901 (2017).
5. Dludla, P. V. *et al.* Metformin and heart failure-related outcomes in patients with or without diabetes: A systematic review of randomized controlled trials. *Heart Fail. Rev.* **26**, 1437–1445. https://doi.org/10.1007/s10741-020-09942-y (2021).
6. Aguilar, D., Chan, W., Bozkurt, B., Ramasubbu, K. & Deswal, A. Metformin use and mortality in ambulatory patients with diabetes and heart failure. *Circ. Heart Fail.* **4**, 53–58. https://doi.org/10.1161/circheartfailure.110.952556 (2011).
7. MacDonald, M. R. *et al.* Treatment of type 2 diabetes and outcomes in patients with heart failure: A nested case-control study from the U.K. general practice research database. *Diabetes Care* **33**, 1213–1218. https://doi.org/10.2337/dc09-2227 (2010).
8. Effect of intensive blood-glucose control with metformin on complications in overweight patients with type 2 diabetes (UKPDS 34). UK Prospective Diabetes Study (UKPDS) Group. *Lancet* **352**, 854–865 (1998).
9. Shah, D. D., Fonarow, G. C. & Horwich, T. B. Metformin therapy and outcomes in patients with advanced systolic heart failure and diabetes. *J. Cardiac Fail.* **16**, 200–206. https://doi.org/10.1016/j.cardfail.2009.10.022 (2010).
10. Cosentino, F. *et al.* 2019 ESC Guidelines on diabetes, pre-diabetes, and cardiovascular diseases developed in collaboration with the EASD. *Eur. Heart J.* **41**, 255–323. https://doi.org/10.1093/eurheartj/ehz486 (2020).
11. Lang, R. M. *et al.* Recommendations for chamber quantification. *Eur. J. Echocardiogr.* **7**, 79–108. https://doi.org/10.1016/j.euje.2005.12.014 (2006).
12. Aaronson, K. D. *et al.* Development and prospective validation of a clinical index to predict survival in ambulatory patients referred for cardiac transplant evaluation. *Circulation* **95**, 2660–2667. https://doi.org/10.1161/01.cir.95.12.2660 (1997).
13. Inzucchi, S. E., Masoudi, F. A. & McGuire, D. K. Metformin in heart failure. *Diabetes Care* **30**, e129. https://doi.org/10.2337/dc07-1686 (2007).
14. Tseng, C. H. Metformin use is associated with a lower risk of hospitalization for heart failure in patients with type 2 diabetes mellitus: A retrospective cohort analysis. *J. Am. Heart Assoc.* **8**, e011640. https://doi.org/10.1161/jaha.118.011640 (2019).
15. Bergmark, B. A. *et al.* Metformin use and clinical outcomes among patients with diabetes mellitus with or without heart failure or kidney dysfunction: Observations from the SAVOR-TIMI 53 trial. *Circulation* **140**, 1004–1014. https://doi.org/10.1161/circulationaha.119.040144 (2019).
16. Inzucchi, S. E. *et al.* Insulin-sensitizing antihyperglycemic drugs and mortality after acute myocardial infarction: Insights from the National Heart Care Project. *Diabetes Care* **28**, 1680–1689. https://doi.org/10.2337/diacare.28.7.1680 (2005).
17. Masoudi, F. A. *et al.* Thiazolidinediones, metformin, and outcomes in older patients with diabetes and heart failure: An observational study. *Circulation* **111**, 583–590. https://doi.org/10.1161/01.cir.0000154542.13412.b1 (2005).
18. Eurich, D. T., Majumdar, S. R., McAlister, F. A., Tsuyuki, R. T. & Johnson, J. A. Improved clinical outcomes associated with metformin in patients with diabetes and heart failure. *Diabetes Care* **28**, 2345–2351. https://doi.org/10.2337/diacare.28.10.2345 (2005).
19. Evans, J. M. *et al.* Effect of Metformin on mortality in patients with heart failure and type 2 diabetes mellitus. *Am. J. Cardiol.* **106**, 1006–1010. https://doi.org/10.1016/j.amjcard.2010.05.031 (2010).

20. Roussel, R. *et al.* Metformin use and mortality among patients with diabetes and atherothrombosis. *Arch. Intern. Med.* **170**, 1892–1899. https://doi.org/10.1001/archinternmed.2010.409 (2010).
21. Andersson, C. *et al.* Metformin treatment is associated with a low risk of mortality in diabetic patients with heart failure: A retrospective nationwide cohort study. *Diabetologia* **53**, 2546–2553. https://doi.org/10.1007/s00125-010-1906-6 (2010).
22. Romero, S. P. *et al.* Metformin therapy and prognosis of patients with heart failure and new-onset diabetes mellitus. A propensity-matched study in the community. *Int. J. Cardiol.* **166**, 404–412. https://doi.org/10.1016/j.ijcard.2011.10.141 (2013).
23. Tinetti, M. E., McAvay, G., Trentalange, M., Cohen, A. B. & Allore, H. G. Association between guideline recommended drugs and death in older adults with multiple chronic conditions: Population based cohort study. *BMJ (Clin. Res. Ed.)* **351**, h4984. https://doi.org/10.1136/bmj.h4984 (2015).
24. Weir, D. L., McAlister, F. A., Senthilselvan, A., Minhas-Sandhu, J. K. & Eurich, D. T. Sitagliptin use in patients with diabetes and heart failure: A population-based retrospective cohort study. *JACC. Heart Fail.* **2**, 573–582. https://doi.org/10.1016/j.jchf.2014.04.005 (2014).
25. Eurich, D. T. *et al.* Metformin treatment in diabetes and heart failure: When academic equipoise meets clinical reality. *Trials* **10**, 12. https://doi.org/10.1186/1745-6215-10-12 (2009).
26. Owen, M. R., Doran, E. & Halestrap, A. P. Evidence that metformin exerts its anti-diabetic effects through inhibition of complex 1 of the mitochondrial respiratory chain. *Biochem. J.* **348**(Pt 3), 607–614 (2000).
27. El-Mir, M. Y. *et al.* Dimethylbiguanide inhibits cell respiration via an indirect effect targeted on the respiratory chain complex I. *J. Biol. Chem.* **275**, 223–228. https://doi.org/10.1074/jbc.275.1.223 (2000).
28. Kanamori, H. *et al.* Metformin enhances autophagy and provides cardioprotection in δ-sarcoglycan deficiency-induced dilated cardiomyopathy. *Circ. Heart Fail.* **12**, e005418. https://doi.org/10.1161/circheartfailure.118.005418 (2019).
29. Larsen, A. H. *et al.* A randomised, double-blind, placebo-controlled trial of metformin on myocardial efficiency in insulin-resistant chronic heart failure patients without diabetes. *Eur. J. Heart Fail.* **22**, 1628–1637. https://doi.org/10.1002/ejhf.1656 (2020).
30. Wu, H. *et al.* Metformin alters the gut microbiome of individuals with treatment-naive type 2 diabetes, contributing to the therapeutic effects of the drug. *Nat. Med.* **23**, 850–858. https://doi.org/10.1038/nm.4345 (2017).
31. He, K. *et al.* The effect of metformin therapy on incidence and prognosis in prostate cancer: A systematic review and meta-analysis. *Sci. Rep.* **9**, 2218. https://doi.org/10.1038/s41598-018-38285-w (2019).
32. Anselmino, L. E. *et al.* Repositioning metformin and propranolol for colorectal and triple negative breast cancers treatment. *Sci. Rep.* **11**, 8091. https://doi.org/10.1038/s41598-021-87525-z (2021).
33. Meijers, W. C. *et al.* Heart failure stimulates tumor growth by circulating factors. *Circulation* **138**, 678–691. https://doi.org/10.1161/circulationaha.117.030816 (2018).
34. Banke, A. *et al.* Incidence of cancer in patients with chronic heart failure: A long-term follow-up study. *Eur. J. Heart Fail.* **18**, 260–266. https://doi.org/10.1002/ejhf.472 (2016).
35. Holman, R. R., Paul, S. K., Bethel, M. A., Matthews, D. R. & Neil, H. A. 10-year follow-up of intensive glucose control in type 2 diabetes. *N. Engl. J. Med.* **359**, 1577–1589. https://doi.org/10.1056/NEJMoa0806470 (2008).
36. Cameron, A. R. *et al.* Anti-inflammatory effects of metformin irrespective of diabetes status. *Circ. Res.* **119**, 652–665. https://doi.org/10.1161/circresaha.116.308445 (2016).
37. Mohan, M. *et al.* A randomized controlled trial of metformin on left ventricular hypertrophy in patients with coronary artery disease without diabetes: The MET-REMODEL trial. *Eur. Heart J.* **40**, 3409–3417. https://doi.org/10.1093/eurheartj/ehz203 (2019).
38. Santos-Gallego, C. G. *et al.* Empagliflozin ameliorates adverse left ventricular remodeling in nondiabetic heart failure by enhancing myocardial energetics. *J. Am. Coll. Cardiol.* **73**, 1931–1944. https://doi.org/10.1016/j.jacc.2019.01.056 (2019).
39. Coll, A. P. *et al.* GDF15 mediates the effects of metformin on body weight and energy balance. *Nature* **578**, 444–448. https://doi.org/10.1038/s41586-019-1911-y (2020).
40. Benes, J. *et al.* The role of GDF-15 in heart failure patients with chronic kidney disease. *Can. J. Cardiol.* **35**, 462–470. https://doi.org/10.1016/j.cjca.2018.12.027 (2019).
41. Monzo, L. *et al.* Myocardial ketone body utilization in patients with heart failure: The impact of oral ketone ester. *Metab. Clin. Exp.* **115**, 154452. https://doi.org/10.1016/j.metabol.2020.154452 (2021).
42. Nielsen, R. *et al.* Cardiovascular effects of treatment with the ketone body 3-hydroxybutyrate in chronic heart failure patients. *Circulation* **139**, 2129–2141. https://doi.org/10.1161/circulationaha.118.036459 (2019).
43. Konopka, A. R. *et al.* Hyperglucagonemia mitigates the effect of metformin on glucose production in prediabetes. *Cell Rep.* **23**, 2532. https://doi.org/10.1016/j.celrep.2018.05.027 (2018).
44. Landstedt-Hallin, L., Englund, A., Adamson, U. & Lins, P. E. Increased QT dispersion during hypoglycaemia in patients with type 2 diabetes mellitus. *J. Intern. Med.* **246**, 299–307. https://doi.org/10.1046/j.1365-2796.1999.00528.x (1999).
45. Rector, T. S., Kubo, S. H. & Cohn, J. N. Validity of the Minnesota living with heart failure questionnaire as a measure of therapeutic response to enalapril or placebo. *Am. J. Cardiol.* **71**, 1106–1107. https://doi.org/10.1016/0002-9149(93)90582-w (1993).
46. Benes, J. *et al.* The effect of three major co-morbidities on quality of life and outcome of patients with heart failure with reduced ejection fraction. *ESC Heart Fail.* https://doi.org/10.1002/ehf2.13227 (2021).
47. McMurray, J. J. V. *et al.* Dapagliflozin in patients with heart failure and reduced ejection fraction. *N. Engl. J. Med.* **381**, 1995–2008. https://doi.org/10.1056/NEJMoa1911303 (2019).
48. Packer, M. *et al.* Cardiovascular and renal outcomes with empagliflozin in heart failure. *N. Engl. J. Med.* **383**, 1413–1424. https://doi.org/10.1056/NEJMoa2022190 (2020).
49. Anker, S. D. *et al.* Effect of empagliflozin on cardiovascular and renal outcomes in patients with heart failure by baseline diabetes status: Results from the EMPEROR-reduced trial. *Circulation* **143**, 337–349. https://doi.org/10.1161/circulationaha.120.051824 (2021).
50. Gebrie, D., Getnet, D. & Manyazewal, T. Cardiovascular safety and efficacy of metformin-SGLT2i versus metformin-sulfonylureas in type 2 diabetes: Systematic review and meta-analysis of randomized controlled trials. *Sci. Rep.* **11**, 137. https://doi.org/10.1038/s41598-020-80603-8 (2021).

Author contributions

J.B., M.K. and K.K. participated in the enrollment of patients, performed echocardiography, analyzed the data and wrote the manuscript. P.W. analyzed the data and revised the manuscript for important intellectual content. J.K., J.F. and P.J. performed laboratory analyses and revised the manuscript. M.H., L.H. and E.H. participated in the enrollment of patients and performed follow-up. T.P., J.K. and V.M. designed the study, participated in data analysis, interpretation and manuscript preparation.

Funding

This work was supported by Ministry of Health, Czech Republic—conceptual development of research organization (Institute for Clinical and Experimental Medicine—IKEM) [IN 00023001] and by Grants NV19-02-00130, NV 19-09-00125, NU21-02-00402 and by the project National Institute for Research of Metabolic and

Cardiovascular Diseases (Programme EXCELES, Project No. LX22NPO5104) - Funded by the European Union - Next Generation EU.

Competing interests

Josef Kautzner is a member of Advisory Boards for Bayer, Boehringer Ingelheim, Daiichi Sankyo, Biosense Webster, Medtronic and St Jude Medical (Abbott). He has received speaker honoraria from the above-mentioned companies and from Biotronik, Mylan, Pfizer and Pro Med. Petr Jarolim received research support from Abbott Laboratories, Amgen Inc., AstraZeneca LP, Beckman Coulter, Daiichi Sankyo, Inc., GlaxoSmithKline, Merck & Co., Inc., Roche Diagnostics Corporation, Takeda Global Research and Development Center and Waters Technologies Corporation and speaker honoraria from Roche Diagnostics Corporation. All other authors have no competing interest to declare.

Additional information

Supplementary Information The online version contains supplementary material available at https://doi.org/10.1038/s41598-022-17327-4.

Correspondence and requests for materials should be addressed to J.B.

Reprints and permissions information is available at www.nature.com/reprints.

Publisher's note Springer Nature remains neutral with regard to jurisdictional claims in published maps and institutional affiliations.

P. Ošťádal et al.

Aortic stenosis and mitral regurgitation modify the effect of venoarterial extracorporeal membrane oxygenation on left ventricularfunction in cardiogenic shock

Scientific reports
Impact Factor: 4.997

rejstřík

scientific reports

Check for updates

OPEN

Aortic stenosis and mitral regurgitation modify the effect of venoarterial extracorporeal membrane oxygenation on left ventricular function in cardiogenic shock

Petr Ostadal[1]✉, Dagmar Vondrakova[1], Michaela Popkova[2], Matej Hrachovina[2], Andreas Kruger[1], Marek Janotka[1], Jan Naar[1], Otomar Kittnar[2], Petr Neuzil[1] & Mikulas Mlcek[2]

Venoarterial extracorporeal membrane oxygenation (VA-ECMO) is widely used in the treatment of patients experiencing cardiogenic shock (CS). However, increased VA-ECMO blood flow (EBF) may significantly impair left ventricular (LV) performance. The objective of the present study was to assess the effect of VA-ECMO on LV function in acute CS with concomitant severe aortic stenosis (AS) or mitral regurgitation (MR) in a porcine model. Eight female swine (45 kg) underwent VA-ECMO implantation under general anaesthesia and mechanical ventilation. Acute CS was induced by global myocardial hypoxia. Subsequently, severe AS was simulated by obstruction of the aortic valve, while severe MR was induced by mechanical destruction of the mitral valve. Haemodynamic and LV performance variables were measured at different rates of EBF rates (ranging from 1 to 4 L/min), using arterial and venous catheters, a pulmonary artery catheter, and LV pressure–volume catheter. Data are expressed as median (interquartile range). Myocardial hypoxia resulted in declines in cardiac output to 2.7 (1.9–3.1) L/min and LV ejection fraction to 15.2% (10.5–19.3%). In severe AS, increasing EBF from 1 to 4 L/min was associated with a significant elevation in mean arterial pressure (MAP), from 33.5 (24.2–34.9) to 56.0 (51.9–73.3) mmHg ($P < 0.01$). However, LV volumes (end-diastolic, end-systolic, stroke) remained unchanged, and LV end-diastolic pressure (LVEDP) significantly decreased from 24.9 (21.2–40.0) to 19.1 (15.2–29.0) mmHg ($P < 0.01$). In severe MR, increasing EBF resulted in a significant elevation in MAP from 49.0 (28.0–53.4) to 72.5 (51.4–77.1) mmHg ($P < 0.01$); LV volumes remained stable and LVEDP increased from 17.1 (13.7–19.1) to 20.8 (16.3–25.6) mmHg ($P < 0.01$). Results of this study indicate that the presence of valvular heart disease may alleviate negative effect of VA-ECMO on LV performance in CS. Severe AS fully protected against LV overload, and partial protection was also detected with severe MR, although at the cost of increased LVEDP and, thus, higher risk for pulmonary oedema.

Abbreviations

AS	Aortic stenosis
CO	Cardiac output
CO_2	Carbon dioxide
CS	Cardiogenic shock
EBF	Extracorporeal blood flow
IV	Intravenous
LV	Left ventricle

[1]Cardiovascular Center, Na Homolce Hospital, Roentgenova 2, 15000 Prague, Czech Republic. [2]Department of Physiology, First Faculty of Medicine, Charles University in Prague, Prague, Czech Republic. ✉email: ostadal.petr@gmail.com

LVEDP	Left ventricular end-diastolic pressure
LVEDV	Left ventricular end-diastolic volume
LVEF	Left ventricular ejection fraction
LVESV	Left ventricular end-systolic volume
LVSV	Left ventricular stroke volume
MAP	Mean arterial pressure
MR	Mitral regurgitation
NIRS	Near-infrared spectroscopy
$PaCO_2$	Partial pressure of CO_2
PaO_2	Partial pressure of oxygen
PV	Pressure-volume
SpO_2	Oxygen saturation
VA-ECMO	Venoarterial extracorporeal membrane oxygenation

Extracorporeal membrane oxygenation in the venoarterial configuration (VA-ECMO) is an established method that offers circulatory support in the most severe conditions of circulatory failure, including cardiogenic shock (CS). However, evidence supporting the use of VA-ECMO in CS is insufficient, with promising results only from retrospective or small randomized studies[1,2]; nevertheless, large multicenter trials are ongoing[3–5].

Insertion of VA-ECMO in case of circulatory collapse enables rapid restoration and maintenance of adequate tissue perfusion; however, it may be associated with unfavorable consequences for the failing myocardium because the outflow part increases not only arterial blood pressure but also left ventricular (LV) afterload[6]. The increased afterload may cause LV overload and further reduction of LV performance, especially if the LV systolic function is already severely compromised. The unfavorable effect of increased extracorporeal blood flow (EBF) on LV performance during ECMO therapy has been described in several experimental and clinical studies[7–15]. Progressive LV overload is associated with increased left atrial pressure and frequently with subsequent severe pulmonary oedema, resulting in a critical condition that often requires urgent intervention (e.g., LV unloading)[16,17].

In the presence of severe valvular heart disease VA-ECMO may, however, influence LV function in a different manner[18]. In particular, aortic stenosis (AS) or mitral regurgitation (MR) are not infrequent causes or modulators of severe CS requiring mechanical circulatory support[18–20]. The effect of VA-ECMO on LV function in CS with AS or MR has not been described. The aim of our study was, therefore, to assess LV functional variables at different VA-ECMO blood flow levels in a porcine model of acute CS with severe AS or MR.

Methods

Animal model. Eight female swine (*Sus scrofa domestica*, Large White × Landrace crossbreed), four to five months of age, and a mean body weight of 45 kg were used. Full details of the animal model used in the present study has been reported earlier[21].

Briefly, after a 24 h fasting, general anaesthesia was induced by administration of midazolam (0.3 mg/kg intramuscular) and ketamine hydrochloride (15–20 mg/kg intramuscular). Initial propofol and morphine boluses (2 mg/kg intravenous [IV] and 0.1–0.2 mg/kg IV, respectively) were administered, followed by orotracheal intubation. Continuous IV infusions of propofol (6–10 mg/kg/h) and morphine (0.1–0.2 mg/kg/h) were used to maintain anaesthesia. The depth was adjusted according to physiological parameters, pupillary photoreactions, corneal and palpebral reflexes, lacrimation, and spontaneous movements[21].

Potassium chloride (2 mEq/kg), in conjunction with general anaesthesia overdose, was used to euthanize the animals at the conclusion of the experiment.

Bilateral femoral (arterial and venous), carotid and jugular approaches were used for multiple sheath insertions using a standard percutaneous Seldinger technique. An initial rapid IV infusion of 1000 mL normal saline was administered after anaesthesia induction to correct hypovolemia caused by 24 h of fasting, followed by continuous IV drip at a rate of 100–500 mL/h to reach and maintain a mean right atrial pressure of 5–7 mmHg. An unfractionated heparin IV bolus (100 U/kg) was administered after vascular sheaths placement, followed by continuous IV infusion of 50 U/kg/h to maintain activated clotting time of 200–250 s. Values were monitored every hour using a microcoagulation system (Hemochron Jr Signature Plus Microcoagulation System, ITC, Piscataway, NJ, USA)[21].

Ventilation was provided using a ventilator (Hamilton G5, Hamilton Medical AG, Switzerland) set to the INTELLiVENT–Adaptive Support Ventilation mode. The ventilator was set to maintain an oxygen saturation (SpO_2) of 95–99% and an end-tidal carbon dioxide (CO_2) pressure of 4.8–5.6 kPa[21].

VA-ECMO. The VA-ECMO setting used in our study has already been described elsewhere[7,21]. The ECMO circuit consisted of a console (Cardiohelp, Getinge, Germany), centrifugal blood pump and tubing set, a membrane oxygenator (Getinge, Germany), and a mechanical gas blender (Sechrist Industries, Inc, Anaheim, CA, USA). A venous cannula (21 Fr, Getinge, Germany) and arterial cannula (15 Fr, Getinge, Germany) were inserted percutaneously using the standard Seldinger technique into the femoral vein and artery. The venous inflow cannula was inserted into the right atrium (the tip position was verified using fluoroscopy), and the femoral arterial outflow cannula was inserted into the femoral artery with the tip placed in the descending aorta. Blood gas values leaving the oxygenator were continuously monitored (CDI™ Blood Parameter Monitoring System 500, Terumo Cardiovascular Systems Corporation, Elkton, MD, USA). The oxygen/air flow was repeatedly adjusted to maintain a partial pressure of oxygen (PaO_2) and partial pressure of CO_2 ($PaCO_2$) in the ranges of 10–15 kPa, and 4.0–6.5 kPa, respectively. The EBF rate was set to 1 L/min to prevent circuit coagulation until the start of the experiment[7,21].

Vital functions and haemodynamic monitoring. Vital functions and haemodynamic monitoring used in our study has been described previously[7,21]. Briefly, arterial pressure was measured using standard invasive methods with fluid-filled pressure transducers (Truwave, Edwards Lifesciences LLC, USA) through a pigtail catheter inserted into the aortic arch. A Swan-Ganz catheter was inserted into the pulmonary artery via the femoral vein. Electrocardiographic parameters, heart rate (HR), invasive blood pressures (aortic arch and central vein), pulse oximetry, capnometry, and invasive central venous SpO_2 were continuously monitored in all animals (Monitor Life Scope TR, Nihon Kohden, Japan; and Vigilance II, Edwards Lifesciences, USA). Four-channel NIRS (i.e., near-infrared spectroscopy) oximetry (INVOS, Medtronic, Minneapolis, MN, USA) was used to monitor regional tissue perfusion (brain, front limbs, body, hind limb); the threshold for the detection of hypoperfusion was 40%[7,21].

Pressure–volume analysis. A pressure–volume (PV) conductance catheter (Scisense 7 Fr VSL Pigtail, Transonic, Ithaca, NY, USA) was inserted into the left ventricle from the left carotid artery through the aortic valve to monitor cardiac performance during induction and maintenance of CS as described elsewhere[7,22]. Correct positioning was assessed radiographically and by verifying optimal PV loop morphology. The catheter was connected to the PV unit (Scisense ADV 500, Transonic, USA) and operated in the admittance mode. The volume was calibrated according to baseline pulmonary thermodilution (Combo CCO catheter, Edwards Lifesciences, Irvine, CA, USA). PV values were recorded continuously during the experiment. At each EBF level, values from five loops were taken at end-expiration, averaged, and used for further analysis. The collected PV data included LV end-diastolic pressure (LVEDP), LV end-diastolic volume (LVEDV), LV end-systolic volume (LVESV), dP/dt_{max}, and arterial elastance (Ea)[7,22].

LV stroke volume (LVSV) was calculated as LVSV = LVEDV – LVESV; LV ejection fraction (LVEF) was calculated as LVEF = LVSV/LVEDV; cardiac output (CO) was calculated as CO = LVSV × HR; and cardiac index (CI) was calculated as CI = CO/body surface area[7,22].

Cardiogenic shock (CS) model. After initiation of ECMO, the animals were stabilized for 10 min. During this time period, oxygen/air flow and fluid infusion rate were repeatedly adjusted to reach and maintain target PaO_2, $PaCO_2$, and right atrial pressure. Mechanical ventilation was subsequently switched to the CMV mode (respiratory rate, 5 breaths/min; inspiratory volume, 100 mL; and fraction of inspired oxygen, 0.21), which precipitated severe hypoxemia in the blood entering the left chambers of the heart and, in turn, caused tissue hypoxia in all tissues perfused by LV ejections, including the coronary arteries. The resulting global myocardial hypoxia rapidly lowered cardiac contractility, LVEF, and arterial blood pressure. Concurrently, the lower body was perfused with fully oxygenated blood from ECMO entering the circulation via the femoral artery. During the hypoxic period, EBF was gradually increased to maintain a mean arterial pressure (MAP) > 60 mmHg, thereby ensuring adequate perfusion pressure. After approximately 1 h of myocardial hypoxia, the haemodynamic criteria for severe CS were fulfilled, including LVEF, which decreased to < 30%, and CO, which decreased to < 3.5 L/min. Thereafter, continuous perfusion of the heart with hypoxaemic blood maintained advanced myocardial dysfunction and severely compromised haemodynamic function. If cardiac performance decreased further with a risk for circulation collapse, the target level of CS severity was adjusted with a partial increase in ventilation[21].

AS. Severe AS was simulated by the insertion of a valvuloplasty balloon (True, BD Biosciences, Franklin Lakes, NJ, USA) across the aortic valve with subsequent stepwise inflation under fluoroscopic and ultrasound control to reach transaortic peak pressure gradient ˃ 40 mmHg. The valvuloplasty balloon was removed after the measurements.

MR. Mechanical destruction of the mitral valve leaflets and/or chordae tendineae was performed under fluoroscopic and ultrasound guidance using endoscopic grasping forceps (Olympus, Tokyo, Japan) inserted via the femoral vein and trans-septal approach to the left atrium. Development of severe MR was confirmed using echocardiography.

Experimental protocol. Figure 1 outlines the experimental protocol that is similar to our previous studies[7,22]. After the placement of all catheters and the establishment of ECMO, the animals were permitted to stabilize for 10 min. CS was induced using global myocardial hypoxia, as described above. Following the occurrence of signs of tissue hypoperfusion (NIRS oximetry, < 40%) and an additional 10 min of stabilization, AS was simulated as described above, and the EBF rate was then set to 4 L/min and gradually decreased by 1 L/min every 5 min. Once an EBF rate of 1 L/min was achieved, it was maintained for 10 min. Subsequently, the EBF rate was gradually increased by 1 L/min every 5 min. At an EBF rate of 4 L/min, the animals were stabilized again for 10 min, and a second cycle of stepwise EBF decrease and increase was performed. After the measurements with AS were completed, the valvuloplasty balloon was removed from the aortic valve and MR was created (as described above) followed by 10 min stabilization. Subsequently, an additional two cycles of stepwise EBF decrease and increase were performed to record data for MR (Fig. 1). LV performance variables were analyzed at the end of each 5 min interval (four data sets per animal), and a mean value was calculated and used in further analysis.

Statistical analysis. Data are expressed as median (interquartile range). The Friedman test was used to compare values at different levels of EBF; differences with $P < 0.05$ were considered to be statistically significant. All statistical analyses were performed using GraphPad Prism version 8.4 (GraphPad, San Diego, CA, USA).

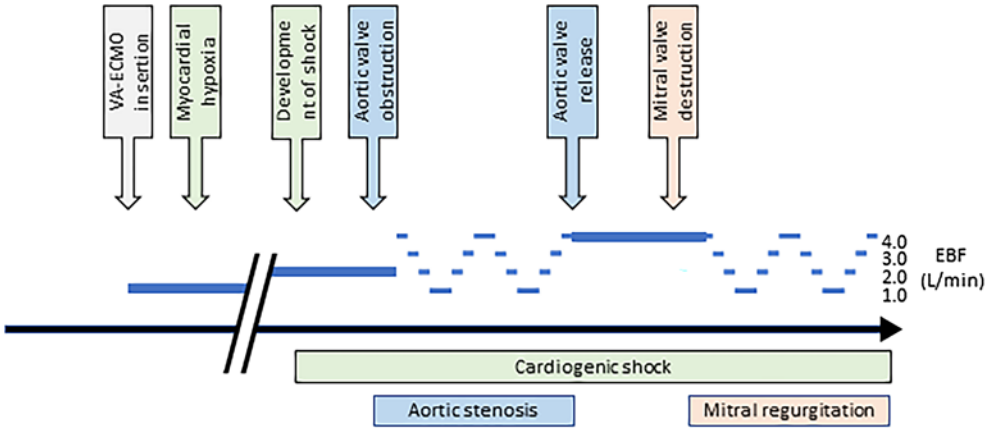

Figure 1. Schematic illustration of the experimental protocol. VA-ECMO, veno-arterial extracorporeal membrane oxygenation; EBF, extravascular blood flow.

Variable	Baseline	Cardiogenic shock	P-value
MAP (mmHg)	90.2 (80.6–98.8)	47.6 (38.9–54.2)	< 0.01
CO (L/min)	6.1 (5.2–7.4)	2.7 (1.9–3.1)	< 0.01
CI (L/min/m^2)	6.9 (5.8–8.3)	3.0 (2.1–3.48)	< 0.01
SV (mL)	72.2 (68.5–75.1)	22.2 (15.4–29.2)	< 0.01
HR (beats/min)	89.0 (79.1–104.9)	109.6 (98.5–124.2)	< 0.01
LVEF (%)	55.5 (53.3–59.0)	15.2 (10.5–19.3)	< 0.01

Table 1. Major hemodynamic variables at baseline and after the development of cardiogenic shock. Data presented as median (interquartile range) unless otherwise indicated. *CO* cardiac output, *HR* heart rate, *LVEF* left ventricular ejection fraction, *MAP* mean arterial pressure, *SV* stroke volume.

Ethics approval and consent to participate. This study was approved by the Charles University First Faculty of Medicine Institutional Animal Care and Use Committee, and was performed at the Animal Laboratory, Department of Physiology, First Faculty of Medicine, Charles University in Prague and Na Homolce Hospital, Prague, Czech Republic, in accordance with Act No 246/1992 Coll., for the protection of animals against cruelty. The investigation and protocol conformed to the Guide for the Care and Use of Laboratory Animals published by the United States National Institutes of Health (Publication No. 85-23, revised 1985). The study is reported in accordance with ARRIVE guidelines (https://arriveguidelines.org).

Results

Baseline characteristics. All animals survived and completed all protocol-defined procedures. Myocardial hypoxia resulted in a marked decline in MAP, CO, CI, LVSV and LVEF, while HR significantly increased (Table 1).

AS. The stepwise increase in EBF was associated with a significant rise in MAP: 33.5 mmHg (24.2–34.9 mmHg) at EBF 1 L/min; 38.4 mmHg (36.9–44.9 mmHg) at EBF 2 L/min; 48.2 mmHg (45.4–61.3 mmHg) at EBF 3 L/min; and 56.0 mmHg (51.9–73.3 mmHg) at EBF 4 L/min ($P<0.01$) (Fig. 2A). LV volume variables (LVEDV, LVESV, LVSV), LVEF, dP/dt_{max} and Ea remained stable at different levels of EBF (Fig. 2B–G). LVEDP significantly decreased with increasing levels of EBF: 24.9 mmHg (21.2–40.0 mmHg) at EBF 1 L/min; 23.6 mmHg (19.7–33.5 mmHg) at EBF 2 L/min; 20.5 mmHg (18.0–33.4 mmHg) at EBF 3 L/min; and 19.1 mmHg (15.2–29.0 mmHg) at EBF 4 L/min ($P<0.01$) (Fig. 2H). The median aortic valve pressure gradient achieved significantly dropped with increasing levels of EBF, from 45.2 mmHg (33.0–74.8 mmHg) at EBF 1 L/min to 32.1 mmHg (25.1–39.6 mmHg) at EBF 4 L/min ($P<0.01$) (Fig. 2I).

MR. A gradual increase in EBF resulted in a significant elevation in MAP: 49.0 mmHg (28.0–53.4 mmHg) at EBF 1 L/min; 56.9 mmHg (39.0–64.0 mmHg) at EBF 2 L/min; 72.5 mmHg (51.4–77.1 mmHg) at EBF 3 L/min; and 84.0 mmHg (62.4–89.6 mmHg) at EBF 4 L/min ($P<0.01$) (Fig. 3A). LV volume variables (LVEDV, LVESV, LVSV), LVEF and dP/dt_{max} remained stable at different EBF rates (Fig. 3B–F). Median Ea increased from 1.5 mmHg/mL (0.4–1.6 mmHg/mL) at EBF 1 L/min to 2.5 mmHg/mL (0.4–2.7 mmHg/mL) at EBF 4 L/min ($P<0.01$) (Fig. 3G). Median LVEDP significantly rose with increasing EBF: 17.1 mmHg (13.7–19.1 mmHg) at

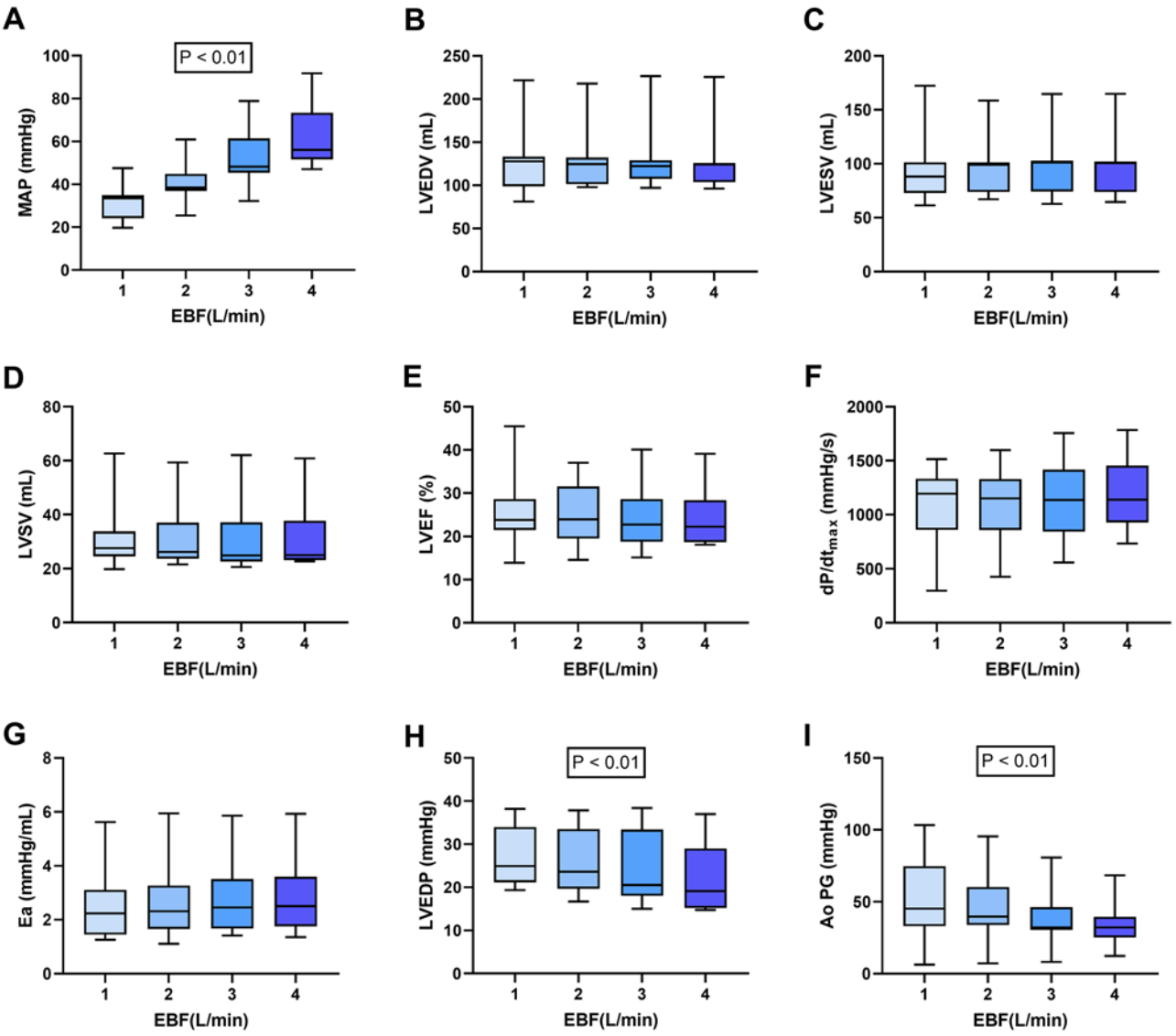

Figure 2. Comparison of the effect of different levels of venoarterial extracorporeal membrane oxygenation (VA-ECMO) blood flow (EBF) on hemodynamic and left ventricular performance parameters in a porcine model of cardiogenic shock with aortic stenosis. (**A**) MAP, mean arterial pressure; (**B**) LVEDV, left ventricle end-diastolic volume; (**C**) LVESV, left ventricle end-systolic volume; (**D**) LVSV, left ventricle stroke volume; (**E**) LVEF, left ventricle ejection fraction; (**F**) dP/dt_{max}; (**G**) Ea, arterial elastance; (**H**) LVEDP, left ventricle end-diastolic pressure; (**I**) AoPG, peak aortic pressure gradient.

EBF 1 L/min; 18.5 mmHg (14.5–19.9 mmHg) at EBF 2 L/min; 19.6 mmHg (15.0–22.4 mmHg) at EBF 3 L/min; and 20.8 mmHg (16.3–25.6 mmHg) at EBF 4 L/min ($P<0.01$) (Fig. 3H).

Discussion

To the best of our knowledge, the present study was the first to directly address the effect of VA-ECMO on LV function in CS with AS or MR. There were two major findings. First, in CS with AS, the effect of increased VA-ECMO blood flow on LV performance parameters was either neutral (LVEDV, LVESV, LVSV, LVEF) or even beneficial (LVEDP decrease). Second, in CS with MR, increased EBF, MAP and Ea did not affect LV volume variables (i.e., LVEDV, LVESV, LVSV, LVEF), but increased LVEDP. Therefore, AS prevented LV overload and partial protection was observed also with MR, at the cost of higher LVEDP.

There are numerous factors that can influence or modulate the effect of VA-ECMO on LV performance including severity of LV dysfunction, EBF rate, use of vasopressors, inotropes, mechanical ventilation setting, presence of right heart failure, and the competence of the heart valves. Valvular heart disease is often present in patients with CS, either with causal relationship or as a concomitant and modulating disease. Severe AS can be a cause of CS, especially if decompensated with LV systolic dysfunction, or contribute to shock in case of acute myocardial injury of other etiology (e.g., myocardial infarction or myocarditis). Additionally, acute MR

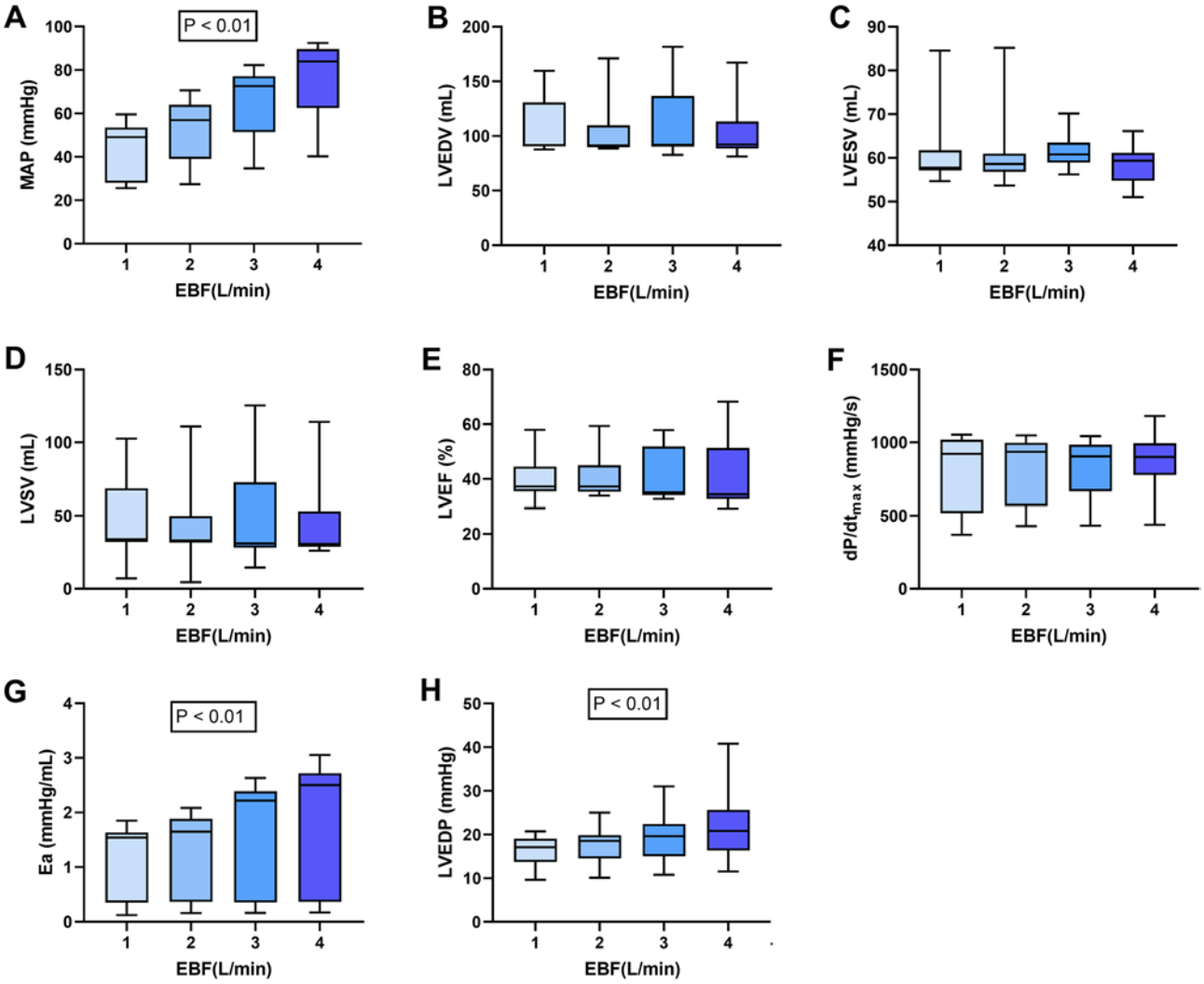

Figure 3. Comparison of the effect of different levels of venoarterial extracorporeal membrane oxygenation (VA-ECMO) blood flow (EBF) on hemodynamic and left ventricular performance parameters in a porcine model of cardiogenic shock with mitral regurgitation. (**A**) MAP, mean arterial pressure; (**B**) LVEDV, left ventricle end-diastolic volume; (**C**) LVESV, left ventricle end-systolic volume; (**D**) LVSV, left ventricle stroke volume; (**E**) LVEF, left ventricle ejection fraction; (**F**) dP/dtmax; (**G**) Ea, arterial elastance; (**H**) LVEDP, left ventricle end-diastolic pressure.

can clinically manifest as CS, and severe MR is often present as concomitant disease as a result of LV dilatation in advanced heart failure[16–18].

Increased VA-ECMO blood flow in CS with severe LV dysfunction and competent valves predominantly increases LVESV and reduces LVSV and LVEF; this phenomenon is largely explained by increased LV afterload at higher EBF rates[7,14,22]. However, if severe AS is present, LV afterload is determined almost entirely by obstruction of the aortic valve and increased VA-ECMO blood flow does not translate into an elevation in LV afterload as demonstrated in our study where Ea was not significantly changed. This could also be a reason why we did not observe any changes in LV volumes with increasing EBF during the simulation of AS. Moreover, decreased preload caused by increased blood drainage from the right atrium at higher EBF can be responsible for reduced LVEDP in our study. Therefore, our data indicate that, in CS with severe AS, VA-ECMO restores systemic circulation and, at the same time, unloades the left ventricle, prevents LV overload, and reduces the risk for pulmonary oedema. In clinical practice, VA-ECMO is frequently used as circulatory support in CS with AS[23–27], and our data support this approach from the haemodynamic perspective.

The situation is different in CS with severe MR. Increased EBF is associated with higher Ea and an incompetent mitral valve enables translation of the effect of increased LV afterload to the left atrium. We did not record regurgitation volumes; however, we speculate that increased LV afterload at higher EBF resulted in increased regurgitation volume, which would fully explain our observation of unchanged LVESV and LVSV together with increased LVEDP. Importantly, higher LVEDP is associated with an increased risk for subsequent pulmonary oedema. Thus, preservation of LV function (LV volumes and LVEF) in CS with MR does not necessarily lead to stable haemodynamic conditions but more likely increased congestion. This effect could be even greater in

predominantly LV failure where preserved RV would contribute to increased LV preload, hence increased LVEPD. Additionally, atrial septostomy (transseptal puncture), that we had to performe when introducing MR model, may have aleviated pulmonary congestion to some extent by venting left atrium[28]. Furthermore, because LVSV was calculated from the PV loop and includes both transaortic flow volume and mitral regurgitation volume, stable LVSV does not reflect reduced transaortic flow and thus lower native CO at higher EBF. Our results, therefore, support the recommendation to not use VA-ECMO alone in MR but rather in combination with other devices such as the Impella system[18].

Our study had several limitations. We used a model of CS caused by global hypoxia that affects not only the left but also the right ventricle, causing severe biventricular systolic dysfunction. Therefore, our model differs from other large animal models of acute heart failure, which are primarily based on the development of myocardial infarction by coronary artery occlusion; however, it reflects frequent clinical scenarios. On the other hand, acute MR or AS usually do not result in immediate right ventricular systolic dysfunction and therefore, hemodynamic consequences of cardiogenic shock caused by acute myocardial infarction may be different then in shock caused by hypoxia affecting both ventricles. Furthermore, LV ejections in our model supply with the hypoxemic blood not only coronary arteries but also carotid arteries at least during the initial phases of the hypoxic period. Hypoxic brain damage could therefore be anticipated. We cannot exclude that cerebral hypoxia may have influenced some of the mechanisms of central regulation of blood circulation. Moreover, we focused on the acute effects of VA-ECMO on haemodynamic and LV performance variables. We speculate that, especially in severe MR, long-term use of VA-ECMO may result in an increase in LV volumes and LV dilatation. A specific limitation of our study is also the non-administration of vasopressors even at very low blood pressure, which is not in accordance with clinical practice. Another important limitation of our study is the simulation of AS by balloon obstruction of aortic valve and MR by mechanical destruction of the mitral valve which does not reflect the processes that happen in real-life valvular heart disease patients with varying degrees of aortic valve opening area, and where the mitral valve is usually not destructed, but tethered and dilated (or showing prolapsing or flail segments), leading to significant variations in the degree of MR. Both AS and MR in our study were also simulated sequentially in each individual animal; however, since the aortic valve obstruction was completely reversible and preceded the development of MR, it is unlikely that the observations in MR were significantly influenced by previous AS simulation. Our study also includes only eight experimental animals; however, changes in MAP and LV performance variables were uniformly expressed across all individual subjects. Finally, our experimental study was conducted in young and otherwise healthy animals. Therefore, caution is advised in translating our results to clinical scenarios involving patients with advanced heart failure, LV remodelling, and comorbidities.

Conclusion

Results of the present study indicate that the presence of valvular heart disease may alleviate the negative effect of VA-ECMO on LV performance. In CS with severe AS, VA-ECMO restored systemic circulation together with LV unloading and prevention of pulmonary oedema. In acute CS with severe MR, the restoration of systemic blood flow was associated with acutely preserved LV volumes and LVEF at the cost of increased LVEDP and, thus, higher risk for pulmonary oedema.

Data availability

The datasets used and/or analysed during the current study are available from the corresponding author on reasonable request.

Received: 17 July 2022; Accepted: 28 September 2022
Published online: 12 October 2022

References

1. Combes, A. *et al.* Outcomes and long-term quality-of-life of patients supported by extracorporeal membrane oxygenation for refractory cardiogenic shock. *Crit. Care Med.* **36**(5), 1404–1411 (2008).
2. Lackermair, K. *et al.* Outcome of patients treated with extracorporeal life support in cardiogenic shock complicating acute myocardial infarction: 1-year result from the ECLS-Shock study. *Clin. Res. Cardiol.* **110**(9), 1412–1420 (2021).
3. Ostadal, P. *et al.* Extra corporeal membrane oxygenation in the therapy of cardiogenic shock (ECMO-CS): Rationale and design of the multicenter randomized trial. *Eur. J. Heart Fail.* **19**(Suppl 2), 124–127 (2017).
4. Thiele, H. *et al.* Extracorporeal life support in patients with acute myocardial infarction complicated by cardiogenic shock—Design and rationale of the ECLS-SHOCK trial. *Am. Heart J.* **234**, 1–11 (2021).
5. Banning, A. S. *et al.* Veno-arterial extracorporeal membrane oxygenation (ECMO) in patients with cardiogenic shock: Rationale and design of the randomised, multicentre, open-label EURO SHOCK trial. *EuroIntervention* **16**(15), e1227–e1236 (2021).
6. Fuhrman, B. P., Hernan, L. J., Rotta, A. T., Heard, C. M. & Rosenkranz, E. R. Pathophysiology of cardiac extracorporeal membrane oxygenation. *Artif. Organs* **23**(11), 966–969 (1999).
7. Ostadal, P. *et al.* Increasing venoarterial extracorporeal membrane oxygenation flow negatively affects left ventricular performance in a porcine model of cardiogenic shock. *J. Transl. Med.* **13**, 266 (2015).
8. Hirschl, R. B., Heiss, K. F. & Bartlett, R. H. Severe myocardial dysfunction during extracorporeal membrane oxygenation. *J. Pediatr. Surg.* **27**(1), 48–53 (1992).
9. Kimball, T. R. *et al.* Changes in cardiac function during extracorporeal membrane oxygenation for persistent pulmonary hypertension in the newborn infant. *J. Pediatr.* **118**(3), 431–436 (1991).
10. Berdjis, F., Takahashi, M. & Lewis, A. B. Left ventricular performance in neonates on extracorporeal membrane oxygenation. *Pediatr. Cardiol.* **13**(3), 141–145 (1992).
11. Pyles, L. A., Gustafson, R. A., Fortney, J. & Einzig, S. Extracorporeal membrane oxygenation induced cardiac dysfunction in newborn lambs. *J. Cardiovasc. Transl. Res.* **3**(6), 625–634 (2010).
12. Shen, I. *et al.* Effect of extracorporeal membrane oxygenation on left ventricular function of swine. *Ann. Thorac. Surg.* **71**(3), 862–867 (2001).

13. Shen, I. *et al.* Left ventricular dysfunction during extracorporeal membrane oxygenation in a hypoxemic swine model. *Ann. Thorac. Surg.* **71**(3), 868–871 (2001).
14. Aissaoui, N. *et al.* Two-dimensional strain rate and Doppler tissue myocardial velocities: analysis by echocardiography of hemodynamic and functional changes of the failed left ventricle during different degrees of extracorporeal life support. *J. Am. Soc. Echocardiogr.* **25**(6), 632–640 (2012).
15. Hala, P. *et al.* Increasing venoarterial extracorporeal membrane oxygenation flow puts higher demands on left ventricular work in a porcine model of chronic heart failure. *J. Transl. Med.* **18**(1), 75 (2020).
16. Ricarte Bratti, J.P., Cavayas, Y.A., Noly, P.E., Serri, K., Lamarche, Y. Modalities of left ventricle decompression during VA-ECMO therapy. *Membranes (Basel)*. 2021, **11**(3).
17. Lusebrink, E. *et al.* Prevention and treatment of pulmonary congestion in patients undergoing venoarterial extracorporeal membrane oxygenation for cardiogenic shock. *Eur. Heart J.* **41**(38), 3753–3761 (2020).
18. Villablanca, P. *et al.* Mechanical circulatory support in cardiogenic shock due to structural heart disease. *Interv. Cardiol. Clin.* **10**(2), 221–234 (2021).
19. Harjola, V. P. *et al.* Clinical picture and risk prediction of short-term mortality in cardiogenic shock. *Eur. J. Heart Fail.* **17**(5), 501–509 (2015).
20. Bonello, L. *et al.* Etiology and prognosis of cardiogenic shock in a secondary center without surgical back-up. *Cardiol. Res. Pract.* **2019**, 3869603 (2019).
21. Ostadal, P. *et al.* Novel porcine model of acute severe cardiogenic shock developed by upper-body hypoxia. *Physiol. Res.* **65**(4), 711–715 (2016).
22. Ostadal, P. *et al.* Electrocardiogram-synchronized pulsatile extracorporeal life support preserves left ventricular function and coronary flow in a porcine model of cardiogenic shock. *PLoS ONE* **13**(4), e0196321 (2018).
23. Raffa, G. M. *et al.* Group EiTI: In-hospital outcomes after emergency or prophylactic veno-arterial extracorporeal membrane oxygenation during transcatheter aortic valve implantation: A comprehensive review of the literature. *Perfusion* **34**(5), 354–363 (2019).
24. Uehara, K. *et al.* Use of extracorporeal membrane oxygenation in complicated transcatheter aortic valve replacement. *Gen. Thorac. Cardiovasc. Surg.* **65**(6), 329–336 (2017).
25. Makdisi, G., Makdisi, P. B. & Wang, I. W. Use of extracorporeal membranous oxygenator in transcatheter aortic valve replacement. *Ann. Transl. Med.* **4**(16), 306 (2016).
26. Husser, O. *et al.* Emergency and prophylactic use of miniaturized veno-arterial extracorporeal membrane oxygenation in transcatheter aortic valve implantation. *Catheter. Cardiovasc. Interv.* **82**(4), E542-551 (2013).
27. Banjac, I. *et al.* Extracorporeal membrane oxygenation as a procedural rescue strategy for transcatheter aortic valve replacement cardiac complications. *ASAIO J.* **62**(1), e1-4 (2016).
28. Mlcek, M. *et al.* Atrial septostomy for left ventricular unloading during extracorporeal membrane oxygenation for cardiogenic shock: Animal model. *JACC Cardiovasc. Interv.* **14**(24), 2698–2707 (2021).

Author contributions

P.O., M.M., D.V., P.N.: study conception and design; M.P., M.H., A.K., M.J., J.N.: data acquisition, analysis, and interpretation; P.O.: manuscript draft; D.V., O.K., P.N.: critical revision; M.M.: final approval of the manuscript. All authors have read and approved the manuscript submitted for publication.

Funding

This study was supported by an Institutional Grant MH CZ-DRO (Nemocnice Na Homolce—NNH, 00023884) IG150501.

Competing interests

PO received speaker's fee from Edwards, Getinge, Xenios. Other authors do not have competing interest.

Additional information

Correspondence and requests for materials should be addressed to P.O.

Reprints and permissions information is available at www.nature.com/reprints.

Publisher's note Springer Nature remains neutral with regard to jurisdictional claims in published maps and institutional affiliations.

L. Opatřil et al.

Stress pulmonary circulation parameters assessed by a cardiovascular magnetic resonance in patients after a heart transplant

Scientific reports
Impact Factor: 4.997

scientific reports

Check for updates

OPEN

Stress pulmonary circulation parameters assessed by a cardiovascular magnetic resonance in patients after a heart transplant

Lukáš Opatřil[1,2,3], Roman Panovsky[1,2,3,4]✉, Mary Mojica-Pisciotti[2], Jan Máchal[2,5], Jan Krejčí[1,3], Tomáš Holeček[2,6], Lucia Masárová[1,2,3], Věra Feitová[2,6], Július Godava[1], Vladimír Kincl[1,2,3], Tomáš Kepák[2,7], Gabriela Závodná[3] & Lenka Špinarová[1,3]

Rest pulmonary circulation parameters such as pulmonary transit time (PTT), heart rate corrected PTT (PTTc) and pulmonary transit beats (PTB) can be evaluated using several methods, including the first-pass perfusion from cardiovascular magnetic resonance. As previously published, up to 58% of patients after HTx have diastolic dysfunction detectable only in stress conditions. By using adenosine stress perfusion images, stress analogues of the mentioned parameters can be assessed. By dividing stress to rest biomarkers, potential new ratio parameters (PTT ratio and PTTc ratio) can be obtained. The objectives were to (1) provide more evidence about stress pulmonary circulation biomarkers, (2) present stress to rest ratio parameters, and (3) assess these biomarkers in patients with presumed diastolic dysfunction after heart transplant (HTx) and in childhood cancer survivors (CCS) without any signs of diastolic dysfunction. In this retrospective study, 48 patients after HTx, divided into subgroups based on echocardiographic signs of diastolic dysfunction (41 without, 7 with) and 39 CCS were enrolled. PTT was defined as the difference between the onset time of the signal intensity increase in the left and the right ventricle. PTT in rest conditions were without significant differences when comparing the CCS and HTx subgroup without diastolic dysfunction (4.96 ± 0.93 s vs. 5.51 ± 1.14 s, p = 0.063) or with diastolic dysfunction (4.96 ± 0.93 s vs. 6.04 ± 1.13 s, p = 0.13). However, in stress conditions, both PTT and PTTc were significantly lower in the CCS group than in the HTx subgroups, (PTT: 3.76 ± 0.78 s vs. 4.82 ± 1.03 s, p < 0.001; 5.52 ± 1.56 s, p = 0.002). PTT ratio and PTTc ratio were below 1 in all groups. In conclusion, stress pulmonary circulation parameters obtained from CMR showed prolonged PTT and PTTc in HTx groups compared to CCS, which corresponds with the presumption of underlying diastolic dysfunction. The ratio parameters were less than 1.

Abbreviations

BMI	Body mass index
b-TFE	Balanced turbo field echo
CCS	Childhood cancer survivors
CMR	Cardiovascular magnetic resonance
CNS	Central nervous system
CO	Cardiac output

[1]First Department of Internal Medicine and Cardioangiology, St. Anne's University Hospital, Pekarska 53, 656 91 Brno, Czech Republic. [2]International Clinical Research Centre, St. Anne's University Hospital, Brno, Czech Republic. [3]Faculty of Medicine, Masaryk University, Brno, Czech Republic. [4]First Department of Internal Medicine and Cardioangiology, International Clinical Research Centre, Faculty of Medicine, Masaryk University, St. Anne's University Hospital, Brno, Czech Republic. [5]Department of Pathophysiology, Faculty of Medicine, Masaryk University, Brno, Czech Republic. [6]Department of Medical Imaging, St. Anne's University Hospital, Brno, Czech Republic. [7]Department of Paediatric Oncology, University Hospital Brno, Brno, Czech Republic. ✉email: panovsky@fnusa.cz

DD	Diastolic diameter
DD LV	Left ventricular diastolic diameter
HCM	Hypertrophic cardiomyopathy
HR	Heart rate
HTx	Heart transplant
HTx_A	Heart transplant without diastolic dysfunction subgroup
HTx_B	Heart transplant with diastolic dysfunction subgroup
IR-TFE	Inversion-recovery turbo field echo
LA	Left atrium
LAP	Left atrial pressure
LGE	Late gadolinium enhancement
LV	Left ventricle
LVEF	Left ventricular ejection fraction
LV LGE	Left ventricular late gadolinium enhancement
LVOT	Left ventricular outflow tract
LV SV	Left ventricular stroke volume
MRI	Magnetic resonance imaging
PBVI	Pulmonary blood volume index
PCWP	Pulmonary capillary wedge pressure
PH	Pulmonary hypertension
PSIR	Phase-sensitive inversion recovery
PTB	Pulmonary transit beats
PTB_S	Stress pulmonary transit beats
PTT	Pulmonary transit time
PTTc	Bazett's formula corrected pulmonary transit time
PTT_S	Stress pulmonary transit time
PTTc_S	Bazett's formula corrected stress pulmonary transit time
PTT ratio	Pulmonary transit time ratio
PTTc ratio	Bazett's formula corrected pulmonary transit time ratio
ROIs	Regions of interest
RV	Right ventricle
RV SV	Right ventricular systolic volume
SAX	Short-axis
SI	Signal intensity
sPAP	Systolic pulmonary artery pressure
SSFP	Steady-state free precession
TE	Echo time
TR	Repetition time
TTE	Transthoracic echocardiography

Pulmonary circulation biomarkers obtained with non-invasive methods are not new themselves. Acquired by different modalities, including radionuclide imaging[1], contrast-enhanced transthoracic or transesophageal echocardiography[2,3], or computed tomography[4], they have been studied for decades.

One of the latest techniques to assess pulmonary circulation parameters is magnetic resonance imaging (MRI). Firstly, through MRI angiography[5], and later on by the first-pass perfusion from cardiovascular magnetic resonance (CMR)[6–8]. The latter option offers advantages such as using an already employed sequence and opens new opportunities with retrospective studies, although data are still limited.

From the analysis of rest perfusion images, biomarkers such as pulmonary transit time (PTT), pulmonary transit beats (PTB) and pulmonary blood volume index (PBVI), can be obtained. Likewise, by using adenosine stress perfusion images, their analogues, the stress pulmonary transit time (PTT_S) and the stress pulmonary transit beats (PTB_S), can also be determined. To our knowledge, so far, just one article reported stress parameters, but only in hypertrophic cardiomyopathy (HCM)[7].

PTT has already shown to be increased in both heart failure with reduced and preserved ejection fraction[6,9]. As previously published by Meluzin et al.[10], by pulmonary capillary wedge pressure acquired by right heart catheterization, 16% of patients after heart transplant (HTx) showed signs of diastolic dysfunction in rest condition, but in stress condition, another 58% showed these signs[10]. Therefore, we hypothesise that in a population after HTx, the stress biomarkers will be prolonged compared to a group of patients without any signs of systolic or diastolic function impairment.

We further assume that in a healthy population, the stress pulmonary transit biomarkers should be shorter and assessing not only the absolute values of rest and stress parameters, but also their corresponding ratio could be valuable.

As far as we know, these biomarkers have not been studied before on patients after HTx or in the childhood cancer survivors (CCS).

This study aimed to (1) provide more evidence about stress pulmonary circulation biomarkers, (2) present and investigate stress to rest ratio parameters, and (3) assess these biomarkers in patients with presumed diastolic dysfunction after heart transplant (HTx) and in CCS without diastolic dysfunction.

Inclusion criteria		Exclusion criteria	
HTx	CCS	HTx	CCS
1 year ± 30 days after HTx	Adults after cardiotoxic chemotherapy in childhood	sPAP > 40 mmHg	sPAP > 40 mmHg
Stress CMR perfusion available	Stress CMR perfusion available	–	Any signs of systolic or diastolic impairment
Echocardiographic examination including E/E', E/A measurement and pulmonary systolic artery pressure assessment	Echocardiographic examination including E/E', E/A measurement and pulmonary systolic artery pressure assessment		-
≤ 30 days between CMR and echocardiography	≤ 30 days between CMR and echocardiography		

Table 1. Inclusion and exclusion criteria. *CMR* cardiovascular magnetic resonance, *CCS* childhood cancer survivors, *HTx* heart transplant group, *sPAP* systolic pulmonary artery pressure.

Methods

Study design and population. This retrospective study was performed in accordance with the Declaration of Helsinki (2000) of the World Medical Association. The Ethics Committee of the Faculty of Medicine, Masaryk University, confirmed that this study has been performed on data of patients already participating in other research studies with signed Informed Consent and therefore, according to the Czech legislation, no specific new approval of the ethics committee was required.

In this retrospective study, 48 subjects after HTx and 39 CCS patients were included. Detailed inclusion and exclusion criteria are shown in Table 1.

The HTx group consisted of patients who underwent HTx for different diagnoses and were being monitored at our center. In the first year after transplantation, a detailed follow-up, including myocardial biopsies and other examinations, took place. During the first-year check-up, they underwent more thorough examinations with CMR, including a stress perfusion test.

The CCS group were patients after cardiotoxic chemotherapy in young or adolescent age treated at the paediatric oncology. Patients were treated with anthracyclines in 74.3%, the rest with Cisplatin and high dose Carboplatin. In terms of specific drugs, 93% of patients treated with anthracyclines received Doxorubicin. All subjects were examined and monitored at our department between the years 2016 and 2020. Only patients that after a thorough examination including transthoracic echocardiography (TTE) and CMR methods showed no signs of systolic or diastolic function impairment or another cardiac pathology were enrolled.

Inclusion criteria required a CMR examination with contrast methods and stress perfusion and TTE without signs of pulmonary hypertension (PH) within 30 days of CMR. Stress perfusions were indicated to exclude coronary artery disease, since it was already detected in some patients treated with anthracyclines or alkylating agents[11,12] and were performed as part of the study.

Patients in the HTx group were divided into subgroups based on the presence of diastolic dysfunction signs from TTE.

Transthoracic echocardiography. All patients underwent the standard TTE exam, and all examinations were performed by experienced cardiologists in our center and according to the established guidelines.

Signs of PH were defined in accordance with 2015 guidelines[13] as estimated pulmonary systolic artery pressure above 40 mmHg, calculated from tricuspid regurgitation jet velocity. The left ventricular diastolic dysfunction was defined as the presence of a grade II or higher diastolic dysfunction assessed by Doppler echocardiography of transmitral velocities of transmitral flow and tissue Doppler imaging of mitral annular velocity.

CMR protocol. The CMR studies were performed similarly as in the case of previous articles from our workplace[14]—with the standard protocol using 1.5 T scanners (Ingenia, Philips Medical Systems, Best, The Netherlands) equipped with 5- and 32-element phased-array receiver coils allowing for the use of parallel acquisition techniques in the supine position in repeated breath-hold. Functional imaging using balanced steady-state free precession (SSFP, b-TFE) cine sequences included four-chamber, two-chamber and left ventricular outflow tract (LVOT) long-axis views, and a short-axis (SAX) stack from the cardiac base to the apex in the plane perpendicular to the LV long axis. Wall motion abnormalities were visually assessed. LV functional and morphological parameters were calculated from the SAX stack using the summation-of-disc methods following the recommendations on post-processing evaluation from the Society for Cardiovascular Magnetic Resonance[15].

Late gadolinium enhancement (LGE) images in all long-axis views and the SAX stack were acquired 10 min after an intravenous bolus of a total 0.2 mmol/kg (stress and rest dual-boluses for perfusion and the bolus of remaining contrast injected after the rest perfusion) of the gadolinium-based contrast agent gadobutrol (Gadovist, Bayer-Schering Pharma, Germany) using inversion-recovery turbo field echo sequence (IR-TFE) and, in case of doubt, also by phase-sensitive inversion recovery (PSIR) TFE. Both 2-dimensional and 3-dimensional data acquisitions were performed. LGE was defined as an area of visually identified contrast enhancement higher than the mean signal intensity of an adjacent area of the reference myocardium.

CMR stress perfusion. CMR first-pass contrast-enhanced myocardial perfusion images were acquired by a b-TFE sequence in three SAX sections (basilar, midventricular, and apical) with these parameters: field of view 300 × 300 mm, reconstruction matrix 224, slice thickness 10 mm, acquisition voxel size 2.5 × 2.5 mm, time to repetition (TR) ≈ 2.2 ms, echo time (TE) ≈ 1.1 ms, flip angle 50°, SENSE factor 2.3, number of dynamics = 90,

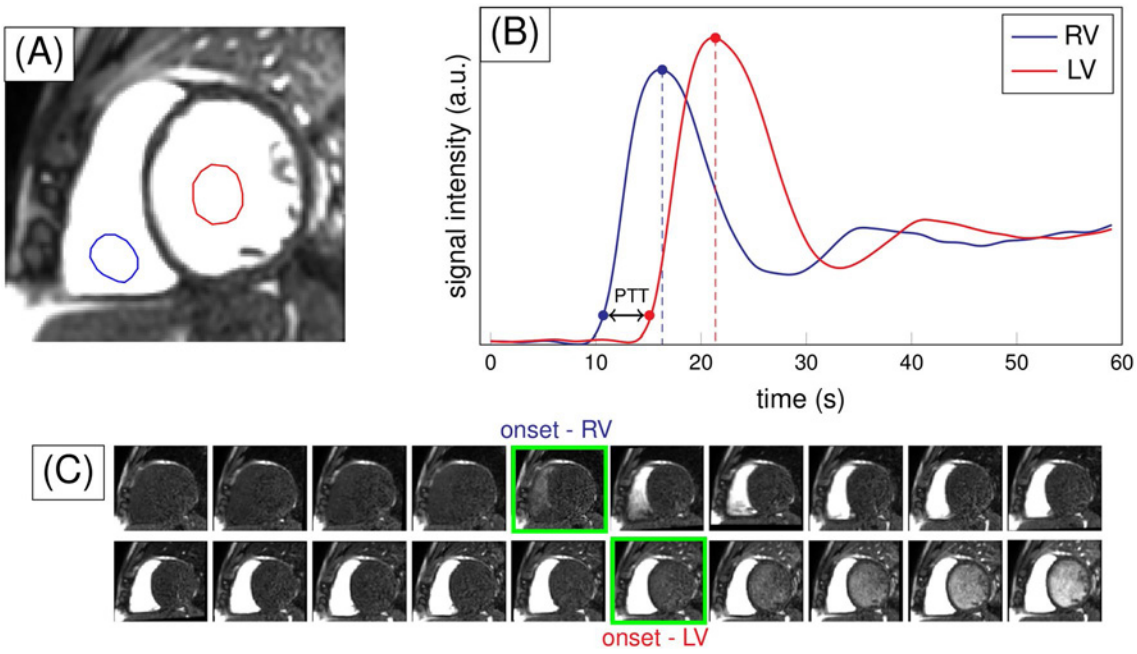

Figure 1. Schematics of the calculation of pulmonary transit time (PTT). (**A**) Region of interests manually traced in the right ventricle (RV, blue) and the left ventricle (LV, red). (**B**) Simulated data of the signal intensity (SI) vs time for the RV and LV. The maxima of the SI are marked. The PTT is the difference between the onsets, determined as the signal at 10% of the maximum values. (**C**) Example of the detection of the onset points in the corrected images. Only a fraction of the images is shown.

non-shared saturation prepulse. Stress perfusion was acquired after a 4 min adenosine infusion at 140 µg/kg/min. Rest perfusion was acquired 10 min after the stress perfusion with the same parameters. MR perfusion was performed during a dual-bolus administration of gadolinium-based contrast agent gadobutrol. The dual-bolus protocol was adapted from Ishida et al.[16]. A volume and rate of 0.005 mmol/kg and 4 ml/s for the pre-bolus and 0.05 mmol/kg and 4 ml/s for the main-bolus were used. Stress and rest volumes and rates were matched.

Pulmonary circulation biomarkers analyses. The PTT values were estimated from SAX rest and stress first-pass perfusion images, using an in-house developed algorithm implemented in MATLAB® 9.8 (R2020a) (The Mathworks Inc., Natick, MA, USA). The images were acquired without breath-hold. The analysis starts with applying a motion correction algorithm to optimize imaging registration and avoid potential contamination from pixels in the blood pool. The algorithm initially performs a rigid transformation to improve the misalignment present in the images and ease the following registration steps. Subsequently, an affine transformation, optimized according to the One Plus One Evolutionary strategy[17], is applied. The method generates a modification in the image using a current transformation (parent) and a newer one (descendant). Then, it estimates the similarity value, and according to it, keeps the parent or the descendant for a new evolutionary step. Finally, the algorithm uses mutual information as a similarity criterion[18]. The registration accuracy is visually assessed. Regions of interest (ROIs) in the right ventricle (RV) and the LV are manually traced in both the rest and stress corrected images for the mid-ventricular slice and, in case of repetitive misregistration, in the basal one. The ROIs automatically propagate throughout the stack of images, their average is computed in each one, and signal intensity (SI) curves vs time are obtained. The algorithm recognizes the maximum SI value in each case and determines a threshold (5–10% of the maximum) for establishing the onset SI. The measurement was done considering the main bolus of the dual bolus technique and confirmed with the pre-bolus. PTT was defined as the difference between the onset time in the LV and the RV, and PTB is the number of frames between these times (see Fig. 1). The PBVI, in ml/m^2, was calculated as the product of the PTB and the RV stroke volume (RV SV), divided by the body surface area[8].

The pulmonary transit time ratio (PTT ratio) and pulmonary transit time ratio with heart rate (HR) correction (PTTc ratio) were calculated.

Where applicable, Bazett's formula ([19]), commonly used to standardize the QT interval across different heart rates, was used to correct the values for HR as previously reported by Ricci et al.[7]. The formula considers a PTT or PTT_S at a given heart rate and normalizes it by the square root of the corresponding RR interval per second, i.e., $\sqrt{}$ (RR interval/1 s)[19]. Therefore, the corrected parameters are PTTc (s) = PTT (s)/ $\sqrt{}$ (RR interval/1 s) and PTTc_S (s) = PTT_S (s)/ $\sqrt{}$ (RR interval/1 s). Ratio parameters (PTT ratio and PTTc ratio) were calculated as stress parameters divided by rest parameters; therefore, PTT ratio = PTT_S/ PTT and PTTc ratio = PTTc_S/ PTTc.

Statistical analysis. The categorical data were compared using the χ^2 test. In case the null hypothesis was refuted, a series of three Fisher exact tests followed by Bonferroni correction was employed. The continuous data

	CCS	HTx_A	HTx_B	HTx	p (CCS vs. HTx_A)	p (CCS vs. HTx_B)	p (HT_A vs. HTx_B)	p (CCS vs. HTx)
Clinical parameters								
Number of patients	39	41	7	48	NA	NA	NA	NA
Age (years)	24. 7 ± 4.6	51.4 ± 12	51.2 ± 14	51.4 ± 12.1	**< 0.001**	**< 0.001**	> 0.99	**< 0.001**
Height	172.7 ± 7.3	175.6 ± 8.9	172.7 ± 10.3	175.2 ± 9.2	0.31	> 0.99	0.8	0.15
Weight (kg)	68.1 ± 14	84.5 ± 15.5	89.6 ± 13.8	85.2 ± 15.5	**< 0.001**	**0.02**	0.79	**< 0.001**
Gender (male), n (%)	30 (77)	34 (83)	6 (86)	40 (83)	0.60	> 0.99	> 0.99	0.59
BMI (kg/m^2)	22.8 ± 4.3	27.3 ± 4.1	30.0 ± 3.8	27.7 ± 4.1	**< 0.001**	**0.004**	0.44	**< 0.001**
LVEF (%)	62.7 ± 5.8	62.7 ± 4.8	59.7 ± 6.6	62.3 ± 5.1	0.91	0.47	0.57	0.41
E/A ratio	1.56 ± 0.46	1.62 ± 0.4	1.92 ± 0.79	1.66 ± 0.48	0.98	0.48	0.51	0.31
E/E´ ratio	6.12 ± 1.19	8.7 ± 1.81	14 ± 7.9	9.58 ± 3.98	**< 0.001**	**< 0.001**	**< 0.001**	**< 0.001**
DD LV (mm)	42.03 ± 4.38	45.88 ± 4.92	45.29 ± 3.77	45.79 ± 4.74	**< 0.001**	0.37	0.97	**< 0.001**
CMR parameters								
LVEF (%)	60 ± 6	69.7 ± 6.7	59.6 ± 10.7	68.2 ± 8.1	**< 0.001**	0.99	**0.018**	**< 0.001**
LV SV (mL)	78.5 ± 18.5	68.1 ± 15.3	60 ± 14.3	66.9 ± 15.3	**0.021**	0.11	0.64	**0.002**
RV SV (%)	74.7 ± 16.9	70.3 ± 15.8	59.4 ± 15.4	68.7 ± 16.1	0.46	0.19	0.43	0.096
LV LGE, n (%)	0 (0)	5 (12)	2 (28.6)	7 (15)	NA	NA	NA	NA
Heart rate (bpm), rest	74.1 ± 13.4	82.2 ± 11.9	84.9 ± 9.8	82.1 ± 11.6	**0.016**	0.26	0.92	**0.002**
Heart rate (bpm), stress	103.5 ± 17.1	91.1 ± 10.1	91.1 ± 12.7	91.1 ± 10.3	**< 0.001**	0.22	> 0.99	**< 0.001**
Rest cardiac output (L/min)	5.33 ± 1.53	5.76 ± 1.24	6.36 ± 1.25	5.87 ± 1.27	0.65	0.48	0.72	0.23
Stress cardiac output (L/min)	11.62 ± 2.08	8.11 ± 1.64	8.22 ± 1.88	8.13 ± 1.87	**0.002**	0.53	0.91	**< 0.001**
Adenosine-induced perfusion defects, n (%)	0 (0)	2 (4.9)	0 (0)	2 (4.2)	NA	NA	NA	NA

Table 2. Baseline clinical, TTE and CMR parameters. Values are presented as mean ± SD unless otherwise indicated. Statistically significant p values are in bold. *BMI* body mass index, *LVEF* left ventricular ejection fraction, *LV SV* left ventricular stroke volume, *DD LV* left ventricular diastolic diameter, *RV SV* right ventricular systolic volume, *LV LGE* left ventricular late gadolinium enhancement, *TTE* transthoracic echocardiography, *CMR* cardiovascular magnetic resonance, *CCS* childhood cancer survivors, *HTx* heart transplant group, *HTx_A* heart transplant without diastolic dysfunction subgroup, *HTx_B* heart transplant with diastolic dysfunction subgroup.

generally followed the Gaussian distribution, as assessed by the Kolmogorov–Smirnov test and visual inspection of histograms. In the case of R-R intervals, square root transformation was applied. One-way ANOVA was used to compare the groups, followed by Tukey Post-hoc test for unequal N. Discrete data (PTB, PTB_S) were assessed using the Kruskal–Wallis test and the Dunn Post-hoc test. In all cases, $\alpha = 0.05$ was used to define a statistically significant result.

Results

Patient's population. Basic clinical, TTE and CMR group characteristics are summarized in Table 2.

In the CCS group, no patient showed signs of diastolic dysfunction. The most common indications for treatment were Hodgkin lymphoma (11 patients, 28%) followed by Non-Hodgkin lymphoma (9 patients, 23%) and acute lymphocytic leukaemia (7 patients, 18%).

In the HTx group, seven patients showed grade II or higher diastolic dysfunction. The HTx population was divided based on the presence of diastolic dysfunction as a subgroup without (HTx_A) and another with (HTx_B).

The most common indication for HTx was dilated cardiomyopathy (30 patients, 63%), followed by ischemic heart disease (7 patients, 15%).

Since the number of patients included in HTx_B subgroup was relatively low, we also compared the whole HTx group with the CCS.

Pulmonary circulation biomarkers. The retrospective analysis of biomarkers was successful in all cases, and no adverse effects of adenosine application were observed.The CCS patients showed biomarker values as follows: PTT 4.96 ± 0.93 s, PTB 5.82 ± 0.91, PTT_S 3.76 ± 0.78 s, for the HTx group: PTT 5.59 ± 1.14 s, PTB 7.40 ± 1.65, PTT_S 4.92 ± 1.13 s, for the HTx_A population: PTT 5.51 ± 1.14 s, PTB 7.22 ± 1.62, PTT_S 4.82 ± 1.03 s and lastly for HTx_B population: PTT 6.04 ± 1.13 s, PTB 8.43 ± 1.51 and PTT_S 5.52 ± 1.56 s. Both PTTc and PTB in the CCS group were significantly lower than in the HTx and both HTx_A and the HTx_B subgroups. PTT showed significantly lower values only in the case of HTx and CCS group, when comparing to subgroups lower values without statistical significance were shown. In the case of stress parameters, both PTT_S and PTTc_S were significantly lower in the CCS group than in the HTx groups. The comparison between HTx_A and HTx_B shows trend toward lower values in the first group but without statistical significance. The PTT ratio was significantly lower in the CCS than in the HTx group and HTx_A subgroup.

	CCS	HTx_A	HTx_B	HTx	p (CCS vs. HTx_A)	p (CCS vs. HTx_B)	p (HT_A vs. HTx_B)	p (CCS vs. HTx)
PTT (s)	4.96 ± 0.93	5.51 ± 1.14	6.04 ± 1.13	5.59 ± 1.14	0.063	0.13	0.61	**0.007**
PTTc (s)	5.45 ± 0.87	6.41 ± 1.3	7.15 ± 1.2	6.52 ± 1.30	**< 0.001**	**0.015**	0.44	**< 0.001**
PTB	5.82 ± 0.91	7.22 ± 1.62	8.43 ± 1.51	7.40 ± 1.65	**< 0.001**	**< 0.001**	0.38	**< 0.001**
PBVI (mL/m^2)	238.98 ± 51.88	252.39 ± 64.32	245.26 ± 71.09	241.78 ± 64.60	0.58	0.98	0.97	0.32
PTT_S (s)	3.76 ± 0.78	4.82 ± 1.03	5.52 ± 1.56	4.92 ± 1.13	**< 0.001**	**0.003**	0.37	**< 0.001**
PTTc_S (s)	4.89 ± 0.89	5.9 ± 1.14	6.71 ± 1.63	6.02 ± 1.24	**< 0.001**	**0.006**	0.33	**< 0.001**
PTB_S	6.46 ± 1.07	6.85 ± 1.51	7.86 ± 2.04	7.00 ± 1.61	0.78	0.20	0.65	0.13
PTT ratio	0.77 ± 0.14	0.88 ± 0.14	0.91 ± 0.14	0.89 ± 0.14	**0.002**	0.18	0.96	**< 0.001**
PTTc ratio	0.91 ± 0.16	0.93 ± 0.16	0.93 ± 0.13	0.93 ± 0.15	0.80	0.96	< 0.99	0.51

Table 3. Pulmonary circulation biomarkers. Values are presented as mean ± SD unless otherwise indicated. Statistically significant p values are in bold. *PTT* pulmonary transit time, *PTTc* Bazett's formula corrected pulmonary transit time, *PTB* pulmonary transit beats, *PBVI* pulmonary blood volume index, *PTT_S* stress pulmonary transit time, *PTTc_S* Bazett's formula stress pulmonary transit time, *PTB_S* stress pulmonary transit beats, *PTT ratio* pulmonary transition time ratio, *PTTc ratio* Bazett's formula corrected pulmonary transition time ratio, *HTx* heart transplant group, *HTx_A* heart transplant without diastolic dysfunction subgroup, *HTx_B* heart transplant with diastolic dysfunction subgroup.

In addition, PTT-derived parameters did not significantly correlate with cardiac output (CO) at rest, but correlated with the stress CO. There was a difference between the CCS and the HTx group and HTx_A subgroup in the values of stress CO. There was no difference in the resting values.

The complete results are summarized in Table 3. Boxplots for rest and stress transition times and derived ratio parameters are shown in Fig. 2.

Rest parameters. The average PTT in the CCS group was not significantly lower neither in the HTx_A (4.96 ± 0.93 s vs. 5.51 ± 1.14 s, p = 0.063) nor the HTx_B group (4.96 ± 0.93 s vs. 6.04 ± 1.13 s, p = 0.13). Although values were lower in the HTx_A subgroup than the HTx_B, the differences did not meet conventional levels of statistical significance.

PTTc, on the other hand, was significantly lower in both cases (5.45 ± 0.87 s (CCS) vs. 6.41 ± 1.3 s, p < 0.001 (HTx_A) and vs. 7.15 ± 1.2 s, p = 0.015 (HTx_B) and the same applies for PTB (5.82 ± 0.91 (CCS) vs. 7.22 ± 1.62, p < 0.001 (HTx_A) and vs. 8.43 ± 1.51, p < 0.001 (HTx_B)). The comparison between HTx_A and HTx_B shows lower values in the first group but without statistical significance. There were no differences in PBVI values.

When comparing CCS and the HTx group as whole, the results copy those of comparing CCS and HTx_A subgroup with 1 exception—PTT was significantly prolonged in the HTx group.

Stress parameters. Both PTT_S and PTTc_S were significantly lower in the CCS group than in the HTx groups: PTT_S 3.76 ± 0.78 s (CCS) vs. 4.82 ± 1.03 s, p < 0.001 (HTx_A) and vs. 5.52 ± 1.56 s, p = 0.003 (HTx_B) and PTTc_S: 4.89 ± 0.89 s (CCS) vs. 5.9 ± 1.14, p < 0.001 (HTx_A) and vs. 6.71 ± 1.63, p = 0.006 (HTx_B).

PTB_S showed lower values in the CCS group, but without statistical significance (6.46 ± 1.07 (CCS) vs. 6.85 ± 1.51, p = 0.78 (HTx_A) and vs. 7.86 ± 2.04, p = 0.19 (HTx_B). Similarly to the rest parameters, the comparison between HTx_A and HTx_B shows lower parameters in the first group, but without statistical significance.

Comparison of CCS and HTx group shows the same results as in the HTx_A group, both PTT_S and PTTc_S were significantly lower in the CCS group, PTB_S showed lower values without statistical significance.

Ratio parameters. The PTT ratio was significantly lower in the CCS than in the HTx_A subgroup (0.77 ± 0.14 vs. 0.88 ± 0.14, p = 0.002) and HTx group as well (0.77 ± 0.14 vs. 0.89 ± 0.14, p < 0.001). Lower parameters without statistical significances were shown when comparing the CCS and the HTx_B groups (0.77 ± 0.14 vs. 0.91 ± 0.14, p = 0.20). Although there were no significant differences between the groups in the case of the PTTc ratio, the PTT ratio and the PTTc ratio were below 1 in all groups, which means PTT_S times were shorter than the rest values.

Regarding the BMI, no statistical significance in any group or parameter was found with only 1 exception—a positive correlation of BMI with PTTc ratio in the CCS group (r = 0.49, p = 0.002). In addition, age did not correlate with PTT-derived parameters in any group (all r values < 0.2, all p values > 0.05).

Discussion

The main goals of this study were to provide more evidence about pulmonary circulation parameters acquired by first-pass perfusion CMR, to investigate stress parameters in the HTx population as a potential marker of diastolic dysfunction and to compare rest and stress parameters and present ratio parameters as potential new biomarkers. The main finding was that stress pulmonary circulation times with and without Bazett's formula correction were shorter than rest times contrary to the only published article including stress data[7]. Additionally, more data about pulmonary circulation parameters in new populations and ratio parameters were presented.

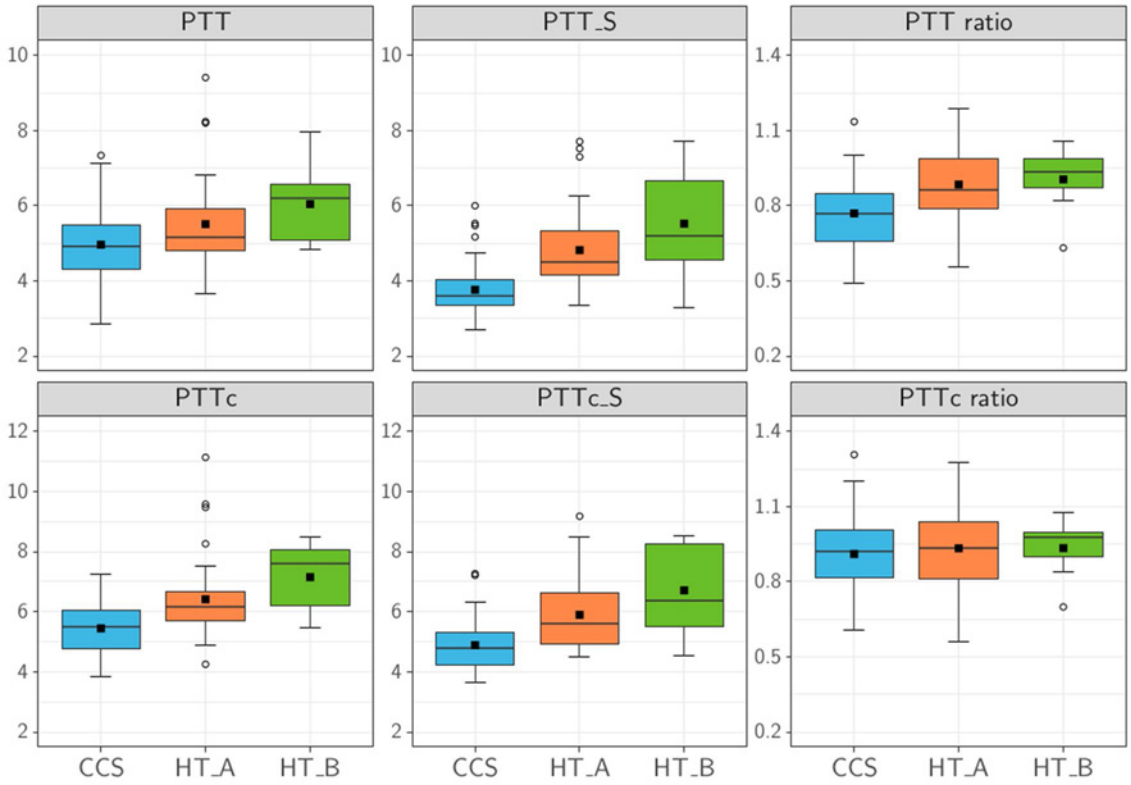

Figure 2. Pulmonary transit time parameters including stress and ratio biomarkers. The figure shows the comparison of pulmonary transit time (PTT) (s), stress pulmonary transit time (PTT_S) (s), pulmonary transit time ratio (PTT ratio) and heart rate corrected derived parameters (PTTc (s), PTTc_S (s) and PTTc ratio). Statistical analysis followed the corresponding methods section, $\alpha = 0.05$ defined a statistically significant result. The average PTT in the childhood cancer survivors (CCS) group was not significantly lower than in the heart transplant without diastolic dysfunction subgroup (HTx_A) or heart transplant with diastolic dysfunction subgroup (HTx_B). PTTc, on the other hand, was significantly lower in both cases. Both PTT_S and PTTc_S were significantly lower in the CCS group than in the HTx subgroups. Stress transition times were shorter than rest times, and therefore ratio parameters were below 1 in all groups.

Since ratio biomarkers are calculated as the ratio of stress and rest values, they describe the heart reaction to adenosine-induced pharmacological stress.

In previously published data[7], only HR corrected PTT time was assessed from stress biomarkers and it showed prolongation or no change compared to HR corrected PTT rest time. In the whole study population of 69 HCM patients, the results showed overall prolongation of PTT stress time. When divided into subgroups based on left atrial pressure (LAP), the corrected PTT stress was prolonged in patients with normal LAP, and in increased LAP, the values stayed roughly the same. Therefore, the calculated corrected PTT ratio would have been higher than 1 or close to 1 for this population.

In this study, all presented groups had PTT and PTTc ratios lower than 1, and therefore stress biomarkers were shorter, which is in contrary. One explanation could be based on the diastolic dysfunction in the HCM group. However, this difference is certainly a matter of discussion. Although adenosine indeed induces vasodilation in pulmonary circulation as the authors claim[7], its overall effect on the myocardium and circulation itself is still debatable and more complex. The HR increase is well documented[20,21], and our data are no exception. However, its effect on contractility is quite controversial. Some studies showed a positive outcome on contractility[22] or stated it affects beta-receptors as well[23], while others claim it has an indirect effect on contractility but no beta-receptor activity[24]. Apart from a direct reaction on the myocardium, recent reports focused on its repercussions in the central nervous system (CNS), mainly in the *nucleus tractus solitarius* but other parts of CNS as well[25], and its possible influence on baroreflex via CNS[26]. However, most of the studies were on rats or mice models or isolated myocardial cells, and for example, the effect on baroreflex could be indirect via hypotension from vasodilatation resulting in increasing HR and contractility of the myocardium. This truly complex problem is quite beyond the scope of this paper to discuss in all the possibilities.

Overall, we presume that in a healthy population, stress biomarkers such as PTT_S should be shorter than their rest analogues, therefore, ratio biomarkers should be less than 1, and they could be potentially used as additional markers of the myocardial reserve and/or diastolic dysfunction. However, further research, including a comprehensive healthy population, is needed.

We hypothesized underlying diastolic function impairment in patients after HTx and the feasibilty of using pulmonary circulation and potentially ratio parameters to assess it. During diastole, the LV receives blood from

the left atrium (LA). LV diastolic dysfunction leads to the impairment of its filling function, therefore filling pressure in the LV is increased, which leads to increased pressure in the LA as well. This corresponds with increasing of the pulmonary capillary wedge pressure (PCWP). When PCWP is increased, the whole process of blood circulating through the pulmonary circulation is supposedly impaired as well, resulting in longer PTT times. This mechanism is supposedly more appreciable in stress conditions, which agrees with our results and also possibly explains the difference in stress CO between CCS and HTx_A.

As Meluzin et al. reported[10]—16% of HTx subjects had signs of diastolic dysfunction in rest conditions (14.6% in this study), but other 58% showed signs of diastolic impairment in stress conditions[10]. While the difference in PTT was not significant, PTTc, PTT_S and PTTc_S were significantly lower in the CCS group than the HTx_A subgroup, which follows our assumption. In addition, both rest and stress transit times reported by Ricci et al. in HCM patients were higher[7]. Since LV hypertrophy in HCM patients is most commonly paired with diastolic dysfunction, these results further strengthenour assumptions.

The lower PTT ratio, while constant PTTc ratio between groups, could be influenced by the difference in HR and the results could be affected by the heart denervation in the HTx population, but that would not explain the tendency to higher values in the HTx_B group with diastolic dysfunction as to the HTx_A. Combined with the prolongation of stress parameters, and thus ratio parameters around 1 or more, as reported by Ricci et al. in HCM patients[7], this further-more points to diastolic function impairment as the explanation.

However, additional studies with different populations are necessary to confirm these results.

In all cases, no statistically significant differences were found when comparing the HTx_A and the HTx_B groups. However, in cases such as for the PTTc (6.41 ± 1.3 s vs. 7.15 ± 1.2 s, $p = 0.44$) or PTTc_S (5.9 ± 1.14 s vs. 6.71 ± 1.63 s, $p = 0.33$), a tendency towards lower values in HTx_A was observed. This is limited by the number of patients included in the HTx_B group. Although this number of patients with diastolic dysfunction included was relatively small, impacting the implications of the results, the proposed method illustrates the feasibility of including pulmonary circulation biomarkers as an additional method to assess diastolic dysfunction.

Since the limited number of subjects in HTx_B subgroup, HTx group as whole was included and compared with CCS group—the results resembled the comparison of CCS and HTx_A group with the exemption of the PTT, which was significantly longer in the HTx group. This result further documents an assumption of the influence of an underlying dysfunction.

It is not completely clear whether to prefer HR-corrected PTT times or not. In Ricci's study, both rest times and only corrected stress PTT times were reported[7], and in Houard et al.[6] no HR correction was applied at all. We believe both alternatives are justified. While PTB could be a form of overriding the effect of HR in counting the number of cycles, for the stress parameters and ratios, we think that both possibilities are valid and should be acquired.

It is also possible to evaluate these biomarkers from the peak-to-peak time interval in the signal intensity curve. However, we opted for the onset assessment because the first appearance of the contrast showed good reproducibility.

To our knowledge, only one other study acquiring pulmonary circulation stress biomarkers was published to date, and therefore, with 87 patients included, this is one of the first larger CMR-based studies involving stress circulation parameters. However, more studies have to be made to confirm our results, including different groups with reduced LVEF, other diagnoses, and an aged-match healthy control group, although applying adenosine to a healthy control group could prove ethically problematic. On the other hand, when using the presented or an earlier developed method, a center with a relatively high number of stress perfusions could comfortably conduct other studies retrospectively to gather more data about stress circulation biomarkers. As far as we know, these parameters have never been studied before in CCS or HTx patient groups.

Study limitations. We acknowledge there are limitations to this study. It was a single-center retrospective study, but arguably the principal constrain is the participant's selection: CCS and HTx. CCS cannot be reffered to as a healthy control group. Although in thorough examinations no signs of systolic or diastolic function impairment, other pathological results or any other cardiac function impairment were observed, patients included underwent potentially cardiotoxic chemotherapy. Their comparability is further limited by basic clinical parameters, mainly age and BMI. However, in neither group the age correlated with pulmonary circulation biomarkers, and the BMI correlated only with the PTTc ratio in the CCS group. Also, selecting patients after HTx could lead to bias with the adenosine effect on a denervated heart. Data on using adenosine or regadenoson on subjects after HTx is limited. In older studies, a hypersensitivity was described[27], but it seems safe to administer it[28]. A newer study from Spain showed its use in the case of stress perfusion as well, although HTx patients presented a lower myocardial perfusion reserve index in comparison to healthy controls[29]. Furthermore, although the number of participants with diastolic dysfunction (HTx_B group) was low, impacting the implications of the results, the proposed method illustrates the feasibility of including pulmonary circulation biomarkers as a potential additional approach to assess diastolic dysfunction.

Ethics approval and consent to participate. This retrospective study was performed in accordance with the Declaration of Helsinki (2000) of the World Medical Association. The Ethics Committee of the Faculty of Medicine, Masaryk University, confrmed under reference number 02082021, that this study has been performed on data of patients already participating in other research studies with signed Informed Consent about using their data anonymously for research purposes and therefore according to the Czech legislation, no specific new approval of the ethics committee was required. Only participants who signed written Informed Consent about using their data anonymously for research purposes were enrolled in the study. No patient from potentially vulnerable group was enrolled in the study.

Conclusions

The study provided more evidence about pulmonary circulation parameters acquired by first-pass perfusion CMR, investigated stress parameters in an HTx population as a potential marker of diastolic dysfunction and presented ratio parameters as potential new biomarkers.

The results showed lower values of PTTc, PTT_S and PTTc_S in the CCS group, corresponding with the presumption of underlying diastolic dysfunction in HTx patients. As assumed, contrary to the data published for HCM patients[7], both PTT_S and PTTc_S times were shorter than their rest analogues in all groups, and therefore the PTT ratio and the PTTc ratio were less than 1.

Data availability

The datasets analysed during the current study are available from the corresponding author upon reasonable request.

Received: 8 July 2021; Accepted: 21 March 2022
Published online: 12 April 2022

References

1. Slutsky, R. A., Bhargava, V. & Higgins, C. B. Pulmonary circulation time: Comparison of mean, median, peak, and onset (appearance) values using indocyanine green and first-transit radionuclide techniques. *Am. Heart J.* **106**(1 Pt 1), 41–45 (1983).
2. de Lepper, A. G. W. *et al.* Noninvasive pulmonary transit time: A new parameter for general cardiac performance. *Echocardiography* **34**(8), 1138–1145 (2017).
3. Herold, I. H. F. *et al.* Pulmonary blood volume measured by contrast enhanced ultrasound: A comparison with transpulmonary thermodilution. *Br. J. Anaesth.* **115**(1), 53–60 (2015).
4. Colin, G. C. *et al.* Pulmonary hypertension detection by computed tomography pulmonary transit time in heart failure with reduced ejection fraction. *Eur. Heart J. Cardiovasc. Imaging* **21**(11), 1291–1298 (2020).
5. Shors, S. M. *et al.* Heart failure: Evaluation of cardiopulmonary transit times with time-resolved MR angiography. *Radiology* **229**(3), 743–748 (2003).
6. Houard, L. *et al.* Prognostic value of pulmonary transit time by cardiac magnetic resonance on mortality and heart failure hospitalization in patients with advanced heart failure and reduced ejection fraction. *Circ. Cardiovasc. Imaging* **14**(1), e011680 (2021).
7. Ricci, F. *et al.* Pulmonary blood volume index as a quantitative biomarker of haemodynamic congestion in hypertrophic cardiomyopathy. *Eur. Heart J. Cardiovasc. Imaging* **20**(12), 1368–1376 (2019).
8. Ricci, F. *et al.* Prognostic value of pulmonary blood volume by first-pass contrast-enhanced CMR in heart failure outpatients: The PROVE-HF study. *Eur. Heart J. Cardiovasc. Imaging* **19**(8), 896–904 (2018).
9. Cao, J. J., Li, L., McLaughlin, J. & Passick, M. Prolonged central circulation transit time in patients with HFpEF and HFrEF by magnetic resonance imaging. *Eur. Heart J. Cardiovasc. Imaging* **19**(3), 339–346 (2018).
10. Meluzin, J. *et al.* High prevalence of exercise-induced heart failure with normal ejection fraction in post-heart transplant patients. *Biomed. Pap.* **158**(2), 295–302 (2014).
11. Mulrooney, D. A. *et al.* Cardiac outcomes in a cohort of adult survivors of childhood and adolescent cancer: Retrospective analysis of the Childhood Cancer Survivor Study cohort. *BMJ* **339**, b4606 (2009).
12. Yeh, E. T. H. *et al.* Cardiovascular complications of cancer therapy. *Circulation* **109**(25), 3122–3131 (2004).
13. 2015 ESC/ERS Guidelines for the diagnosis and treatment of pulmonary hypertension | European Heart Journal | Oxford Academic [Internet]. https://academic.oup.com/eurheartj/article/37/1/67/2887599. Accessed 28 Mar 2021.
14. Panovský, R. *et al.* Cardiac profile of the Czech population of Duchenne muscular dystrophy patients: A cardiovascular magnetic resonance study with T1 mapping. *Orphanet J. Rare Dis.* **14**(1), 10 (2019).
15. Schulz-Menger, J. *et al.* Standardized image interpretation and post processing in cardiovascular magnetic resonance: Society for Cardiovascular Magnetic Resonance (SCMR) board of trustees task force on standardized post processing. *J. Cardiovasc. Magn. Reson.* **1**(15), 35 (2013).
16. Ishida, M. *et al.* Development of a universal dual-bolus injection scheme for the quantitative assessment of myocardial perfusion cardiovascular magnetic resonance. *J. Cardiovasc. Magn. Reson.* **13**(1), 28 (2011).
17. Styner, M., Brechbuhler, C., Szckely, G. & Gerig, G. Parametric estimate of intensity inhomogeneities applied to MRI. *IEEE Trans. Med. Imaging* **19**(3), 153–165 (2000).
18. Pluim, J. P. W., Maintz, J. B. A. & Viergever, M. A. Mutual-information-based registration of medical images: A survey. *IEEE Trans. Med. Imaging* **22**(8), 986–1004 (2003).
19. Bazett, H. C. An analysis of the time-relations of electrocardiogram. *Heart* **7**, 353 (1920).
20. Wilson, R. F., Wyche, K., Christensen, B. V., Zimmer, S. & Laxson, D. D. Effects of adenosine on human coronary arterial circulation. *Circulation* **82**(5), 1595–1606 (1990).
21. Salerno, M. *et al.* Adenosine stress cardiovascular magnetic resonance with variable-density spiral pulse sequences accurately detects coronary artery disease. *Circ. Cardiovasc. Imaging* **7**(4), 639–646 (2014).
22. Monahan, T. S., Sawmiller, D. R., Fenton, R. A. & Dobson, J. G. Adenosine A2a-receptor activation increases contractility in isolated perfused hearts. *Am. J. Physiol. Heart Circ. Physiol.* **279**(4), H1472–H1481 (2000).
23. Hori, M. & Kitakaze, M. Adenosine, the heart, and coronary circulation. *Hypertension* **18**(5), 565–574 (1991).
24. Chandrasekera, P. C., McIntosh, V. J., Cao, F. X. & Lasley, R. D. Differential effects of adenosine A2a and A2b receptors on cardiac contractility. *Am. J. Physiol. Heart Circ. Physiol.* **299**(6), H2082–H2089 (2010).
25. Costa, M. A., Matsumoto, J. P. P., Carrettiero, D. C. & Fior-Chadi, D. R. Adenosine A1 and A2a receptors modulate the nitrergic system in cell culture from dorsomedial medulla oblongata. *Auton. Neurosci.* **229**, 102737 (2020).
26. Tian, L. *et al.* Blockade of adenosine A1 receptor in nucleus tractus solitarius attenuates baroreflex sensitivity response to dexmedetomidine in rats. *Brain Res.* **1743**, 146949 (2020).
27. Ellenbogen, K. A., Thames, M. D., DiMarco, J. P., Sheehan, H. & Lerman, B. B. Electrophysiological effects of adenosine in the transplanted human heart. Evidence of supersensitivity. *Circulation* **81**(3), 821–828 (1990).
28. Flyer, J. N. *et al.* Prospective study of adenosine on atrioventricular nodal conduction in pediatric and young adult patients after heart transplantation. *Circulation* **135**(25), 2485–2493 (2017).
29. Jiménez-Jaso, J. M. *et al.* Valoración del índice de reserva de perfusión miocárdica por resonancia magnética en pacientes con trasplante cardíaco. *Radiologia* **62**(6), 493–501 (2020).

Author contributions

L.O., R.P., J.K. and L.S. were the main designers of this study. L.O. was the major contributor in writing the manuscript. J.M. performed the statistical analysis. L.M., J.G., T.K. and V.K. contributed to patient recruitment, inclusion and revised the article critically. V.F. and T.H. performed CMR examinations and assisted with CMR data analysis. M.M.P. coded the algorithm for the CMR images processing and M.M.P. with G.Z. performed the data analysis. All authors read, reviewed and approved the final manuscript.

Funding

The work was supported by the European Regional Development Fund—project ENOCH (No. CZ.02.1.01/0.0/0.0/16_019/0000868) and by the project "New trends in diagnostics and therapy of cardiomyopathies" number MUNI/A/1685/2020 with the support of the Specific University Research Grant, as provided by the Ministry of Education, Youth and Sports of the Czech Republic in the year 2021.

Competing interests

The authors declare no competing interests.

Additional information

Correspondence and requests for materials should be addressed to R.P.

Reprints and permissions information is available at www.nature.com/reprints.

Publisher's note Springer Nature remains neutral with regard to jurisdictional claims in published maps and institutional affiliations.

C. Štěchovský et al.

Comparison of 30-Day Outcomes after Carotid Artery Stenting in Patients with Near-Occlusion and Severe Stenosis: A PropensityScore Matching Analysis

AJNR Am J Neuroradiol
Impact Factor: 4.966

Comparison of 30-Day Outcomes after Carotid Artery Stenting in Patients with Near-Occlusion and Severe Stenosis: A Propensity Score Matching Analysis

C. Štěchovský, K. Hulíková Tesárková, P. Hájek, M. Horváth, E. Hansvenclová, and J. Veselka

ABSTRACT

BACKGROUND AND PURPOSE: Carotid artery near-occlusion is a type of severe stenosis with complete or partial distal luminal collapse and intracranial collaterals. This study aimed to compare 30-day outcomes and 10-year survival in patients undergoing carotid artery stenting for near-occlusion with a control group of patients with severe stenosis.

MATERIALS AND METHODS: We used data from a registry of 639 patients who underwent 789 carotid artery stenting procedures between 2005 and 2021. The primary end point was any stroke or death within 30 days after carotid artery stenting. Patients were matched using propensity scores based on 6 variables.

RESULTS: Propensity score matching yielded 84 subjects in the near-occlusion group matched with 168 subjects in the control group. In the matched cohort, the primary end point occurred in 7 (8.3%) and 11 (6.6%) patients in the near-occlusion and control groups, respectively ($P = .611$). In the unmatched cohort, the primary end point occurred in 7 (8.3%) and 19 (4.1%) patients ($P = .101$). Survival in the near-occlusion group versus the control group in the matched cohort at 5 and 10 years was 69.8% (95% CI, 58.0%–78.8%) versus 77.3% (95% CI, 70.0%–83.1%) and 53.3% (95% CI, 39.9%–65.0%) versus 53.3% (95% CI, 44.5%–61.4%) (log-rank, $P = .798$).

CONCLUSIONS: Carotid stent placement in patients with ICA near-occlusion was not associated with an increased 30-day risk of stroke or death compared with severe stenosis. Survival up to 10 years after carotid artery stenting was similar in both groups.

ABBREVIATIONS: CAS = carotid artery stenting; ECA = external carotid artery; ESC = European Society of Cardiology; ESVS = European Society for Vascular Surgery

Carotid artery near-occlusion is a type of severe stenosis with complete or incomplete distal luminal collapse and intracranial collaterals.[1] Various terms have been used to describe near-occlusion: subtotal stenosis or occlusion, functional occlusion, string sign, slim sign, critical stenosis, and others.[2] Calculating the percentage stenosis for ICA near-occlusion according to the NASCET criteria[3,4] is a fallacious approach. Near-occlusion can be confused with complete occlusion or severe stenosis when imaging with CTA or sonography is suboptimal.[4] The multitude of terms, subtle variation in the definition, and diagnostic ambiguity lead to uncertainty about the true incidence, prognosis, and optimal treatment of ICA near-occlusion. Some early observational studies[5,6] suggested that near-occlusion carries a high risk of stroke and should be promptly recognized and treated by endarterectomy. This suggestion was later negated by the re-analysis of the NASCET and the European Carotid Surgery Trial.[3,7] Patients with near-occlusion were either excluded or not assessed or reported in further randomized clinical trials comparing surgery or conservative treatment of asymptomatic stenosis.[2] Both current European and American guidelines state that there is no clear evidence that endarterectomy or carotid artery stenting (CAS) prevents stroke in patients with near-occlusion of the ICA.[8,9] Another position paper admits that the prognoses of asymptomatic near-occlusion and periprocedural risks of CAS or endarterectomy are unknown.[10] A recent meta-analysis showed that the 30-day risk of stroke or death after endarterectomy or CAS for symptomatic ICA near-occlusion was 2%.[11]

In this study, we report 30-day outcomes after CAS in patients with ICA near-occlusion and compare them with a control group of patients with severe stenosis after CAS using a propensity score matching analysis. Additionally, we report 10-year survival after CAS.

Received March 2, 2022; accepted after revision June 17.

From the Department of Cardiology (C.Š., P.H., M.H., E.H., J.V.), Second Faculty of Medicine, Charles University, Motol University Hospital, Prague, Czech Republic; and Department of Demography and Geodemography (K.H.T.), Faculty of Science, Charles University, Prague, Czech Republic.

Please address correspondence to Cyril Štěchovský, MD, Department of Cardiology, Motol University Hospital, V Uvalu 84, 150 06, Prague, Czech Republic; e-mail: stechovsky@gmail.com

Indicates article with online supplemental data.

http://dx.doi.org/10.3174/ajnr.A7598

Table 1: Patient characteristics

	Unmatched Cohort			Matched Cohort		
	Near-Occlusion (n = 84 Patients)	Control Group (n = 460 Patients)	P Value	Near-Occlusion (n = 84 Patients)	Control Group (n = 168 Patients)	P Value
Age (mean) (yr)	70.3 (SD, 9.7)	68.6 (SD, 8.3)	.091	70.3 (SD, 9.7)	70.2 (SD, 7.7)	.943
Men	68%	65%	.620	68%	64%	.576
Current smokers	43%	40%	.629	43%	37%	.411
Arterial hypertension	88%	88%	1.000	88%	88%	1.000
Total plasma cholesterol level (mean) (mmol/L)	4.4 (SD, 1.1)	4.2 (SD, 1.0)	.126	4.4 (SD, 1.1)	4.4 (SD, 1.1)	.664
LDL cholesterol level (mean) (mmol/L)	2.6 (SD, 0.9)	2.4 (SD, 0.8)	.171	2.6 (SD, 0.9)	2.5 (SD, 0.9)	.629
HDL cholesterol level (mean) (mmol/L)	1.06 (SD, 0.31)	1.09 (SD, 0.33)	.695	1.06 (SD, 0.31)	1.09 (SD, 0.33)	.659
Plasma triglyceride level (mean) (mmol/L)	1.93 (SD, 1.2)	1.8 (SD, 1.1)	.638	1.93 (SD, 1.2)	1.78 (SD, 1.0)	.614
CRP level (median) (IQR) (mg/L)	3.6 (1.1–8.6)	2.3 (0.8–5.5)	.008	3.6 (1.1–8.6)	2.1 (0.9–4.9)	.010
Body mass index (mean)	28.6 (SD, 4.8)	28.1 (SD, 4.4)	.483	28.6 (SD, 4.8)	28.0 (SD, 4.1)	.540
Diabetes	33%	42%	.184	33%	37%	.676
Chronic kidney disease	27%	22%	.324	27%	24%	.644
Chronic bronchopulmonary disease	14%	13%	.723	14%	15%	1.000
Peripheral arterial disease	32%	39%	.271	32%	33%	.888
Heart failure with reduced ejection fraction	15%	11%	.320	15%	11%	.374
Previous coronary artery bypass	20%	18%	.649	20%	17%	.490
Need for heart surgery within 30 days	5%	9%	.281	5%	10%	.224
Previous myocardial infarction	24%	28%	.506	24%	30%	.302
Previous percutaneous coronary artery intervention	23%	32%	.094	23%	24%	.876
Known multivessel coronary artery disease	39%	40%	1.000	39%	35%	.490
Previous stroke	37%	30%	.252	37%	40%	.683
Ipsilateral cerebral ischemic symptoms in the past month	37%	21%	.003	37%	33%	.577
Ipsilateral cerebral ischemic symptoms in the past 6 months (ie, symptomatic stenosis)	45%	29%	.005	45%	46%	.894
Patients with ≥1 risk factors for endarterectomy[a]	82%	80%	.766	82%	82%	1.000

Note:—IQR indicates interquartile range; CRP, C-reactive protein.
[a] One of the following: left ventricle ejection fraction of ≤40%, chronic bronchopulmonary disease, prior myocardial infarction, coronary artery bypass grafts, or age 75 years or older.

MATERIALS AND METHODS

We retrospectively analyzed data from a single-center (Motol University Hospital) registry of 639 patients who underwent 789 CAS procedures between 2005 and 2021. Patients who had bilateral CAS or CAS for in-stent restenosis were excluded from the analysis. Some of the patients were included in previous studies.[12-16]

Patient Assessment, Procedure, and Follow-up

Patients were referred to carotid angiography and CAS by a neurologist, cardiologist, or vascular surgeon on the basis of Doppler sonography and/or CTA. Patient characteristics are listed in Table 1, and their medication before CAS is found in the Online Supplemental Data. Stenosis was quantified angiographically according to the NASCET criteria.[3] Inclusion criteria were symptomatic (≥50%) or asymptomatic (≥70%) stenosis of the ICA in a patient who was considered eligible for CAS. Carotid stenosis was considered symptomatic if the patient had a stroke, TIA, or amaurosis fugax ipsilateral to the stenosis in the previous 6 months. All patients provided written informed consent for the procedure. Procedures were performed via the femoral artery using a 7F or 8F guiding catheter or a long 6F sheath. The antithrombotic regimen included administration of 500 mg of aspirin and 300 mg of clopidogrel before CAS in naïve patients; a bolus of heparin (70 IU/kg) was administrated at the beginning of CAS. Types and manufacturers of stents and embolic protection devices were at the operator's discretion and current availability. Detailed angiographic and procedural characteristics are listed in the Online Supplemental Data. After CAS, patients were examined by a physician, and all symptomatic patients were examined by a neurologist. Postprocedural CTA or MR imaging was performed in all cases of clinically suspected stroke. Patients were discharged with dual antiplatelet therapy for 1 month and single antiplatelet therapy and high-dose statin therapy life-long. Follow-up consisted of a history and review of medical documentation if the patient had neurologic symptoms and Doppler sonography at 1, 6, and 12 months after CAS. Information about vital status was retrieved from the National Death Index. In the deceased patients, cause of death was adjudicated as cardiovascular or noncardiovascular. The study was conducted in accordance with the Declaration of Helsinki principles.

Definitions and End Points

Patients in the registry were divided into near-occlusion and control groups. Angiographic criteria described in the NASCET[2,3] were used to distinguish near-occlusion from conventional stenosis: 1) partial or complete collapse of the distal lumen (diameter of the ipsilateral distal ICA less than that of the contralateral distal ICA), 2) diameter of ipsilateral distal ICA less than that of the ipsilateral external carotid artery (ECA), 3) delayed filling of the ipsilateral distal ICA, and 4) intracranial collaterals (Fig 1). Two

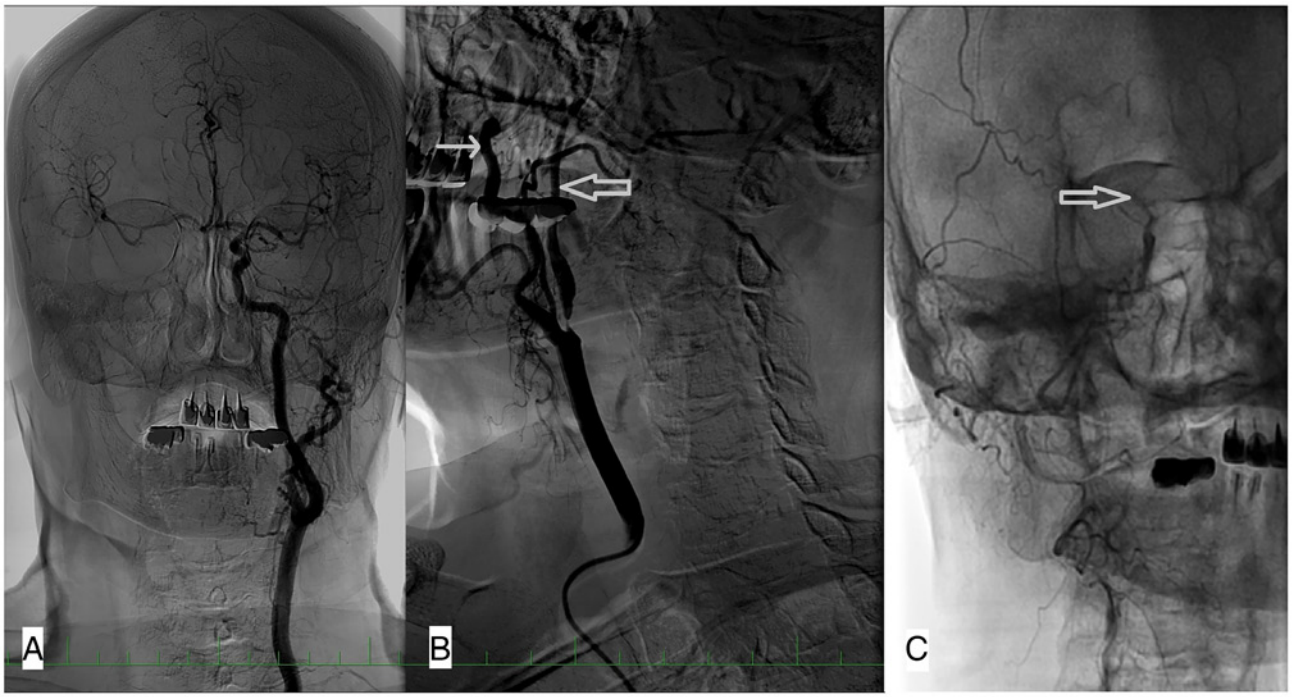

FIG 1. An angiogram in a patient with right ICA near-occlusion. *A*, In a selective angiogram of the left carotid artery, no stenosis is present; the diameter of the ICA is larger than that of the ECA; and there is rapid filling of the intracranial circulation and intracranial collaterals to the right ACA and MCA. *B*, Near-occlusion of the right ICA. The diameter of the distal ICA (*thick arrow*) is smaller than that of the ECA (*thin arrow*) and much smaller than that of the contralateral ICA. Late filling of the distal ICA. *C*, In the late phase of the angiogram, the contrast filling stops at the level of carotid siphon (*thick arrow*). The intracranial circulation is not visualized because the contrast is diluted by collateral flow. ACA indicates anterior cerebral artery.

of the 4 criteria were required for the diagnosis. In patients without acute neurologic symptomatology, intracranial collaterals must always be present in the near-occlusion. The primary end point consisted of any stroke or death within 30 days after CAS. Ischemic stroke was defined as an acute neurologic event with focal symptoms, lasting for ≥24 hours. Minor stroke was defined as a new neurologic deficit that resolved within 30 days without any limiting disability (≤1 on the mRS) or return to baseline status. Major stroke was defined as a new neurologic deficit with persisting disability (≥2 on mRS). TIA was defined as an episode of new neurologic dysfunction attributed to focal cerebral ischemia, with resolution within 24 hours.

Statistical Analysis

Statistical analyses were performed using SAS software, Version 9.4 (SAS Institute). Data are presented as means (SD) or median and interquartile range or counts and proportions. The Student *t* test or Mann-Whitney *U* test was used to evaluate the difference among continuous variables, and the Fisher exact test was used for the evaluation among categoric variables. Kaplan-Meier survival analysis was used to estimate long-term survival in patients after CAS with 95% confidence intervals. Given the inherent differences between patients with near-occlusion and the control group, using the logit model, we calculated propensity scores for the following variables as covariates: age, sex, total plasma cholesterol, diabetes, previous percutaneous coronary intervention, and ipsilateral cerebral ischemic symptoms in the past 6 months. Other potential covariates were confirmed as nonsignificant or highly correlated to other variables. Matching on the propensity scores was performed using the 1:2 nearest neighbor method without replacement.[17,18] A 2-sided *P* value ≤ .05 was considered to indicate statistical significance.

RESULTS

A total of 544 patients were analyzed, 84 (15%) in the near-occlusion group and 460 (85%) in the control group. Propensity score matching yielded 84 subjects in the near-occlusion group matched with 168 subjects in the control group (Table 1 and Online Supplemental Data). Patients in the unmatched cohort with near-occlusion had symptomatic stenosis significantly more often, higher median C-reactive protein levels, used less statin therapy, had longer fluoroscopic times, and more often required predilation ($P < .05$ for all) (Table 1 and Online Supplemental Data). After matching, patients with near-occlusion had significantly higher median C-reactive protein levels and longer fluoroscopy time and more often required predilation ($P < .05$ for all) (Table 1 and Online Supplemental Data).

Data on major adverse in-hospital and 30-day events were available in 544 (100%) and 527 (97%) patients, respectively. Vital status at the end of the follow-up was available in all patients from the National Death Index. In the unmatched cohort, the primary end point occurred in 7 (8.3%) patients in the near-occlusion group and 19 (4.1%) patients in the control group ($P = .101$) and in the matched cohort in 7 (8.3%) and 11 (6.6%) patients ($P = .611$). Individual components of the end point are summarized in Table 2. In the matched subgroup of symptomatic patients, the primary end

Table 2: Thirty-day major adverse events and long-term follow-up

	Unmatched Cohort			Matched Cohort		
	Near-Occlusion (n = 84 Patients)	Control Group (n = 460 Patients)	P Value	Near-Occlusion (n = 84 Patients)	Control Group (n = 168 Patients)	P Value
TIA during hospitalization (No.) (%)	6 (7.1)	12 (2.6)	.045	6 (7.1)	7 (4.2)	.368
A, Minor stroke during hospitalization (No.) (%)	3 (3.6)	5 (1.1)	.111	3 (3.6)	3 (1.8)	.404
B, Major stroke during hospitalization (No.) (%)	1 (1.2)	6 (1.3)	1.000	1 (1.2)	4 (2.4)	.668
Hyperperfusion syndrome during hospitalization (No.) (%)	0	2 (0.4)	1.000	0	0	
Myocardial infarction during hospitalization (No.) (%)	1 (1.2)	0	.154	1 (1.2)	0	.333
Death during hospitalization (No.) (%)	2 (2.4)	2 (0.4)	.115	2 (2.4)	0	.110
C, Minor stroke in 30-day hospitalization (No.) (%)	0	4 (0.9)	1.000	0	2 (1.2)	.554
D, Major stroke in 30-day hospitalization (No.) (%)	1 (1.2)	2 (0.4)	.396	1 (1.2)	1 (0.6)	1.000
E, Death in 30 days (including during hospitalization) (No.) (%)	3 (3.6)	3 (0.7)	.050	3 (3.6)	1 (0.6)	.109
Primary end point: A + B + C + D + E (No.) (%)	7 (8.3)	19 (4.1)	.101	7 (8.3)	11 (6.6)	.611
Re-intervention for restenosis during follow-up (No.) (%)	9 (10.7)	19 (4.1)	.026	9 (10.7)	6 (3.6)	.044
All-cause mortality during follow-up (No.) (%)	33 (39.3)	202 (43.9)	.473	33 (39.3)	76 (45.2)	.419
Cardiovascular death (No.) (%)	25 (29.8)	129 (28.0)	.792	25 (29.8)	53 (31.6)	.885
Noncardiovascular death (No.) (%)	6 (7.1)	64 (13.9)	.110	6 (7.1)	19 (11.3)	.374
Unknown death (No.) (%)	2 (2.4)	9 (2.0)	.682	2 (2.4)	4 (2.4)	1.000
Mortality per 100 patient-years	6.6	6.8		6.6	6.5	

Note:—TIA indicates transient ischemic attack.

point occurred in 4 (10.5%) patients in the near-occlusion group and 7 (9%) patients in the control group (P = .748). In the asymptomatic patients, the primary end point occurred in 3 (6.5%) patients in the near-occlusion group and 4 (4.4%) patients in the control group (P = .688). The results for the symptomatic and asymptomatic patients are summarized in the Online Supplemental Data.

In the unmatched cohort, the mean follow-up was 5.9 (SD, 4.1) years in the near-occlusion group and 6.5 (SD, 4.1) years in the control group, which yielded 499 and 2980 patient-years of follow-up. Thirty-three (39.3%) patients in the near-occlusion group and 202 (43.9%) patients in the control group died (P = .473), which translated into 6.6 and 6.8 deaths per 100 patient-years, respectively. In the matched cohort, the mean follow-up was 5.9 (SD, 4.1) years in the near-occlusion group and 7.0 (SD, 4.2) years in the control group, which yielded 499 and 1176 patient-years of follow-up. In the matched cohort, 33 (39.3%) patients in the near-occlusion group and 76 (45.2%) patients in the control group died (P = .419), which translated into 6.6 and 6.5 deaths per 100 patient-years, respectively. In the matched cohort, survival in the near-occlusion group versus the control group at 5 and 10 years was 69.8% (95% CI, 58.0%–78.8%) versus 77.3% (95% CI, 70.0%–83.1%) and 53.3% (95% CI, 39.9%–65.0%) versus 53.3% (95% CI, 44.5%–61.4%) (log-rank, P = .798) (Fig 2*A*). In the unmatched cohort, survival at 5 and 10 years was similar (log-rank, P = .996) (Fig 2*B*).

During the follow-up, 9 (10.7%) patients and 19 (4.1%) patients underwent re-intervention for in-stent restenosis in the near-occlusion and control groups, respectively (P = .026) (Fig 3*A*). After matching, the difference was still statistically significant, 10.7% versus 3.6% (P = .044) (Fig 3*B*).

DISCUSSION

Results of our observational study suggest that patients with near-occlusion had a high incidence of stroke or death within 30 days after CAS (8.3%) and high annual mortality (6.7%). However, the risk was not significantly different from that of severe stenosis after the adjustment using the propensity score matching. Although we observed a trend toward higher periprocedural risk in the near-occlusion group, which was numerically 2-fold, it did not reach statistical significance. The difference in the primary end points was even smaller after the adjustment. We believe that this difference is due to the higher proportion of symptomatic patients in the near-occlusion group. However, it could be related to the number of patients in the registry and confounders. The NASCET and European Carotid Surgery Trial included 262 cases of near-occlusion.[3,7] The risk of perioperative stroke and death was similar in near-occlusion (5.4%) and 70%–99% stenosis (6.2%),[19] and lower periprocedural risks have been reported since then.[11] Later, trials comparing endarterectomy and CAS either excluded patients with near-occlusion or did not assess near-occlusion. The real-world registry might provide valuable information about the early risk of CAS for near-occlusion in a population of patients with high cardiovascular comorbidity that is not typically represented in randomized trials. Given the differences in the population

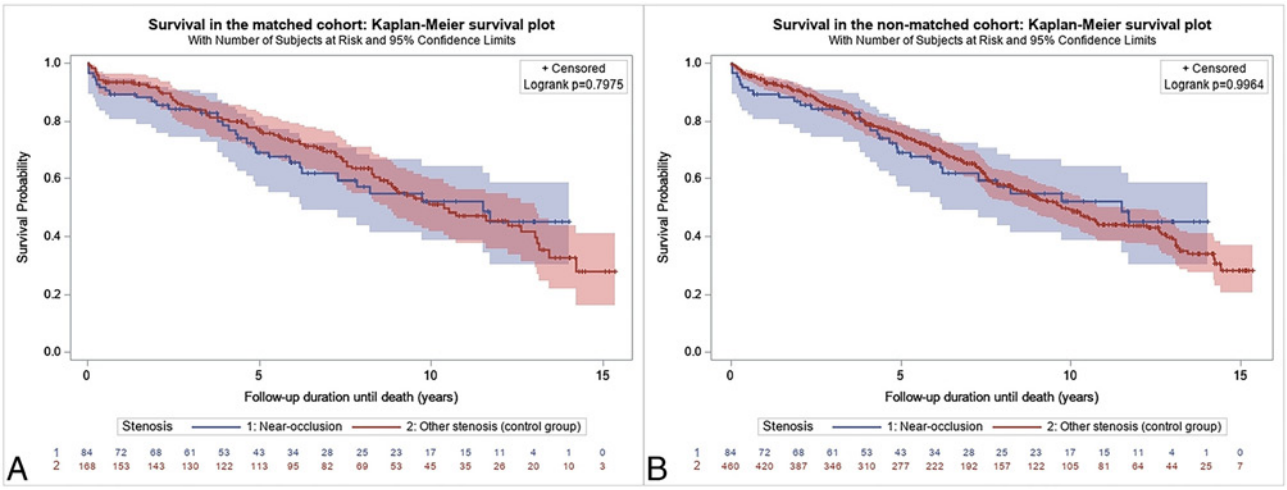

FIG 2. Kaplan-Meier estimate of 10-year survival after carotid stent placement in the near-occlusion-versus-control groups in the matched (*A*) and unmatched (*B*) cohorts.

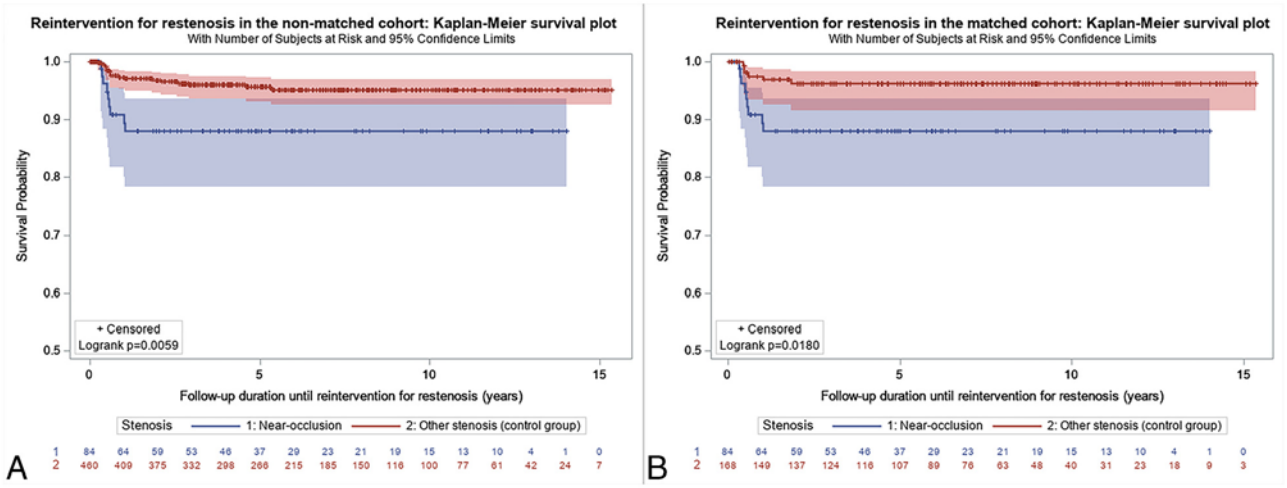

FIG 3. Kaplan-Meier estimate of freedom from re-intervention for in-stent restenosis after carotid stent placement in the near-occlusion-versus-control groups in the unmatched (*A*) and matched (*B*) cohorts.

of patients with near-occlusion and conventional severe stenosis and a most notably higher incidence of symptomatic stenosis in the near-occlusion group, we decided to compare the groups with the propensity score matching analysis to balance the baseline characteristics in both groups and lower the risk of selection bias.

The high periprocedural risk of stroke in ICA near-occlusion might be explained by the slow flow of blood distal to the lesion, which promotes in situ thrombosis that is embolized during CAS or protrudes through the stent struts and embolizes in the early postprocedural period. Angiography might not be able to distinguish ruptured atherosclerotic plaque with mural thrombus or mural thrombus in the distal ICA. Some cases of near-occlusion are actually recanalized thrombotic occlusions. Indeed, Hirata et al[20] reported that those old, organized thrombi were more frequently found in the endarterectomy specimens from near-occlusions than in high-grade stenoses. In our study, the 30-day stroke or death rate in the near-occlusion group (8.3%) was higher than that in a recent meta-analysis of some 703 patients with near-occlusion (226 underwent CAS; the 30-day stroke or death rate was 2.2%).[11] Individual observational studies included in the meta-analysis reported a 30-day stroke or death rate after CAS between 0% and 7%.[21-25] These studies had only 1 arm and did not compare the risk of CAS for near-occlusion with that in a control group. The high variability in the reported periprocedural risks might reflect different baseline characteristics and selection of patients rather than procedural techniques. It is also possible that the periprocedural stroke and death risk reported in the meta-analysis by Meershoek et al[11] underestimated the true risk because of bias in the reporting of small observational studies with unfavorable results.

The high all-cause mortality rate in our study is in contrast to the much lower mortality in the long-term follow-up of a recent, large, randomized Second Asymptomatic Carotid Surgery Trial (ACST-2: 330 deaths in 1811 patients randomized to CAS with a mean follow-up of 5 years and an annual mortality of ≈3.6%).[26] On the other hand, a study that analyzed data from Medicare

beneficiaries treated with CAS reported a mortality rate of 8.0% per year after the periprocedural period.[27] This study included older patients than in our registry, but other baseline characteristics were similar, with high cardiovascular comorbidity. These differences indicate that clinical trials enroll populations different from high-risk patients in whom the investigated technique is used in clinical practice.

We should carefully consider performing CAS in a patient with ICA near-occlusion, given the substantial periprocedural risk and life expectancy that might be shorter than 5 years reported by the European Society of Cardiology (ESC) and the European Society for Vascular Surgery (ESVS).[28] Meershoek et al[29] suggested that although the initial approach to symptomatic near-occlusion with full distal luminal collapse should be conservative, patients with recurrent events may be treated with endarterectomy. There is a need for further studies that could be based on large registries like the mandatory German Carotid National Registry.[30] We believe that the treatment of patients with ICA near-occlusion is one of the important topics in the field of carotid interventions that will require continued research before more evidence-based recommendations can be made.

The study is not without limitations. First, data were collected from a single center for 16 years. Although operators and procedural techniques remained unchanged, protection devices and stents changed across time. Referral of patients for carotid angiography and the criteria for selection of patients who would benefit from CAS changed during that time, with updated ESC/ESVS guidelines and results of randomized controlled trials.[26,28] The proportion of patients with near-occlusion and conventional stenosis who were selected for CAS compared with endarterectomy or medical therapy is unknown. Our results cannot be generalized to all patients with ICA near-occlusion. Second, propensity score matching is associated with inherent limitations. Although the matched cohort might seem well-balanced for baseline characteristics, there is always a risk of confounding bias. Third, we did not systematically collect data on major adverse cardiovascular events beyond the 30-day period after CAS; therefore, we reported only data on long-term survival.

CONCLUSIONS

Carotid stent placement in patients with ICA near-occlusion was not associated with an increased 30-day risk of stroke or death compared with severe stenosis. Survival up to 10 years after CAS was similar in both groups.

Disclosure forms provided by the authors are available with the full text and PDF of this article at www.ajnr.org.

REFERENCES

1. Fox AJ, Eliasziw M, Rothwell PM, et al. **Identification, prognosis, and management of patients with carotid artery near occlusion.** *AJNR Am J Neuroradiol* 2005;26:2086–94 Medline
2. Johansson E, Fox AJ. **Carotid near-occlusion: a comprehensive review, Part 1: definition, terminology, and diagnosis.** *AJNR Am J Neuroradiol* 2016;37:2–10 CrossRef Medline
3. Morgenstern LB, Fox AJ, Sharpe BL, et al. **The risks and benefits of carotid endarterectomy in patients with near occlusion of the carotid artery: North American Symptomatic Carotid Endarterectomy Trial (NASCET) group.** *Neurology* 1997;48:911–15 CrossRef Medline
4. Bartlett ES, Walters TD, Symons SP, et al. **Quantification of carotid stenosis on CT angiography.** *AJNR Am J Neuroradiol* 2006;27:13–19 Medline
5. Ringelstein EB, Berg-Dammer E, Zeumer H. **The so-called atheromatous pseudo-occlusion of the internal carotid artery: a diagnostic and therapeutical challenge.** *Neuroradiology* 1983;25:147–55 CrossRef Medline
6. O'Leary DH, Mattle H, Potter JE. **Atheromatous pseudo-occlusion of the internal carotid artery.** *Stroke* 1989;20:1168–73 CrossRef Medline
7. Rothwell PM, Gutnikov SA, Warlow CP. **Reanalysis of the final results of the European Carotid Surgery Trial.** *Stroke* 2003;34:514–23 CrossRef Medline
8. Bonati LH, Kakkos S, Berkefeld J, et al. **European Stroke Organisation guideline on endarterectomy and stenting for carotid artery stenosis.** *Eur Stroke J* 2021;6:I–XLVII CrossRef Medline
9. Kleindorfer DO, Towfighi A, Chaturvedi S, et al. **2021 Guideline for the Prevention of Stroke in Patients with Stroke and Transient Ischemic Attack: a Guideline From the American Heart Association/American Stroke Association.** *Stroke* 2021;52:e364–467 CrossRef Medline
10. Johansson E, Fox AJ. **Carotid near-occlusion: a comprehensive review, Part 2: prognosis and treatment, pathophysiology, confusions, and areas for improvement.** *AJNR Am J Neuroradiol* 2016;37:200–04 CrossRef Medline
11. Meershoek AJ, de Vries EE, Veen D, et al; NEON study group. **Meta-analysis of the outcomes of treatment of internal carotid artery near occlusion.** *Br J Surg* 2019;106:665–71 CrossRef Medline
12. Veselka J, Hajek P, Štěchovský C, et al. **Long-term survival of carotid stenting patients with regard to single- or double-vessel carotid artery disease: a propensity score matching analysis.** *Arch Med Sci* 2021;17:849–55 CrossRef Medline
13. Štěchovský C, Hájek P, Horváth M, et al. **Near-infrared spectroscopy combined with intravascular ultrasound in carotid arteries.** *Int J Cardiovasc Imaging* 2016;32:181–88 CrossRef Medline
14. Štěchovský C, Hájek P, Horváth M, et al. **Effect of stenting on the near-infrared spectroscopy-derived lipid core burden index of carotid artery plaque.** *Eurointervention* 2019;15:e289–96 CrossRef Medline
15. Veselka J, Špacõek M, Horváth M, et al. **Impact of coexisting multivessel coronary artery disease on short-term outcomes and long-term survival of patients treated with carotid stenting.** *Arch Med Sci* 2016;12:760–65 CrossRef Medline
16. Veselka J, Cerná D, Zimolová P, et al. **Feasibility, safety, and early outcomes of direct carotid artery stent implantation with use of the FilterWire EZ Embolic Protection System.** *Catheter Cardiovasc Interv* 2009;73:733–38 CrossRef Medline
17. Rosenbaum PR, Rubin DB. **Constructing a control group using multivariate matched sampling methods that incorporate the propensity score.** *The American Statistican* 1985;39:33–38 CrossRef
18. Fraeman KH. **An introduction to implementing propensity score matching with SAS.** NESUG 2010: Applications Development. https://www.lexjansen.com/nesug/nesug10/ad/ad05.pdf. Accessed September 07, 2021
19. Rothwell PM, Eliasziw M, Gutnikov SA, et al. **Analysis of pooled data from the randomised controlled trials of endarterectomy for symptomatic carotid stenosis.** *Lancet* 2003;361:107–16 CrossRef Medline
20. Hirata Y, Sakata N, Inoue T, et al. **Histopathological features with angiographic correlates of internal carotid artery pseudo-occlusion: impact of plaque compositions—clinical article.** *J Neurosurg* 2011;115:350–58 CrossRef Medline
21. Oka F, Ishihara H, Kato S, et al. **Cerebral hemodynamic benefits after carotid artery stenting in patients with near occlusion.** *J Vasc Surg* 2013;58:1512–17 CrossRef Medline
22. González A, Gil-Peralta A, Mayol A, et al. **Internal carotid artery stenting in patients with near occlusion: 30-day and long-term outcome.** *AJNR Am J Neuroradiol* 2011;32:252–58 CrossRef Medline

23. Matsuda Y, Terada T, Okada H, et al. **Angiographic characteristics of pseudo-occlusion of the internal carotid artery before and after stenting.** *Neurosurgery* 2016;79:832– 38 CrossRef Medline
24. Son S, Choi DS, Kim SK, et al. **Carotid artery stenting in patients with near occlusion: a single-center experience and comparison with recent studies.** *Clin Neurol Neurosurg* 2013;115:1976–81 CrossRef Medline
25. Sakamoto S, Kiura Y, Kajihara Y, et al. **Carotid artery stenting using the proximal or dual protection method for near occlusion of the cervical internal carotid artery.** *Neurosurg Rev* 2013;36:551–58 CrossRef Medline
26. Halliday A, Bulbulia R, Bonati LH, et al; ACST-2 Collaborative Group. **Second asymptomatic carotid surgery trial (ACST-2): a randomised comparison of carotid artery stenting versus carotid endarterectomy.** *Lancet* 2021;398:1065–73 CrossRef Medline
27. Jalbert JJ, Nguyen LL, Gerhard-Herman MD, et al. **Outcomes after carotid artery stenting in Medicare beneficiaries, 2005 to 2009.** *JAMA Neurol* 2015;72:276–86 CrossRef Medline
28. Aboyans V, Ricco JB, Bartelink MEL, ESC Scientific Document Group, et al. **2017 ESC Guidelines on the Diagnosis and Treatment of Peripheral Arterial Diseases, in collaboration with the European Society for Vascular Surgery (ESVS): document covering atherosclerotic disease of extracranial carotid and vertebral, mesenteric, renal, upper and lower extremity arteries endorsed by: the European Stroke Organization (ESO), the Task Force for the Diagnosis and Treatment of Peripheral Arterial Diseases of the European Society of Cardiology (ESC) and of the European Society for Vascular Surgery (ESVS).** *Eur Heart J* 2018;39:763–816 CrossRef Medline
29. Meershoek AJ, Vonken EP, Nederkoorn PJ, et al. **Carotid endarterectomy in patients with recurrent symptoms associated with an ipsilateral carotid artery near occlusion with full collapse.** *J Neurol* 2018;265:1900–05 CrossRef Medline
30. Kallmayer MA, Tsantilas P, Knappich C, et al. **Patient characteristics and outcomes of carotid endarterectomy and carotid artery stenting: analysis of the German mandatory national quality assurance registry - 2003 to 2014.** *J Cardiovasc Surg (Torino)* 2015;56:827–36 Medline

M. Pešl et al.

hESC derived cardiomyocyte biosensor to detect the different types of arrhythmogenic properties of drugs

Anal Chim Acta
Impact Factor: 4.9

rejstřík

Analytica Chimica Acta 1216 (2022) 339959

Contents lists available at ScienceDirect

Analytica Chimica Acta

journal homepage: www.elsevier.com/locate/aca

hESC derived cardiomyocyte biosensor to detect the different types of arrhythmogenic properties of drugs

Roberto Pivato [a,b], Simon Klimovic [b,c,d], Daniil Kabanov [c,d], Filip Sverák [a,b], Martin Pesl [a,b,e], Jan Pribyl [d,**], Vladimir Rotrekl [a,b,*]

[a] Department of Biology, Faculty of Medicine, Masaryk University, Kamenice 5, 625 00, Brno, Czech Republic
[b] International Clinical Research Center at St. Anne's University Hospital, Pekarská 53, 65691, Brno, Czech Republic
[c] Department of Biochemistry, Faculty of Science, Masaryk University, Kamenice 753/5, 625 00, Brno, Czech Republic
[d] Central European Institute for Technology, Masaryk University, Kamenice 753/5, 625 00, Brno, Czech Republic
[e] First Department of Internal Medicine - Cardioangiology, Faculty of Medicine, Masaryk University and St. Anne's University Hospital, Pekarská 53, 65691, Brno, Czech Republic

HIGHLIGHTS

- CBB consists of dual human stem cell-derived CMs cluster forming conductive syncytium.
- AFM based CBB presents relevant arrhythmic response suitable for arrhythmia detection.
- Dual cluster syncytium is able to spontaneously mimic phenotypes present in the neonatal heart.
- CBB derived from patients' specific hiPSCs possesses high potential for precision medicine.

GRAPHICAL ABSTRACT

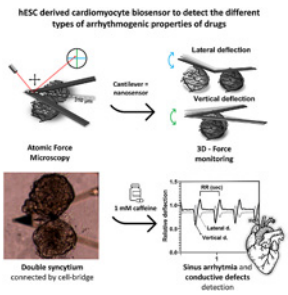

ARTICLE INFO

Keywords:
Cell-based biosensor
Atomic force microscopy
Human embryonic stem cells
Cardiac arrhythmia
Cardiomyocytes
Caffeine

ABSTRACT

In the present work, we introduce a new cell-based biosensor for detecting arrhythmias based on a novel utilization of the combination of the Atomic Force Microscope (AFM) lateral force measurement as a nanosensor with a dual 3D cardiomyocyte syncytium. Two spontaneously coupled clusters of cardiomyocytes form this.

The syncytium's functional contraction behavior was assessed using video sequences analyzed with Musclemotion ImageJ/Fiji software, and immunocytochemistry evaluated phenotype composition.

The application of caffeine solution induced arrhythmia as a model drug, and its spontaneous resolution was monitored by AFM lateral force recording and interpretation and calcium fluorescence imaging as a reference method describing non-synchronized contractions of cardiomyocytes.

The phenotypic analysis revealed the syncytium as a functional contractile and conduction cardiac behavior model. Calcium fluorescence imaging was used to validate that AFM fully enabled to discriminate cardiac arrhythmias in this *in vitro* cellular model. The described novel 3D hESCs-based cellular biosensor is suitable to detect arrhythmic events on the level of cardiac contractile and conduction tissue cellular model. The resulting

* Corresponding author. Department of Biology, Faculty of Medicine, Masaryk University, Kamenice 5, 625 00, Brno, Czech Republic.
** Corresponding author.
E-mail addresses: jan.pribyl@ceitec.muni.cz (J. Pribyl), vrotrekl@med.muni.cz (V. Rotrekl).

https://doi.org/10.1016/j.aca.2022.339959
Received 23 February 2022; Received in revised form 16 May 2022; Accepted 17 May 2022
Available online 20 May 2022
0003-2670/

biosensor allows for screening of arrhythmogenic properties of tailored drugs enabling its use in precision medicine.

1. Introduction

Introduction of induced pluripotent stem cells (iPSCs)-derived cardiomyocytes (CM) allowed the wide development of cell-based biosensors (CBBs). This leap allowed quantification of CMs biomechanical and biochemical properties to study response to various treatments or cardiomyopathies [1]. Sensors are usually based on the multi-electrode array (MEA) [2–4], impedance-based assays (ECIS, xCELLigence®) [5,6], piezoresistive sensor [7] or atomic force microscopy (AFM) [8].

AFM, belonging to the scanning probe microscopy, was at the beginning used predominantly in material research and engineering. Overcoming difficulties related to biological samples allowed it to become a frequently used tool in life sciences. AFM was used to characterize the cell properties, such as phenotype [9,10], cell growth [11] and stiffness of living cells [12]. Moreover, AFM was successfully used as a sensitive cell-based biosensor (CBB), capable of detecting contractile movements of the cardiac cells [13] and their clusters (embryonic bodies EBs) [8], or combined with MEA [14]. Additionally, arrhythmic (i.e., non-periodical) events in the natural beating pattern, often connected with cardiac non-functionality and heart failure, can be identified in the recorded data by adding drugs or other bioactive molecules [15]. AFM microscopy can also be easily combined with other methods such as optical or fluorescence microscopy, as they often create a single unit with AFM [16]. AFM can be further combined with Raman spectroscopy [17], and others to bring a multiparametric description of cardiac cell functions. The main limitation is the need for proper cell adhesion on the surface and maintaining conditions such as a liquid medium and physiological temperature [18].

Cardiac cells within the sinus node generate action potentials spontaneously (cardiac automaticity). This spontaneous activity is retrieved by diastolic depolarization, which brings the membrane potential to the threshold and triggers an impulse propagating through the cardiac conduction system. Cardiac arrhythmia is defined as a deviation from the regular electrical activation of heart contraction, originating in the sinus node [19]. Human heart rate above 100 BPM is tachycardia, and around 50–60 and lower is bradycardia, arrhythmia often presents irregularly [20]. The most prevalent type of arrhythmia is atrial fibrillation (AF), affecting more than 33 million people worldwide, with an estimated increase of 2–3 times by 2050 [21]. AF aggravates the risk of stroke, heart failure, and all-cause mortality [22]. Recent studies say atrial fibrillation is independently associated with an increased risk of sudden cardiac death [23]. The mechanisms of cardiac arrhythmias are divided into two categories - abnormal or enhanced formation of ectopic impulses and conduction disturbances. In a structurally normal heart, the ectopic beats seldom progress to sustained arrhythmia. Thus, conduction disturbances in the myocardial tissue are crucial.

A large body of commonly utilized substances and even drugs causing arrhythmias – i.e., antianginals, antibiotics, narcotics, or bronchodilators [24]. A widely available chemical compound with proarrhythmic effects is caffeine [25] Caffeine acts as a nonselective inhibitor of A1 and A2A adenosine receptors at the cellular level. Cardiovascular effects of caffeine include an increase in blood pressure, changes in heart rate, and neuroendocrine effects. These effects find reason in the blockade of adenosine receptors, causing an increase in intracellular calcium concentrations, the release of norepinephrine, and the sensitization of dopamine receptors [26]. In clinical practice, caffeine finds application alone, e.g., in selected cases of hypotension [27] or in combination with analgesics due to its vasoconstricting and anti-inflammatory effects [26,28]. Due to the high prevalence of arrhythmias in the population, their difficult therapy, it is appropriate to address this abnormality burdening the normal functioning of the heart also at the cellular level. This approach is well served by the presented CBB, which can help describe the arrhythmia, its formation, the treatment, and possibly the effect of therapeutical drugs, as even the treatment medication may cause adverse side effects.

Most of the available cell models are based on single cells or smaller clusters of cells, both of which produce unstable signals [29]. Other models are based on cell monolayers, such as the model proposed by Lian et al. [30]. The major limitation of these monolayer models is that the environment in which cells are grown does not allow to form 3D syncytia with sufficient similarity to physiological tissues [31]. Monolayers present a significantly reduced extracellular matrix, connections between cells only at the periphery of the cells, and the answer to drugs is uniform in all cells. Therefore, 3D models such as embryoid bodies (EBs) are more indicated. EBs are 3D aggregates of cells that imitate structures of the developing embryo and can be differentiated from different lineages such as human embryonic stem cells (hESCs) or patient-specific human induced pluripotent stem cells (hiPSCs), enabling their use in precision medicine [32]. In the present work, hESCs were used. The rationale for using hESCs is that they represent a standard in the field and they do not carry the burden of somatic mutations or reprogramming-induced epigenetic effects [33].

In the present work, we introduce a new biosensor setup based on a combination of atomic force microscope with the hESC derived CMs, where the microcantilever of the microscope creates a sensitive transducer to study cardiac arrhythmias. Computational analysis of image sequences served as a reference method to monitor synchronization of the arrhythmic beating of two cell clusters connected by cardiac conduction-like syncytium. Moreover, the fluorescence calcium imaging supports data obtained by the biosensor setup. The arrhythmic events were induced by caffeine solution. The use of the biosensor setup for a detailed description of the arrhythmia initiation, progression, and termination is presented and discussed.

2. Materials and methods

2.1. Cell lines, cultivation, and differentiation into embryoid bodies

Human embryonic stem cell (hESCs) CCTL14 and CCTL 12 were used in the present work. These cell lines have been derived in Masaryk University, Brno, approved by Ministry of Education of the Czech Republic (MSMT approval no.14648/2016-5) and were previously characterized and described [34].

Cell lines have been maintained on the feeder layer of mouse embryonic fibroblasts (mEF), that have been inactivated mitotically by irradiation as previously described [35].

Cardiac differentiation was performed as described in Ref. [36].

2.2. Cultivation dish preparation and EBs seeding

Standard 30 mm cultivation dishes (TPP, cat no. 93040) and low 35 mm ibidi μ-Dishes (ibidi, cat. no. 80136) had to be modified with an agarose-based mask to increase the probability of seeding two differentiated embryoid bodies next to each other. Consequently, we delimited the area to let the EBs adhere when the following protocol was employed. A 0.5 ml Eppendorf tube was cut to obtain 4 mm external diameter sections. The prepared sections were fixed to the bottom of the cultivation dish with a double-sided scotch. The remaining space in the dish was filled with a 1 mm thick layer of 1% agarose dissolved in PBS. Agarose solution created gel after 20 min of incubation at RT. The addition of 1 ml of PBS stabilized the gel layer after another 10 min. The plastic mask was then removed, the dishes were closed and sealed with a

parafilm. The whole process was finished with sterilization by gamma-irradiation at 100 Gy. Dishes were stored for a maximum of one week at 4° Celsius.

The dish was washed twice with PBS prior to seeding the EBs. The bottom of the holes created by the masking process was coated with 0,1% gelatin for at least 30 min at 37 °C and 5% CO_2 to promote the cell adhesion. Then, the excess gelatin was removed, 1 ml of cultivation medium was added, and two differentiated EBs were seeded. Thus, prepared samples were left for at least 24 h in a standard CO_2 incubator to produce adhered double-EB structure.

2.3. Processing of video sequences

After seeding of EBs, the development of beating synchronization was monitored in real-time by analyzing sequences of optical images. Monitoring was performed by the everyday acquisition of 20-s videos on the Zeiss LSM 700 microscope in the bright field and processing them using ImageJ/Fiji macro Musclemotion (see supplementary material) [37].

2.4. Atomic force microscopy

For mechanic contraction measurements Atomic Force Microscopy (AFM) method (JPK Nanowizard 3, JPK-Bruker) was used as described before [8]. In a liquid environment, measurements were conducted in force spectroscopy mode (1 nN setpoint) using MLCT-C cantilever (Bruker). The cantilever was chosen based on its dimensions, allowing it to land on both EBs simultaneously (see Fig. 1). Partially coated cantilevers from silicon nitride were used due to their properties when measuring in liquid. 30 mm cultivation Petri dishes containing either distilled water for calibration or double EB were placed to the motorized stage with a pre-heated Petri dish heater to 37 °C. The laser reflection sum was maximized before each experiment, and the laser detector was centered. After that, cantilever sensitivity and stiffness via the contact-free method in Bruker-JPK software were determined. Vertical and lateral deflection data was collected in 100 Hz frequency as mechanocardiograms (MCG). Sampling frequency was chosen three times higher than the frequency required to sample the fastest event in the QRS complex. Vertical deflection provided information about the R-R interval and its immediate response to caffeine. Beating frequency was calculated as 60s divided by average R-R interval in seconds during post processing. The lateral (horizontal) deflection representing the complex movement of the syncytium was used to report on the different defects of EB synchronization. Each sample was measured for 1 min in a standard cultivation medium (MEF), followed by 1-min measurements of cells treated with 1 mM caffeine in MEF in 0, 5, and 10 after the addition of treatment. Experiments to assess the effect of caffeine (Sigma Aldrich, cat. No. C-0750) on our syncytium has been performed 24 h after synchronization of the syncytium.

Data analysis obtained from AFM was based on the combination of

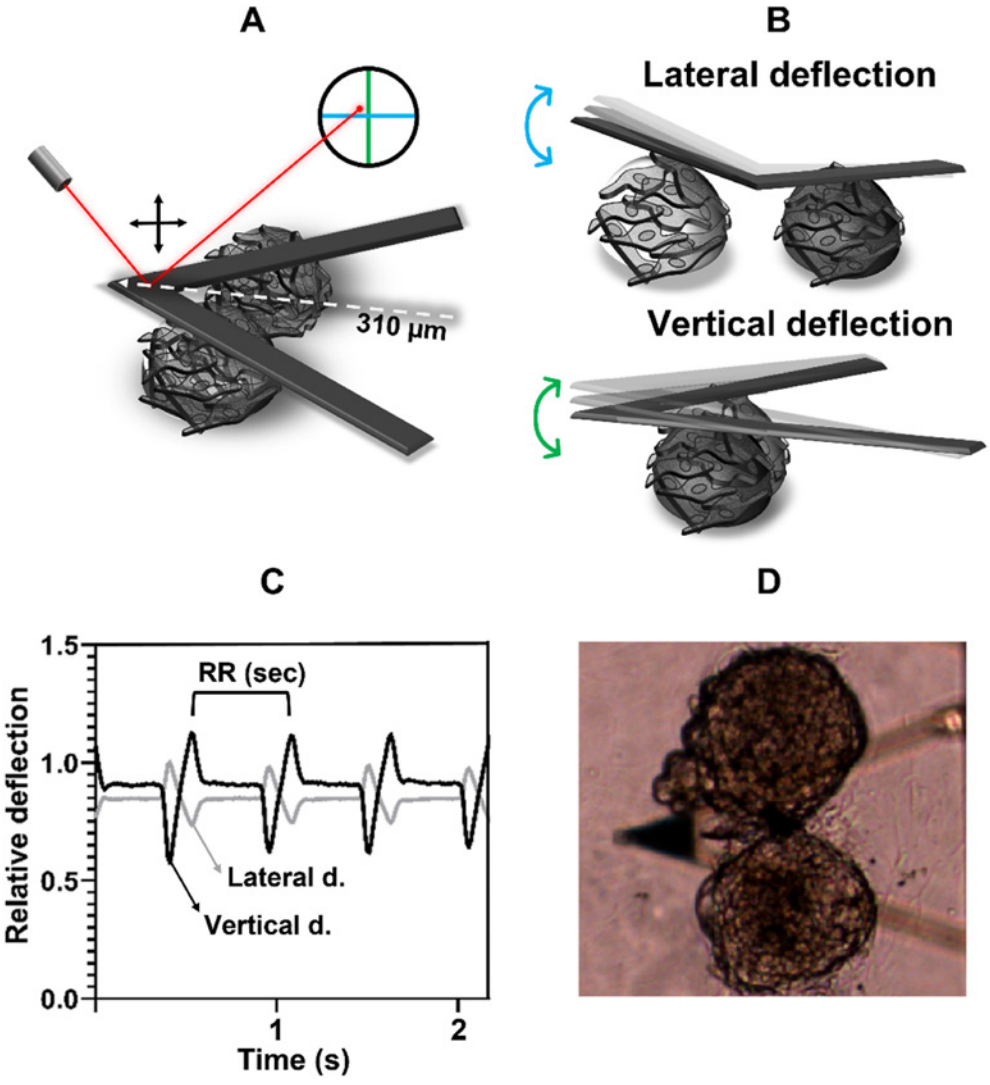

Fig. 1. (A) - Schematic description of the AFM methodological approach. The soft silicon-nitride lever measures the contraction movement of the double-EB in both planes, (B) as lateral and vertical force change deflection of the cantilever. (C) – Representative mechanocardiogram with indicated vertical, lateral synchronized deflection and RR length in seconds (D) - Real image from the top optical microscope captures the cantilever in contact with both EBs, magnification 10×. (For interpretation of the references to color in this figure legend, the reader is referred to the Web version of this article.)

average RR length, the distance between two R peaks, and standard deviation of the average RR length in vertical and lateral deflection data (Fig. 1B, D). These values, recorded for each time point, have been normalized concerning the values registered in standard cultivation medium, i.e., without caffeine. Variation of RR length indicates the onset of tachycardia or bradycardia. The onset of arrhythmic events was assessed by comparing the standard deviation value computed after caffeine treatment concerning the value registered in the standard cultivation medium. Data extraction was performed employing our python script [38]. Analysis of typical MCG curve recorded by AFM is shown in Fig. S1.

2.5. Ca^{2+} imaging

The fluorescence staining of cytoplasmic calcium with Fluo-4-AM (Invitrogen, cat. no. F14201) dye was used as a supportive analysis of the contraction movements. This allowed for monitoring of the contraction by measuring the Ca^{2+} release from sarcoplasmic reticulum. The samples of double EBs were prepared with the same protocol as for AFM measurements; the Ca^{2+} imaging experiments were performed 24 h after syncytium synchronization.

The staining protocol was adopted from the literature [39] Briefly, 1.5 μM Fluo-4-AM solution in DMSO was added to the cultivation medium. EBs were then incubated for at least 30 min at 37 °C and 5% CO_2 in the dark. No washing of the fluorescence dye was necessary.

The measurement of Ca^{2+} fluorescence was performed on Zeiss LSM 700 confocal microscope using software Zen Black. Here, line scan analysis was performed (1000 Hz) by placing the line across our syncytium to cover its full length.

Line scans were then processed on ImageJ/Fiji [40]. Two regions of interest (ROIs) were applied, one over each EB, and evaluated was each ROI average intensity of the fluorescence signal for every timepoint. Data extracted were then plotted in GraphPad software (GraphPad Software) to analyze the evolution of the mutual interaction between the two EBs in real-time.

2.6. Immunocytochemistry

To unravel the cellular phenotypes composing our syncytium, immunocytochemistry analysis for three markers was performed. Vimentin (Santa Cruz Biotechnologies, cat. no. sc-7557, dilution 1:250) as a marker of fibroblasts [41]; Discoidin Domain Receptor 2 (DDR2-Santa Cruz Biotechnologies, cat. no. sc-81707, dilution 1:100) marker of cardiac fibroblasts [42]; Cardiac Troponin T (cTnT- R&D Systems, cat. no. MAB1874, dilution 1:100) marker of CMs [43].

Briefly, the samples were fixed in ice-cold paraformaldehyde, after permeabilization with 0.2% Triton X, blocking with 2.5% BSA solution in PBS buffer containing 0.1% Tween detergent followed. The incubation of samples with primary antibodies was performed overnight at 4 °C. The following day, the secondary antibodies were applied, and cover glasses were mounted on the Mowiol® 4–88 (Sigma, cat. no. 9002-89-5) layer with DAPI (Thermo Fisher Scientific, cat. no. 62248). Secondary antibodies labeled with the Alexa Fluor 488 (Invitrogen, cat. no. A-21202) and Alexa Fluor 594 (Invitrogen, cat. no. A-21203) dyes were both applied in dilution 1:500.

3. Results and discussion

In this study, we presented a new stem cell-based model for the study of cardiac arrhythmias coupled with AFM forming together a biosensor capable of detecting arrhythmogenic properties of drugs. Starting from hESCs, we have been able to form a suspension of hESC's clusters which were differentiated into CMs syncytium. Two such clusters seeded on adherent plate in vicinity spontaneously formed electrically connected syncytium presenting fundamental phenotypes of the human myocardium and its conductive system. Formation of the syncytium, beating synchronization, and study of arrhythmia monitored by the AFM and calcium release are presented and discussed in the following chapter.

3.1. Formation and characterization of functional syncytium

In this work, two beating clusters were seeded in the vicinity on an adhesive surface allowing cell outgrowth from the EBs. The adhesive surface was previously shown to inhibit cardiogenesis via SRC-family kinases [44], promote cell migration [45], and fibroblast proliferation [46]. To investigate the cellular composition of the conductive cell layer connecting the two synchronized EBs, staining of vimentin and discoidin domain receptor 2 (DDR2) was visualized by confocal microscopy (Fig. 2). A positive signal for vimentin evenly spread across the cell layer suggested the presence of fibroblast cells. Most cells between the two EBs ('a bridge') proved to be positive for DDR 2, a specific marker of cardiac fibroblasts. The presence of cardiac fibroblasts has been previously shown to be a key factor in the onset of cardiac syncytia synchronization [47]. Cardiac fibroblasts are also crucial in forming tissue-like architecture [48]. Finally, the syncytium and the bridge were positively stained for cTnT, structural CMse protein, and synchronization of the contractions of the two EBs was observed on day 4. Considering the hESC-derived CMs have a similar phenotype as fetal/-neonatal CMs [49] the composition of the connecting cell layer may resemble the composition of the human fetal heart [50].

Two EBs were seeded in proximity, thus creating a functional syncytium "bridge" during the following days. Sets of EBs with the suboptimal distance between each other were excluded. The beat rate and synchronicity of the EB pairs were observed in time for 4 days from seeding. Syncytia formed by the two EBs connected by conductive cell layer (Fig. 1) with fully synchronized beating were observed at day four for all analyzed samples (Fig. 3; 10 EB sets were analyzed).

The unification of the beating frequency of the two EBs and the synchronization of their beats was associated with cell outgrowth on adhesive tissue culture dishes, stemming from both EBs. Correlation between the amount of the cellular outgrowth and synchronization of the beating was observed, suggesting the formation of a conductive cell layer between the EBs. The cell outgrowth was fundamental for the synchronization of the syncytium. Synchronization may come from the excitable cardiac fibroblast population [47] or gap junctions formed between adjacent CMs [51].

3.2. Detection of caffeine-induced arrhythmia by AFM based biosensor and Fluo-4

An extremely sensitive setup based on the microcantilever of AFM acting as a nanosensor was used to analyze the contractile properties of both EBs (Fig. 1). Recorded data were analyzed for both vertical (beating frequency) and horizontal (synchronization) deflections (Fig. 4). Caffeine was used to induce arrhythmic events.

Caffeine addition induced shortening of the RR interval and thus the increase in the beat rate of the syncytium (Fig. 4). This was reflected by both the change in vertical and lateral deflection (Fig. 4a, c). Calculated standard deviation reports on the irregularity/arrhythmic events. A significant increase in standard deviation was observed immediately after caffeine injection (Fig. 4b and d, time 0 min) in comparison to other time points, suggesting an arrhythmic event induced by the caffeine. The caffeine-induced increase in standard deviation was observed for both the lateral and the vertical deflection.

The decrease in average RR length is comparable for vertical and lateral deflection after the addition of caffeine (Table S1), witnessing that the chronotropic effect of caffeine increases with time. The standard deviation of the RR interval, on the other side, increases only immediately after the addition of caffeine in both the vertical and lateral deflection, while it is lower than the control value in all other time intervals (Table S1). The increase in RR standard deviation at time 0 suggests that RR standard deviation reports the caffeine-induced beat rate

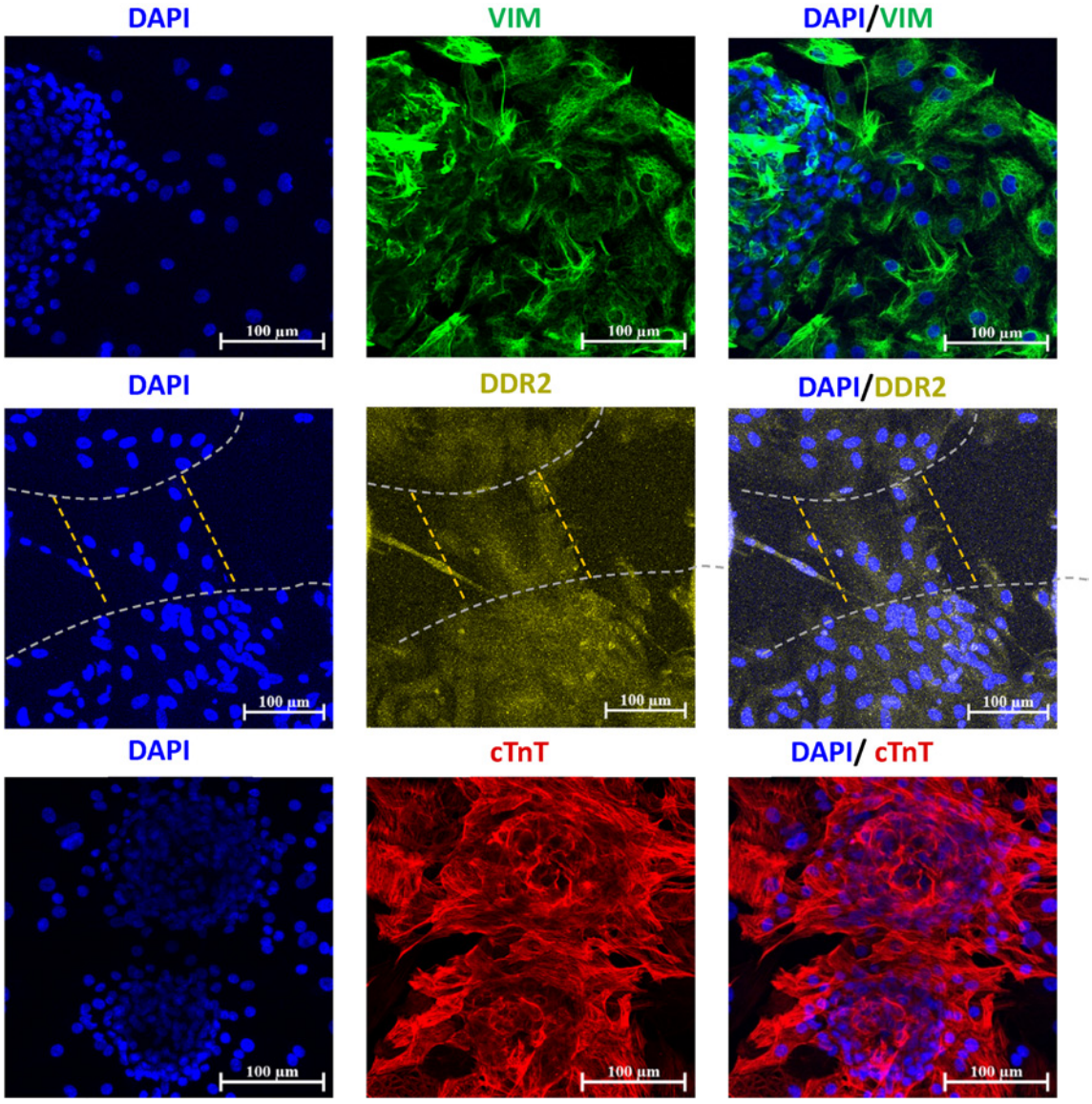

Fig. 2. Cell composition of the connective cell layer between the two adjacent EBs 'a bridge'. The cell layer formed by cell outgrowth from the two EBs on the adhesive surface was stained for the presence of the fibroblast marker vimentin (green), cardiac fibroblast marker DDR2 (yellow), and cardiomyocyte marker cTnT (red). The yellow color was obtained in postprocessing. Orange dashed line helps to recognize connecting 'bridge'; the grey dashed line visualizes partial contours of both EBs. (For interpretation of the references to color in this figure legend, the reader is referred to the Web version of this article.)

irregularity (vertical movement) and EBs' synchronization irregularity (lateral movement).

Further, caffeine affected the synchronization of vertical and lateral displacement of the AFM cantilever (Fig. 5). The lateral and vertical deflection peaks followed each other closely before adding caffeine, suggesting the spread of contraction waves through the syncytium (Fig. 5A). Adding caffeine caused a series of small peeks (independent lateral and vertical deflections) and ultimately resulted in complete dyssynchrony of the lateral and vertical movement (Fig. 5B). That suggests arrhythmic-like events caused by defects in signal spreading through the bridge of cells between the two EBs, resulting in the irregular beat of the two EBs (Fig. 5B).

The addition of caffeine induced the loss of synchrony between lateral and vertical deflection resulting in the displacement of the cantilever in both directions (for detail see Fig. 5C).

The novel double EB biosensor benefits from atomic force microscopy's real-time measuring mechanical response. Measuring the displacement of a soft cantilever in time gave us information about both cellular clusters' lateral and vertical movements. We hypothesized that vertical movement reports on the beat rate of the whole syncytium while lateral movement can record excitation waves spreading across the double EB set up and report on asynchronous events due to irregular beat of the adjacent EBs.

To validate our hypothesis, our model consisting of two EBs connected in syncytium was subjected to measurement of intracellular cytosolic Ca^{2+} employing fluorescent calcium-sensitive detector Fluo-4. The line scan across the two EBs and their connective layer allowed for the observation of synchronization of the two EBs (Fig. 6C, D, F). Caffeine induced a progressive increase of beat rate sound with the observation by AFM. The whole syncytium presents a higher beat rate in caffeine's presence than the MEF media without the caffeine. Caffeine further induced beat rate irregularities and beating discrepancies between the two EBs suggesting the presence of synchronization defects of the two EBs in the double EB biosensor (Fig. 6C and D). Fig. 6 also shows a different pacing part of one of the clusters compared to the contraction rate of the syncytium (Fig. 6E and F). To validate our hypothesis, our model consisting of two EBs connected in syncytium was subjected to measurement of intracellular cytosolic Ca^{2+} employing fluorescent

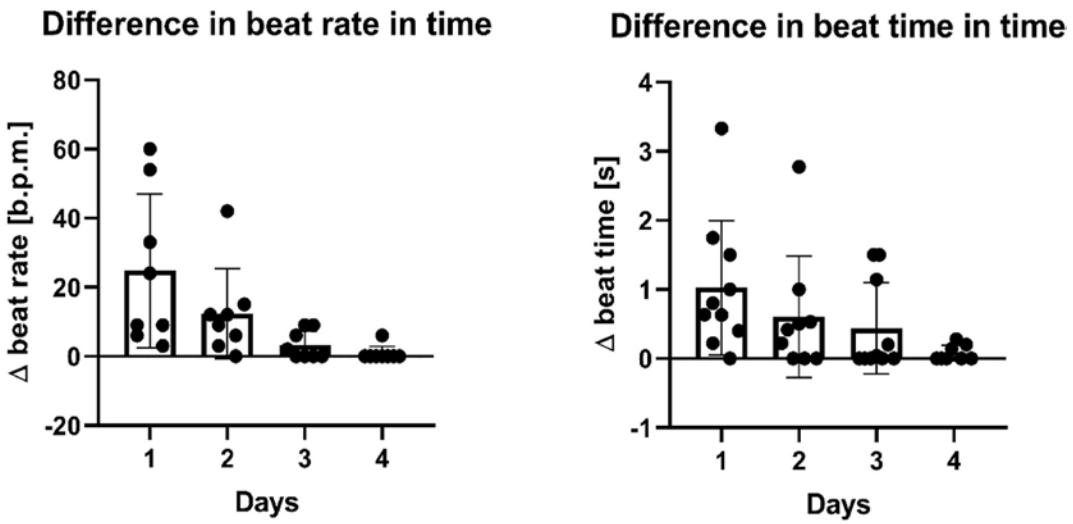

Fig. 3. Synchronization of the syncytium. The evolution of the difference between contraction frequency (Δ beat rate) of the two EBs is plotted against time (days) in panel A. Difference between total times of contraction of the two EBs (Δ beat time) is plotted against time (days) in panel B. The two graphs show that full synchronization of the syncytium was achieved on day 4, as they developed a common beating frequency and synchronized their beating. N = 10.

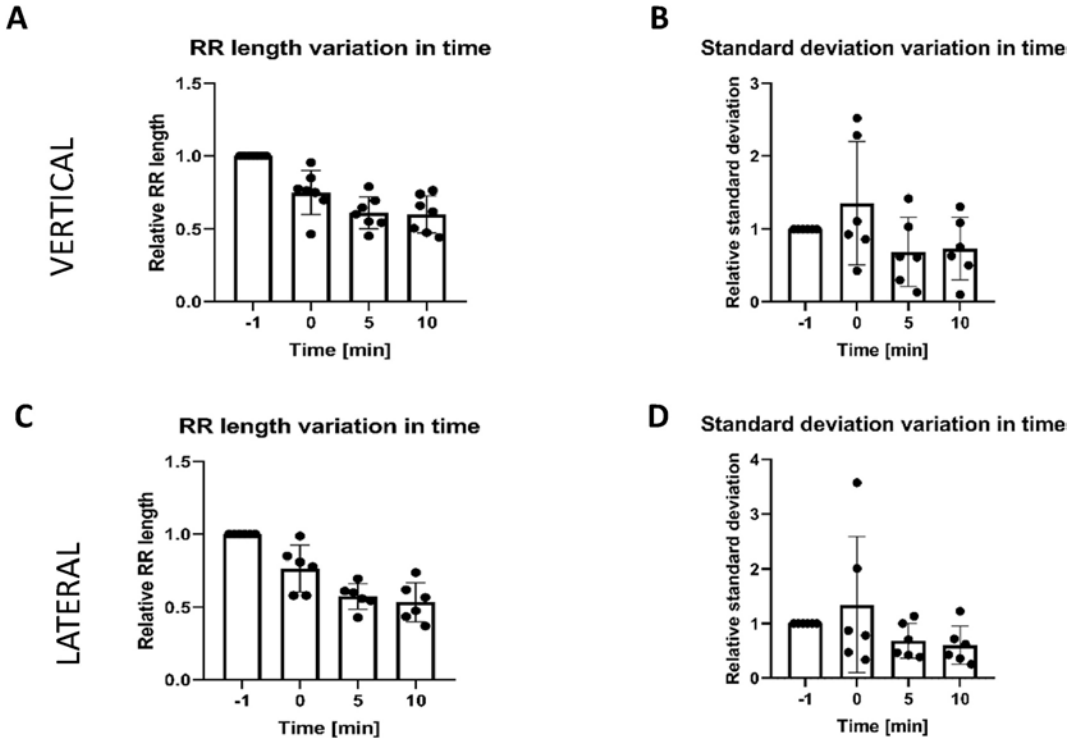

Fig. 4. AFM analysis of the caffeine induced changes in vertical and lateral displacement. Time -1 min indicates measurements conducted in MEF media without caffeine. Caffeine was added at 0 min with subsequent measurements at 5 and 10 min. The vertical displacement (VERTICAL) and lateral displacement (LATERAL) were analyzed. The frequencies of the vertical and lateral movement reporting on the chronotropic effect of caffeine are shown on panels A and C, while the variation of the movement in time is plotted as standard deviation values on panels A and B. Both average RR length and standard deviation have been normalized to the average RR length and standard deviation value before caffeine addition. In both cases, the RR length decreases in time, and the standard deviation increases right after adding caffeine medium.

calcium-sensitive detector Fluo-4. The line scan across the two EBs and their connective layer allowed for the observation of synchronization of the two EBs (Fig. 6B, D, F). Caffeine induced a progressive increase of beat rate sound with the observation by AFM. The syncytium presents a higher beat rate in caffeine's presence than the MEF media without the caffeine. Caffeine further induced beat rate irregularities and beating discrepancies between the two EBs suggesting the presence of synchronization defects of the two EBs in the double EB biosensor (Fig. 6C and D).

As already mentioned, in the present work, we used a 3D model derived from the model used by Ref. [52]. Our model and the single EB model agree on the arrhythmic response caused by caffeine except for the stop-and-go effect not observed in the double EB setup. Moreover, the single EB presents a lower degree of complexity as it does not allow to characterize the effects of chemical compounds on the conductive system employing AFM. Indeed, differentiated EBs present a

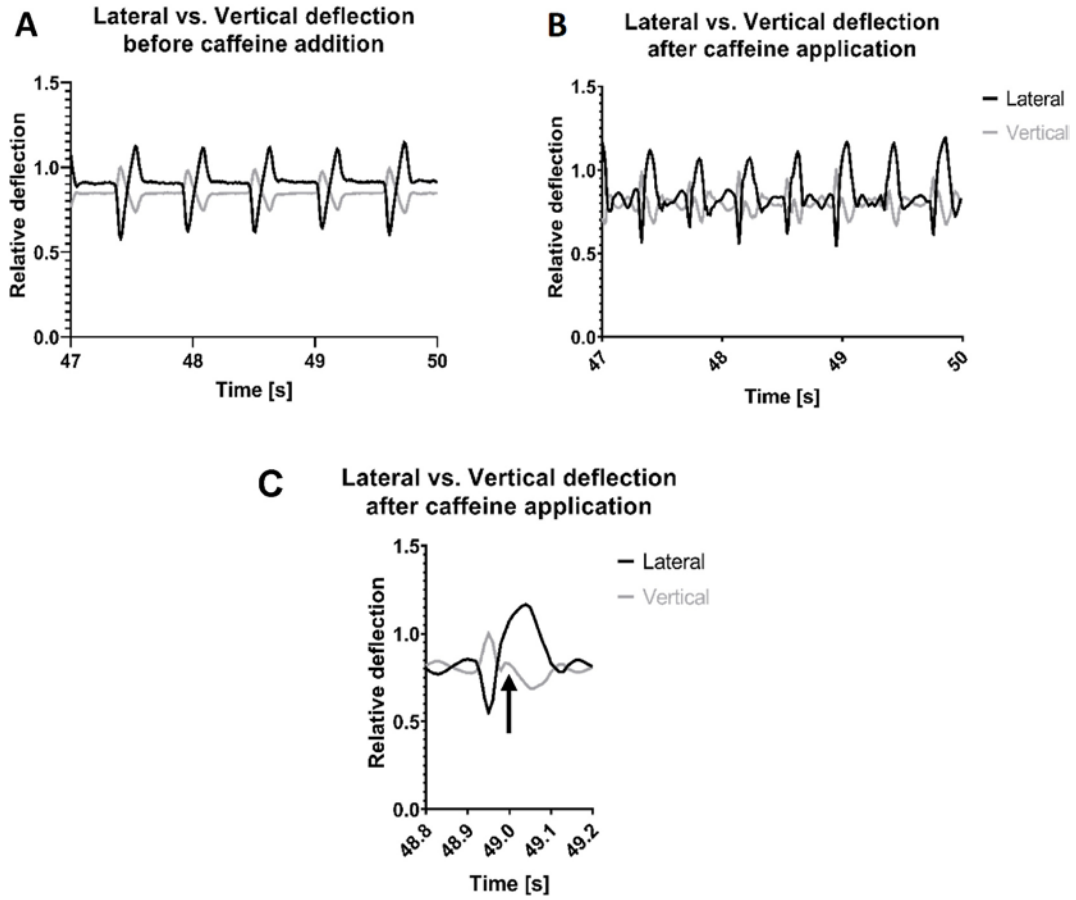

Fig. 5. Caffeine-induced dyssynchrony of the lateral and vertical deflections. Comparison of lateral and vertical deflection before caffeine addition (panel a) and after caffeine addition (panel b). In standard culture medium, vertical and lateral deflection appears to be synchronized with slight time shifts. Caffeine induced irregular small deflections and dyssynchrony of lateral and vertical displacements. (c) Detail of the comparison between vertical and lateral deflection after the application of caffeine. The arrow indicates the instant where dyssynchrony is detected.

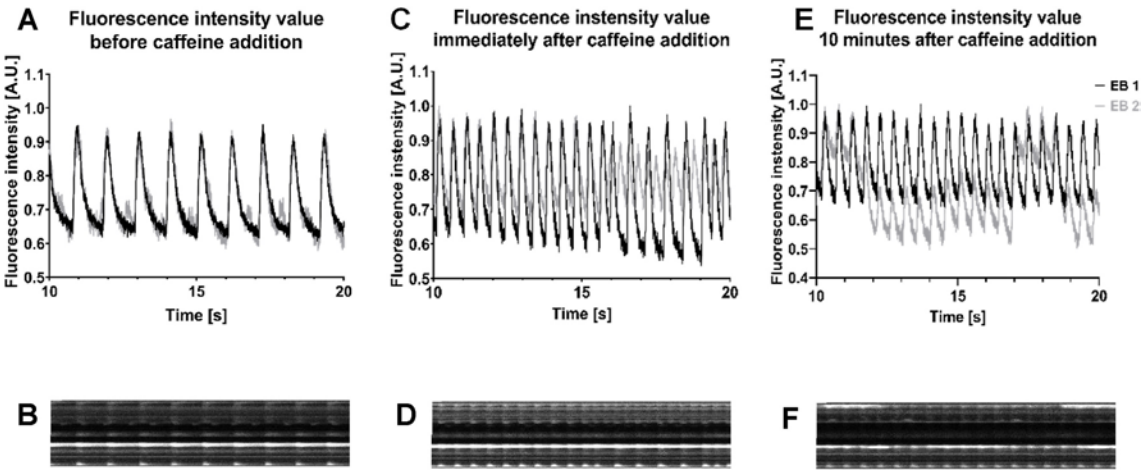

Fig. 6. Calcium imaging analysis of caffeine-induced synchronization defects of the double EB biosensor. Evaluation of the time evolution of the synchronicity of the two EBs (EB1 in black and EB2 in grey) of the double EB biosensor by line scan in high sampling frequency. Panels a and b show representative data of the double EB biosensor in MEF media (control). Panels c to f show three types of beat rate and synchronization defects after caffeine addition. Each curve and image represent 10 s recording before (panels A and B) and after caffeine addition (panels C to F).

combination of atrial, ventricular, and nodal CMs [53] Our model can detect rhythm abnormalities on vertical deflection and conductive disorders on a horizontal deflection by comparing vertical and lateral deflection. In the present study, a conductive defect caused by caffeine equals either ventricular or atrial fibrillation-like behavior and a decrease of contractile function. This is a precise picture of proarrhythmogenic loss of complementarity and sequentiality between vertical and horizontal deflection patterns. This proves that our detection method based on AFM is suitably sensitive for detecting arrhythmic events.

The introduction of the effects caused by the conductive cardiac system and the complex behavior of caffeine represents an advantage of our model compared to 2D models. However, the arrhythmic response of our syncytium is coherent with planar models present in the literature, whether analyzing tachycardia-like [54,55], fibrillation-like [56] or conductive anomalies [57] response.

On the other hand, the multicellular system may constitute an eventual limitation as a dual model cannot discreet single-cell phenotype as other 3D [58] or 2D [59] models, thus increasing the difficulty of studying the contribution of single cellular phenotypes on the arrhythmic response. The phenotype is a known hurdle in the process of drug screening [49]. Further, we must acknowledge that our system is unlikely to contain Purkinje bundles, the anatomical structure of the cardiac conduction system, responsible for certain kinds of arrhythmias and it' development [60]. Thus, the involvement of direct Purkinje cells generation from hESCs by cAMP signaling activation [61] might be the next step in developing a complex cardiac conduction system model.

Nevertheless, using this model has a crucial advantage. As a matter of fact, for the differentiation of EBs, it is possible to use both hESCs and hiPSCs [43]. The use of hiPSCs could be used in the future to introduce patient-specific models that would allow ad hoc drug screening [62] to select the most appropriate anti-arrhythmic drug for a given patient/pathology.

AFM also comes with limitations as the samples need to adhere, and the question of sterility comes to mind when measuring for a longer time. Some alternatives can be used for mechanical responses measurements, such as traction force microscopy or optical tweezers [63–65]. Those two, however, lack a straightforward sample preparation in the case of the former or are experimentally complex in the case of the latter. Methods based on image processing software such as Musclemotion [37], Myocyter [66] and others, offer a non-invasive way to measure mechanical response; however, they lack the sensitivity of AFM and information about contraction force. Moreover, optical methods lack exact recognition of CMs cultivated *in vitro* due to their immature morphology compared to isolated CMs and often require dissociation of the syncytium [67]. Compared to AFM, calcium imaging required sophisticated image/video postprocessing and analysis. Finally, impedance assay methods were also used for mechanical contraction measurements [68], but it's unclear whether this method would be feasible with two EBs. Some methods are probing contractile properties in the context of cellular electrophysiology rather than mechanobiology. Those methods include fluorescence voltage-sensitive or calcium-sensitive dyes, arguably suitable for this model, though, become toxic for the cells after a given time [69–71]. Compared to AFM, fluorescent calcium indicators require an incubation period and the intracellular presence of the indicator may interfere with cell physiology. Nevertheless, the fluorescent methods can serve as complementary methods.

On the other hand, a multi-electrode array (MEA) is suitable for this model as each EB can sit on a different electrode, allowing simultaneous field potential monitoring of both EBs. Still, such measurement would be complicated by adhering EBs exactly on the electrode. Optimization in this regard, for example, by different types of coating, is very desirable, as this method can be easily combined with AFM. This MEA-AFM setup would give us complex information about electro-mechanical coupling [14], together with the detection of arrhythmic events demonstrated in this paper.

4. Conclusion

Dual cluster CBB using human stem cell-derived CMs based model presents relevant arrhythmic response and confirms AFM as a suitable device for arrhythmia detection.

Dual cluster syncytium can spontaneously mimic phenotypes present in the neonatal heart, yet its heterogeneity might constitute a limitation. On the other hand, this model already possesses high potential for patient-specific drug screening as future application as patients' hiPSCs derived beating EBs have already been successfully differentiated.

CRediT authorship contribution statement

Roberto Pivato: Methodology, Investigation, Writing – original draft. **Simon Klimovic:** Methodology, Investigation. **Daniil Kabanov:** Data curation. **Filip Sverák:** Data curation. **Martin Pesl:** Writing – review & editing. **Jan Pribyl:** Writing – review & editing, Supervision. **Vladimir Rotrekl:** Conceptualization, Writing – review & editing, Supervision.

Declaration of competing interest

The authors declare that they have no known competing financial interests or personal relationships that could have appeared to influence the work reported in this paper.

Acknowledgments

The European Regional Development Fund supports this project – Project ENOCH (No. CZ.02.1.01/0.0/0.0/16_019/0000868) and by Brno Ph.D. Talent Scholarship, funded by the Brno City Municipality.

CIISB, Instruct-CZ Centre of Instruct-ERIC EU consortium, funded by MEYS CR infrastructure project LM2018127, is gratefully acknowledged for the financial support of the measurements at the CF Nanobiotechnology.

Ministry of Health of the Czech Republic, grant NU20-06-00156 has financially supported this work.

Appendix A. Supplementary data

Supplementary data to this article can be found online at https://doi.org/10.1016/j.aca.2022.339959.

References

[1] N. Gupta, V. Renugopalakrishnan, D. Liepmann, R. Paulmurugan, B.D. Malhotra, Cell-based biosensors: recent trends, challenges and future perspectives, Biosens. Bioelectron. 141 (2019) 111435, https://doi.org/10.1016/J.BIOS.2019.111435.

[2] H. Izumi-Nakaseko, M. Hagiwara-Nagasawa, A.T. Naito, A. Goto, K. Chiba, Y. Sekino, Y. Kanda, A. Sugiyama, Application of human induced pluripotent stem cell-derived cardiomyocytes sheets with microelectrode array system to estimate antiarrhythmic properties of multi-ion channel blockers, J. Pharmacol. Sci. 137 (2018) 372–378, https://doi.org/10.1016/J.JPHS.2018.07.011.

[3] D. Jans, G. Callewaert, O. Krylychkina, L. Hoffman, F. Gullo, D. Prodanov, D. Braeken, Action potential-based MEA platform for in vitro screening of drug-induced cardiotoxicity using human iPSCs and rat neonatal myocytes, J. Pharmacol. Toxicol. Methods 87 (2017) 48–52, https://doi.org/10.1016/J.VASCN.2017.05.003.

[4] L. Wang, L. Liu, X. Li, N. Magome, K. Agladze, Y. Chen, Multi-electrode monitoring of guided excitation in patterned cardiomyocytes, Microelectron. Eng. 111 (2013) 267–271, https://doi.org/10.1016/J.MEE.2012.11.018.

[5] Q. Wang, K. Su, L. Hu, L. Zou, T. Wang, L. Zhuang, N. Hu, P. Wang, A novel and functional assay for pharmacological effects of marine toxins, saxitoxin and tetrodotoxin by cardiomyocyte-based impedance biosensor, Sensor. Actuator. B Chem. 209 (2015) 828–837, https://doi.org/10.1016/J.SNB.2014.11.150.

[6] S. Fleischer, H.G. Jahnke, E. Fritsche, M. Girard, A.A. Robitzki, Comprehensive human stem cell differentiation in a 2D and 3D mode to cardiomyocytes for long-term cultivation and multiparametric monitoring on a multimodal microelectrode array setup, Biosens. Bioelectron. 126 (2019) 624–631, https://doi.org/10.1016/J.BIOS.2018.10.061.

[7] D.S. Kim, Y.J. Jeong, B.K. Lee, A. Shanmugasundaram, D.W. Lee, Piezoresistive sensor-integrated PDMS cantilever: a new class of device for measuring the drug-induced changes in the mechanical activity of cardiomyocytes, Sensor. Actuator. B Chem. 240 (2017) 566–572, https://doi.org/10.1016/J.SNB.2016.08.167.

[8] M. Pesl, J. Pribyl, I. Acimovic, A. Vilotic, S. Jelinkova, A. Salykin, A. Lacampagne, P. Dvorak, A.C. Meli, P. Skladal, V. Rotrekl, Atomic force microscopy combined with human pluripotent stem cell derived cardiomyocytes for biomechanical sensing, Biosens. Bioelectron. 85 (2016), https://doi.org/10.1016/j.bios.2016.05.073.

[9] M. Pesl, J. Pribyl, G. Caluori, V. Cmiel, I. Acimovic, S. Jelinkova, P. Dvorak, Z. Starek, P. Skladal, V. Rotrekl, Phenotypic assays for analyses of pluripotent stem cell–derived cardiomyocytes, J. Mol. Recogn. 30 (2017) 1–14, https://doi.org/10.1002/jmr.2602.

[10] S. Warrier, A.E. Belevych, M. Ruse, R.L. Eckert, M. Zaccolo, T. Pozzan, R.D. Harvey, β-adrenergic- and muscarinic receptor-induced changes in cAMP activity in adult cardiac myocytes detected with FRET-based biosensor, Am. J. Physiol. Cell Physiol. 289 (2005) 455–461, https://doi.org/10.1152/ajpcell.00058.2005.

[11] T. Wang, N. Hu, J. Cao, J. Wu, K. Su, P. Wang, A cardiomyocyte-based biosensor for antiarrhythmic drug evaluation by simultaneously monitoring cell growth and beating, Biosens. Bioelectron. 49 (2013) 9–13, https://doi.org/10.1016/j.bios.2013.04.039.

[12] B.O. Alunda, Y.J. Lee, Review: cantilever-based sensors for high speed atomic force microscopy, Sensors 20 (2020) 1–39, https://doi.org/10.3390/S20174784.

[13] H. Liu, S. Yu, H. Zhang, J. Xu, Angiogenesis impairment in diabetes: role of methylglyoxal-induced receptor for advanced glycation endproducts, autophagy and vascular endothelial growth factor receptor 2, PLoS One 7 (2012), https://doi.org/10.1371/journal.pone.0046720.

[14] G. Caluori, J. Pribyl, M. Pesl, S. Jelinkova, V. Rotrekl, P. Skladal, R. Raiteri, Non-invasive electromechanical cell-based biosensors for improved investigation of 3D cardiac models, Biosens. Bioelectron. (2019) 124–125, https://doi.org/10.1016/j.bios.2018.10.021.

[15] N. Gupta, V. Renugopalakrishnan, D. Liepmann, R. Paulmurugan, B.D. Malhotra, Cell-based biosensors: recent trends, challenges and future perspectives, Biosens. Bioelectron. 141 (2019) 111435, https://doi.org/10.1016/j.bios.2019.111435.

[16] N.A. Geisse, AFM and combined optical techniques, Mater. Today 12 (2009) 40–45, https://doi.org/10.1016/S1369-7021(09)70201-9.

[17] M. Miletić, S. Aškrabić, J. Rüger, B. Vasić, L. Koricánac, A.S. Mondol, J. Dellith, J. Popp, I.W. Schie, Z. Dohčević-Mitrović, Combined Raman and AFM detection of changes in HeLa cervical cancer cells induced by CeO2 nanoparticles – molecular and morphological perspectives, Analyst 145 (2020) 3983–3995, https://doi.org/10.1039/C9AN02518A.

[18] J. Domke, W.J. Parak, M. George, H.E. Gaub, M. Radmacher, Mapping the mechanical pulse of single cardiomyocytes with the atomic force microscope, Eur. Biophys. J. 28 (1999) 179–186, https://doi.org/10.1007/s002490050198.

[19] C. Antzelevitch, A. Burashnikov, Overview of basic mechanisms of cardiac arrhythmia, Card. Electrophys. Clin. 3 (2011) 23–45, https://doi.org/10.1016/j.ccep.2010.10.012.

[20] S.M. Al-Khatib, W.G. Stevenson, M.J. Ackerman, W.J. Bryant, D.J. Callans, A. B. Curtis, B.J. Deal, T. Dickfeld, M.E. Field, G.C. Fonarow, A.M. Gillis, C.B. Granger, S.C. Hammill, M.A. Hlatky, J.A. Joglar, G.N. Kay, D.D. Matlock, R.J. Myerburg, R. L. Page, AHA/ACC/HRS guideline for management of patients with ventricular arrhythmias and the prevention of sudden cardiac death: executive summary: a report of the American college of cardiology/American heart association task force on clinical practice guidelines and the heart rhythm society, 2018, Heart Rhythm 15 (2017) e190, https://doi.org/10.1016/j.hrthm.2017.10.035. e252.

[21] S.S. Chugh, R. Havmoeller, K. Narayanan, D. Singh, M. Rienstra, E.J. Benjamin, R. F. Gillum, Y.H. Kim, J.H. McAnulty, Z.J. Zheng, M.H. Forouzanfar, M. Naghavi, G. A. Mensah, M. Ezzati, C.J.L. Murray, Worldwide epidemiology of atrial fibrillation: a global burden of disease 2010 study, Circulation 129 (2014) 837–847, https://doi.org/10.1161/CIRCULATIONAHA.113.005119.

[22] C.T. January, L.S. Wann, J.S. Alpert, H. Calkins, J.E. Cigarroa, J.C. Cleveland, J. B. Conti, P.T. Ellinor, M.D. Ezekowitz, M.E. Field, K.T. Murray, R.L. Sacco, W. G. Stevenson, P.J. Tchou, C.M. Tracy, J.L. Anderson, J.L. Halperin, N.M. Albert, B. Bozkurt, R.G. Brindis, M.A. Creager, L.H. Curtis, D. DeMets, R.A. Guyton, J. S. Hochman, R.J. Kovacs, E.M. Ohman, S.J. Pressler, F.W. Sellke, W.K. Shen, C. W. Yancy, AHA/ACC/HRS Guideline for the Management of Patients with Atrial Fibrillation: Executive Summary: A Report of the American College of Cardiology/American Heart Association Task Force on Practice Guidelines and the Heart Rhythm Society, 2014, https://doi.org/10.1161/CIR.0000000000000040, 2014.

[23] L.Y. Chen, N. Sotoodehnia, P. Bůžková, F.L. Lopez, L.M. Yee, S.R. Heckbert, R. Prineas, E.Z. Soliman, S. Adabag, S. Konety, A.R. Folsom, D. Siscovick, A. Alonso, Atrial fibrillation and the risk of sudden cardiac death: the atherosclerosis risk in communities study and cardiovascular health study, JAMA Intern. Med. 173 (2013) 29–35, https://doi.org/10.1001/2013.jamainternmed.744.

[24] B.J. Barnes, J.M. Hollands, Drug-induced arrhythmias, Crit. Care Med. 38 (2010), https://doi.org/10.1097/CCM.0b013e3181de112a.

[25] A. Voskoboinik, J.M. Kalman, P.M. Kistler, Caffeine and arrhythmias: time to grind the data, JACC (J. Am. Coll. Cardiol.): Clinic. Electrophys. 4 (2018) 425–432, https://doi.org/10.1016/j.jacep.2018.01.012.

[26] J.W. Daly, D. Shi, O. Nikodijevic, K.A. Jacobson, The role of adenosine receptors in the central action of caffeine, Caffeine and Behavior: current Views & Research Trends, Curr. Views Res. Trends 7 (2020) 1–31, https://doi.org/10.4324/9780429271038-1.

[27] J. Sawynok, Pharmacological rationale for the clinical use of caffeine, Drugs 49 (1995) 37–50, https://doi.org/10.2165/00003495-199549010-00004.

[28] J.L. Temple, C. Bernard, S.E. Lipshultz, J.D. Czachor, J.A. Westphal, M.A. Mestre, The safety of ingested caffeine: a comprehensive review, Front. Psychiatr. 8 (2017) 1–19, https://doi.org/10.3389/fpsyt.2017.00080.

[29] P. Wu, G. Deng, X. Sai, H. Guo, H. Huang, P. Zhu, Maturation strategies and limitations of induced pluripotent stem cell-derived cardiomyocytes, Biosci. Rep. 41 (2021) 1–16, https://doi.org/10.1042/BSR20200833.

[30] X. Lian, C. Hsiao, G. Wilson, K. Zhu, L.B. Hazeltine, S.M. Azarin, K.K. Raval, J. Zhang, T.J. Kamp, S.P. Palecek, Robust cardiomyocyte differentiation from human pluripotent stem cells via temporal modulation of canonical Wnt signaling, Proc. Natl. Acad. Sci. U. S. A. 109 (2012), https://doi.org/10.1073/pnas.1200250109.

[31] C. Zuppinger, 3D culture for cardiac cells, Biochim. Biophys. Acta Mol. Cell Res. 1863 (2016) 1873, https://doi.org/10.1016/j.bbamcr.2015.11.036. –1881.

[32] G. Pettinato, X. Wen, N. Zhang, Formation of well-defined embryoid bodies from dissociated human induced pluripotent stem cells using microfabricated cell-repellent microwell arrays, Sci. Rep. 4 (2014), https://doi.org/10.1038/srep07402.

[33] S. Kobold, A. Guhr, A. Kurtz, P. Löser, Human embryonic and induced pluripotent stem cell research trends: complementation and diversification of the field, Stem Cell Rep. 4 (2015) 914–925, https://doi.org/10.1016/j.stemcr.2015.03.002.

[34] O. Adewumi, B. Aflatoonian, L. Ahrlund-Richter, M. Amit, P.W. Andrews, G. Beighton, P.A. Bello, N. Benvenisty, L.S. Berry, S. Bevan, B. Blum, J. Brooking, K. G. Chen, A.B.H. Choo, G.A. Churchill, M. Corbel, I. Damjanov, J.S. Draper, P. Dvorak, K. Emanuelsson, R.A. Fleck, A. Ford, K. Gertow, M. Gertsenstein, P. J. Gokhale, R.S. Hamilton, A. Hampl, L.E. Healy, O. Hovatta, J. Hyllner, M. P. Imreh, J. Itskovitz-Eldor, J. Jackson, J.L. Johnson, M. Jones, K. Kee, B.L. King, B. B. Knowles, M. Lako, F. Lebrin, B.S. Mallon, D. Manning, Y. Mayshar, R.D. G. McKay, A.E. Michalska, M. Mikkola, M. Mileikovsky, S.L. Minger, H.D. Moore, C.L. Mummery, A. Nagy, N. Nakatsuji, C.M. O'Brien, S.K.W. Oh, C. Olsson, T. Otonkoski, K.Y. Park, R. Passier, H. Patel, M. Patel, R. Pedersen, M.F. Pera, M. S. Piekarczyk, R.A.R. Pera, B.E. Reubinoff, A.J. Robins, J. Rossant, P. Rugg-Gunn, T.C. Schulz, H. Semb, E.S. Sherrer, H. Siemen, G.N. Stacey, M. Stojkovic, H. Suemori, J. Szatkiewicz, T. Turetsky, T. Tuuri, S. Van Den Brink, K. Vintersten, S. Vuoristo, D. Ward, T.A. Weaver, L.A. Young, W. Zhang, Characterization of human embryonic stem cell lines by the International Stem Cell Initiative, Nat. Biotechnol. 25 (2007) 803–816, https://doi.org/10.1038/nbt1318.

[35] S. Jelinkova, P. Fojtik, A. Kohutova, A. Vilotic, L. Marková, M. Pesl, T. Jurakova, M. Kruta, J. Vrbsky, R. Gaillyova, I. Valášková, I. Frák, A. Lacampagne, G. Forte, P. Dvorak, A.C. Meli, V. Rotrekl, Dystrophin deficiency leads to genomic instability in human pluripotent stem cells via NO synthase-induced oxidative stress, Cells 8 (2019) 53, https://doi.org/10.3390/cells8010053.

[36] S. Jelinkova, A. Vilotic, J. Pribyl, F. Aimond, A. Salykin, I. Acimovic, M. Pesl, G. Caluori, S. Klimovic, T. Urban, H. Dobrovolna, V. Soska, P. Skladal, A. Lacampagne, P. Dvorak, A.C. Meli, V. Rotrekl, DMD pluripotent stem cell derived cardiac cells recapitulate in vitro human cardiac pathophysiology, Front. Bioeng. Biotechnol. 8 (2020), https://doi.org/10.3389/fbioe.2020.00535.

[37] L. Sala, B.J. Van Meer, L.G.J. Tertoolen, J. Bakkers, M. Bellin, R.P. Davis, C. Denning, M.A.E. Dieben, T. Eschenhagen, E. Giacomelli, C. Grandela, A. Hansen, E.R. Holman, M.R.M. Jongbloed, S.M. Kamel, C.D. Koopman, Q. Lachaud, I. Mannhardt, M.P.H. Mol, D. Mosqueira, V.V. Orlova, R. Passier, M.C. Ribeiro, U. Saleem, G.L. Smith, F.L. Burton, C.L. Mummery, Musclemotion: a versatile open software tool to quantify cardiomyocyte and cardiac muscle contraction in vitro and in vivo, Circ. Res. 122 (2018), https://doi.org/10.1161/CIRCRESAHA.117.312067 e5–e16.

[38] D. Kabanov, CardioScripts: scripts for calculations of cardiac data such as MEA results and calcium sparks. https://github.com/DaniilKabanov/CardioScripts. (Accessed 12 January 2022).

[39] S. Klimovic, M. Scurek, M. Pesl, D. Beckerova, S. Jelinkova, T. Urban, Z. Starek, M. Bebarova, J. Pribyl, V. Rotrekl, K. Brat, Aminophylline Induces Two Types of Arrhythmic Events in Human Pluripotent Stem Cell-Derived Cardiomyocytes - Dataset, 2021. https://zenodo.org/record/4552607.

[40] J. Schindelin, I. Arganda-Carreras, E. Frise, V. Kaynig, M. Longair, T. Pietzsch, S. Preibisch, C. Rueden, S. Saalfeld, B. Schmid, J.Y. Tinevez, D.J. White, V. Hartenstein, K. Eliceiri, P. Tomancak, A. Cardona, Fiji: an open-source platform for biological-image analysis, Nat. Methods 9 (2012) 7, https://doi.org/10.1038/nmeth.2019, 9 (2012) 676–682.

[41] E. Tarbit, I. Singh, J.N. Peart, R.B. Rose'Meyer, Biomarkers for the identification of cardiac fibroblast and myofibroblast cells, Heart Fail. Rev. 24 (2019) 1–15, https://doi.org/10.1007/s10741-018-9720-1.

[42] P. Camelliti, T.K. Borg, P. Kohl, Structural and functional characterisation of cardiac fibroblasts, Cardiovasc. Res. 65 (2005) 40–51, https://doi.org/10.1016/j.cardiores.2004.08.020.

[43] S. Jelinkova, A. Vilotic, J. Pribyl, F. Aimond, A. Salykin, I. Acimovic, M. Pesl, G. Caluori, S. Klimovic, T. Urban, H. Dobrovolna, V. Soska, P. Skladal, A. Lacampagne, P. Dvorak, A.C. Meli, V. Rotrekl, DMD pluripotent stem cell derived cardiac cells recapitulate in vitro human cardiac pathophysiology, Front. Bioeng. Biotechnol. 8 (2020) 1–19, https://doi.org/10.3389/fbioe.2020.00535.

[44] X. Zhang, C. Simerly, C. Hartnett, G. Schatten, T.E. Smithgall, Src-family tyrosine kinase activities are essential for differentiation of human embryonic stem cells, Stem Cell Res. 13 (2014) 379, https://doi.org/10.1016/J.SCR.2014.09.007.

[45] J. Liu, C. Huang, X. Zhan, Src is required for cell migration and shape changes induced by fibroblast growth factor 1, Oncogene 18 (1999) 48, https://doi.org/10.1038/sj.onc.1203050, 18 (1999) 6700–6706.

[46] D.M. Kilkenny, J.v. Rocheleau, J. Price, M.B. Reich, G.G. Miller, c-Src regulation of fibroblast growth factor-induced proliferation in murine embryonic fibroblasts, J. Biol. Chem. 278 (2003) 17448–17454, https://doi.org/10.1074/JBC.M209698200.

[47] Y. Jang, S.C. Choi, D.S. Lim, J.H. Kim, J. Kim, Y. Park, Modulating cardiomyocyte and fibroblast interaction using layer-by-layer deposition facilitates synchronisation of cardiac macro tissues, Soft Matter 16 (2020) 428–434, https://doi.org/10.1039/c9sm01531k.

[48] A. Eder, I. Vollert, A. Hansen, T. Eschenhagen, Human engineered heart tissue as a model system for drug testing, Adv. Drug Deliv. Rev. 96 (2016) 214–224, https://doi.org/10.1016/j.addr.2015.05.010.

[49] L. Sala, M. Bellin, C.L. Mummery, Integrating cardiomyocytes from human pluripotent stem cells in safety pharmacology: has the time come? Br. J. Pharmacol. 174 (2017) 3749–3765, https://doi.org/10.1111/bph.13577.

[50] J.M. Dewing, V. Saunders, I. O'Kelly, D.I. Wilson, Defining cardiac cell populations and relative cellular composition of the early fetal human heart, bioRxiv (2021) 2021, 10.21.465281.
[51] Y. Aratyn-Schaus, F.S. Pasqualini, H. Yuan, M.L. McCain, G.J.C. Ye, S.P. Sheehy, P. H. Campbell, K.K. Parker, Coupling primary and stem cell-derived cardiomyocytes in an in vitro model of cardiac cell therapy, JCB (J. Cell Biol.) 212 (2016) 389–397, https://doi.org/10.1083/jcb.201508026.
[52] M. Pesl, I. Acimovic, J. Pribyl, R. Hezova, A. Vilotic, J. Fauconnier, J. Vrbsky, P. Kruzliak, P. Skladal, T. Kara, V. Rotrekl, A. Lacampagne, P. Dvorak, A.C. Meli, Forced aggregation and defined factors allow highly uniform-sized embryoid bodies and functional cardiomyocytes from human embryonic and induced pluripotent stem cells, Heart Ves. 29 (2014), https://doi.org/10.1007/s00380-013-0436-9.
[53] N. Naumova, L. Iop, Bioengineering the cardiac conduction system: advances in cellular, gene, and tissue engineering for heart rhythm regeneration, Front. Bioeng. Biotechnol. 9 (2021) 1–21, https://doi.org/10.3389/fbioe.2021.673477.
[54] R. Balasubramaniam, S. Chawla, A.A. Grace, C.L.H. Huang, Caffeine-induced arrhythmias in murine hearts parallel changes in cellular Ca2+ homeostasis, Am. J. Physiol. Heart Circ. Physiol. 289 (2005) 1584–1593, https://doi.org/10.1152/ajpheart.01250.2004.
[55] W. Korohoda, A. Jurkiewicz, I. Figiel, J. Czyz, A new model for the research into rhythmic contraction activity of cardiomyocytes in vitro, Biochem. Cell. Biol. 73 (1995) 431–439, https://doi.org/10.1139/o95-050.
[56] S. Shafaattalab, E. Lin, E. Christidi, H. Huang, Y. Nartiss, A. Garcia, J. Lee, S. Protze, G. Keller, L. Brunham, G.F. Tibbits, Z. Laksman, Ibrutinib displays atrial-specific toxicity in human stem cell-derived cardiomyocytes, Stem Cell Rep. 12 (2019) 996–1006, https://doi.org/10.1016/j.stemcr.2019.03.011.
[57] H. Satoh, Positive and negative chronotropic effects of caffeine in spontaneously beating rabbit sino-atrial node cells, Gen. Pharmacol. 24 (1993) 1223–1230, https://doi.org/10.1016/0306-3623(93)90372-5.
[58] M. Kawatou, H. Masumoto, H. Fukushima, G. Morinaga, R. Sakata, T. Ashihara, J. K. Yamashita, Modelling Torsade de Pointes arrhythmias in vitro in 3D human iPS cell-engineered heart tissue, Nat. Commun. 8 (2017) 1–11, https://doi.org/10.1038/s41467-017-01125-y.
[59] M. Gharanei, S. Shafaattalab, S. Sangha, M. Gunawan, Z. Laksman, L. Hove-Madsen, G.F. Tibbits, Atrial-specific hiPSC-derived cardiomyocytes in drug discovery and disease modeling, Methods (2021), https://doi.org/10.1016/j.ymeth.2021.06.009.
[60] K.H.W.J.T. Tusscher, A.V. Panfilov, Modelling of the ventricular conduction system, Prog. Biophys. Mol. Biol. 96 (2008) 152–170, https://doi.org/10.1016/j.pbiomolbio.2007.07.026.
[61] S.Y. Tsai, K. Maass, J. Lu, G.I. Fishman, S. Chen, T. Evans, Efficient generation of cardiac Purkinje cells from ESCs by activating cAMP signaling, Stem Cell Rep. 4 (2015) 1089–1102, https://doi.org/10.1016/j.stemcr.2015.04.015.
[62] S. Kussauer, R. David, H. Lemcke, hiPSCs derived cardiac cells for drug and toxicity screening and disease modeling: what micro- electrode-array analyses can tell us, Cells 8 (2019) 1331, https://doi.org/10.3390/CELLS8111331, 8 (2019) 1331.
[63] C. Arbore, L. Perego, M. Sergides, M. Capitanio, Probing force in living cells with optical tweezers: from single-molecule mechanics to cell mechanotransduction, Biophys. Rev. 11 (2019) 765–782, https://doi.org/10.1007/s12551-019-00599-y.
[64] M. Lekka, K. Gnanachandran, A. Kubiak, T. Zieliński, J. Zemła, Traction force microscopy – measuring the forces exerted by cells, Micron 150 (2021), https://doi.org/10.1016/j.micron.2021.103138.
[65] J.A. Schaefer, R.T. Tranquillo, Tissue contraction force microscopy for optimization of engineered cardiac tissue, tissue engineering - Part C: methods, 22, https://doi.org/10.1089/ten.tec.2015.0220, 2016, 76-83.
[66] T. Grune, C. Ott, S. Häseli, A. Höhn, T. Jung, The "MYOCYTER" – convert cellular and cardiac contractions into numbers with ImageJ, Sci. Rep. 9 (2019) 1–13, https://doi.org/10.1038/s41598-019-51676-x.
[67] M.L. Rodriguez, B.T. Graham, L.M. Pabon, S.J. Han, C.E. Murry, N.J. Sniadecki, Measuring the contractile forces of human induced pluripotent stem cell-derived cardiomyocytes with arrays of microposts, J. Biomech. Eng. 136 (2014), https://doi.org/10.1115/1.4027145.
[68] H.G. Jahnke, D. Steel, S. Fleischer, D. Seidel, R. Kurz, S. Vinz, K. Dahlenborg, P. Sartipy, A.A. Robitzki, A novel 3D label-free monitoring system of hES-derived cardiomyocyte clusters: a step forward to in vitro cardiotoxicity testing, PLoS One 8 (2013) 1–9, https://doi.org/10.1371/journal.pone.0068971.
[69] A. Ahola, R.P. Pölönen, K. Aalto-Setälä, J. Hyttinen, Simultaneous measurement of contraction and calcium transients in stem cell derived cardiomyocytes, Ann. Biomed. Eng. 46 (2018) 148–158, https://doi.org/10.1007/s10439-017-1933-2.
[70] S. Guatimosim, C. Guatimosim, L.S. Song, Imaging calcium sparks in cardiac myocytes, Methods Mol. Biol. 689 (2011) 205–214, https://doi.org/10.1007/978-1-60761-950-5_12.
[71] T.J. Herron, P. Lee, J. Jalife, Optical imaging of voltage and calcium in cardiac cells & tissues, Circ. Res. 110 (2012) 609–623, https://doi.org/10.1161/CIRCRESAHA.111.247494.

P. Kala et al.

Endothelin type A receptor blockade attenuates aorto-caval fistula-induced heart failure in rats with angiotensin II-dependenthypertension

J Hypertens
Impact Factor: 4.844

rejstřík

Original Article

OPEN

Endothelin type A receptor blockade attenuates aorto-caval fistula-induced heart failure in rats with angiotensin II-dependent hypertension

Petr Kala[a,b], Olga Gawrys[a,c], Matúš Miklovic[a], Zdenka Vanourková[a], Petra Skaroupková[a], Sárka Jíchová[a], Janusz Sadowski[c], Elzbieta Kompanowska-Jezierska[c], Agnieszka Walkowska[c], Josef Veselka[b], Miloš Táborsky[d], Hana Maxová[e], Ivana Vanecková[f], and Ludek Cervenka[a,d]

Objective: Evaluation of the effect of endothelin type A (ET_A) receptor blockade on the course of volume-overload heart failure in rats with angiotensin II-dependent hypertension.

Methods: Ren-2 renin transgenic rats (TGR) were used as a model of hypertension. Heart failure was induced by creating an aorto-caval fistula (ACF). Selective ET_A receptor blockade was achieved by atrasentan. For comparison, other rat groups received trandolapril, an angiotensin-converting enzyme inhibitor (ACEi). Animals first underwent ACF creation and 2 weeks later the treatment with atrasentan or trandolapril, alone or combined, was applied; the follow-up period was 20 weeks.

Results: Eighteen days after creating ACF, untreated TGR began to die, and none was alive by day 79. Both atrasentan and trandolapril treatment improved the survival rate, ultimately to 56% (18 of 31 animals) and 69% (22 of 32 animals), respectively. Combined ACEi and ET_A receptor blockade improved the final survival rate to 52% (17 of 33 animals). The effects of the three treatment regimens on the survival rate did not significantly differ. All three treatment regimens suppressed the development of cardiac hypertrophy and lung congestion, decreased left ventricle (LV) end-diastolic volume and LV end-diastolic pressure, and improved LV systolic contractility in ACF TGR as compared with their untreated counterparts.

Conclusion: The treatment with ET_A receptor antagonist delays the onset of decompensation of volume-overload heart failure and improves the survival rate in hypertensive TGR with ACF-induced heart failure. However, the addition of ET_A receptor blockade did not enhance the beneficial effects beyond those obtained with standard treatment with ACEi alone.

Keywords: endothelin system, hypertension, Ren-2 renin transgenic rat, renin–angiotensin system, volume-overload heart failure

Abbreviations: ACE, angiotensin-converting enzyme; ACF, aorto-caval fistula; ACEi, angiotensin-converting enzyme inhibitor; ANG II, angiotensin II; ANG 1–7, angiotensin-(1–7); $(+dP/dt)_{max}$, maximum rates of pressure rise; $(-dP/dt)_{max}$, maximum rates of pressure fall; ESPVR, end-systolic pressure–volume relationship; ET_A, endothelin type A; ET-1, endothelin 1; HanSD, Hannover Sprague-Dawley rats; LV, left ventricle; LVEDP, left ventricle end-diastolic pressure; LVEDV, left ventricle end-diastolic volume; PRSW, preload recruitable stroke work; RAAS, renin–angiotensin–aldosterone system; RV, right ventricle; SNS, sympathetic nervous system; TGR, Ren-2 renin transgenic rats; TPR, total peripheral resistance

INTRODUCTION

Over the past 40 years, substantial progress has been made in the treatment of acute coronary syndromes. However, many surviving patients still develop substantial myocardial damage eventually leading to heart failure [1]. Heart failure has become a major public health problem [2,3]; despite the availability of multiple therapeutic measures and recent pharmacological advances, the prognosis remains bleak [2,4–7]. Inappropriately activated renin–angiotensin–aldosterone system (RAAS) is crucial for the progression of heart failure and blockade thereof has become a cornerstone component of the treatment. However, in the advanced phase of heart failure its effectiveness is limited [2,6–9], which was conspicuous in patients who had been hypertensive before the onset of

Journal of Hypertension 2023, 41:99–114

[a]Center for Experimental Medicine, Institute for Clinical and Experimental Medicine, [b]Department of Cardiology, University Hospital Motol and 2nd Faculty of Medicine, Charles University, Prague, Czech Republic, [c]Department of Renal and Body Fluid Physiology, Mossakowski Medical Research Institute, Polish Academy of Science, Warsaw, Poland, [d]Department of Internal Medicine I, Cardiology, University Hospital Olomouc and Palacky University, Olomouc, [e]Department of Pathophysiology, 2nd Faculty of Medicine, Charles University and [f]Institute of Physiology of the Czech Academy of Sciences, Prague, Czech Republic

Correspondence to Petr Kala, MD, PhD, Center for Experimental Medicine, Institute for Clinical and Experimental Medicine; Department of Cardiology, University Hospital Motol and 2nd Faculty of Medicine, Charles University, Prague, Czech Republic.
E-mail: petr.kala@lfmotol.cuni.cz

Received 1 May 2022 **Revised** 6 August 2022 **Accepted** 7 September 2022

DOI:10.1097/HJH.0000000000003307

heart failure [10–12]. Remarkably, in heart failure induced by volume overload, RAAS inhibition did not attenuate eccentric remodeling of the left ventricle (LV) or improve its systolic function [13–15]. Therefore, new therapeutic strategies for the treatment of heart failure are urgently needed and should be preceded by focused experimental studies [6,16].

It has long been proposed that persistent inappropriate activation of various neurohormonal systems underlies the progression of heart failure ('neurohormonal model of heart failure pathophysiology' [17–19]). More recently considerable attention was focused on the endothelin system and its most important peptide: endothelin-1 (ET-1) [20]. ET-1 via endothelin type A (ET_A) receptors induces vasoconstriction; activation of endothelin type B receptors leads to vasodilatation and natriuresis. Inappropriate activation of ET_A receptors is thought important in the pathophysiology of cardiovascular and renal diseases [20–25]. The endothelin system in the kidney and heart was shown to be markedly activated in animals with heart failure [26,27], and its prolonged upregulation proved maladaptive [22,24,25].

Therefore, the upregulated endothelin system might be an important target for therapeutic intervention in heart failure [22,24,25]. Indeed, Sakai *et al.* [28] reported that in heart failure post myocardial infarction long-term ET_A blockade improved the survival rate, an analogy to the improvement obtained with angiotensin-converting enzyme (ACE) inhibition which resulted in the introduction of angiotensin-converting enzyme inhibitor (ACEi) as a gold standard therapy of heart failure [29]. However, application of the endothelin system blockade yielded controversial results [21,22,30–32], and the effects in heart failure patients, admittedly receiving nonselective endothelin receptor antagonist (bosentan) or presumably selective ET_A antagonist (darusentan) were disappointing: early fluid retention actually leading to worsening of heart failure was a common finding [33–35]. In the landmark ENABLE study (Endothelin Antagonism with Bosentan and Lowering of Events) [36] endothelin receptor antagonist treatment was not recommended in heart failure patients; however, the pertinent experimental studies should continue [37]. Evidently, the effects of genuinely selective ET_A receptor blockade on the natural course of heart failure have not yet been evaluated [21–25]. The availability of orally active and indisputably selective ET_A receptor antagonist, atrasentan [21], enables exploration of this issue [21,22,25,38–41].

The rat model of volume overload induced by the creation of the aorto-caval fistula (ACF) reasonably well mimics human heart failure [13,15,42–47] and is officially recommended for preclinical studies [48,49]. The Ren-2 renin transgenic rat (TGR) model combines endogenous activation of the RAAS and hypertension [50,51], the two factors critical for the progression of heart failure [18,19,52,53]. We have shown that TGR with ACF exhibited markedly enhanced heart failure-related mortality [15,45,47]. Taking advantage of such suitable experimental research models and the availability of a highly selective ET_A receptor antagonist, we evaluated the effects of chronic atrasentan treatment on morbidity and mortality in ACF TGR.

To explore in more detail a possible role of interaction of the RAAS and endothelin system and sympathetic nervous system (SNS) [18,54–56] in the pathophysiology of ACF-induced heart failure, kidney tissue concentrations of angiotensin II (ANG II), ET-1 and norepinephrine were measured. In addition, in critical time-points of the experiments, we assessed the cardiac structure and function, using echocardiography and invasive pressure–volume analysis of the LV.

METHODS

Ethical approval, animals, heart failure model, and pharmacological therapeutic regimes

The studies were performed in accordance with guidelines and practices established by the Animal Care and Use Committee of the Institute for Clinical and Experimental Medicine, Prague, which accord with the European Convention on Animal Protection and Guidelines on Research Animal Use and approved by the Ministry of Health of the Czech Republic (project decision 26306/2020-4/OVZ). Heterozygous TGR were generated by breeding male homozygous TGR with female homozygous Hannover Sprague-Dawley (HanSD) rats. Male TGR and HanSD rats, at the initial age of 9 weeks, derived from several litters, were randomly assigned to experimental groups to make sure that the animals from a single litter did not prevail in any group. To obtain reliable data regarding the effects of two treatment regimens on the survival rate, high initial *n* values were used (not so for sham-operated animals) to enable a valid comparison of the long-term survival rate. Such required n values were established using the statistical power analysis method developed by Cohen [57].

Rats were anesthetized (tiletamine + zolazepam, Virbac SA, Carros Cedex, France, 8 mg/kg; and xylasine, Spofa, Czech Republic, 4 mg/kg intramuscularly) and heart failure was induced by volume overload caused by ACF created using needle technique as employed and validated by many investigators, including our own group [13,15,42–47,58,59].

Trandolapril (2 mg/l in drinking water; Gopten; Abbott, Prague, Czech Republic), was used to inhibit ACE because in our previous studies and here in preliminary experiments we demonstrated that at this dose the ACEi, trandolapril, provided maximal blockade of the RAAS and was well tolerated both by rats with ACF-induced heart failure and by sham-operated animals [15,47,59]. ET_A receptor blockade was achieved with atrasentan (5 mg/kg per day in drinking water; Abbott, Illinois, USA). The dose of atrasentan was adjusted weekly to actual water intake; such dosage was previously found to effectively block ET_A receptors [39,40].

Detailed experimental design

The whole experimental design of the study, with a presentation of the detailed time sequence of experimental maneuvers and different treatment regimes, is given in Fig. 1.

Series 1: Effects of treatment with endothelin type A receptor antagonist and angiotensin-converting enzyme inhibitor, alone or combined, on the survival rate and albuminuria

Animals underwent either sham-operation or ACF creation and were left without treatment for 2 weeks. At this time point (day 0) they were assigned to the following experimental groups:

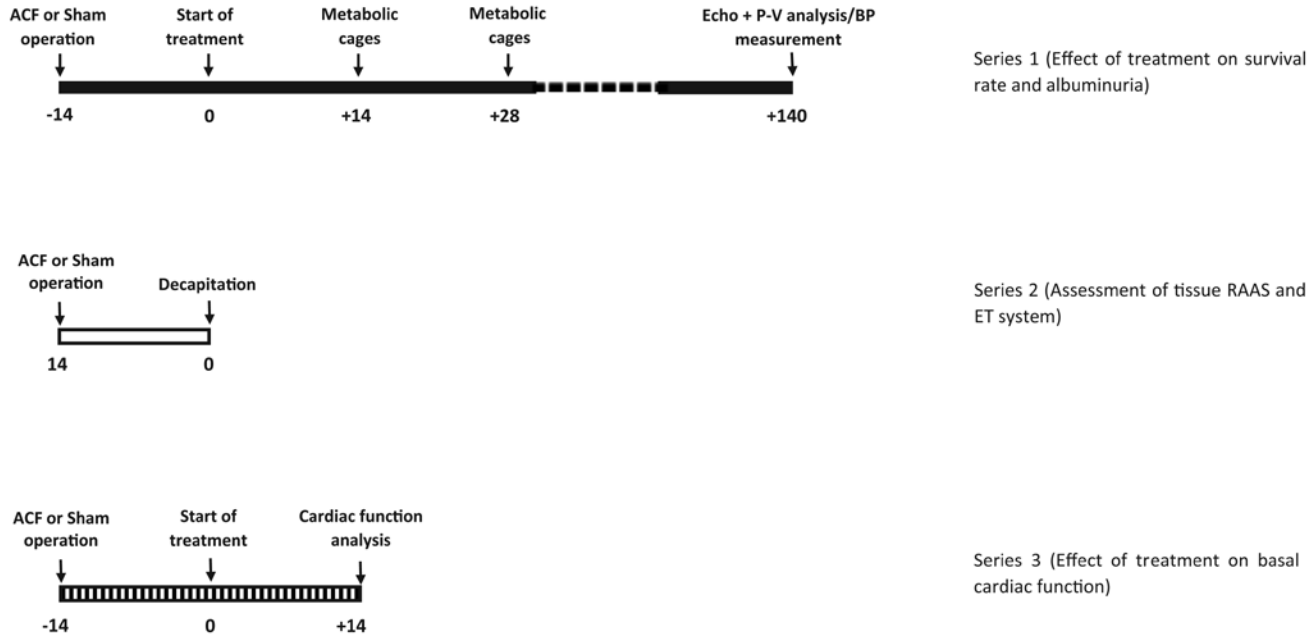

FIGURE 1 The experimental design of the whole study, delineating the time sequence of experimental maneuvers and different treatment regimes.

Group 1: Sham-operated HanSD rats + placebo (initial $n = 12$).
Group 2: Sham-operated TGR + placebo (initial $n = 14$).
Group 3: ACF TGR + placebo (i.e., untreated ACF TGR) (initial $n = 30$).
Group 4: ACF TGR + ET_A receptor antagonist (initial $n = 31$).
Group 5: ACF TGR + ACEi (initial $n = 32$).
Group 6: ACF TGR + ACEi + ET_A receptor antagonist (initial $n = 33$).

The follow-up period was 20 weeks. At the end of the experiment (on day +140), the survived rats were anesthetized and echocardiography was performed. Subsequently, LV functions were invasively assessed by employing pressure–volume analysis by techniques and protocols developed and validated for mice and rats by Pacher *et al.* [60]. This method was employed almost 10 years ago in our laboratory and it is routinely used in our studies evaluating cardiac functions in rats. Detailed descriptions can be found in numerous of our previous studies [15,47,61,62]. Briefly, rats were anesthetized with long-term anesthesia (thiopental sodium, 50 mg/kg, intraperitoneally, VAUB Pharma a.s., Roztoky, Czech Republic) commonly used for pressure–volume analysis [60]. Before the pressure–volume analysis, echocardiography was performed. Rats were intubated with a plastic cannula to ensure chest relaxation during the whole operation. The left jugular vein was cannulated for securing central venous access for solutions administration as required. A balloon catheter (LeMaitre Single Lumen Embolectomy Catheter, 2F, Burlington, Massachusetts, USA) was inserted under ultrasonic control via the right jugular vein to the vena cava inferior, below the diaphragm to maintain the best position for preload reduction. Just before the pressure–volume measurement of the LV, the conductance and pressure signals of the Millar pressure–volume catheter (Millar, 2F, Houston, Texas, USA) were calibrated using MPVS software (V2.2, Millar) according to the manufacturer's instructions. Functions of the LV were invasively assessed by a pressure–volume catheter introduced into the LV via the right carotid artery as described in previous studies [15,47,61,62]. For basal measurements, pancuronium (1 mg/kg, intravenously, Inresa Arzneimittel, Freiburg, Germany) was administered through the cannulated left jugular vein and rinsed with a bolus of saline to reduce noisiness in the signal caused by breathing. For effective determination of cardiac functions, the preload reductions were performed by slowly inflating the balloon catheter with aqua pour injection. Volume signal was calibrated by end-diastolic and end-systolic volume obtained shortly before invasive recordings. Data from pressure–volume loops were captured and analyzed in LabChart Pro software (ADInstruments, Bella Vista, New South Wales, Australia).

Series 2: Assessment of angiotensin II, endothelin-1, angiotensin 1–7, and norepinephrine levels and organ weights in the early phase after aorto-caval fistula-induced heart failure

Animals underwent either sham-operation or ACF creation and were left without treatment for 2 weeks and then were killed by decapitation. Whole kidney ANG II, angiotensin 1–7 (ANG 1–7) and norepinephrine levels, and ET-1 concentrations in the kidney cortex, kidney papilla, and lung tissue were measured, as described in our previous studies [38,39,45–47,51,63,64]. The following experimental groups ($n = 11$ each) were investigated:

Group 1: Sham-operated HanSD rats.
Group 2: Sham-operated TGR.
Group 3: ACF TGR.

Series 3: Effects of 2-week treatment with endothelin type A receptor antagonist and angiotensin-converting enzyme inhibitor, alone or combined, on basal cardiac function assessed by echocardiography and by pressure–volume analysis

Animals were prepared as described in series 1 and 2, and at week 0 the pharmacological treatment was applied for a period of 2 weeks. On day +14, the measurements were performed in the following groups:

Group 1: Sham-operated HanSD rats + placebo ($n = 7$).
Group 2: Sham-operated TGR + placebo (initial $n = 7$).
Group 3: ACF TGR + placebo (i.e., untreated ACF TGR) ($n = 10$).
Group 4: ACF TGR + ET_A receptor antagonist ($n = 9$).
Group 5: ACF TGR + ACEi ($n = 9$).
Group 6: ACF TGR + ACEi + ET_A receptor antagonist ($n = 9$).

Statistical analysis

Statistical analysis of the data was performed using GraphPad Prism software (Graph Pad Software, San Diego, California, USA). Comparison of survival curves was performed by log-rank (Mantel-Cox) test followed by Gehan-Breslow-Wilcoxon test. Statistical comparison of other results was made by Student's *t* test, Wilcoxon's signed-rank test for unpaired data, or one-way analysis of variance when appropriate. The values are expressed as the means ± standard error of the mean and n represents the number of animals. A *P* value less than 0.05 was considered statistically significant.

RESULTS

Effects of treatment with endothelin type A receptor antagonist and angiotensin-converting enzyme inhibitor, alone or combined, on the survival rate and albuminuria

All sham-operated HanSD rats and TGR survived until the end of the study, and for clarity of presentation they are omitted from Fig. 2. As shown in Fig. 2a, untreated ACF TGR definitely began to die from day +14 (4 weeks after the creation of ACF), and by day +65 all the animals were dead. ET_A receptor antagonist and ACEi, applied alone, improved survival: the final rate was 56% (18 of 31 animals) and 69% (22 of 32 animals), respectively. With the combined treatment the final survival rate was 52% (17 of 33 animals). The three variants of treatment did not significantly differ in their effectiveness.

At the start of the treatment (2 weeks after sham-operation or creation of ACF), the sham-operated TGR showed about 35-fold higher albuminuria than observed in sham-operated HanSD rats (Fig. 2b). Significantly, the creation of ACF caused a significant about 65% decrease in albuminuria in TGR in this period. Albuminuria modestly but significantly increased throughout the study in sham-operated animals, in parallel with increasing age but, surprisingly, such age-dependent rise was relatively more pronounced in sham-operated HanSD rats. All three treatments reduced albuminuria in ACF TGR, but combined ACE and ET_A receptor blockade was the most effective. Remarkably, in ACF TGR receiving the combined treatment albuminuria was even 22-fold lower than in sham-operated HanSD rats (0.236 ± 0.02 vs. 5.14 ± 0.27 mg/24 h, $P < 0.05$).

Tissue angiotensin II, angiotensin 1–7, norepinephrine, and endothelin-1 levels and organ weights in the early phase after aorto-caval fistula-induced heart failure

Two weeks after the creation of ACF, TGR displayed a further increase in cardiac LV hypertrophy when compared with sham-operated TGR, and marked right ventricle (RV) hypertrophy (Table 1). In addition, ACF TGR displayed substantial lung congestion (increased wet lung weight) without significant differences in body, kidney, and liver weight.

Two weeks after the creation of ACF or sham-operation tissue concentrations of ANG II, ANG 1–7, norepinephrine, and ET-1 were as shown in Fig. 3. Sham-operated TGR showed higher kidney ANG II levels compared with sham-operated HanSD rats (Fig. 3a). Dissimilarly, kidney ANG 1–7 concentrations did not differ (Fig. 3b). Evidently, the intrarenal balance between the vasodilator and vasoconstrictor axes of the RAAS (expressed as the ratio of ANG 1–7 to ANG II) was shifted toward the vasoconstrictor axis. Kidney ANG II levels tended to be higher in ACF TGR (NS), however, the creation of ACF distinctly increased kidney ANG 1–7 levels. This marked increase resulted in a considerable increase in the ANG 1–7/ANG II ratio, up to the level found in sham-operated HanSD rats. There were no significant differences in kidney norepinephrine concentrations between experimental groups (Fig. 3c). Nor were there any significant between-group differences in the concentrations of ET-1 in the kidney cortex, kidney papilla, and lung tissue (Fig. 3d–f).

Effects of 2-weeks' treatment with endothelin type A receptor antagonist and angiotensin-converting enzyme inhibitor, alone or combined, on basal cardiac function assessed by echocardiography and by pressure–volume analysis

Sham-operated TGR displayed whole cardiac and LV hypertrophy as compared with sham-operated HanSD rats (Table 2). In TGR the hypertrophy was slightly but significantly greater than observed at week 0 (Table 1). Untreated ACF TGR displayed, again, bilateral cardiac hypertrophy that strikingly progressed over 2 weeks. The final increase above the values from week 0 (see Table 1) was by 27, 16, and 45% in the case of whole cardiac, LV, and RV hypertrophy, respectively. All treatment regimens substantially attenuated the degree of hypertrophy in ACF TGR; the concurrent lung weight decrease suggested attenuation of lung congestion.

Evaluation of cardiac structure and function by echocardiography showed that sham-operated TGR displayed higher LV anterior and posterior wall thickness and the LV relative wall thickness as compared with sham-operated HanSD rats (Table 3), showing effects of hypertension and

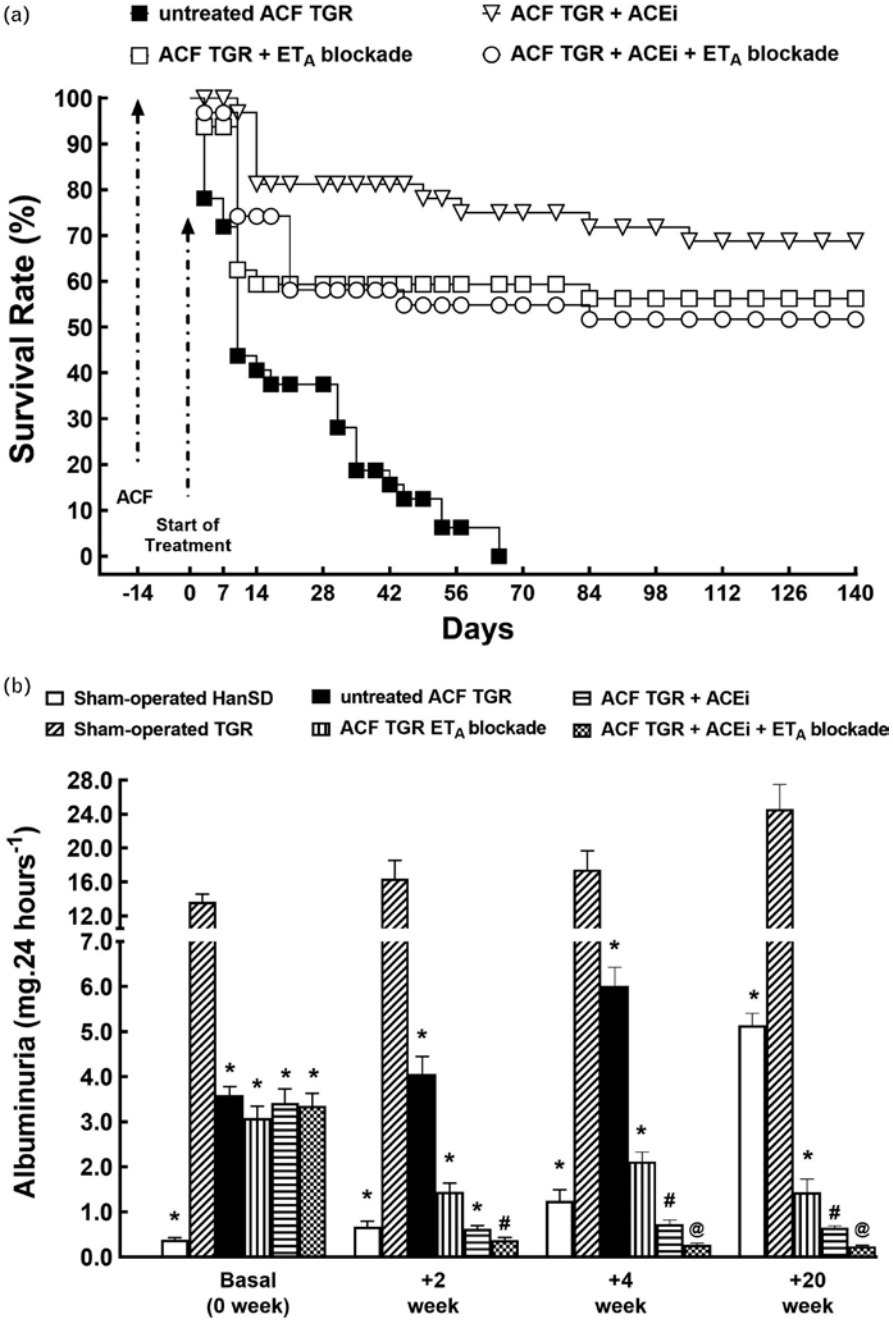

FIGURE 2 Effects of treatment on survival and albuminuria. The survival rate (a) and albuminuria (b) in sham-operated transgene-negative Hannover Sprague-Dawley rats, sham-operated heterozygous Ren-2 renin transgenic rats, and Ren-2 renin transgenic rats with aorto-caval fistula, treated with endothelin type A receptor antagonist, or with angiotensin-converting enzyme inhibitor, alone or combined. $^{*}P < 0.05$ versus sham-operated Ren-2 renin transgenic rats. $^{**}P < 0.05$ versus sham-operated Hannover Sprague-Dawley rats. $^{***}P < 0.05$ versus all other groups.

LV cardiac hypertrophy. Otherwise, there were no structural and functional LV changes or significant differences between sham-operated TGR and sham-operated HanSD rats. Nor were there any significant differences in RV parameters between sham-operated TGR and sham-operated HanSD rats. Untreated ACF TGR had increased stroke volume and cardiac output (a consequence of the shunt), strikingly increased LV and RV diameters, and decreased LV anterior and posterior wall thickness and LV relative wall thickness (indices of eccentric cardiac hypertrophy). In addition, untreated ACF TGR displayed decreased LV ejection fraction and LV fractional shortening as compared with sham-operated TGR (impairment of LV systolic function). In contrast, at this stage, untreated ACF TGR did not show any impairment of RV systolic function as seen from the normal RV ejection fraction. The treatment with ET_A receptor antagonist alone or ACEi alone reduced both the LV and RV diameters but did not change the LV wall thickness and systolic function of the LV in ACF TGR. Notably, combined treatment with ACEi and ET_A receptor antagonists did not

TABLE 1. Organ weights 2 weeks after the creation of the aorto-caval fistula or sham-operation, that is, before initiation of treatment protocols (week 0)

	Group		
	HanSD + water	TGR + water	ACF TGR + water
Tibia length (mm)	38.1 ± 0.3	37.9 ± 0.2	37.8 ± 0.3
Whole heart weight (mg)/tibia length (mm)	34.67 ± 0.64	43.54 ± 0.46*	54.26 ± 0.88**
LV weight (mg)/tibia length (mm)	24.91 ± 0.17	32.74 ± 0.51*	35.53 ± 0.62**
RV weight (mg)/tibia length (mm)	5.93 ± 0.16	6.31 ± 0.29	10.40 ± 0.48**
Lung weight (mg)/tibia length (mm)	44.41 ± 0.86	46.72 ± 1.08	78.79 ± 1.14**
Kidney weight (mg)/tibia length (mm)	37.01 ± 0.76	38.79 ± 0.69	40.08 ± 1.09
Liver weight (mg)/tibia length (mm)	410 ± 13	420 ± 18	421 ± 16

The values are the means ± SEM. ACF, aorto-caval fistula; HanSD, Hannover Sprague-Dawley rats; LV, left ventricle; RV, right ventricle; TGR, Ren-2 renin transgenic rats.
*$P < 0.05$ vs. sham-operated HanSD rats.
**$P < 0.05$ vs. TGR + water.

modify the LV and RV diameters but further decreased the LV anterior and posterior wall thickness and LV relative wall thickness and, unexpectedly, decreased RV ejection fraction.

On the evaluation of cardiac function by the invasive hemodynamics method (Figs. 4 and 5) sham-operated TGR showed, on one side, higher LV peak pressure (Fig. 4a), maximum rates of pressure rise $(+dP/dt)_{max}$ (Fig. 4d) and end-systolic pressure–volume relationship (ESPVR) (Fig. 5a) and of the total peripheral resistance (TPR) (Fig. 5d) and, on the other side, lower maximum rates of pressure fall $(-dP/dt)_{max}$ (Fig. 4e) and LV wall stress (Fig. 5f) as compared with sham-operated HanSD rats. These results are in line with the degree of hypertension and LV cardiac hypertrophy in sham-operated TGR. Untreated ACF TGR displayed significant decreases in LV peak pressure, $(+dP/dt)_{max}$, $(-dP/dt)_{max}$ (Fig. 4d and e), ESPVR, and preload recruitable stroke work (PRSW) (Fig. 5a and c), and increased LV relaxation constant tau (Fig. 4f) as compared with sham-operated TGR. This indicated impairment of load-dependent as well as load-independent LV systolic function and also of the LV diastolic function. Moreover, untreated ACF TGR showed a marked decrease in TPR (Fig. 5d), and particularly prominent increases in LV end-diastolic pressure (LVEDP), LV end-diastolic volume (LVEDV) (Fig. 4b and c), total power output (Fig. 5e) and LV wall stress (Fig. 5f), as compared with sham-operated TGR. Each of the three treatments decreased LVEDP, LVEDV, LV relaxation constant tau, and LV wall stress and increased $(+dP/dt)_{max}$ in ACF TGR but did not alter $(-dP/dt)_{max}$ and ESPVR. ET_A receptor blockade, applied alone or with ACEi, increased PRSW (Fig. 5c) or decreased end-diastolic pressure–volume relationship (Fig. 5b). Finally, only the combined treatment further decreased TPR in ACF TGR (Fig. 5d).

Effects of 20-weeks' treatment with endothelin type A receptor antagonist and angiotensin-converting enzyme inhibitor, alone or combined, on organ weights and cardiac function assessed by echocardiography and by pressure–volume analysis

Table 4 collects organ weights from animals that survived until the end of the study (22 weeks after sham-operation or creation of ACF and after 20-weeks' treatment). The values of whole, LV, and RV weights in the ACF TGR that were treated either with ET_A receptor antagonist alone or with ACEi alone were similar with those in untreated ACF TGR in the early phase (4 weeks after the creation of ACF). On the other hand, the extent of lung congestion was lower than observed in untreated ACF TGR (Table 2). Combined treatment with ACEi and ET_A receptor antagonist in ACF TGR significantly reduced the bilateral cardiac hypertrophy and lung congestion when compared with ACF TGR treated with ET_A receptor antagonist alone or with ACEi alone.

Table 5 presents an evaluation of cardiac structure and function by echocardiography, again, in the animals that survived until the end of the study. Irrespective of the treatment applied, all ACF TGR groups displayed increases in LV and RV diameters that were even greater than those measured in untreated ACF TGR in the early phase (4 weeks after induction of ACF, see Table 3). In addition, in each of ACF TGR treatment groups, the decreases in LV ejection fraction and LV fractional shortening were more pronounced than those observed in the early phase (see Table 3). Moreover, in contrast to the early phase, all ACF TGR groups exhibited impairment of RV systolic function. Significantly, the treatment regimens that included ET_A receptor blockade, alone and combined with ACEi, attenuated the increases in RV diameters and impairment of RV systolic function. Figs. 6 and 7 present an evaluation of cardiac function by the invasive hemodynamics method in animals that survived until the end of the study. All the values for sham-operated HanSD and sham-operated TGR were similar as observed in the early phase (see Figs. 4 and 5). All ACF TGR groups subjected to treatment showed similar load-sensitive values of systolic and diastolic function as well as of load-independent contractile function. Remarkably, the combined treatment with ACEi and ET_A receptor antagonist normalized LVEDP in ACF TGR (Fig. 6b) and brought them to levels observed in sham-operated TGR, however, without affecting LVEDV (Fig. 6c). Moreover, there were no significant differences in TPR, total power output and LV wall stress between ACF TGR groups subjected to different treatments (Fig. 7d–f).

DISCUSSION

We found that both ET_A receptor blockade and ACE inhibition substantially reduced the extremely high heart failure-related mortality in ACF TGR. This agrees with the

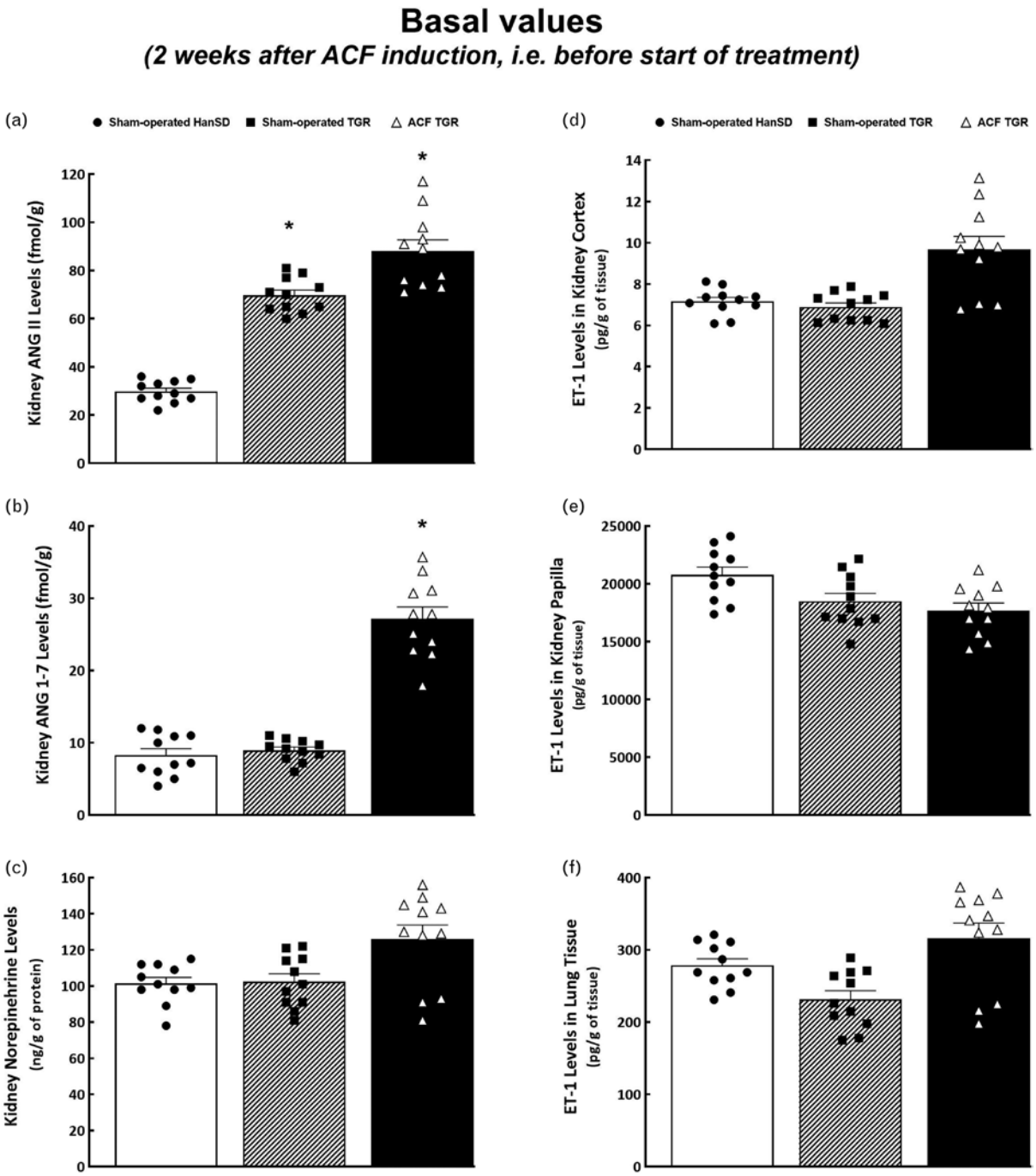

FIGURE 3 Tissue levels of angiotensin II (a), angiotensin 1–7 (b), norepinephrine (c), endothelin-1 (d) in kidney cortex, endothelin-1 in kidney papilla (e), and endothelin-1 in lung tissue (f) in sham-operated transgene-negative Hannover Sprague-Dawley rats, sham-operated heterozygous Ren-2 renin transgenic rats, and Ren-2 renin transgenic rats with aorto-caval fistula 2 weeks after the creation of the aorto-caval fistula or sham-operation. $^{*}P < 0.05$ versus sham-operated Hannover Sprague-Dawley rats.

proposal that the blockade of ET_A receptors might be an important target for therapeutic intervention in heart failure, at least in its volume-overload variant. A similar favorable action of ACEi (improvement of survival, attenuation of albuminuria, etc.) indicates that even though early activation of the vasoconstrictor/sodium retaining axis of the RAAS may be beneficial, its long-term pleiotropic actions are detrimental and contribute to the progression of heart failure.

Since both treatment regimens substantially delayed the heart failure-related morbidity and mortality in ACF TGR, we hypothesized that combined treatment with trandolapril and atrasentan should provide additive protective actions. However, this hypothesis has not been corroborated: the results of the combined therapy did not significantly differ from those of either single treatment. Therefore, one should consider individual aspects of heart failure-related morbidity as related to interaction at various levels of the RAAS and

TABLE 2. Organ weights 4 weeks after the creation of the aorto-caval fistula or sham-operation and after 2 weeks' treatment with endothelin type A receptor antagonist and angiotensin-converting enzyme inhibitor, alone or combined (week + 2)

	Group					
	HanSD + water	TGR + water	ACF TGR + water	ACF TGR + ACEi	ACF TGR + ET_A antagonist	ACF TGR + ACEi + ET_A antagonist
Tibia length (mm)	37.9 ± 0.3	38.1 ± 0.2	37.8 ± 0.2	38.1 ± 0.2	38.1 ± 0.3	37.9 ± 0.2
Whole heart weight (mg)/tibia length (mm)	37.21 ± 0.54	48.47 ± 0.98*	69.03 ± 1.18**	54.33 ± 1.15***	47.91 ± 0.75***	54.79 ± 2.04***
LV weight (mg)/tibia length (mm)	24.12 ± 0.11	35.12 ± 0.91*	41.09 ± 0.92**	33.96 ± 0.68***	30.81 ± 0.59***	35.06 ± 1.35***
RV weight (mg)/tibia length (mm)	7.28 ± 0.19	7.46 ± 0.25	15.09 ± 0.39**	12.05 ± 0.17***	9.92 ± 0.24***	10.75 ± 0.31***
Lung weight (mg)/tibia length (mm)	48.96 ± 1.06	48.52 ± 1.29	75.11 ± 1.38**	61.91 ± 1.27***	57.29 ± 1.29***	61.52 ± 1.33***
Kidney weight (mg)/tibia length (mm)	40.14 ± 0.41	42.19 ± 1.29	40.08 ± 1.09	38.92 ± 1.36	39.14 ± 1.08	38.99 ± 0.91
Liver weight (mg)/tibia length (mm)	437 ± 19	459 ± 17	445 ± 26	439 ± 26	444 ± 23	433 ± 27

The values are the means ± SEM. ACEi, angiotensin-converting enzyme inhibitor; ACF, aorto-caval fistula; ET_A, endothelin type A; HanSD, Hannover Sprague-Dawley rats; LV, left ventricle; RV, right ventricle; TGR, Ren-2 renin transgenic rats.
*$P < 0.05$ vs. sham-operated HanSD rats.
**$P < 0.05$ vs. TGR + water.
***$P < 0.05$ vs. ACF TGR + water.

endothelin systems [65,66]. ANG II can stimulate ET-1 release by various cell types [67–69] and vice versa, ET-1 stimulates ANG II formation [65,70]. Indeed, in TGR after 5/6 renal ablation (5/6 NX), RAAS inhibition decreased ET-1 levels similarly as observed in animals treated with ET_A receptor antagonist [38]. Evidently, some of the beneficial effects of the blockade of one system can also be partially mediated, indirectly, by inhibition of the other system.

Notably, the combined treatment exhibited more pronounced effect on albuminuria and was more effective in reducing bilateral cardiac hypertrophy and lung congestion. Since albuminuria and cardiac hypertrophy are independent risk factors for cardiovascular morbidity and mortality (including heart failure-related mortality) [3,7,10,64,71–73], greater beneficial effects of the combined treatment might provide additional protection. To make this conclusive, studies using long-term treatment protocols (e.g. 40 weeks) are required. Nevertheless, the present results strongly suggest a benefit of dual inhibition of the RAAS and ET_A system in chronic kidney disease, heart failure, and similar disorders. If so, understanding the underlying mechanism(s) is important.

To address this issue, we examined the effects of the three treatments (atrasentan, trandolapril, or both combined) on cardiac function after 2-weeks' treatment, at a time when untreated animals were showing high mortality. Untreated ACF TGR not only exhibited bilateral cardiac hypertrophy and prominent eccentric chamber remodeling but also an impairment of load-sensitive systolic and diastolic function and load-independent contractile function of the LV, which confirmed the view that the ACF-induced model of heart failure well represents heart failure with reduced ejection fraction elicited by chronic volume-overload insult [48,49,74].

TABLE 3. Echocardiographic analysis performed 4 weeks after the creation of the aorto-caval fistula or sham-operation and after 2 weeks' treatment with endothelin type A receptor antagonist and angiotensin-converting enzyme inhibitor, alone or combined (week + 2)

	Group					
	HanSD + water	TGR + water	ACF TGR + water	ACF TGR + ACEi	ACF TGR + ET_A antagonist	ACF TGR + ACEi + ET_A antagonist
Heart rate (s^{-1})	381 ± 16	379 ± 11	369 ± 9	368 ± 8	372 ± 9	377 ± 16
LV diastolic diameter (mm)	6.44 ± 0.12	6.14 ± 0.13	9.89 ± 0.21*	8.74 ± 0.21**	8.54 ± 0.23**	10.53 ± 0.23*
LV systolic diameter (mm)	3.32 ± 0.12	3. 07 ± 0.12	6.01 ± 0.22*	5.22 ± 0.17**	4.97 ± 0.22**	6.22 ± 0.22*
LV anterior wall thickness in diastole (mm)	2.04 ± 0.04	2.82 ± 0.04***	2.11 ± 0.05*	2.06 ± 0.04*	2.01 ± 0.03*	1.66 ± 0.05**
LV posterior wall thickness in diastole (mm)	2.18 ± 0.05	3.17 ± 0.08***	2.29 ± 0.08*	2.29 ± 0.05*	2.15 ± 0.05*	1.86 ± 0.04**
LV relative wall thickness	0.62 ± 0.02	1.05 ± 0.06***	0.42 ± 0.03*	0.44 ± 0.03*	0.51 ± 0.04*	0.35 ± 0.01*
LV ejection fraction (%)	79.2 ± 1.2	80.6 ± 0.9	65.2 ± 0.9*	64.8 ± 1.3*	70.9 ± 1.3*	68.9 ± 1.4*
LV fractional shortening (%)	50.5 ± 1.4	51.5 ± 0.7	38.8 ± 1.1*	39.3 ± 1.1*	42.2 ± 1.2*	41.1 ± 1.5*
LV stroke volume (μl)	149 ± 5.4	146 ± 7.9	384 ± 19*	334 ± 14*	303 ± 14*	373 ± 21*
Cardiac output (ml/min)	61.1 ± 1.5	59.8 ± 3.6	135.7 ± 5.6*	121.5 ± 6.6*	114.6 ± 4.4*	152.9 ± 8.8*
RV diastolic diameter (mm)	3.21 ± 0.07	3.16 ± 0.08	5.71 ± 0.33*	5.02 ± 0.21*	3.94 ± 0.09**	5.75 ± 0.22*
RV systolic diameter (mm)	3.05 ± 0.04	2.55 ± 0.11	5.04 ± 0.31*	3.56 ± 0.21**	3.49 ± 0.07**	5.31 ± 0.19*
RV ejection fraction (%)	57.7 ± 1.7	55.1 ± 2.1	51.1 ± 2.8	50.9 ± 2.4	52.1 ± 2.5	37.7 ± 2.1**

The values are the means ± SEM. ACEi, angiotensin-converting enzyme inhibitor; ACF, aorto-caval fistula; ET_A, endothelin type A; HanSD, Hannover Sprague-Dawley rats; LV, left ventricle; RV, right ventricle; TGR, Ren-2 renin transgenic rats.
*$P < 0.05$ vs. TGR + water.
**$P < 0.05$ vs. ACF TGR + water.
***$P < 0.05$ vs. sham-operated HanSD rats.

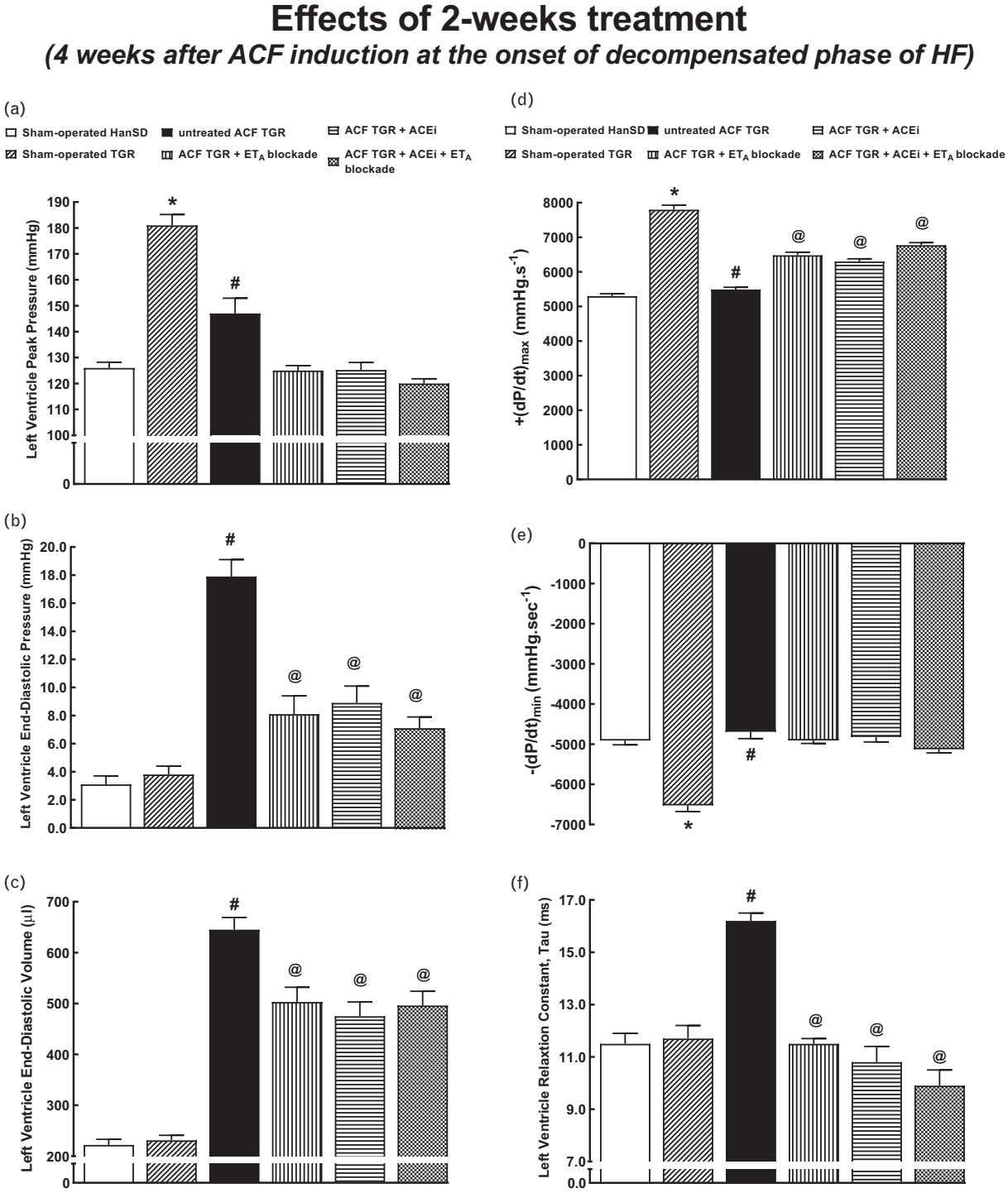

FIGURE 4 Left ventricle cardiac function assessment by invasive hemodynamic analysis performed 4 weeks after the creation of the aorto-caval fistula, that is, 2 weeks after initiation of treatments in sham-operated transgene-negative Hannover Sprague-Dawley rats, sham-operated heterozygous Ren-2 renin transgenic rats and Ren-2 renin transgenic rats with aorto-caval fistula, treated with either endothelin type A receptor antagonist alone or with angiotensin-converting enzyme inhibitor alone or with the combination of endothelin type A receptor antagonist and angiotensin-converting enzyme inhibitor. Left ventricle peak pressure (a), left ventricle end-diastolic pressure (b), left ventricle end-diastolic volume (c), maximum rates of pressure rise $(+dP/dt)_{max}$ (d), maximum rates of pressure fall $(-dP/dt)_{max}$ (e), left ventricle relaxation constant tau (f). $^{*}P < 0.05$ sham-operated Ren-2 renin transgenic rats versus sham-operated Hannover Sprague-Dawley rats. $^{**}P < 0.05$ untreated aorto-caval fistula Ren-2 renin transgenic rats versus sham-operated Ren-2 renin transgenic rats. $^{***}P < 0.05$ treated aorto-caval fistula Ren-2 renin transgenic rats versus untreated aorto-caval fistula Ren-2 renin transgenic rats.

We hypothesized that the beneficial effects of the treatment regimens on long-term survival were preferentially mediated by cardiac mechanisms, in agreement with the recent evidence that 15 weeks' ACEi treatment significantly improved LV ejection fraction in ACF TGR [59]. Here we found that ACF TGR which survived until the end of the study and had been exposed to 20 weeks' treatment exhibited impaired load-dependent as well as load-

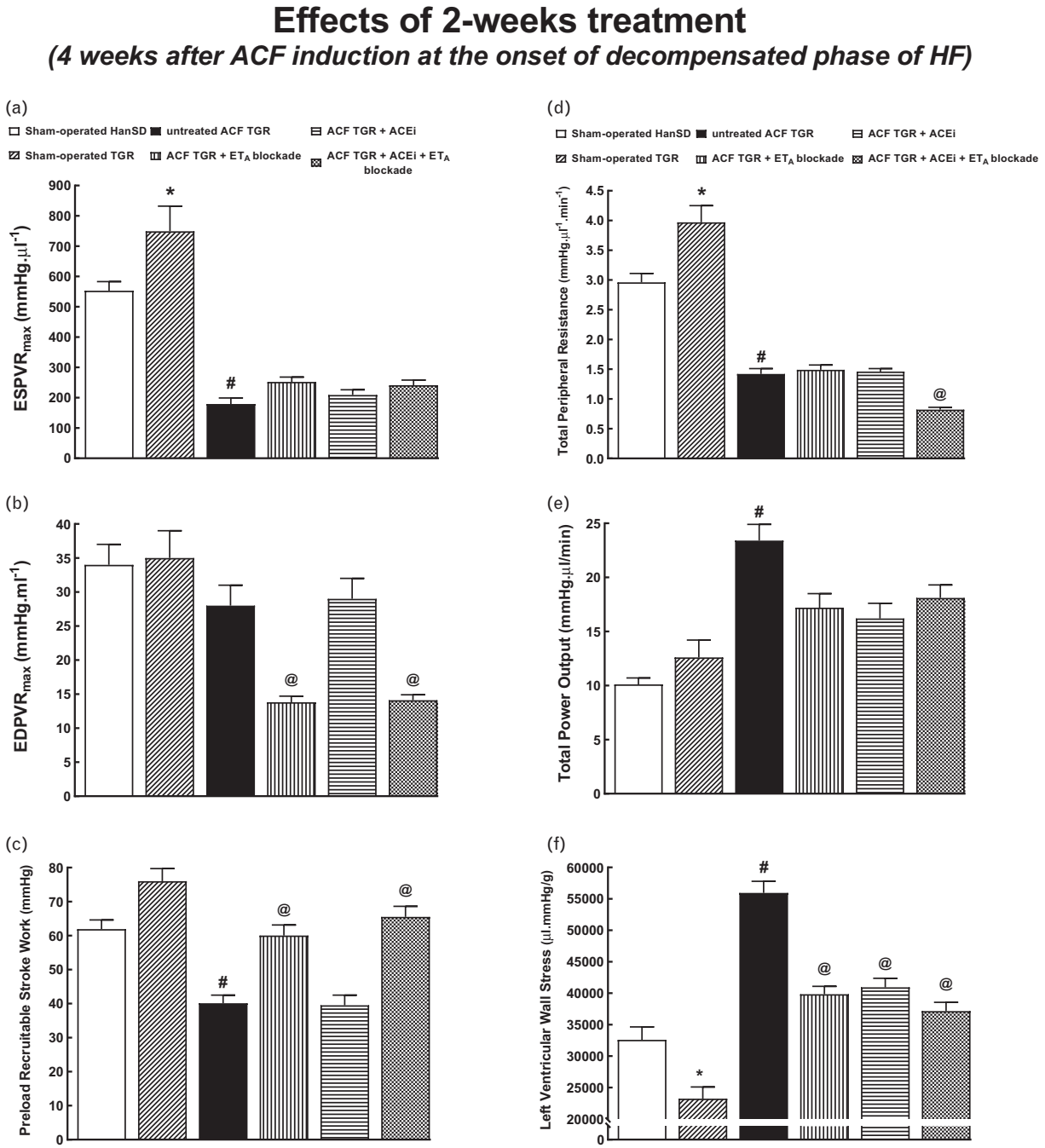

FIGURE 5 Left ventricle cardiac function assessment by invasive hemodynamic analysis performed 4 weeks after the creation of the aorto-caval fistula, that is, 2 weeks after initiation of treatments in sham-operated transgene-negative Hannover Sprague-Dawley rats, sham-operated heterozygous Ren-2 renin transgenic rats and Ren-2 renin transgenic rats with aorto-caval fistula, treated with either endothelin type A receptor antagonist alone or with angiotensin-converting enzyme inhibitor alone or with the combination of endothelin type A receptor antagonist and angiotensin-converting enzyme inhibitor. End-systolic pressure–volume relationship (a), end-diastolic pressure–volume relationship (b), preload recruitable stroke work (c), total peripheral resistance (d), total power output (e), and left ventricle wall stress (f). $^{*}P < 0.05$ sham-operated Ren-2 renin transgenic rats versus sham-operated Hannover Sprague-Dawley rats. $^{**}P < 0.05$ untreated aorto-caval fistula Ren-2 renin transgenic rats versus sham-operated Ren-2 renin transgenic rats. $^{***}P < 0.05$ treated aorto-caval fistula Ren-2 renin transgenic rats versus untreated aorto-caval fistula Ren-2 renin transgenic rats.

independent LV contractility. Moreover, irrespective of the treatment variant actually applied, they exhibited markedly increased LV wall stress, bilateral cardiac hypertrophy, and lung congestion. This could reflect a complete failure of our treatment regimens to improve cardiac morphology and function. However, it should be noticed that the data cannot be compared with those obtained at the same time from untreated ACF TGR because all of the latter died 10 weeks earlier. However, if we used for the comparison of the untreated ACF TGR in the early phase of heart failure (Table 2), we find that whole heart, LV, and RV weights and lung weights in the groups treated with either inhibitor for 20 weeks (see Table 4) are similar as in untreated ACF TGR, and with the combined treatment they are even lower.

TABLE 4. Organ weights determined 22 weeks after the creation of the aorto-caval fistula or sham-operation and after 20-weeks' treatment with endothelin type A receptor antagonist and angiotensin-converting enzyme inhibitor, alone or combined (week + 20)

	Group				
	HanSD + water	TGR + water	ACF TGR + ACEi	ACF TGR + ET_A antagonist	ACF TGR + ACEi + ET_A antagonist
Tibia length (mm)	43.6 ± 0.2	43.5 ± 0.3	43.9 ± 0.4	43.6 ± 0.3	43.4 ± 0.5
Whole heart weight (mg)/tibia length (mm)	32.44 ± 0.51	46.52 ± 0.99*	64.95 ± 1.09**	68.89 ± 0.53**	56.87 ± 0.49***
LV weight (mg)/tibia length (mm)	26.31 ± 0.21	33.96 ± 0.74*	39.11 ± 0.28**	40.37 ± 0.43**	34.48 ± 0.32***
RV weight (mg)/tibia length (mm)	7.44 ± 0.24	7.51 ± 0.18	15.27 ± 0.38**	16.58 ± 0.42**	12.09 ± 0.21***
Lung weight (mg)/tibia length (mm)	47.93 ± 1.09	47.66 ± 1.13	63.19 ± 1.21**	69.92 ± 2.27**	54.19 ± 0.68***
Kidney weight (mg)/tibia length (mm)	41.89 ± 1.02	41.56 ± 1.22	39.86 ± 1.17	41.89 ± 1.24	40.19 ± 0.97
Liver weight (mg)/tibia length (mm)	451 ± 17	441 ± 23	434 ± 29	438 ± 28	442 ± 25

The values are the means ± SEM. ACEi, angiotensin-converting enzyme inhibitor; ACF, aorto-caval fistula; ET_A, endothelin type A; HanSD, Hannover Sprague-Dawley rats; LV, left ventricle; RV, right ventricle; TGR, Ren-2 renin transgenic rats.
*$P < 0.05$ vs. sham-operated HanSD rats.
**$P < 0.05$ vs. TGR + water.
***$P < 0.05$ vs. ACF TGR + ACEi and vs. ACF TGR + ET_A antagonist.

Apparently, the eccentric cardiac remodeling and cardiac hypertrophy related to the enhanced cardiac output (blood recirculation through the fistula) progressed during the study. This was also supported by the data on cardiac function obtained by pressure–volume analysis: the respective values for ACF TGR treated for 20 weeks were similar to those found in untreated ACF TGR in the early phase after ACF-induced heart failure. Furthermore, the combined treatment reduced LVEDP to levels observed in sham-operated TGR.

Overall, each of the treatment regimens applied within the long-term protocol (20 weeks) improved cardiac morphology, systolic and diastolic function of the LV and reduced lung congestion. Most probably, the beneficial effects on the survival rate observed with atresan or trandolapril, alone or combined, are mostly mediated by cardiac mechanisms. This notion is further supported by the effectiveness of 2-weeks' treatment on cardiac morphology and function. At the onset of heart failure decompensation (when untreated rats were beginning to die) all treatment regimens substantially attenuated bilateral cardiac hypertrophy and lung congestion, reduced LVEDP, LVEDV, LV wall stress, and improved LV systolic contractility.

What was the degree of activation of the intrarenal neurohormonal systems in the earliest phase of ACF-induced heart failure? Two weeks after ACF creation, just before the treatment was initiated, ACF TGR did not display any significant increase in kidney ANG II levels. This suggests no substantial activation of the intrarenal vasoconstrictor/sodium retaining axis of the RAAS. In contrast, elevated kidney ANG 1–7 and increased ANG 1–7/ANG II ratio indicates activation of the intrarenal vasodilator/natriuretic axis of the RAAS. There was no increase in kidney norepinephrine concentration, that is, an absence of substantial activation of the intrarenal SNS. In addition, ACF TGR did not show increased concentrations of ET-1 in the renal cortex, papilla, and lung tissue, which suggests no substantial activation of the tissue endothelin system.

TABLE 5. Echocardiographic analysis performed 22 weeks after the creation of the aorto-caval fistula or sham-operation, and after 20 weeks' treatment with endothelin type A receptor antagonist and angiotensin-converting enzyme inhibitor, alone or combined (week + 20)

	Group				
	HanSD + water	TGR + water	ACF TGR + ACEi	ACF TGR + ET_A antagonist	ACF TGR + ACEi + ET_A antagonist
Heart rate (s^{-1})	376 ± 11	375 ± 11	368 ± 8	353 ± 11	347 ± 16
LV diastolic diameter (mm)	6.91 ± 0.21	7.01 ± 0.21	11.78 ± 0.33*	11.58 ± 0.39*	11.51 ± 0.17*
LV systolic diameter (mm)	3.74 ± 0.18	4.31 ± 0.39	7.77 ± 0.27*	7.85 ± 0.38*	7.69 ± 0.23*
LV anterior wall thickness in diastole (mm)	2.12 ± 0.05	3.08 ± 0.06**	2.03 ± 0.05*	2.16 ± 0.09*	1.84 ± 0.07*
LV posterior wall thickness in diastole (mm)	2.51 ± 0.06	3.12 ± 0.09**	2.05 ± 0.05*	2.19 ± 0.05*	1.94 ± 0.07*
LV relative wall thickness	0.71 ± 0.04	0.92 ± 0.04**	0.35 ± 0.02*	0.40 ± 0.03*	0.37 ± 0.03*
LV ejection fraction (%)	73.6 ± 1.7	72.5 ± 2.1	51.1 ± 1.6*	53.1 ± 2.3*	56.4 ± 1.9*
LV fractional shortening (%)	47.1 ± 1.5	46.1 ± 1.3	30.3 ± 0.7*	32.5 ± 1.5*	32.4 ± 1.3*
LV stroke volume (μl)	182 ± 10	178 ± 9	429 ± 21*	449 ± 31*	404 ± 28*
Cardiac output (ml/min)	64.3 ± 1.3	65.6 ± 3.2	162 ± 5.2*	157 ± 11*	149 ± 12*
RV diastolic diameter (mm)	3.09 ± 0.14	3.06 ± 0.09	6.69 ± 0.21*	5.38 ± 0.43***	5.61 ± 0.36***
RV systolic diameter (mm)	2.41 ± 0.11	2.39 ± 0.09	6.05 ± 0.12*	4.57 ± 0.28***	4.52 ± 0.27***
RV ejection fraction (%)	67.9 ± 3.9	65.7 ± 3.2	31.9 ± 1.1*	49.3 ± 2.7***	48.7 ± 2.2***

The values are the means ± SEM. ACEi, angiotensin-converting enzyme inhibitor; ACF, aorto-caval fistula; ET_A, endothelin type A; HanSD, Hannover Sprague-Dawley rats; LV, left ventricle; RV, right ventricle; TGR, Ren-2 renin transgenic rats.
*$P < 0.05$ vs. TGR + water.
**$P < 0.05$ vs. sham-operated HanSD rats.
***$P < 0.05$ vs. ACF TGR + ACEi.

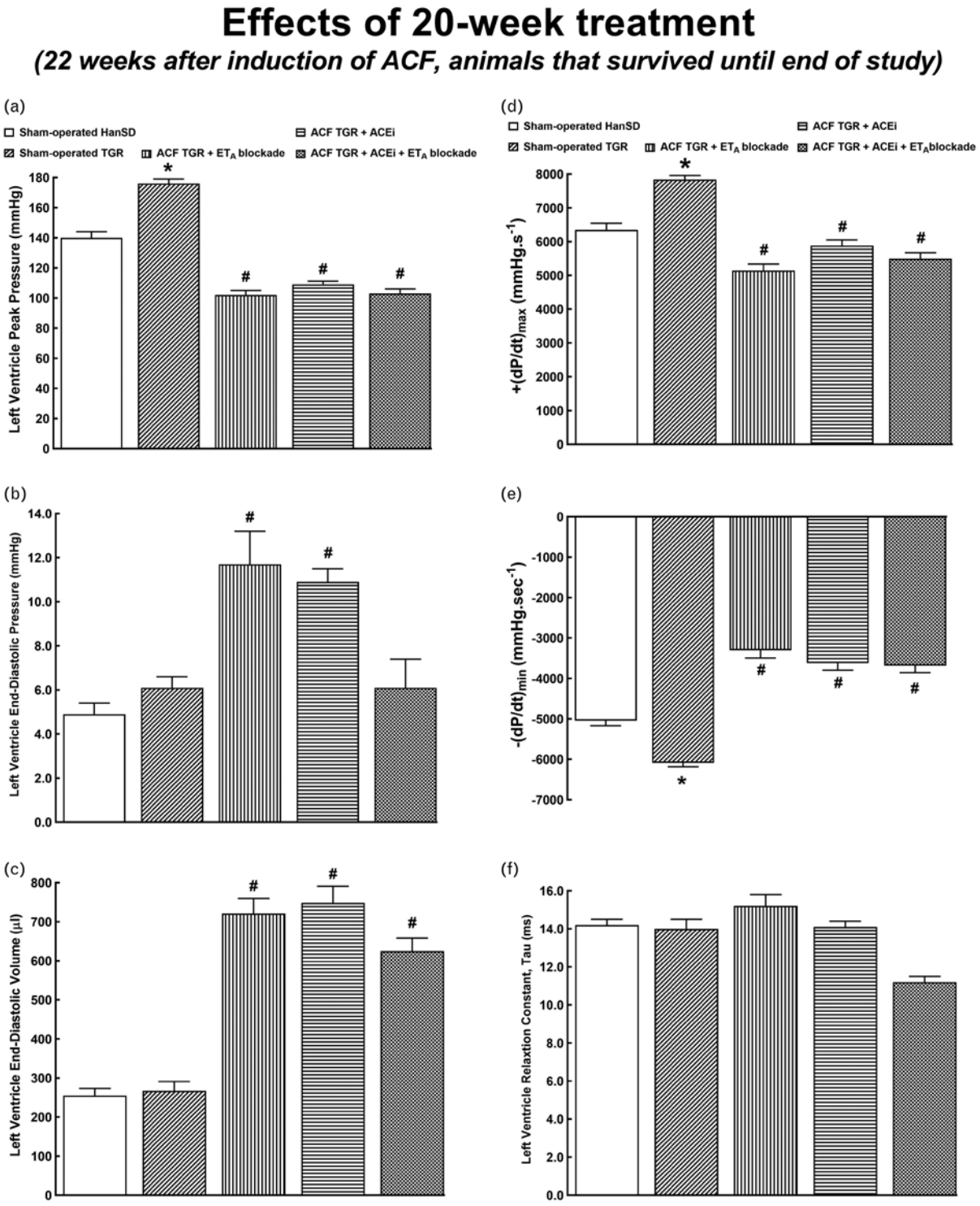

FIGURE 6 Part 1 of the left ventricle cardiac function assessment by invasive hemodynamic analysis performed 22 weeks after the creation of the aorto-caval fistula, that is, 20 weeks after initiation of treatments in sham-operated transgene-negative Hannover Sprague-Dawley rats, sham-operated heterozygous Ren-2 renin transgenic rats and Ren-2 renin transgenic rats with aorto-caval fistula, treated with either endothelin type A receptor antagonist alone or with angiotensin-converting enzyme inhibitor alone or with the combination of endothelin type A receptor antagonist and angiotensin-converting enzyme inhibitor. Left ventricle peak pressure (a), left ventricle end-diastolic pressure (b), left ventricle end-diastolic volume (c), maximum rates of pressure rise $(+dP/dt)_{max}$ (d), maximum rates of pressure fall $(-dP/dt)_{max}$ (e), left ventricle relaxation constant tau (f). $^{*}P < 0.05$ sham-operated Ren-2 renin transgenic rats versus sham-operated Hannover Sprague-Dawley rats. $^{***}P < 0.05$ treated aorto-caval fistula Ren-2 renin transgenic rats versus sham-operated Ren-2 renin transgenic rats.

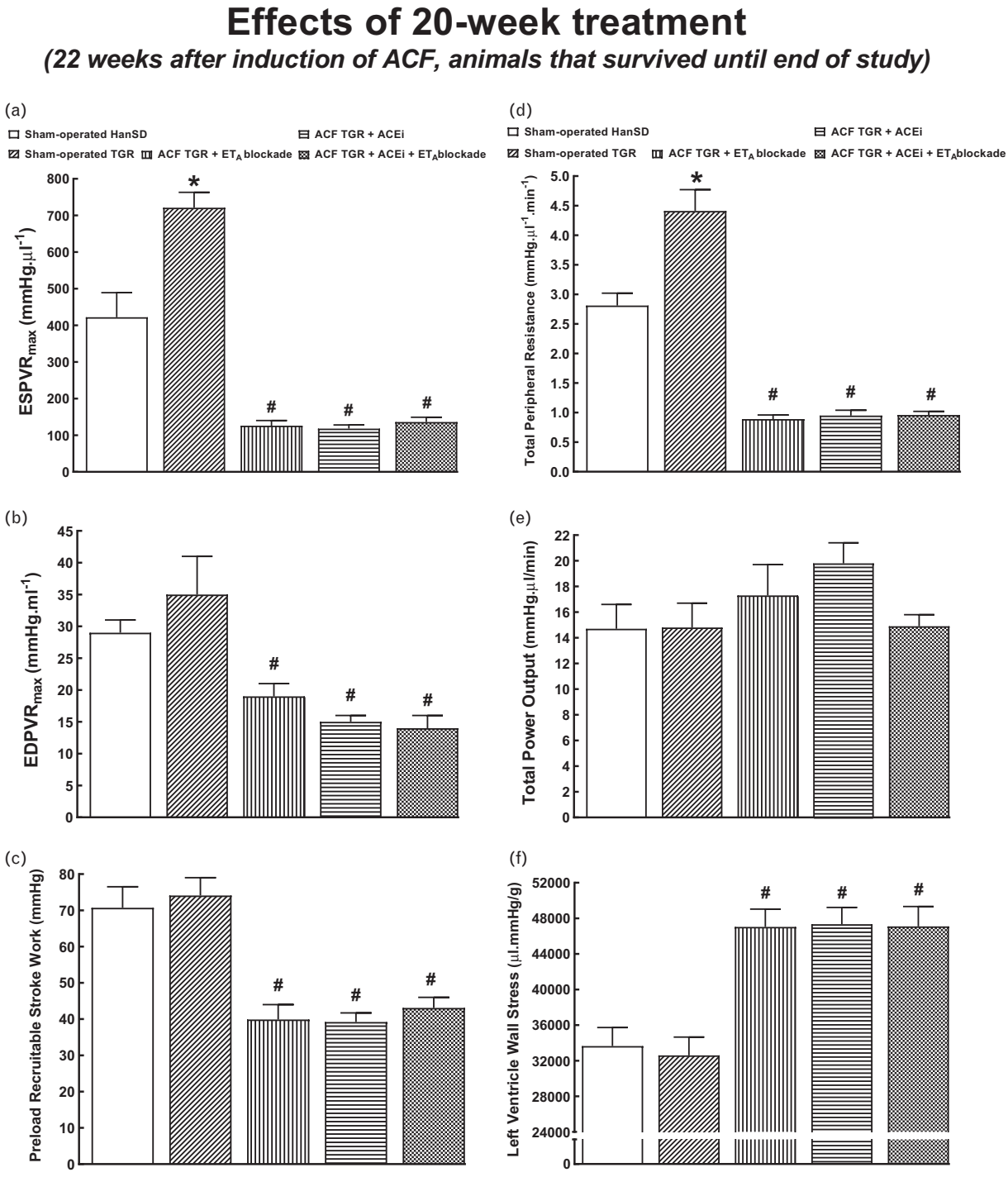

FIGURE 7 Part 2 of the left ventricle cardiac function assessment by invasive hemodynamic analysis performed 22 weeks after the creation of the aorto-caval fistula, that is, 20 weeks after initiation of treatments in sham-operated transgene-negative Hannover Sprague-Dawley rats, sham-operated heterozygous Ren-2 renin transgenic rats and Ren-2 renin transgenic rats with aorto-caval fistula, treated with either endothelin type A receptor antagonist alone or with angiotensin-converting enzyme inhibitor alone or with the combination of endothelin type A receptor antagonist and angiotensin-converting enzyme inhibitor. End-systolic pressure–volume relationship (a), end-diastolic pressure–volume relationship (b), preload recruitable stroke work (c), total peripheral resistance (d), total power output (e), and left ventricle wall stress (f). $^{*}P < 0.05$ sham-operated Ren-2 renin transgenic rats versus sham-operated Hannover Sprague-Dawley rats. $^{**}P < 0.05$ treated aorto-caval fistula Ren-2 renin transgenic rats versus sham-operated Ren-2 renin transgenic rats.

Evidently, in the very early phase of volume-overload heart failure, ACF TGR did not show intrarenal activation of the vasoconstrictor/sodium retaining axis of the RAAS, SNS, or endothelin system. However, there was a marked activation of the intrarenal vasodilator/natriuretic axis of the RAAS.

The evidence that kidney activity of RAAS, SNS, and endothelin system is not increased in ACF TGR seems incompatible with the neurohormonal theory of the pathophysiology of heart failure, which proposes that in heart failure the activity of the RAAS and SNS is increased and

compensates for the initial insult, even though in the long run such hyperactivity is known to be deleterious and critically contributes to the progression of heart failure [17–19,54–56]. In addition, the present results are at variance with our earlier report on an increased plasma and kidney RAAS and SNS activity in hypertensive rats [15,59,75]. However, this was so 5 weeks after the creation of ACF, in the phase of advanced heart failure decompensation, with 60% mortality (Fig. 5). All this accords with the neurohormonal concept that during the progression of heart failure the neurohormonal activity does increase and counteracts the cardiac function impairment (yet in the long run such inappropriate activation becomes extremely deleterious [17–19,54–56,76]). Briefly, in the very early phase of high-output heart failure, the sodium retaining activity of the RAAS is not apparent. However, in our ACF TGR, kidney ANG 1–7 and the ANG 1–7/ANG II ratio was increased. Evidently, the ACE2/ANG 1–7/Mas receptor axis of the RAAS, which counteracts the effects of the classical RAAS axis [77], was substantially activated. Taken together, since ANG 1–7 is the most important component of the ACE2/ANG 1–7/Mas axis, its activation was presumably the first compensatory event in response to ACF creation, preceding the activation of the vasoconstrictor/sodium retaining axis of the RAAS, SNS, and endothelin system. We believe that this counteracted the subsequently increased activity of the RAAS, SNS, and endothelin systems and attenuated their long-term deleterious influence, in agreement with the proposed role of ANG 1–7, particularly under conditions of elevated kidney ANG II levels [77,78], and with the recent evidence that the elevated ANG 1–7/ANG II ratio predicts a beneficial outcome of heart failure [79].

Limitations of the study

One limitation of the current study is the application of the ACF TGR model. On the other hand, its major advantage is that the rats are highly hypertensive and display marked systemic and intrarenal activation of the RAAS [50,51], thus they exhibit two most important risk factors for the progression of heart failure [18,19,52,53]. However, the model is sometimes regarded 'nonnatural' and the progression of heart failure is thought excessively accelerated. Moreover, the creation of the ACF is associated with a profound decrease in total peripheral resistance and a subsequent decrease in blood pressure: evidently, the initial increase in cardiac output cannot compensate the decrease in TPR. It must also be admitted that the ACF TGR model mimics heart failure dependent on chronic volume overload, a condition affecting only 5–7% of heart failure patients. Most of them suffer from severe mitral insufficiency which is resistant to treatment [3].

It is also admitted that all our series which evaluated cardiac functions were performed in long-term anesthetized and surgically stressed animals, which must have caused the increased activity of neurohormonal systems, particularly of the RAAS and SNS. Possibly, the resultant changes in neurohumoral and volume status could alter cardiac function to some extent, both in healthy animals and in those with ACF-induced heart failure. However, we demonstrated previously, in the initial comprehensive reference study and in our previous studies [15,47,61,62] that long-term anesthesia (isoflurane or barbiturates) and surgical procedures do not deteriorate the stability of animals. Therefore, despite such potential drawbacks the pressure–volume analyses are now accepted as a golden standard approach for the evaluation of cardiac function in mice and rats.

In conclusion, our results showed that, first, even in the absence of pronounced activation of the tissue endothelin system in the early phase of volume-overload heart failure, ET_A receptor blockade delays the onset of heart failure decompensation and improves the survival in ACF TGR. Second, the beneficial effects of each of the treatment regimens on long-term survival are most probably mediated by partial recovery of cardiac function, specifically by attenuation of bilateral cardiac hypertrophy, of lung congestion, by reducing LVEDP, LVEDV, LV wall stress, and also by improving LV systolic contractility. Third, the addition of ET_A receptor blockade did not increase the protection against heart failure-related mortality in ACF TGR beyond the improvement obtained with the treatment with ACEi alone.

On the whole, our results suggest that targeting the endothelin system should again be considered for the treatment of heart failure, at least of its volume-overload variant, and in individuals with background hypertension and enhanced RAAS activity.

ACKNOWLEDGEMENTS

Previous presentations: none.

The current study was supported by the project National Institute for Research of Metabolic and Cardiovascular Diseases (Program EXCELES, Project No. LX22NPO5104) – funded by the European Union – Next Generation EU.

The current study was also supported by the Ministry of Health of the Czech Republic grant number 20-02-00052 awarded to H.M. and P.K. was supported by the Grant Agency of Charles University, grant number 68121.

Conflicts of interest

There are no conflicts of interest.

REFERENCES

1. Bulluck H, Yellon DM, Hausenloy DJ. Reducing myocardial infarct size: challenges and future opportunities. *Heart* 2016; 102:341–348.
2. Ponikowski P, Voors AA, Anker SD, Bueno H, Cleland JG, Coats AJ, *et al.*, Authors/Task Force Members. 2016 ESC Guidelines for the diagnosis and treatment of acute and chronic heart failure: The Task Force for the diagnosis and treatment of acute and chronic heart failure of the European Society of Cardiology (ESC). Developed with the special contribution of the Heart Failure Association (HFA) of the ESC. *Eur Heart J* 2016; 37:2129–2200.
3. Savarese G, Becher PM, Lund LH, Seferovic P, Rosano GMC, Coats A. Global burden of heart failure: A comprehensive and updated review of epidemiology. *Cardiovasc Res* 2022;cvac013; doi: 10.1093/cvr/cvac013.
4. Kassi M, Hannawi B, Trachtenberg B. Recent advances in heart failure. *Curr Opin Cardiol* 2018; 33:249–256.
5. Rangawwami J, Bhalla V, Blair JEA, Chang TI, Costa S, Lentine KL, *et al.* American Heart Association Council on the Kidney in Cardiovascular Disease and Council on Clinical Cardiology. *Circulation* 2019; 139: e840–e878.
6. McDonagh TS, Metra M, Adamo A, Gardner RS, Baumbach A, Bohm M, *et al.* 2021 ESC Guidelines for the diagnosis and treatment of acute and chronic heart failure. *Eur Heart J* 2021; 42:3599–3726.

7. Murphy SP, Ibrahim NE, Januzzi J Jr. Heart failure with reduced ejection fraction. *JAMA* 2020; 324:488–504.
8. The CONSENSUS Trial Study Group. Effects of enalapril on mortality in severe congestive heart failure. Results of the Cooperative North Scandinavian Enalapril Survival Study (CONSENSUS). *N Engl J Med* 1987; 316:1429–1435.
9. Yusuf S, Pitt B, Davis CE, Hood WB Jr, Cohn JN, SOLVD Investigators. Effect of enalapril on mortality and the development of heart failure in asymptomatic patients with reduced left ventricular ejection fractions. *N Engl J Med* 1992; 327:658–691.
10. Messerli FH, Rimoldi SF, Bangalore S. The transition from hypertension to heart failure. *JACC Heart Failure* 2017; 8:543–551.
11. Pfeffer MA. Heart failure and hypertension: importance of prevention. *Med Clin North Am* 2017; 101:19–28.
12. Pinho-Gomes AC, Azevedo L, Bidel Z, Nazarzadeh M, Canoy D, Copland E, *et al*. Effects of blood pressure-lowering drugs in heart failure: a systemic review and meta-analysis of randomized controlled trials. *J Hypertens* 2019; 37:1757–1767.
13. Ryan TD, Rothstein EC, Aban I, Tallaj JA, Hussain A, Lucchesi PA, *et al*. Left ventricular eccentric remodellin and matrix loss are mediated by bradykinin and precede cardiomyocyte elongation in rats with volume overload. *J Am Coll Cardiol* 2007; 49:811–821.
14. Plante E, Lachance D, Beaudoin J, Champetier S, Roussel E, Arsenault M, *et al*. Comparative study of vasodilators in an animal mode of chronic volume overload caused by severe aortic regurgitation. *Circ Heart Fail* 2009; 2:25–32.
15. Červenka L, Melenovský V, Husková Z, Škaroupková P, Nishiyama A, Sadowski J. Inhibition of soluble epoxide hydrolase counteracts the development of renal dysfunction and progression of congestive heart failure in Ren-2 transgenic hypertensive rats with aorto-caval fistula. *Clin Exp Pharmacol Physiol* 2015; 42:795–807.
16. Ciccarelli M, Dawson D, Falcao-Pires I, Giacca M, Hamdani N, Heymans S, *et al*. Reciprocal organ interactions during heart failure: a position paper from the ESC Working Group on Myocardial Function. *Cardiovas Res* 2021; 117:2416–2433.
17. Packer M. How should physicians view heart failure? The philosophical and physiological evolution of three conceptual models of the disease. *Am J Cardiol* 1993; 71:3C–11C.
18. Dube P, Weber KT. Congestive heart failure: pathophysiologic consequences of neurohormonal activation and the potential for recovery: Part I. *Am J Med Sci* 2011; 342:348–351.
19. Mann DL, Felker GM. Mechanisms and models in heart failure. *A Transl Approach Circ Res* 2021; 128:1435–1450.
20. Yanagisawa M, Kurihara H, Kimura S, Tomobe Y, Kobayashi M, Mitsui Y, *et al*. A novel potent vasoconstrictor peptide produced by vascular endothelial cells. *Nature* 1988; 332:411–415.
21. Davenport AP, Hyndman KA, Dhaun N, Southan C, Kohan DE, Pollkock JS, *et al*. Endothelin. *Pharmacol Rev* 2016; 68:357–418.
22. Dhaun NJ, Webb DJ. Endothelins in cardiovascular biology and therapeutics. *Nat Review Cardiol* 2019; 16:491–502.
23. Barton M, Yanagisawa M. Endothelin: 30 years from discovery to therapy. *Hypertension* 2019; 74:1232–1265.
24. Miyauchi T, Sakai S. Endothelin and the heart in health and diseases. *Peptides* 2019; 111:77–88.
25. Eroglu E, Kocyigit I, Linholm B. The endothelin system as target for therapeutic interventions in cardiovascular and renal disease. *Clin Chimi Acta* 2020; 506:92–106.
26. Kobayashi T, Miyauchi T, Sakai S, Kobayashi M, Yamaguchi I, Goto K, *et al*. Expression of endothelin-1, ETA and ETB receptors, and ECE and distribution of endothelin-1 in failing heart. *Am J Physiol* 1999; 276: H1197–H1206.
27. Motte S, van Beneden R, Mottet J, Rondelet B, Mathieu M, Havaux X, *et al*. Early activation of cardia and renal endothelin systems in experimental heart failure. *Am J Physiol* 2003; 285:H2482–H2491.
28. Sakai S, Miyauchi T, Kobayashi M, Yamaguchi I, Goto K, Sugishita Y. Inhibition of myocardial endothelin pathway improves long-term survival in heart failure. *Nature* 1996; 384:353–355.
29. Pfeffer MA, Pfeffer JM, Steinberg C, Finn P. Survival after an experimental myocardial infarction: beneficial effects of long-term therapy with captopril. *Circulation* 1985; 2:406–412.
30. Mulder P, Boujedainin H, Richard V, Henry JP, Renet S, Munter K, *et al*. Long-term survival and hemodynamics after endothelin-A receptor antagonism and angiotensin-converting enzyme inhibition in rats with chronic heart failure. Monotherapy versus combination therapy. *Circulation* 2002; 106:1159–1164.
31. Lee DS, Nguyen QT, Lapointe N, Austin F, Ohlsson A, Tu JV, *et al*. Meta-analysis of the effects of endothelin receptor blockade on survival in experimental heart failure. *J Card Fail* 2003; 9:368–374.
32. Xia QG, Reinecke A, Dorenkamp M, Daemen MJ, Simon R, Unger T. Effects of endothelin ET_A receptor blocker LU 135252 on cardiac remodeling and survival in a hypertensive rat model of chronic heart failure. *Acta Pharmacol Sin* 2006; 27:1417–1422.
33. Luscher TF, Enseleit F, Pacher R, Mitrovic V, Schulze MR, Willenbrock R, *et al*. Hemodynamic and neurohormonal effects of selective endothelin A (ET_A) receptor blockade in chronic heart failure. The heart failure ET_A receptor blockade trial (HEAT). *Circulation* 2002; 106:2666–2672.
34. Anand I, McMurray J, Cohn JN, Konstam MA, Notter T, Quitzaou K, *et al*. Long-term effects of darusentan on left-ventricular remodeling and clinical outcomes in EndothelinA Receptor Antagonist Trial in Heart Failure (EARTH): randomized, double-blind, placebo-controlled trial. *Lancet* 2004; 364:347–354.
35. Mann JFE, Green D, Jamerson K, Ruilope LM, Kuranoff SJ, Littke T, *et al*. Avosentan for over diabetic nephropathy. *J Am Soc Nephrol* 2010; 21:527–535.
36. Packer M, McMurray JJV, Krum H, Kiowski W, Massie BM, Caspi A, *et al*. Long-term effect on endothelin receptor antagonism with bosentan on the morbidity and mortality of patients with severe chronic heart failure. Primary results of the ENABLE trials. *J Am Col Cardiol HF* 2017; 5:317–326.
37. Gottlieb SS, Theory fact. Revisiting association and causation. *J Am Col Cardiol HF* 2017; 5:327–328.
38. Čertíková Chábová V, Vernerová Z, Kujal P, Husková Z, Škaroupková P, Tesař V, *et al*. Addition of ETA receptor blockade increases renoprotection provided by renin–angiotensin system blockade in 5/6 nephrectomized Ren-2 transgenic rats. *Life Sci* 2014; 118:297–305.
39. Sedláková L, Čertíková Chábová V, Doleželová Š, Škaroupková P, Kopkan L, Husková Z, *et al*. Renin-angiotensin system blockade alone or combined with ETA receptor blockade: effects on the course of chronic kidney disease in 5/6 nephrectomized Ren-2 transgenic hypertensive rats. *Clin Exp Hypertens* 2017; 39:183–195.
40. Vaněčková I, Hojná S, Vernerová Z, Kadlecová M, Rauchová H, Kompanowska-Jezierska E, *et al*. Renoprotection provided by additional diuretic treatment in partially nephrectomized Ren-2 transgenic rats subjected to the combined RAS and ETA blockade. *Front Physiol* 2019; 10:1145.
41. Heerspinkg HJ, Parving HH, Andress DL, Bakris G, Correa-Rotter R, Hou FF, *et al*. Atresantan and renal events in patients with type 2 diabetes and chronic kidney disease (SONAR): a double-blind, randomized, placebo-controlled trial. *Lancet* 2019; 393:1937–1947.
42. Brower GL, Levick SP, Janicki JS. Differential effects of prevention and reversal treatment with Lisinopril on left ventricular remodeling in a rat model of heart failure. *Heart Lung Circ* 2015; 24:919–924.
43. Oliver-Dussault C, Ascah A, Marcil M, Matas J, Picard S, Pibarot P, *et al*. Early predictors of cardiac decompensation in experimental volume overload. *Mol Cell Biochem* 2010; 338:271–281.
44. Abassi Z, Goltsmna I, Karram T, Winaver J, Horrman A. Aortocaval fistula in rat: a unique model of volume-overload congestive heart failure and cardiac hypertrophy. *J Biomed Biotechnol* 2011; 2011:729497.
45. Honetschlagerová Z, Gawrys O, Jíchová Š, Škaroupková P, Kikerlová S, Vaňourková Z, *et al*. Renal sympathetic denervation attenuates congestive heart failure in angiotensin II-dependent hypertension: studies with Ren-2 transgenic hypertensive rats with aorto-caval fistula. *Kidney Blood Press Res* 2021; 46:95–113.
46. Honetschlagerová Z, Škaroupková P, Kikerlová S, Husková Z, Maxová H, Melenovský V, *et al*. Effects of renal sympathetic denervation on the course of congestive heart failure combined with chronic kidney disease: insight from studies with fawn-hooded hypertensive rats with volume overload induced using aorto-caval fistula. *Clin Exp Hypertens* 2021; 43:522–535.
47. Kala P, Miklovič M, Jíchová Š, Škaroupková P, Vaňourková Z, Maxová H, *et al*. Effects of Epoxyeicosatrienoic acid-enhancing therapy on the course of congestive heart failure in angiotensin II-dependent rat hypertension: from mRNA analysis towards functional in vivo evaluation. *Biomedicines* 2021; 9:1053.

48. Houser SR, Margulies KB, Murphy AM, Spinale FG, Francis GS, Prabhu SD. Animal models of heart failure: a scientific statement from the American Heart Association. *Circ Res* 2012; 111:131–150.
49. Riehle C, Bauersachs J. Small animals models of heart failure. *Cardiovasc Res* 2019; 115:1838–1849.
50. Mullins JJ, Peters J, Ganten D. Fulminant hypertension in transgenic rats harboring the mouse Ren-2 gene. *Nature* 1990; 344:541–544.
51. Husková Z, Kramer HJ, Vaňourková Z, Červenka L. Effects of changes in sodium balance on plasma and kidney angiotensin II levels in anesthetized and conscious Ren-2 transgenic rats. *J Hypertens* 2006; 24:517–522.
52. Sobieraj P, Nisson PM, Kahan T. Heart failure events in a clinical trial on arterial hypertension: new insights into the SPRINT trial. *Hypertension* 2021; 78:1241–1247.
53. Aimo A, Vergaro G, Passion C, Clerico A. Evaluation of pathophysiological relationship between renin-angiotensin systems in cardiovascular disorders: from theory to routine clinical practice in patients with heart failure. *Crit Rev Clin Lab Sci* 2021; 1:1–16.
54. Antoine S, Vaidya G, Imam H, Villarreal D. Pathophysiologic mechanisms in heart failure: role of the sympathetic nervous system. *Am J Med Sci* 2017; 353:27–30.
55. Floras JS. The 2021 Carl Ludwig Lecture. Unsympathetic autonomic regulation in heart failure: patients-inspired insights. *Am J Physiol* 2021; 321:R338–R351.
56. Grassi G, Mancia G, Esler M. Central and peripheral sympathetic activation in heart failure. *Cardiovas Res* 2022; 8:1857–1871.
57. Cohen J. Some issue in power analysis. In: Cohen J, editor. *Statistical power analysis for behavioral sciences*, 2nd ed. Oxford, UK: Routledge; 2013. pp. 531–542.
58. Wang X, Ren B, Liu S, Sentex E, Tappia PS, Dhalla NS. Characterization of cardiac hypertrophy and heart failure due to volume overload in the rat. *J Appl Physiol* 2003; 94:752–763.
59. Kratky V, Vanourkova Z, Sykora M, Szeiffova Bacova B, Hruskova Z, Kikerlova S, *et al.* AT1 receptor blocker, but not an ACE inhibitor, prevents kidneys from hypoperfusion during congestive heart failure in normotensive and hypertensive rats. *Sci Rep* 2021; 11:4271.
60. Pacher P, Nagayama T, Mukhopadhyay P, Bátkai S, Kass DA. Measurement of cardiac function using pressure–volume conductance catheter technique in mice and rats. *Nat Protoc* 2008; 3:1422–1434.
61. Kala P, Bartušková H, Pit'ha J, Vaňourková Z, Kikerlová S, Jíchová Š, *et al.* Deleterious effects of hyperactivity of the renin-angiotensin system and hypertension on the course of chemotherapy-induced heart failure after doxorubicin administration: a study in Ren-2 transgenic rats. *Int J Mol Sci* 2020; 21:9337.
62. Havlenova T, Skaroupkova P, Miklovic M, Behounek M, Chmel M, Jarkovaska D, *et al.* Right versus left ventricular remodeling in heart failure due to chronic volume overload. *Sci Rep* 2021; 11:17136.
63. Opočenský M, Kramer HJ, Bäcker A, Vernerová Z, Eis V, Červenka L, *et al.* Late-onset endothelin-A receptor blockade reduces podocyte injury in homozygous Ren-2 rats despite severe hypertension. *Hypertension* 2006; 48:965–971.
64. Husková Z, Kopkan L, Červenková L, Doleželová Š, Vaňourková Z, Škaroupková P, *et al.* Intrarenal alterations of the angiotensin-converting type 2/angiotensin 1-7 complex of the renin-angiotensin system do not alter the course of malignant hypertension in Cyp1a1-Ren-2 transgenic rats. *Clin Exp Pharmacol Physiol* 2016; 43:438–449.
65. Kohno M, Horio T, Ikeda M, Yokowa K, Fukui T, Yasunari K, *et al.* Angiotensin II stimulates endothelin-1 secretion in cultured rat mesangial cells. *Kidney Int* 1992; 42:860–866.
66. Barton M, Shaw S, d'Uscio LV, Moreau P, Luscher T. Angiotensin II increases vascular and renal endothelin-1 and functional endothelin-converting enzyme activity in vivo: role of ET_A receptors of endothelin regulation. *Biochem Biophys Res Commun* 1997; 238:861–865.
67. Kawaguchi H, Sawa H, Yasuda H. Effects of endothelin on angiotensin converting enzyme activity in cultured pulmonary artery endothelial cells. *J Hypertens* 1991; 9:171–174.
68. Stehouwer CDA, Smulders YM. Microalbuminuria and risk for cardiovascular disease: analysis of potential mechanisms. *J Am Soc Nephrol* 2006; 17:2106–2111.
69. Currie G, Delles C. Proteinuria and its relation to cardiovascular disease. *Int J Nephrol Renovas Dis* 2014; 7:13–24.
70. Liang W, Liu Q, Wang Q-y. Yu H, Yu J. Albuminuria and dipstick proteinuria for predicting mortality in heart failure: a systematic review and meta-analyses. *Front Cardiovas Med* 2021; 8:665831.
71. Rossi GP, Sacchetto A, Cesari M, Pessina AC. Interactions between endothelin-1 and the renin–angiotensin–aldosterone system. *Cardiovasc Res* 1999; 43:300–307.
72. Komers R, Plotkin H. Dual inhibition of renin-angiotensin-aldosterone system and endothelin-1 in treatment of chronic kidney disease. *Am J Physiol* 2016; 310:R877–R884.
73. Emori T, Hirata Y, Ohta K, Kanno K, Eguchi S, Imai T, *et al.* Cellular mechanisms of endothelin-1 release by angiotensin and vasopressin. *Hypertension* 1991; 18:165–170.
74. Ho KKL, Pinsky JL, Kannel WB, Levy D. The epidemiology of heart failure: the Framingham study. *J Am Coll Cardiol* 1993; 22 (Supplement A):6A–13A.
75. Pilz PM, Ward JE, Chang WT, Kiss A, Bateh E, Jha A, *et al.* Large and small animal models of heart failure with reduced ejection fraction. *Circ Res* 2022; 130:1888–1905.
76. Vacková Š, Kikerlová S, Melenovský V, Kolář F, Imig JD, Kompanowska-Jezierska E, *et al.* Altered renal vascular responsiveness to vasoactive agents in rats with angiotensin II-dependent hypertension and congestive heart failure. *Kidney Blood Press Res* 2019; 44:792–809.
77. Santos RAS, Sampaion WO, Alzamora AC, Motta-Santos D, Alenina N, Bader M, *et al.* The ACE2/angiotensin-(1-7)/Mas axis of the renin–angiotensin system: focus on the angiotensin-(1-7). *Physiol Rev* 2018; 98:505–553.
78. Bürgelová M, Kramer HJ, Teplan V, Thumová M, Červenka L. Effects of angiotensin-(1-7) blockade on renal function in rats with enhanced intrarenal ANG II activity. *Kidney Int* 2005; 67:1453–1461.
79. Wang K, Basu R, Poglitsch M, Bakal JA, Stat P, Oudit GY. Elevated angiotensin 1-7/angiotensin II ratio predicts favorable outcomes in patients with heart failure. *Circ Heart Fail* 2020; 13:e006939.

J. Plášek et al.

The Agreement of a Two- and a Three-Dimensional Speckle-Tracking Global Longitudinal Strain

J Clin Med
Impact Factor: 4.242

‹ rejstřík

Journal of
Clinical Medicine

MDPI

Article

The Agreement of a Two- and a Three-Dimensional Speckle-Tracking Global Longitudinal Strain

Jiří Plášek [1,2,3,*], Tomáš Rychlý [2,3], Diana Drieniková [1,2], Ondřej Cisovský [2,3], Tomáš Grézl [1,3], Miroslav Homza [2,3] and Jan Václavík [1,3]

[1] Department of Internal Medicine and Cardiology, University Hospital Ostrava, 708 52 Ostrava, Czech Republic; diana.drienikova@fno.cz (D.D.); tomasgrezl@gmail.com (T.G.); jan.vacalvik@fno.cz (J.V.)
[2] Benedor Cardiology Outpatient Clinic Ltd., 708 00 Ostrava, Czech Republic; info@benedor.cz (T.R.); ondrej.ciso@gmail.com (O.C.); mirek.homza@centrum.cz (M.H.)
[3] Faculty of Medicine, University of Ostrava, 703 00 Ostrava, Czech Republic
* Correspondence: jiri.plasek@fno.cz; Tel.: +40-776-658-598

Abstract: Background: Two-dimensional (2D) and three-dimensional (3D) speckle-tracking echocardiography (STE) enables assessment of myocardial function. Here, we examined the agreement between 2D and 3D STE measurement of a global longitudinal strain (GLS) in patients with normal left ventricle, reduced ejection fraction, and cardiac pacing. Methods: Our analysis included 90 consecutive patients (59% males; average age: 73.2 ± 11.2 years) examined between May 2019–December 2020, with valid 2D and 3D loops for further speckle-tracking strain analysis. Linear regression, Pearson correlation, and a Bland–Altman plot were used to quantify the association between 2D and 3D GLS and related segments, using the 17-segment American Heart Association (AHA) model. Analyses were performed in the entire study group and subgroups. Intra- and inter-observer variability of 2D and 3D GLS measurement was also performed in all participants. Results: We observed a strong correlation between 2D and 3D GLS measurements (R = 0.76, $p < 0.001$), which was higher in males (R = 0.78, $p < 0.001$) than females (R = 0.69, $p < 0.001$). Associated segment correlation was poor (R = 0.2–0.5, $p < 0.01$). The correlation between 2D and 3D GLS was weaker in individuals with ventricular pacing of >50% (R = 0.62, $p < 0.001$) than <50% (R = 0.8, $p < 0.001$), and in patients with LVEF of <35% (R = 0.69, $p = 0.002$) than >35% (R = 0.72, $p < 0.001$). Intra-observer variability for 2D and 3D GLS was 2 and 2.3%, respectively. Inter-observer variability for 2D and 3D GLS was 3.8 and 3.6%, respectively Conclusion: Overall 2D and 3D GLS were closely associated but not when analyzed per segment. It seems that GLS comparison is more representative of global shortening than local displacement. Right ventricular pacing and reduced left ventricular ejection fraction were associated with a reduced correlation between 2D and 3D GLS.

Keywords: global longitudinal strain; 17-segment AHA model; deformation imaging; three-dimensional echocardiography; speckle-tracking echocardiography

Citation: Plášek, J.; Rychlý, T.; Drieniková, D.; Cisovský, O.; Grézl, T.; Homza, M.; Václavík, J. The Agreement of a Two- and a Three-Dimensional Speckle-Tracking Global Longitudinal Strain. *J. Clin. Med.* **2022**, *11*, 2402. https://doi.org/10.3390/jcm11092402

Academic Editors: Francesca Bursi and Giovanni Benfari

Received: 24 March 2022
Accepted: 23 April 2022
Published: 25 April 2022

Publisher's Note: MDPI stays neutral with regard to jurisdictional claims in published maps and institutional affiliations.

1. Introduction

Speckle-tracking echocardiography (STE) is a promising method for non-invasive myocardial deformation analysis [1]. Compared to magnetic resonance imaging (MRI), two-dimensional (2D) STE enables angle-independent and reliable measurement of left ventricular dimensions and strains [1]. Despite years of research showing advantages over conventional parameters, 2D STE is not commonly used in clinical practice, except for cardio-oncology [2]. Reasons include that the analysis is time-consuming, a lack of standardization, inter-vendor differences, and the need for manual adjustments to the cardiac regions of interest [3–5]. Moreover, different modalities such as 2D STE, three-dimensional (3D) STE, and cardiac MRI are available to acquire myocardial strain measurements, raising questions regarding the agreement between methods [4,5].

Two-dimensional STE has been validated against MRI tagging, as a gold standard of deformation analysis [1,6]. However, based on the expert consensus statement, there is no true gold standard technique for non-invasive quantification of left ventricular (LV) mechanics [7]. MRI tagged myocardial strain showed an excellent correlation to 2D STE [1], similar to the agreement previously described between tissue Doppler imaging (TDI)-based strain and MRI-tagging [8].

Two-dimensional STE enables feasible assessment of global and regional myocardial function [5]. The model is reconstructed and segmented from three 2D planes, in contrast to 3D volumetric speckle-tracking analysis. Three-dimensional STE is an emerging ultrasonographic modality that may provide us with more physiological, and probably faster, analysis of myocardial deformation. The results of 3D STE should be cautiously evaluated. Compared to 2D STE, 3D STE involves a considerably lower average frame rate and a higher level of automatization of the analysis. Therefore, there remains a need to examine the agreement between 2D and 3D STE.

Global longitudinal strain (GLS) predominantly reflects the contractile function of the subendocardium and subepicardium of the left ventricular wall due to myofiber orientation [9]. Notably, the subendocardium is more susceptible to both ischemia/stunning and mechanical overload related to either valvular disease or aging [9–11]. Therefore, GLS is likely to decrease in early stages of various cardiac diseases [9]. GLS is rarely systematically used, although it is reliable, and it has a reproducible parameter, even when compared to left ventricular ejection fraction (LVEF) [12].

Based on its reliability, sensitivity, and reproducibility, GLS was the main parameter investigated in our present study. We aimed to analyze the level of agreement between GLS measured by 2D vs. 3D STE and its reproducibility. Gender-related influences on left ventricular mechanics in individuals free of heart failure have been recently described [13]. Therefore, separate analyses for males and females were also performed.

2. Materials and Methods

2.1. Patients

For this study, we retrospectively enrolled echocardiographic examinations from 90 consecutive patients, who were scheduled for routine evaluation. Incomplete loops and/or inadequate image quality for 2D and 3D STE led to exclusion from the study. Patients with atrial fibrillation at the time of the image acquisition were also excluded from the study. The study sample comprised of patients with various cardiovascular diseases to assess the correlation between 2D and 3D STE across a real-life patient population. This study was approved by the institutional review board of University Hospital Ostrava and conducted in accordance with the Helsinki Declaration. The need for informed consent was waived for this study.

2.2. Echocardiography

Two-dimensional grayscale echocardiography was performed using a Vivid E95 scanner (GE Vingmed Ultrasound, Horten, Norway). The frame rate was >50/s for 2D STE, and >25/s for 3D STE. Images were analyzed using EchoPAC version 203 revision 73 (GE Vingmed Ultrasound, Horten, Norway). The endocardial border was traced at end-systole, and the thickness of the region of interest (ROI) was adjusted to include most of the myocardium, while avoiding stationary speckles near the pericardium. From the 3060 analyzed segments of the 17-segment AHA model, a total of 136 segments (4.4%) were excluded from the analysis due to an inability to track.

For 2D STE, we used automatic function imaging (AFI) of the EchoPAC (Figure 1). The AFI feature involves the manual placement of markers on each side of the mitral annulus and left ventricular (LV) apex in three standard apical views. Next, the program automatically tracks the endocardial border and calculates the myocardial (ROI). When necessary, manual adjustments were made to the ROI and/or the endocardial/epicardial borders, which are important for the strain analysis (Figure 1).

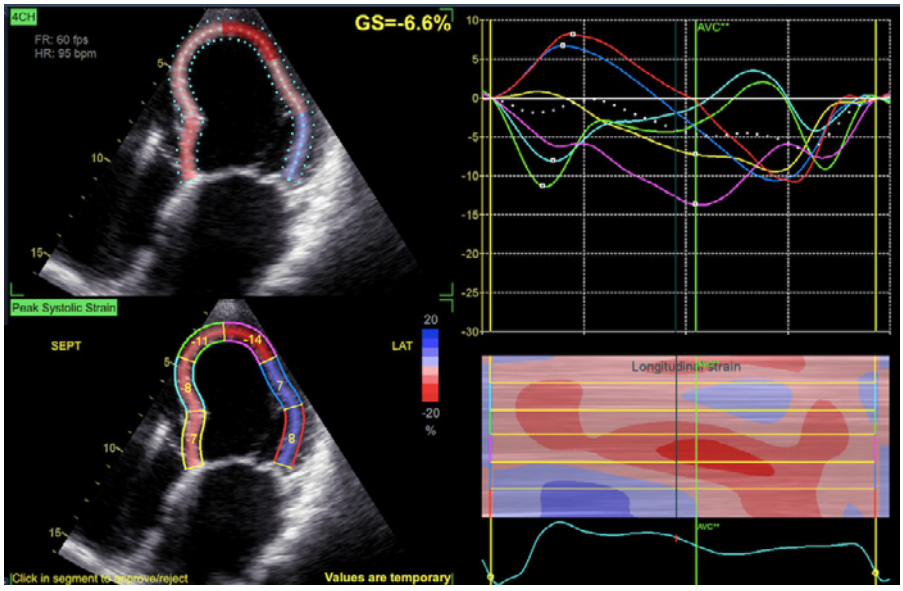

Figure 1. Four–chamber view of automatic function imaging (AFI), peak systolic strain is visualized in the left lower part, global strain in the left upper part and corresponding waveforms in the right upper part, right lower part visualize surface extrapolated color mapped strain.

For 3D STE analysis, we used the automatic left ventricular quantification function (AutoLVQ) of EchoPAC. Topographic markers were placed in the middle of the mitral valve and the LV apex. The endocardial border was automatically delineated, and manual adjustments were made when necessary. For both 2D and 3D STE, end-diastole and end-systole were determined by automatic identification of the aortic valve opening and closing, and manual adjustments were made when necessary. All the 2D and 3D global longitudinal strain values were calculated using the software, and presented as a 17-segment bull's eye model (Figure 2).

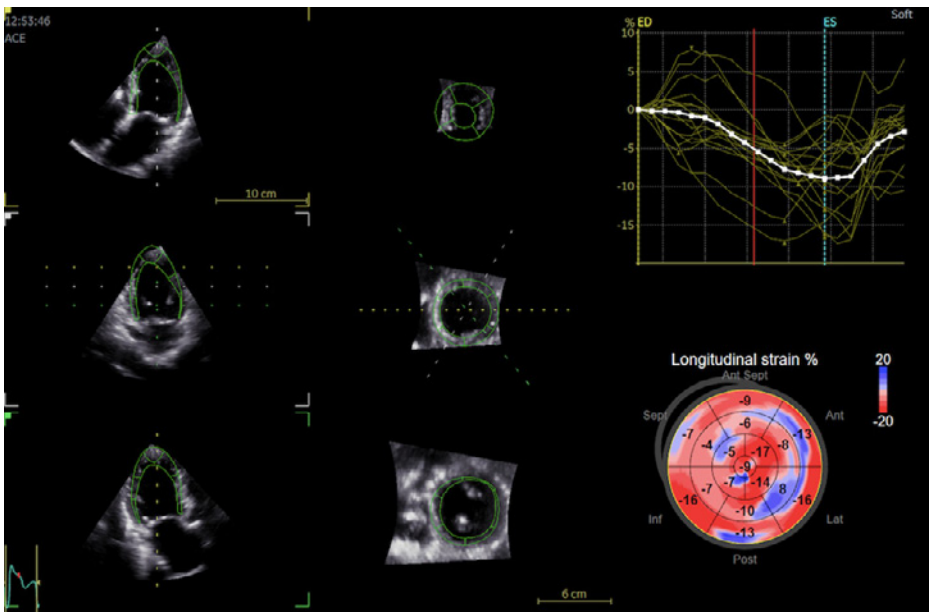

Figure 2. Automatic left ventricular quantification (AutoLVQ) plane after segmentation process with bull's eye reconstruction of 3D global longitudinal strain. Red color and more negative number means better contractility as opposed to positive numbers and blue colour.

2.3. Statistics

Continuous variables were expressed as mean ± standard deviation, and compared by *t*-test or Mann–Whitney U test, as appropriate. Categorical variables were expressed as percentages, and compared by the chi-square test, Fisher's exact test, or logistic regression, as appropriate. We investigated the association of 2D GLS with 3D GLS using linear regression analysis, Pearson's, Spearman correlation, and a Bland-Altman plot. A two-tailed α value of <0.05 was considered statistically significant—except for the test of equality of covariance matrices, for which $p < 0.005$ was considered significant. Normal distribution of the data was assessed by Shapiro–Wilk's test. The majority of analyses were performed on the entire group of patients, some analyses were performed separately for males and females. All analyses were performed using IBM SPSS for MAC version 23 (IBM, New York, NY, USA) and MS Excel (Redmond, Washington, DC, USA) for MAC version 16.5.

2.4. Reproducibility Analysis

Intra- and inter-observer variability of 2D and 3D GLS measurement was tested in all subjects. Intra-observer variability was tested by repeated measurements four or more weeks apart with blinding to the original dataset. To test inter-observer variability, a second experienced operator evaluated the loops with no access to the original dataset. Intra- and interobserver variability is presented as mean percentage error, and it was calculated as an absolute difference between the two measurements.

3. Results

Our analysis included a total of 90 patients. Table 1 shows the baseline clinical characteristics, including gender differences. Except for LVEF, heart failure, and CABG, there were no meaningful differences between males and females. Females were less represented in the whole patient sample (41%). Mean value of 2D and 3D GLS was -10.6 ± 4.2 and -10.5 ± 4.1, respectively. A Shapiro–Wilk's test ($p > 0.05$) and visual inspection of the histograms, normal Q-Q plots and box plots showed that the data (2D, 3D GLS) are approximately normally distributed for both males and females. There were very few outliers in the 2D and 3D GLS dataset. Since they were not due to data entry error, and they do not affect the assumptions made in the analysis or the results, they were not removed from the analysis.

We observed an overall strong positive correlation between 2D GLS and 3D GLS (Pearson's R = 0.76, $p < 0.001$, Spearman $\rho = 0.74$, $p < 0.001$) (Figure 3). Separate analyses revealed that this correlation coefficient was numerically greater in males (Pearson's R = 0.78, $p < 0.001$, Spearman $\rho = 0.75$, $p < 0.001$) and lesser in females (R = 0.69, $p < 0.001$, Spearman $\rho = 0.66$, $p < 0.001$), though this difference was not significant. A Bland–Altman analysis demonstrated a small bias (0.1%) and moderate limits of agreement (SD: 2.9%) between 2D and 3D GLS (Figure 4).

Analysis of every 2D vs. 3D segment of the 17-segment AHA model revealed a poor associated segment correlation, with R and ρ values ranging from 0.2 to 0.5 ($p < 0.01$) (Table 2). Not all the segments even reached the level of significance. The anteroseptal segments seem to produce a higher correlation between 2D and 3D GLS irrespective whether they were apical, middle, or basal (Table 2). The correlation between 2D and 3D GLS was weaker among individuals with >50% ventricular pacing (R = 0.62, $p < 0.001$) than in individuals with <50% ventricular pacing or no pacing (R = 0.8, $p < 0.001$) (Figure 5, Table 3). Moreover, the correlation and regression coefficients between 2D vs. 3D GLS were lower with LVEF < 35% (R = 0.69, $p = 0.002$) than LVEF > 35% (R = 0.72, $p < 0.001$) (Figure 6, Table 3). Other clinical or paraclinical parameters did not influence the level of correlation between 2D and 3D GLS. Intra-observer variability for 2D and 3D GLS was 2 and 2.3%, respectively. Inter-observer variability for 2D and 3D GLS was 3.8 and 3.6%, respectively.

Table 1. Baseline characteristics of the study population.

	Total Population	Males	Females	*p* Value
	N = 90	N = 53	N = 37	
Age (years)	73.2 ± 11.2	70.5 ± 12.3	76.7 ± 8.3	0.681
Males (%)	59	-	-	
Body weight (kg)	85.1 ± 18.4	91.4 ± 16.5	77 ± 17.7	0.882
Body height (cm)	169.1 ± 9.9	175.5 ± 6.4	160.7 ± 7	0.068
Body mass index (kg/m^2)	29.6 ± 5.4	29.5 ± 4.6	29.8 ± 6.4	0.92
LV EF	48 ± 12.7	45 ± 12.9	51 ± 11.8	0.039
Coronary artery disease (%)	46.5	49	43.2	0.269
Hyperlipoproteinemia (%)	52.6	55.1	48.6	0.726
Myocardial infarction (%)	27.9	32.7	21.6	0.744
Peripheral arterial disease (%)	4.7	8.2	2.7	0.660
Hypertension (%)	79.1	73	86.5	0.371
Heart failure (%)	8.1	18.0	10.8	0.021
Diabetes mellitus (%)	25.6	24.5	27	0.732
Previous stroke/TIA (%)	9.3	10.2	8.1	0.585
COPD (%)	8.1	8.2	8.1	0.314
DCM	8.1	10.2	5.4	0.27
HCM	1.2	2	0	N/A
CABG (%)	16.3	24.5	5.4	0.027
PM (%)	38	32	48	0.656

Indices are shown as mean ± standard deviation or proportion in percentages and compared for male and females.; CABG, Coronary artery by-pass graft; COPD, Chronic obstructive pulmonary disease; DCM, dilated cardiomyopathy; EF, ejection fraction; HCM, hypertrophic cardiomyopathy; LV, left ventricle; N/A, not applicable; PM, pacemaker; TIA, transient ischemic attack.

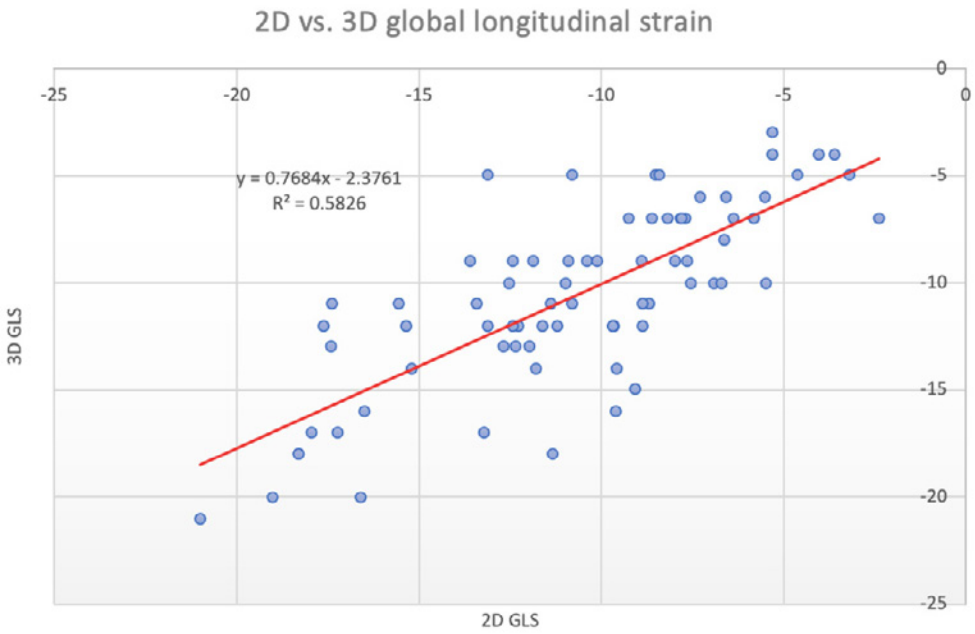

Figure 3. Scatter plot of 2D vs. 3D global longitudinal strain, linear regression equation displayed in the left upper section.

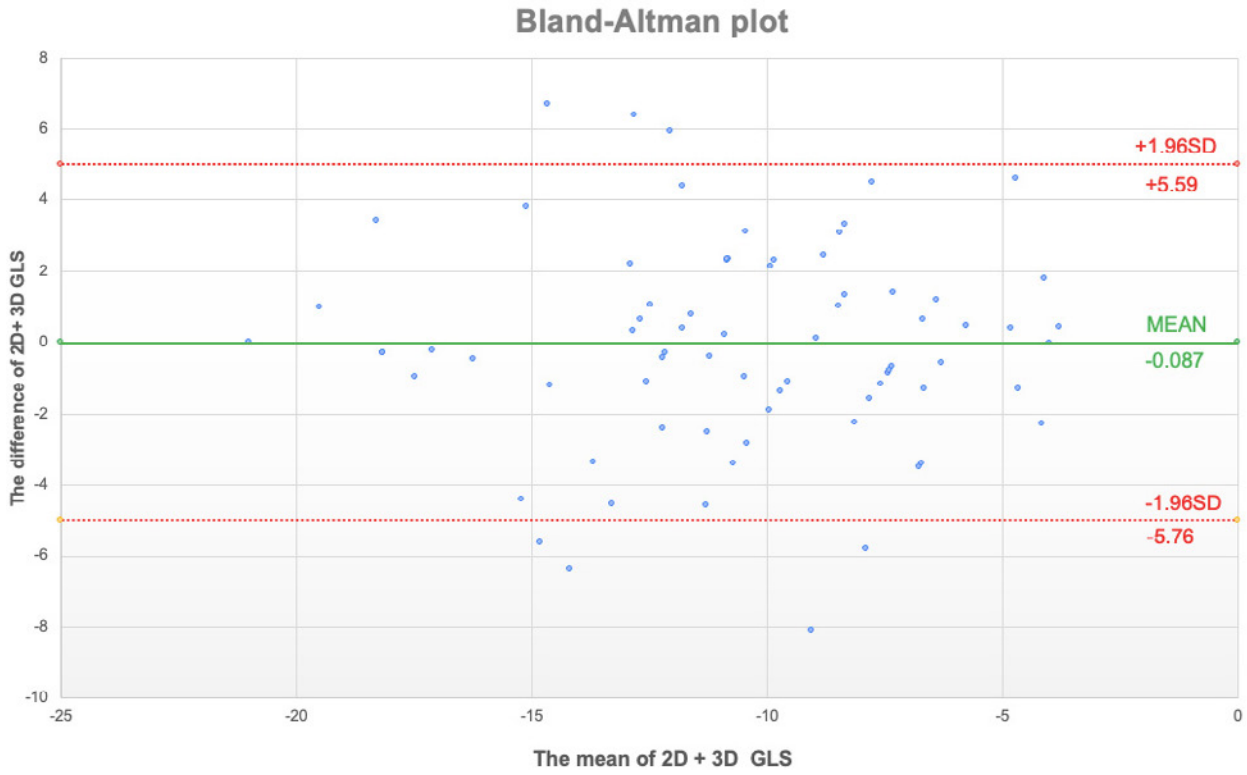

Figure 4. Bland–Altman plot of mean values of 2D + 3D global longitudinal strain (GLS, *x* axis) and the difference between 2D and 3D GLS. Upper and lower limit of agreement displayed as red dotted line with respective values.

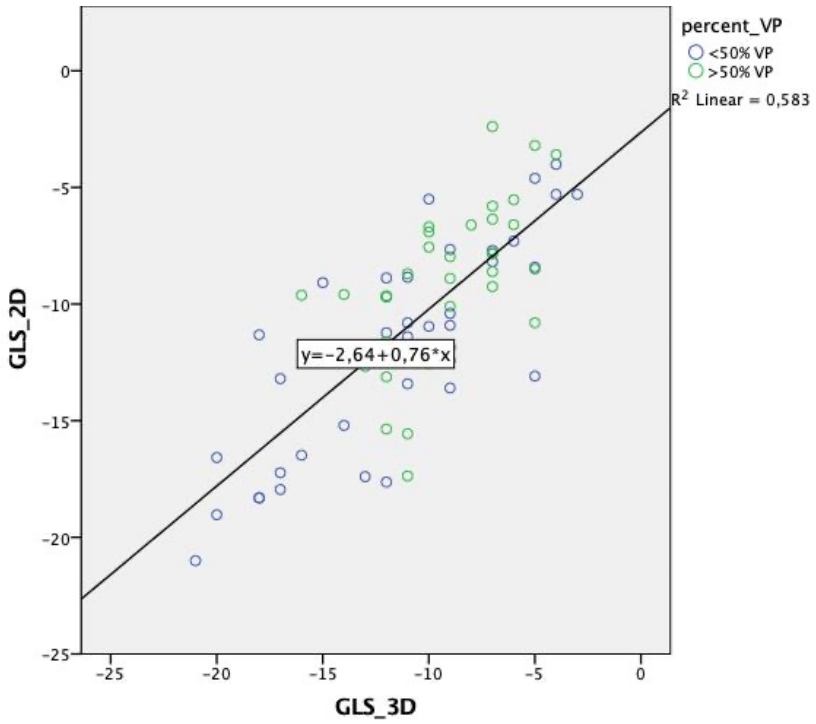

Figure 5. Scatter plot of 2D vs. 3D global longitudinal strain. Sorted by the amount of right ventricular pacing (VP) with displayed regression equation.

Table 2. Comparison of 2D vs. 3D global longitudinal strain, analyzed on entire group and separately by gender.

2D vs. 3D GLS	LINEAR REGRESSION + PEARSON'S AND SPEARMAN CORRELATION																				
	ALL							MALES							FEMALES						
	SLOPE ± SEM	**R**	***p***	**r**	***p***	**ρ**	***p***	**SLOPE ± SEM**	**R**	***p***	**r**	***p***	**ρ**	***p***	**SLOPE ± SEM**	**R**	***p***	**ρ**	***p***	**r**	***p***
	0.77 ± 0.27	**0.76**	**<0.001**	**0.76**	**<0.001**	**0.74**	**<0.001**	**0.82 ± 0.35**	**0.78**	**<0.001**	**0.78**	**<0.001**	**0.75**	**<0.001**	**0.69 ± 0.39**	**0.69**	**<0.001**	**0.66**	**<0.001**	**0.69**	**<0.001**
Seg.1	0.38 ± 0.39	0.27	0.019	0.27	0.02	0.32	0.005	0.36 ± 0.36	0.16	0.3	0.18	0.23	0.42	0.006	0.26 ± 0.57	0.15	0.41	0.23	0.218	0.16	0.40
Seg.2	0.66 ± 0.52	0.55	<0.001	0.55	<0.001	0.50	<0.001	0.79 ± 0.51	0.54	<0.001	0.54	<0.001	0.57	<0.001	0.58 ± 1.03	0.58	<0.001	0.47	0.009	0.58	<0.001
Seg.3	0.12 ± 0.59	0.18	0.123	0.20	0.09	0.23	0.053	0.29 ± 0.74	0.3	0.05	0.32	0.04	0.36	0.018	0.09 ± 0.91	0.07	0.715	0.06	0.740	0.08	0.682
Seg.4	0.46 ± 0.60	0.35	0.002	0.35	0.002	0.35	0.002	0.46 ± 0.82	0.35	0.023	0.35	0.02	0.34	0.027	0.44 ± 089	0.33	0.075	0.30	0.104	0.32	0.086
Seg.5	0.42 ± 0.68	0.318	0.006	0.30	0.009	0.35	0.002	0.38 ± 0.79	0.26	0.096	0.24	0.119	0.25	0.116	0.50 ± 1.19	0.40	0.03	0.46	0.011	0.39	0.03
Seg.6	0.05 ± 0.60	0.068	0.569	0.04	0.733	0.12	0.327	−0.01 ± 0.65	0.05	0.750	0.01	0.970	0.13	0.413	0.06 ± 1.11	0.06	0.745	0.06	0.754	0.06	0.753
Seg.7	0.50 ± 0.43	0.44	<0.001	0.44	<0.001	0.48	<0.001	0.43 ± 0.60	0.42	0.006	0.42	0.004	0.51	0.001	0.61 ± 0.57	0.432	0.019	0.49	0.007	0.43	0.016
Seg.8	0.44 ± 0.48	0.47	<0.001	0.47	<0.001	0.56	<0.001	0.59 ± 0.54	0.53	<0.001	0.53	<0.001	0.56	<0.001	0.33 ± 0.88	0.42	0.024	0.51	0.004	0.41	0.02
Seg.9	0.50 ± 0.47	0.41	<0.001	0.41	<0.001	0.33	0.005	0.57 ± 0.59	0.49	0.001	0.49	0.001	0.45	0.003	0.40 ± 0.76	0.32	0.086	0.22	0.251	0.31	0.09
Seg.10	0.32 ± 0.52	0.27	0.02	0.27	0.02	0.35	0.002	0.59 ± 0.65	0.53	<0.001	0.52	<0.001	0.62	<0.001	−0.1 ± 0.85	0.04	0.850	0.631	0.091	0.05	0.794
Seg.11	0.531 ± 0.528	0.45	<0.001	0.45	<0.001	0.50	<0.001	0.63 ± 0.63	0.51	<0.001	0.50	<0.001	0.55	<0.001	0.36 ± 0.91	0.36	0.05	0.31	0.1	0.37	0.04
Seg.12	0.50 ± 0.52	0.45	<0.001	0.45	<0.001	0.39	0.001	0.60 ± 0.59	0.54	<0.001	0.54	<0.001	0.51	0.001	0.39 ± 0.92	0.36	0.05	0.28	0.229	0.37	0.04
Seg.13	0.29 ± 0.65	0.48	<0.001	0.48	<0.001	0.58	<0.001	0.37 ± 0.75	0.51	<0.001	0.51	<0.001	0.62	<0.001	0.16 ± 1.15	0.38	0.05	0.49	0.007	0.37	0.04
Seg.14	0.46 ± 0.66	0.52	<0.001	0.52	<0.001	0.50	<0.001	0.56 ± 0.75	0.56	<0.001	0.57	<0.001	0.56	<0.001	0.39 ± 1.18	0.49	0.007	0.43	0.017	0.49	0.006
Seg.15	0.23 ± 0.61	0.32	0.007	0.26	0.03	0.31	0.007	0.28 ± 0.75	0.42	0.006	0.31	0.05	0.37	0.016	0.17 ± 1.01	0.23	0.220	0.19	0.376	0.2	0.291
Seg.16	0.14 ± 0.56	0.19	0.103	0.18	0.129	0.135	0.257	0.33 ± 0.75	0.45	0.003	0.42	0.006	0.36	0.018	−0.15 ± 0.76	0.17	0.359	0.25	0.190	0.17	0.361
Seg.17	0.27 ± 0.49	0.3	0.01	0.29	0.01	0.26	0.028	0.42 ± 0.66	0.47	0.002	0.44	0.003	0.40	0.773	0.03 ± 0.71	0.04	0.830	0.05	0.773	0.03	0.877

Indices are shown as mean ± standard error of the mean (SEM);2D, Two-dimensional;3D, Three-dimensional; GLS, Global longitudinal strain; values of Pearson's correlation coefficient (r) and linear regression coefficient (R) coincide while the data are in the same units, thus "naturally" normalized; ρ stands for Spearman correlation.

Table 3. 2D and 3D global longitudinal strain, subgroup analysis.

	N	R	*p* Value
LV EF < 35%	17	0.699	0.002
LV EF > 35%	73	0.727	<0.001
VP > 50%	41	0.62	<0.001
VP < 50%	49	0.8	<0.001

EF, Ejection fraction; LV, Left ventricle; VP, Ventricular pacing, R—person's correlation coefficient.

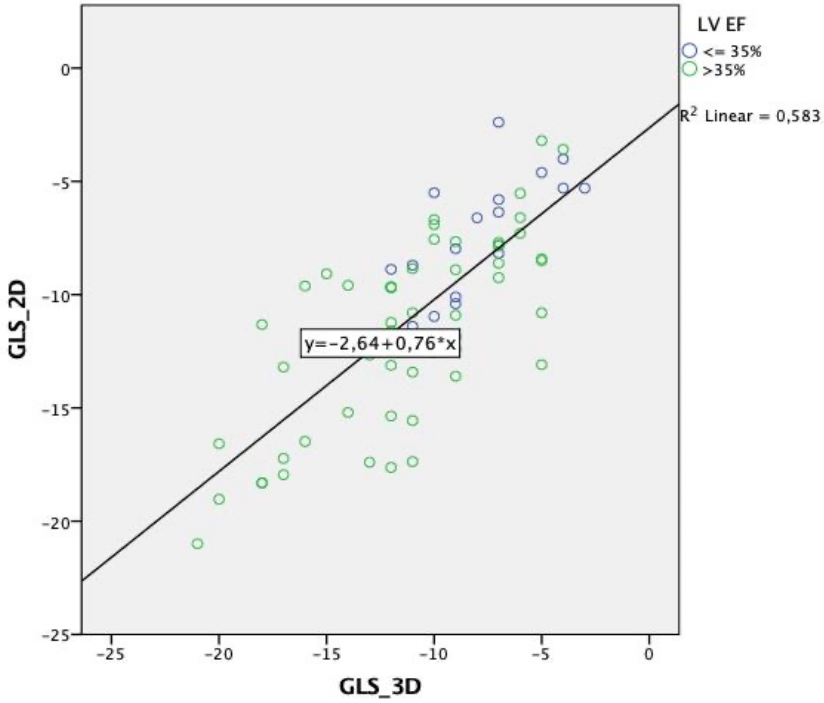

Figure 6. Scatter plot of 2D vs. 3D global longitudinal strain sorted by left ventricular ejection fraction (LV EF) with displayed regression equation.

4. Discussion

The main findings of our retrospective analysis can be summarized as follows: (1) we found a high agreement between the two-dimensional and the three-dimensional global longitudinal strain, (2) segmental agreement between the 2D and the 3D strain was poor, (3) the degree of agreement differed between genders, though not significantly, and (4) cardiac pacing and reduced LVEF were associated with a lower numerical correlation between the two-dimensional and the three-dimensional global longitudinal strain.

4.1. Previous Studies

Two-dimensional speckle-tracking echocardiography has been proven to be efficient and reliable for the quantification of regional and global LV myocardial motion in different clinical scenarios, yet it has some limitations [1,3–6,9,12]. Three-dimensional speckle-tracking echocardiography has attracted interest because it may overcome the "out of plane" movement limitation of 2D STE. However, the greater complexity of 3D STE acquisition and image analysis make it vulnerable to low image quality, tracking artifacts, and low frame rate interactions. Although it has been shown that 3D STE performance is not compromised by frame rates as low as 18–25 frame/s [14].

Many recent comparative studies have examined 2D STE, 3D STE, and MRI tagging or feature tracking, showing varying results. Altman et al. conducted a trial comparing different 2D STE and 3D STE measures, and they found that GLS was similar between 2D and 3D modes (-14 ± 4 vs. -13 ± 3, non-significant) [15]. Another trial evaluated the

agreement between 3D and 2D speckle-tracking GLS, and it found a Pearson correlation of 0.95 [16]. On the other hand, a comparison of 2D vs. 3D GLS detected a correlation coefficient of only 0.4 in healthy volunteers, compared to 0.9 in patients with mitral stenosis [6]. Another study reported a good correlation between GLS determined by cardiac magnetic resonance feature tracking (CMRFT) compared to 2DSTE (r = 0.83) and 3DSTE (r = 0.87) [17]. In one investigation, GLS values were consistently lower in the 3D mode compared to the 2D mode, and the sensitivity for predicting coronary artery disease was 80% for 2D GLS compared to 93% for 3D GLS [18]. Notably, 3D strain data were acquired faster than 2D data (2.2 ± 1 vs. 3 ± 1 min, respectively) [18].

In addition, Mirea et al. [19] showed significant 2D segmental strain variation of up to 4.5%, though the parameters from each vendor correlated to the mean of all vendors ranging from 0.58 to 0.81 [19].

The varying levels of agreement between 2D and 3D strain data may be explained by the different vendors, intra- and interobserver variability, differences in patient comorbidities and gender, cine loop image quality, and the magnitude of manual adjustments.

4.2. Current Study

To the best of our knowledge, no prior studies have compared 2D and 3D GLS between segments of the 17-segment AHA model. Surprisingly, although we found a high overall agreement between 2D and 3D GLS, the numerical correlation per segment was quite low. This is probably due to the different manner of acquisition and the segmentation processes. In the 3D mode, the calculation originates from the volumetric matrix. On the contrary, in the 2D mode, an extrapolation is created from three 2D apical planes. Moreover, we may speculate that the strain segment annotation differs between 2D and 3D mode, which could explain why there was a generally strong correlation between the two modes overall, but not per segment. On the other hand, there is some pattern to the level of correlation related to broader areas of the myocardium. Particularly anterior and anteroseptal areas demonstrated higher 2D vs. 3D GLS correlation than the rest of the heart. We may only speculate that better visualization of anterior and septal areas, which are usually in the direct beam of the ultrasound transducer, may lead to more reliable speckle tracking acquisition. On the lateral, posterior, and inferior myocardial wall the tracked border may more easily depart from the visible boundary [20]. A study by Patrianakos et al. showed a good agreement of segmental 2D STE in apical segments and a poor correlation of basal segments obtained using two different echocardiography devices [21].

Low 2D vs. 3D segmental agreement may be also caused by different mechanisms of tracking.

The sensitivity of the 3D tracking is expected to be lower in comparison with 2D tracking due to a lower resolution, thus bigger speckles to track. Also, 3D tracking corresponds to surface shortening as opposed to 2D, which represents linear shortening [22]. Since LV deformation involves a combination of apex-to-base movement, thickening, and simultaneous twisting, speckles exhibit genuine 3D motion, which 2D STE cannot account for as compared to 3D STE [22].

After the publication of the first inter-vendor study demasking a significant difference of 3.7% strain units [4], software adjustments were made to improve the inter-vendor GLS agreement [23]. This could be achieved by giving more weight to the global shortening in detriment to the local displacement.

In our study, we also found that a low LVEF of <35% and a significant amount (>50%) of right ventricular pacing were associated with a decreased correlation between 2D and 3D GLS. Both factors have the same denominator of asynchronous and/or impaired ventricular contraction. It has been also shown that the left ventricle geometry may act as a confounder. A significant reduction of GLS could be compensated by a small increase in global circumferential strain, wall thickness, and/or reduced LV diameter [24]. We may speculate that more complex 3D myocardial motion during pacing and with reduced LVEF may enhance the difference between 2D and 3D tracking based on "out of plane" motion.

Of note, the reproducibility of our GLS measurements was comparable to both of the inter-vendor trials [3,4] but higher than in the trial by Altman et al. [15]. Therefore, it is less likely that intra- or inter-observer variability meaningfully accounted for 2D and 3D strain variability in our trial.

Finally, our study is more hypothesis-generating than completely enlightening the association of GLS and segmental strain data. Comparison of 2D and 3D global and segmental strain data warrants further systematic prospective studies utilizing reference modality (CMR), computer simulated data to begin with and/or different vendor agreement studies.

4.3. Implications

Our observations may have implications for clinical practice. The global longitudinal strain is a reliable and a reproducible measure of myocardial deformation, even when assessed using different modes of acquisition (2D vs. 3D). On the contrary, caution should be paid when evaluating segmental strain data, which may significantly differ between 2D and 3D modes of tracking. It seems that GLS is more representative of global shortening than local displacement. In patients with a reduced left ventricular ejection fraction and a significant amount of right ventricular pacing, strain data must be evaluated cautiously.

4.4. Limitations

The study has several limitations. First, it was a retrospective study, and many aspects of the acquisition were not prespecified. Moreover, the agreement between the 2D and the 3D strain was determined purely based on echocardiographic methods, without comparison to the "golden standard" reference of MRI tagging or feature tracking. Notably, although there is no real golden standard for myocardial deformation, MRI is historically considered the most accurate and reliable method. In addition, we studied patients with heterogenous cardiovascular diseases.

5. Conclusions

We found that 2D and 3D GLS measurements exhibited a close overall agreement, but not when analyzed per segment according to the 17-segment AHA model. It seems that GLS is more representative of global shortening than local displacement. Moreover, high levels of right ventricular pacing and a reduced left ventricular ejection fraction were associated with a numerically lower correlation between 2D and 3D GLS. Therefore, strain data in patients with reduced ejection fraction and right ventricular pacing have to be evaluated with caution.

Author Contributions: Conceptualization, J.P.; methodology, J.P. and O.C.; validation, J.V. and T.G.; formal analysis, J.P.; image acquisition J.P., T.G., T.R., O.C. and D.D.; resources, M.H. and T.R.; data curation, J.P., T.R. and D.D. writing—original draft preparation, J.P.; writing—review and editing, J.V. and O.C.; visualization, J.P.; supervision, J.V. and M.H.; project administration, T.R.; funding acquisition, J.P. All authors have read and agreed to the published version of the manuscript.

Funding: This research was funded by University of Ostrava, Czech Republic, grant number SGS01/LF/2020 and the APC was funded by the Ministry of Health, Czech Republic; MH CZ—DRO (FNOs/2021).

Institutional Review Board Statement: The study was conducted in accordance with the Declaration of Helsinki and approved by the Institutional Review Board (or Ethics Committee) of University Hospital Ostrava on 25 February 2021 with reference number 174/2021.

Informed Consent Statement: Patients' written informed consent was waived by the Institutional Review Board due to the retrospective manner of the study. Moreover the written consent with data analysis and publication is part of image acquisition consent.

Data Availability Statement: The data that support the findings of this study are available from the corresponding author upon reasonable request and with compliance to the General Data Protection Regulation.

Conflicts of Interest: The authors declare no conflict of interest.

References

1. Amundsen, B.H.; Helle-Valle, T.; Edvardsen, T.; Torp, H.; Crosby, J.; Lyseggen, E.; Støylen, A.; Ihlen, H.; Lima, J.A.; Smiseth, O.A.; et al. Noninvasive myocardial strain measurement by speckle tracking echocardiography: Validation against sonomicrometry and tagged magnetic resonance imaging. *J. Am. Coll. Cardiol.* **2006**, *47*, 789–793. [CrossRef] [PubMed]
2. Curigliano, G.; Lenihan, D.; Fradley, M.; Ganatra, S.; Barac, A.; Blaes, A.; Herrmann, J.; Porter, C.; Lyon, A.R.; Lancellotti, P.; et al. Management of cardiac disease in cancer patients throughout oncological treatment: ESMO consensus recommendations. *Ann. Oncol.* **2020**, *31*, 171–190. [CrossRef] [PubMed]
3. Argyle, R.A.; Ray, S.G. Stress and strain: Double trouble or useful tool? *Eur. J. Echocardiogr.* **2009**, *10*, 716–722. [CrossRef] [PubMed]
4. Farsalinos, K.E.; Daraban, A.M.; Ünlü, S.; Thomas, J.D.; Badano, L.P.; Voigt, J.U. Head-to-head comparison of global longitudinal strain measurements among nine different vendors:The EACVI/ASE inter-vendor comparison study. *J. Am. Soc. Echocardiogr.* **2015**, *28*, 1171–1181. [CrossRef] [PubMed]
5. Mirea, O.; Pagourelias, E.D.; Duchenne, J.; Bogaert, J.; Thomas, J.D.; Badano, L.P.; Voigt, J.U. Intervendor Differences in the Accuracy of detecting regional functional abnormalities: A report from the EACVI-ASE strain standardization task force. *JACC Cardiovasc. Imaging* **2018**, *11*, 25–34. [CrossRef] [PubMed]
6. Poyraz, E.; Tugba, K.O.; Güvenç, R.C.; Güvenç, T.S. Correlation and agreement between 2D and 3D speckle-tracking echocardiography for left ventricular volumetric, strain, and rotational parameters in healthy volunteers and in patients with mild mitral stenosis. *Echocardiography* **2019**, *36*, 897–904. [CrossRef] [PubMed]
7. Mor-Avi, V.; Lang, R.M.; Badano, L.P.; Belohlavek, M.; Cardim, N.M.; Derumeaux, G.; Galderisi, M.; Marwick, T.; Nagueh, S.F.; Sengupta, P.P.; et al. Current and evolving echocardiographic techniques for the quantitative evaluation of cardiac mechanics: ASE/EAE consensus statement on methodology and indications endorsed by the Japanese Society of Echocardiography. *J. Am. Soc. Echocardiogr.* **2011**, *24*, 277–313. [CrossRef] [PubMed]
8. Edvardsen, T.; Gerber, B.L.; Garot, J.; Bluemke, D.A.; Lima, J.A.; Smiseth, O.A. Quantitative assessment of intrinsic regional myocardial deformation by Doppler strain rate echocardiography in humans: Validation against three-dimensional tagged magnetic resonance imaging. *Circulation* **2002**, *106*, 50–56. [CrossRef]
9. Lumens, J.; Prinzen, F.W.; Delhaas, T. Longitudinal strain: "Think globally track locally". *JACC Cardiovasc. Imaging* **2015**, *8*, 1360–1363. [CrossRef]
10. Mazhari, R.; Omens, J.H.; Pavelec, R.S.; Covell, J.W.; McCulloch, A.D. Transmural distribution of threedimensional systolic strains in stunned myocardium. *Circulation* **2001**, *104*, 336–341. [CrossRef]
11. Lumens, J.; Delhaas, T.; Arts, T.; Cowan, B.R.; Young, A.A. Impaired subendocardial contractile myofiber function in asymptomatic aged humans, as detected using MRI. *Am. J. Physiol. Heart Circ. Physiol.* **2006**, *291*, H1573–H1579. [CrossRef]
12. Karlsen, S.; Dahlslett, T.; Grenne, B.; Sjøli, B.; Smiseth, O.; Edvardsen, T.; Brunvand, H. Global longitudinal strain is more reproducible measure of left ventricular function than ejection fraction regardless of echocardiographic training. *Cardiovasc. Ultrasound* **2019**, *17*, 18. [CrossRef] [PubMed]
13. Hung, C.h.L.; Gonçalves, A.; Shah, A.M.; Cheng, S.; Kitzman, D.; Scott, S.D. Age and gender-related influences on left ventricular mechanics in elderly individuals free of prevalent heart failure: The atherosclerosis risk in communities study. *Circ. Cardiovasc. Imaging* **2017**, *10*, e004510. [CrossRef]
14. Yodwut, C.; Weinert, L.; Klas, B.; Lang, R.M.; Mor-Avi, V. Effects of frame rate on three-dimensiona speckle tracking-based measurements of myocardial deformation. *J. Am. Soc. Echocardiogr.* **2012**, *25*, 978–985. [CrossRef] [PubMed]
15. Altman, M.; Bergerot, C.; Aussoleil, A.; Davidsen, E.S.; Sibellas, F.; Ovize, M.; Bonnefoy-Cudraz, E.; Thibault, H.; Derumeaux, G. Assesment of left ventricular systolic function by deformation imaging derived from speckle tracking: A comparison between 2D and 3D echo modalities. *Eur. Heart J. Cardiovasc. Imaging* **2014**, *15*, 316–323. [CrossRef] [PubMed]
16. Trache, T.; Stöbe, S.; Tarr, A.; Pfeiffer, D.; Hagendorff, A. The agreement between 3D, standard 2D and triplane 2D speckle tracking: Effects of image quality and 3D volume rate. *Echo Res. Pract.* **2014**, *1*, 71–83. [CrossRef]
17. Obokata, M.; Nagata, Y.; Wu, V.C.; Kado, Y.; Kurabayashi, M.; Otsuji, Y.; Takeuchi, M. Direct comparison of cardiac magnetic resonance feature tracking and 2D/3D echoardiography speckle tracking for evaluation of global left ventricular strain. *Eur. Heart J. Cardiovasc. Imaging* **2016**, *17*, 525–532. [CrossRef]
18. Dillikar, M.V.; Venkateshvaran, A.; Barooah, B.; Varyani, R.; Kini, P.; Dash, P.K.; Sola, S. Three dimensional versus two dimensional strain for assessment of myocardial function: A case series. *J. Indian Acad. Echocrdiogr. Cardiovsc. Imaging* **2017**, *1*, 18–23.
19. Mirea, O.; Pagourelias, E.D.; Duchenne, J.; Bogaert, J.; Thomas, J.D.; Badano, L.P.; Voigt, J.U. Variability and reproducibility of segmental longitudinal strain measurement: A report from the EACVI-ASE strain standardization task force. *JACC Cardiovasc. Imaging* **2018**, *11*, 15–24. [CrossRef]
20. Pedrizzetti, G.; Claus, P.; Kilner, P.J.; Nagel, E. Principles of cardiovascular magnetic resonance feature tracking and echocardiographic speckle tracking for informed clinical use. *J. Cardiovasc. Magn. Reson.* **2016**, *18*, 51. [CrossRef]
21. Patrianakos, A.P.; Zacharaki, A.A.; Kalogerakis, A.; Solidakis, G.; Parthenakis, F.I.; Vardas, P.E. Two-dimensional global and segmental longitudinal strain: Are the results from software in different high-end ultrasound systems comparable? *Echo Res. Pract.* **2015**, *2*, 29–39. [CrossRef] [PubMed]

22. Muraru, D.; Niero, A.; Rodriguez-Zanella Cherata, D.; Badano, L. Three-dimensional speckle-tracking echocardiography- benefits and limitations of integrating myocardial mechanics with three-dimensional imaging. *Cardiovasc. Diagn Ther.* **2018**, *8*, 101–117. [CrossRef] [PubMed]
23. Castel, A.L.; Menet, A.; Ennezat, P.V.; Delelis, F.; Le Goffic, C.; Binda, C.; Guerbaai, R.A.; Levy, F.; Graux, P.; Tribouilloy, C.; et al. Global longitudinal strain software upgrade: Implications for intervendor consistency and longitudinal imaging studies. *Arch. Cardiovasc. Dis.* **2016**, *109*, 22–30. [CrossRef]
24. Stokke, T.M.; Hasselberg, N.E.; Smedsrud, M.K.; Sarvari, S.I.; Haugaa, K.H.; Smiseth, O.A.; Edvardsen, T.; Remme, E.W. Geometry as a confounder when assessing ventricular systolic function: Comparison between ejection fraction and strain. *J. Am. Coll. Cardiol.* **2017**, *70*, 942–954. [CrossRef] [PubMed]

M. Pešl et al.

Reduced Radiation Exposure Protocol during Computer Tomography of the Left Atrium Prior to Catheter Ablation in Patients withAtrial Fibrillation

Diagnostics (Basel)
Impact Factor: 3.39

‹ rejstřík

diagnostics

MDPI

Article

Reduced Radiation Exposure Protocol during Computer Tomography of the Left Atrium Prior to Catheter Ablation in Patients with Atrial Fibrillation

Tomasz Jadczyk [1,2,†], Jiri Wolf [1,3,†], Martin Pesl [1,3,4,†], Filip Soucek [1,3], Frantisek Lehar [1,3], Jiri Jez [1,3], Tomas Kulik [1,3], Bohdan Tyshchenko [5], Silvie Belaskova [5,6], Petr Ourednicek [6,7], Guido Caluori [1,8,9,10], Miroslav Novak [3] and Zdenek Starek [1,3,*]

1 Interventional Cardiac Electrophysiology Group, International Clinical Research Center, St. Anne's University Hospital Brno, 656 91 Brno, Czech Republic; tomasz.jadczyk@gmail.com (T.J.); jiri.wolf@philips.com (J.W.); martin.pesl@fnusa.cz (M.P.); filip.soucek@fnusa.cz (F.S.); frantisek.lehar@fnusa.cz (F.L.); jiri.jez@fnusa.cz (J.J.); kulikt@gmail.com (T.K.); guido.cal87@gmail.com (G.C.)
2 Department of Cardiology and Structural Heart Diseases, Medical University of Silesia, 40-635 Katowice, Poland
3 1st Department of Internal Medicine—Cardioangiology, St. Anne's University Hospital Brno, 656 91 Brno, Czech Republic; miroslav.novak@fnusa.cz
4 Department of Biology, Faculty of Medicine, Masaryk University, 625 00 Brno, Czech Republic
5 Biostatistics, International Clinical Research Center, St. Anne's University Hospital Brno, 656 91 Brno, Czech Republic; tishchenko.b.m@gmail.com (B.T.); silvie.belaskova@fnusa.cz (S.B.)
6 Institute of Mathematics and Statistics, Masaryk University, 611 37 Brno, Czech Republic; petr.ourednicek@philips.com
7 Department of Medical Imaging, Faculty of Medicine, St. Anne's University Hospital Brno, Masaryk University, 656 91 Brno, Czech Republic
8 Nanotechnology, CEITEC, Masaryk University, 625 00 Brno, Czech Republic
9 IHU Liryc Electrophysiology and Heart Modeling Institute, Fondation Bordeaux Université, 33600 Pessac, France
10 INSERM, UMR 1045, Cardiothoracic Research Center of Bordeaux, University Bordeaux, 33600 Pessac, France
* Correspondence: zdenek.starek@fnusa.cz; Tel.: +420-543-182-189
† These authors contributed equally to this work.

Abstract: (1) Background: Computer tomography (CT) is an imaging modality used in the pre-planning of radiofrequency catheter ablation (RFA) procedure in patients with cardiac arrhythmias. However, it is associated with a considerable ionizing radiation dose for patients. This study aims to develop and validate low-dose CT scanning protocols of the left atrium (LA) for RFA guidance. (2) Methods: 68 patients scheduled for RFA of atrial fibrillation were sequentially assigned to four groups of ECG-gated scanning protocols, based on the set tube current (TC): Group A (n = 20, TC = 33 mAs), Group B (n = 18, TC = 67 mAs), Group C (n = 10, TC = 135 mAs), and control Group D (n = 20, TC = 600 mAs). We used a 256-row multidetector CT with body weight-dependent tube voltage of 80 kVp (<70 kg), 100 kVp (70–90 kg), and 120 kVp (>90 kg). We evaluated scanning parameters including radiation dose, total scanning procedure time and signal-to-noise ratio (SNR). (3) Results: The average effective radiation dose (ED) was lower in Group A in comparison to Group B, C and D (0.83 (0.76–1.10), 1.55 (1.36–1.67), 2.91 (2.32–2.96) and 9.35 (8.00–10.04) mSv, $p < 0.05$). The total amount of contrast media was not significantly different between groups. The mean SNR was 6.5 (5.8–7.3), 7.1 (5.7–8.2), 10.8 (10.1–11.3), and 12.2 (9.9–15.7) for Group A, B, C and D, respectively. The comparisons of SNR in group A vs. B and C vs. D were without significant differences. (4) Conclusions: Optimized pre-ablation CT scanning protocols of the LA can reduce an average ED by 88.7%. Three dimensional (3D) models created with the lowest radiation protocol are useful for the integration of electro-anatomic-guided RFA procedures.

Keywords: computed tomography; catheter ablation; radiation

Citation: Jadczyk, T.; Wolf, J.; Pesl, M.; Soucek, F.; Lehar, F.; Jez, J.; Kulik, T.; Tyshchenko, B.; Belaskova, S.; Ourednicek, P.; et al. Reduced Radiation Exposure Protocol during Computer Tomography of the Left Atrium Prior to Catheter Ablation in Patients with Atrial Fibrillation. *Diagnostics* **2022**, *12*, 612. https://doi.org/10.3390/diagnostics12030612

Academic Editor: Vasileios Vassilikos

Received: 18 January 2022
Accepted: 23 February 2022
Published: 1 March 2022

1. Introduction

Despite great technological progress in the management of patients with atrial fibrillation (AF), pulmonary vein isolation (PVI) with catheter ablation might be a challenging task even for an experienced operator. Structural variabilities of the left atrium (LA) and pulmonary veins (PVs) can include LA enlargement, thepresence of LA diverticulum, additional PVs with variant anatomy of the ostia (observed in 40% of patients undergoing ablation) [1], and early-branching [2,3]. Thus, it is convenient to support electroanatomic mapping (EAM)-guided radiofrequency ablation (RFA) procedures with additional imaging of the LA, such as 3D computed tomography (CT) [4–7]. Moreover, cardiac CT allows the assessment of LA appendage for the presence of thrombus further reducing the risk of complications [8]. However, despite the significant clinical usability of CT-generated LA models, this technique is associated with substantial ionizing radiation and contrast agent exposure for patients. Thus, new scanning protocols are required to improve patient safety.

We designed low-dose LA CT scanning protocols and validated them using a standard on-site hospital CT scanner, to show the feasibility and applicability in everyday clinical workflow. Furthermore, CT-generated LA models were co-registered with the EAM system for guidance of AF catheter ablation. We validated three prospectively gated axial protocols (group A–C) with standard on-site helical scan protocol as a control (group D, data collected retrospectively).

2. Materials and Methods

This ambispective single-center open study was designed to compare four pre-ablation CT scanning protocols of LA with regards to radiation dose, contrast media volume and total scanning procedure time. The CT-generated models were assessed qualitatively and semi-quantitatively by the operator's opinion and evaluation of signal-to-noise ratio (SNR). The adequacy of the low-dose CT scanning protocol was estimated with: (1) application of a reduced effective radiation dose (ED); (2) appropriate 3D representation of LA and PV anatomy; and (3) possibility to integrate the CT model with EAM to support PVI procedures.

2.1. Study Population

Between October 2015 and May 2017, sixty-eight (68) patients with drug-resistant paroxysmal and persistent AF referred for catheter ablation were enrolled in the study. Exclusion criteria were: (1) allergy to iodine-containing contrast medium, (2) contraindication to anticoagulant therapy, (3) inability to follow instructions to hold one's breath, (4) renal failure requiring dialysis or GFR < 30 mL/min/1.73 m^2, (5) severe mitral regurgitation (to preserve homogenous contrast filling of LA), (6) LA thrombus, (7) pregnancy and (8) hemodynamic instability requiring intravenous inotropes.

During the prospective phase of the ambispective study, the individuals were grouped and underwent pre-ablation CT scanning of the LA according to one of the protocols designed with respect to the desired tube current (TC): Group A (TC = 33 mAs), Group B (TC = 67 mAs), Group C (TC = 135 mAs). In the retrospective phase of the ambispective study, we collected patients in control group D (TC = 600 mAs) from a hospital database as a scanning protocol reference routinely used at the Department of Radiology, International Clinical Research Center, St. Anne's University Hospital Brno, Czech Republic (retrospective scanning). Detailed characterizations of each scanning protocol A–D are presented in Table S1.

2.2. Scanning Procedure

The examinations were performed on a 256-slice scanner (Brilliance iCT 256; Philips Healthcare, Best, The Netherlands). Scanning protocols differed regarding body weight-dependent tube voltage and tube current with collimation automatically adapted to the length of the scan area. Prospective scans A–C applied half of the full rotation angle needed for data collection and not used overlapping angle in the time of diastole of cardiac cycle. In retrospective helical protocol D, the pitch factor was automatically calculated based on the patient's heart rate. Additionally, multicycle technology was used to reach maximum temporal resolution. Specifically, all CT scanning protocols were subdivided into three sections, based on patient weight, to allow the appropriate quality of imaging. Peak tube voltages of 80 kVp, 100 kVp, and 120 kVp were adapted according to patient body weight categories of <70 kg, 70–90 kg, and >90 kg, respectively. Tube time-current product (in mAs) was the same across the three sections of each scanning protocol and defined the inclusion of patients to the relative study group. All images were reconstructed with the same level of hybrid iterative reconstruction (hIR, iDose4, level 7). A detailed characterizations of each parameter are presented in Table S1. In the axial scan, slice thickness was 0.625 mm. All prospective scans were conducted with zero tolerance to avoid additional doses. Planned CT dose index (CTDI) is shown in Table S1. In this study, we have not used any other dose modulation techniques to further decrease dose radiation. To determine an exact field of interest (FOI) for contrast scan, we performed ultralow dose native prospective calcium scoring scan in each patient—weight-adjusted scans parameters of 120 kVp and a minimum tube current of 10 mAs, Table S1. The dose length product (DLP) of the LA and PV scans were recorded from CT scanner display or dose report. The effective radiation dose was calculated using the equation:

$$ED = kDLP, \quad (1)$$

where k = 0.017 mSv $\times$ mGy^{-1} $\times$ cm^{-1} for the cardiac CT [9].

Figure 1 shows examples of LA images performed using Group A–D scanning protocols.

2.3. Pre-Scanning Settings

Patients were instructed to maintain a normal breathing cycle throughout the study but were asked to follow the operator's verbal commands for breath-hold during active CT scanning. All patients were imaged in a supine position with their arms raised above their heads. Isocentering of the LA was obtained from the anteroposterior and left lateral X-ray views. In all protocols, the target area of interest (LA and surroundings) was precisely located before the start of the scanning procedure by using a standard dual CT radiograph (a surview) (Figure 2a) and ultralow-dose calcium scoring (Figure 2b). After precise focusing on an LA, a contrast agent tracker was placed in the middle of the LA (Figure 2c) and data acquisition was launched. The total amount of Iomeron 400 contrast (Bracco Imaging S.p.A., Milano, Italy) was calculated individually according to patient weight (0.75 mL/kg). Contrast agent was administered into peripheral veins using the angiographic injection system (Mark-V ProVis, Medrad, Inc., Indianola, PA, USA) with the following modality: (i) 50 mL of contrast agent was injected at 5 mL/s rate; (ii) the rest of the contrast agent was injected at 4 mL/s; (iii) 50 mL of saline was injected at 5 mL/s. The start of the scanning phase was triggered by the tracker threshold set to 110 Hounsfield units (HU) (Figure 2c).

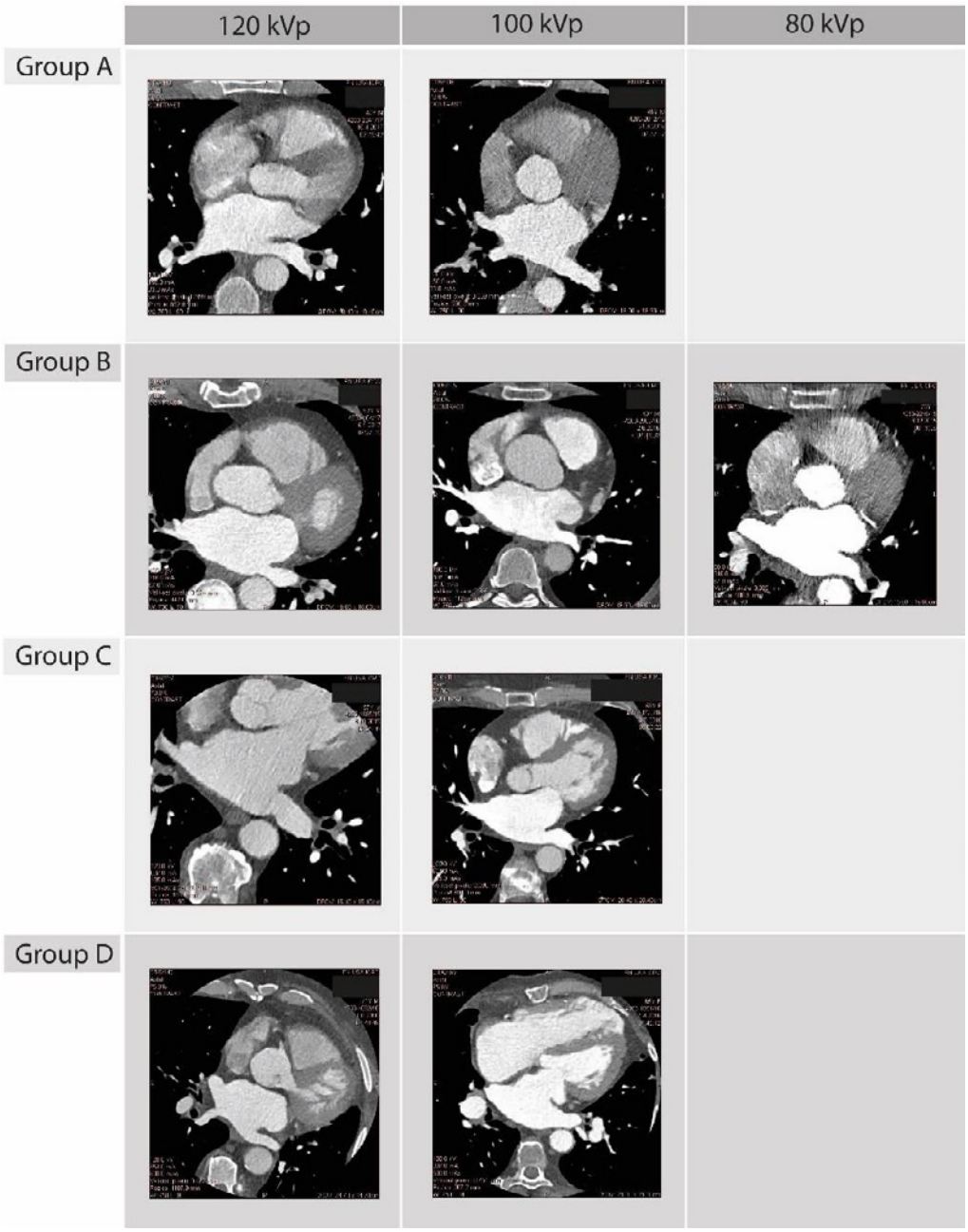

Figure 1. Examples of LA images performed using Group A–D scanning protocols. A 256-row multidetector CT with body weight-dependent tube voltage of 80 kVp (<70 kg), 100 kVp (70–90 kg), and 120 kVp (>90 kg) was used with tube current of 33 mAs, 67 mAs, 135 mAs and 600 mAs for Group A–D, respectively.

2.4. 3D Left Atrium Model Segmentation and Image Quality Assessment

EP Navigator® 3D image integration tool (Philips Healthcare, Hamburg, Germany) was used to segment CT data. Images were post-processed by an electrophysiology technician with 10 years of experience in cardiac CT analysis. The computer-derived 3D model of the LA was evaluated by two independent electrophysiologists who had over 8 years of cardiac CT reading experience. Image quality was semi-quantitatively categorized using a 3-point Likert scale: (1) excellent—LA contour and all PVs were recognized and segmented automatically; (2) useful—LA contour recognized but some of PVs needed to be segmented manually; and (3) inadequate—LA contour and/or PVs were not recognized properly, 3D reconstruction was not feasible or the details were not interpretable [10]. After the segmen-

tation process, both electrophysiologists evaluated LA models individually. Grading was concordant (agreement) if both physicians gave the same mark.

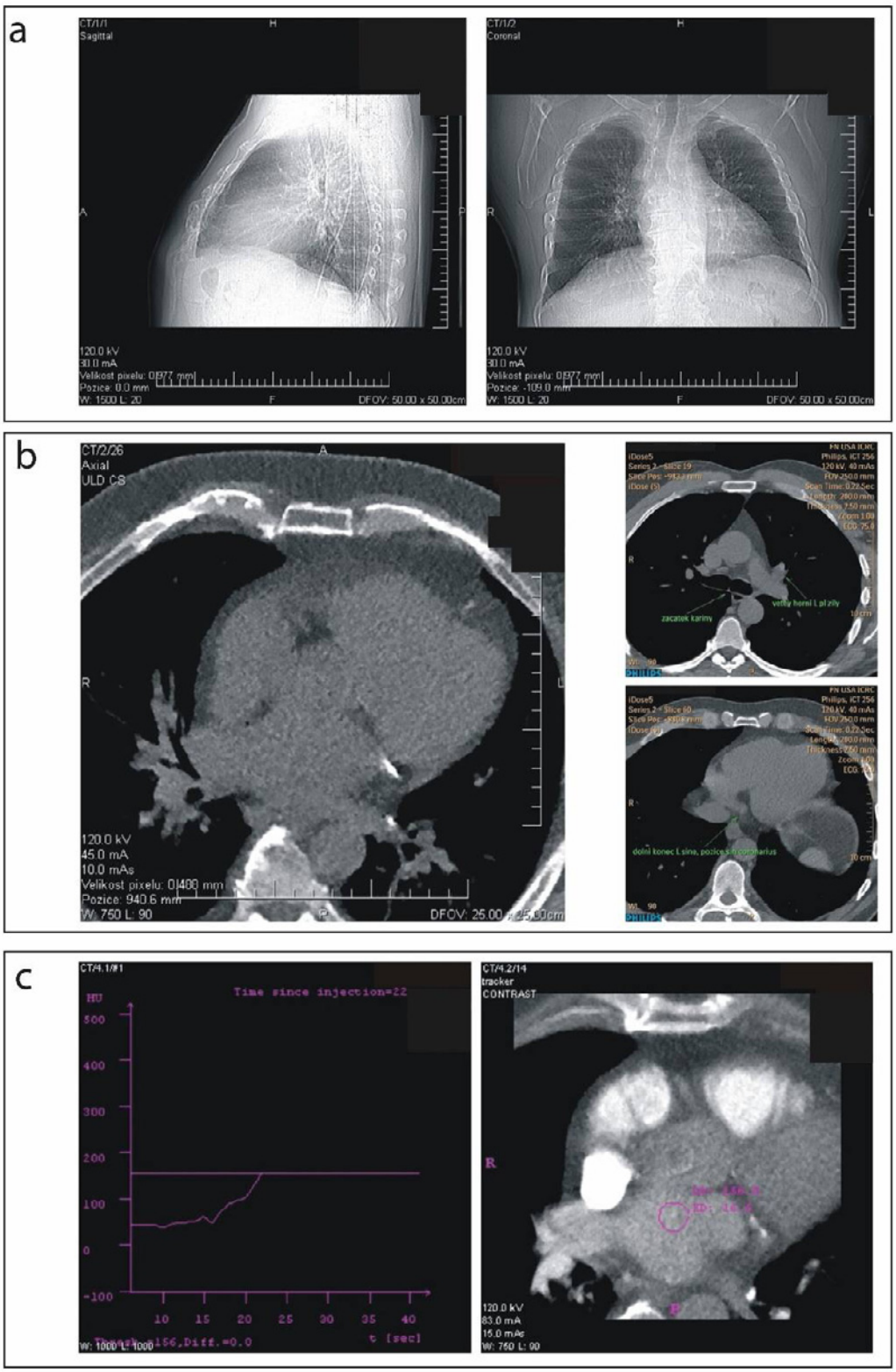

Figure 2. (**a**) Dual surview (scout in the two cross-sections); (**b**) ultra-low-dose calcium scoring; (**c**) setting of contrast agent tracker.

Quantitative assessment was performed based on the intraluminal attenuation (IA) with standard deviation (noise) in the LA. The same measurement position was chosen in all three planes (frontal, sagittal, transversal) with circular ROIs (1 cm^2) placed in the center of LA. SNR was calculated as [11]:

$$\text{SNR} = \text{IA}/\text{noise}. \quad (2)$$

2.5. CT-EAM Integration and Procedural Usefulness

The resulting LA models were integrated with the electroanatomical map using the EnSite Verismo Segmentation Tool, a component of the EnSite Velocity cardiac mapping system (Abbott Laboratories, Chicago, IL, USA). Integration was considered successful if the LA model was imported to the EAM system without errors and the operator confirmed the completeness of the import process. Procedural usefulness was assessed by the electrophysiologist performing the PVI using dichotomous categorization to (1) Useful or (2) Not useful.

2.6. Statistical Analysis

The Shapiro–Wilk test was used to assess the normal distribution of data. For the normal distribution, data were analyzed by ANOVA, followed by the Scheffe test for comparison of samples, and are presented as mean ± standard deviations (SD). The Kruskal–Wallis test, followed by Dunn's multiple comparison test (Benjamini–Hochberg-corrected p-value < 0.05), was applied for ordinal data, which is presented as medians (25th–75th IQR). A generalized linear model (GLM) for binomial response variable and logit link function was computed to predict software successful integration (categorical variable) in relation to different protocols tested in the present study. Statistical analysis was carried out using SAS (Copyright © 2017, SAS Institute Inc., Cary, NC, USA).

3. Results

Baseline patient characteristics are presented in Table 1. The median age of the study population was 61.0 (53.3–68.0) years with a numerically higher number of males among all participants (79.6%). The median body mass index (BMI) of all participants was 30.8 (26.8–32.6). Between the groups, there were no statistically significant differences in age, sex, or BMI. The four groups were homogeneous in terms of cardiovascular risk factors. RFA procedures were successful in all patients. No procedural complications were noted during CT scanning and intervention. During CT scanning, sinus rhythm was present in 32 patients and AF in 36 individuals. There was no statistically significant difference in heart rhythm distribution between groups (p = 0.241).

3.1. Dose Results

Data acquisition by 256-row MDCT was successful in all 68 patients (100%). The ECG-gated prospective axial protocol with 33 mAs tube current (Group A) allowed reduction of DLP and corresponding ED to 48.6 (44.5–64.8) mGy × cm and 0.83 (0.76–1.10) mSv, respectively, with the lowest ED value of 0.83 mSv using 80 kVp tube voltage. In comparison, radiation doses in Groups B, C and D were significantly higher at 1.55 (1.36–1.67), 2.91 (2.32–2.96) and 9.35 (8.00–10.04) mSv, respectively). The total scanning procedure time and amount of contrast media were not statistically different among the groups; details are presented in Table 2.

Table 1. Patient characteristics.

	Group A (n = 20)	Group B (n = 18)	Group C (n = 10)	Group D (n = 20)	p-Value
Age (years)	61.0 (53.0–68.0)	62.0 (56.0–66.0)	56.0 (49.0–68.0)	63.0 (58.0–69.0)	0.333
Male, n (%)	17 (85)	16 (89)	7 (70)	14 (70)	0.392
BMI (kg/m^2)	28.0 (26.4–33.8)	30.6 (26.3–34.0)	31.1 (28.1–32.0)	30.0 (27.7–32.2)	0.947
Diabetes mellitus (yes), n (%)	6 (30)	4 (22)	1 (10)	2 (10)	0.354
Hypertension (yes), n (%)	12 (60)	12 (67)	4 (40)	11 (55)	0.578
Dyslipidemia (yes), n (%)	10 (50)	6 (33)	6 (60)	8 (40)	0.514
Ischemic heart diseases (yes), n (%)	3 (15)	4 (22)	1 (10)	3 (15)	0.848
TEE, LA diameter (mm)	54.0 (46.0–60.0)	48.5 (45.0–52.5)	52.2 (47.0–58.0)	46 (40.0–55.0)	0.227
Preimaging heart rhythm, SR, n (%)	8 (40)	8 (44)	3 (30)	13 (65)	0.241

AF = atrial fibrillation; BMI = body mass index; LA = left atrium; SR = sinus rhythm; TEE = trans-esophageal echocardiography Data presented as median (25th; 75th IQR) or percentage (%).

Table 2. CT procedure characteristics.

	Group A (n = 20)	Group B (n = 18)	Group C (n = 10)	Group D (n = 20)	p-Value					
					A vs. B	A vs. C	A vs. D	B vs. C	B vs. D	C vs. D
DLP (mGy × cm)	48.6 (44.5–64.8)	90.9 (79.8–98.1)	171.2 (131.4–174.2)	550.2 (470.7–590.7)	<0.0001	<0.0001	<0.0001	<0.0001	<0.0001	<0.0001
Effective radiation dose (mSv) [§]	0.83 (0.76–1.10)	1.55 (1.36–1.67)	2.91 (2.23–2.96)	9.35 (8.00–10.04)	<0.0001	<0.0001	<0.0001	<0.0001	<0.0001	<0.0001
Total scanning procedure time (min) [#]	8.0 (7.0–11.5)	7.0 (7.0–9.0)	8.0 (7.0–11.9)	10.0 (8.0–11.0)	NS.	NS	<0.0001	NS	<0.0001	0.003
Contrast media volume (ml) [#]	66.5 (60.0–78.5)	70.5 (64.0–75.0)	76.0 (67.0–80.0)	100.0 (80.0–100.0)	NS	NS	NS	NS	NS	NS
IA ± noise (HU)	386.5 (317.2–469.6)	370.1 (280.4–451.3)	378.0 (332.0–424.0)	341.2 (306.9–97.9)	NS	NS	NS	NS	NS	NS
SNR	6.5 (5.8–7.3)	7.1 (5.7–8.2)	10.8 (10.1–11.3)	12.2 (9.9–15.7)	NS	<0.001	<0.0001	0.0004	<0.0001	n.s.

IA = intraluminal attenuation; CT = computer tomography; DLP = dose length product; HU—Hounsfield unit; SNR = signal-to-noise ratio; NS. = not significant; Data presented as median (25th–75th IQR); [§] conversion coefficient factor k = 0.017 mSv × mGy^{-1} × cm^{-1}; [#] Kruskal-Wallis test not statistically significant.

3.2. Quality of 3D Left Atrium Models, CT-EAM Integration and Procedural Usefulness

Successful image segmentation and reconstruction were achieved in all cases. For all 68 LA scans, there was full agreement in image quality scoring between both electrophysiologists. Overall, LA 3D models were graded excellent in 53 cases (77.94%) and useful in 15 cases (22.06%), with eight requiring minimal manual segmentation (up to 8 min for the presence of three right PVs), while four cases required up to 15 min of manual processing (due to contrast presence in the right atrium). No model was found to be inadequate.

Specifically for Group A, which presented the lowest radiation dose, 14 of 20 scans (70%) were graded excellent, and only one required advanced manual processing as defined above. Furthermore, heart rhythm did not affect the 3D reconstruction process and final model quality. There were no statistically significant differences between scanning protocols in terms of integration of CT images with the EAM system (p = 0.296).

In our GLM of image integration into the EAM software, Group D was considered as a control, and odds ratios estimated across the comparisons were Group C vs. Group D protocol (OR = 0.123; 95% CI 0.011–1386; p = 0.6320), Group B vs. Group D protocol (OR = 0.137; 95% CI 0.014–1.311; p = 0.3904) and Group A vs. Group D protocol (OR = 0.123; 95% CI 0.013–1.138; p = 0.267. Other models were considered with adjusted effects for BMI, cardiac rhythm and age, yet none of these additional parameters made any significant change in the test. The odds ratio estimated were: A vs. D protocol OR = 0.408; 95% CI

0.034–4.852 with $p = 0.789$; B protocol vs. D protocol OR = 0.423; 95% CI 0.035–5.058 with $p = 0.843$; C protocol vs. D protocol is OR = 0.286; 95% CI 0.019–4.284 with $p = 0.450$.

The resulting 3D LA models were used to support the EAM procedure either as a parallel view of the electroanatomical map and 3D model of LA (Figure 3a–d, left panels) or as a direct fusion of the 3D LA model with the electroanatomical map (Figure 3a–d, right panels). Both methods provided additional information about complex LA anatomy for electrophysiologists. Anatomical accuracy was reassessed through the whole procedure, and no discordance was reported. Based on the operator's opinion, all CT-generated models were procedurally useful and supportive for RFA including 12 cases (17.64%) requiring additional manual segmentation.

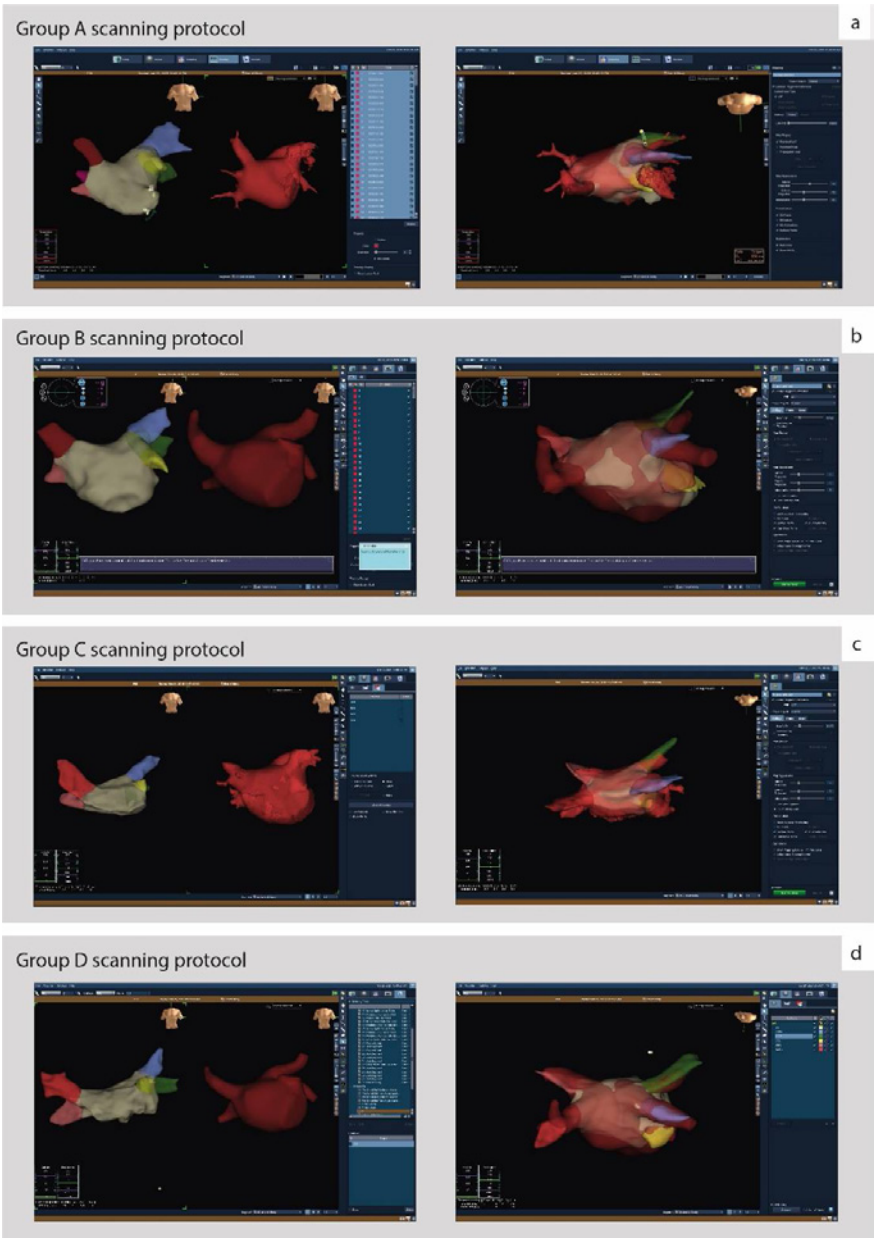

Figure 3. Parallel views of 3D electroanatomical maps with CT-generated LA models. From left to right, each subfigure represents the patient's electroanatomical maps (beige with PVs colorized), the corresponding CT LA model (red) and the fusion of the two. (**a**) Group A (current tube 33 mAs); (**b**) Group B (current tube 67 mAs); (**c**) Group C (current tube 135 mAs); (**d**) Group D (current tube 600 mAs).

Among all scanning protocols, the SNR was the highest in Group D (12.2 (9.9–15.7) reaching statistical significance in comparison to Group A (6.5 (5.8–7.3)) and Group B (7.1 (5.7–8.2), p <0.0001 Mean SNR was, 7.1 (5.7–8.2), 10.8 (10.1–11.3), and) for Groups A, B, C, and D, respectively ($p < 0.0001$ for group A vs. C and B vs. C). The comparisons of SNR in group A vs. B and C vs. D were without significant difference. Moreover, there was no statistically significant difference between standard hospital scanning protocols applied in Group D and C protocols. SNR, IA, and noise values are presented in Table 2.

4. Discussion

The rapid growth of AF prevalence in the elderly European population indicates there will be an estimated ≥14.4 million patients affected by this arrhythmia by the year 2060 [12]. The present demographic scenario is reflected by the number of individuals referred to PVI by EAM-guided catheter ablation [13]. Compensating for LA/PVs anatomical variability [14], which might reduce therapy efficacy and increase procedural time, different imaging modalities have been used to facilitate RFA procedures [4,15–17] including CT. Currently, CT scanners with excellent spatial resolution are widely distributed and could be helpful for detailed pre-procedural planning in cardiac electrophysiology. However, despite its great clinical utility [5,18], this imaging technique is associated with substantial radiation and potential long-term cancer risks due to ionizing radiation [19]. Thus, in the present study, we described low-dose CT scanning protocols that can be implemented on the standard on-site hospital CT scanner for pre-RFA imaging of LA and EAM-CT co-registration and fusion. Previously, various CT protocols have been developed, including non-ECG gated scanning, retrospective and prospective ECG-triggered axial scanning (Step & Shoot Cardiac) [20,21], dual-source high-pitch spiral scanning [22,23], adaptive statistical iterative reconstruction algorithm (ASIR; GE Healthcare, Milwaukee, WI, USA) and model-based iterative reconstruction (MBIR) technology [24]. The ECG-gated 64-row CT generates a relatively high radiation dose (13.4 mSv) requiring substantial contrast volume for adequate LA image quality. In comparison, non-ECG gated 64-row CT allows the reduction of the radiation dose to 4.6 mSv [20]. Furthermore, Annoni et al. used the MBIR algorithm to improve image quality with ED reduction to 0.4 mSv. However, applied technology required high computing power and a long reconstruction time [24]. In our study, comparing to the results reported by Annoni et al., calcium score imaging accounted for 29% of the ED and was implemented to plan FOI precisely. Importantly, there is a chance to further reduce ED by omitting this step, while determining FOI from a dual surview scan. Moreover, we used a co-efficient factor k = 0.017 mSv × mGy^{-1} × cm^{-1}, while Annoni et al. [24] and Fahlenkamp et al. [11] applied k = 0.014 mSv × mGy^{-1} × cm^{-1}. As computationally modeled, for a patient with the lowest DLP achieved in our study, we could reduce ED to 0.31 mSv (k = 0.014 mSv × mGy^{-1} × cm^{-1}). Notably, further optimization of the scanning protocol can be achieved using dedicated software for mathematical modeling of the lowest SNR to assess noise threshold acceptable by 3D reconstruction workstation, which is a goal for a further investigation. A merger of CT-reconstructed 3D models of the LA with the EAM system is an excellent supportive tool providing anatomic orientation in real-time. In our study, a fusion of the 3D LA model with the EnSite Velocity was possible in all cases. After registration of the 3D CT image to the EAM map, the LA models were consistently continuously oriented at the same angles the electroanatomical reconstruction. Moreover, the 3D image could be clipped manually for independent internal view assessment.

The resulting CT images provided valuable anatomical information enabling favorable logistics and seamless utilization in the electrophysiology laboratory. Optimization of the LA CT scanning protocol is a promising approach for reducing patients' radiation exposure as well as increasing therapeutic efficacy due to better anatomical orientation during mapping and ablation. Primarily, the present study has a practical aspect, supporting the better utilization of available on-site hospital resources for workflow improvement and sustaining the quality of diagnostic and interventional electrophysiology procedures.

It is worth noting that the application of cardiac CT expends beyond supporting ablation procedures. This imaging tool is used in clinical settings to diagnose procedural complications (i.e., LA dissection) [25], confirm/exclude the presence of thrombus [8] and plan structural heart disease procedures [26]. Parallelly, cardiac CT can be used to quantify coronary calcification burden stratifying asymptomatic patients with low and intermediate risk of cardiovascular events [27]. In this aspect, the expert review on this imaging technique highlights its predictive value beyond the traditional Framingham risk score [28]. The aforementioned examples confirm a wide range of clinical applicability and rationalize the broader clinical utilization of cardiac CT.

Limitations: This is a single-center study with only one imaging modality evaluated. An additional comparison with 3D rotational angiography, cardiac magnetic resonance, and intracardiac echocardiography would provide a more detailed understanding of a preferable diagnostic strategy. Despite detailed characteristics of low-dose scanning protocols, neither acute procedural data nor follow-up data were presented. Therefore, no conclusion on mid- and long-term outcomes can be made. Due to the relatively small number of patients enrolled in the study, larger, multicenter clinical trials are needed to confirm the promising presented findings.

5. Conclusions

Optimized left atrium CT scan protocols using hIR allow the creation of quality 3D models of the LA with a reduction in the average ED by 86.2%. Newly developed scanning protocols are simple to implement and could be applied to the standard CT workstation. Low-dose CT-generated 3D models are non-inferior to routinely used models in terms of usefulness for 3D EAM integration and guidance during RFA procedures.

Supplementary Materials: The following supporting information can be downloaded at: https://www.mdpi.com/article/10.3390/diagnostics12030612/s1, Table S1: CT scanning protocols.

Author Contributions: Conceptualization, Z.S. and J.W.; methodology, J.W., P.O. and Z.S.; formal analysis, J.W., P.O., T.J. and G.C.; investigation, J.W., M.P., F.S., F.L. and J.J.; data curation and statistics T.K., B.T., S.B. and P.O.; writing—original draft preparation, T.J.; writing—review and editing, M.P., S.B. and Z.S.; supervision, Z.S. and M.N.; funding acquisition, M.N. and Z.S. All authors have read and agreed to the published version of the manuscript.

Funding: This work was supported by project No. CZ.02.1.01/0.0/0.0/16_019/0000868 "ENOCH" from European Regional Development Fund. Statutory funds of the Medical University of Silesia in Poland (PCN-1-005/N/0/K and PCN-1-073/N/1/K), specific research funds of Faculty of Medicine, Masaryk University, project nr. MUNI/A/1462/2021 and Anneliese and Mieczysław Koćwin Foundation Scholarship (T.J.).

Institutional Review Board Statement: The study was approved by the Ethics Committee of the St. Anne's Hospital in Brno, Czech Republic (reference number 68V/2014, approved on 11 November 2014) and performed at the Department of Cardiovascular Diseases and Department of Radiology, St. Anne's Hospital in Brno, Czech Republic. The study adhered to the principles of the Declaration of Helsinki.

Informed Consent Statement: Informed consent was obtained from all subjects involved in the study.

Conflicts of Interest: Petr Ourednicek is a clinical scientist at Philips, Best, The Netherlands. Other authors declare no conflict of interest.

References

1. Kato, R.; Lickfett, L.; Meininger, G.; Dickfeld, T.; Wu, R.; Juang, G.; Angkeow, P.; LaCorte, J.; Bluemke, D.; Berger, R.; et al. Pulmonary vein anatomy in patients undergoing catheter ablation of atrial fibrillation: Lessons learned by use of magnetic resonance imaging. *Circulation* **2003**, *107*, 2004–2010. [CrossRef]
2. Chen, J.; Yang, Z.-G.; Xu, H.-Y.; Shi, K.; Long, Q.-H.; Guo, Y.-K. Assessments of pulmonary vein and left atrial anatomical variants in atrial fibrillation patients for catheter ablation with cardiac CT. *Eur. Radiol.* **2017**, *27*, 660–670. [CrossRef]

3. Skowerski, M.; Wozniak-Skowerska, I.; Hoffmann, A.; Nowak, S.; Skowerski, T.; Sosnowski, M.; Wnuk-Wojnar, A.M.; Mizia-Stec, K. Pulmonary vein anatomy variants as a biomarker of atrial fi-brillation—CT angiography evaluation. *BMC Cardiovasc. Disord.* **2018**, *18*, 146. [CrossRef]
4. Anand, R.; Gorev, M.; Poghosyan, H.; Pothier, L.; Matkins, J.; Kotler, G.; Moroz, S.; Armstrong, J.; Nemtsov, S.V.; Orlov, M.V. Prospective randomized comparison of rotational angiography with three-dimensional reconstruction and computed tomography merged with electro-anatomical mapping: A two center atrial fibrillation ablation study. *J. Interv. Card. Electrophysiol.* **2016**, *46*, 71–79. [CrossRef]
5. Dong, J.; Calkins, H.; Solomon, S.B.; Lai, S.; Dalal, D.; Lardo, A.; Brem, E.; Preiss, A.; Berger, R.D.; Halperin, H.; et al. Integrated electroanatomic mapping with three-dimensional computed tomo-graphic images for real-time guided ablations. *Circulation* **2006**, *113*, 186–194. [CrossRef] [PubMed]
6. Kistler, P.; Rajappan, K.; Harris, S.; Earley, M.J.; Richmond, L.; Sporton, S.C.; Schilling, R.J. The impact of image integration on catheter ablation of atrial fibrillation using electroanatomic mapping: A prospective randomized study. *Eur. Heart J.* **2008**, *29*, 3029–3036. [CrossRef] [PubMed]
7. Richmond, L.; Rajappan, K.; Voth, E.; Rangavajhala, V.; Earley, M.J.; Thomas, G.; Harris, S.; Sporton, S.C.; Schilling, R.J. Validation of Computed Tomography Image Integration into the EnSite NavX Mapping System to Perform Catheter Ablation of Atrial Fibrillation. *J. Cardiovasc. Electrophysiol.* **2008**, *19*, 821–827. [CrossRef]
8. Park, J.J. Computed Tomography for Assessment of Left Atrial Appendage Function. *Korean Circ. J.* **2019**, *49*, 181–182. [CrossRef]
9. Protection, R. The 2007 Recommendations of the International Commission on Radiological Protection. ICRP Publication 103. *Ann. ICRP* **2007**, *37*, 1–332.
10. Wolf, J.; Stárek, Z.; Jež, J.; Lehar, F.; Lukasova, M.; Kulik, T.; Novak, M. Rotational angiography of left ventricle to guide ventricular tachycardia ablation. *Int. J. Cardiovasc. Imaging* **2015**, *31*, 899–904. [CrossRef] [PubMed]
11. Fahlenkamp, U.L.; Diaz Ramirez, I.; Wagner, M.; Schwenke, C.; Huppertz, A.; Hamm, B.; Lembcke, A. Image quality of low-radiation dose left atrial CT using filtered back projection and an iterative reconstruction algorithm: Intra-individual comparison in unselected patients undergoing pul-monary vein isolation. *Acta Radiol.* **2018**, *59*, 161–169. [CrossRef] [PubMed]
12. Di Carlo, A.; Bellino, L.; Consoli, D.; Mori, F.; Zaninelli, A.; Baldereschi, M.; Cattarinussi, A.; D'Alfonso, M.G.; Gradia, C.; Sgherzi, B.; et al. Prevalence of atrial fibrillation in the Italian elderly population and projections from 2020 to 2060 for Italy and the European Union: The FAI Project. *EP Eur.* **2019**, *21*, 1468–1475. [CrossRef] [PubMed]
13. Kirchhof, P.; Benussi, S.; Kotecha, D.; Ahlsson, A.; Atar, D.; Casadei, B.; Castella, M.; Diener, H.C.; Heidbuchel, H.; Hendriks, J.; et al. 2016 ESC Guidelines for the management of atrial fibrillation developed in col-laboration with EACTS. *Eur. Heart J.* **2016**, *37*, 2893–2962. [CrossRef] [PubMed]
14. Hunter, R.J.; Ginks, M.; Ang, R.; Diab, I.; Goromonzi, F.C.; Page, S.; Baker, V.; Richmond, L.; Tayebjee, M.; Sporton, S.; et al. Impact of variant pulmonary vein anatomy and image integration on long-term out-come after catheter ablation for atrial fibrillation. *Europace* **2010**, *12*, 1691–1697. [CrossRef]
15. Malchano, Z.J.; Neuzil, P.; Cury, R.C.; Holmvang, G.; Weichet, J.; Schmidt, E.J.; Ruskin, J.N.; Reddy, V.Y. Integration of Cardiac CT/MR Imaging with Three-Dimensional Electroanatomical Mapping to Guide Catheter Manipulation in the Left Atrium: Implications for Catheter Ablation of Atrial Fibrillation. *J. Cardiovasc. Electrophysiol.* **2006**, *17*, 1221–1229. [CrossRef]
16. Mah, D.Y.; Miyake, C.Y.; Sherwin, E.D.; Walsh, A.; Anderson, M.J.; Western, K.; Abrams, D.; Alexander, M.E.; Cecchin, F.; Walsh, E.P.; et al. The use of an integrated electroanatomic mapping system and intracardiac echocardiography to reduce radiation exposure in children and young adults undergoing ablation of supraventricular tachycardia. *Europace* **2013**, *16*, 277–283. [CrossRef]
17. Stárek, Z.; Lehar, F.; Jež, J.; Wolf, J.; Novak, M. 3D X-ray imaging methods in support catheter ablations of cardiac arrhythmias. *Int. J. Cardiovasc. Imaging* **2014**, *30*, 1207–1223. [CrossRef]
18. Tian, J.; Jeudy, J.; Smith, M.F.; Jimenez, A.; Yin, X.; Bruce, P.A.; Lei, P.; Turgeman, A.; Abbo, A.; Shekhar, R.; et al. Three-Dimensional Contrast-Enhanced Multidetector CT for Anatomic, Dynamic, and Perfusion Characterization of Abnormal Myocardium To Guide Ventricular Tachycardia Ablations. *Circ. Arrhythmia Electrophysiol.* **2010**, *3*, 496–504. [CrossRef]
19. Picano, E.; Vano, E. The Radiation Issue in Cardiology: The time for action is now. *Cardiovasc. Ultrasound* **2011**, *9*, 35. [CrossRef]
20. Wagner, M.; Butler, C.; Rief, M.; Beling, M.; Durmus, T.; Huppertz, A.; Voigt, A.; Baumann, G.; Hamm, B.; Lembcke, A.; et al. Comparison of non-gated vs. electrocardiogram-gated 64-detector-row computed tomography for integrated electroanatomic mapping in patients undergoing pulmonary vein isolation. *Europace* **2010**, *12*, 1090–1097. [CrossRef]
21. Hlaihel, C.; Boussel, L.; Cochet, H.; Roch, J.A.; Coulon, P.; Walker, M.J.; Douek, P.C. Dose and image quality comparison between prospectively gated axial and retro-spectively gated helical coronary CT angiography. *Br. J. Radiol.* **2011**, *84*, 51–57. [CrossRef] [PubMed]
22. Thai, W.-E.; Wai, B.; Lin, K.; Cheng, T.; Heist, E.K.; Hoffmann, U.; Singh, J.P.; Truong, Q.A. Pulmonary Venous Anatomy Imaging with Low-Dose, Prospectively ECG-Triggered, High-Pitch 128-Slice Dual-Source Computed Tomography. *Circ. Arrhythmia Electrophysiol.* **2012**, *5*, 521–530. [CrossRef] [PubMed]
23. Iwayama, T.; Arimoto, T.; Ishigaki, D.; Hashimoto, N.; Kumagai, Y.; Koyama, Y.; Kiribayashi, N.; Netsu, S.; Nishiyama, S.; Takahashi, H.; et al. The Clinical Value of Nongated Dual-Source Computed Tomography in Atrial Fibrillation Catheter Ablation. *J. Cardiovasc. Electrophysiol.* **2015**, *27*, 34–40. [CrossRef] [PubMed]

24. Annoni, A.D.; Andreini, D.; Pontone, G.; Formenti, A.; Petullà, M.; Consiglio, E.; Nobili, E.; Baggiano, A.; Conte, E.; Mushtaq, S.; et al. Ultra-low-dose CT for left atrium and pulmonary veins imaging using new model-based iterative reconstruction algorithm. *Eur. Heart J.—Cardiovasc. Imaging* **2015**, *16*, 1366–1373. [CrossRef] [PubMed]
25. Cereda, A.F.; de Luca, F.; Lanzone, A.M.; Cottini, M.; Pastori, L.; Sangiorgi, G. Case report and systematic review of iatrogenic left atrial dissection in different cardiovascular specialties: A common treatment for an uncommon complication? *Catheter. Cardiovasc. Interv.* **2020**, *95*, E30–E36. [CrossRef]
26. Thériault-Lauzier, P.; Spaziano, M.; Vaquerizo, B.; Buithieu, J.; Martucci, G.; Piazza, N. Computed Tomography for Structural Heart Disease and Interventions. *Interv. Cardiol.* **2015**, *10*, 149–154. [CrossRef]
27. Oudkerk, M.; Stillman, A.E.; Halliburton, S.S.; Kalender, W.A.; Möhlenkamp, S.; McCollough, C.H.; Vliegenthart, R.; Shaw, L.J.; Stanford, W.; Taylor, A.J.; et al. Coronary artery calcium screening: Current status and recommendations from the European Society of Cardiac Radiology and North American Society for Cardiovascular Imaging. *Int. J. Cardiovasc. Imaging* **2008**, *24*, 645–671. [CrossRef]
28. Hecht, H.S. Coronary artery calcium scanning: Past, present, and future. *JACC Cardiovasc. Imaging* **2015**, *8*, 579–596. [CrossRef]

J. Veselka et al.

Prediction of sudden cardiac arrest after alcohol septal ablation for hypertrophic obstructive cardiomyopathy: ASA-SCARRE RiskScore

Am J Cardiol
Impact Factor: 3.133

‹ rejstřík

Prediction of Sudden Cardiac Arrest After Alcohol Septal Ablation for Hypertrophic Obstructive Cardiomyopathy: ASA-SCARRE Risk Score

Josef Veselka, MD, PhD[a,*], Max Liebregts, MD, PhD[b], Robert Cooper, MBChB[c], Lothar Faber, MD, PhD[d], Jaroslav Januska, MD[e], Maksim Kashtanov, MD, PhD[f], Klara Hulikova Tesarkova, RNDr, PhD[g], Peter Riis Hansen, MD, DMSc, PhD[h], Hubert Seggewiss, MD[i], Eugene Shloydo, MD, PhD[j], Kirill Popov, MD[j], Eva Hansvenclova[a], Eva Polakova, MD[a], Jurriën ten Berg, MD, PhD[b], Rodney Hilton Stables, MA, MD, BM BCh[c], Jiri Jarkovsky, RNDr, PhD[k], and Jiri Bonaventura, MD, PhD[a]

This study aimed to derive a new score, the Alcohol Septal Ablation-Sudden Cardiac ARREst (ASA-SCARRE) risk score, that can be easily used to evaluate the risk of sudden cardiac arrest events (sudden cardiac death, resuscitation, or appropriate implantable cardioverter-defibrillator discharge) after alcohol septal ablation (ASA) in patients with hypertrophic obstructive cardiomyopathy. We analyzed 1,834 patients from the Euro-ASA registry (49% men, mean age 57 ± 14 years) who were followed up for 5.0 ± 4.3 years (9,202 patient-years) after ASA. A total of 65 patients (3.5%) experienced sudden cardiac arrest events, translating to 0.72 events per 100 patient-years. The independent predictors of sudden cardiac arrest events were septum thickness before ASA (hazard ratio 1.09 per 1 mm, 95% confidence interval 1.04 to 1.14, p <0.001) and left ventricular outflow tract (LVOT) gradient at the last clinical checkup (hazard ratio 1.01 per 1 mm Hg, 95% confidence interval 1.01 to 1.02, p = 0.002). The following ASA-SCARRE risk scores were derived and independently predicted long-term risk of sudden cardiac arrest events: "0" for both LVOT gradient <30 mmHg and baseline septum thickness <20 mm; "1" for LVOT gradient ≥30 mm Hg or baseline septum thickness ≥20 mm; and "2" for both LVOT gradient ≥30 mm Hg and baseline septum thickness ≥20 mm. The C statistic of the ASA-SCARRE risk score was 0.684 (SE 0.030). In conclusion, the ASA-SCARRE risk score may be a useful and easily available clinical tool to predict risk of sudden cardiac arrest events after ASA in patients with hypertrophic obstructive cardiomyopathy. **(Am J Cardiol 2022;00:1−7)**

Introduction

Alcohol septal ablation (ASA) is effective for relief of left ventricular (LV) outflow tract (LVOT) obstruction in symptomatic patients with hypertrophic obstructive cardiomyopathy (HOCM).[1] During the procedure, a small amount of alcohol is injected into ≥1 septal branch, leading to local myocardial necrosis, shrinking of basal septum, and consequent widening of the LVOT and alleviation of symptoms. The long-term clinical course of patients who undergo ASA is not completely known, and some patients remain at risk of sudden cardiac death. The contemporary risk-scoring algorithms for patients with hypertrophic cardiomyopathy (HCM) have not been dedicated specifically to patients after ASA.[2−9] Therefore, we analyzed data from the Euro-ASA registry and derived a new model that can be easily used to evaluate the risk of sudden cardiac arrest: the Alcohol Septal Ablation-Sudden Cardiac ARREst (ASA-SCARRE) risk score.

Methods

We evaluated a total of 1,834 symptomatic patients with HOCM who underwent ASA and were recorded in the multicenter Euro-ASA registry between 1996 and 2021. Procedures were performed in 10 tertiary invasive centers in 6 European countries (Germany, Czech Republic, Denmark, The Netherlands, United Kingdom, and Russian Federation) by experienced interventional cardiologists. All patients had been prospectively included in institutional

[a]Department of Cardiology, University Hospital Motol, Second Medical School, Charles University, Prague, Czech Republic; [b]Department of Cardiology, St. Antonius Hospital Nieuwegein, Nieuwegein, The Netherlands; [c]Institute of Cardiovascular Medicine and Science, Liverpool Heart and Chest Hospital, Liverpool, United Kingdom; [d]Department of Cardiology, Ruhr University Bochum, Bochum, Germany; [e]Cardiocentre Podlesi, Trinec, Czech Republic; [f]Department of Endovascular Therapy, Sverdlovsk Regional Hospital No. 1 and Ural Federal University, Yekaterinburg, Russian Federation; [g]Department of Demography and Geodemography, Faculty of Science, Charles University, Prague, Czech Republic; [h]Department of Cardiology, Herlev and Gentofte Hospital, Hellerup, Denmark; [i]Comprehensive Heart Failure Center, University Clinic Wuerzburg, Wuerzburg, Germany; [j]Department of Cardiology, City Hospital No. 2, St. Petersburg, Russian Federation; and [k]Institute of Biostatistics and Analyses, Faculty of Medicine and Faculty of Science, Masaryk University, Brno, Czech Republic. Manuscript received June 23, 2022; revised manuscript received and accepted August 17, 2022.

See page 6 for disclosure information.

*Corresponding author: Tel +420 224434900; fax +420 224434920.
E-mail address: veselka.josef@seznam.cz (J. Veselka).

0002-9149/
https://doi.org/10.1016/j.amjcard.2022.08.028

registries and subsequently in the Euro-ASA registry. Results from the registry have been published in the past.[8,9]

The diagnosis of HOCM was based on typical clinical, electrocardiographic, transthoracic echocardiographic, and/or cardiac magnetic resonance imaging features.[1–9] Maximal LVOT gradient was measured at rest using continuous-wave Doppler echocardiography. Septum thickness was measured in the parasternal short- and long-axis planes using 2-dimensional echocardiography.

The indications for interventional treatment were limiting symptoms despite pharmacotherapy. The final decision regarding septal reduction therapy (myectomy or ASA) was made after multidisciplinary assessment and detailed discussions with the patient.

We recorded clinical, demographic, electrocardiographic, and echocardiographic data and symptoms at baseline before ASA. Patients were assessed 3 to 6 months after ASA and every year thereafter. The indications for repeated septal reduction procedure were at the discretion of each participating cardiologist/center.

For the evaluation of long-term risk of sudden cardiac arrest events, we excluded all patients who experienced such events within 30 days after ASA to differentiate between possible ASA-related events caused by periprocedural complications and the long-term risk of sudden cardiac arrest.

All clinical adverse events were confirmed by reviewing the medical records and the national databases of deaths (Czech Republic, Denmark, and Russian Federation) or updated by clinical examination (the last clinical checkup), telephone call, or e-communication. The study was performed in compliance with the Declaration of Helsinki.

Sudden cardiac arrest events were defined as cardiac death after witnessed unexpected collapse; nocturnal death; or death within 1 hour of new symptoms, successful cardiopulmonary resuscitation, or appropriate implantable cardioverter-defibrillator (ICD) discharge.

We examined (1) occurrence of 30-day and long-term sudden cardiac arrest events; (2) independent predictors of sudden cardiac arrest events during long-term follow-up; and (3) a prediction model of cardiac arrest events, the ASA-SCARRE risk score.

Traditional and established risk factors of sudden death have not been available in all patients. Therefore, an unexplained syncope, LV apical aneurysm, LV dysfunction, or family history of sudden death have not been included in the analysis.

All data were reviewed and analyzed by 2 experienced research statisticians. Data were presented as means ± SDs for continuous variables and as counts and proportions for categorical variables. Mann-Whitney *U* and Student's *t* tests were used to assess the differences between continuous variables, and chi-square test was used for categorical variables. Cox proportional hazards model was used to identify predictors of sudden cardiac arrest events. Based on previous studies,[8–16] the following variables with potential impact on the outcome were included in multivariable analysis: age; septum thickness before ASA; LV end-diastolic diameter/septum thickness before ASA; left atrial diameter at last clinical checkup; LVOT gradient at last clinical checkup; and alcohol volume injected during ASA. The multivariable analysis was performed using the Cox proportional hazard model. Parameters included in the final model were selected by forward stepwise selection based on Wald test. The binarized variables of the final model were summed into scores with possible range of 0 to 2. Because of censored data, the cutoffs of parameters and overall predictive power of the model were set by time-dependent receiver operating characteristic curve analysis. Internal validation of the final model was made using three-fold cross-validation. The long-term survival was evaluated by the Kaplan−Meier method; statistical significance of differences in survival among groups of patients was evaluated using log-rank test. A $p < 0.05$ was considered statistically significant. All reported p values were 2-sided. The statistical software SAS, version 9.4 (SAS, NC), was used for the analyses, specifically, the PHREG procedure for the Cox regression and calculation of the C statistics and LIFETEST procedure for the Kaplan−Meier analysis.

Results

We performed ASA in 1,871 patients. A total of 37 patients (2%) were excluded from the long-term analysis because of occurrence of a sudden cardiac arrest event within 30 days after ASA; 15 of these patients (0.8%) died and 22 (1.2%) experienced electrical cardioversion or appropriate ICD discharge. We analyzed long-term outcomes of 1,834 patients (Table 1) who were followed for survival for 5.0 ± 4.3 years (9,202 patient-years). Of these, 212 patients (12%) died; this translated to 2.30 deaths per 100 patient-years (Figure 1). The last clinical checkup was 4.9 ± 4.3 years after ASA.

A total of 65 patients (3.5%) experienced sudden cardiac arrest events, representing 0.72 events per 100 patient-years (Figure 1). Of these, 37 patients (57%) died, 11 (17%) were successfully resuscitated, and 25 (38%) experienced appropriate ICD discharge.

According to the prespecified multivariable analysis, independent predictors of the occurrence of sudden cardiac arrest events were septal thickness before ASA (hazard ratio [HR] 1.09 per 1 mm in septal thickness, 95% confidence interval [CI] 1.04 to 1.14, $p < 0.001$) and LVOT gradient at the last clinical checkup (HR 1.01 per 1 mm Hg in LVOT gradient, 95% CI 1.01 to 1.02, $p = 0.002$).

ASA-SCARRE risk scores were defined such that a score of "0" represented LVOT gradient <30 mm Hg and baseline septum thickness <20 mm, a score of "1" represented LVOT gradient ≥30 mmHg or baseline septum thickness ≥20 mm, and a score of "2" represented both LVOT gradient ≥30 mm Hg and baseline septum thickness ≥20 mm (Tables 1 and 2).

Survival analyses for the 3 groups with ASA-SCARRE risk scores of 0, 1, and 2 are presented Figure 1, Table 3. The ASA-SCARRE risk scores predicted low (approximately 0.4% per year), moderate (approximately 0.7% per year), and high (approximately 2% per year) risk of sudden cardiac arrest, respectively (Table 3). Based on the time-dependent receiver operating characteristic curve analysis, the sensitivities/specificities of the model for score cutoffs ≥1 and 2 at the mean follow-up time (5.0 years) were 0.85/0.38 and 0.29/0.90, respectively. The Harrell's C statistic of the ASA-SCARRE risk score was 0.684 (SE 0.030)

Table 1
Clinical and echocardiographic characteristics of the cohort divided according to the ASA-SCARRE risk score at baseline and at the last checkup

	Score 0 n = 672	Score 1 n = 959	Score 2 n = 203	All cohort n = 1834
Age, years	59±12	57±14	56±15	57±14
Males, n (%)	329 (49)	485 (51)	91 (45)	905 (49)
Total alcohol volume at 1st ASA*, ml	1.9±1.0	2.0±1.0	1.9±0.9	2.0±1.0
Total alcohol volume at 1st ASA* + re-ASA, ml	2.0±1.1	2.2±1.2	2.1±1.3	2.1±1.2
Pacemaker				
Baseline, n (%)	20 (3)	29 (3)	8 (4)	57 (3)
Last clinical check-up, n (%)	105 (16)	137 (14)	22 (11)	264 (14)
ICD*				
Baseline, n (%)	15 (2)	39 (4)	8 (4)	62 (3)
Last clinical check-up, n (%)	28 (4)	64 (7)	19 (9)	111 (6)
Dyspnea, NYHA* class				
Baseline	2.6±0.6	2.8±0.6	2.7±0.6	2.7±0.6
Last clinical check-up	1.3±0.8	1.4±0.8	1.6±0.9	1.4±0.8
NYHA* class III/IV				
Baseline, n (%)	442 (66)	690 (72)	135 (67)	1267 (69)
Last clinical check-up, n (%)	54 (8)	79 (8)	29 (14)	162 (9)
Angina, CCS* class				
Baseline	1.1±1.2	1.1±1.1	1.0±1.1	1.1±1.2
Last clinical check-up	0.5±0.8	0.5±0.8	0.6±0.7	0.5±0.8
LVOT* gradient at rest, mmHg				
Baseline	61±33	68±35	88±39	68±36
Last clinical check-up	10±6	14±15	52±30	17±20
Last gradient ≥ 30 mmHg, n (%)	0	81 (8)	203 (100)	284 (15)
LVOT* gradient decrease (%)	78±19	75±24	31±51	71±30
LV* diameter, mm				
Baseline	44.7±5.5	44.0±6.7	44.3±6.8	44.3±6.3
Last clinical check-up	45.8±5.3	46.2±6.3	46.6±6.2	46.1±6.0
LV* ejection fraction, %				
Baseline	70±8	70±8	69±9	70±8
Last clinical check-up	67±8	66±8	66±9	66±8
Septum thickness, mm				
Baseline	17.5±1.5	22.6±3.7	23.3±3.1	20.8±4.0
Last clinical check-up	13.8±3.0	16.4±4.2	19.1±4.2	15.8±4.2
LV* diameter/septum thickness				
Baseline	2.6±0.4	2.0±0.4	1.9±0.4	2.2±0.5
Last clinical check-up	3.5±1.1	3.0±1.0	2.6±0.9	3.2±1.1
Left atrium diameter, mm				
Baseline	44.7±5.5	44.0±6.7	44.3±6.8	44.3±6.3
Last clinical check-up	45.8±5.3	46.2±6.3	46.6±6.2	46.1±6.0
Mean follow-up duration, years	5.2±4.1	5.1±4.5	4.0±4.1	5.0±4.3

* ASA = alcohol septal ablation; CCS = Canadian Cardiovascular Association; IQR = interquartile range; LV = left ventricular; LVOT = left ventricular outflow tract; NYHA = New York Heart Association.

(Figure 2). The highest prediction strength of the model was during the first years after ASA (approximately 0.8 during the first 2 years of follow-up) (Figure 3). In threefold internal cross-validation, the range of the C statistic from all computations was 0.643 to 0.724.

ASA-SCARRE score was 0 in 32% of cases, 1 in 52% of cases, and 2 in 16% of cases. A total of 170 patients (9%) underwent re-ASA, and 43 patients (2%) primarily treated by ASA subsequently underwent surgical myectomy.

Discussion

As far as we know, this is the first study to generate a prediction model of sudden cardiac arrest risk after ASA. The most important findings were that (1) after exclusion of patients with periprocedural ASA complications (2% of the study population), the occurrence of sudden cardiac arrest events was 0.72 per 100 patient-years; however, the first event was fatal in more than half of the patients; (2) based on 2 independent risk predictors (septum thickness before ASA and LVOT gradient at last clinical checkup), we derived a risk model (the ASA-SCARRE risk score) for prediction of low (0.4% per year), moderate (0.7% per year), and high (2% per year) risk of sudden cardiac arrest; and (3) the ASA-SCARRE risk score is simple, intuitive, and has a reasonable predictive performance. Therefore, the proposed risk score may have potential clinical utility for improvement of risk stratification and provide a simple tool for clinicians to better communicate expected long-term outcome after ASA with patients and their families.

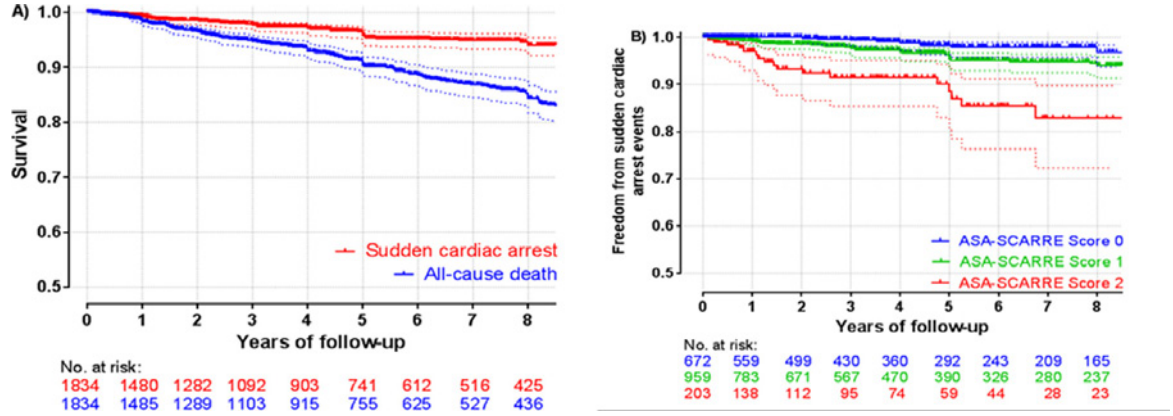

Figure 1. (*A*) Freedom from all-cause death and sudden cardiac arrest events (with 95% confidence intervals) after alcohol septal ablation in patients with hypertrophic obstructive cardiomyopathy; (*B*) freedom from sudden cardiac arrest events (with 95% confidence intervals), according to ASA-SCARRE risk score.

Sudden cardiac death is the most dreaded complication of HCM.[2–7] The current approach for risk stratification recommended by both European and United States guidelines on HCM is based on several consistent observations demonstrating that age, cardiac morphology (LV hypertrophy, LV aneurysms, increased left atrial diameter, and replacement fibrosis), LV function (increased LVOT gradient, systolic and diastolic dysfunction, and arrhythmias), patient history of syncopes, and family history of sudden death are key factors that increase the risk of sudden cardiac death.[5,6] Specifically, the American College of Cardiology/American Heart Association approach to adult patients with HCM is based on major risk factors (family history of sudden death, massive LV hypertrophy, syncope, apical aneurysm, and systolic dysfunction), and if one or more of these are present, ICD implantation should be considered.[6] The European Society of Cardiology model calculates 5-year risk based on 7 above-mentioned factors and divides patients into 3 groups with a subsequent recommendation to implant, consider, or not implant ICD.[5] Both algorithms have been repeatedly validated and, despite some criticism, have contributed significantly to appropriate selection of patients for ICD implantation and the current low rate of HCM-related sudden cardiac deaths.[2–4,7] Recently, a machine-learning-based risk stratification model for ventricular tachycardia and heart failure in patients with HCM has been proposed and may suggest a new direction for future risk management in patients with HCM.[17]

Patients treated with ASA represent a specific subgroup of patients with HOCM defined by limiting symptoms,

Table 2
Definition of the Alcohol Septal Ablation-Sudden Cardiac ARREst (ASA-SCARRE) risk score

Risk factors		Score
IVS prior to ASA	<20 mm	0
	≥20 mm	1
LVOT gradient at last clinical check-up	<30 mmHg	0
	≥30 mmHg	1
Total score		
Low risk	IVS <20 mm and LVOT gradient <30 mmHg	0
Moderate risk	IVS ≥20 mm or LVOT gradient ≥30 mmHg	1
High risk	IVS ≥20 mm and LVOT gradient ≥30 mmHg	2

IVS = septum thickness; LVOT = left ventricular outflow tract.

Table 3
Freedom from sudden cardiac arrest events after alcohol septal ablation according to the Alcohol Septal Ablation-Sudden Cardiac ARREst (ASA-SCARRE) risk score

Score	1-year survival (95% CI)	5-year survival (95% CI)	10-year survival (95% CI)	p Value	HR	p Value
0	1	0.98 (0.97-0.99)	0.96 (0.93-0.98)	<0.001	1.00	-
1	0.99 (0.98-1.00)	0.96 (0.95-0.98)	0.93 (0.90-0.95)		2.15 (1.12-4.14)	0.022
2	0.97 (0.93-0.99)	0.90 (0.82-0.94)	0.80 (0.68-0.88)		6.54 (3.12-13.70)	<0.001

HR = hazard ratio.

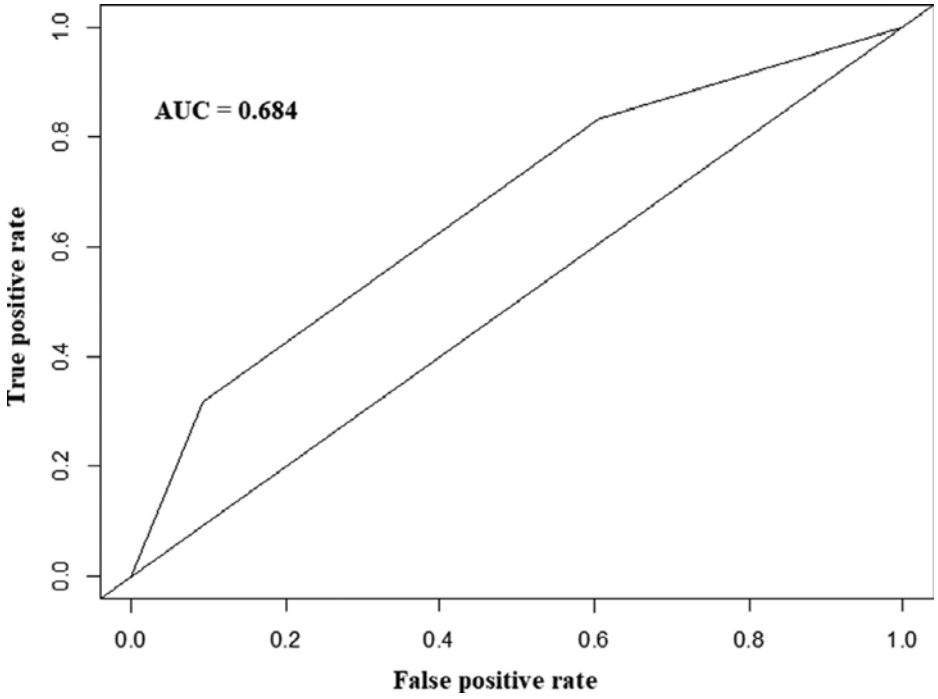

Figure 2. ROC of ASA-SCARRE risk score. ROC, receiver operating characteristic.

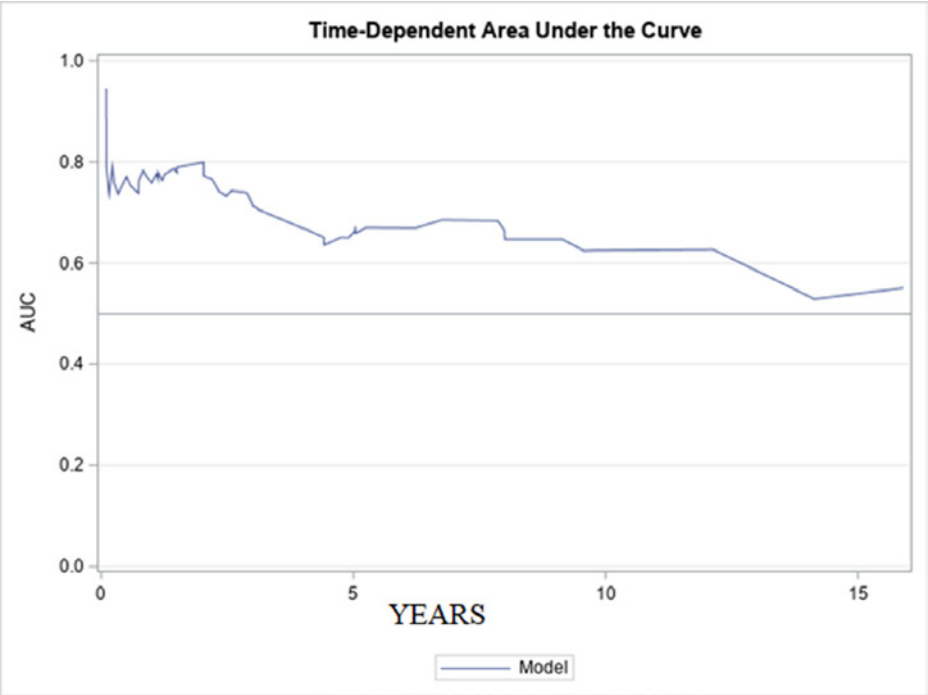

Figure 3. Time-dependent AUC representing the level of ROC for each value of time (in years) after ASA. AUC = area under the curve; ROC, receiver operating characteristic.

severe LVOT obstruction, and significant septal LV hypertrophy. Five years ago, in a cohort of patients treated with ASA (n = 844), Liebregts et al[4] validated all available recommendations dealing with prediction of sudden death in patients with HCM published between 2003 and 2014 and found modest performances (C statistic 0.58 to 0.61). One of the reasons for this finding may be that patients treated with ASA were underrepresented (3%, n =100 patients) in the analyses that generated European algorithm for risk stratification in HCM.[2]

LVOT gradient and LV hypertrophy have repeatedly been determined to be strong predictors of outcome after ASA.[9–14] Therefore, it is not surprising that we identified these 2 variables as strong independent risk factors. Subsequently, we incorporated them into a simple and readily available ASA-SCARRE risk prediction model. The model

achieved a C statistic of 0.684, with ensuing threefold internal cross-validation of 0.643 to 0.724, suggesting the possibility of clinical use.

Notably, the presented model suggests that in symptomatic patients who underwent ASA, we should aim at maximal LVOT gradient reduction, as this may reduce the risk of sudden cardiac arrest. This also further enhances the observations that high residual LVOT gradients increase the risk of sudden cardiac arrest[10,11] and provides support for the idea that actively treating this hemodynamic abnormality can affect the outcomes.

In contrast to previous models,[5,6] our intention in the present study was not to categorize patients into risk groups aimed at indication for ICD therapy but to provide an easily accessible and memorable score estimating risk of sudden cardiac arrest after ASA. We emphasize that the risk should be carefully interpreted within each patient's clinical context, including the presence of other established risk factors for sudden cardiac death such as family history of sudden death, syncope, LV dysfunction, or ventricular tachycardia. These factors were not included in our study because they were not available for all patients. However, they should definitely be considered, especially in patients with low scores.

There are some limitations of this study. First, dichotomizing of continuous variables such as interventricular septum thickness or LVOT gradient may involve borderline values in some specific patients, impairing the objectivity of evaluation. Second, although the model was derived from (to the best of our knowledge) the largest ASA outcome cohort reported to date (approximately 1,800 patients), and patients were followed for 5 years (approximately 9,200 patient-years), the number of patients with sudden cardiac arrest events was relatively low (n = 65). Nevertheless, the results are consistent with previous reports demonstrating a significant risk linked with baseline LV hypertrophy and LVOT obstruction.[9–14] Furthermore, the annual rate of sudden cardiac arrest events observed in this study (0.7% per year) was similar to that reported in the large HCM cohorts.[2,11,18] Third, an external validation study should be performed in a large and geographically diverse cohort recruited also from non-European centers.[19,20] However, although this model lacks external validation, its results clearly show that special attention should be paid to elimination of residual LVOT gradient and that we should not hesitate to use repeated septal reduction procedure and/or myosin inhibitor therapy.[21–23] Fourth, because several concomitant diseases—coronary artery disease, for example —affecting sudden cardiac death may exist in patients with HOCM, some mortality assessed as HCM-related may stem from different causes. Indeed, we speculate that this confound may be among the reasons for the limited long-term performance of all current sudden cardiac death risk models in these patients.[3,4] In conclusion, the ASA-SCARRE risk score may be a useful and easily available clinical tool to predict long-term sudden cardiac arrest events after ASA in patients with HOCM.

Disclosures

The authors have no conflict of interests to declare.

1. Sigwart U. Non-surgical myocardial reduction for hypertrophic obstructive cardiomyopathy. *Lancet* 1995;346:211–214.
2. O'Mahony C, Jichi F, Pavlou M, Monserrat L, Anastasakis A, Rapezzi C, Biagini E, Gimeno JR, Limongelli G, McKenna WJ, Omar RZ, Elliott PM. Hypertrophic Cardiomyopathy Outcomes Investigators. A novel clinical risk prediction model for sudden cardiac death in hypertrophic cardiomyopathy (HCM risk-SCD). *Eur Heart J* 2014;35:2010–2020.
3. O'Mahony C, Akhtar MM, Anastasiou Z, Guttmann OP, Vriesendorp PA, Michels M, Magrì D, Autore C, Fernández A, Ochoa JP, Leong KMW, Varnava AM, Monserrat L, Anastasakis A, Garcia-Pavia P, Rapezzi C, Biagini E, Gimeno JR, Limongelli G, Omar RZ, Elliott PM. Effectiveness of the 2014 European Society of Cardiology guideline on sudden cardiac death in hypertrophic cardiomyopathy: a systematic review and meta-analysis. *Heart* 2019;105:623–631.
4. Liebregts M, Faber L, Jensen MK, Vriesendorp PA, Hansen PR, Seggewiss H, Horstkotte D, Adlova R, Michels M, Bundgaard H, ten Berg JM, Veselka J. Validation of the HCM Risk-SCD model in patients with hypertrophic cardiomyopathy following alcohol septal ablation. *Europace* 2018;20:f198–f203.
5. Elliott PM, Anastakis A, Borger MA, Borggrefe M, Cecchi F, Charron P, Hagege AA, Lafont A, Limongelli G, Mahrholdt H, McKenna WJ, Mogensen J, Nihoyannopoulos P, Nistri S, Pieper PG, Pieske B, Rapezzi C, Rutten FH, Tillmanns C, Watkins H. 2014 ESC guidelines on diagnosis and management of hypertrophic cardiomyopathy: the Task Force for the Diagnosis and Management of Hypertrophic Cardiomyopathy of the European Society of Cardiology (ESC). *Eur Heart J* 2014;35:2733–2779.
6. Ommen SR, Mital S, Burke MA, Day SM, Deswal A, Elliott P, Evanovich LL, Hung J, Joglar JA, Kantor P, Kimmelstiel C, Kittleson M, Link MS, Maron MS, Martinez MW, Miyake CY, Schaff HV, Semsarian C, Sorajja P. 2020 AHA/ACC guideline for the diagnosis and treatment of patients with hypertrophic cardiomyopathy: executive summary: a report of the American College of Cardiology/American Heart Association Joint Committee on clinical practice guideline. *Circulation* 2020;142:e533–e557.
7. Rowin EJ, Burrows A, Madias C, Estes NAM III, Link MS, Maron MS, Maron BJ. Long-term outcome in high-risk patients with hypertrophic cardiomyopathy after primary prevention defibrillator implants. *Circ Arrhythm Electrophysiol* 2020;13:e008123.
8. Veselka J, Jensen MK, Liebregts M, Januska J, Krejci J, Bartel T, Dabrowski M, Hansen PR, Almaas VM, Seggewiss H, Horstkotte D, Tomasov P, Adlova R, Bundgaard H, Steggerda R, ten Berg J, Faber L. Long-term clinical outcome after alcohol septal ablation for obstructive hypertrophic cardiomyopathy: results from the Euro-ASA registry. *Eur Heart J* 2016;37:1517–1523.
9. Veselka J, Jensen M, Liebregts M, Cooper RM, Januska J, Kashtanov M, Dabrowski M, Hansen PR, Seggewiss H, Hansvenclova E, Bundgaard H, ten Berg J, Hilton Stables R, Faber L. Alcohol septal ablation in patients with severe septal hypertrophy. *Heart* 2020;106:462–466.
10. Veselka J, Tomašov P, Januška J, Krejčí J, Adlová R. Obstruction after alcohol septal ablation is associated with cardiovascular mortality events. *Heart* 2016;102:1793–1796.
11. Elliott PM, Gimeno JR, Tomé MT, Shah J, Ward D, Thaman R, Mogensen J, McKenna WJ. Left ventricular outflow tract obstruction and sudden death risk in patients with hypertrophic cardiomyopathy. *Eur Heart J* 2006;27:1933–1941.
12. Spirito P, Bellone P, Harris KM, Bernabo P, Bruzzi P, Maron BJ. Magnitude of left ventricular hypertrophy and risk of sudden death in hypertrophic cardiomyopathy. *N Engl J Med* 2000;342:1778–1785.
13. Jensen MK, Jacobsson L, Almaas V, van Buuren F, Hansen PR, Hansen TF, Aakhus S, Eriksson MJ, Bundgaard H, Faber L. Influence of septal thickness on the clinical outcome after alcohol septal ablation in hypertrophic cardiomyopathy. *Circ Cardiovasc Interv* 2016;9:e003214.
14. Yazaki K, Suzuki A, Shiga T, Minami Y, Arai K, Ashihara K, Shoda M, Hagiwara N. Left intraventricular pressure gradient in hypertrophic cardiomyopathy patients receiving implantable cardioverter-defibrillators for primary prevention. *BMC Cardiovasc Disord* 2021;21:106.
15. El-Sabawi B, Nishimura RA, Barsness GW, Cha YM, Geske JB, Eleid MF. Temporal occurrence of arrhythmic complications after alcohol septal ablation. *Circ Cardiovasc Interv* 2020;13:e008540.
16. Veselka J, Lawrenz T, Stellbrink C, Zemanek D, Branny M, Januska J, Groch L, Dimitrow P, Krejci J, Dabrowski M, Mizera S, Kuhn H. Low

incidence of procedure-related major adverse cardiac events after alcohol septal ablation for symptomatic hypertrophic obstructive cardiomyopathy. *Can J Cardiol* 2013;29:1415–1421.
17. Smole T, Žunkovič B, Pičulin M, Kokalj E, Robnik-Šikonja M, Kukar M, Fotiadis DI, Pezoulas VC, Tachos NS, Barlocco F, Mazzarotto F, Popović D, Maier L, Velicki L, MacGowan GA, Olivotto I, Filipović N, Jakovljević DG, Bosnić Z. A machine learning-based risk stratification model for ventricular tachycardia and heart failure in hypertrophic cardiomyopathy. *Comput Biol Med* 2021;135:104648.
18. Rowin EJ, Maron MS, Wells S, Patel PP, Koethe BC, Maron BJ. Impact of sex on clinical course and survival in contemporary treatment era for hypertrophic cardiomyopathy. *J Am Heart Assoc* 2019;8:e012041.
19. Nauffal V, Marstrand P, Han L, Parikh VN, Helms AS, Ingles J, Jacoby D, Lakdawala NK, Kapur S, Michels M, Owens AT, Ashley EA, Pereira AC, Rossano JW, Saberi S, Semsarian C, Ware JS, Wittekind SG, Day S, Olivotto I, Ho CY. Worldwide differences in primary prevention implantable cardioverter defibrillator utilization and outcomes in hypertrophic cardiomyopathy. *Eur Heart J* 2021;42:3932–3944.
20. Veselka J, Faber L, Jensen MK, Cooper R, Januska J, Krejci J, Bartel T, Dabrowski M, Hansen PR, Almaas VM, Seggewiss H, Horstkotte D, Adlova R, Bundgaard H, ten Berg J, Liebregts M. Effect of institutional experience on outcomes of alcohol septal ablation for hypertrophic obstructive cardiomyopathy. *Can J Cardiol* 2018;34:16–22.
21. Nagueh SF, Groves BM, Schwartz L, Smith KM, Wang A, Bach RG, Nielsen C, Leya F, Buergler JM, Rowe SK, Woo A, Maldonado YM, Spencer WH III. Alcohol septal ablation for the treatment of hypertrophic obstructive cardiomyopathy. A multicenter North American registry. *J Am Coll Cardiol* 2011;58:2322–2328.
22. Veselka J, Faber L, Liebregts M, Cooper R, Januska J, Krejci J, Dabrowski M, Hansen PR, Seggewiss H, Horstkotte D, Hansvenclova E, Bundgaard H, ten Berg J, Jensen MK. Long-term outcome of repeated septal reduction therapy after alcohol septal ablation for hypertrophic obstructive cardiomyopathy: insight from the Euro-ASA registry. *Arch Med Sci* 2020;16:1239–1242.
23. Panza JA, Naidu SS. Historical perspectives in the evolution of hypertrophic cardiomyopathy. *Cardiol Clin* 2019;37:1–10.

P. Stojadinović et al.

The hemodynamic effect of simulated atrial fibrillation on left ventricular function

J Cardiovasc Electrophysiol
Impact Factor: 2.942

Received: 7 July 2022 | Revised: 27 August 2022 | Accepted: 1 September 2022

DOI: 10.1111/jce.15669

ORIGINAL ARTICLES

WILEY

The hemodynamic effect of simulated atrial fibrillation on left ventricular function

Predrag Stojadinović MD[1,2] | Aslesha Deshraju MD[2] | Dan Wichterle MD, PhD[1,3] | Masato Fukunaga MD[1] | Petr Peichl MD, PhD[1] | Josef Kautzner MD, PhD[1] | Marek Šramko MD, PhD[1,2,3]

[1]Institute for Clinical and Experimental Medicine, Prague, Czech Republic

[2]Institute of Physiology, First Faculty of Medicine, Charles University, Prague, Czech Republic

[3]2nd Department of Medicine—Department of Cardiovascular Medicine, First Faculty of Medicine, Charles University, Prague, Czech Republic

Correspondence

Predrag Stojadinović, MD, Institute for Clinical and Experimental Medicine (IKEM), Vídeňská 1958/9, 140 21 Prague, Czech Republic.
Email: stop@ikem.cz

Disclosures: Marek Šramko has received speaker honoraria from Biotronik and an educational grant from Boston Scientific. Josef Kautzner reports personal fees from Bayer, Biosense Webster, Boehringer Ingelheim, Medtronic, and St. Jude Medical (Abbott) for participation in scientific advisory boards, and has received speaker honoraria from Bayer, Biosense Webster, Biotronik, Boehringer Ingelheim, CathVision, Medtronic, Mylan, Organon, Pfizer, ProMed, and St. Jude Medical (Abbott). Petr Peichl has received speaker honoraria from St. Jude Medical (Abbott) and has served as a consultant for Biotronik and Boston Scientific. Other authors: No disclosures.

Funding information

National Institute for Research of Metabolic and Cardiovascular Diseases (Programme EXCELES, Project No. LX22NPO5104) - Funded by the European Union - Next Generation EU

Abstract

Introduction: Atrial fibrillation (AF) is the most common sustained arrhythmia in humans. The onset of the arrhythmia can significantly impair cardiac function. This hemodynamic deterioration has been explained by several mechanisms such as the loss of atrial contraction, shortening of ventricular filling, or heart rhythm irregularity. This study sought to evaluate the relative hemodynamic contribution of each of these components during in vivo simulated human AF.

Methods: Twelve patients undergoing catheter ablation for paroxysmal AF were paced simultaneously from the proximal coronary sinus and the His bundle region according to prescribed sequences of irregular R–R intervals with the average rate of 90 and 130 bpm, which were extracted from the database of digital ECG recordings of AF from other patients. The simulated AF was compared to regular atrial pacing with spontaneous atrioventricular conduction and regular simultaneous atrioventricular pacing at the same heart rate. Beat-by-beat left atrial and left ventricular pressures, including LV dP/dT and Tau index were assessed by direct invasive measurement; beat-by-beat stroke volume and cardiac output (index) were assessed by simultaneous pulse-wave doppler intracardiac echocardiography.

Results: Simulated AF led to significant impairment of left ventricular systolic and diastolic function. Both loss of atrial contraction and heart rate irregularity significantly contributed to hemodynamic impairment. This effect was pronounced with increasing heart rate.

Conclusion: Our findings strengthen the rationale for therapeutic strategies aiming at rhythm control and heart rate regularization in patients with AF.

KEYWORDS

arrhythmia, atrial fibrillation, hemodynamics, his bundle pacing

Abbreviations: AF, atrial fibrillation; AV, atrioventricular; CI, cardiac index; CO, cardiac output; HB, His bundle; HR, heart rate; ICE, intracardiac echocardiography; LA, left atrium; LAP, left atrial pressure; LV, left ventricle; LVEDP, end-diastolic pressure; RV, right ventricle; SBP, systolic blood pressure; SDRR, standard deviation of R-R intervals; SV, stroke volume; VTI, velocity-time integral.

1 | INTRODUCTION

Atrial fibrillation (AF) is the most common sustained arrhythmia affecting 2% of people.[1] It can significantly impair the cardiac performance, which can clinically manifest with a spectrum ranging from mild symptoms to severe heart failure. The deleterious hemodynamic effect of AF has been explained by several pathophysiological mechanisms, including the loss of atrial kick, shortening of left ventricular (LV) diastolic filling, or heart rhythm irregularity causing neurohumoral activation.[2–7] However, the relative hemodynamic contribution of each of these mechanisms has not yet been elucidated, mainly because of the lack of a realistic hemodynamic model of human AF. On the other hand, a better understanding of the individual hemodynamic components of AF can have important clinical implications, especially for individualized nonpharmacological therapeutic strategies aiming at rate or rhythm control.

This study aimed to evaluate the relative contribution of the main hemodynamic effects of AF to the impairment of cardiac function during simulated arrhythmia. To this end, we used our previously validated in vivo model of human AF that allows us to reproduce the hemodynamics in AF by simultaneous atrial and His bundle pacing, using prescribed sequences of irregular R–R intervals extracted from the database of digital ECG recordings of AF from other patients.[8] We hypothesized that the loss of atrial contraction, heart rhythm irregularity, and shortening of LV diastolic filling by tachycardia would all independently impair cardiac performance and that these alterations would be augmented at a higher heart rate (HR).

2 | METHODS

2.1 | Study population and catheter ablation

The study included 12 patients who were indicated for catheter ablation of paroxysmal AF and maintained a stable sinus rhythm, documented by telemetric monitoring, for at least 24 h before the procedure. The required sample size was estimated based on previous studies.[2,3,5] According to our previously described protocol, the ablation procedures were performed under conscious sedation with fentanyl and midazolam.[9] Electrical isolation of the pulmonary venous ostia was performed by 3.5-mm irrigation-tip radiofrequency catheter (Navistar Thermocool; Biosense Webster), using the support of a three-dimensional electroanatomical mapping system (CARTO; Biosense Webster) The hemodynamic study was performed at the end of the ablation procedure during a stable sinus rhythm. The study was approved by the institutional ethics committee (docket ID 845/14), and all patients signed informed consent to the investigation.

2.2 | Instrumentation

A steerable decapolar catheter for atrial pacing was introduced into the coronary sinus (CS). A 6-French fluid-filled pigtail catheter was introduced into the LV cavity through a transseptal sheath via the femoral vein approach. The ablation catheter was positioned at the His bundle (HB) on the right ventricular (RV) side of the interventricular septum. Stable His bundle capture was confirmed by consistently narrow QRS complex while pacing and this site was tagged on the three-dimensional mapping system. Finally, an intracardiac echocardiography (ICE) probe (AcuNav; Siemens Medical Solutions) was positioned via the femoral vein approach in the RV outflow tract to achieve a perpendicular view of the aortic valve and a parallel view of the proximal part of the ascending aorta (Figure 1).

2.3 | Cardiac pacing

Cardiac pacing was performed by a dedicated external cardiac stimulator (MicroPace), which was connected to a purpose-made electronic device that controlled the pacing sequence (further referred to as the "sequence controller").[8] The sequence controller was programmed to generate square-shaped trigger pulses (2 V/20 ms) to emulate the predefined R–R intervals. These pulses were sensed through an ECG input of the external cardiac stimulator that was set to triggered mode and that with negligible delay generated stimulation pulses (~10 V) through a splitter to the catheters in the CS and at the HB to achieve simultaneous atrioventricular (AV) pacing. The resulting QRS duration on the surface ECG was 126 ± 13 ms. The reproducibility of this method for simulation of LV hemodynamics in AF has been previously described.[8]

2.4 | Hemodynamic study

Hemodynamic parameters were assessed during four different pacing configurations, each of them with a mean HR of 90 and 130 bpm: (1) regular pacing from the CS to simulate normal sinus rhythm, (2) regular simultaneous AV pacing from the CS, and HB to evaluate the loss of atrial systole without impeding the natural electric activation of the ventricles, (3) irregular simultaneous AV pacing according to prescribed R–R sequences with R–R interval standard deviation (SDRR) of 20% (i.e., "less irregular" simulated AF), and (4) irregular simultaneous AV pacing according to prescribed R–R sequences with an SDRR of 30% (i.e., "more irregular" simulated AF) (Figure 2).

Each pacing episode lasted 2 min and was followed by a stabilization period of 30 s of regular CS pacing with the same rate. The stabilization period was excluded from the hemodynamic analysis. All patients were paced according to the same set of R–R sequences, but the order of the pacing episodes was random for each patient. The irregular R–R sequences for simulated AF were obtained from a database of Holter ECG recordings in patients with persistent AF (http://physionet.org, the Long-Term AF Database). Representative segments of AF with the desired duration, mean HR, and SDRR were selected with the help of a custom program written in

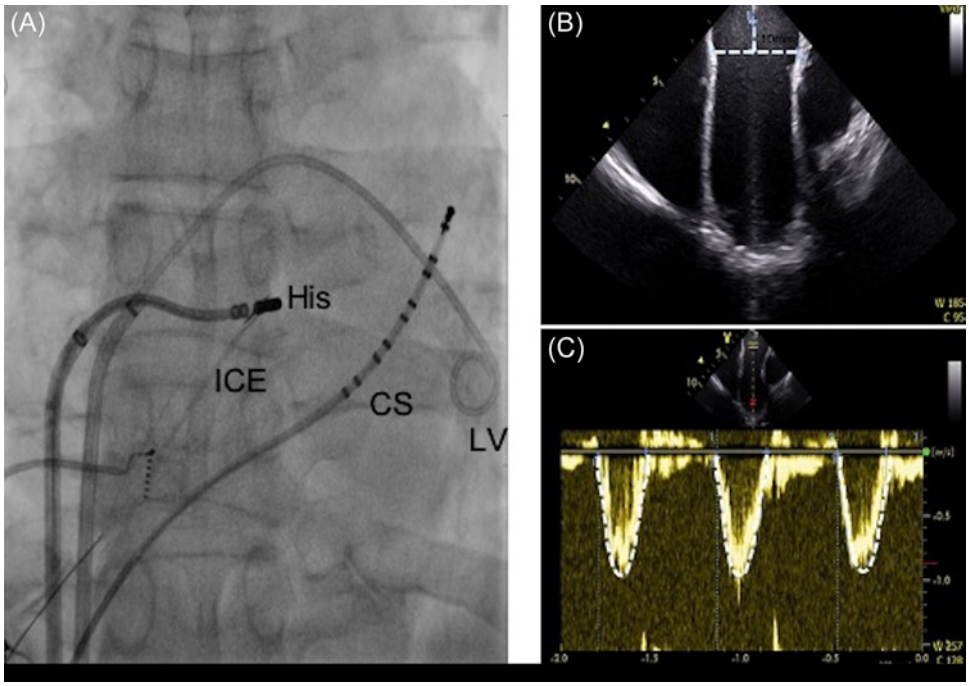

FIGURE 1 Stroke volume assessment by ICE. Fluoroscopic image of catheter setting (A). The aortic valve and ascending aorta were visualized by ICE in a long axis. The diameter of the aorta was measured at 10 mm above the aortic cusps (B). VTI was delineated manually at the level of the aortic root and was averaged over the entire pacing episode (C). In all cases, the angle of incidence during the measurement of VTI was <5°. CS, decapolar catheter introduced to the coronary sinus for atrial pacing; His, mapping catheter used for the pacing of the His bundle; ICE, intracardiac echocardiography probe, LV, pigtail catheter in the left ventricle.

FIGURE 2 Atrial fibrillation cycle length histograms. Histograms of the R–R interval that were used to simulate distinct types of atrial fibrillation: slow (90/min), fast (130/min), more regular (SDRR = 20%), and more irregular (SDRR = 30%). Means are represented by red lines. AF, atrial fibrillation, SDRR, standard deviation of R–R intervals.

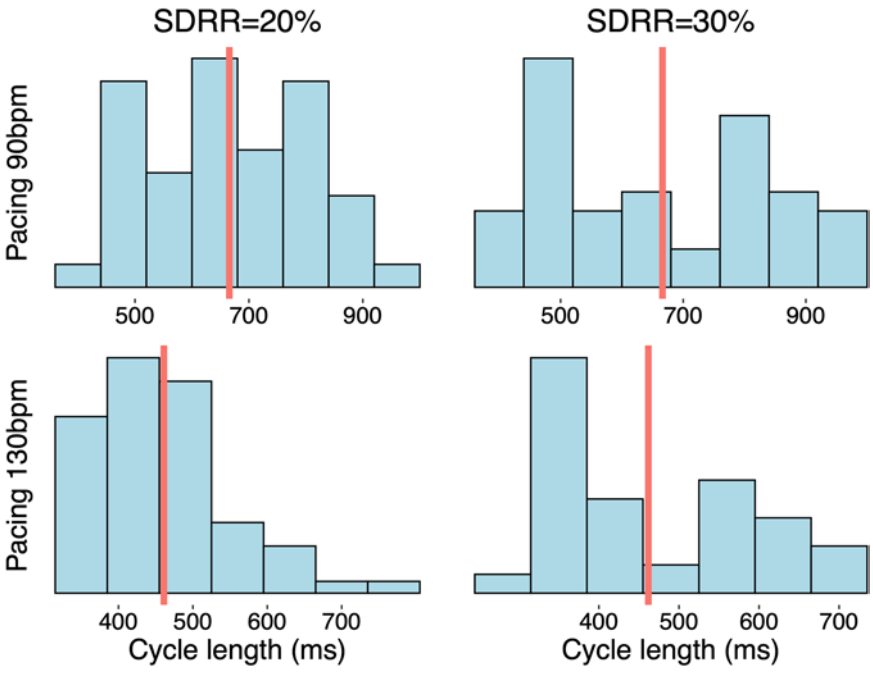

Matlab (MathWorks) that enabled automated search and reviewing of the database.

Evaluated hemodynamic parameters included: (1) blood pressure (SBP), LV end-diastolic pressure (LVEDP), LV dP/dT max, and Tau index measured with pigtail catheter in the LV, (2) mean left atrium (LA) pressure measured by the transseptal sheath in the LA, and (3) cardiac output (CO) and cardiac index (CI) were measured simultaneously by pulse-wave Doppler ICE in the ascending aorta (Figure 1).

2.5 | Data acquisition and analysis

Trigger pulses from the sequence controller, surface ECG, and analogue blood pressure signals from the LA and LV were recorded at 1000 Hz by data acquisition hardware (Powerlab; ADInstruments). The data were analyzed in LabChart 7 (ADInstruments). SBP, LVEDP, mean LA pressure, maximum LV dP/dT, and Tau index were obtained beat-by-beat, and the values were averaged over each two-min pacing episode.

Video output from ICE (the pulse-wave Doppler in the ascending aorta) was recorded to a computer with a resolution of 640 × 480 pixels and 30 frames/s and synchronized with blood pressure signals by the Video Capture Module in LabChart (ADInstruments). The recorded video loops were processed in ImageJ (http://ImageJ.net, the Fiji distribution). For each cardiac cycle, the envelope of the pulse-wave Doppler signal from the ascending aorta was manually outlined to obtain the velocity-time integral (VTI). The beat-by-beat VTI values were averaged over the entire two-min pacing episode. Stroke volume (SV) was calculated from the mean VTI and diameter of the ascending aorta at the sampling volume, according to the formula: $SV = \pi \times (\text{aorta diameter}/2)^2 \times VTI$.

2.6 | Statistical analysis

Statistical analyses were conducted in R (http://www.R-project.org). Continuous variables are displayed in means ± standard deviation. Hemodynamic changes within the individual patients were compared by paired *t* test with Holm's correction for repeated measurements. Between-group comparisons were performed using analysis of variance (ANOVA) with the Tukey post hoc test. A value of $p < .05$ was considered significant.

TABLE 1 Baseline characteristics of the study population

	N = 12
Age (years)	59 ± 5
Male gender	8 (67%)
Body mass index (kg/m^2)	29 ± 3
Arterial hypertension	6 (50%)
Diabetes mellitus	2 (16%)
History of stroke	2 (16%)
Antiarrhythmic drugs	5 (41%)
CHA2DS2-VASc score	1.7 ± 1.5
Left ventricular ejection fraction (%)	55 ± 9
Left atrial volume (ml/m^2)	39 ± 9

Note: Data are provided as means ± standard deviations or counts (proportions).

TABLE 2 Hemodynamic parameters during different pacing modes

	Pacing mode			
	Atrial regular	AV regular	AF (SDRR = 20%)	AF (SDRR = 30%)
Pacing 90 bpm				
SBP (mmHg)	142.1 ± 16.7	138.5 ± 14.4	131.9 ± 15.5	128.6 ± 15.9
LVEDP (mmHg)	12.0 ± 4.1	11.8 ± 4.2	15.2 ± 4.2	17.0 ± 3.6
LAP (mmHg)	9.6 ± 3.7	10.8 ± 4.1	11.8 ± 4.3	12.9 ± 4
LV dP/dT (mmHg/s)	2017 ± 302	1848 ± 320	1904 ± 315	1870 ± 329
Tau (ms)	39.2 ± 11.2	39.2 ± 10	50.6 ± 12.8	62.5 ± 11.9
SV (ml)	82.8 ± 10	74.4 ± 7.3	63 ± 10.7	63 ± 12.2
CI (L/min/m^2)	3.5 ± 0.4	3.1 ± 0.2	2.6 ± 0.4	2.6 ± 0.5
Pacing 130 bpm				
SBP (mmHg)	141.1 ± 20.8	124.1 ± 15.6**	116.6 ± 17.4***	114.8 ± 18.1
LVEDP (mmHg)	13.5 ± 3.7	14.7 ± 4.6	19.1 ± 5.5*	21.2 ± 6.7***
LAP (mmHg)	10.2 ± 4.8*	14 ± 3.5	14.6 ± 3.9	15.7 ± 3.8**
LV dP/dT (mmHg/s)	2300 ± 476*	1996 ± 383	1857 ± 380	1808 ± 402
Tau (ms)	41.5 ± 13.1	42.6 ± 13.1	61.6 ± 15.4**	71.4 ± 14.4**
SV (ml)	73.7 ± 12.9	50.8 ± 8.4***	41.7 ± 8.6***	42.6 ± 9.1***
CI (L/min/m^2)	4.5 ± 0.8**	3.1 ± 0.5	2.5 ± 0.5	2.6 ± 0.6

Note: Data are provided as means ± standard deviations.

Abbreviations: AF, atrial fibrillation; AV, atrio-ventricular; CI, cardiac index, LV, left ventricular; LAP, left atrial pressure; LV, left ventricular; LVEDP, left ventricular end-diastolic pressure; SBP, systolic blood pressure; SDRR, standard deviation of R–R intervals; SV, stroke volume.

The significance level for the comparison between pacing 90 bpm and pacing 130 bpm within the same pacing mode is indicated as follows:

*$p \le .05$; **$p \le .01$; ***$p \le .001$ by paired *t* test.

3 | RESULTS

The hemodynamic study was completed on all 12 patients. Their baseline characteristics are summarized in Table 1. No procedure-related clinical complications occurred. Measurement of the LV pressure was available in all 12 patients, and assessment of CI by ICE was obtained in the last 8 patients.

3.1 | The effect of loss of atrial contraction

Compared to regular atrial pacing, regular simultaneous AV pacing significantly impeded LV contractility, which was reflected by decreased SV, CI, LV dP/dT, and SBP, both at 90 and 130 bpm (Tables 2 and 3, Figure 3A,B). Regular simultaneous AV pacing at 130 bpm also significantly impeded LV diastolic function, leading to an increase in the mean LA pressure.

3.2 | The effect of heart rhythm irregularity

Compared to regular simultaneous AV pacing, irregular simultaneous AV pacing (SDRR of 20%) significantly impeded LV diastolic function, which was reflected by increased Tau and LVEDP at 90 and 130 bpm (Table 2, Figure 3A,B). The increase of Tau was further pronounced during the more irregular AF pacing (SDRR of 30%) compared to the less irregular AF pacing (SDRR of 20%).

Compared to regular simultaneous AV pacing, AF pacing also significantly impeded LV contractility, which was reflected by decreased SV, CI, and SBP at both HR, and by decreased LV dP/dT at 130 bpm. Compared to the less irregular AF pacing, the more irregular AF pacing led to a more pronounced decrease of SBP at 90 bpm and a more pronounced change in Tau index at both pacing rates, while there were no differences in SV and CI. Compared to the regular simultaneous AV pacing, the mean LA pressure increased significantly only during the more irregular AF pacing at both pacing rates.

3.3 | The effect of fast HR

An increase of HR from 90 to 130/min during regular atrial pacing was accompanied by an expected increase in CI without affecting SV and LV diastolic function (Table 2). However, increased HR during regular AV pacing or AF pacing led to a significant decrease in SV, while the CI remained unchanged thanks to the compensation by tachycardia (Table 2). Moreover,

TABLE 3 Relative percent difference between pacing modes

	Relative percent difference			
	Atrial regular vs. AV regular	AV regular vs. AF (SDRR = 20%)	Atrial regular vs. AF (SDRR = 20%)	AF (SDRR = 20%) vs. AF (SDRR = 30%)
Pacing 90 bpm				
SBP (mmHg)	−2.5**	−4.8*	−7.2***	−2.5*
LVEDP (mmHg)	−2.1	28.9*	26.2*	11.9
LAP (mmHg)	11.8	9.4	22.3	9.6
LV dP/dT (mmHg/s)	−8.4*	3.1	−5.6*	−1.8
Tau (ms)	0	29.1*	29.1*	23.5***
SV (ml)	−10.2*	−15.3**	−24*	0
CI (L/min/m^2)	−10.3*	−15.2**	−24**	0.2
Pacing 130 bpm				
SBP (mmHg)	−12.1**	−6*	−17.4***	−1.6
LVEDP (mmHg)	8.7	30.3	41.6**	10.8
LAP (mmHg)	36.6***	4.1	42.2*	7.8
LV dP/dT (mmHg/s)	−13.2**	−6.9*	−19.2***	−2.7
Tau (ms)	2.7	44.6**	48.6**	15.9*
SV (ml)	−31.1**	−17.8**	−43.3***	2
CI (L/min/m^2)	−31**	−17.9**	−43.4***	2.4

Note: Abbreviations are the same as in Table 2.

The significance level for the difference is indicated as follows:

*$p \le .05$; **$p \le .01$; ***$p \le .001$ by paired t test with Holm's correction for repeated measurements.

the adverse hemodynamic impact of the loss of atrial contraction and heart rhythm irregularity on LV contractility and diastolic function was more pronounced at a higher HR (Tables 2 and 3).

4 | DISCUSSION

4.1 | Main findings

This study used a realistic in vivo model of human AF to evaluate the hemodynamic consequences of AF. The study demonstrated the negative impact of AF on various parameters of LV systolic and diastolic function. The loss of effective atrial contraction and heart rhythm irregularity significantly contributed to the adverse hemodynamics. Tachycardia itself augmented the impact of the loss of atrial kick and heart rhythm irregularity.

4.2 | Previous studies

Two earlier studies observed an improvement of CO by 23%–56% after electrical cardioversion of AF to sinus rhythm.[6,10] The magnitude of the increase of CO was similar to the decrease of CO we observed during the induction of simulated AF. The impact of the loss of atrial "kick" on the LV filling has been demonstrated by two

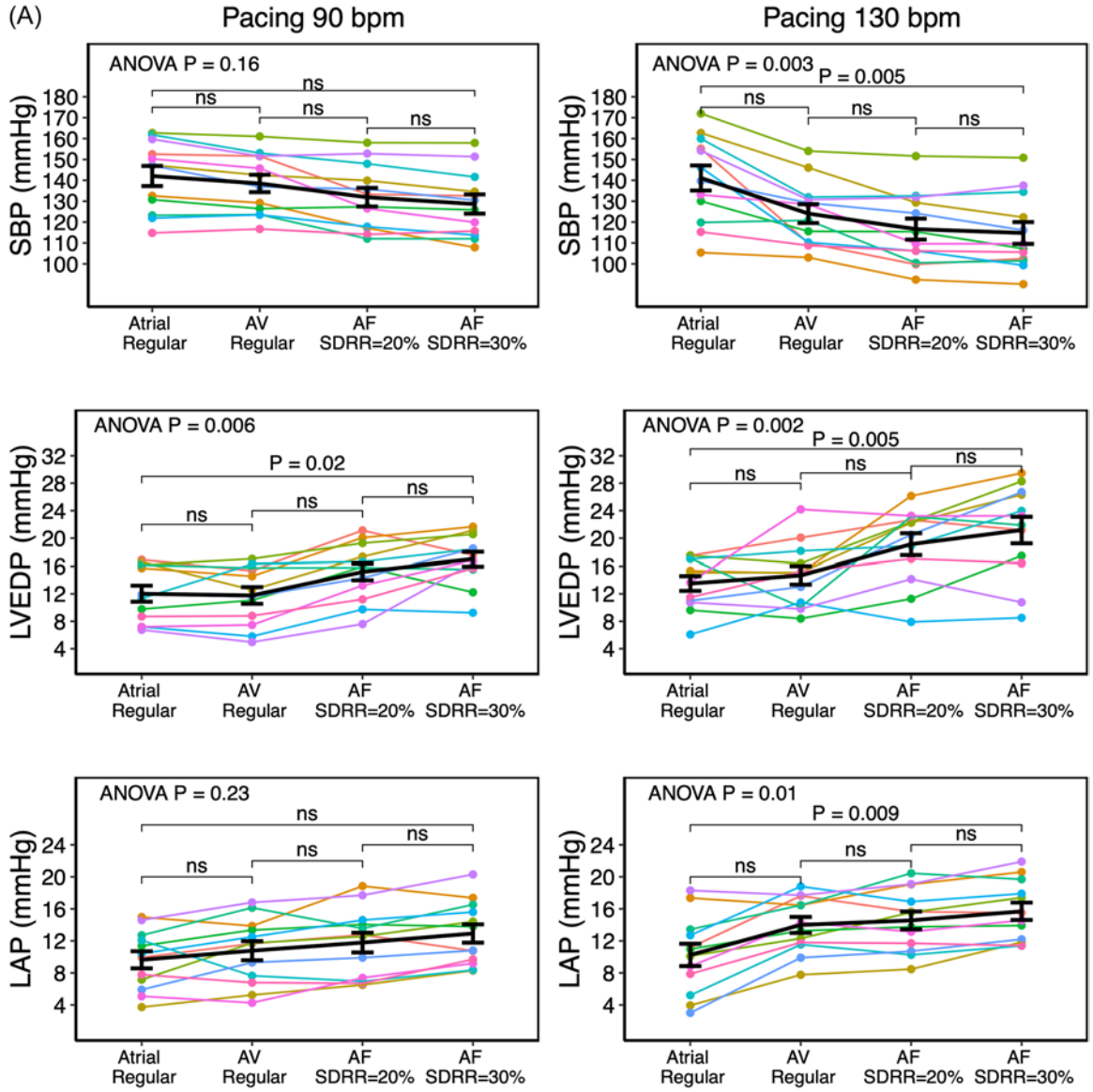

FIGURE 3 (A, B) The effect of individual pacing episodes on the hemodynamic parameters. Color lines connect the values for each patient. Black lines with error bars represent group means and standard errors. The group means were compared using analysis of variance (ANOVA) with the Tukey post hoc test. AF, atrial fibrillation, AV, atrioventricular, LAP, left atrial pressure, LVEDP, left ventricular end-diastolic pressure; SBP, systolic blood pressure; SDRR, standard deviation of R–R intervals.

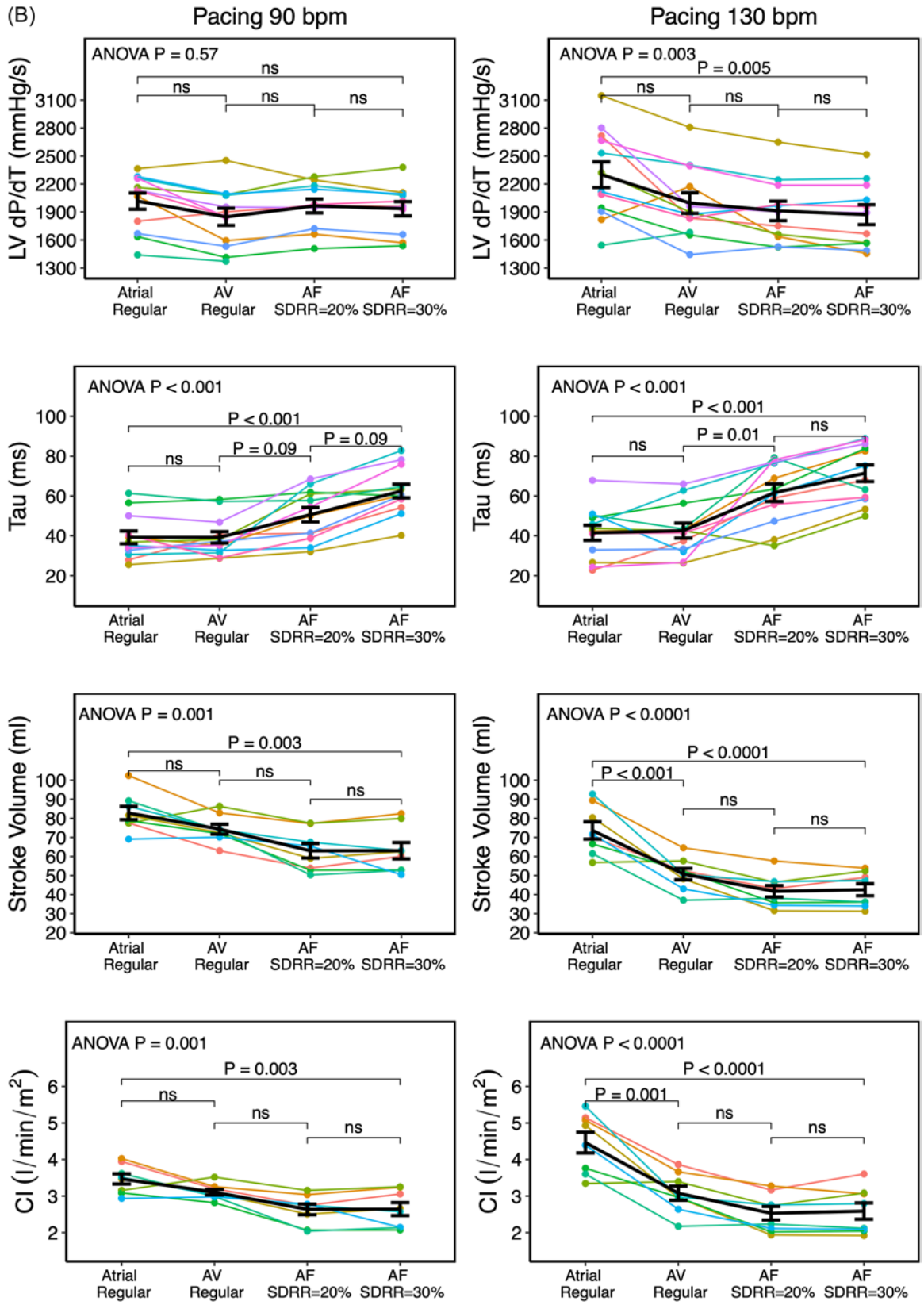

FIGURE 3 Continued

studies using simultaneous AV pacing in patients with sinus rhythm.[11,12] Our study corroborates these studies by the finding of a decreased SV by 10%–31% attributable to simultaneous AV pacing. Altogether, these findings underline the hemodynamic superiority of the sinus rhythm over AF, regardless of the actual HR.

The hemodynamic impact of heart rhythm irregularity was evaluated by two studies using RV pacing in patients with permanent AF who underwent ablation of the AV node.[3,5] The authors attributed to the heart rhythm irregularity a decrease of CO by 12% and 21%, respectively. These values are comparable to our finding of reduced CO by 15%–18% when comparing irregular AV pacing with regular AV pacing. We can only speculate whether the detrimental hemodynamic effect of heart rhythm irregularity could be related to the impairment of LV filling, changes in myocyte calcium handling, or neurohormonal activation.[3,13,14]

Of note, RV pacing alone can impair LV function.[15] This bias was partially overcome by the study of Melenovsky et al.,[16] which performed irregular pacing through exposed electrodes of a biventricular pacemaker in patients with chronic heart failure. A key feature of our hemodynamic model was the use of HB pacing, which enabled even more natural activation of the LV.

4.3 | Clinical implications

From a clinical perspective, results from this study provide the rationale to support strategies aiming at restoration and maintenance of sinus rhythm, such as electrical cardioversion, antiarrhythmic drugs, and catheter ablation. Patients in whom sinus rhythm cannot be achieved could benefit not only from rate control but also from the regularization of the heart rhythm by permanent selective HB pacing combined with AV node ablation.

4.4 | Study limitations

Our study investigated only acute hemodynamic changes during AF, not accounting for possible long-term compensatory mechanisms. The hemodynamics was not investigated during the patients' native (induced) AF. Such a design would not allow the evaluation of the hemodynamics of AF independently from the HR. Furthermore, our study included patients with preserved LV ejection fraction. It is conceivable that the hemodynamic impact of AF would be even more pronounced in patients with chronic LV systolic dysfunction. Measurement of CI by ICE was performed only in the last eight patients due to technical difficulties with the hardware setup in the first four patients. Nevertheless, the changes in CI were prominent enough to allow for an adequate statistical comparison by a paired *t* test.

Moreover, sinus rhythm was simulated by pacing from the proximal CS instead of the high RA to avoid catheter displacement during rapid pacing and to avoid atrial ectopic beats by mechanical irritation. This could have resulted in a slightly shorter AV delay during RA pacing, although the site of RA stimulation did not affect the hemodynamics during stimulated AF.

Another potential limitation is the absence of autonomic blockade during the study protocol, which could have theoretically altered the hemodynamics by sympathetic stimulation. To account for this potential bias, we applied different pacing sequences in random order and calculated the average values of the hemodynamic variables from repeated measurements. Moreover, each change in the pacing sequence included a blanking period of regular pacing to stabilize the hemodynamics.

5 | CONCLUSION

This study demonstrated the detrimental hemodynamic effect of AF and described the independent contribution of the absence of atrial kick, heart rhythm irregularity, and increased HR. These findings provide the translational basis for rhythm-control strategies in patients with AF and HR regularization strategies by permanent HB pacing if sinus rhythm cannot be maintained.

AUTHOR CONTRIBUTIONS

Substantial contributions to the conception and design or the acquisition, analysis, or interpretation of the data: Predrag Stojadinović, Aslesha Deshraju, Dan Wichterle, Masato Fukunaga, and Marek Šramko. *Substantial contributions to the drafting of the articles or critical revision for important intellectual content*: Predrag Stojadinović, Dan Wichterle, Petr Peichl, Josef Kautzner, and Marek Šramko. *Final approval of the version to be published*: Josef Kautzner and Marek Šramko. *Agreement to be accountable for all aspects of the work in ensuring that questions related to the accuracy or integrity of any part of the article are appropriately investigated and resolved*: Predrag Stojadinović and Marek Šramko.

ACKNOWLEDGMENT

This study was supported by the project National Institute for Research of Metabolic and Cardiovascular Diseases (Programme EXCELES, Project No. LX22NPO5104)—Funded by the European Union—Next Generation EU.

DATA AVAILABILITY STATEMENT

The data that support the findings of this study are available on request from the corresponding author. The data are not publicly available due to privacy or ethical restrictions.

ORCID

Predrag Stojadinović http://orcid.org/0000-0002-1487-5823
Dan Wichterle http://orcid.org/0000-0002-0448-5143
Masato Fukunaga http://orcid.org/0000-0002-0230-4556

REFERENCES

1. Hindricks G, Potpara T, Dagres N, et al. 2020 ESC guidelines for the diagnosis and management of atrial fibrillation developed in collaboration with the European Association for Cardio-Thoracic Surgery (EACTS): the Task Force for the diagnosis and management of atrial fibrillation of the European Society of Cardiology (ESC) developed with the special contribution of the European Heart Rhythm Association (EHRA) of the ESC. *Eur Heart J*. 2021;42(5):373-498.
2. Raymond RJ, Lee AJ, Messineo FC, Manning WJ, Silverman DI. Cardiac performance early after cardioversion from atrial fibrillation. *Am Heart J*. 1998;136(3):435-442.
3. Clark DM, Plumb VJ, Epstein AE, Kay GN. Hemodynamic effects of an irregular sequence of ventricular cycle lengths during atrial fibrillation. *J Am Coll Cardiol*. 1997;30(4):1039-1045.
4. Naito M, David D, Michelson EL, Schaffenburg M, Dreifus LS. The hemodynamic consequences of cardiac arrhythmias: evaluation of the relative roles of abnormal atrioventricular sequencing, irregularity of ventricular rhythm and atrial fibrillation in a canine model. *Am Heart J*. 1983;106(2):284-291.
5. Daoud EG, Weiss R, Bahu M, et al. Effect of an irregular ventricular rhythm on cardiac output. *Am J Cardiol*. 1996;78(12):1433-1436.
6. Shapiro W, Klein G. Alterations in cardiac function immediately following electrical conversion of atrial fibrillation to normal sinus rhythm. *Circulation*. 1968;38(6):1074-1084.
7. Sramko M, Wichterle D, Melenovsky V, et al. Independent effect of atrial fibrillation on natriuretic peptide release. *Clin Res Cardiol*. 2019;108(2):142-149.
8. Sramko M, Wichterle D, Kautzner J. Feasibility of in-vivo simulation of acute hemodynamics in human atrial fibrillation. *PLoS One*. 2016;11(10):e0165241.
9. Sramko M, Peichl P, Wichterle D, et al. A novel biomarker-based approach for the detection of asymptomatic brain injury during catheter ablation of atrial fibrillation. *J Cardiovasc Electrophysiol*. 2014;25(4):349-354.
10. Orlando JR, van Herick R, Aronow WS, Olson HG. Hemodynamics and echocardiograms before and after cardioversion of atrial fibrillation to normal sinus rhythm. *Chest*. 1979;76(5):521-526.
11. Mitchel H, Gupta N, Payne M. Influence of atrial systole on effective ventricular stroke volume. *Circ Res*. 1965;17:11-18.
12. Benchimol A, Duenas A, Liggett MS, Dimond EG. Contribution of atrial systole to the cardiac function at a fixed and at a variable ventricular rate. *Am J Cardiol*. 1965;16:11-21.
13. Samet P. Hemodynamic sequelae of cardiac arrhythmias. *Circulation*. 1973;47(2):399-407. doi:10.1161/01.cir.47.2.399
14. Gosselink AT, Blanksma PK, Crijns HJ, et al. Left ventricular beat-to-beat performance in atrial fibrillation: contribution of Frank–Starling mechanism after short rather than long RR intervals. *J Am Coll Cardiol*. 1995;26(6):1516-1521.
15. Lieberman R, Padeletti L, Schreuder J, et al. Ventricular pacing lead location alters systemic hemodynamics and left ventricular function in patients with and without reduced ejection fraction. *J Am Coll Cardiol*. 2006;48(8):1634-1641.
16. Melenovsky V, Hay I, Fetics BJ, et al. Functional impact of rate irregularity in patients with heart failure and atrial fibrillation receiving cardiac resynchronization therapy. *Eur Heart J*. 2005;26(7):705-711.

How to cite this article: Stojadinović P, Deshraju A, Wichterle D, et al. The hemodynamic effect of simulated atrial fibrillation on left ventricular function. *J Cardiovasc Electrophysiol*. 2022;33:2569-2577. doi:10.1111/jce.15669